Analysis of metabolic mutants of Clostridium acetobutylicum by a global and quantitative systems biology approach

Minyeong Yoo

Université de Toulouse

THÈSE

En vue de l'obtention du

DOCTORAT DE L'UNIVERSITÉ DE TOULOUSE

Délivré par :
Institut National des Sciences Appliquées de Toulouse (INSA Toulouse)

Discipline ou spécialité :

Microbiologie et Biocatalyse Industrielles

Présentée et soutenue par :
YOO Minyeong

le : vendredi 13 mai 2016

Titre :

Etude de mutants du métabolisme de Clostridium acetobutylicum par une approche globale et quantitative de biologie des systèmes

---

JURY

Nicholas Lindley Directeur de recherche, CNRS, Toulouse
Hans Geiselmann Professeur, Université Joseph Fourier, Saint-Martin-d'Hères
Lee Lynd Professeur, Dartmouth college, NH, USA
Henri-Pierre Fierobe Directeur de recherche, CNRS, Marseille
Isabelle Meynial-Salles Examinateur Maître de conférences, HDR, INSA, Toulouse

---

Ecole doctorale :
Sciences Ecologiques, Vétérinaires, Agronomiques et Bioingénieries (SEVAB)

Unité de recherche :
Laboratoire d'Ingénierie des Systèmes Biologiques et des Procédés

Directeur(s) de Thèse :

Philippe Soucaille

Rapporteurs :
Hans Geiselmann
Lee Lynd

Titre en français: Etude de mutants du métabolisme de Clostridium acetobutylicum par une approche globale et quantitative de biologie des systèms

Title in English: Analysis of metabolic mutants of Clostridium acetobutylicum by a global and quantitative systems biology approach

Résumé de la thèse

Clostridium acetobutylicum, une bactérie anaérobie stricte, à Gram positif et sporulante est maintenant considérée comme l'organisme modèle pour l'étude du métabolisme complexe des Clostridies solvantogènes. Néanmoins, malgré de nombreuses études sur le sujet, les mécanismes moléculaires impliqués dans l'induction de solvantogénèse ne sont pas encore totalement compris. Une souche témoin et trois mutants métaboliques simples avec une délétion dans les phases codantes de gènes clés impliqués dans les formations d'acides / de solvants, à savoir *ΔadhE1*, *ΔadhE2* et *ΔbukΔptb300*, ont été analysés par une approche globale à l'échelle du système pour mieux caractériser la régulation de la formation de solvant chez *C. acetobutylicum* d'un point de vue physiologique.

Tout d'abord, la souche témoin *ΔCA_C1502Δupp* a été cultivée en chemostat limité en phosphate sous trois états métaboliques différents: l'acidogénèse, la solvantogénèse, et l'alcoologénèse. Les cultures ont été analysées par une approche de transcriptomique et de protéomique quantitative associée à une analyse fluxomique, basée sur un modèle l'échelle du génome, *i*Cac967, développé au cours de la thèse. Cette étude a permis de mesurer le nombre de molécules d'ARNm par cellule pour tous les gènes dans les trois conditions métaboliques ainsi que le nombre de molécules de protéines cytosoliques par cellule pour environ 700 gènes dans au moins une des trois conditions de régime permanent.

ΔadhE1 et *ΔadhE2* ont été analysés ensemble et comparés à la souche témoin dans les mêmes conditions par une analyse transcriptomique et fluxomique globale. En condition solvantogène, seul le mutant *ΔadhE1* présentait des changements significatifs montrant une diminution de la production de butanol et des changements d'expression au niveau transcriptionel dans de

nombreux gènes. En particulier, *adhE2* était surexprimé montrant qu'AdhE2 peut remplacer partiellement AdhE1 pour la production de butanol en solvantogénèse. En condition alcoologène, seul le mutant *ΔadhE2* a montré des changements frappants dans l'expression des gènes et des flux métaboliques, avec notamment une perte totale de la production de butanol. Il est par conséquent démontré que AdhE2 est essentiel pour la production de butanol en alcoologénèse et que les flux métaboliques ont été réorientés vers la formation du butyrate. En condition acidogène, les flux métaboliques n'ont pas été significativement modifiés chez les deux mutants, mise à part la perte complète de la formation de butanol chez *ΔadhE2*, mais de manière surprenante des changements importants ont été observés, par analyse transcriptionnelle, dans l'expression de nombreux gènes. En outre, la plupart des gènes sur- ou sous-exprimés de manière significative dans cette condition physiologique, le sont pour les deux mutants.

Le mutant *ΔbukΔptb300* a également été analysé et comparé à la souche témoin dans les mêmes conditions par une analyse transcriptomique et fluxomique globale. En condition acidogène, le principal métabolite était le butanol et un nouveau composé est aussi produit qui a été identifié comme étant du 2-hydroxy-valérate. En condition solvantogène, une augmentation de la production de butanol a été obtenue par rapport à la souche de contrôle et un rendement très élevé de formation de butanol a été atteint. En condition alcoologène, le produit principal était le lactate. En outre, au niveau transcriptionnel, *adhE2* connu comme un gène exprimé spécifiquement en alcoologénèse, était étonnamment fortement exprimé dans tous les états métaboliques chez le mutant.

Mot clés: *Clostridium acetobutylicum*, Mutants métaboliques, Biologie des systèmes

Abstract

Clostridium acetobutylicum, a Gram-positive, strictly anaerobic, spore-forming bacterium is now considered as the model organism for the study of the complex metabolism of solventogenic Clostridia. Nevertheless, the molecular mechanisms involved in the induction of solventogenesis are not totally understood. A control strain and three single metabolic mutants with in frame deletion in key genes involved in acid/solvent formations, namely Δ*adhE1*, Δ*adhE2*, and Δ*buk*Δ*ptb300*, were analyzed by a system scale approach to better characterize the regulation of solvent formation in *C. acetobutylicum* from a physiological point of view.

First of all, the control strain Δ*CA_C1502*Δ*upp* was cultured in phosphate-limited chemostat under three different metabolic states, acidogenesis, solventogenesis, and alcohologenesis. The cultures were analyzed by a quantitative transciptomic and proteomic approach, and finally associated with a fluxomic analysis, based on the reconstructed genome-scale model, *i*Cac967 developed during the thesis. This study provided the number of mRNA molecules per cell for all genes under the three metabolic conditions as well as the number of cytosolic protein molecules per cell for approximately 700 genes under at least one of the three steady-state conditions.

Δ*adhE1* and Δ*adhE2* were analyzed together to be compared to the control strain under same conditions in transcriptomic and fluxomic level. Under solventogenesis, only Δ*adhE1* mutant exhibited significant changes showing decreased butanol production and transcriptional expression changes in numerous genes. In particular, *adhE2* was overexpressed; thus, AdhE2 can partially replace AdhE1 for butanol production under solventogenesis. Under alcohologenesis, only Δ*adhE2* mutant exhibited striking changes in gene expression and

metabolic fluxes, and butanol production was completely lost. Therefore, it was demonstrated that AdhE2 is essential for butanol production and thus metabolic fluxes were redirected toward butyrate formation. Under acidogenesis, metabolic fluxes were not significantly changed in both mutants except the complete loss of butanol formation in Δ*adhE2*, but numerous changes in gene expression were observed. Furthermore, most of the significantly up- or down-regulated genes under this condition showed the same pattern of change in both mutants.

Δ*buk*Δ*ptb300* was also analyzed to be compared to the control strain under same conditions in transcriptomic and fluxomic level. Under acidogenic conditions the primary metabolite was butanol and a new compound, 2-hydroxy-valerate was produced while under solventogenesis, increased butanol production was obtained compared to control strain under same condition and a very high yield of butanol formation was reached. Under alcohologenesis, the major product was lactate. Furthermore, at the transcriptional level, *adhE2* known as a gene specifically expressed in alcohologenesis, was surprisingly highly expressed in all the metabolic states in the mutant.

Key words: *Clostridium acetobutylicum*, Metabolic mutants, Systems biology

List of contents

List of figures

List of supplementary figures

Figure S3.3. Metabolic flux map of *ΔadhE1* under acidogenesis (A), *ΔadhE2* under acidogenesis (B), *ΔadhE1* under solventogenesis (C), *ΔadhE2* under solventogenesis (D), *ΔadhE1* under alcohologenesis (E), *ΔadhE2* under alcohologenesis (F)

Figure S4.1. Butanol pathway analysis of control (A) and *ΔbukΔptb* (B) under acidogenesis, solventogenesis, and alcohologenesis

Figure S4.2 Metabolic flux map of control and ΔbukΔptb300 strains under three metabolic states

List of tables

List of supplementary tables

Table S3.6. Four-fold increased or decreased genes under alcohologenesis in *ΔadhE1*

Table S3.7. Four-fold increased or decreased genes under alcohologenesis in *ΔadhE2*

Table S4.1. Four-fold increased genes under acidogenesis in *ΔbukΔptb*

Table S4.2. Four-fold decreased genes under acidogenesis in *ΔbukΔptb*

Table S4.3. Four-fold increased genes under solventogenesis in *ΔbukΔptb*

Table S4.4. Four-fold decreased genes under solventogenesis in *ΔbukΔptb*

Table S4.5. Four-fold increased genes under alcohologenesis in *ΔbukΔptb*

Table S4.6. Four-fold decreased genes under alcohologenesis in *ΔbukΔptb*

Abbreviations

Aad: aldehyde/alcohol dehydrogenase, adhE

ABE: acetone-butanol-ethanol

AdhE: aldehyde/alcohol dehydrogenase

Ack: acetate kinase

Adc: acetoacetatedecarboxylase

ADP: adenosine-5’ diphosphate

AlsD: alpha-acetolatate decarboxylase

AlsS: acetolactate synthase

ATP: adenosine-5’ triphosphate

Bcd: butyryl-CoAdehydrogenase

Bdh: butanol dehydrogenase

bp: base pair

B.subtilis: Bacilus subtilis

Buk: butyrate kinase

C .acetobutylicum: Clostridium acetobutylicum

C. kluyveri: Clostridium kluyveri

CO_2: carbon dioxide

CoA: coenzyme A

Crt: crotonase

Ctrl: control

CtfAB: acetoacetyl-CoA:acyl-CoA transferase

DNA: deoxyribonucleic acid

E. coli: Escherichia coli

EtfA: Electron transferring factor A

EtfB: Electron transferring factor B

Fd: ferrdoxin

FRT: FLP recognition target

GDH: glycerol dehydrogenase

GDH: glutamate dehydrogenase

GAPDH: glyceraldehyde 3-phosphate dehydrogenase

GOGAT: glutamine 2-oxoglutarate aminotransferase

H_2: dihydrogen

Hbd: 3-hydroxybutyryl-CoA dehydrogenase

HPLC: High performance liquid chromatography

kb: Kilobase

Km: Michaelis constant

Ldh: Lactate dehydrogenase

M: molar

mL: milliliter

mM: millimolar

mmol: millimole

mol: mole

mRNA: messenger RNA

nm: nanometer

NAD^+/NADH: nicotinamide adenine dinucleotide (oxidized/reduced form)

$NADP^+$/NADPH: Nicotinamide adenine dinucleotide phosphate (oxidized/reduced form)

OD: optical density

ORF: open reading frame

P: phosphate

PCR: polymerase chain reaction

Pfor: pyruvate:ferredoxin oxidoreductase

Pta: phosphotransacetylase

Ptb: phosphotransbutyrylase

PTS: phosphotransferase system

RID: refractive index detector

RBS: ribosome binding site

RNA: ribonucleic acid

Thl: thiolase

UV: ultraviolet

Vmax: maximum velocity

WT: Wild type

Acknowldegments and Declaration

This thesis was financially supported by the European Community's Seventh Framework Program "CLOSTNET" (PEOPLE-ITN-2008-237942). All the experiments done by myself were performed at LISBP, INSA Toulouse.

The following experiments in this thesis were carried out by other people:

All the experiments related to proteomics and enzyme assay for control strain – Metabolic explorer

DNA microarray experiment and normalization – Lidwine Trouilh and Sophie Lamarre

Construction of *ΔbukΔptb* – Christian Croux

Introduction and objectives of the work

A renewed interest in the development of biofuels is emerging as a result of a variety of factors including dwindling crude oil reserves, concerns over the environmental impact of fossil fuels and threats to national security potentially limiting access to resources. In recent years, biofuels have been predominantly sourced from crops, resulting in competition for limited food resources and land; bacterial fermentation has been considered a possible answer to this problem. One of the best-studied bacteria for biofuel production is *Clostridium acetobutylicum*. Clostridia are strictly anaerobic, Gram-positive and form highly-resistant spores. Many of the clostridial species, such as *Clostridium difficile* and *Clostridium botulinum*, are highly pathogenic and cause devastating diseases. Some, however, like *C. acetobutylicum* which was first isolated from corn in 1912 by Chaim Weizmann, are harmless to humans, animals and plants and make a wide range of useful chemicals.

The metabolism of *C. acetobutylicum* is characterized by the so called as acetone-butanol-ethanol (ABE) fermentation. Since butanol is a more efficient biofuel than many other solvents such as ethanol, much research is currently focused on this bacterium. In batch culture, the primary metabolism of *C. acetobutylicum* comprises two characteristic phases: acidogenesis and solventogenesis. During the transition phase the generation of the solvents acetone, butanol and ethanol is induced while the acids acetate and butyrate start to be re-consumed. In phosphate-limited chemostat cultures on the other hand, *C. acetobutylicum* can be maintained in three different stable metabolic states without cellular differentiation: acidogenic (producing acetate and butyrate) when grown at neutral pH with glucose; solventogenic (producing acetone, butanol, and ethanol) when grown at low pH with glucose; and alcohologenic (forming butanol and ethanol but not acetone) when grown at neutral pH under conditions of high

NAD(P)H availability. Though the metabolic pathways leading to solvent and acid production are clearly defined [10], the mechanisms governing the different metabolic states and the contribution of the different enzymes to the metabolic fluxes are still poorly understood. The first objective of this thesis was to develop and/or improved current omics tools in order to apply a quantitative systems biology approach to better understand the physiology of *C. acetobutylicum*. For this purpose, an improved genome-scale model will be constructed based on experimentally validated biochemical data with the aim to gain accurate fluxomic data. In addition, a quantitative transcriptomic method will be adapted to access to mRNA molecules per cell. Similarly, a quantitative, label free, gel free proteomic method will be developed/adapted to measure cytoplasmic proteins molecules per cell. Once those methods will be operational they will be used for the physiological characterization of a control strain *C. acetobutylicum ΔCA_C1502Δupp*, which has been engineered for rapid gene knockout and gene knockin.

The second objective of this thesis will be to analyze and understand the roles of two adhE genes encoding bifunctional aldehyde-alcohol dehydrogenases, adhE1 and adh E2, in butanol production under each of the three stable metabolic states. To perform this work, individual metabolic mutants, ΔadhE1 and ΔadhE2 will be constructed and submitted to a systems biology approach under the three metabolic condition.

Finally, the last objective of this thesis will be to analyze the metabolic flexibility of *C. acetobutylicum* in response to a deletion of the genes encoding the butyrate formation pathway. Thus a *C. acetobutylicum ΔbukΔptb* mutant will be constructed and analyze by the same system scale approach used to characterize the control and the ΔadhE mutant strains.

It is expected that this work should improve our understanding of the physiology of *C. acetobutylicum* as well as provide new targets to metabolically engineered this microorganism

to produce only n-butanol which has never been achieved yet by any research group or company.

Chapter 1

Literature Review

1.1 History of solvent production by *Clostridium acetobutylicum*

In 1862, butanol production from microbial fermentation was reported with the description of "Vibrion butyrique" firstly by Louis Pasteur (Pasteur, 1862). About 40 years later, in 1905, a first report of fermentative production of acetone was described by Franz Schardinger (Schardinger, 1905). Microbial fermentation dealing with solvents formation led to further investigations early in the 20th century and in 1926 the first publication naming *Clostridium acetobutylicum*, for the production of butanol.(McCoy *et al.*, 1926, Dürre, 2008) was published. Prior to publication of this name, natural production of solvents by this bacterium has already received attention from not only academia but also industry. For instance, in the collaboration between Strange & Graham, Ltd. and Chaim Weizmann employed by the University of Manchester in United Kingdom, *C. acetobutylicum* was first isolated in 1912 (Dürre, 2004, Haus *et al.*, 2011), and a fermentation process of this bacterium was patented in 1915 (Dürre, 2008, Weizmann, 1915).

Around that time, United Kingdom urgently required acetone to make cordite replacing gunpowder for World War I (WWI), which broke out in August 1914, and this condition boosted studies on *C. acetobutylicum* specifically for acetone production. Weizmann refused to be rewarded by the government of United Kingdom, but showed wish for Jewish home in Palestine. Weizmann became the leader of the whole Zionist organization, and finally he was installed as the first president of the State of Israel (Jones & Woods, 1986a).

The cessation of WWII brought on a rapid reduction of acetone demand but butanol, an unwanted by-product of the Weizmann process, began to gain interest for the production of synthetic rubber. Biological production of butanol was maintained until increased prices of fermentative substrates resulted in a petrochemical process more economical than the biological one. However, finite petroleum resources gave rise to increase of cost, and the

biological production of butanol, regained interest (Dürre, 2011, Dürre, 2007, Dürre, 2008) as a chemical and a potential biofuel. Butanol is a much suitable biofuel than ethanol for several reasons: butanol is less corrosive and less hydroscopic, it has a higher energy density and less enthalpy of vaporization. Those features allow this biofuel to be used with current pipelines and engines (Lee *et al.*, 2008b, Zingaro & Terry Papoutsakis, 2013).

1.2 Metabolism of *C. acetobutylicum*

C. acetobutylicum is a Gram-positive, obligate anaerobic, non-pathogenic, low-GC-content and spore-forming bacterium which can produce mixtures of organic acids and/or solvents from various sugars and polysaccharides. This bacterium has a 4-Mb chromosome and a large plasmid pSol1 (210 kb), carrying the genes needed for solvents production, and loss of this plasmid was associated with degeneration (defined as "the process whereby Clostridium acetobutylicum ATCC 824 loses the capacity to produce acetone and butanol after repeated vegetative transfers or in continuous culture" by Cornillot et al.) (Cornillot *et al.*, 1997a, Cornillot *et al.*, 1997b) of the strain.

In batch cultures, *C. acetobutylicum* usually shows two distinct phases, an acidogenic (production of acetic and butyric acids as the major products) phase and a solventogenic (production of butanol, acetone and ethanol as the major products) phase.

In continuous cultures, three different metabolic states of *C. acetobutylicum* can be observed depending on pH and availability of NAD(P)H: i) an acidogenic state (production of acetic and butyric acids), ii) a solventogenic state (production of acetone, butanol, and ethanol) and iii) an alcohologenic state (formation of butanol and ethanol but not acetone) (Girbal & Soucaille, 1994b, Girbal *et al.*, 1995e).

1.2.1 Central metabolic pathway

Glucose (hexose) is degraded to pyruvate via Embden-Meyerhof-Parnas pathway (EMP pathway), while pentoses are converted to pyruvate by the pentose phosphate pathway (Ezeji *et al.*, 2007).

Pyruvate is oxidized to acetyl-coenzyme A (acetyl-CoA) by pyruvate ferredoxin oxidoreductase (PFOR). This oxidative decarboxylation consists of several reactions. The oxidation of pyruvate is coupled to the reduction of ferredoxin (Fd) an iron-sulfur protein. Reduced ferredoxin (FdH_2) is then reoxidized and Fd is regenerated through hydrogen production by hydrogenase with protons as electron acceptors ($2H^+ \rightarrow H_2$)(Rao & Mutharasan, 1987).

The electron flow is differently directed depending on the metabolic phase and the demand for NAD(P)H. During the acidogenic phase, the NADH produced in the EMP pathway is higher than the NADH consumed in the butyrate pathway and the excess is used by NADH-ferredoxin reductase to reduced ferredoxin. Both this reduced ferredoxin and the one produced from the decarboxylation of pyruvate are reoxidized by the hydrogenase to produce hydrogen and the H_2/CO_2 ratio is then higher than one. On the contrary, during the solventogenic phase, the NAD(P)H consumed in alcohol formation is higher than the NAD(P)H produced in the EMP pathway and part of the reduced ferredoxin produced by the PFOR is used by the Fd-NAD^+ reductase to produce NAD(P)H. Under this phase the $H_2/C0_2$ ratio is then lower than one hydrogen production is reduced (Gorwa *et al.*, 1996) .

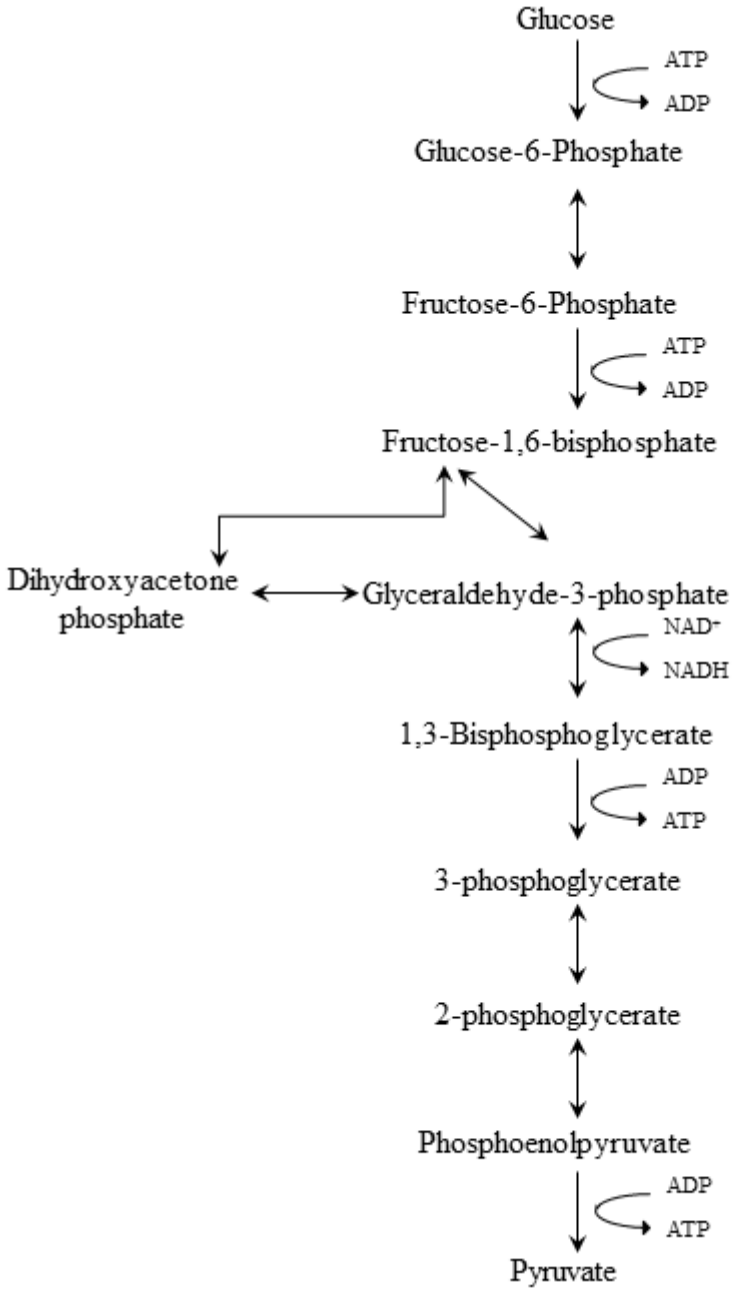

Figure 1.1. Glycolysis (EMP pathway) in *C. acetobutylicum*

source: (Nelson *et al.*, 2008)

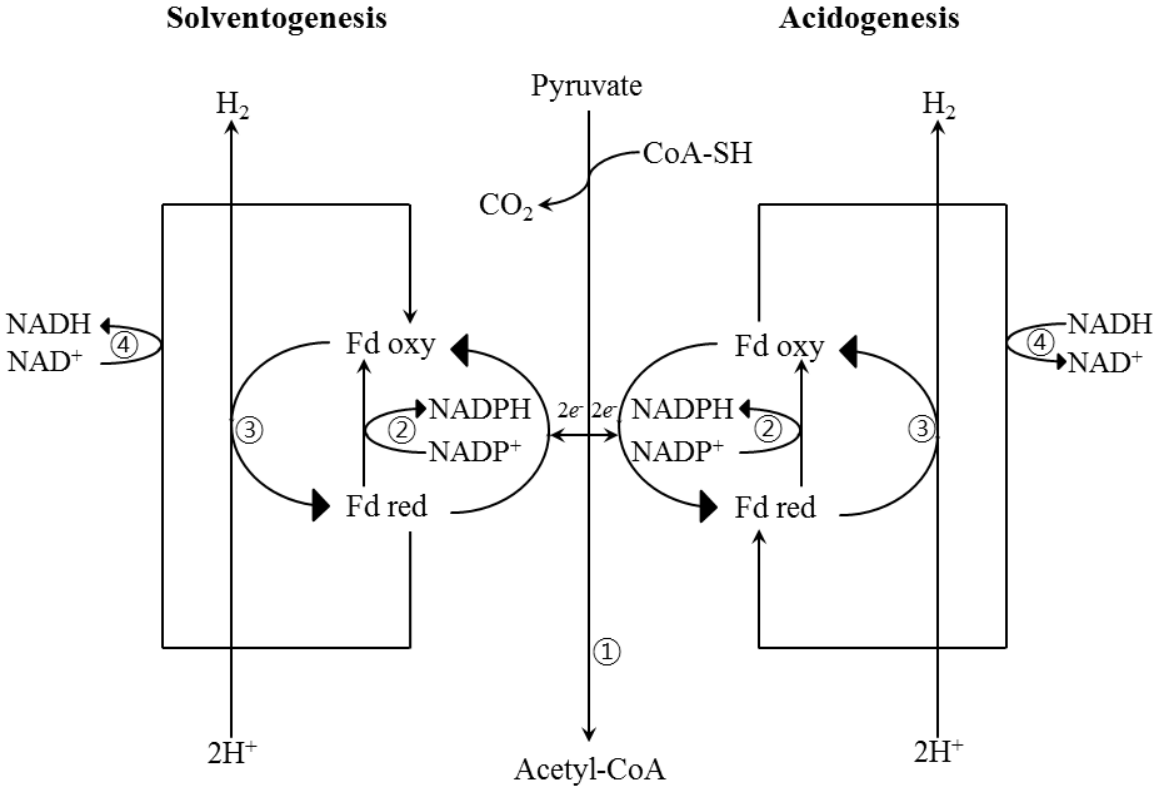

Figure 1.2. The breakdown of pyruvate to acetyl-CoA and electrons flux in *C. acetobutylicum*. ①Pyruvate ferredoxin oxidoreductase; ②Ferredoxin NADPH oxydoreductase; ③Hydrogenase; ④Ferredoxin NADH oxydoreductase

Source: (Girbal, 1994)

1.2.2 Acids formation pathway

Acetyl-CoA is a key intermediate that is produced from the decarboxylation of pyruvate by PFOR. In the acetic acid formation pathway, acetyl-CoA is converted to acetyl-phosphate (acetyl-P) by phosphotransacetylase (encoded by *pta*), and then acetyl-P is dephosphorylated by acetate kinase to produce acetate and ATP. In the butyric acid formation pathway, acetyl-CoA is converted into acetoacetyl-CoA by thiolase (encoded by *thlA*). The conversion of acetoacetyl-CoA into 3-hydroxybutyryl-CoA is carried out by 3-hydroxybutyryl-CoA

dehydrogenase (encoded by *hbd*) with NADH consumption. Then crotonase (encoded by *crt*) converts 3-hydroxybutyryl-CoA into crotonyl-CoA. This intermediate is then reduced by butyryl-CoA dehydrogenase (encoded by *bcd*, *etfA* and *etfB*) complex. At this step, butyryl-CoA formation is coupled to the oxidation of 2 NADH and the reduction of 1 ferredoxin (Li *et al.*, 2008, Lee *et al.*, 2008a). Butyryl CoA is converted into butyryl-phosphate (butyryl-P) by phosphotransbutyrylase (encoded by *ptb*) and butyryl-P is dephosphorylated by butyrate kinase (encoded by *buk*) to produce butyric acid and ATP.

Lactic acid (a minor product under normal condition) can be produced by lactate dehydrogenase (encoded by *ldh*) from pyruvate and NADH. . Lactic acid formation pathway is less efficient for energy generation than the two other acid production pathways., (Jones & Woods, 1986a).

1.2.3 Solvents formation pathway

At the end of the exponential growth phase, when acetate and butyrate accumulate, and pH of culture medium decreased, the acids previously produced, are re-consumed and solvent production begin. Even though sprorulation is not indispensable for solvent production, the initiation of sprorulation process occurs simultaneously (Lutke-Eversloh & Bahl, 2011a). For the solvent production pathways, the key intermediates are acetyl-CoA and butyryl-CoA (Jones & Woods, 1986a).

The first step of acetone formation is coupled to acetic and butyric re-consumption as they are respectively converted to acetyl-CoA and butyryl-CoA by the CoA transferase (encoded by *ctfAB*) during the conversion of acetoacetyl-CoA to acetoacetate. Acetoacetate is then decarboxylated by the acetoacetate decarboxylase (encoded by *adc*) to produce acetone and

carbon dioxide.

In solventogenic conditions, acetyl-CoA and butyryl-CoA are converted respectively to ethanol and butanol by the bifunctional aldehyde/alcohol dehydrogenase (encoded by *adhE*, also known as *aad*). Acetaldehyde and butyraldehyde can also be converted to ethanol and Butanol by NADP+ dependent butanol dehydrogenase (encoded by *bdhB*)

In alcohologenic conditions, acetyl-CoA and butyryl-CoA are converted respectively to ethanol and butanol by a bifunctional aldehyde/alcohol dehydrogenase (encoded by *adhE2*) (Fontaine *et al.*, 2002a).

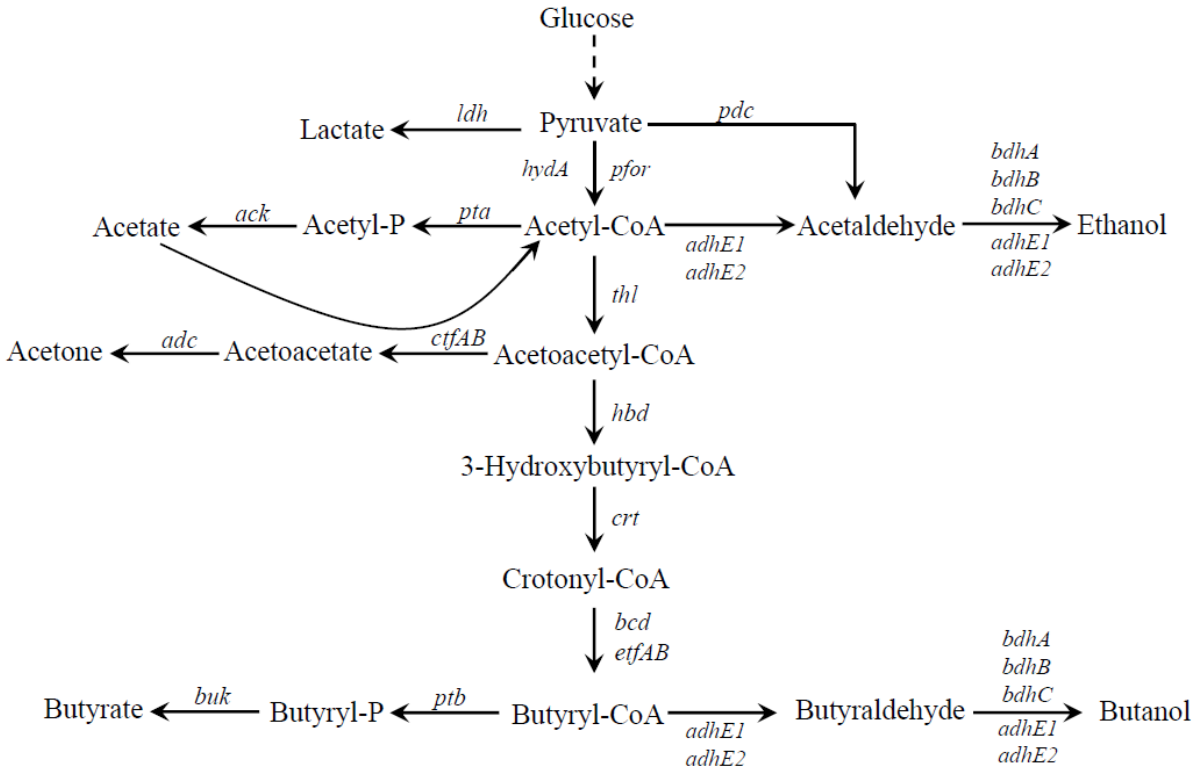

Figure 1.3. Acidogenic and solventogenic metabolic pathways in *C. acetobutylicum*.

The corresponding enzymes are abbreviated and written in red letters as follows

Fd red,Ferrdoxin reductase; AlsS,acetolactate synthase; AlsD,alpha-acetolatate decarboxylase; Pfor,pyruvate:ferredoxinoxidoreductase; Pta,phosphotransacetylase; Ack,acetate kinase;

AdhE,aldehyde/alcohol dehydrogenase; CtfAB,acetoacetyl-CoA:acyl-CoA transferase; Adc,acetoacetate decarboxylase; Thl,thiolase; Hbd,3-hydroxybutyryl-CoA dehydrogenase; Crt,crotonase; Bcd,butyryl-CoA dehydrogenase; Ptb,phosphotransbutyrylase; Buk,butyrate kinase; Bdh,butanol dehydrogenase

.

Table1.1. Key enzymes of metabolic pathway in *C. acetobutylicum*

Source:(Hönicke *et al.*, 2012, Nölling *et al.*, 2001)

Enzyme	Gene	Locus tag	Note
Pyruvate ferredoxin oxidoreductase	*pfor*	CA_C2229	pflB 0980 in Lee et al. (Lee *et al.*, 2008b)
Hydrogenase	*hydA*	CA_C0028	
Phosphotransacetylase	*pta*	CA_C1742	
Acetate kinase	*ack*	CA_C1743	
Thiolase	*thl*	CA_C2873	
3-hydroxybutyryl-CoA dehydrogenase	*hbd*	CA_C2708	
Crotonase	*crt*	CA_C2712	
Butyryl-CoA dehydrogenase	*bcd*	CA_C2711	
Phosphotransbutyrylase	*ptb*	CA_C3076	
Butyrate kinase	*buk*	CA_C3075	
CoA transferase	*ctfAB*	CA_P0163-4	
Acetoacetate decarboxylase	*adc*	CA_P0165	
Aldehyde/alcohol dehydrogenase	*adhE1*	CA_P0162	
Aldehyde/alcohol dehydrogenase	*adhE2*	CA_P0035	
Butanol dehydrogenase	*bdhAB*	CA_C3298-9	
Lactate dehydrogenase	*ldh1*	CA_C0267	

1.3 Regulation of solventogenesis in chemostat cultures

Like other bacteria, *C. acetobutylicum* requires inorganic substances, and energy-generating carbon sources for growth (Monot *et al.*, 1982). In order to sustain bacterial populations indefinitely, limiting one nutrient's concentration at a low value with an accompanying maintenance of high values of all other nutrients is the best way (Novick & Szilard, 1950) to get a stable chemostat culture.

Many studies regarding metabolism of *C. acetobutylicum* show poor reproducibility as they were carried out in batch cultures. Chemostat cultures run under defined and steady state conditions are favored fermentation method to maximize reproducibility in virtue of keeping endogeneous and exogenous parameters, such as specific cell growth rate, specific substrates consumption rates, and specific production rates constant *(Janssen et al., 2010a).*

According to Girbal et al. (Girbal *et al.*, 1995a), *C. acetobutylicum* can be stably maintained in solventogenic state, in glucose fed chemostat cultures maintained at a pH of 4.4 while when the pH was increased to 6.5 a stable acidogenic state was obtained. In solventogenic state, 50% of fed carbon was recovered as solvents whereas in acidogenic state 50% of fed carbon was recovered as acids. In solventogenic and acidogenic states, the sum of the adenylated nucleotides concentrations were constant, while the ATP/ADP ratio was 2.6-fold higher in solventogenesis than in acidogenesis. However, the $NADH/NAD^+$ ratios were similar for both cultures. Furthermore, solventogenic cells maintain a high ΔpH (1.1) while acidogenic cells keep a low ΔpH (0.1). Linked to these differences in ΔpHs, solventogenic cells are associated to a high intracellular butyrate concentration while acidogenic cells have a lower concentration.

To summarize, cells in solventogenic state were characterized by i) a low $NADH/NAD^+$ ratio, ii) a high ATP/ADP ratio, and iii) a high intracellular butyrate concentration. On the other

hand, cells in acidogenic state were characterized by i) a low NADH/NAD^+ ratio, ⅱ) a low ATP/ADP ratio, and ⅲ) a lower intracellular butyrate concentration

Butanol production in solventogenic state is linked to i) the high NAD(P)H-dependent butyraldehyde dehydrogenase activities and ii) a high NADPH-dependent butanol dehydrogenase activity. Acetone production in solventogenic state is associated to i) a high CoA transferase activity, with a preference for acetate as co-substrate, and a 10-fold increased in aceroacetate decarboxylase activity compared with acidogenesis. In terms of hydrogenase acitivity, both hydrogen evolution and uptake activities were lower in solventogenesis, specifically hydrogen evolution activity was much more decreased than hydrogen uptake activity. The ferredoxin NAD(P)+ reductase activities were not detected in solventogenesis in contrast to acidogenesis (Girbal *et al.*, 1995a).

1.4 Regulation of alcohologenesis in chemostat cultures

Alcohologenesis is a particular metabolic state that can be obtained in chemostat cultures maintained at neutral pH and by supplying ⅰ) of mixture of glucose and glycerol, a more reduced carbon source than glucose, or ⅱ) glucose and artificial electron carriers such as Neutral red and Methyl viologen which can replace ferredoxin in the oxidoreduction reactions of *C. acetobutylicum* (Vasconcelos *et al.*, 1994, Girbal *et al.*, 1995d, Fontaine *et al.*, 2002a).

In comparison to acidogenesis, in alcohologenesis, growth on substrates mixtures of glucose and glycerol (molar ration 1.98/1), consumption of glycerol produces twice the amount of NADH than consumption of glucose for same amount of carbon, and the resultant reducing

equivalent excess was not used for molecular hydrogen production, moreover, reduced ferredoxin released from pyruvate ferredoxin oxidoreductase was oxidized to generate NADH, consequently less hydrogen was produced. Intracellular NADH/NAD^+ ratio was increased and in terms of phosphorylation, the ATP/ADP ratio was high compared to acidogenesis although the ATP+ADP pool remained constant. When glycerol was used by *C. acetobutylicum*, high intracellular NADH and ATP were distinctively observed. In alcohologenic state, intracellular pH of *C. acetobutylicum* cells was lower than extracellular pH, i.e. ΔpH (-0.315) is negative, in contrast to acidogenic state, which showed positive ΔpH (0.1). The assumption that hydrogenase is associated to the alkalization of cytoplasm is based on the fact that two protons are required for molecular hydrogen formation with reduced ferredoxin (Girbal *et al.*, 1994a). Since carbon monoxide, a hydrogenase inhibitor, supplied to acidogenic culture resulted in negative ΔpH, the roles of hydrogenase for proton consumption and ΔpH generation at neutral pH was verified. Associtated to this negative ΔpH, intracellular butyrate concentration was low.

To summarize, cells in alcohologenic state were characterized by i) a high NADH/NAD^+ ratio, ii) a high ATP/ADP ratio, and iii) a low intracellular butyrate concentration

In terms of enzyme activities on high NADH/NAD^+, glyceraldehyde-3-phosphate dehydrogenase (GAPDH) revealed significantly inhibited activity; in contrast, glycerol dehydrogenase (GDH) was not influenced notably by the increase NADH/NAD^+ ratio.

Butanol production in solventogenic state is linked to i) the high NADH-dependent butyraldehyde dehydrogenase activities and ii) a high NADH-dependent butanol dehydrogenase activity. The absence of acetone production in alcohologenic state is associated to low CoA transferase aceroacetate decarboxylase activities.

The electron flow is redirected from molecular hydrogen production to the reductions of

NADH consumed in the the alcohol production pathways due to high ferredoxin NAD^+ reductase activities and low NADH ferredoxin reductase activities. When an for alcohologenic metabolism was obtained by the addition of Neutral red in chemostat cultures (Girbal *et al.*, 1995d) pyruvate ferredoxin oxidoreductase and NADH ferredoxin reductase activities were not affected, however the ferredoxin NAD reductase activity increased and hydrogen evolution activity decreased compared to acidogenic cultures. Recently, the redox-sensing protein Rex (CAC2713) was reported to be a transcriptional repressor of key central metabolic genes of *C. acetobutylicum* (Wietzke & Bahl, 2012). Rex repression is released by high $NADH/NAD^+$ ratio. In fact Rex is a transcriptional repressor of genes involved in lactate, butyryl-CoA, and alcohol formation. The *rex* mutant, *C. acetobutylicum rex::*int(95), showed significant increased ethanol production and slightly increased butanol formation, while the amount of acetone produced was decreased compared to wild type.

Figure.1.4. Transcriptional unit of rex in *C. acetobutylicum*. Source: (Wietzke & Bahl, 2012)

1.5 Developments of genome-scale models of *C. acetobutylicum*

Since *C. acetobutylicum* genome has been sequenced (Nölling *et al.*, 2001), and as it is a model organism of solventogenic clostridia (Lutke-Eversloh & Bahl, 2011a), genome-scale model of this organism have been developed by several groups.

In 2008, two different reconstructed genome-scale models (GSMs) of *C. acetobutylicum* were developed by the group of Eleftherios Terry Papoutsakis in a two-parts serial publication (Senger & Papoutsakis, 2008a, Senger & Papoutsakis, 2008b) and by the group of Sang Yup Lee (Lee *et al.*, 2008a), respectively. Four years later, a third GSM of *C. acetobutylicum* was

developed with more reactions and more metabolites than the previous GSMs by the group of Senger who was one of the authors of the first GSM of *C. acetobutylicum* (Senger & Papoutsakis, 2008a, Senger & Papoutsakis, 2008b).

Genome-scale models accompany the practical use of flux balance analysis (FBA), a mathematical method based on linear programming for analysis of metabolite flow through metabolic systems, via two-dimensional stochiometric matrix (Orth *et al.*, 2010, Senger & Papoutsakis, 2008a, Lee *et al.*, 2008a, Schilling *et al.*, 1999).

In order to minimize the extent of the steady state flux distribution solution space of FBA, not only the maximization of the specific growth rate (Edwards *et al.*, 2001) but also thermodynamic based (Henry *et al.*, 2007) or regulatory event considered (Covert *et al.*, 2001) flux constraints have been developed.

The first two GSMs of *C. acetobutylicum* did not reflect the study concerning complete, bifurcated Tricarboxylic Acid (TCA) Cycle in *C. acetobutylicum* by Systems-level Metabolic Flux Profiling (Amador-Noguez *et al.*, 2010), because they were developed and published earlier, then the two genome-scale models applied an incomplete TCA Cycle based on genome sequencing data (Nölling *et al.*, 2001) whereas the third GSM reflect the complete TCA cycle. However, a conflict result was reported by Au et al.(Au *et al.*, 2014) that TCA cycle of *C. acetobutylicum* is incomplete and this incomplete cycle was reflected in the fourth GSM of *C. acetobutylicum* by Dash et al. (Dash *et al.*, 2014), which integrated transcriptomic data of stress conditions to compare *in silico* and experimental data. Before the publications of those GSMs of *C. acetobutylicum*, the GSM of *Bacillus subtilis*, endospore forming and showing high similarity to Clostridia but facultative unlike Clostridia was published (Oh *et al.*, 2007) and contributed to *C. acetobutylicum* model reconstructions afterward.

Computerized metabolic network reconstructions, founded on enzyme homology searches, call for the use of universal metabolic network topology from metabolic pathway databases like Kyoto Encyclopedia of Genes and Genomes (KEGG) (Kanehisa *et al.*, 2006), MetaCyc (Caspi *et al.*, 2006), and The Institute for Genomic Research (TIGR) etc (Senger & Papoutsakis, 2008a, Lee *et al.*, 2008a). Algorithms have been developed to supplement non-perfect genome annotation owing to gaps from missing enzymes, reaction reversibility, unlike notations for the same genes and metabolites, and cofactor particularities (Senger & Papoutsakis, 2008a, Lee *et al.*, 2008a) that give rise to non-functional metabolic network. A gap-filling process is required for those reasons, and is carried out using publications and literatures along with experimental data (Breitling *et al.*, 2008).

Biomass equation of the GSM of Senger and Papoutsakis was based on the platform built for *Staphylococcus aureus* N315 (Heinemann *et al.*, 2005). Biomass was set as a sum of: RNA, DNA, protein, lipids, cell wall, and solute pools of the cytoplasm. The average DNA constitution was founded on the nucleotide constituents of the chromosome and the pSOL1 megaplasmid. The average protein and RNA constituents were derived from their analysis of known Open Reading Frames (ORFs). In the case of GSM of Lee et al., building blocks of individual major molecule of the cell, for instance, amino acids, fatty acids, and nucleic acids (Feist *et al.*, 2007) were formed based on precursors. They assumed that macromolecular constitution and solute pools were same with that of *B. subtilis* (Oh *et al.*, 2007). The average nucleotides constitution was based on genome sequences (Borodina *et al.*, 2005). Amino acid and cell wall constitution were determined (Amino acid: at Korea Basic Science Institute, cell wall: at Deutsche Sammlung von Mikroorganismen und Zellkulturen GmbH) based on the analysis of *C. acetobutylicum* in batch cultures in defined medium.

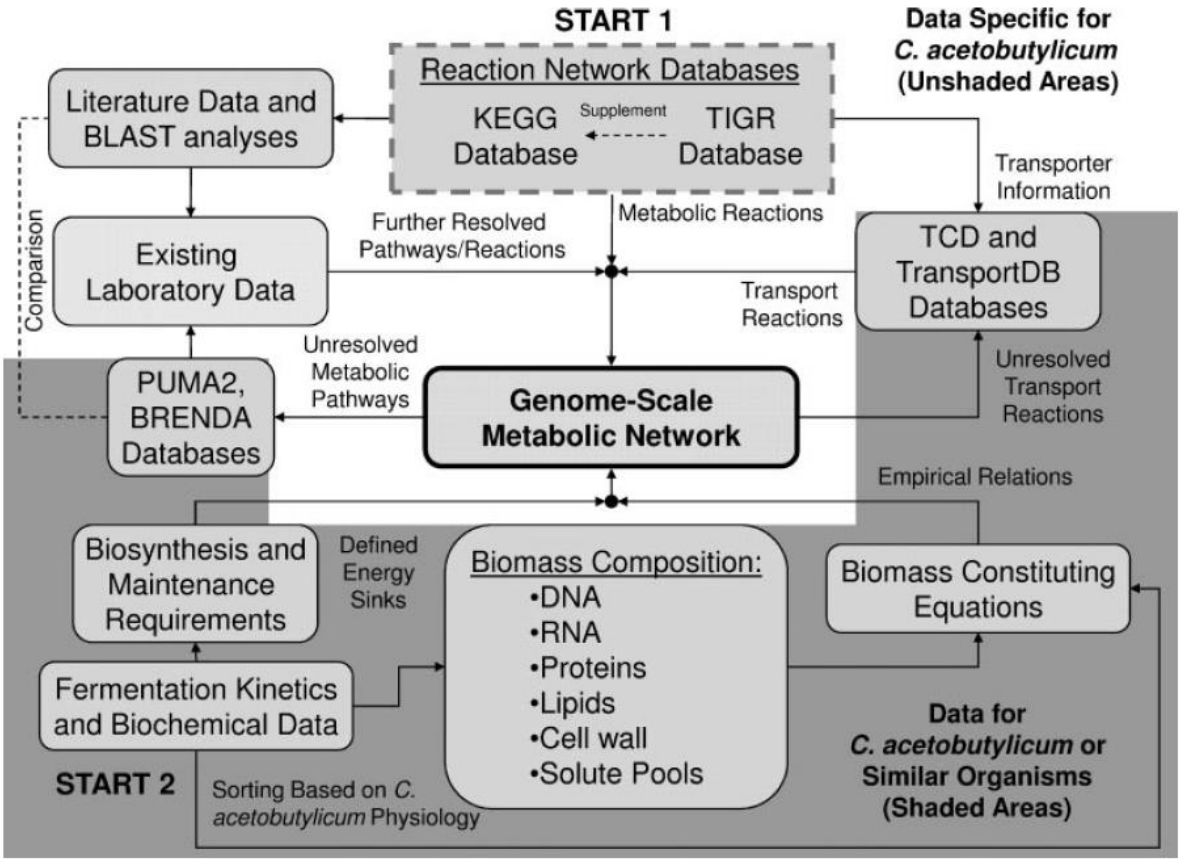

Figure 1.5. Flow diagram of iterative construction of the genome-scale metabolic network described in the first genome-scale model of *C. acetobutylicum*.

White background: data obtained from resources specific to *C. acetobutylicum*.

Dark gray background: data compiled from resources specific to *C. acetobutylicum* and supplemented with information obtained from similar organisms, other clostridia, *B. subtilis*, *S. aureus*, and *E. coli.*

Source: (Senger & Papoutsakis, 2008a)

1.6 Genetic tools for *C. acetobutylicum*

Analytical tools

Transcriptome analysis

Due to the importance of the transition of metabolic state from acidogenesis to solventogenesis, several attempts to identify transcriptional alterations have been made. Since it was considered that genes coding for proteins involved in sporulation such as Spo0A (the general sporulation regulator in Gram-positive bacteria) also influence on regulation of solventogenesis, the preceded transcriptomics in batch cultures were focused on key proteins for sporulation as well as solvent formation (Alsaker & Papoutsakis, 2005, Jones *et al.*, 2008a). But the transcriptomic analysis of metabolic switch in chemostat of *C. acetobutylicum* demonstrated that sporulation is not a requisite for solventogenesis by showing no significant changes in *spo* genes expression between acidogenesis and solventogenesis (Grimmler *et al.*, 2011a).

The simultaneous proteomic and transcriptomic analysis of *C. acetobutylicum* in phosphate limited acidogenic and solventogenic chemostat cultures were first reported in 2010 (Janssen *et al.*, 2010a). These transcriptomic data were compared with previous transcriptomic data of *C. acetobutylicum* in batch cultures (Alsaker & Papoutsakis, 2005, Jones *et al.*, 2008a), and showed distinct transcriptional expression changes between acidogenesis and solventogenesis of CAP0036 and CAP0037, in contrast to negligible expression in batch culture.

Proteome analysis

The study described above (Janssen *et al.*, 2010a) analyzed proteomic data first and confirmed by a transcriptomic analysis the changes in expression of genes coding for the proteins showing significant changes between acidogenesis and solventogenesis. Sullivan and Bennett also

published a proteomic analysis to compare wild type and Spo0A mutant protein expression (Sullivan & Bennett, 2006). Their results verify the correlation of previously reported RNA (Tomas *et al.*, 2003a) and proteomic profiles of the gene expression protein (RpoA). In addition, Post-translational modification of several proteins was identified by observation of the appearance at plural locations on the 2-DE gel. To optimize proteomic analysis of *C. acetobutylicum*, a Standard Operating Procedure (SOP) (Schwarz *et al.*, 2007) and Proteome reference map of *C. acetobutylicum* (Mao *et al.*, 2010) were reported in 2007 and 2010, respectively.

Metabolome analysis

Two representative metabolomic studies of *C. acetobutylicum* were reported by the group of Joshua D. Rabinowitz (Amador-Noguez *et al.*, 2010, Amador-Noguez *et al.*, 2011). To fulfill these studies, metabolomics (LC-MS/MS, NMR), isotope tracers, and quantitative flux modeling were used. The metabolomics published in 2010 (Amador-Noguez *et al.*, 2010) answered to the question regarding how TCA cycle directs in spite of lack of obvious key enzymes annotation through providing evidence of bifurcated TCA cycle. The matabolomic level analysis of acidogenic-solventogenic transition showed notable alterations of glycolysis, TCA cycles, and amino acids biosynthesis as well as acidogenic/solventogenic pathways (Amador-Noguez *et al.*, 2011).

Engineering tools

Genetic engineering of *C. acetobutylicum* has been considered difficult because transformation of this organism is not happening naturally and was interfered by the restriction endonuclease

Cac824I (Mermelstein & Papoutsakis, 1993), and unstable single-crossover integrative knock out mutants by non-replicative plasmids had been obtained in spite of substantial efforts (Lehmann *et al.*, 2012a, Papoutsakis, 2008). Hence the initial trials for engineering were focused upon gene knock down by the antisense RNA method (Desai & Papoutsakis, 1999). In 2007, two Targetron-system based genetic engineering methods were published by different groups (Heap *et al.*, 2007b, Shao *et al.*, 2007). The ClosTron system was developed based on the mobile group II intron of *Lactococcus lactis* (Ll.ltrB) (Karberg *et al.*, 2001), and has been applied to functional genomic study of solventogenic Clostridia as well. The group II introns are self-splicing conceivable RNA molecules, encode multi-domain, able to be retargeted after splicing, therefore worked as a template for particular insertion into the gene (Lehmann *et al.*, 2012a). Two allelic exchange methods have been developed to replace or delete gene in Clostridia (Croux *et al.*, 2012). At least two marker genes are carried by the replicative vectors for these methods, and the marker genes can be removed by eliminating resistance cassettes to make marker-less strains (Figure 1.6).

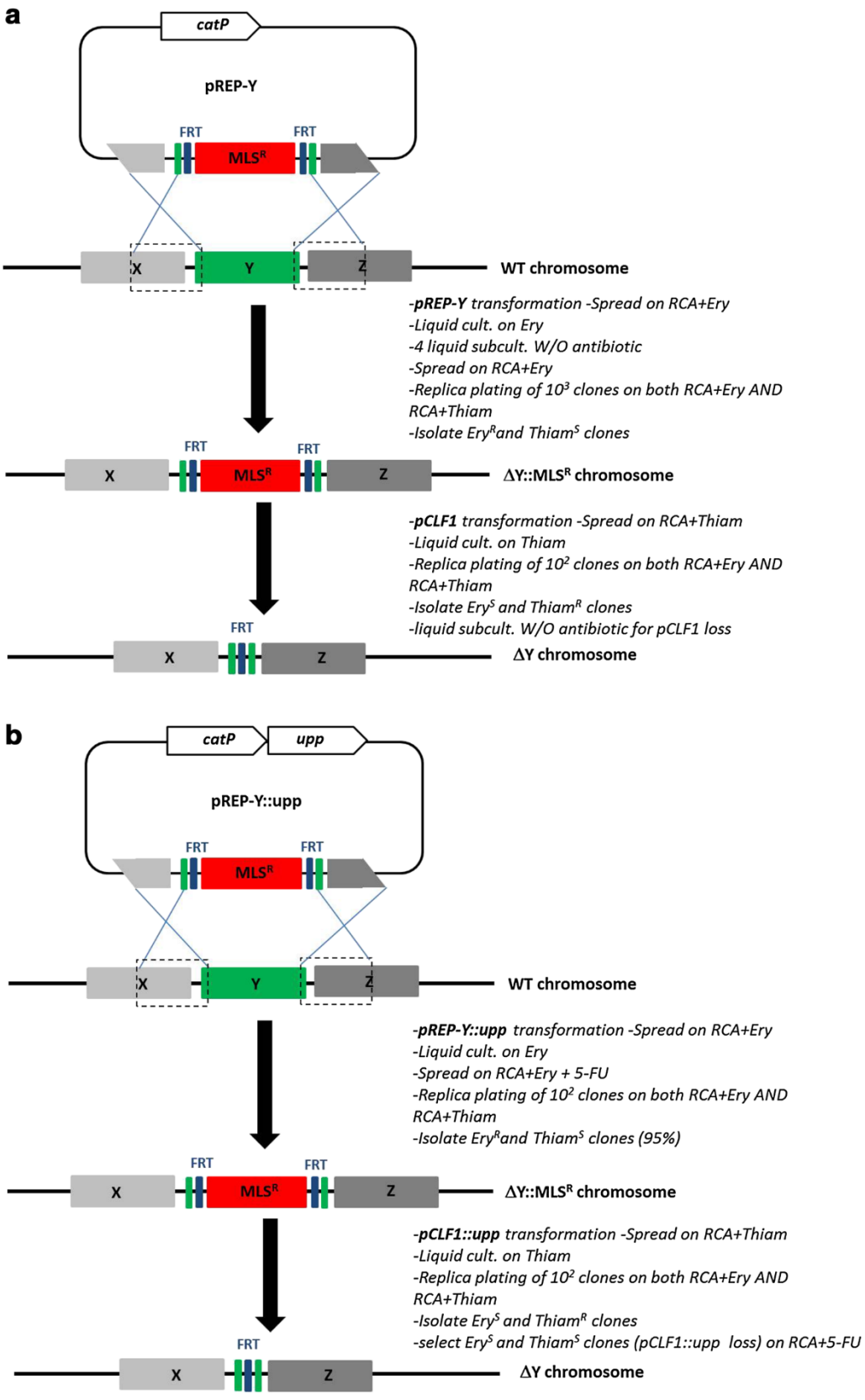
a
catP
pREP-Y
FRT
MLS^R
FRT
X
Y
Z
WT chromosome
-pREP-Y transformation -Spread on RCA+Ery
-Liquid cult. on Ery
-4 liquid subcult. W/O antibiotic
-Spread on RCA+Ery
-Replica plating of 10^3 clones on both RCA+Ery AND RCA+Thiam
-Isolate Ery^R and Thiam^S clones
ΔY::MLS^R chromosome
-pCLF1 transformation -Spread on RCA+Thiam
-Liquid cult. on Thiam
-Replica plating of 10^2 clones on both RCA+Ery AND RCA+Thiam
-Isolate Ery^S and Thiam^R clones
-liquid subcult. W/O antibiotic for pCLF1 loss
ΔY chromosome
b
catP
upp
pREP-Y::upp
WT chromosome
-pREP-Y::upp transformation -Spread on RCA+Ery
-Liquid cult. on Ery
-Spread on RCA+Ery + 5-FU
-Replica plating of 10^2 clones on both RCA+Ery AND RCA+Thiam
-Isolate Ery^R and Thiam^S clones (95%)
ΔY::MLS^R chromosome
-pCLF1::upp transformation -Spread on RCA+Thiam
-Liquid cult. on Thiam
-Replica plating of 10^2 clones on both RCA+Ery AND RCA+Thiam
-Isolate Ery^S and Thiam^R clones
-select Ery^S and Thiam^S clones (pCLF1::upp loss) on RCA+5-FU
ΔY chromosome

Figure.1.6. Gene replacement via allelic exchange. To delete *Y* locus, the MLS^R marker was introduced with the FLP recombinase. The *X* and *Z* genes represent the immediately upstream and downstram regions of homology incorporated into the replicative plasmid used for the double-crossover event (~ 1 kbp each). **A:** Initial strategy used for the construction of the *Δcac1502* and *Δcac1502Δupp* strains, **B**: counter-selection strategy with the 5-FU/*upp* system.

Source: (Croux *et al.*, 2016)

1.7 Metabolic mutants of *C. acetobutylicum*

In 1996, the first reports regarding single-gene knockout mutants of *C. acetobutylicum*, *adhE1*, *pta*, *buk* mutants, (Green *et al.*, 1996, Green & Bennett, 1996, Lutke-Eversloh, 2014b) were published. These publications reported that despite disruption of *buk* or *pta*, butyric or acetic acids formations were not completely suppressed. Inactivation of *adhE1* brought out reduced alcohol production. However, those mutants were obtained by single-crossover integration and were demonstrated to be unstable in the absence of a selective pressure.

After the development of ClosTron system, a number of metabolic mutants have been constructed. The group of Nigel P. Minton published a paper about targeted mutagenesis of *C. acetobutylicum*, which showed batch fermentation profiles of *ptb*, *ack*, *adhE1*, *adhE2*, *bdhA*, *bdhB*, *ctfA*, *ctfB*, *adc*, CAP0059 mutants. *thlA* or *hydA* mutants were not obtained by this group in spite of repeated trials (Cooksley *et al.*, 2012). In addition, Honicke et al., constructed by this method several metabolic mutants including a *ptb* mutant which were characterized by a transcriptomic analysis (Honicke *et al.*, 2014a).

Targetron technique also led to aggressive attempts for construction of metabolic mutants of *C. acetobutylicum*. Shao et al. obtained a *buk* and a *solR* (encoding a putative sol operon

repressor (Nair *et al.*, 1999)) mutant after the modification of a targetron plasmid to produce the suitable plasmid (pSY6) for *C. acetobutylicum* (Shao *et al.*, 2007). Jang et al. succeeded in obtaining a multiple genes disrupted mutant strain in *pta*, *buk*, *ctfB*, *adhE1* and also claimed to obtain a *hydA* mutant using TargeTron although i) the accomplishment of *hydA* mutant is known to be hardly approachable (Jang *et al.*, 2014b) and ii) this mutant still produced hydrogen.

Constructions of metabolic mutants of *C. acetobutylicum* are not restricted to gene disruption, introduction of foreign genes for production of valuable metabolites is also an active area. For example, isopropanol, a non-natural product of *C. acetobutylicum*, has been able to be formed with butanol and ethanol by metabolically engineered mutants of *C. acetobutylicum* (Dusseaux *et al.*, 2013, Lee *et al.*, 2012).

Chapter 2

Results and discussion part 1- Control strain

A quantitative system-scale characterization of the metabolism of *Clostridium acetobutylicum*

Published in mBio 2015, 6(6):e01808-01815

Abstract

Engineering industrial microorganisms for ambitious applications, for example, the production of second-generation biofuel such as butanol, is impeded by a lack of knowledge of primary metabolism and its regulation. A quantitative system-scale analysis was applied to the biofuel-producing bacterium *Clostridium acetobutylicum*, a microorganism used for the industrial production of solvent. An improved genome-scale model, *i*Cac967, was first developed based on thorough biochemical characterizations of 15 key metabolic enzymes and on extensive literature analysis to acquire accurate fluxomic data. In parallel, quantitative transcriptomic and proteomic analyses were performed to assess the number of mRNA molecules per cell for all genes under acidogenic, solventogenic and alcohologenic steady-state conditions as well as the number of cytosolic protein molecules per cell for approximately 700 genes under at least one of the three steady-state conditions. A complete fluxomic, transcriptomic and proteomic analysis applied to different metabolic states allowed us to better understand the regulation of primary metabolism. Moreover, this analysis enabled the functional characterization of numerous enzymes involved in primary metabolism, including (i) the enzymes involved in the two different butanol pathways and their cofactor specificities, (ii) the primary hydrogenase and its redox partner, (iii) the major butyryl-CoA dehydrogenase and (iv) the major glyceraldehyde-3-phosphate dehydrogenase. This study provides important information for further metabolic engineering *C. acetobutylicum* to develop a commercial process for the production of n-butanol.

Importance

Currently, there is a resurgence of interest in *Clostridium acetobutylicum*, the biocatalyst of the historical Weizmann process, to produce n-butanol for use both as a bulk chemical and as

a renewable alternative transportation fuel. To develop a commercial process for the production of n-butanol via a metabolic engineering approach, it is necessary to better characterize both the primary metabolism of *C. acetobutylicum* and its regulation. Here we apply a quantitative system-scale analysis to acidogenic, solventogenic and alcohologenic steady-state *C. acetobutylicum* cells and report for the first time quantitative transcriptomic, proteomic and fluxomic data. This approach allows for a better understanding of the regulation of primary metabolism and for the functional characterization of numerous enzymes involved in primary metabolism.

Introduction

Clostridium acetobutylicum is a gram-positive, spore-forming anaerobic bacterium capable of converting various sugars and polysaccharides to organic acids (acetate and butyrate) and solvents (acetone, butanol, and ethanol). Due to its importance in the industrial production of the bulk chemicals acetone and butanol (Jones, 2001, Jones & Woods, 1986b, Jones *et al.*, 1982) and its potential use in the production of n-butanol, a promising bio-based liquid fuel with several advantages over ethanol (Durre, 2007, Ni & Sun, 2009), much research has focused on understanding i) the regulation of solvent formation (Vasconcelos *et al.*, 1994, Girbal & Soucaille, 1994b, Girbal *et al.*, 1995c, Girbal *et al.*, 1995a, Girbal & Soucaille, 1998b, Wiesenborn *et al.*, 1989b, Wiesenborn *et al.*, 1989a, Sauer & Dürre, 1995), ii) the ability to tolerate butanol (Janssen *et al.*, 2012a, Schwarz *et al.*, 2012, Wang *et al.*, 2013a, Venkataramanan *et al.*, 2013), and iii) the molecular mechanism of strain degeneration *in C. acetobutylicum* (Cornillot & Soucaille, 1996, Cornillot *et al.*, 1997b). The complete genome sequence of *C. acetobutylicum* ATCC 824 has been published (Nolling *et al.*, 2001), and numerous transcriptomic and proteomic studies have been performed to date (Alsaker & Papoutsakis, 2005, Janssen *et al.*, 2010a, Jones *et al.*, 2008a, Sullivan & Bennett, 2006, Tomas *et al.*, 2003a, Schaffer *et al.*, 2002). Although most of these transcriptomic studies have been performed using two-color microarrays (Tomas *et al.*, 2003a, Paredes *et al.*, 2007, Servinsky *et al.*, 2010, Grimmler *et al.*, 2010), RNA deep sequencing (RNA-seq) has recently been used, allowing a more accurate quantification of transcripts as well as the determination of transcription start sites and 5' untranslated sequences (5'UTRs) (Venkataramanan *et al.*, 2013, Tan *et al.*, 2015). With regard to proteomic studies of *C. acetobutylicum*, 2-Dimensional gel electrophoresis (2-DGE) (Mao *et al.*, 2010, Janssen *et al.*, 2010a, Mao *et al.*, 2011, Jang *et al.*, 2014a, Sullivan & Bennett, 2006) is typically employed. 2-DGE is popular and generates substantially valuable data; however, limitations of this method, such as low

reproducibility, narrow dynamic range and low throughput remain (Magdeldin *et al.*, 2014). Recently more quantitative approaches have been developed using 2D-LC-MS-MS (Sivagnanam *et al.*, 2011) or iTRAQ tags (Hou *et al.*, 2013).

In general, transcriptomic and/or proteomic studies of *C. acetobutylicum* have been focused on understanding i) the transcriptional program underlying spore formation (Jones *et al.*, 2008a, Alsaker & Papoutsakis, 2005), ii) the response or adaptation to butanol and butyrate stress (Janssen *et al.*, 2012a, Schwarz *et al.*, 2012, Wang *et al.*, 2013a, Venkataramanan *et al.*, 2013), and iii) the regulation of primary metabolism (Alsaker & Papoutsakis, 2005, Jones *et al.*, 2008a, Tomas *et al.*, 2003a, Sivagnanam *et al.*, 2011, Grimmler *et al.*, 2011c, Janssen *et al.*, 2010a)

Furthermore, to elucidate the molecular mechanisms of endospore formation, microarrays (Jones *et al.*, 2008a, Alsaker & Papoutsakis, 2005) have been used extensively in combination with the down-regulation of sigma factors by antisense RNA (Jones *et al.*, 2008a) or inactivation by gene knockout (Tracy *et al.*, 2011, Jones *et al.*, 2011). Initially, investigation of the response of *C. acetobutylicum* to butanol and butyrate stress have employed microarrays (Janssen *et al.*, 2012a, Schwarz *et al.*, 2012, Wang *et al.*, 2013a) followed by RNA deep sequencing (RNA-seq) to quantify both mRNA and small non-coding RNAs (sRNA) (Venkataramanan *et al.*, 2013) and quantitative transcriptomic and proteomic approaches were later combined (Venkataramanan *et al.*, 2015). Based on one of these studies (Wang *et al.*, 2013a), regulons and DNA-binding motifs of stress-related transcription factors as well as transcriptional regulators controlling stress-responsive amino acid and purine metabolism and their regulons have been identified. Furthermore, integrative proteomic-transcriptomic analysis has revealed the complex expression patterns of a large fraction of the proteome that could only be explained by involving specific molecular mechanisms of post-transcriptional regulation (Venkataramanan *et al.*, 2015).

The regulation of solvent formation in *C. acetobutylicum* has been extensively studied in batch cultures using transcriptomic (Alsaker & Papoutsakis, 2005, Jones *et al.*, 2008a, Tomas *et al.*, 2003a) and/or a proteomic approaches (Sullivan & Bennett, 2006, Sivagnanam *et al.*, 2011). Despite the valuable insights achieved in those studies, many physiological parameters, such as specific growth rates, specific glucose consumption rates, pH, and cellular differentiation as well as butyrate and butanol stress change with time making it difficult to understand many details of the expression pattern.

In phosphate-limited chemostat cultures, *C. acetobutylicum* can be maintained in three different stable metabolic states (Bahl *et al.*, 1982b, Girbal *et al.*, 1995a, Girbal & Soucaille, 1998b, Vasconcelos *et al.*, 1994, Girbal *et al.*, 1995c) without cellular differentiation (Grimmler *et al.*, 2011c): acidogenic (producing acetate and butyrate) when grown at neutral pH on glucose; solventogenic (producing acetone, butanol, and ethanol) when grown at low pH on glucose; and alcohologenic (forming butanol and ethanol but not acetone) when grown at neutral pH under conditions of high NAD(P)H availability. Indeed, because the cells are maintained at steady-state conditions with constant endogenous and exogenous parameters such as a specific growth rate and specific substrate consumption rate, chemostat culture is the preferred fermentation method by which to achieve standardized conditions with a maximum degree of reproducibility. Transcriptional analysis of the transition from an acidogenic to a solventogenic state (Grimmler *et al.*, 2011c) as well as transcriptomic and proteomic analyses of acidogenic and solventogenic (Janssen *et al.*, 2010a) phosphate-limited chemostat cultures has already been performed using two-color microarrays for transcriptomic analysis and 2-DGE for proteomic, methods that are semi-quantitative. However, a systems biology approach, combining more than two quantitative "omic" analyses of chemostat cultures of *C. acetobutylicum*, has never been performed.

Therefore, the aim of this study was to apply a quantitative system-scale analysis to acidogenic, solventogenic and alcohologenic steady-state *C. acetobutylicum* cells to provide new insight into the metabolism of this bacterium. We first developed an improved genome-scale model (GSM), including a thorough biochemical characterization of 15 key metabolic enzymes, to obtain accurate fluxomic data. We then applied quantitative transcriptomic and proteomic approaches to better characterize the distribution of carbon and electron fluxes under different physiological conditions and the regulation of *C. acetobutylicum* metabolism.

Results and discussion

Improving upon current GSMs for metabolic flux analysis.

The *i*Cac967 model for *C. acetobutylicum* ATCC 824 spans 967 genes and includes 1,058 metabolites participating in 1,231 reactions (Table 1, Dataset S1). All reactions are elementally and charge balanced. The *i*Cac967 model is the result of an extensive literature analysis associated with the biochemical characterization of many key metabolic enzymes in an attempt to better understand the distribution of carbon and electron fluxes. The previously uncharacterized butyryl-CoA dehydrogenase (Bcd) encoded by *bcd-etfB-etfA* (CA_C2711, CA_C2710, CA_C2709) (Boynton *et al.*, 1996) was biochemically characterized via homologous expression of the encoding operon in *C. acetobutylicum* and the purification of the enzyme complex (Table 2, Fig. S1). We demonstrated that the butyryl-CoA dehydrogenase of *C. acetobutylicum* is a strictly NADH dependent enzyme and that ferredoxin is needed for the reaction to proceed. To study the stoichiometry of the reaction, the concentrations of NADH (Fig. S1A) and crotonyl-CoA (Fig. S1B) were modulated using constant concentrations of purified ferredoxin (CA_C0303) and hydrogenase (CA_C0028). Based on the initial slope in Fig. S1B, it was calculated that in the presence of excess crotonyl-CoA, 2.15 mol of NADH was required for the formation of 1 mol of H_2; from the

initial slope in Fig. S1A, it was calculated that in the presence of excess NADH, 1.25 mol of crotonyl-CoA was required for the formation of 1 mol of H_2. The results indicate that under fully coupled conditions, approximately 1 mol of ferredoxin is reduced by 2 mol of NADH and 1 mol of crotonyl-CoA, similar to the butyryl-CoA dehydrogenase of *Clostridium kluyveri* (Li *et al.*, 2008). Although the possibility that this enzyme might consume 2 mol of NADH and produce one mol of reduced ferredoxin in *C. acetobutylicum* was previously presented as a hypothesis (Sillers *et al.*, 2008a), it has not been demonstrated to date nor has it been integrated in the recently published GSMs (Dash *et al.*, 2014, McAnulty *et al.*, 2012). This result has strong implications for the distribution of electron fluxes, as discussed below in the metabolic flux analysis section.

The second key enzyme that remained uncharacterized was the bifunctional alcohol-aldehyde dehydrogenase (AdhE1 or Aad, encoded by CA_P0162), an enzyme involved in the last two steps of butanol and ethanol formation during solventogenic culturing of *C. acetobutylicum* (Nair *et al.*, 1994a, Fischer *et al.*, 1993). First, *adhE1* and *adhE2* (as a positive control) were individually heterologously expressed in *E. coli*, after which AdhE1 and AdhE2 were purified as tag-free proteins (Table 2) for biochemical characterization. We demonstrated that *in vitro*, AdhE1 possesses high NADH-dependent butyraldehyde dehydrogenase activity but surprisingly very low butanol dehydrogenase activity with both NADH and NADPH; in contrast, AdhE2 possesses both high butyraldehyde and butanol dehydrogenase activities with NADH. The three potential alcohol dehydrogenases, BdhA, BdhB and BdhC (Walter *et al.*, 1992), encoded by *bdhA*, *bdhB* and *bdhC* (CA_C3299, CA_C3298, and CA_C3392), were heterologously expressed in *E. coli* and then characterized after purification as tag-free proteins (Table 2). The three enzymes were demonstrated to be primarily NADPH dependent butanol dehydrogenases, results do not agree with the previous characterizations of BDHI and BDHII (later demonstrated to be encoded by *bdhA* and *bdhB*), which were reported to be

NADH dependent (Welch *et al.*, 1989, Walter *et al.*, 1992). However, in agreement with our findings, all of the key amino acids of the two GGGS motifs at positions 37–40 and 93–96 involved in the NADPH binding of YqhD, a strictly NADPH-dependent alcohol dehydrogenase (Sulzenbacher *et al.*, 2004), are perfectly conserved in the three *C. acetobutylicum* alcohol dehydrogenases. Furthermore, these results are also in line with previously published data from two different research groups (Dürre *et al.*, 1987, Girbal *et al.*, 1995a) showing that in a crude extract of solventogenic *C. acetobutylicum* cultures, the butanol dehydrogenase activity measured in the physiological direction is mainly NADPH dependent. As discussed below, *C. acetobutylicum* must utilize at least one of these alcohol dehydrogenases to produce butanol and ethanol under solventogenic conditions, which implies that one mole of NADPH is needed for each mole of butanol and ethanol produced under solventogenic conditions.

The cofactor specificity of the ammonium assimilation pathway that proceeds via glutamine 2-oxoglutarate aminotransferase (GOGAT) encoded by *gltA* and *gltB* (CA_C1673 and CA_C1674), and glutamate dehydrogenase (GDH) encoded by *gdh* (CA_C0737) was also characterized. The *gltA-gltB* and *gdh* genes were expressed in *C. acetobutylicum* and *E. coli* respectively, and GOGAT and GDH were purified (Table 2). Both enzymes were found to be NADH-dependent, in contrast to the corresponding enzymes in *E. coli*, which are NADPH dependent (Schmidt & Jervis, 1980, Sakamoto *et al.*, 1975).

The functions of the three genes (CA_C0970, CA_C0971 and CA_C0972) proposed (Amador-Noguez *et al.*, 2010) to encode the first three steps of the oxidative branch of the tricarboxylic acid (TCA) cycle were unambiguously characterized. CA_C0970, CA_C0971 and CA_C0972 were individually expressed in *E. coli*, and their gene products were purified (Table 2); the genes were demonstrated to encode a *Re*-citrate synthase (CitA), an aconitase (CitB) and an NADH dependent isocitrate dehydrogenase (CitC), respectively.

Finally, we characterized the cofactor specificity of the two malic enzymes encoded by CA_C1589 and CA_C1596, two almost identical genes that differ only by two nucleotides. Not surprisingly, the specific activities of the two purified enzymes are almost identical and both enzymes are NADH dependent (Table 2).

The *i*Cac967 model statistics and those of all other published models for *C. acetobutylicum* (Senger & Papoutsakis, 2008a, Senger & Papoutsakis, 2008b, Lee *et al.*, 2008a, McAnulty *et al.*, 2012, Dash *et al.*, 2014) are shown in Table 1. *i*Cac967 has 20% more genes than the most recently published model by Dash et al. (Dash *et al.*, 2014) but fewer metabolites and reactions, as some reactions described by these authors were not validated by our extensive literature analysis or were inappropriate in the context of anaerobic metabolism, for example, R0013 ($NADPH + O_2 + H^+ + 2\text{-Octaprenylphenol} \rightarrow H_2O + NADP^+ + 2\text{-Octaprenyl-6-hydroxyphenol}$) and R0293 ($H_2O + O_2 + \text{Sarcosine} \rightarrow H_2O_2 + \text{Glycine} + \text{Formaldehyde}$). Furthermore, we applied our GSM to the butyrate kinase knock-out mutant (Harris *et al.*, 2000b) and the M5 degenerate strain (Lee *et al.*, 2009) (that has lost the pSOL1 plasmid) and successfully predicted their phenotypes (Table S1).

Quantitative transcriptomic and proteomic analyses of *C. acetobutylicum* under stable acidogenic, solventogenic and alcohologenic conditions

General considerations.

Quantitative transcriptomic and proteomic analyses were performed on phosphate-limited chemostat cultures of *C. acetobutylicum* maintained in three different stable metabolic states: acidogenic, solventogenic and alcohologenic (Girbal & Soucaille, 1998b, Vasconcelos *et al.*, 1994, Girbal & Soucaille, 1994b, Girbal *et al.*, 1995a). The total amount of DNA, RNA and protein contents (expressed in g/g dry cell weight (DCW)) and the number of cells per g DCW were experimentally determined for each steady-state condition under phosphate

limitation at a dilution rate of 0.05 h^{-1}. These numbers were not significantly different among the steady-state conditions, in agreement with previous studies (Neidhardt & Umbarger, 1996, Pramanik & Keasling, 1997) on *E. coli* that have shown that the biomass composition is not dependent on the carbon source but is strictly dependent on the specific growth rate. According to all of the values, the average contents of DNA (1.92 ± 0.03), mRNA (9.41 ± 0.94 × 10^3) and protein (6.26 ± 0.18 ×10^6) molecules per cell were calculated. Noticeably, the total number of mRNA molecules per cell was only 2.4 times higher than the total number of ORFs (3916). In *E. coli* the situation was even worst with a total number of mRNA molecules per cell (1380) 3 times lower than the total number of ORFs (4194) (Neidhardt & Umbarger, 1996).

For each gene, we sought to quantify the number of mRNA molecules per cell. For this purpose, we used Agilent's One-Color microarray-based gene expression analysis, as a recent study (Miller *et al.*, 2014) demonstrated a linear relationship between the amounts of transcript determined by this method and by the RNA-seq method. The minimum number of mRNA molecules per cell detected was around 0.06 while the maximum number was around 80. It was observed that a large number of genes have less than 0.2 mRNA molecules per cell (for 37.1%, 36.8 % and 37.2% of the genes under respectively acidogenic, solventogenic and alcohologenic conditions). This result indicates that for these genes, there is either i) heterogeneity among different cells, such that some cells contain one transcript and others do not, or ii) a high mRNA degradation rate. Genes that showed a value of mRNA molecules per cell <0.2 under all three conditions were excluded from further analysis.

The purpose of this study was also to quantify the number of cytoplasmic protein molecules per cell. Different quantitative methods using either 2D-protein-gels (Schaffer *et al.*, 2002), or peptide analysis by two-dimensional high-performance liquid chromatography (2D HPLC) coupled with tandem mass spectrometry (MS/MS) with peptide labeling (Hou *et al.*, 2013)

have been developed for *C. acetobutylicum*. In collaboration with the Waters Company, we adapted a recently published method (Foster *et al.*, 2015) using label-free peptide analysis after shotgun trypsin hydrolysis of cytosolic proteins. For approximately 700 cytosolic proteins, it was possible to quantify the number of protein molecules per cell in the at least one of the three steady-states. This number is approximately 4 times higher than the number of cytosolic proteins detected in phosphate- limited acidogenic and solventogenic chemostat cultures by Jansen et al. (Janssen *et al.*, 2010a), but similar to the number of cytosolic protein detected by Venkataramanan et al. (Venkataramanan *et al.*, 2015) by iTRAQ. Furthermore, the minimum number of protein molecules per cell detected was around 200 while the maximum number was approximately 300 000. For 96 % of the cytosolic proteins that could be quantified, a linear relationship was obtained, with an $R^2 > 0.9$, when the numbers of protein molecules per cell were plotted against the numbers of mRNA molecules per cell, (Dataset S2). This result indicated that for steady-state continuous cultures run at the same specific growth rate and with the same total amount of carbon supplied, the rate of protein turnover is proportional to the mRNA content for 96% of the genes. This result is not necessary surprising, as it has previously been shown for other microorganisms such as *E. coli* (Bremer & Dennis, 1996) that the number of ribosomes and tRNAs per cell are dependent on the specific growth rate and not on the carbon source. The absolute protein synthesis rates for approximately 700 genes were calculated by assuming that the rate of protein degradation is negligible compared to the rate of protein synthesis (Dataset S2). These values varied from 0.0007 s^{-1} for CA_C3723 (*ssb* encoding a single-stranded DNA-binding protein) to 0.95 s^{-1} for CA_C0877 (*cfa* encoding a cyclopropane fatty acid synthase). Interestingly, the rate of protein synthesis appears to correlate inversely with the average number of mRNA molecules per cell (Dataset S2).

Comparison of solventogenic versus acidogenic steady-state cells.

Solventogenic cells were first comprehensively compared to acidogenic cells via quantitative transcriptomic and proteomic analyses. The complete transcriptomic and proteomic results are provided in Dataset S2. A similar study in phosphate-limited chemostat cultures was previously performed by Jansen et al. (Janssen *et al.*, 2010a) using semi-quantitative transcriptomic (two-color microarrays) and proteomic (2DGE) methods. Among the 95 genes shown by Jansen et al. to be up-regulated, we qualitatively confirmed up-regulation for 68; among the 53 genes shown by Jansen et al. to be down-regulated, we qualitatively confirmed down-regulation for 27. What might explain the differences between the two studies? First, the culture conditions were slightly different in terms of dilution rate ($0.075 h^{-1}$ for Jansen et al, $0.05\ h^{-1}$ in our study), phosphate limitation (0.5 mM for Jansen et al, 0.7 mM in our study) as well as the pH of the acidogenic culture (5.7 for Jansen et al., 6.3 in our study), leading to a higher amount of glucose consumed and thus a higher amount of products formed in our study. We are confident regarding the validity of our results because we found agreement quantitatively with the transcriptomic data whenever proteins were detected by our method and thus quantitative proteomic data were available. Below, we discuss these data in more detail and striking differences in mRNA molecules per cell are highlighted in Fig. S2A.

In total, 64 genes matched the significance criteria of $\geq$ 4.0-fold higher expression in solventogenesis versus acidogenesis as well as > 0.2 mRNA molecules per cell under at least one of the two conditions (Table S2). In particular, high values (~80–150-fold) were documented for the *sol* operon genes (CA_P0162–CA_P0164) and confirmed by the proteomic analysis, in agreement with i) the requirement of AdhE1 and CoA-transferase subunits for the production of solvents under solventogenic conditions (Fischer *et al.*, 1993, Fontaine *et al.*, 2002a, Nair *et al.*, 1994a, Wiesenborn *et al.*, 1989a) and ii) the previous study by Janssen et al.(Janssen *et al.*, 2010a). Elevated upregulation (4–40-fold) of genes involved

in serine biosynthesis (CA_C0014–0015), seryl-tRNA synthesis (CA_C0017) and arginine biosynthesis (CA_C2388) was detected at the mRNA level and confirmed by the proteomic analysis, in agreement with a previous metabolomic study in batch culture (Amador-Noguez *et al.*, 2011), that reported higher intracellular concentrations of serine and arginine in solventogenic cells. Interestingly, all these genes were previously shown to be upregulated in response to butanol stress (Wang *et al.*, 2013a), although these results were not confirmed by proteomic analysis (Venkataramanan *et al.*, 2015). In addition, an ~4–8-fold up-regulation of genes involved in purine biosynthesis (CA_C1392–1395, CA_C1655, and CA_C2445) was detected at the mRNA level and confirmed by the proteomic analysis. Similar to the study by Janssen et al.(Janssen *et al.*, 2010a), an ~5-fold upregulation of a gluconate dehydrogenase (CA_C2607) was detected; however, as this protein was not detected, this was not confirmed by proteomic analysis.

As reported in previous studies (Grimmler *et al.*, 2011c, Janssen *et al.*, 2010a), elevated up-regulations (~4–16-fold) of the genes involved in the production of i) a non-functional cellulosome (CA_C0910–CA_C0918 and CA_C0561) (Nolling *et al.*, 2001, Sabathé *et al.*, 2002) and ii) non-cellulosomal pectate lyase-encoding genes (CA_P0056, CA_C0574) at the mRNA level. However, these results could not be verified by proteomic analysis, as exoproteome analysis was not performed in this study. All these genes, except CA_P0056, were also shown to be up-regulated in response to a butanol stress (Wang *et al.*, 2013a). Importantly, *spo0A* (CA_C2071), encoding a regulator of sporulation and solvent production (Harris *et al.*, 2002, Ravagnani *et al.*, 2000b, Thormann *et al.*, 2002), showed an increase in expression at the level of both mRNA and protein molecules per cell. This increased expression does not agree with previous chemostat culture studies by Grimmler et al. (Grimmler *et al.*, 2011c) and Janssen et al. (Janssen *et al.*, 2010a), but does agree with batch culture studies (Tomas *et al.*, 2003a, Alsaker & Papoutsakis, 2005) and also supports the

common notion of Spo0A acting as a master regulator of solventogenesis. *hsp18* (CA_C3714), encoding gene product involved in solvent tolerance (Tomas *et al.*, 2004), also exhibited an ~4.5-fold increase in mRNA and protein molecules per cell, in agreement with a previous butanol stress study (Venkataramanan *et al.*, 2015). A striking difference between the study of Janssen et al. and ours was observed with regard to the level of this chaperone, which in contrast to our study showing an ~4.5-fold increase under solventogenesis, was decreased (~5-fold) in the study by Janssen et al.(Janssen *et al.*, 2010a). Nonetheless, this difference appears to be due to the limitation of 2-DGE, because 3 different proteins could be detected in the "Hsp18 spot" and transcriptional changes in hsp18 did not correlated with the proteomic data (Janssen *et al.*, 2010a); in contrast, our quantitative transcriptomic and proteomic data showed good correlation ($R^2 > 0.9$).

The detailed results of the 45 ORFs that exhibited ≥ 4.0-fold decreases in numbers of mRNA molecules per cell under solventogenic versus acidogenic conditions and of a number with mRNA molecules per cell > 0.2 under at least one of the two conditions are given in Table S2. Significantly, in this metabolic state, various genes involved in the assimilation of different carbon sources were down-regulated. For example, the highest decrease (~6–70-fold) at the mRNA level was observed for genes (CA_C0422–0426) involved in sucrose transport, metabolism and the regulation of these genes, which was confirmed by the proteomic analysis. In addition, two genes involved in mannan (CA_C0332) and maltose metabolism (CA_C0533) exhibited 4- and 10-fold decreases, respectively, in their mRNA levels. Because acidogenic culture reached glucose limitation but a small amount of glucose remained in solventogenic culture (similar to our previous publication (Girbal *et al.*, 1995a)), this phenomenon can be explained by a release of catabolite repression in acidogenic cultures. The similar high expression observed for CA_C0422–0426, CA_C0332, and C A_C0533 in alcohologenic and acidogenic cultures that were glucose limited is in agreement

with this hypothesis. Two genes located on the megaplasmid pSOL1 (CA_P0036 and CA_P0037), encoding a cytosolic protein of unknown function and a potential transcriptional regulator, respectively, exhibited particularly high scores corresponding to an ~60–70-fold decrease, which is in good agreement with the proteomic data and the previous study by Janssen et al.(Janssen *et al.*, 2010a). Interestingly, under all conditions, these two proteins are present at a 1 to 1 molar ratio. Furthermore, three genes involved in cysteine (CA_C2783) and methionine (CA_C1825 and CA_C0390) biosynthesis exhibited ~5-fold decreases in their numbers of mRNA and protein molecules per cell in agreement with a previous metabolomics study by Amador-Noguez et al. (Amador-Noguez *et al.*, 2011), showing a ~5-fold decreased in intracellular methionine in solventogenesis.

Comparison of alcohologenic versus acidogenic steady-state cells.

Alcohologenic cells were comprehensively compared to acidogenic cells by quantitative transcriptomic and proteomic analyses. The complete transcriptomic results are listed in Dataset S2, and striking differences are highlighted in Fig. S2B. In total, 52 genes matched the significance criteria of ≥ 4.0-fold higher expression in alcohologenesis versus acidogenesis as well as > 0.2 mRNA molecules per cell under at least one of the two conditions (Table S3). In particular, high values (~55–520-fold) were documented for the gene cluster coding for glycerol transport and utilization (CA_C1319–CA_C1323) and confirmed by the proteomic analysis, in agreement with the requirement of GlpK (glycerol kinase) and GlpAB (glycerol-3-phosphate dehydrogenase) for glycerol utilization in alcohologenic metabolism (Vasconcelos *et al.*, 1994, Girbal *et al.*, 1995a). High up-regulation (160-fold) of *adhE2* (CA_P0035), which is involved in alcohol production under alcohologenic conditions (Fontaine *et al.*, 2002a), was detected and correlated with a high AdhE2 protein concentration. Interestingly, CA_C3486, which encodes a multimeric

flavodoxin, was also highly expressed (~6-fold) and may participate in redistribution of the electron flux in favor of butanol under alcohologenic conditions. Of note, an ~20–70-fold up-regulation of a gene cluster involved in sulfate transport, reduction and incorporation to produce cysteine (CA_C0102–0110), ~4-fold up-regulation of *cysK* (CA_C2235), which is also involved in cysteine synthesis, and ~7–10-fold upregulation of an operon (CA_C3325–3327) involved in cysteine transport were detected at the mRNA level and confirmed by the proteomic analysis for the cytosolic proteins detected (CA_C0102-0104, CA_C0107, CA_C0109-0110, CA_C2235 and CA_C3327). All of these genes/operon were shown to possess a CymR-binding site in their promoter regions, and some have been shown to be up-regulated in response to butanol stress (Wang *et al.*, 2013a).

An ~3–5-fold up-regulation of an operon involved in histidine synthesis and histidyl-tRNA synthesis (CA_C0935–0943) and 5-fold up-regulation of a gene involved in arginine biosynthesis (CA_C2388) were also detected at the mRNA level and confirmed by the proteomic analysis. These genes were also shown to be upregulated under solventogenic conditions and in response to butanol stress (Wang *et al.*, 2013a).

The detailed results of the 64 ORFs that exhibited a ≥ 4.0-fold decrease in transcript levels under alcohologenic versus acidogenic conditions and > 0.2 mRNA molecules per cell under at least one of the two conditions are given in Table S3. The highest decrease (~70-fold) at the mRNA level was observed for an operon (CA_C0427–0430) involved in glycerol-3-phosphate transport and coding for a glycerophosphoryl diester phosphodiesterase, which was confirmed by the cytosolic protein analysis. As observed under solventogenic conditions, CA_P0036 and CA_P0037 exhibited ~40–50-fold lower expression levels, which agrees well with the proteomic data. Furthermore, an operon involved in phosphate uptake (CA_C1705–1709), an operon encoding an indolepyruvate ferredoxin oxidoreductase (CA_C2000–2001) and a gene encoding a pyruvate decarboxylase (CA_P0025) exhibited ~80–350-fold, ~4–5-

fold and ~4-fold decreases, respectively, at the mRNA level, confirmed by the proteomic analysis. Additionally, two clusters of genes involved in fatty acid biosynthesis/degradation (CA_C2004–2017) exhibited ~3.5–6-fold decreases at the mRNA level, a result that was confirmed by the proteomic analysis.

Metabolic flux analysis of *C. acetobutylicum* under stable acidogenic, solventogenic and alcohologenic conditions.

To perform a metabolic flux analysis of *C. acetobutylicum* under stable acidogenic, solventogenic and alcohologenic conditions, *i*Cac967 was combined with our transcriptomic and proteomic data. As a first simple example, we present how the gene responsible for pyruvate ferredoxin oxidoreductase (PFOR) activity was identified. This gene encodes a key enzyme in the glycolytic pathway that decarboxylates pyruvate to produce reduced ferredoxin, CO_2 and acetyl-CoA. Two putative PFOR-encoding genes (CA_C2229 and CA_C2499) were identified in our GSM (Dataset S1). Under all conditions, only CA_C2229 was transcribed (average of 56 mRNA molecules per cell) and translated (average of 166,000 protein molecules per cell).

As a second simple example, we present how the main enzyme responsible for crotony-CoA reduction to butyryl-CoA was identified. Two different enzymes can potentially catalyze this reaction: the BCD complex encoded by *bcd*, *etfB*, *etfA* (CA_C2711, CA_C2710, CA_C2709) which consumes two moles of NADH and produces one mole of reduced ferredoxin (Fig.S1) and TER (trans-2-enoyl-CoA reductase) encoded by (CA_C0642) which only consumes one mole of NADH (Hu *et al.*, 2013). In all conditions, *bcd* was much more transcribed than CA_C0642 (67 versus 1.2 mRNA molecules per cell) and in terms of proteins BCD was detected (average of 113,000 protein molecules per cell) whereas TER was below the detection limit of the method.

As a complex example, we also present the actors in the different butanol pathways and their cofactor specificities. Five proteins can potentially be involved in the last two steps of butanol formation. AdhE1 retains only NADH dependent aldehyde dehydrogenase activity, whereas AdhE2 is a bifunctional NADH dependent aldehyde-alcohol dehydrogenase (Fontaine *et al.*, 2002a); BdhA, BdhB and BdhC are NADPH dependent alcohol dehydrogenases. For each of the three conditions and for each of the aforementioned genes and their corresponding proteins, the number of mRNA molecules per cell and the number of protein molecules per cell were measured. The percent of the total butanol flux due to each of the five enzymes was calculated by assuming that all five enzymes function at their Vmax and using the amount of each protein per cell. The results are presented in Fig. 1. Under acidogenic conditions, the entire butyraldehyde dehydrogenase flux is due to AdhE2, whereas the butanol dehydrogenase flux is primarily due to BdhB and BdhA. Under solventogenic conditions, the butyraldehyde dehydrogenase flux is largely due to AdhE1, whereas the butanol dehydrogenase flux is primarily due to BdhB, BdhA and BdhC, in decreasing order of activity. Finally, under alcohologenic conditions, all of the flux of butyraldehyde dehydrogenase activity and most of that of butanol dehydrogenase activity are due to AdhE2. In summary, the last two steps of butanol production consume one mole of NADH and one mole of NADPH under acidogenic and solventogenic conditions and two moles of NADH under alcohologenic conditions.

These results have strong implications for the distribution of electron fluxes and the use of reduced ferredoxin under the respective studied conditions. Under acidogenic conditions, reduced ferredoxin is primarily used to produce hydrogen, and only a small fraction is used to produce the NADH needed for butyrate formation and the NADPH needed for anabolic reactions (Fig. 2A). However, under alcohologenic conditions, reduced ferredoxin is primarily used to produce the NADH needed for alcohol formation (Fig. 2C) Under

solventogenic conditions, although reduced ferredoxin is predominantly utilized for hydrogen production, a significant amount is used for the NADPH formation needed for the final step of alcohol formation by BdhB, BdhA and BdhC, as *C. acetobutylicum* has no oxidative pentose phosphate pathway (*zwf*, encoding glucose 6-phosphate-dehydrogenase, is absent) to produce NADPH (Fig. 2B and Fig.3). Although the enzymes converting reduced ferredoxin to NADPH or NADH, namely ferredoxin-$NADP^+$ reductase and ferredoxin-NAD^+ reductase, and their corresponding genes are unknown, they likely play key roles in alcohol formation under solventogenic and alcohologenic conditions, respectively.

A fourth example of metabolic flux analysis is the identification of the hydrogen production pathway. Three hydrogenases are potentially involved: two Fe-Fe hydrogenases, HydA (encoded by CA_C0028) and HydB (encoded by CA_C3230), and one Ni-Fe hydrogenase, HupSL (encoded by CA_P0141–0142). The *hydB* and the *hupSL* genes are not expressed under all three conditions, nor were the HydB and HupSL proteins detected by quantitative proteomic analysis. As HydA is the only hydrogenase present, how can the lower observed flux in H_2 production under solventogenic and alcohologenic conditions (compared to acidogenic conditions) be explained? Under solventogenic conditions, there is a 3-fold decrease in the expression of *hydA*; this is associated with a 2-fold decrease in the expression of *fdx1* (CA_C0303), which encodes the primary ferredoxin, the key redox partner for the hydrogenase. As these results were confirmed by the proteomic analysis, they may explain the 1.3-fold decrease in H_2 production under solventogenic conditions compared to acidogenic conditions (Fig. 2B). Nonetheless, under alcohologenic conditions a 1.7-fold decrease in H_2 production (compared to acidogenic conditions) is associated with a 1.8-fold higher expression of *hydA*, a 3-fold decrease in the expression of *fdx1*, and a 6-fold increase in the expression of CA_C3486, which encodes a multimeric flavodoxin, another potential redox partner for the hydrogenase. In fact, the reduced multimeric flavodoxin may be a better

substrate for the ferredoxin-NAD^+ reductase than for the primary hydrogenase, as was previously shown for reduced neutral red (Girbal *et al.*, 1995c). This result would explain the low flux in hydrogen production and the high flux in ferredoxin-NAD^+ reductase production under alcohologenic metabolism obtained either through growth in glucose-glycerol mixtures or in glucose in the presence of neutral red (Girbal *et al.*, 1995c).

A fifth example of metabolic flux analysis is the glyceraldehyde-3-phosphate oxidation pathway. Two glyceraldehyde-3-phosphate dehydrogenases are potentially involved: GapC (encoded by CA_C0709) (Schreiber & Durre, 1999), which phosphorylates and produces NADH, and GapN (encoded by CA_C3657) (Iddar *et al.*, 2002), which is non-phosphorylating and produces NADPH. For each of the three conditions and each of the genes studied, the numbers of mRNA molecules and protein molecules per cell were measured. The percent of the total glycolytic flux due to each of the enzymes was calculated by assuming that both enzymes function at their previously published Vmax levels (Schreiber & Durre, 1999, Iddar *et al.*, 2002) and using the amount of each protein per cell. Herein, results are only presented for solventogenic metabolism, though qualitatively, the conclusions were the same for all conditions: *gapN* is poorly expressed compared to *gapC* (0.56 versus 66 mRNA molecules per cell; 3,500 versus 190,000 protein molecules per cell) (Dataset S2), and GapN would be responsible for less than 5% of the glycolytic flux.

Two fluxes involved in anaplerotic reactions, namely, that for pyruvate carboxylase (encoded by CA_C2660) and NADH-dependent malic enzymes (encoded by CA_C1589 and CA_C1596), could not be solved for using our GSM analysis coupled with transcriptomic and proteomic analyses. All of the genes studied were transcribed and translated under all conditions, and because all fermentations occurred under a high partial pressure of CO_2, malic enzymes could function in both malate production from pyruvate and malate decarboxylation to pyruvate, depending on the NADH/NAD^+ and pyruvate/malate ratios.

Using 13C-labeling in a *C. acetobutylicum* batch culture, Au et al. (Au *et al.*, 2014) demonstrated that malic enzymes function in the malate-to-pyruvate direction but that this flux accounted for less than 5% of the pyruvate carboxylase flux. In Fig.3 and Fig.S3, the anaplerotic fluxes presented are net anaplerotic fluxes, which were attributed to pyruvate carboxylase.

The flux in the oxidative branch of the TCA cycle was much higher than that in the reductive branch (Fig.3 and Fig.S3). In agreement with the 13C-labeling flux data reported by Amador-Noguez et al. (Amador-Noguez *et al.*, 2010), who demonstrated the flux from oxaloacetate to malate, but in contrast to the report by Au et al. (Au *et al.*, 2014), in which no flux could be measured through this enzyme, under all three conditions, we measured ~1,000 malate dehydrogenase (CA_C0566) protein molecules per cell that could catalyze the first step of the TCA reductive branch (Dataset S2).

Conclusion

In this work, an improved GSM containing new and validated biochemical data was developed in conjunction with quantitative transcriptomic and proteomic analyses to obtain accurate fluxomic data. These "omics" data allowed for i) the determination of the distribution of carbon and electron fluxes, ii) the elucidation of the different genes/enzymes involved in the primary metabolism of *C. acetobutylicum* and iii) a better understanding of the regulation of *C. acetobutylicum* primary metabolism under different physiological conditions. The information provided in this study will be important for the further metabolic engineering of *C. acetobutylicum* to develop a commercial process for the production of n-butanol.

2.5 Materials and Methods

Chemicals and other reagents

All chemicals were of reagent grade and were purchased from Sigma-Aldrich Chimie (Saint Quentin Fallavier, France) or from VWR Prolabo (Fontenay Sous Bois, France). All gases used for gas flushing of the medium and for the anaerobic chamber were of the highest purity available and were obtained from Air Liquide (Paris, France). All restriction enzymes and Crimson Taq DNA polymerase used for colony PCR were supplied by New England Biolabs (MA, USA) and were used according to the manufacturer's instructions. DNA fragments for vector constructions were amplified using Phusion High-Fidelity DNA polymerase (New England Biolabs).

Culture conditions

Batch culture

All liquid cultures of *C. acetobutylicum* ATCC 824 *ΔCA_C1502 Δupp* (Soucaille *et al.*, 2014) were performed in 30 mL or 60 mL glass vials under strict anaerobic conditions in clostridium growth medium (CGM), as described previously (Roos *et al.*, 1985), or in synthetic medium (MS), as described previously (Vasconcelos *et al.*, 1994). *C. acetobutylicum* was stored in spore form at -20 °C after sporulation in MS medium. Heat-shock was performed for spore germination by immersing the bottle into a water bath at 80 °C for 15 minutes.

Continuous culture

The conditions described previously by Vasconcelos et al. (Vasconcelos *et al.*, 1994) and Girbal et al. (Girbal *et al.*, 1995a) were used for the phosphate-limited continuous culture of *C. acetobutylicum* fed a constant total carbon amount of 995 mM. The cultures were

maintained under acidogenesis (pH 6.3, 995 mM of carbon from glucose), solventogenesis (pH 4.4, 995 mM of carbon from glucose) and alcohologenesis (pH 6.3, 498 mM of carbon from glucose and 498 mM of carbon from glycerol).

RNA extraction & microarray

For transcriptomic analysis, 3 mL samples were collected from chemostat cultures and immediately frozen in liquid nitrogen. The frozen cell cultures were ground promptly with 2-mercaptoethanol in a liquid nitrogen-cooled mortar. RNA was extracted using an RNeasy Midi kit (Qiagen, Courtaboeuf, France) following the manufacturer's instructions with the supplementation of DNase treatment using RNase-Free DNase Set (Qiagen). RNA quantity and composition were analyzed using an Agilent 2100 Bioanalyzer (Agilent Technologies, Massy, France) and a NanoDrop ND-1000 spectrophotometer (Labtech France, Paris, France) at 260 nm and 280 nm. All microarray procedures were performed according to the manufacturer’s protocol (Agilent One-Color Microarray-Based Exon Analysis). Briefly, the RNAs were labeled with a Low Input Quick Amp Labeling kit and hybridized following a one-color microarray-based gene expression analysis protocol. The slides were scanned using a Tecan MS200 scanner and analyzed using Feature Extraction V.11.5.1.1.

Protein extraction and analysis

For proteomic analysis, 20 mL samples were collected from chemostat cultures and treated according to the standard operating procedures developed by Schwarz et al. (Schwarz *et al.*, 2007) for the extraction of intracellular proteins, except that PMSF was not added. Samples of 200 µg of each of the lyophilized protein extracts were dissolved at 80 °C in 100 µl of 0.1% RapiGest (Waters) in water. Disulfide bonds were reduced with the addition of dithiothreitol (DTT) at 2 mM and incubation at 60 °C for 15 minutes. Cysteine residues were

carboxyamidomethylated with the addition of iodoacetamide to a concentration of 10 mM and incubated in the dark at room temperature. Proteolytic digestion was performed with trypsin (10 µg/ml) at 37 °C for 12 hours. Protein hydrolysates were acidified with 5 µl of concentrated trifluoroacetic acid (TFA), incubated at 37 °C for 20 minutes, and centrifuged at 18,000 g for 2 minutes to remove the RapiGest precipitate. The supernatant was collected. Post-digestion samples at a concentration of 2 µg/µl were mixed at a ratio of 1:1 with 40 fmol/µl phosphorylase B internal standard tryptic digest in 200 mM ammonium formate buffer.

Quantitative two-dimensional reversed-phase liquid chromatography-tandem mass spectrometry (LC/LC-MS/MS) was performed at a high-low pH reversed-phase/reversed-phase configuration using a nano-Acquity ultra-performance liquid chromatography (UPLC)/UPLC system (Waters Corp.) coupled with a Synapt G2 HDMS mass spectrometer (Waters Corp.) and nano-electrospray ionization, as previously described by Foster et al. (Foster *et al.*, 2015).

Raw MS data were processed either using a Mascot Distiller (version 2.4.3.1) for peptide and protein identification and isobaric quantification or using a Progenesis QI (Nonlinear Dynamics, United Kingdom) for label-free quantification. The MS/MS spectra were searched against the UniProt *Clostridium acetobutylicum* database using the Mascot search engine (version 2.4.1) with the following search parameters: full tryptic specificity, up to two missed cleavage sites, carbamidomethylation of cysteine residues as a fixed modification, and N-terminal methionine oxidation as a variable modification.

Determination of DNA, mRNA, and protein contents

DNA and protein contents were measured in cells grown in a chemostat culture after centrifugation (4,000 g, 10 min, 4 °C) and washed twice with Milli-Q water. Protein content

was determined via the Biuret method (Peterson, 1983). The DNA content was determined after incubation with perchloric acid (0.5 M, 70 to 80 °C, 15 to 20 min), as described by Hanson and Phillips (Hanson & Phillips, 1981). The RNA content was determined using the protocol described above for the microarrays.

Measurement of fermentation parameters

Biomass concentration was determined both by counting the number of cells per ml, as previously described (Ferras *et al.*, 1986) and by the DCW method after centrifugation (16,000 g, 5 min, room temperature), two washes with Milli-Q water, and drying under vacuum at 80 °C. The concentrations of glucose, glycerol, acetate, butyrate, lactate, pyruvate, acetoin, acetone, ethanol, and butanol were determined based on high-performance liquid chromatography (HPLC), as described by Dusséaux et al. (Dusseaux *et al.*, 2013), except that the concentration of H_2SO_4 was changed to 0.5 mM, as required for mobile phase optimization. The concentrations of formate and fumarate were measured using a formate assay kit (Sigma-Aldrich) and a fumarate assay kit (Sigma-Aldrich), according to the manufacturer's instructions.

Material and method regarding metabolic enzyme expression and purification

This information is provided as supplementary material.

GEO data deposit

The microarray data can be accessed at GEO through accession number GSE69973.

Acknowledgments

We thank Professor Jean-Louis Uribelarrea, Sophie Lamarre and Lidwine Trouilh for help

with the data analysis. This work was financially supported by the European Community's Seventh Framework Program "CLOSTNET" (PEOPLE-ITN-2008-237942) to Minyeong Yoo.

Figure legends

FIG 2.1. Butanol pathway analysis under acidogenesis (A), solventogenesis (B), and alcohologenesis (C). (Left) Numbers of mRNA (blue) and protein (green) molecules per cell for the five enzymes potentially involved in butanol production.

(Right) Activity distributions of the five enzymes are shown for each step under the arrows. The primary cofactors used for each step are shown over the arrows. Butanol flux is indicated under the word 'butanol'.

FIG 2.2. Electron flux map: acidogenesis (A), solventogenesis (B), alcohologenesis (C). The hydrogenase (red), ferredoxin-NAD+reductase (blue) and ferredoxin-NADP+(green) *in vivo* fluxes are presented. All values are normalized to the flux of the initial carbon source (mmol/gDCW/h). Glucose flux is normalized as 100 for acidogenesisand solventogenesis, and the sum of glucose and half of the glycerol normalized as 100 for alcohologenesis

FIG 2.3. Metabolic flux map of *C. acetobutylicum* in solventogenesis. All values are normalized to flux of initial carbon source, glucose (mmol/gDCW/h). Metabolic flux maps of *C. acetobutylicum* in acidogenesis and in alcohologenesis are presented in Fig. S3.

Table 2.1. Comparison of genome-scale models (GSMs) of *C. acetobutylicum*. The numbers of genes, reactions, and metabolites present in four previous GSMs of *C. acetobutylicum* and *i*Cac967 are shown.

Model statics	**Senger et al. (56, 57)**	**Lee et al. (58)**	**McAnulty et al. (46)**	**Dash et al. (45)**	***i*Cac967**
Genes	474	432	490	802	967
Reactions	552	502	794	1462	1231
Metabolites	422	479	707	1137	1058

Table 2.2. Activities of purified key metabolic enzymes.

Locus Number	Gene Name	Enzyme Activity	Activity (U/mg)*
CA_C3299	*bdhA*	Butanol dehydrogenase	NADH (0.15±0.05) ; NADPH (2.57±0.45)
CA_C3298	*bdhB*	Butanol dehydrogenase	NADH (0.18±0.02) ; NADPH (2.95±0.36)
CA_C3392	*bdhC*	Butanol dehydrogenase	NADH (0.24±0.04); NADPH (2.21±0.41)
CA_P0162	*adhE1*	Butanol dehydrogenase	NADH (0.04±0.02) ; NADPH (not detected)
CA_P0035	*adhE2*	Butanol dehydrogenase	NADH (4.8±0.42) ; NADPH (0.12±0.01)
CA_P0162	*adhE1*	Butyraldehyde dehydrogenase	NADH (2.27±0.21) ; NADPH (0.08±0.01)

CA_P0035	*adhE2*	Butyraldehyde dehydrogenase	NADH (2.5±0.31); NADPH (0.07±0.01)
CA_C2711-2709	*bcd-etfB-etfA*	Butyryl-CoA dehydrogenase	NADH (0.569±0.08); NADPH (not detected)
CA_C1673-1674	*gltA/gltB*	Glutamate synthase	NADH (0.61±0.16) ; NADPH (0.051+0.01)
CA_C0737	*gdh*	Glutamate dehydrogenase	NADH (41.2.±3.4); NADPH (0.12±0.01)
CA_C0970	*citA*	*Re*-citrate synthase	(1.9±0.14)
CA_C0971	*citB*	Aconitase	(6.5.±0.52)
CA_C0972	*citC*	Isocitrate dehydrogenase	NADH (104±6.8); NADPH (7.1±0.43)
CA_C1589	*malS1*	Malic enzyme	NADH (156±9.6); NADPH (3.4±0.24)

			NADH (142±12.7);
CA_C1596	*malS2*	Malic enzyme	NADPH
			(2.9±0.34)

*One Unit is the amount of enzyme that consumes one μmole of substrate per minute

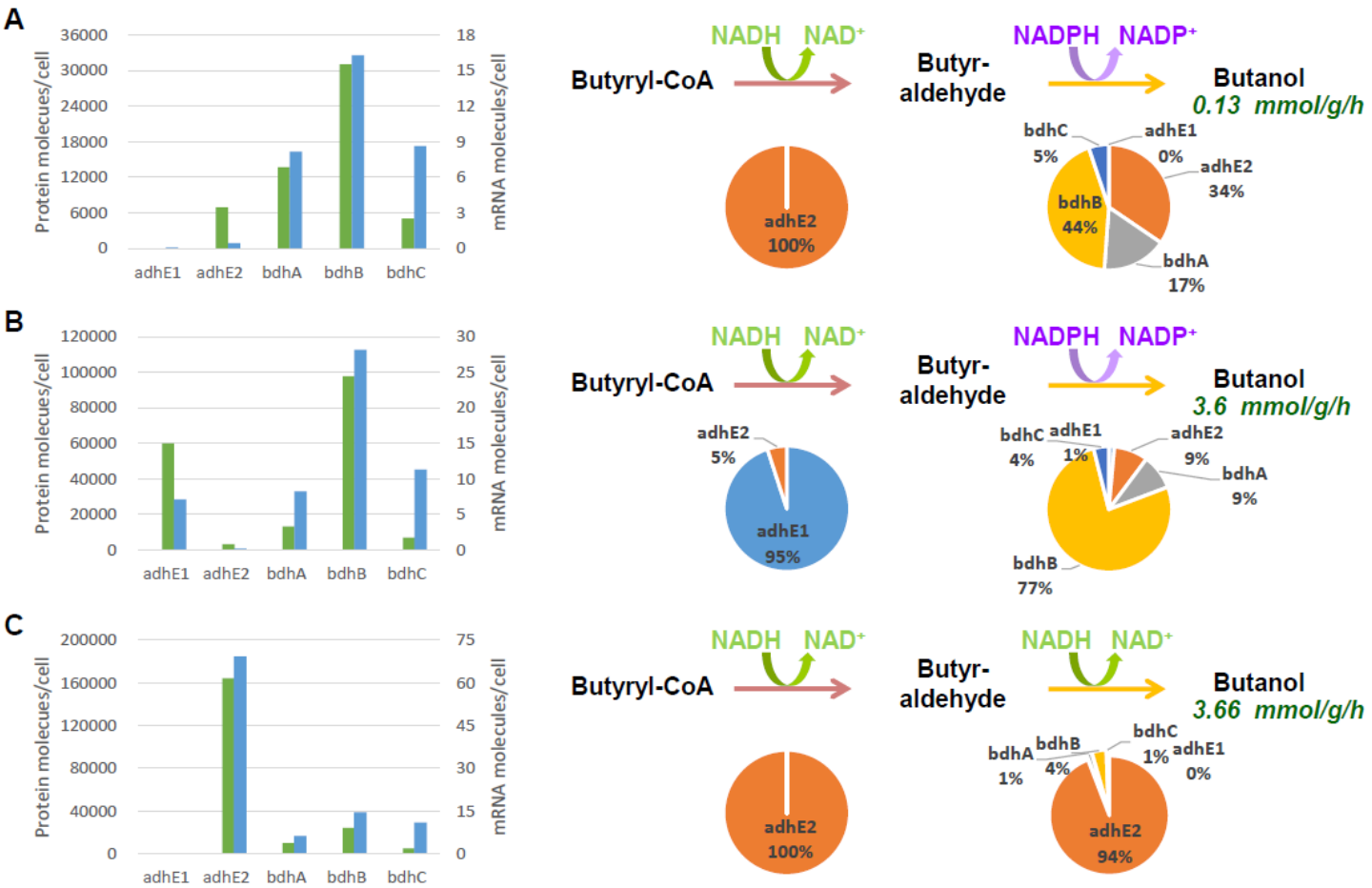

FIG 2.1. Butanol pathway analysis under acidogenesis (A), solventogenesis (B), and alcohologenesis (C). (Left) Numbers of mRNA (blue) and protein (green) molecules per cell for the five enzymes potentially involved in butanol production. (Right) Activity distributions of

the five enzymes are shown for each step under the arrows. The primary cofactors used for each step are shown over the arrows. Butanol flux is indicated under the word ‘butanol’.

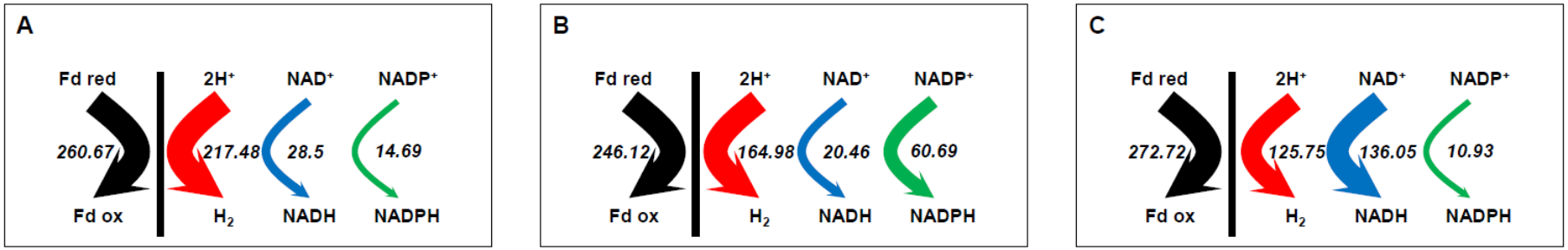

FIG 2.2. Electron flux map: acidogenesis (A), solventogenesis (B), alcohologenesis (C). The hydrogenase (red), ferredoxin-NAD^+ reductase (blue) and ferredoxin-$NADP^+$ (green) *in vivo* fluxes are presented. All values are normalized to the flux of the initial carbon source (mmol/gDCW/h). Glucose flux is normalized as 100 for acidogenesisand solventogenesis, and the sum of glucose and half of the glycerol normalized as 100 for alcohologenesis

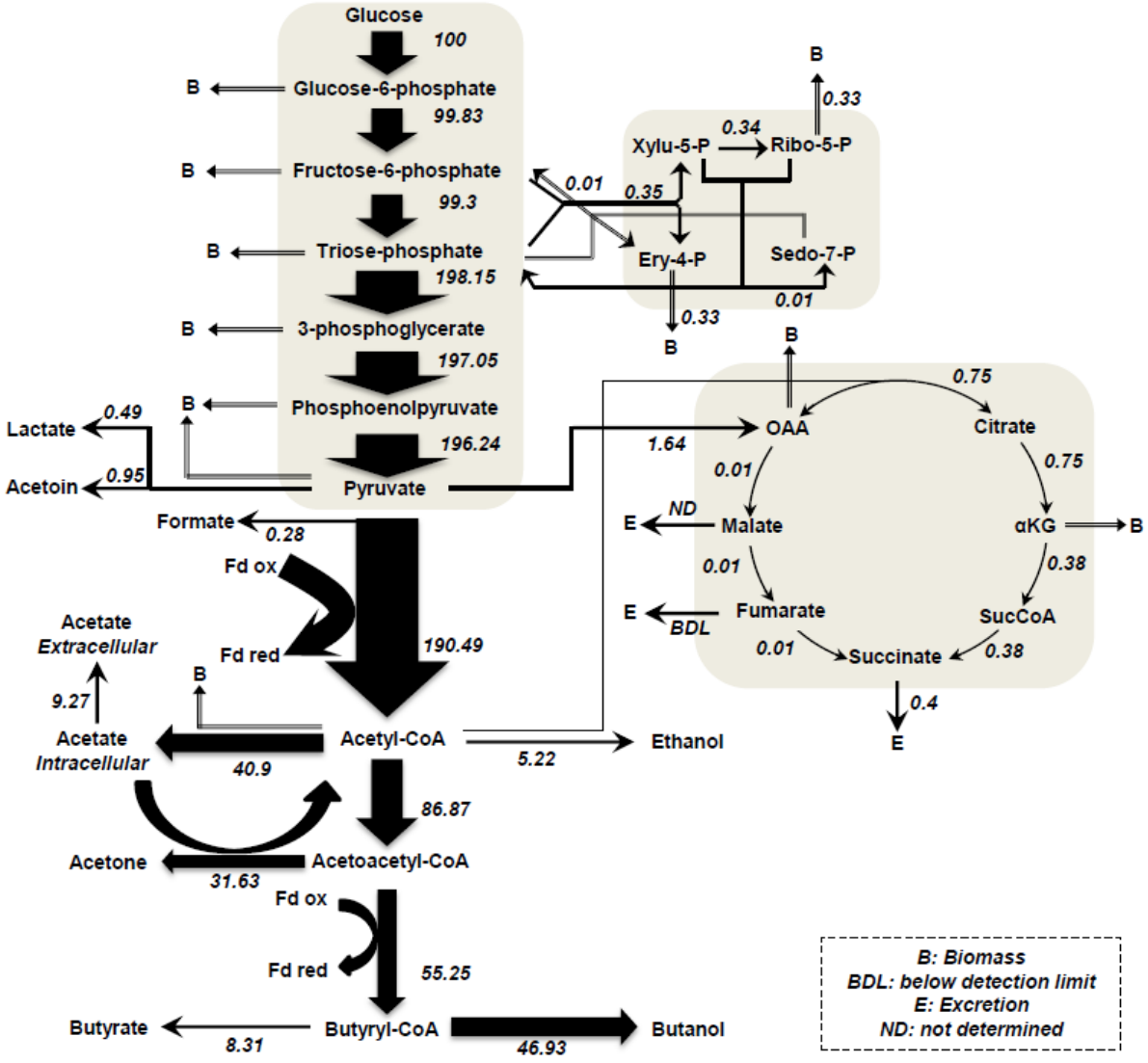

FIG 2.3. Metabolic flux map of *C. acetobutylicum* in solventogenesis. All values are normalized to flux of initial carbon source, glucose (mmol/gDCW/h). Metabolic flux maps of *C. acetobutylicum* in acidogenesis and in alcohologenesis are presented in Fig. S3.

SI Materials and Methods

Expression and Purification of key metabolic enzymes.

All the genes encoding key metabolic enzymes to be biochemically characterized in this study (except the genes encoding the butyryl-CoA dehydrogenase and the glutamine 2-oxoglutarate aminotransferase) were expressed in *E. coli* BL21 (DE3) and the proteins were purified using a Profinity eXact Protein Purification System, following the recommendations of the manufacturer (Biorad). To express the genes of interest in the pPAL7 vector, the gene fragments were amplified from *C. acetobutylicum* ATCC 824 total genomic DNA by PCR using the respective specific primers. After gel purification, the resulting fragments were digested either by *SpeI or NcoI* at 5' end and by *BclI or BamHI* at 3' end and directly cloned into the pPAL7 vector previously digested by *SpeI or NcoI* and by *BamHI* to yield the different pPAL7 expression plasmids , which were validated by sequencing.

E. coli BL21(DE3) Codon plus cells harboring the different pPAL7 plasmids were grown anaerobically in TB medium in the presence of 50µg/mL carbenicillin and 30µg/mL chloramphenicol at 30 °C to OD_{550} ~0.45, and then induced with 100µM IPTG for 4hr at 30 °C. After centrifugation in the anaerobic glove box, the cell lysate was obtained by sonication of the resuspended pellet in oxygen free bind/wash buffer (0.1 M sodium phosphate buffer, pH 7.2) supplemented with 0.2 mM $ZnSO_4$ in the case of *bdhA* (CA_C3299), *bdhB* (CA_C3298) and *bdhC* (CA_C3392) or with 0.2 mM $MnCl_2$ in the case of *citA* (CA_C0970), *citC* (CA_C0972), *malS1* (CA_C1589) and *malS2* (CA_C1596). The tag-free proteins were prepared under anaerobic conditions using a Profinity eXact Protein Purification System according to the standard protocol. After binding and washing of the Profinity eXact mini spin column, the proteolytic activity of the affinity matrix was activated by applying 2 columns volumes of oxygen free 0.1 M sodium phosphate buffer (pH 7.2, containing 0.1 M sodium

fluoride) and incubating for 30 min to allow cleavage of the tag from the protein, prior to releasing of the tag-free protein from the mini-spin column by centrifugation in the anaerobic glove box. At their N-Terminus, the purified proteins retain a Thr-Ser linker when *SpeI* was used as a cloning site and a Thr-Ser-Thr linker, when *NcoI* was used. Sodium fluoride was eliminated by two consecutive concentration (by ultrafiltration on Amicon Ultra-15 Centrifugal 10 kDa Filter Units)-dilution (into the buffer used for the appropriate assay of each enzymes) steps.

The butyryl-CoA dehydrogenase and the glutamine 2-oxoglutarate aminotransferase encoding genes were expressed in *C. acetobutylicum* ATCC 824 *ΔCA_C1502 Δupp* and the proteins were purified as C-terminal Strep-tagged proteins as previous described (Girbal *et al.*, 2005). To construct the butyryl-CoA dehydrogenase expression plasmid, the *etfB* (CA_C2710), *etfA* (CA_C2711) and *bcd* (CA_C2709) genes were amplified by PCR using *C. acetobutylicum* ATCC 824 total genomic DNA as template and the following couples of primers: Cac2710-D and Cac2710-R, Cac2711-Dand Cac2711-R, and Cac2709-Dand Cac2709-R (Table S3). The first couple of primers was designed to amplify the natural *thlA* RBS region along with the *etfB* gene composed of a *BamH1* restriction site at 5' end and the *SmaI*-long Amino acid linker Streptag-*NarI* sequence at 3' end to allow better yield of purification of the fusion protein as previously described by Lautier et al. (Lautier *et al.*, 2011). The PCR-amplified fragment and the pSOS95 vector were digested with *BamHI* and *NarI*, the resulting fragments were purified on an agarose gel and were ligated to yield the 5.8 kb pCSTLLetfB vector, which was verified by sequencing. The second couple of primers was designed to introduce *FspI* restriction sites at both end of the DNA fragment and to amplify the *etfA* gene with its RBS sequence. The PCR-amplified fragment and the pCSTLLetfB vector were respectively digested by *FspI*, and the fragments were ligated, after purification on an agarose gel and a treatment with Antarctic

phosphatase, yielding the 6.8 kb pCSTLLetfB-etfA vector after verification by sequencing that the *etfA* gene was not mutated.

The third couple of primers was designed to introduce *BamHI* restriction sites at both end of the DNA fragment and to amplify the *bcd* gene with its RBS sequence. The PCR-amplified fragment and the pCSTLLetfB-etfA vector were both digested by *BamHI*, and the resulting fragments were ligated after purification on an agarose gel and a treatment with Antarctic phosphatase, to yield the 8 kb pCSTLLbcd-etfB-etfA vector, which was verified by sequencing that the *bcd* gene was not mutated.

To construct the glutamate synthase expression plasmid, the *gltB* (CA_C1674) and *gltA* (CA_C1673) genes were amplified by PCR with Phusion DNA Polymerase using *C. acetobutylicum* ATCC824 total genomic DNA as template and the following couples of primers: Cac1674-D and Cac1674-R, and Cac1673-D and Cac1673-R (Table S3). The first couple of primers was designed to introduce a *BamHI* and a *SmaI* restriction site at respectively the 5' end and 3' end of the DNA fragment and to amplify the natural *thlA* RBS region along with the *gltB* gene. The PCR-amplified fragment and the 5.8 kb pCSTLLetfB vector were digested with *BamHI* and *SmaI*, the resulting fragments were purified on an agarose gel and were then ligated to yield the 6.5 kb pCSTLLgltB vector, which was verified by sequencing. The second couple of primers was designed to introduce *BamHI* restriction sites at both end of the DNA fragment and to amplify the natural *thlA* RBS region along with the *gltA* gene. The PCR-amplified fragment and the pCSTLLgltB vector were both digested by *BamHI*, and the resulting fragments were ligated after purification on an agarose gel and a treatment with Antarctic phosphatase, to yield the 11 kb pCSTLLgltA-gltB vector. The pCSTLLbcd-etfB-etfA and pCSTLLgltA-gltB vectors were introduced in *C. acetobutylicum* ATCC 824 *ΔCA_C1502 Δupp* by electroporation, respectively. *C. acetobutylicum* recombinant strains

were stored in spore form at -20 °C, being stable for months. Recombinant strains were grown in MS (Vasconcelos *et al.*, 1994) supplemented with erythromycin (40 µg/ml) and calcium carbonate (2 g/l), in a 1.3-liter batch culture maintained at 37 °C and pH 6.5 as previously described (Girbal *et al.*, 2005).

The primers used in this study is below.

Primer name	Sequence (5'-3')
Cap0162-D-NcoI	AAAAA**CCTAGG**atgaaagtcacaacagtaaaggaattagatgaaaaactc
Cap0162-R-BclI	AAAAA**TGATCA**ttaaggttgtttttaaaacaatttatatacatttc
Cap0035-D-NcoI	AAAAA**CCTAGG**atgaaagttacaaatcaaaaagaactaaaacaaaagcta
Cap0035-R-BamHI	AAAAA**GGATCC**ttaaaatgattttatatagatatccttaagttcact
Cac3298-D-SpeI	AAAAA**ACTAGT**atggttgatttcgaatattcaataccaactagaattttt
Cac3298-R-BamHI	AAAAA**GGATCC**ttacacagatttttgaatatttgtaggacttcg
Cac3299-D-SpeI	AAAAA**ACTAGT**atgctaagttttgattattcaataccaactaaagttttt
Cac3299-R-BamHI	AAAAA**GGATCC**ttaataagatttttaaatatctcaagaacatcc
Cac3392-D-SpeI	AAAAA**ACTAGT**atgtataattttgatttttttaacccaacacatatagta
Cac3392-R-BamHI	AAAAA**GGATCC**tttgcggcttactttacattgcaccctctaaaat
Cac0737-D-SpeI	AAAAA**ACTAGT**atggaaattttaaagcatgtaatggatgatgttattaaa

Cac0737-R-BamHI	AAAAA**GGATCC**ttaaaatccaagagaatacatggcttcagcaactttag
Cac0970-D-SpeI	AAAAA**ACTAGT**atgaaagaactaaatctaaaagatgttgaggagccaaat
Cac0970-R-BamHI	AAAAA**GGATCC** ttaactggctcttgtattttcaacatcaattaacta
Cac0971-D-SpeI	AAAAA**ACTAGT**atgggactaacattaactgaaaaaataataaagagtcat
Cac0971-R-BamHI	AAAAA**GGATCC** ttattttgtgtctttttttatctgatttaattttc
Cac0972-D-SpeI	AAAAA**ACTAGT**atgaaaaaaaatcacacaataactcttattcctggagat
Cac0972-R-BamHI	AAAAA**GGATCC** ttatatattctttataacttcattagcaaattcatc
Cac1589/1596-D-SpeI	AAAAA**ACTAGT**atgaataatttaaaaggtttagaattactaagaaatccc
Cac1589-R-BamHI	AAAAA**GGATCC** ttatctatagtatggttcccaaatttcattttcaac
Cac1596-R-BamHI	AAAAA**GGATCC** ttatttatagtatggttcccaaatttcattttcaac
Cac2711-D-FspI	AATAA**TGCGCA**aggagggatttttcaatgaataaagcagattacaagggcg
Cac2711-R-FspI	TAAGT**TGCGCA**attaattattagcagctttaacttgagc
Cac2710-D-BamHI	CCGTA**GGATCC**atcaaaatttaggaggttagttagaatgaatatagt
Cac2710-R-NarI	AAATT**GGCGCC**ttatttttcaaattgaggatgtgaccaactaccaccaccactaccac caccactacccccgggaatatagtgttcttcttttaattttgagacaacatatgc
Cac2709-D-BamHI	AAATT**GGATCC**aggaggtaagtttatatggattttaatttaacaagag
Cac2709-R-BamHI	AAATT**GGATCC**ttatctaaaaatttttcctg

Cac1674-D-BamHI	AAATT**GGATCC**atcaaaatttaggaggttagttagaatggaaaggtaactggatttaaagaatacg
Cac1674-R-smaI	AAATT**CCCGGG**tcctctaagagaagtttctcccataagg
Cac1673-D-BamHI	AAATT**GGATCC**atcaaaatttaggaggttagttagaatgacaagaaatattggatatcctg
Cac1673-R-BamHI	AAATT**GGATCC**ttacatattaactgcagcagc

Enzyme assays

Butanol dehydrogenase and butyraldehyde dehydrogenase activities were measured spectrophotometrically as previously described by Vasconcelos et al. (Vasconcelos *et al.*, 1994) by the rate of NADH or NADPH consumption under anaerobic conditions.

Butyryl-CoA dehydrogenase activity was measured spectrophotometrically as previous described by Li et al. (Li *et al.*, 2008) by the rate of NADH or NADPH consumption under anaerobic conditions. The stoichiometry of the reaction catalyzed by the butyryl-CoA dehydrogenase was determined as previously described by Li et al. (Li *et al.*, 2008) for the enzymes from *Clostridium kluyveri* except that purified ferredoxin (as described by Guerrini et al.(Guerrini *et al.*, 2008)) (encoded by CA_C0303) and hydrogenase (as described by Lautier et al. (Lautier *et al.*, 2011)) (encoded by CA_C0028) from *C. acetobutylicum* were used in place of *Clostridium pasteurianum* ferredoxin and hydrogenase.

Glutamate dehydrogenase activity was measured spectrophotometrically as previous described by Teller et al. (Teller *et al.*, 1992) by the rate of NADH or NADPH production under anaerobic conditions.

Glutamate synthase activity was measured spectrophotometrically as previous described by

Vanoni et al. (Vanoni *et al.*, 1991) by the rate of NADH or NADPH production under anaerobic conditions

The *Re*-citrate synthase activity was measured spectrophotometrically as previous described by Li et al. (Li *et al.*, 2007)(2007) by the rate of formation of the anion of thionitrobenzoate from 5,5'-dithiobis-[2-nitrobenzoic acid] (DTNB, Ellman's reagent) and CoA at 412 nm under anaerobic conditions.

The aconitase activity was measured spectrophotometrically, after treatment with ferrous iron under reducing conditions, as previous described by Dingman and Sonenshein (Dingman & Sonenshein, 1987) by the rate of cis-aconitate formation at 240 nm from isocitrate under anaerobic conditions.

The isocitrate dehydrogenase activity was measured spectrophotometrically as previous described by Wang et al. (Wang *et al.*, 2012) by the rate of NADH or NADPH production under anaerobic conditions at a MnCl2 concentration of 5 mM.

The malic enzyme activity was measured spectrophotometrically as previous described by Stols and Donnelly (Stols & Donnelly, 1997) by the rate of NADH or NADPH production under anaerobic conditions at a MnCl2 concentration of 5 mM.

SI results

Quantitative transcriptomic analysis of *Clostridium acetobutylicum* under different physiological conditions.

Quantitative transcriptomic analyses were performed in phosphate-limited chemostat cultures

of *C. acetobutylicum* maintained in three different stable metabolic states: acidogenic, solventogenic and alcohologenic. Solventogenic and alcohologenic cells were comprehensively compared to acidogenic cells via quantitative transcriptomic analysis. Striking differences are highlighted in Fig. S2A and Fig. S2B, respectively. The numbers of mRNA molecules per cell of genes matching the significance criteria of ≥ 4.0-fold increased expression or ≥ 4.0-fold decreased expression in solventogenesis versus acidogenesis are presented respectively in Table S1. Similarly, the numbers of mRNA molecules per cell of genes matching the significance criteria of ≥ 4.0-fold increased expression or ≥ 4.0-fold decreased expression in alcohologenesis versus acidogenesis are presented respectively in Table S2.

Metabolic flux analysis of *Clostridium acetobutylicum* under different physiological conditions.

To perform a metabolic flux analysis of *C. acetobutylicum* under stable acidogenic, solventogenic and alcohologenic conditions, *i*Cac963 was combined with our transcriptomic and proteomic data. The results are summarized in Fig. S3.

Supplemental material footnotes and figure legends

Table S2.1. *i*Cac967 validation on previously published data

Table S2.2. Genes with ≥ 4.0-fold increased or decreased expression in solventogenesis versus acidogenesis.

Table S2.3. Genes with ≥ 4.0-fold increased or decreased expression in alcohologenesis

versus acidogenesis.

Fig. S2.1. H_2 formation from NADH catalyzed by purified butyryl-CoA dehydrogenase/Etf complex from *C. acetobutylicum* in the presence of hydrogenase (HydA from *C. acetobutylicum*), ferredoxin (Fdx from *C. acetobutylicum*), and crotonyl-CoA. (A) Amount of H_2 formed as a function of the amount of NADH added in the presence of excess amounts of crotonyl-CoA. (B) Amount of H_2 formed as a function of the amount of crotonyl-CoA added in the presence of excess amounts of NADH.

Fig. S2.2. Overview of the transcript levels during solventogenesis versus acidogenesis (A) and alcohologenesis versus acidogenesis (B).

Log expression ratios of solventogenesis to acidogenesis (B) and alcohologenesis to acidogenesis are shown. All genes with log values (as logarithms to the basis of 2) higher than 2 (≥ 4.0-fold increased expression) are significantly induced under solventogenesis (A) and alcohologenesis (B), and genes with a negative log of less than -2 (≥ 4.0-fold decreased expression) were significantly induced in acidogenesis. According to this definition, all genes between the dashed lines were expected to be not significantly influenced.

Fig. S2.3. Metabolic flux map of *C. acetobutylicum* in acidogenesis (A), solventogenesis (B), alcohologenesis (C). All values are normalized to the flux of the initial carbon source (mmol/gDCW/h). Glucose flux is normalized as 100 for acidogenesisand solventogenesis, and the sum of glucose and half of the glycerol normalized as 100 for alcohologenesis.

Fig. S2.4. Carbon source consumption and product profiles of *C. acetobutylicum*. (A) Carbon source consumption. (B) Product profiles. Each histogram indicates different metabolic states: red (acidogenesis), green (solventogenesis), and blue (alcohologenesis).

Dataset S1. Metabolic networks of *C. acetobutylicum*.

Dataset S2. Transcriptomic and Proteomic data.

Supplemental text. Supplemental materials and methods, and results

Table S2.1. *i*Cac967 validation on previously published data

	M5 (pIMP1) experimental[1]	M5 (pIMP1) *i*Cac967	Buk mutant experimental[2]	Buk mutant *i*Cac967
Growth rate (h^{-1})	0.2	0.2	0.3	0.3
Glucose fluxes (mmol/g/h)	21.3	21.3	6.7	6.7
Acetate fluxes (mmol/g/h)	3	3.5	5.6	5.6
Butyrate fluxes (mmol/g/h)	15.5	18.2	0.8	0
Butanol fluxes (mmol/g/h)	0	0	2.7	1.9
Ethanol fluxes (mmol/g/h)	0.15	0	0.3	0.2
Acetone fluxes (mmol/g/h)	0	0	0.3	0
Carbon balance (%)	96	100	130	100

[1] Data source: Harris LM, Desai RP, Welker NE, Papoutsakis ET. 2000. Characterization of recombinant strains of the *Clostridium acetobutylicum* butyrate kinase inactivation mutant: need for new phenomenological models for solventogenesis and butanol inhibition? Biotechnol Bioeng 67:1-11.

[2] Data source: Lee JY, Jang YS, Lee J, Papoutsakis ET, Lee SY. 2009. Metabolic engineering of *Clostridium acetobutylicum* M5 for highly selective butanol production. Biotechnol J 4:1432-1440.

Table S2.2. Genes with ≥ 4.0-fold increased or decreased expression in solventogenesis versus acidogenesis

Gene number	Function	Solventogenesis /Acidogenesis	Acidogenesis mRNA molecules per cell*	Solventogenesis mRNA molecules per cell*	Acidogenesis protein molecules per cell*	Solventogenesis protein molecules per cell*
Increase						
CAC0014	Aminotransferase	28.63	0.13 ± 0.01	3.74 ± 1.51	ND	3840 ± 571
CAC0015	D-3-phosphoglycerate dehydrogenase	36.66	0.17 ± 0.02	6.3 ± 2.56	ND	4834 ± 373
CAC0016	Related to HTH domain of SpoOJ/ParA/ParB/repB family, involved in chromosome partitioning	12.82	0.13 ± 0.01	1.66 ± 1.48	ND	3374 ± 260
CAC0017	Seryl-tRNA synthetase	12.01	0.09 ± 0	1.04 ± 0.51	ND	3704 ± 397
CAC0106	ABC-type probable sulfate transporter, periplasmic binding protein	4.25	0.12 ± 0	0.5 ± 0.17	ND	ND
CAC0110	GTPase, sulfate adenylate transferase subunit 1	5.00	0.14 ± 0.01	0.68 ± 0.31	ND	360 ± 73
CAC0273	2-isopropylmalate synthase	4.08	0.55 ± 0.05	2.23 ± 0.56	2193 ± 53	10381 ± 906
CAC0319	ABC transporter ATP-binding protein	4.74	0.15 ± 0.01	0.72 ± 0.09	ND	ND
CAC0458	Permease	4.77	0.15 ± 0	0.72 ± 0.36	ND	ND
CAC0561	Cellulase CelE ortholog; dockerin domain;	7.82	0.28 ± 0.03	2.21 ± 0.23	ND	ND
CAC0574	Pectate lyase H (FS)	4.55	0.11 ± 0.01	0.48 ± 0.27	ND	ND

CAC0575	Pectate lyase H (FS)	7.55	0.2 ± 0.02	1.54 ± 0.97	ND	ND
CAC0663	Hypothetical protein	5.23	0.61 ± 0.07	3.21 ± 1.53	ND	ND
CAC0718	Ortholog ycnD B.subtilis, nitroreductase	4.31	0.16 ± 0.01	0.67 ± 0.36	ND	1410 ± 434
CAC0910	Probably cellulosomal scaffolding protein precursor, secreted; cellulose-binding and cohesin domain;	15.69	0.22 ± 0.02	3.42 ± 0.98	ND	ND
CAC0911	Possible processive endoglucanase family 48, secreted; CelF ortholog; dockerin domain;	12.87	0.22 ± 0.02	2.85 ± 0.61	ND	ND
CAC0912	Possible non-processive endoglucanase family 5, secreted; CelA homolog secreted; dockerin domain;	13.79	0.21 ± 0.03	2.84 ± 1.01	ND	ND
CAC0913	Possible non-processive endoglucanase family 9, secreted; CelG ortholog; dockerin and cellulose-binding domain;	5.69	0.08 ± 0	0.46 ± 0.08	ND	ND
CAC0914	Cellulosome integrating cohesin-containing protein, secreted;	11.55	0.15 ± 0	1.68 ± 0.79	ND	ND
CAC0915	Endoglucanase A precursor (endo-1,4-beta-glucanase) (cellulase A), secreted; dockerin domain;	5.30	0.08 ± 0	0.42 ± 0.09	ND	ND
CAC0916	Possible non-processive endoglucanase family 9, secreted; CelG ortholog; dockerin and cellulose-	5.95	0.08 ± 0	0.48 ± 0.13	ND	ND

	binding domain;					
CAC0917	and cellulose-binding endoglucanase family 9; CelL ortholog; dockerin domain;	5.05	0.07 ± 0	0.33 ± 0.06	ND	ND
CAC0918	Possible non-processive endoglucanase family 5, ortholog of mannase A, secreted; dockerin domain;	7.99	0.12 ± 0.01	0.97 ± 0.33	ND	ND
CAC0935	Histidyl-tRNA synthetase	5.41	0.94 ± 0.03	5.11 ± 1.24	3476 ± 232	13410 ± 108
CAC1045	Predicted permease	4.01	0.12 ± 0.01	0.5 ± 0.08	ND	ND
CAC1047	Ribonucleotide reductase, vitamin B12-dependent	15.74	0.7 ± 0.07	11.07 ± 1.87	223 ± 41	2714 ± 270
CAC1314	Hypothetical protein	17.94	0.08 ± 0	1.51 ± 0.74	ND	ND
CAC1315	Peptodoglycan-binding domain containing protein	41.25	0.37 ± 0.04	15.14 ± 7.22	ND	ND
CAC1322	Glycerol-3-phosphate dehydrogenase, GLPA	4.49	0.13 ± 0.01	0.57 ± 0.03	ND	ND
CAC1324	Uncharacterized predected metal-binding protein	11.76	0.1 ± 0.01	1.23 ± 1.23	ND	ND
CAC1392	Glutamine phosphoribosylpyrophosphate amidotransferase	8.83	0.53 ± 0.03	4.64 ± 2.93	1666 ± 172	9480 ± 166
CAC1393	Phosphoribosylaminoimidazol (AIR) synthetase	7.76	0.32 ± 0.02	2.51 ± 1.35	707 ± 200	2424 ± 619

CAC1394	Folate-dependent phosphoribosylglycinamide formyltransferase	8.78	0.34 ± 0.02	2.97 ± 1.36	1091 ± 95	7168 ± 826
CAC1395	AICAR transformylase/IMP cyclohydrolase	7.38	0.37 ± 0.01	2.75 ± 1.26	913 ± 117	4756 ± 30
CAC1405	Beta-glucosidase	6.07	6 ± 0.61	36.4 ± 12.51	14695 ± 407	7352 ± 353
CAC1433	Hypothetical protein	4.20	0.19 ± 0.01	0.79 ± 0.19	ND	ND
CAC1547	Thioredoxin, trxA1	∞	0	0.23 ± 0.01	ND	ND
CAC1548	Thioredoxin reductase	7.76	0.13 ± 0	1 ± 0.07	ND	ND
CAC1549	Glutathione peroxidase	5.79	0.12 ± 0	0.69 ± 0.07	ND	ND
CAC1655	bifunctional enzyme phosphoribosylformylglycinamidine (FGAM) synthase (synthetase domain/glutamine amidotransferase domain)	5.09	0.9 ± 0.4	4.6 ± 2.21	6414 ± 65	2482 ± 118
CAC1669	Carbon starvation protein	9.56	0.28 ± 0.03	2.68 ± 0.5	ND	ND
CAC2072	Stage IV sporulation protein B, SpoIVB	∞	0	0.34 ± 0.04	ND	ND
CAC2293	Hypothetical secreted protein	7.38	2.47 ± 0.26	18.21 ± 5.6	ND	ND
CAC2388	N-acetylornithine aminotransferase	4.84	1.44 ± 0.18	6.96 ± 1.03	2529 ± 202	10394 ± 1895
CAC2405	Predicted glycosyltransferase	5.20	0.39 ± 0.02	2.01 ± 0.93	ND	ND
CAC2408	Glycosyltransferase	4.03	0.24 ± 0.03	0.96 ± 0.58	ND	ND
CAC2445	AICAR transformylase domain of	5.92	0.4 ± 0.05	2.34 ± 0.12	1024 ± 155	3397 ± 456

	PurH-like protein					
CAC2446	Hypothetical protein	5.80	0.39 ± 0.06	2.24 ± 0.08	ND	ND
CAC2517	Extracellular neutral metalloprotease, NPRE	4.43	1.63 ± 0.16	7.22 ± 2.02	725 ± 137	3219 ± 180
CAC2607	Short-chain alcohol dehydrogenase family protein	4.94	0.26 ± 0.03	1.31 ± 0.48	ND	ND
CAC2774	Methyl-accepting chemotaxis protein with HAMP domain	8.73	0.37 ± 0.08	3.26 ± 1.36	ND	ND
CAC2959	Galactokinase	6.44	1.35 ± 0.3	8.69 ± 3.42	879 ± 139	4081 ± 387
CAC2960	UDP-galactose 4-epimerase	5.34	0.45 ± 0.09	2.42 ± 0.92	ND	ND
CAC2961	Galactose-1-phosphate uridyltransferase	4.67	0.6 ± 0.04	2.82 ± 0.83	ND	ND
CAC3228	Predicted membrane protein	5.27	0.3 ± 0	1.6 ± 0.16	ND	ND
CAC3280	Possible surface protein, responsible for cell interaction; contains cell adhesion domain and ChW-repeats	6.61	0.55 ± 0.07	3.62 ± 0.79	ND	ND
CAC3327	Amino acid ABC-type transporter, ATPase component	4.61	0.56 ± 0.1	2.56 ± 1.07	ND	1109 ± 436
CAC3612	Hypothetical protein	4.13	0.85 ± 0.07	3.5 ± 1.51	ND	ND
CAC3624	6-pyruvoyl-tetrahydropterin synthase	5.26	0.11 ± 0	0.57 ± 0.09	ND	ND
CAC3714	Molecular chaperone (small heat shock protein), HSP18	4.26	2.95 ± 0.19	12.57 ± 6.78	5945 ± 372	30140 ± 1716
CAP0056	Pectate lyase, secreted,	4.53	0.24 ± 0.03	1.08 ± 0.83	ND	ND

	polysaccharide lyase family					
CAP0162	Aldehyde dehydrogenase (NADH dependent), adhE1	83.38	0.09 ± 0.01	7.1 ± 0.73	ND	59943 ± 1535
CAP0163	Butyrate-acetoacetate COA-transferase subunit A	145.85	0.18 ± 0.02	25.79 ± 2.58	ND	10231 ± 528
CAP0164	Butyrate-acetoacetate COA-transferase subunit B	88.65	0.12 ± 0.02	10.27 ± 1.67	ND	7305 ± 1414
Decrease						
CAC0040	Uncharacterized small conserved protein, homolog of yfjA/yukE B.subtilis	0.10	4.33 ± 0.11	0.45 ± 0.14	ND	ND
CAC0042	Hypothetical protein, CF-1 family	0.18	0.93 ± 0.02	0.17 ± 0.03	ND	ND
CAC0043	Hypothetical protein, CF-3 family	0.23	0.54 ± 0.03	0.12 ± 0.02	ND	ND
CAC0044	Predicted membrane protein	0.22	0.86 ± 0.06	0.19 ± 0.03	ND	ND
CAC0047	Uncharacterized small conserved protein, homolog of yfjA/yukE B.subtilis	0.22	0.77 ± 0.03	0.17 ± 0.02	ND	ND
CAC0048	Hypothetical protein, CF-17 family	0.23	0.73 ± 0.03	0.17 ± 0.02	ND	ND
CAC0332	Beta-mannanase	0.23	2.88 ± 0.53	0.66 ± 0.35	ND	ND
CAC0390	Cystathionine gamma-synthase	0.21	0.69 ± 0.03	0.14 ± 0.02	1170 ± 552	ND
CAC0422	Transcriptional antiterminator licT	0.18	1.08 ± 0.27	0.2 ± 0.05	3862 ± 283	ND
CAC0423	Fusion: PTS system, beta-glucosides	0.01	7.23 ± 1.07	0.1 ± 0.02	7941 ± 803	ND

	specific IIABC component					
CAC0424	Fructokinase	0.03	2.8 ± 0.18	0.08 ± 0.01	24634 ± 503	ND
CAC0425	Sucrase-6-phosphate hydrolase (gene sacA)	0.05	1.55 ± 0.21	0.08 ± 0	2836 ± 720	ND
CAC0426	Transcriptional regulator (HTH_ARAC-domain)	0.13	39.11 ± 2.88	4.98 ± 0.2	ND	ND
CAC0533	Maltose-6'-phosphate glucosidase (glvA)	0.09	4.09 ± 0.58	0.38 ± 0.06	ND	ND
CAC0683	Hypothetical protein	0.20	2.97 ± 0.51	0.6 ± 0.2	ND	ND
CAC0684	CBS domains	0.17	6.86 ± 0.85	1.13 ± 0.39	4862 ± 347	1002 ± 77
CAC0685	Putative Mn transporter, NRAMP family	0.22	2.12 ± 0.14	0.47 ± 0.18	ND	ND
CAC1357	Uncharacterized predicted metal-binding protein	0.21	1.11 ± 0.07	0.24 ± 0.06	ND	ND
CAC1825	Homoserine trans-succinylase	0.15	5.71 ± 0.27	0.83 ± 0.13	5828 ± 36	1430 ± 89
CAC1826	Hypothetical protein	0.17	7.94 ± 0.24	1.36 ± 0.17	ND	ND
CAC1888	Uncharacterized phage related protein	0.00	0.21 ± 0.02	0	ND	ND
CAC1893	ClpP family serine protease, possible phage related	0.00	0.23 ± 0.03	0	ND	ND
CAC1945	Phage related anti-repressor protein	0.00	0.21 ± 0.03	0	ND	ND
CAC2456	Hypothetical protein, CF-40 family	0.17	1.82 ± 0.11	0.31 ± 0.1	ND	ND
CAC2457	Hypothetical protein	0.17	2.06 ± 0.18	0.35 ± 0.11	ND	ND

CAC2783	O-acetylhomoserine sulfhydrylase	0.21	5.91 ± 0.16	1.22 ± 0.15	29805 ± 195	7473 ± 92
CAC2810	Possible glucoamylase (diverged), 15 family	0.24	15.81 ± 1.25	3.82 ± 0.8	ND	ND
CAC3258	Hypothetical protein	0.23	0.67 ± 0.06	0.16 ± 0.05	ND	ND
CAC3264	Uncharacterized conserved protein, YTFJ B.subtilis ortholog	0.25	78.48 ± 1.92	19.59 ± 8.11	23796 ± 2151	5405 ± 1761
CAC3265	Predicted membrane protein	0.12	2.24 ± 0.13	0.27 ± 0.08	ND	ND
CAC3266	Hypothetical protein	0.10	8.71 ± 0.16	0.86 ± 0.22	ND	ND
CAC3267	Specialized sigma subunit of RNA polymerase	0.20	0.78 ± 0.02	0.16 ± 0.02	ND	ND
CAC3274	Possible surface protein, responsible for cell interaction; contains cell adhesion domain and ChW-repeats	0.25	0.32 ± 0.04	0.08 ± 0	ND	ND
CAC3419	S-adenosylmethionine-dependent methyltransferase	0.25	0.72 ± 0.08	0.18 ± 0.04	ND	ND
CAC3522	Hypothetical protein, CF-7 family	0.24	6.64 ± 0.43	1.61 ± 0.82	ND	ND
CAC3523	Hypothetical protein, CF-7 family	0.20	2.36 ± 0.17	0.48 ± 0.23	ND	ND
CAC3524	Hypothetical protein, CF-7 family	0.25	2.35 ± 0.08	0.58 ± 0.3	ND	ND
CAC3582	Hypothetical protein	0.10	1.31 ± 0.13	0.13 ± 0.01	ND	ND
CAC3583	Predicted permease	0.21	0.32 ± 0.03	0.07 ± 0.01	ND	ND
CAC3584	Predicted permease	0.08	1.52 ± 0.22	0.12 ± 0.02	ND	ND
CAC3585	ABC-type transporter, ATPase component	0.07	1.29 ± 0.06	0.1 ± 0.02	ND	ND

CAC3589	Uncharacterized conserved membrane protein, YHGE B.subtilis ortholog	0.22	2.86 ± 0.51	0.62 ± 0.17	ND	ND
CAP0036	Uncharacterized, ortholog of YgaT gene of B.subtillis	0.02	78.48 ± 1.92	1.37 ± 0.3	48818 ± 867	582 ± 130
CAP0037	Uncharacterized, ortholog of YgaS gene of B.subtillis	0.01	78.48 ± 1.92	1.13 ± 0.23	42868 ± 8915	547 ± 92
CAP0038	Uncharacterized conserved protein, YCII family	0.21	0.52 ± 0.04	0.11 ± 0.01	ND	ND

*** Average ± SD were determined from triplicate samples, SD values below 0.01 are written as 0 in the table**

ND, not detected

Table S2.3. Genes with ≥ 4.0-fold increased or decreased expression in alcohologenesis versus acidogenesis

Gene number	Function	Alcohologenesis /Acidogenesis	Acidogenesis mRNA molecules per cell*	Alcohologenesis mRNA molecules per cell*	Acidogenesis protein molecules per cell*	Alcohologenesis protein molecules per cell*
Increase						
CAC0102	O-acetylhomoserine sulfhydrylase	21.60	0.06 ± 0	1.35 ± 0.33	1956 ± 350	14020 ± 4015
CAC0103	Adenylylsulfate kinase	28.07	0.07 ± 0	1.87 ± 0.59	ND	850 ± 20
CAC0104	Adenylylsulfate reductase, subunit A	43.02	0.06 ± 0	2.73 ± 0.89	ND	601 ± 7
CAC0105	Ferredoxin	30.26	0.07 ± 0	2.1 ± 0.75	ND	ND
CAC0106	ABC-type probable sulfate transporter, periplasmic binding protein	22.15	0.12 ± 0	2.6 ± 0.89	ND	ND
CAC0107	ABC-type sulfate transporter, ATPase component	17.34	0.07 ± 0.01	1.22 ± 0.39	ND	738 ± 38
CAC0108	ABC-type probable sulfate transporter, permease protein	30.93	0.07 ± 0	2.18 ± 0.8	ND	ND
CAC0109	Sulfate adenylate transferase, CysD subfamily	43.79	0.08 ± 0	3.7 ± 1.36	ND	1520 ± 272
CAC0110	GTPase, sulfate adenylate transferase subunit 1	74.30	0.14 ± 0.01	10.13 ± 3.45	ND	3752 ± 186
CAC0544	Permease	9.54	0.07 ± 0.01	0.7 ± 0.44	ND	ND
CAC0562	Predicted membrane protein	5.36	1.64 ± 0.1	8.82 ± 5.13	ND	ND
CAC0563	Predicted membrane protein	4.12	0.91 ± 0.07	3.73 ± 2.17	ND	ND
CAC0706	Endo-1,4-beta glucanase (fused to two ricin-B-like domains)	4.33	1.19 ± 0.13	5.15 ± 2.61	ND	ND
CAC0751	Permease	6.77	0.57 ± 0.03	3.86 ± 0.22	ND	ND

CAC0935	Histidyl-tRNA synthetase	5.23	0.94 ± 0.03	4.94 ± 0.65	3476 ± 232	13443 ± 210
CAC0936	ATP phosphoribosyltransferase	4.28	3.88 ± 0.17	16.63 ± 2.55	1608 ± 126	5931 ± 300
CAC0939	Glutamine amidotransferase	4.04	5.16 ± 0.33	20.84 ± 4.17	4120 ± 135	14194 ± 295
CAC1047	Ribonucleotide reductase, vitamin B12-dependent	4.29	0.7 ± 0.07	3.02 ± 0.88	223 ± 41	761 ± 45
CAC1319	Glycerol uptake facilitator protein, GLPF	75.74	0.48 ± 0.05	36.16 ± 8.43	ND	1869 ± 1385
CAC1320	Glycerol-3-phosphate responsive antiterminator (mRNA-binding), GLPP	60.41	0.27 ± 0.01	16.43 ± 3.59	ND	5347 ± 118
CAC1321	Glycerol kinase, GLPK	55.53	0.51 ± 0.01	28.1 ± 6.48	ND	12938 ± 106
CAC1322	Glycerol-3-phosphate dehydrogenase, GLPA	470.61	0.13 ± 0.01	59.87 ± 8.18	ND	64059 ± 1024
CAC1323	NAD(FAD)-dependent dehydrogenase	516.51	0.12 ± 0.01	59.44 ± 8.43	ND	63155 ± 1927
CAC1324	Uncharacterized predected metal-binding protein	390.80	0.1 ± 0.01	41.03 ± 1.56	ND	38905 ± 1985
CAC1554	Heavy-metal-associated domain (N-terminus) and membrane-bounded cytochrome biogenesis cycZ-like domain	8.56	0.3 ± 0	2.54 ± 1.68	ND	ND
CAC2072	Stage IV sporulation protein B, SpoIVB	∞	0	0.38 ± 0.04	ND	ND
CAC2235	Cysteine synthase/cystathionine beta-synthase, CysK	4.42	3.22 ± 0.22	14.22 ± 3.46	2251 ± 246	21962 ± 365
CAC2241	Cation transport P-type ATPase	20.27	0.44 ± 0.04	9 ± 1.1	ND	ND
CAC2242	Predicted transcriptional regulator, arsE family	10.42	0.15 ± 0.03	1.55 ± 0.2	ND	1740 ± 765

CAC2388	N-acetylornithine aminotransferase	4.80	1.44 ± 0.18	6.9 ± 0.09	2529 ± 202	7611 ± 119
CAC2681	Hypothetical protein	11.51	2.9 ± 0.21	33.39 ± 2.37	ND	5548 ± 1098
CAC2682	Hypothetical protein	5.05	0.08 ± 0	0.39 ± 0.02	ND	ND
CAC2872	Predicted membrane protein in FoF1-type ATP synthase operon	4.06	0.51 ± 0.05	2.07 ± 0.2	ND	ND
CAC3274	Possible surface protein, responsible for cell interaction; contains cell adhesion domain and ChW-repeats	4.51	0.32 ± 0.04	1.45 ± 0.95	ND	ND
CAC3325	Periplasmic amino acid binding protein	7.00	0.11 ± 0	0.74 ± 0.22	ND	ND
CAC3326	Amino acid ABC-type transporter, permease component	7.35	0.11 ± 0.01	0.78 ± 0.21	ND	ND
CAC3327	Amino acid ABC-type transporter, ATPase component	9.61	0.56 ± 0.1	5.35 ± 1.21	ND	2009 ± 50
CAC3486	Multimeric flavodoxin WrbA family protein	6.08	0.38 ± 0.05	2.3 ± 1.04	ND	2195 ± 423
CAC3582	Hypothetical protein	8.64	1.31 ± 0.13	11.29 ± 7.71	ND	ND
CAC3583	Predicted permease	7.22	0.32 ± 0.03	2.3 ± 1.58	ND	ND
CAC3584	Predicted permease	6.14	1.52 ± 0.22	9.36 ± 6.38	ND	ND
CAC3585	ABC-type transporter, ATPase component	9.39	1.29 ± 0.06	12.06 ± 8.33	ND	ND
CAC3630	Oligopeptide ABC transporter, permease component	4.65	0.64 ± 0.03	2.97 ± 0.52	ND	ND
CAC3631	Oligopeptide ABC transporter, permease component	4.23	0.81 ± 0.02	3.44 ± 0.58	ND	ND

CAC3632	Oligopeptide ABC transporter, periplasmic substrate-binding component	4.77	1.09 ± 0.12	5.19 ± 0.72	710 ± 141	5534 ± 345
CAC3635	Oligopeptide ABC transporter, ATPase component	5.51	0.69 ± 0.03	3.78 ± 0.37	861 ± 160	4825 ± 329
CAC3636	Oligopeptide ABC transporter, ATPase component	5.82	0.97 ± 0.07	5.66 ± 0.56	ND	ND
CAC3637	Oligopeptide ABC transporter, permease component	4.88	0.47 ± 0.04	2.29 ± 0.14	ND	ND
CAP0030	Isochorismatase	29.41	0.06 ± 0	1.86 ± 1.27	ND	ND
CAP0035	Bifunctional aldehyde/alcohol dehydrogenase (NADH dependent), adhE2	163.14	0.42 ± 0.02	69.21 ± 13.07	6923 ± 2976	164092 ± 2992
CAP0118	Possible xylan degradation enzyme (glycosyl hydrolase family 30-like domain and Ricin B-like domain)	4.21	0.22 ± 0.02	0.92 ± 0.48	ND	ND
Decrease						
CAC0204	Sortase (surface protein transpeptidase), YHCS B.subtilis ortholog	0.12	3.65 ± 0.24	0.44 ± 0.05	ND	ND
CAC0205	Predicted phosphohydrolases, Icc family	0.06	16.4 ± 0.6	1.05 ± 0.18	2101 ± 300	ND
CAC0206	Uncharacterized conserved membrane protein	0.04	5.06 ± 0.47	0.21 ± 0.08	ND	ND
CAC0427	Glycerol-3-phosphate ABC-transporter, permease component	0.00	2.78 ± 0.71	0 ± 0	ND	ND
CAC0428	Sugar permease	0.01	18.83 ± 0.66	0.16 ± 0.03	ND	ND

CAC0429	Glicerol-3-phosphate ABC-transporter, periplasmic component	0.02	4.62 ± 0.09	0.08 ± 0.02	2138 ± 92	ND
CAC0430	Glycerophosphoryl diester phosphodiesterase	0.02	14.78 ± 0.42	0.29 ± 0.04	3203 ± 306	ND
CAC0447	FeoA protein, involved in Fe2+ transport	0.24	2.43 ± 0.06	0.58 ± 0.04	ND	ND
CAC0658	Fe-S oxidoreductase	0.14	0.73 ± 0.04	0.1 ± 0.03	1918 ± 174	ND
CAC0659	Predicted Zn-dependent peptidase	0.17	0.52 ± 0.09	0.09 ± 0.01	ND	ND
CAC0660	Hypothetical protein, CF-26 family	0.13	5.73 ± 0.37	0.74 ± 0.34	ND	ND
CAC0742	Uncharacterized protein, containing predicted phosphatase domain	0.04	12.82 ± 0.38	0.52 ± 0.05	ND	ND
CAC0814	3-oxoacyl-[acyl-carrier-protein] synthase III	0.16	6.25 ± 0.26	1.02 ± 0.46	ND	ND
CAC0843	Ribonuclease precursor (barnase), secreted.	0.06	5.2 ± 0.09	0.3 ± 0.06	3063 ± 661	ND
CAC0844	Barstar-like protein ribonuclease (barnase) inhibitor	0.05	6.01 ± 0.36	0.32 ± 0.07	ND	ND
CAC0946	ComE-like protein, Metallo beta-lactamase superfamily hydrolase, secreted	0.11	7.6 ± 0.56	0.87 ± 0.15	ND	ND
CAC1079	Uncharacterized protein, related to enterotoxins of other Clostridiales	0.23	1.27 ± 0.2	0.3 ± 0.12	ND	ND
CAC1080	Uncharacterized protein, probably surface-located	0.24	20.76 ± 0.39	5.06 ± 3.64	ND	ND
CAC1470	2-Hydroxy-6-Oxo-6-Phenylhexa-2,4-Dienoate hydrolase	0.22	1.15 ± 0.12	0.25 ± 0.03	ND	ND
CAC1699	Uncharacterized protein, YfiH family	0.14	11.56 ± 3.03	1.58 ± 0.94	ND	ND

CAC1700	Response regulator (CheY-like receiver domain and DNA-binding HTH domain)	0.20	12.08 ± 2.2	2.42 ± 1.31	ND	ND
CAC1701	Sensory histidine kinase (with HAMP and PAS domains)	0.21	2.5 ± 0.32	0.53 ± 0.29	ND	ND
CAC1702	Hypothetical protein	0.00	0.43 ± 0.06	0 ± 0	ND	ND
CAC1703	Methyl-accepting chemotaxis protein (fragment)	0.00	0.54 ± 0.04	0 ± 0	ND	ND
CAC1705	Periplasmic phosphate-binding protein	0.00	77.73 ± 1.59	0.27 ± 0.09	62281 ± 4136	2010 ± 404
CAC1706	Phosphate permease	0.01	9.1 ± 0.33	0.08 ± 0.03	ND	ND
CAC1707	Permease component of ATP-dependent phosphate uptake system	0.01	18.82 ± 0.22	0.09 ± 0.01	ND	ND
CAC1708	ATPase component of ABC-type phosphate transport system	0.00	46.67 ± 0.3	0.13 ± 0.01	19924 ± 1530	ND
CAC1709	Phosphate uptake regulator	0.01	10.04 ± 0.58	0.12 ± 0.02	9598 ± 885	ND
CAC1766	Predicted sigma factor	0.23	0.34 ± 0.03	0.08 ± 0.01	ND	ND
CAC1775	Predicted membrane protein	0.18	5.53 ± 0.37	0.97 ± 0.25	2830 ± 288	ND
CAC1996	Hypothetical protein	0.24	1.45 ± 0.16	0.34 ± 0.2	ND	ND
CAC1997	Predicted glycosyltransferase	0.22	1.45 ± 0.03	0.32 ± 0.19	ND	ND
CAC1998	ABC-type transport system, ATPase component	0.22	1.31 ± 0.1	0.29 ± 0.18	5046 ± 469	ND
CAC1999	Uncharacterized protein related to hypothetical protein Cj1507c from Campylobacter jejuni	0.25	1.14 ± 0.07	0.28 ± 0.18	ND	ND
CAC2000	Indolepyruvate ferredoxin oxidoreductase, subunit beta	0.23	1.48 ± 0.05	0.35 ± 0.21	ND	ND

CAC2001	Indolepyruvate ferredoxin oxidoreductase, subunit alpha	0.18	5.57 ± 0.13	1.01 ± 0.66	1806 ± 180	410 ± 61
CAC2004	Siderophore/Surfactin synthetase related protein	0.25	4.01 ± 0.25	0.99 ± 0.69	ND	ND
CAC2005	Siderophore/Surfactin synthetase related protein	0.24	2.22 ± 0.3	0.53 ± 0.35	ND	ND
CAC2007	Predicted glycosyltransferase	0.21	5.87 ± 0.14	1.21 ± 0.84	ND	ND
CAC2008	3-oxoacyl-(acyl-carrier-protein) synthase	0.23	2.25 ± 0.14	0.51 ± 0.33	1612 ± 459	ND
CAC2009	3-Hydroxyacyl-CoA dehydrogenase	0.21	3.83 ± 0.14	0.82 ± 0.57	ND	ND
CAC2010	Predicted Fe-S oxidoreductase	0.22	5.38 ± 0.16	1.18 ± 0.83	2358 ± 436	552 ± 283
CAC2011	Possible 3-oxoacyl-[acyl-carrier-protein] synthase III	0.23	3.32 ± 0.16	0.75 ± 0.46	2349 ± 342	539 ± 309
CAC2012	Enoyl-CoA hydratase	0.25	2.31 ± 0.07	0.58 ± 0.35	869 ± 125	ND
CAC2013	Hypothetical protein	0.25	4.33 ± 0.23	1.06 ± 0.59	ND	ND
CAC2014	Predicted esterase	0.23	5.18 ± 0.07	1.21 ± 0.68	ND	ND
CAC2016	Enoyl-CoA hydratase	0.25	13.81 ± 0.63	3.4 ± 2.07	5825 ± 578	1319 ± 268
CAC2438	Predicted phosphatase	0.25	0.29 ± 0.07	0.07 ± 0.01	ND	ND
CAC2742	Predicted membrane protein	0.00	0.25 ± 0.05	0 ± 0	ND	ND
CAC2743	Predicted permease, YXIO B.subtilis ortholog	0.12	0.82 ± 0.09	0.1 ± 0.01	ND	ND
CAC3264	Uncharacterized conserved protein, YTFJ B.subtilis ortholog	0.19	78.48 ± 1.92	14.67 ± 1.91	23796 ± 2151	3806 ± 580
CAC3265	Predicted membrane protein	0.10	2.24 ± 0.13	0.22 ± 0.05	ND	ND
CAC3266	Hypothetical protein	0.07	8.71 ± 0.16	0.64 ± 0.1	ND	ND

CAC3267	Specialized sigma subunit of RNA polymerase	0.16	0.78 ± 0.02	0.12 ± 0.02	ND	ND
CAC3379	Uncharacterized protein, YQFW B.subtilis homolog	0.03	2.98 ± 2.07	0.09 ± 0.01	ND	ND
CAC3589	Uncharacterized conserved membrane protein, YHGE B.subtilis ortholog	0.22	2.86 ± 0.51	0.62 ± 0.45	ND	ND
CAC3612	Hypothetical protein	0.16	0.85 ± 0.07	0.14 ± 0.04	ND	ND
CAC3685	Predicted membrane protein	0.10	1.48 ± 0.42	0.15 ± 0.08	ND	ND
CAC3686	Metallo-beta-lactamase superfamily hydrolase	0.13	0.77 ± 0.09	0.1 ± 0.04	ND	ND
CAP0025	Pyruvate decarboxylase	0.22	5.6 ± 0.81	1.24 ± 0.51	3036 ± 531	603 ± 260
CAP0026	Hypothetical protein	0.20	18.09 ± 0.83	3.58 ± 1.8	ND	ND
CAP0036	Uncharacterized, ortholog of YgaT gene of B.subtillis	0.03	78.48 ± 1.92	1.99 ± 0.18	48818 ± 867	717 ± 114
CAP0037	Uncharacterized, ortholog of YgaS gene of B.subtillis	0.02	78.48 ± 1.92	1.63 ± 0.11	42868 ± 8915	781 ± 158

*** Average ± SD were determined from triplicate samples, SD values below 0.01 are written as 0 in the table**

ND, not detected

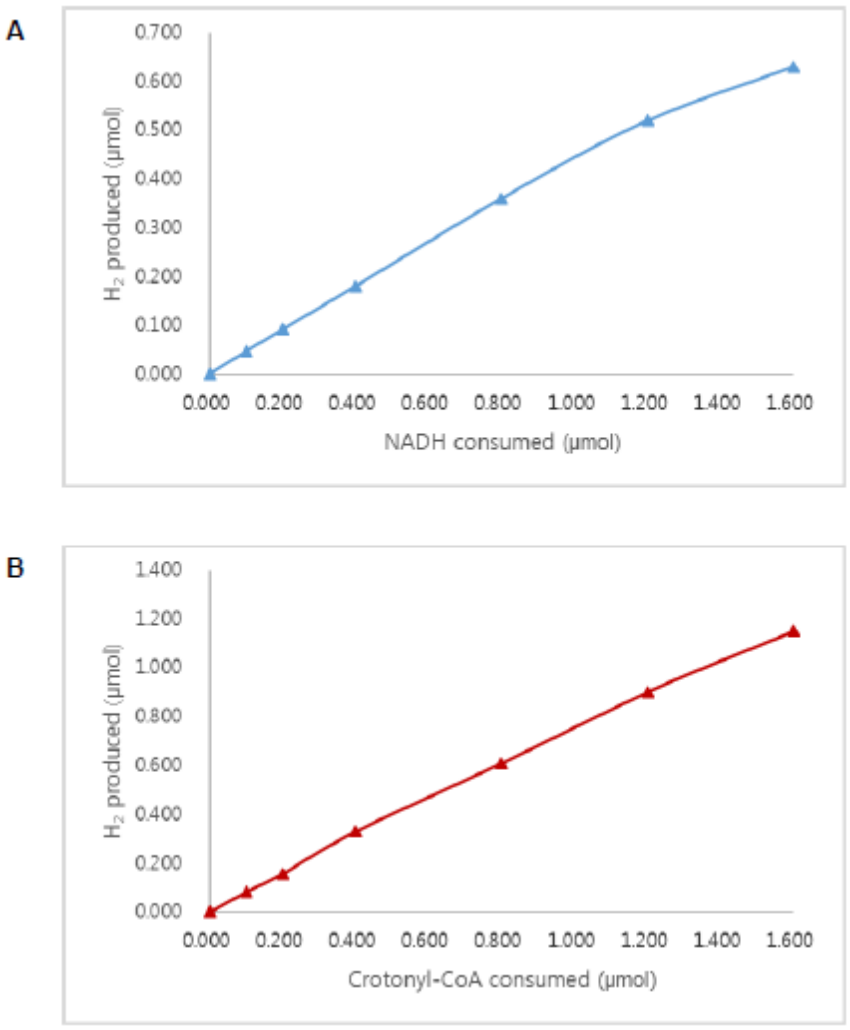

Fig. S2.1. H_2 formation from NADH catalyzed by purified butyryl-CoA dehydrogenase/Etf complex from *C. acetobutylicum* in the presence of hydrogenase (HydA from *C. acetobutylicum*), ferredoxin (Fdx from *C. acetobutylicum*), and crotonyl-CoA. (A) Amount of H_2 formed as a function of the amount of NADH added in the presence of excess amounts of crotonyl-CoA. (B) Amount of H_2 formed as a function of the amount of crotonyl-CoA added in the presence of excess amounts of NADH.

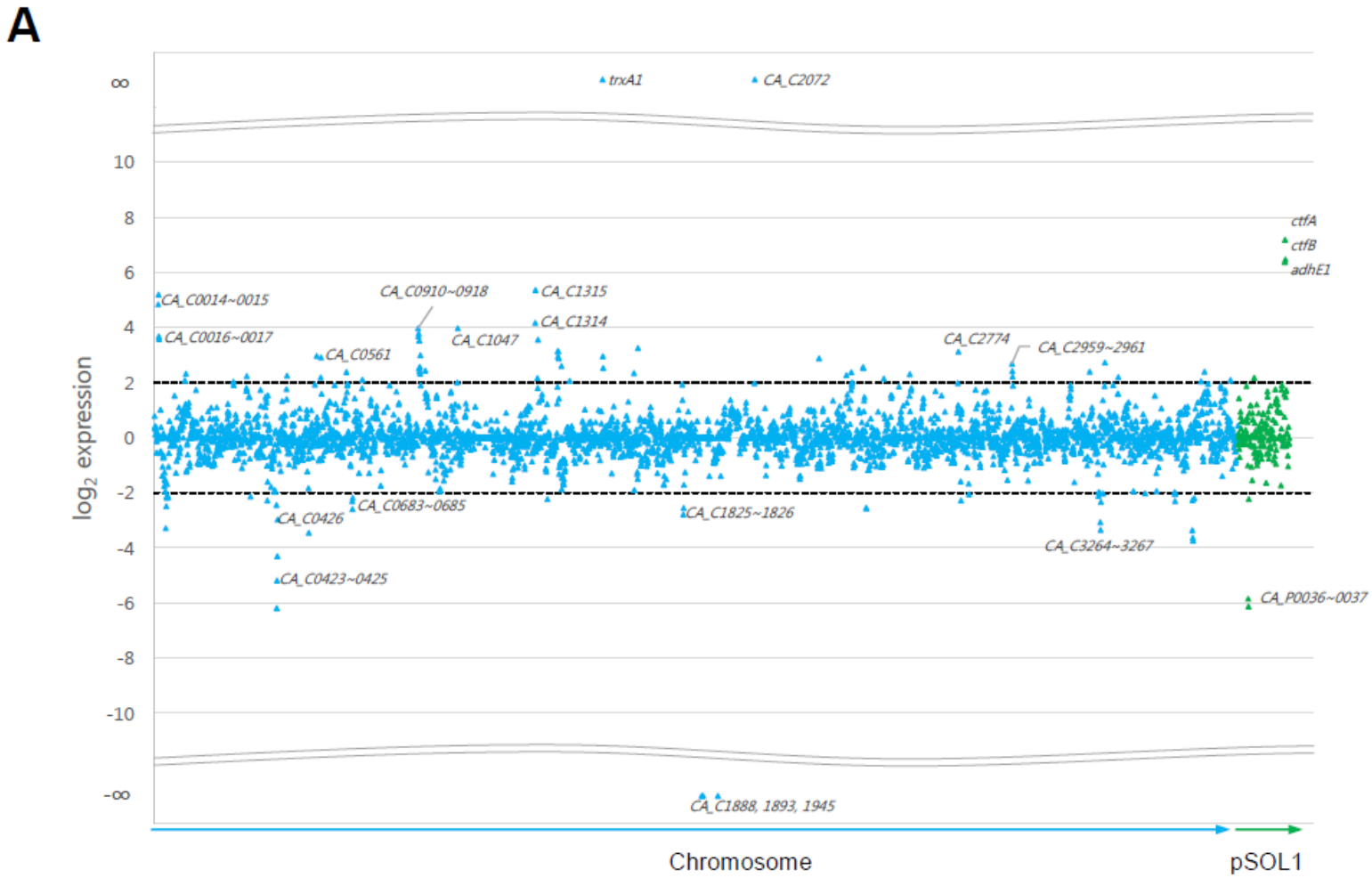
A
∞
10
8
6
4
2
0
-2
-4
-6
-8
-10
-∞
log2 expression
trxA1
CA_C2072
ctfA
ctfB
adhE1
CA_C0014~0015
CA_C0016~0017
CA_C0910~0918
CA_C1315
CA_C1314
CA_C1047
CA_C0561
CA_C2774
CA_C2959~2961
CA_C0426
CA_C0683~0685
CA_C1825~1826
CA_C3264~3267
CA_C0423~0425
CA_P0036~0037
CA_C1888, 1893, 1945
Chromosome
pSOL1

Fig.S2.2

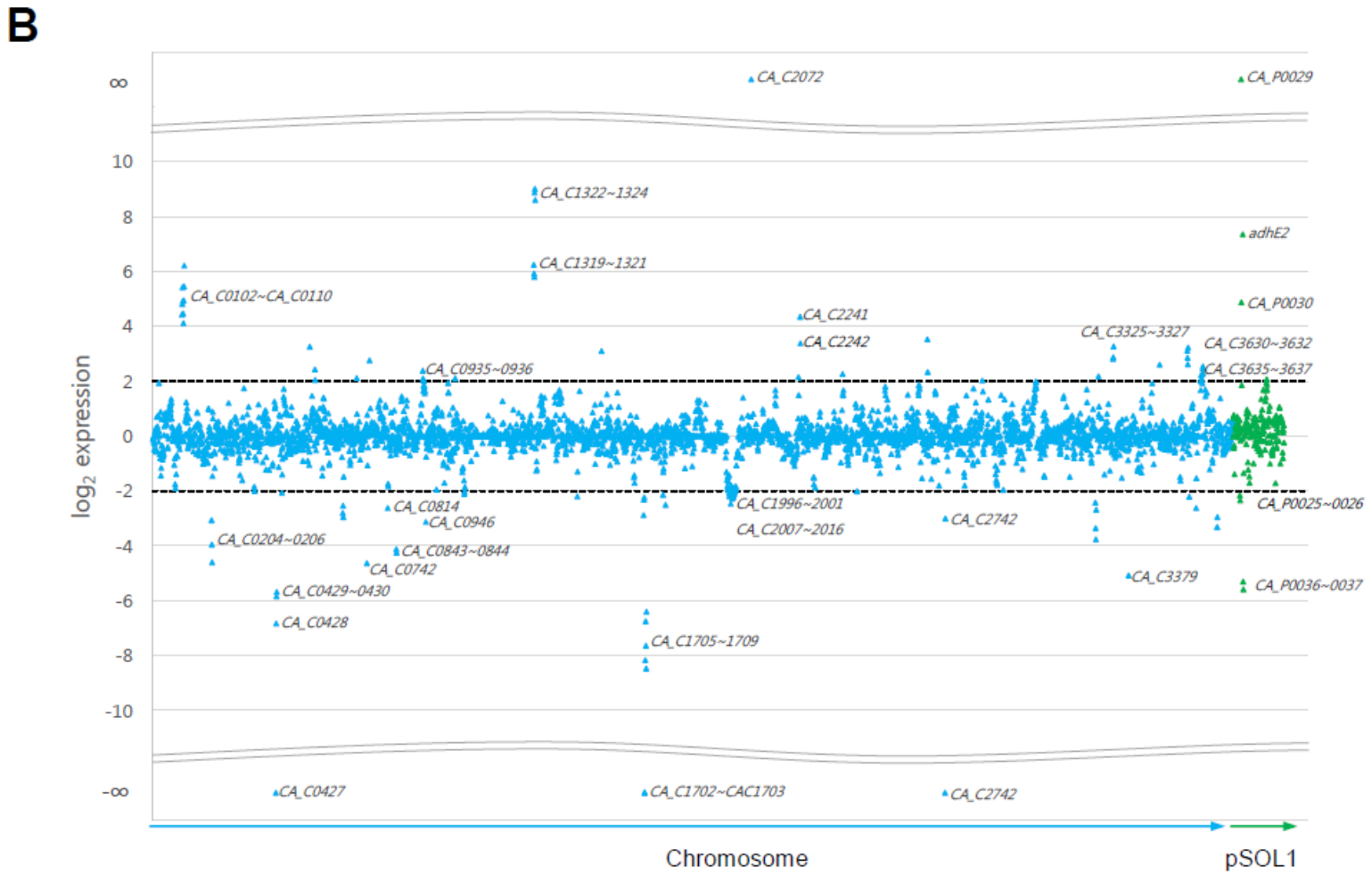
B
log2 expression
∞
10
8
6
4
2
0
-2
-4
-6
-8
-10
-∞
CA_C2072
CA_P0029
CA_C1322~1324
adhE2
CA_C1319~1321
CA_C0102~CA_C0110
CA_P0030
CA_C2241
CA_C2242
CA_C3325~3327
CA_C3630~3632
CA_C3635~3637
CA_C0935~0936
CA_C0814
CA_C0946
CA_C1996~2001
CA_C2007~2016
CA_C2742
CA_P0025~0026
CA_C0204~0206
CA_C0843~0844
CA_C0742
CA_C3379
CA_C0429~0430
CA_P0036~0037
CA_C0428
CA_C1705~1709
CA_C0427
CA_C1702~CAC1703
CA_C2742
Chromosome
pSOL1

Fig.S2.2

Fig. S2.2. Overview of the transcript levels during solventogenesis versus acidogenesis (A) and alcohologenesis versus acidogenesis (B).

Log expression ratios of solventogenesis to acidogenesis (B) and alcohologenesis to acidogenesis are shown. All genes with log values (as logarithms to the basis of 2) higher than 2 (≥ 4.0-fold increased expression) are significantly induced under solventogenesis (A) and alcohologenesis (B), and genes with a negative log of less than -2 (≥ 4.0-fold decreased expression) were significantly induced in acidogenesis. According to this definition, all genes between the dashed lines were expected to be not significantly influenced.

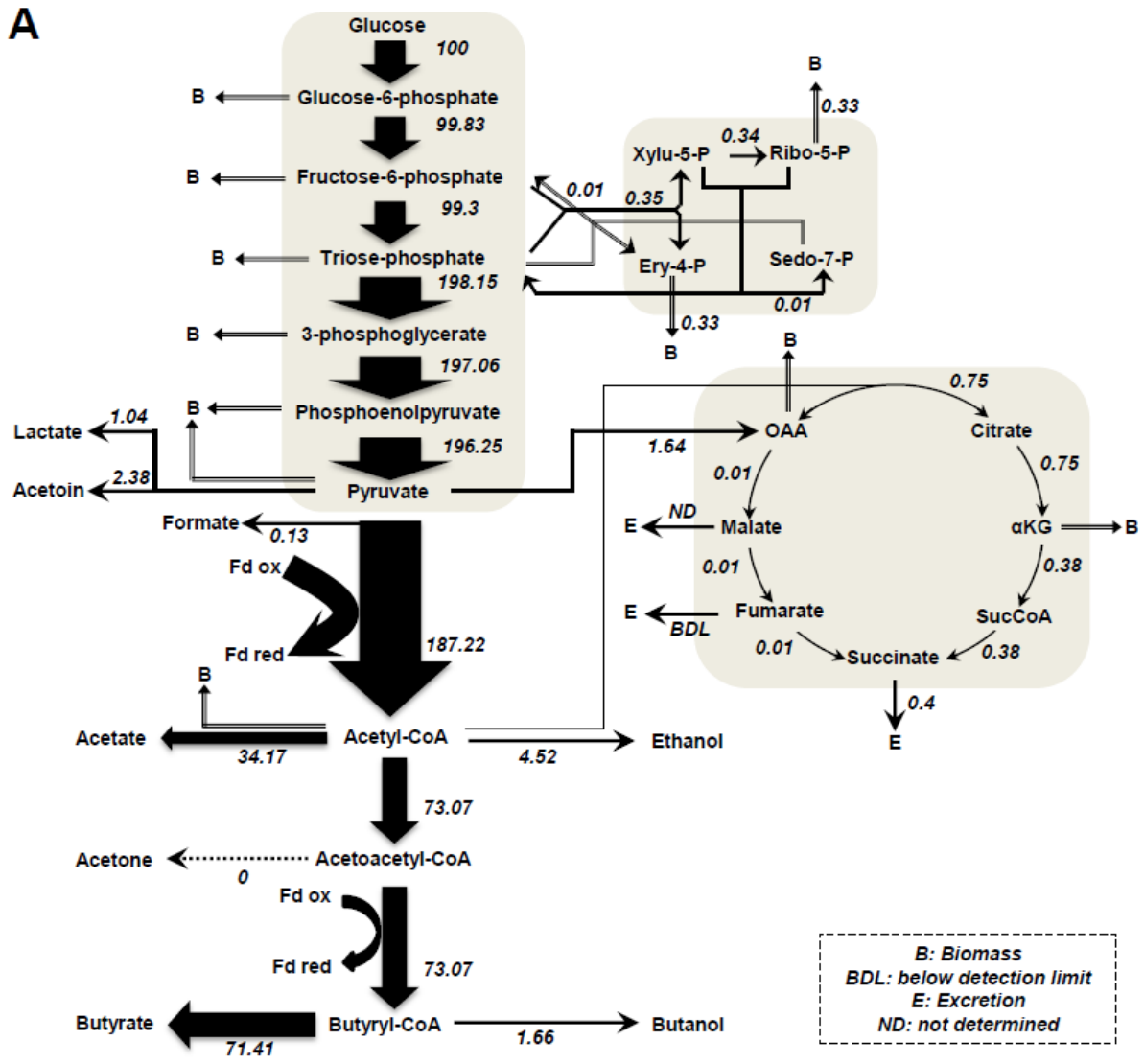

Fig. S2.3. Metabolic flux map of *C. acetobutylicum* in acidogenesis (A), solventogenesis (B), alcohologenesis (C). All values are normalized to the flux of the initial carbon source (mmol/gDCW/h). Glucose flux is normalized as 100 for acidogenesisand solventogenesis, and the sum of glucose and half of the glycerol normalized as 100 for alcohologenesis.

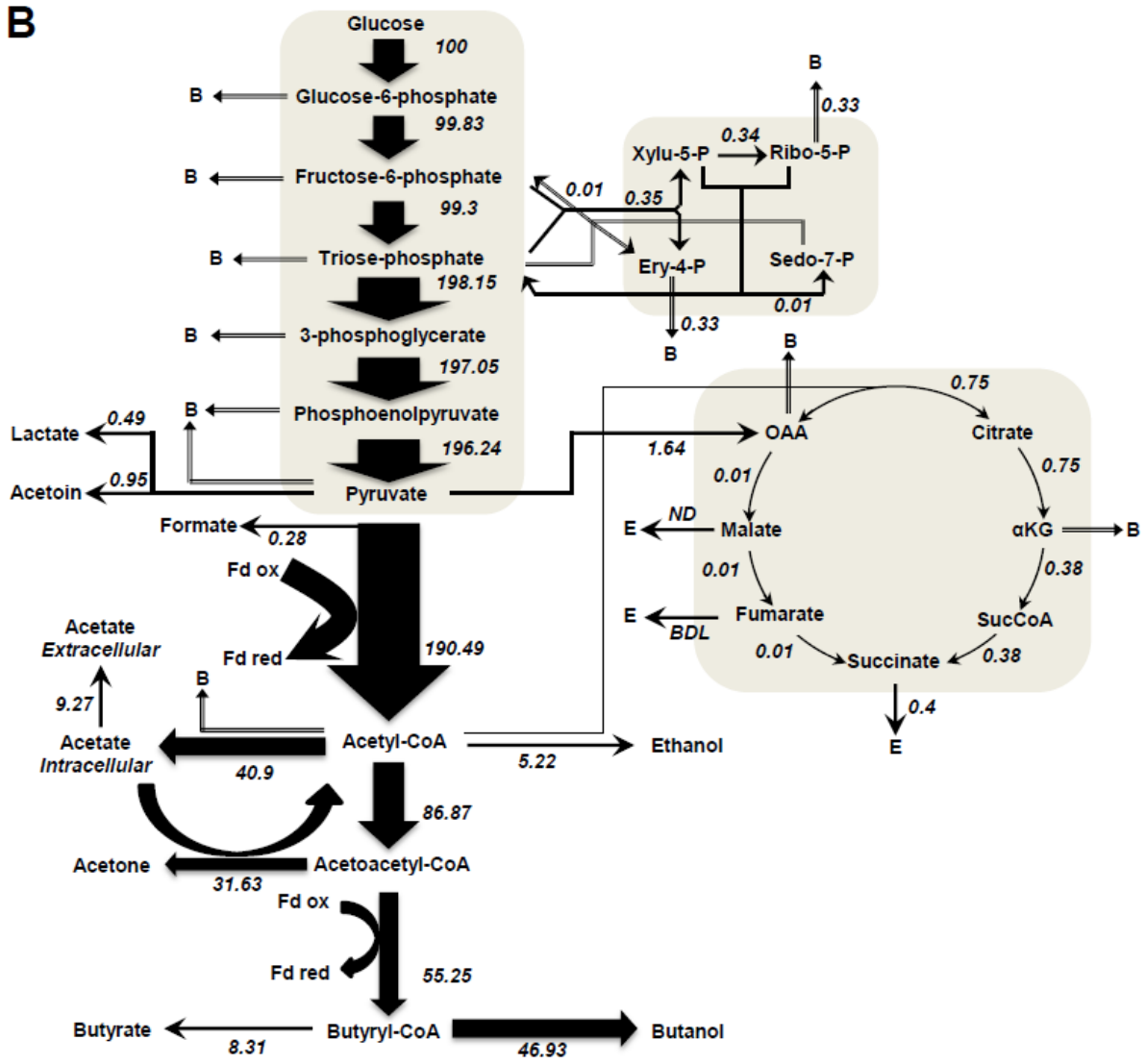

Fig. S2.3. Metabolic flux map of *C. acetobutylicum* in acidogenesis (A), solventogenesis (B), alcohologenesis (C). All values are normalized to the flux of the initial carbon source (mmol/gDCW/h). Glucose flux is normalized as 100 for acidogenesisand solventogenesis, and the sum of glucose and half of the glycerol normalized as 100 for alcohologenesis.

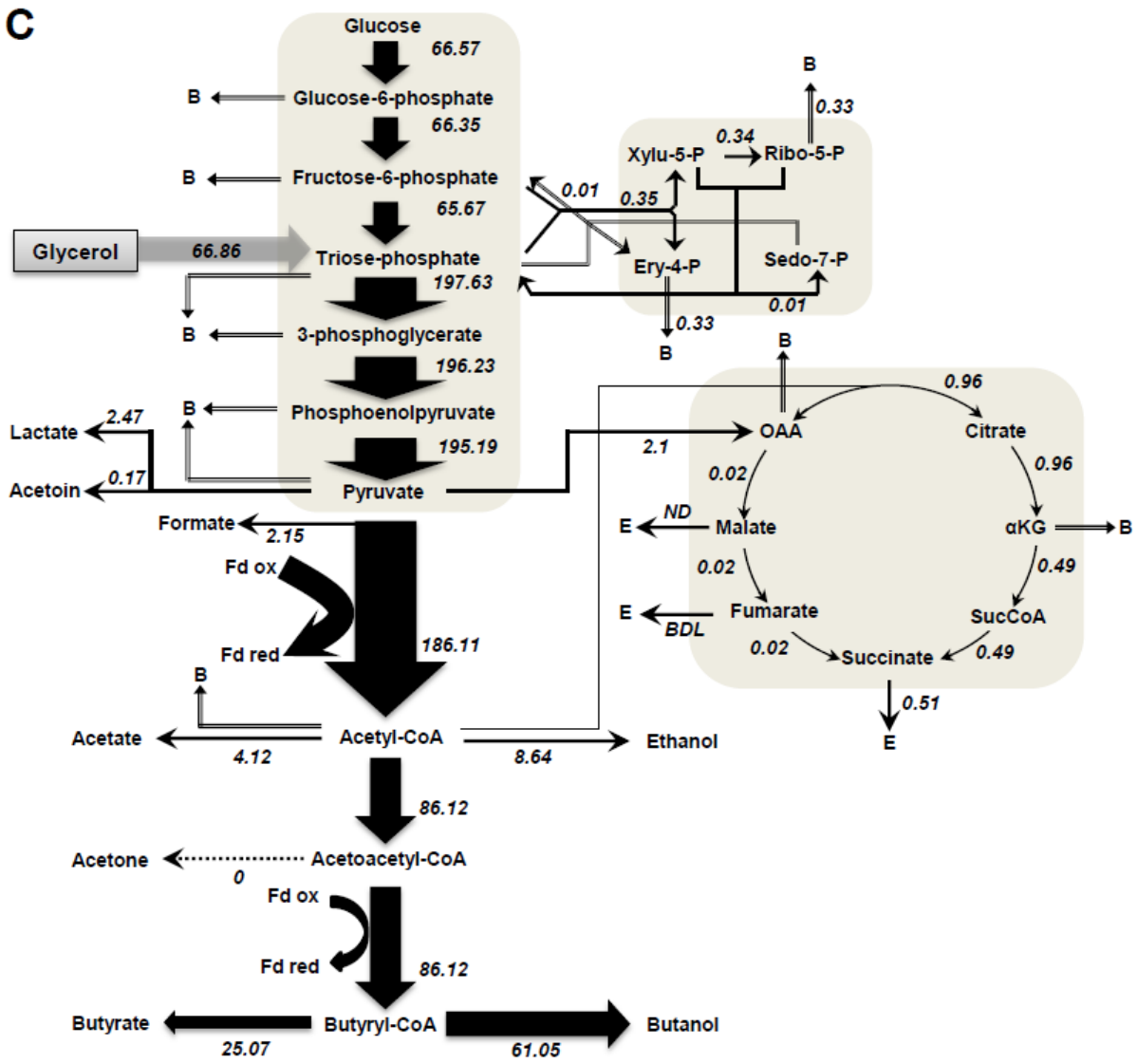

Fig. S2.3. Metabolic flux map of *C. acetobutylicum* in acidogenesis (A), solventogenesis (B), alcohologenesis (C). All values are normalized to the flux of the initial carbon source (mmol/gDCW/h). Glucose flux is normalized as 100 for acidogenesisand solventogenesis, and the sum of glucose and half of the glycerol normalized as 100 for alcohologenesis.

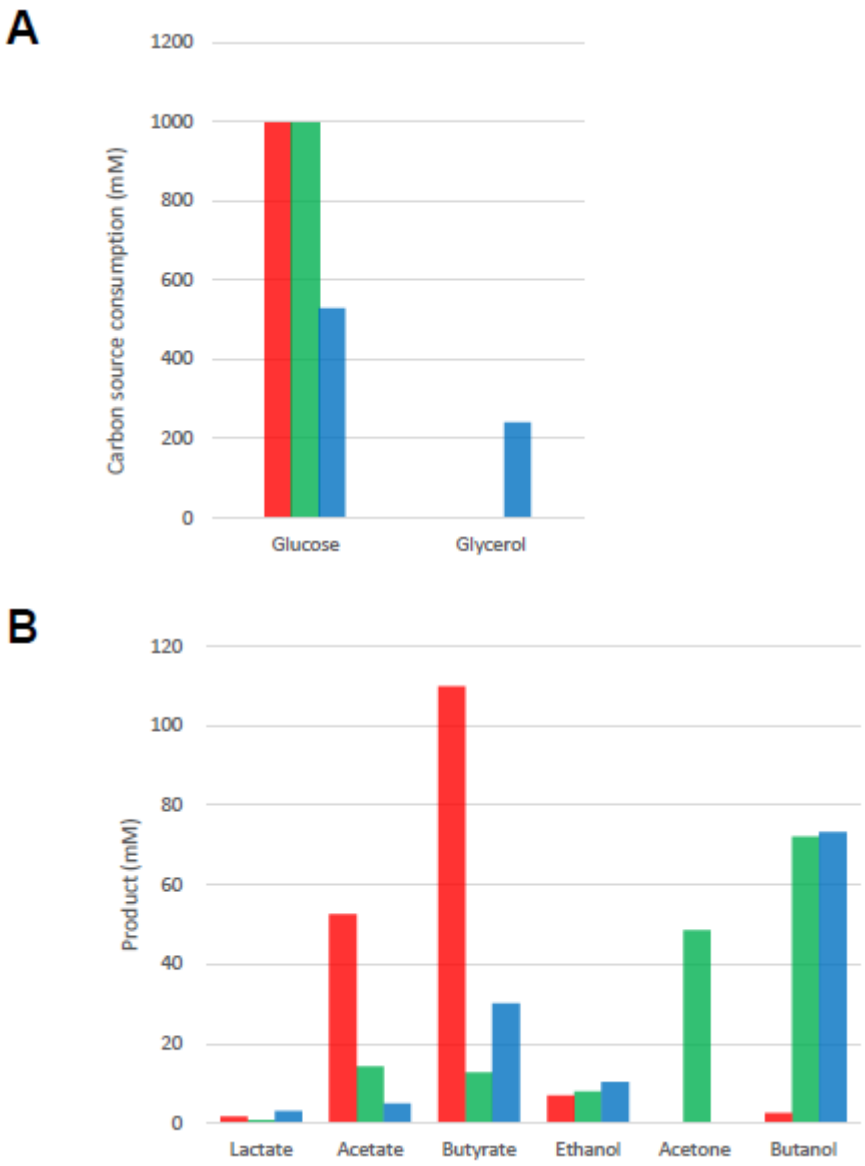

Fig. S2.4. Carbon source consumption and product profiles of *C. acetobutylicum*. (A) Carbon source consumption. (B) Product profiles. Each histogram indicates different metabolic states: red (acidogenesis), green (solventogenesis), and blue (alcohologenesis).

Chapter 3

Results and discussion part 2- Δ*adhE1* and Δ*adhE2* strains

Elucidation of the roles of *adhE1* and *adhE2* in the primary metabolism of *Clostridium acetobutylicum* by combining in-frame gene deletion and a quantitative system-scale approach

Published in Biotechnology for Biofuels 2016, 9:92

Abstract

Background

Clostridium acetobutylicum possesses two homologous *adhE* genes, *adhE1* and *adhE2*, which have been proposed to be responsible for butanol production in solventogenic and alcohologenic cultures, respectively. To investigate their contributions in detail, in-frame deletion mutants of each gene were constructed and subjected to quantitative transcriptomic (mRNA molecules/cell) and fluxomic analyses in acidogenic, solventogenic and alcohologenic chemostat cultures.

Results

Under solventogenesis, compared to the control strain, only Δ*adhE1* mutant exhibited significant changes showing decreased butanol production and transcriptional expression changes in numerous genes. In particular, *adhE2* was overexpressed (126-fold); thus, AdhE2 can partially replace AdhE1 for butanol production (more than 30%) under solventogenesis. Under alcohologenesis, only Δ*adhE2* mutant exhibited striking changes in gene expression and metabolic fluxes, and butanol production was completely lost. Therefore, it was demonstrated that AdhE2 is essential for butanol production and thus metabolic fluxes were redirected toward butyrate formation. Under acidogenesis, metabolic fluxes were not significantly changed in both mutants except the complete loss of butanol formation in Δ*adhE2*, but numerous changes in gene expression were observed. Furthermore, most of the significantly up- or down-regulated genes under this condition showed the same pattern of change in both mutants.

Conclusions

This quantitative system-scale analysis confirms the proposed roles of AdhE1 and AdhE2 in butanol formation that AdhE1 is the key enzyme under solventogenesis, whereas AdhE2 is the key enzyme for butanol formation under acidogenesis and alcohologenesis. Our study also highlights the metabolic flexibility of *C. acetobutylicum* to genetic alterations of its primary metabolism.

Key words

AdhE; butanol; *Clostridium acetobutylicum;* System-scale analysis

Background

Clostridium acetobutylicum is now considered as the model organism for the study of solventogenic Clostridia (Nair *et al.*, 1994a, Lutke-Eversloh & Bahl, 2011a). The superiority of butanol over ethanol as an alternative biofuel has attracted research interest into *C. acetobutylicum* and other recombinant bacteria producing butanol as major products (Atsumi & Liao, 2008a).

In phosphate-limited chemostat cultures, *C. acetobutylicum* can be maintained in three different stable metabolic states (Vasconcelos *et al.*, 1994, Girbal *et al.*, 1995c, Girbal & Soucaille, 1994b, Girbal & Soucaille, 1998b, Bahl *et al.*, 1982b) without cellular differentiation (Grimmler *et al.*, 2011c): acidogenic (producing acetate and butyrate) when grown at neutral pH with glucose; solventogenic (producing acetone, butanol, and ethanol) when grown at low pH with glucose; and alcohologenic (forming butanol and ethanol but not acetone) when grown at neutral pH under conditions of high NAD(P)H availability (Girbal & Soucaille, 1994b, Peguin & Soucaille, 1995a, Girbal *et al.*, 1995c).

AdhE1 (CA_P0162 gene product, also referred to as Aad) has long been considered as an NADH-dependent bifunctional alcohol/aldehyde dehydrogenase responsible for alcohol formation in solventogenic *C. acetobutylicum* cultures (Fischer *et al.*, 1993, Nair *et al.*, 1994a, Lutke-Eversloh & Bahl, 2011a). Recently, however, AdhE1 was purified and shown to have lost most of its alcohol dehydrogenase activity despite its NADH-dependent aldehyde dehydrogenase activity (Yoo *et al.*, 2015).

Prior to the identification of *adhE2* (CA_P0035), the existence of alcohologenesis-specific gene(s) responsible for alcohol formation was predicted because i) there was high NADH-dependent butanol dehydrogenase activity in alcohologenesis versus high NADPH-dependent

butanol dehydrogenase activity in solventogenesis (Girbal & Soucaille, 1998b, Girbal *et al.*, 1995c) and ii) previously identified genes related to butanol production (*bdhA, bdhB, adhE1*) were not induced in alcohologenic cultures (Sauer & Dürre, 1995). The *adhE2* gene is the second aldehyde/alcohol dehydrogenase-encoding gene and is carried by the pSol1 megaplasmid, as is *adhE1* (Fontaine *et al.*, 2002a). The two genes are not clustered, in contrast to the observations for *C. ljungdahlii* (Leang *et al.*, 2013) and their expression patterns differ (Yoo *et al.*, 2015, Grimmler *et al.*, 2011c). *adhE1*, *ctfA* and *ctfB* (CA_P0163 and CA_P0164) form the *sol* operon (Fischer *et al.*, 1993, Nair *et al.*, 1994a); *ctfA* and *ctfB* encode the CoA-transferase responsible for the first step of acetone formation, while the second step, catalyzed by acetoacetate decarboxylase, is encoded by *adc* (CA_P0165), located downstream of the *sol* operon. However, *adc* is transcribed under the control of its own promoter, which is oriented in the opposite direction of the *sol* operon (Fischer *et al.*, 1993).

In the three metabolic states, the contributions of the different enzymes responsible for the butyraldehyde dehydrogenase and butanol dehydrogenase activities to butanol flux has recently been characterized (Yoo *et al.*, 2015). Under acidogenesis, the low butanol flux is catalyzed by AdhE2 (100%) for butyraldehyde dehydrogenase activity, while BdhB and BdhA are responsible for butanol dehydrogenase activity. Under solventogenesis, AdhE1 (95%; the other 5% is contributed by adhE2) is the key player responsible for butyraldehyde dehydrogenase activity, while BdhB, BdhA and BdhC are responsible for butanol dehydrogenase activity. Under alcohologenesis, AdhE2 plays a major role in both butyraldehyde dehydrogenase (100%) and butanol dehydrogenase activities. In the study of Cooksley et al. (Cooksley *et al.*, 2012), *adhE1* and *adhE2* knockout mutants were i) constructed using the ClosTron method (Heap *et al.*, 2007b) and ii) phenotypically characterized in batch culture using Clostridium basal medium (CBMS) without pH adjustment. The *adhE1* knockout mutant obtained in their study

exhibited low ethanol and no butanol formation along with scant acetone production; these findings were consistent with the polar effect of the intron on *ctfAB* transcription (Cooksley *et al.*, 2012). Using the *adhE2* knockout mutant, no alteration of solvent production was observed; however, the *adhE2* knockout mutant has not been evaluated under alcohologenic conditions, under which it is normally thought to play a major role (Fontaine *et al.*, 2002a).

The aim of this study was to perform clean individual in-frame deletions of *adhE1* and *adhE2* to characterize their roles in butanol formation in the three different metabolic states in more detail. Furthermore, to study the metabolic flexibility of *C. acetobutylicum* in response to each of these gene deletions, a complete fluxomic and quantitative transcriptomic analysis was also performed in the three conditions known for the wild type strains: acidogenic, solventogenic and alcohologenic states. The results presented here not only support our previous studies (Fontaine *et al.*, 2002a, Yoo *et al.*, 2015) on the roles of AdhE1 and AdhE2 in butanol formation in different metabolic states but also highlight the metabolic flexibility of *C. acetobutylicum* to genetically alter its primary metabolism.

Results & Discussion

Construction of ΔadhE1 and ΔadhE2 mutant strains

Construction of the *ΔadhE2* mutant was relatively straightforward, as *adhE2* is expressed in a monocistronic operon (Fontaine *et al.*, 2002a) (Fig. 1A). However, the position of *adhE1* as the first gene of the *sol* operon made the construction of *ΔadhE1* more complicated because the transcription of downstream *ctfAB* genes could be affected. Fig. 1B-D show different configurations of the *sol* operon promoter, *ctfAB* genes, and either *catP* cassette with two FRT (Flippase Recognition Target) sites or a single FRT site remaining after Flippase (Flp)-FRT

recombination of the three different types of *ΔadhE1* mutants generated in this study. The first constructed *ΔadhE1* mutant, *ΔCA_C1502ΔuppΔadhE1::catP* (Fig. 1B), was unable to form acetone as predicted because a transcriptional terminator was included in the *catP* cassette, which is located upstream of *ctfAB* encoding the acetoacetyl coenzyme A:acetate/butyrate:coenzyme A transferase that is responsible for the first specific step of acetone formation (Fischer *et al.*, 1993). However, after removing the *catP* cassette from *ΔCA_C1502ΔuppΔadhE1::catP*, acetone production was unexpectedly not recovered in *ΔCA_C1502ΔuppΔadhE1* (Fig. 1C). The presence of the megaplasmid pSOL1 was confirmed by the production of ethanol and butanol under alcohologenic conditions and was attributed to *adhE2* expression. By sequencing the pSOL1 region around the *adhE1* deletion, we confirmed that there was no mutation in the *sol* promoter, *ctfAB* and *adc* (encoding acetoacetate decarboxylase, which is responsible for the last step of acetone production). Based on these results, the possibility of unsuspected early transcriptional termination by the FRT site remaining after *catP* removal was deduced. To confirm the early termination of transcription by an FRT site and to eliminate this polar effect on acetone production, a new plasmid was constructed to position both of the FRT sites carried by the *catP* cassette upstream of the *sol* operon promoter and was used to construct the *ΔadhE1* mutant *ΔCA_C1502ΔuppΔadhE1::catP-A1A4* mutant (Fig. 1D). Consistent with our hypothesis, this last *ΔadhE1* mutant recovered acetone production (Fig. 2, Fig. S3). To the best of our knowledge, the potential role of an FRT site as a transcriptional terminator was reported once in *Salmonella* (Apfel, 2012) and twice in yeast (Waghmare *et al.*, 2003, Storici & Bruschi, 2000), although the FRT site is not generally recognized as possessing this additional activity. However, the high score of the FRT site hit from the "Dimers & Hairpin Loops analysis" in Vector NTI software (Invitrogen) and the detection of this activity upon deleting *adhE1* in *C. acetobutylicum* unambiguously demonstrate that the FRT site can function as a transcriptional

terminator.

Hereafter, *C. acetobutylicum ΔCA_C1502ΔuppΔadhE1::catP-A1A4* (Fig. 1D) is referred to as *ΔadhE1* in all the chemostat culture experiments.

Carbon and electron fluxes of ΔadhE1 and ΔadhE2 mutants under different physiological conditions

The *ΔadhE1* and *ΔadhE2* mutants were first evaluated under acidogenic conditions and compared to previously published data for the control strain (Yoo *et al.*, 2015). All the strains behaved the same, and no significant changes in the metabolic fluxes were recorded (Fig. S3), except that butanol production was completely abolished in the *ΔadhE2* mutant strain (Fig. 2, Fig. S3).

The two mutant strains were then evaluated under solventogenic conditions and compared to previously published data for the control strain (Yoo *et al.*, 2015). The control and *ΔadhE2* strains behaved the same, with no significant change in metabolic fluxes (Fig. S3). However, the *ΔadhE1* mutant exhibited completely different behavior. In the first phase, before the "pseudo steady state" was reached, this mutant exhibited considerable fluctuations in growth, glucose consumption and metabolite profiles. Under "pseudo steady state conditions", the butanol and acetone fluxes were stable, while the butyrate flux showed fluctuations between 2.2 and 2.9 $mmol.g^{-1}.h^{-1}$. In *ΔadhE1*, the butanol, ethanol and acetone fluxes decreased by 60, 49 and 46%, respectively (Fig. S3), compared to the control strain; thus, the acetone and ethanol fluxes were not reduced as greatly as the butanol fluxes. These results support the previously proposed (Fischer *et al.*, 1993, Nair *et al.*, 1994a, Fontaine *et al.*, 2002a, Yoo *et al.*, 2015) key role of AdhE1 in butanol production under solventogenic conditions and demonstrate that an

adhE1 knockout strain with no polar effect on *ctfAB* transcription can still produce acetone. The level of *ctfAB* expression was 3-fold higher in the *adhE1* knockout compared to the control strain. This indicates that the lower flux of acetone production is the result of a control at the enzyme level due to a lower acetoacetyl-CoA concentration and/or higher acetyl-CoA/butyryl-CoA concentrations. The remaining ability of the *ΔadhE1* strain to produce butanol under solventogenesis is explained by the higher *adhE2* expression (~127-fold higher than the control strain, but only 25 mRNA molecules/cell) (Table 1, Dataset S1). For the *ΔadhE1* mutant, the butyrate flux increased by 5-fold compared to the control strain (Fig. S3), although neither *ptb-buk* (CA_C3076–CA_C3075) nor *buk2* (CA_C1660) experienced a significant transcriptional increase (Dataset S1). Thus, flux is controlled at the enzyme level via an increase in the butyryl-CoA pool due to the lower flux in the butanol pathway. However as the AdhE2 level in the mutant is the same as the AdhE1 level in the control (6.31×10^4 versus 5.99×10^4 protein molecules/cell) the lower flux of butanol production can be explained by i) a lower catalytic efficiency of AdhE2 for butyryl-CoA and /or NADH or ii) a lower intracellular pH under solventogenic conditions that would be less optimal for AdhE2 that is normally expressed under alcohologenic conditions at neutral pH. The second hypothesis can be eliminated as the previously measured intracellular pH (Girbal *et al.*, 1995a, Vasconcelos *et al.*, 1994) in solventogenic and alcohologenic cells are relatively close (5.5 and 5.95 respectively) as the ΔpH is inverted (more acidic inside) under alcohologenic conditions (Girbal *et al.*, 1994a). Finally, as we will see below, the fact that ethanol flux is less affected than the butanol flux might be explained by the existence of an ethanol flux through the Pdc (pyruvate decarboxylase, encoded by CA_P0025) and bdhA/BdhB.

The two mutant strains were also evaluated under alcohologenic conditions and compared to previously published data for the control strain (Yoo *et al.*, 2015). The control and *ΔadhE1*

strains behaved the same, with no significant changes in metabolic fluxes (Fig. S3). However, the *ΔadhE2* mutant exhibited completely different behavior; no flux toward butanol was detected, whereas fluxes toward butyrate became the primary fluxes, as opposed to butanol in the control strain (Fig. S3). In addition, acetate levels increased by ~3-fold, and such changes were accompanied by changes in electron fluxes (Fig. 3), which are described in detail below. These phenomena were not observed by Cooksley et al. (Cooksley *et al.*, 2012) with their *adhE2* knockout mutant, as they performed batch fermentation without promoting alcohologenic conditions. As *adhE1* was not expressed under the "alcohologenic conditions" of the *ΔadhE2* mutant, the physiological function of *adhE2* does not appear to be compensated by *adhE1* (Table 1). To verify that loss of the butanol-producing ability under alcohologenesis did not result from loss of the pSOL1 megaplasmid (Cornillot *et al.*, 1997b, Cornillot & Soucaille, 1996) but rather from the deletion of *adhE2*, the culture was switched to solventogenic conditions before the experiment was ended; under solventogenic conditions, high butanol and acetone production fluxes were recovered (data not shown).

The butanol pathway was analyzed for three different conditions in the respective mutants (Fig. S2) by calculating the contribution of each of the five enzymes potentially involved in each of the two steps to the fluxes (see methods for the calculation).

Under acidogenesis, *adhE1* was not expressed, and thus AdhE1 could not replace AdhE2 for the conversion of butyryl-CoA to butyraldehyde in the *ΔadhE2* mutant (Fig. S2). This failure of AdhE1 to replace AdhE2 led to the absence of butanol production in the *ΔadhE1* mutant, which behaved the same as the control strain, leaving AdhE2 responsible for all the conversion. The *ΔadhE1* mutant behaved the same as the control strain with respect to the conversion of butyraldehyde to butanol under these conditions, and AdhE2 (45% of the flux), BdhB (34% of the flux) and BdhA (14% of the flux) were the main contributors (Fig. S2). The *ΔadhE2* mutant

was not analyzed because it does not produce butanol.

Under solventogenesis, AdhE2 replaced AdhE1 for the conversion of butyryl-CoA to butyraldehyde in the *ΔadhE1* mutant, while in the *ΔadhE2* mutant, which behaved the same as the control strain, AdhE1 was responsible for all the conversion. The two main contributors to the conversion of butyraldehyde to butanol under these conditions were AdhE2 (67% of the flux) and BdhB (30% of the flux) in the *ΔadhE1* mutant, while in the *ΔadhE2* mutant, which behaved the same as the control strain, BdhB (75% of the flux) and BdhA (16% of the flux) were the main contributors (Fig. S2).

Under alcohologenesis, *adhE1* was not expressed (Table 1, Dataset S1), and thus AdhE1 could not replace AdhE2 for the conversion of butyryl-CoA to butyraldehyde in the *ΔadhE2* mutant. This failure of AdhE1 to replace AdhE2 led to the absence of butanol production, while in the *ΔadhE1* mutant, which behaved the same as the control strain, AdhE2 was responsible for all the conversion. The *ΔadhE1* mutant behaved the same as the control strain with respect to the conversion of butyraldehyde to butanol under these conditions, and AdhE2 was the main contributor (Fig. S2). The *ΔadhE2* mutant was not analyzed because it does not produce butanol.

Two possible routes are known for the conversion of pyruvate to acetaldehyde in *C. acetobutylicum*: (i) a two-step reaction by pyruvate:ferredoxin oxidoreductase (PFOR) and acetaldehyde dehydrogenase via acetyl-CoA production or (ii) a one-step reaction by pyruvate decarboxylase (Pdc, encoded by CA_P0025) (Atsumi *et al.*, 2008). In the wild-type strain, the former route is considered as the primary pathway (Lehmann & Lutke-Eversloh, 2011, Lutke-Eversloh & Bahl, 2011a). Under acidogenic and alcohologenic conditions of the *ΔadhE2* mutant, ethanol production was observed, but no butanol production was detected (Fig. 2, Fig. S3). As previously reported (Yoo *et al.*, 2015), AdhE1 retains only aldehyde dehydrogenase activity, whereas AdhE2 possesses both aldehyde and alcohol dehydrogenases activities. Thus,

the ethanol production of the *ΔadhE2* mutant suggests that the latter route is active. In other words, Pdc could be functional, and the ethanol dehydrogenase activity in acidogenesis could be due to BdhA, BdhB or BdhC (Table 1).

Because the predominant use of reduced ferredoxin is for hydrogen production (Yoo *et al.*, 2015), no significant effects were observed under acidogenesis in both the *ΔadhE1* and *ΔadhE2* mutants with respect to electron flux (Fig. 3). In addition, solventogenesis of the *ΔadhE2* mutant exhibited similar flux levels to the control strain due to the small contribution of AdhE2 (5% for butyraldehyde dehydrogenase function and 9% for butanol dehydrogenase function) under these conditions in the control strain. However, under the same conditions as for *ΔadhE1*, both the fluxes for NADH, known as the partner of AdhE1 and AdhE2, and for NADPH, known as the partner of BdhA, BdhB, and BdhC, were reduced (by ~2.7-fold and 1.8-fold, respectively) due to decreased carbon fluxes toward alcohols (Fig. 3, Fig. S3). The most striking changes were observed in the *ΔadhE2* mutant under alcohologenesis, in which the primary use of reduced ferredoxin was switched from NADH to hydrogen production. The absence of butanol formation resulted in a ~3.6-fold decreased flux toward NADH production and a 1.7-fold increased flux toward hydrogen production (Fig. 3).

Common criteria used for quantitative transcriptomic analysis

To filter the data from only significant results, the same criteria used to compare the wild-type strain under different physiological conditions (Yoo *et al.*, 2015) were used to compare the mutants to the control strain. The first criterion was > 4.0-fold higher expression or > 4.0-fold lower expression in *ΔadhE1* or *ΔadhE2* than in the control strain under the same physiological condition, and the second criterion was > 0.2 mRNA molecules per cell in at least one of the two strains being compared.

Genes affected by adhE1 or adhE2 deletion under acidogenesis

As alcohols are minor products under acidogenesis, the deletion of *adhE1* or *adhE2* did not significantly alter the metabolic flux map (Fig. S3). However, a surprisingly large number of genes (100 genes increased in Δ*adhE1*, 108 genes decreased in *ΔadhE1*, 119 genes increased in Δ*adhE2*, 170 genes decreased in *ΔadhE2*) showed significant changes in mRNA molecules/cell in response to the deletion of each gene (Table 2). Furthermore, 50 genes (> 4-fold increase) and 87 genes (> 4-fold decrease) revealed the same patterns of change in both the *ΔadhE1* and *ΔadhE*2 mutants (Table 2). The primary metabolism-related genes that influence metabolic fluxes did not exhibit significant changes, whereas mostly subordinate metabolism-related genes were affected (Table S2, S3, and Fig. 4).

Interestingly, a large portion (18 genes showed > a 4-fold increase, and 2 genes showed a > 2.8-fold increase out of 30 genes genes proposed by Wang et al. (Wang *et al.*, 2013a) of the cysteine metabolism regulator (CymR) regulon showed significantly increased expression in both mutants under acidogenesis (CymR regulons are indicated in Table 3). In particular, an operon involved in cysteine and sulfur metabolism (CA_C0102–CA_C0110) showed a > 10-fold increase in both mutants. This operon was reported to respond to butyrate/butanol stresses and to be up-regulated under alcohologenesis in wild-type strains (Alsaker *et al.*, 2010b, Wang *et al.*, 2013a, Yoo *et al.*, 2015) and under solventogenesis in the *Δptb* mutant (Honicke *et al.*, 2014a). In addition, the expression of two putative cysteine ABC transporter operons belonging to the CymR regulon (Alsaker *et al.*, 2010b, Wang *et al.*, 2013a), namely CA_C0878–CA_C0880 and CA_C3325–CA_C3327), was also up-regulated.

A long gene cluster linked to iron/sulfur/molybdenum metabolism (CA_C1988–CA_C2019)

exhibited significantly decreased expression (except for CA_C1988, CA_C1990, CA_C1992 and CA_C1995, for which some values were below the significance criterion of 4-fold but were higher than 3-fold) (Table 3, Dataset S1). A part of this cluster, CA_C1988–CA_C1996, was previously reported to be down-regulated under oxygen-exposed conditions (Hillmann *et al.*, 2009). Moreover, this cluster was shown by Schwarz et al. (Schwarz *et al.*, 2012) to be repressed by butanol stress in an acidogenic chemostat.

Transcriptional changes due to adhE1 or adhE2 deletion under solventogenesis

Under solventogenesis, a drastic change in fluxes was observed in the *ΔadhE1* mutant, while the fluxes remained unchanged in the *ΔadhE2* mutant; additionally, as expected, more genes showed significant changes in *ΔadhE1* than in *ΔadhE2* (Table 2, Table S4, S5). Specifically, in *ΔadhE1,* 55 genes were up-regulated, and 127 genes were down-regulated (Table 2). In *ΔadhE2*, 22 genes were up-regulated, and 17 genes were down-regulated (Table 2). In contrast to the observations previously made under acidogenesis, no gene was significantly increased in both the *ΔadhE1* and *ΔadhE*2 mutants, and only 1 gene (CA_C3612, encoding a hypothetical protein) was significantly decreased in both mutants

In *ΔadhE1*, the CA_C0102–CA_C0110 operon which was shown to be up-regulated in acidogenesis and belongs to the CymR regulon , was also up-regulated by > 18-fold under solventogenesis (Table S4). However, the up-regulation of this operon (under alcohologenesis in the control strain, acidogenesis and solventogenesis in *ΔadhE1*, or acidogenesis in *ΔadhE2*) did not have striking shared features with the main product profile.

Interestingly, expression of the *natAB* operon (CA_C3551–CA_C3550) (> 10-fold), encoding a potential Na^+-ABC transporter, and the *kdp* gene cluster (CA_C3678–CA_C3682), encoding

a potential K^+ transporter (> 20-fold), was highly up-regulated under solventogenesis (Table S4, Dataset S1) in *ΔadhE1*. The *natAB* operon and the *kdp* gene cluster have previously been reported to be up-regulated by both acetate and butyrate stress (Alsaker *et al.*, 2010b). As the ability of the *ΔadhE1* mutant to produce butanol was highly affected and as butyrate and acetate were the primary fermentation products (Fig. 2), this strain struggled to survive under acidic conditions (i.e., under the pH of 4.4 for solventogenesis); consequently, genes involved in ion transport were up-regulated.

The operon CA_P0029–CA_P0030, which potentially encodes a transporter and an isochorismatase, was up-regulated under acidogenesis in both mutants as well as under solventogenesis in *ΔadhE2* (> 20-fold) (Table 2, Table S5). Two neighboring genes, CA_C3604 (*ilvD*), encoding dihydroxyacid dehydratase linked to valine/leucine/isoleucine biosynthesis, and CA_C3605 (*gntP*), encoding high affinity gluconate/L-idonate permease, exhibited striking increases (> 120-fold) (Table S5) in *ΔadhE2*.

As described above, the solventogenic culture of *ΔadhE1* has a lower glucose consumption rate than the control strain (Fig. 2) and consequently more glucose remained unconsumed in the medium. Accordingly, numerous genes related to sugar metabolism were down-regulated under this metabolic state. For instance, all the structural genes on the mannitol phosphotransferase system (PTS)-related operon *mtlARFD* (CA_C0154–CA_C0157) and the mannose PTS-related operon (CA_P0066–CA_P0068) were decreased by > 10-fold (Table S4).

Interestingly, one of two operons encoding a quorum-sensing system and putatively involved in sporulation, CA_C0078–CA_C0079 (*agrBD*) (Steiner *et al.*, 2012a), was strongly down-regulated (infinity- for CA_C0078 and 667-fold for CA_C0078) in *ΔadhE2* relative to the control strain (Table S5). However, the other operon, CA_C0080–CA_C0081 (*agrCA*), did not significantly change (< 3-fold decreases) (Dataset S1). Quantitatively, less than 1 *agrCA*

mRNA molecule was found per cell, whereas more than 1 *agrBD* mRNA molecule was found per cell under all conditions in the control strain (Yoo *et al.*, 2015). These different expression levels are not surprising because *agrBD* and *agrCA* are independently transcribed (Steiner *et al.*, 2012a, Alsaker & Papoutsakis, 2005, Paredes *et al.*, 2004). In addition, *agrBD* was repressed under all conditions in *ΔadhE2*, although the sporulation of this mutant was not affected (Dataset S1).

Transcriptional changes due to adhE1 or adhE2 deletion under alcohologenesis

Under alcohologenesis, a drastic change in fluxes was observed in the *ΔadhE2* mutant, while in the *ΔadhE1* mutant, the fluxes remained unchanged. As expected, more genes showed significant changes in the *ΔadhE2* mutant than in the *ΔadhE1* mutant (Table 2). Specifically, in *ΔadhE1*, only 1 gene was up-regulated (*agrB)*, and 14 genes were down-regulated, while in *ΔadhE2,* 35 genes were up-regulated, and 38 genes were down-regulated.

The most dynamic changes in the *ΔadhE2* mutant were observed in CA_C3604 (*ilvD*, 297-fold) and CA_C3605 (*gntP*, 301-fold) (Table S7). As mentioned previously, these genes were highly up-regulated (> 84-fold) under all the conditions in the *ΔadhE2* mutant (Dataset S1). Interestingly, two genes located immediately downstream of *adhE2*, CA_P0036, which encodes a cytosolic protein of unknown function, and CA_P0037, which encodes a potential transcriptional regulator, exhibited a ~9-fold increase under alcohologenesis (Table S7) in *ΔadhE2.*

A sucrose metabolism operon comprising s*crAKB* (CA_C0423–CA_C0425), encoding a PTS IIBCA domain on a single gene, fructokinase and sucrose-6-P hydrolase (Tangney & Mitchell, 2000, Servinsky *et al.*, 2010), was strikingly down-regulated (> 47-fold) (Table S6). Moreover,

the gene immediately upstream, *scrT* (CA_C0422) (encoding a putative transcriptional antiterminator), and the gene downstream, CA_C0426, encoding a putative AraC-type of regulator, were also decreased, by 9.3-fold and 8-fold, respectively (Talbe S6). The similar expression patterns of CA_C0422, CA_C0426 and *scrAKB* support the hypotheses of previous studies regarding their roles in regulating *scrAKB* (Tangney & Mitchell, 2000, Servinsky *et al.*, 2010).

As expected based on the reduced consumption of glycerol (approximately one-fourth of the control strain) (Fig. 2) in *ΔadhE2*, the gene cluster for glycerol transport and utilization (CA_C1319-CA_C1322) was down-regulated (> 4.3-fold) under these conditions (Table S7).

Most arginine biosynthesis-related genes known to respond negatively to butanol and butyrate stress (Wang *et al.*, 2013a) (i.e., CA_C0316 (*argF/I*), CA_C0973–CA_C0974 (*argGH*), CA_C2389–CA_C2388 (*argBD*), CA_C2390–CA_C2391 (*argCJ*), CA_C2644 (*carB*) and CA_C2645 (*carA*)) were significantly down-regulated (> 4-fold decrease) (Table S7) in *ΔadhE2*. CA_C3486, which encodes a multimeric flavodoxin, was decreased by 4.4-fold in *ΔadhE2* (Table S7), resulting in a loss of butanol production under alcohologenesis. This finding is consistent with the proposed hypothesis (Yoo *et al.*, 2015) that under alcohologenesis, the gene product of CA_C3486 may function as a redox partner between the hydrogenase and ferredoxin-NAD^+ reductase and may participate in the redistribution of electron fluxes in favor of butanol formation.

Conclusions

The results presented here support the hypothesis of the roles of AdhE1 and AdhE2 in butanol formation, namely that AdhE1 is the key enzyme for butanol formation in solventogenesis and that AdhE2 is the key enzyme for butanol formation in alcohologenesis. Furthermore, this study

also demonstrates the metabolic flexibility of *C. acetobutylicum* in response to genetic alteration of its primary metabolism.

Methods

Bacterial strains and plasmid construction

All *C. acetobutylicum* strains used in this study and in the control study were constructed from the *C. acetobutylicum* ATCC 824 Δ*CA_C1502* Δ*upp* mutant strain, which was constructed for rapid gene knockout and gene knockin (Croux *et al.*, 2016). Detailed procedures, including all strains and primers used, are described in the online supporting information (Supplementary experimental procedures).

Culture conditions

All batch cultures were performed under strict anaerobic conditions in synthetic medium (MS), as previously described (Vasconcelos *et al.*, 1994). *C. acetobutylicum* was stored in spore form at -20 °C after sporulation in MS medium. Heat shock was performed for spore germination by immersing the 30 or 60 mL bottle into a water bath at 80 °C for 15 minutes.

All the phosphate-limited continuous cultivations were performed as previously described by Vasconcelos et al. (Vasconcelos *et al.*, 1994) and Girbal et al. (Girbal *et al.*, 1995a) like in the control strain study (Yoo *et al.*, 2015). The chemostat was fed a constant total of 995 mM of carbon and maintained at a dilution rate of 0.05 h^{-1}. The maintained pH of the bioreactor and the supplied carbon sources of each metabolic state were as follows: for acidogenesis, pH 6.3,

with 995 mM of carbon from glucose; for solventogenesis, pH 4.4, with 995 mM of carbon from glucose; and for alcohologenesis, pH 6.3, with 498 mM of carbon from glucose and 498 mM of carbon from glycerol.

RNA extraction & microarray

Total RNA isolation and microarray experiments were performed as previously described (Yoo *et al.*, 2015). Briefly, 3 mL of chemostat cultures was sampled, immediately frozen in liquid nitrogen and ground with 2-mercaptoethanol. RNA was extracted by using an RNeasy Midi kit (Qiagen, Courtaboeuf, France) and RNase-Free DNase Set (Qiagen) per the manufacturer's protocol. The RNA quantity and integrity were monitored using an Agilent 2100 Bioanalyzer (Agilent Technologies, Massy, France) and a NanoDrop ND-1000 spectrophotometer (Labtech France, Paris, France) at 260 nm and 280 nm. All microarray procedures were performed per the manufacturer's protocol (Agilent One-Color Microarray-Based Exon Analysis).

Analytical methods

The optical density at 620 nm (OD620 nm) was monitored and used to calculate the biomass concentration with the correlation factor between dry cell weight and OD620 nm (path length 1 cm) of 0.28, which was experimentally determined from continuous cultures and was used in a control strain study (Yoo *et al.*, 2015). The glucose, glycerol, acetate, butyrate, lactate, pyruvate, acetoin, acetone, ethanol, and butanol concentrations were determined using high-performance liquid chromatography (HPLC), as described by Dusséaux et al. (Dusseaux *et al.*, 2013). The concentration of the eluent H_2SO_4 was changed to 0.5 mM, as this concentration was required to optimize the mobile phase for the control strain study (Yoo *et al.*, 2015).

Calculation of the cytosolic proteins concentration (protein molecules per cell)

In a previously published work (Yoo *et al.*, 2015), we quantified the amount of i) mRNA molecules per cell for all genes and ii) protein molecules per cell (for approximately 700 cytosolic proteins) for steady-state chemostat cultures (at a specific growth rate of $0.05h^{-1}$) of *C. acetobutylicum* under different physiological conditions. For 96 % of the cytosolic proteins that could be quantified, a linear relationship was obtained, with an $R^2 > 0.9$, when the numbers of protein molecules per cell were plotted against the numbers of mRNA molecules per cell. This result indicated that for steady-state continuous cultures run at the same specific growth rate and with the same total amount of carbon supplied, the rate of protein turnover is proportional to the mRNA content for 96% of the genes. As the mutants were cultivated in chemostat culture at the same growth rate ($0.05h^{-1}$), we used the absolute protein synthesis rates previously calculated (Yoo *et al.*, 2015) for each of the 700 genes to calculate the amount of protein molecule per cell for each of these 700 genes in the different mutants. (Dataset S1).

Calculation of the contribution of different enzymes on the butanol flux

The contribution of the 5 proteins potentially involved in the butanol pathway, namely AdhE1, AdhE2, BdhA, BdhB, and BdhC, was made as previously described (Yoo *et al.*, 2015) by assuming that all five enzymes function at their Vmax and using the calculated amount of each protein per cell (Dataset S1).

Declarations

Abbreviations

Flp: flippase; FRT: flippase recognition target; catP: chloramphenicol acetyltransferase

Availability of data and material

Microarray data can be accessed at GEO through accession number GSE69973.

Acknowledgements

We thank Sophie Lamarre, and Lidwine Trouilh for help with the data analysis.

This work was financially supported by the European Community's Seventh Framework Program "CLOSTNET" (PEOPLE-ITN-2008-237942) to Minyeong Yoo.

Authors' contributions

CC, IMS, and PS conceived the study; MY performed all the experimental work. MY and PS performed the data analysis and drafted the manuscript. PS supervised the work. All authors read and approved the final manuscript.

Competing interests

The authors declare that they have no competing interests.

Figure legends

Fig. 3.1. . Construction of *ΔadhE1* and *ΔadhE2*. The single construction of *ΔadhE2* and three different constructions of *ΔadhE1* are described: *ΔCA_C1502ΔuppΔadhE2::catP* (A), *ΔCA_C1502ΔuppΔadhE1::catP* (B), *ΔCA_C1502ΔuppΔadhE1* (C), and *ΔCA_C1502ΔuppΔadhE1::catP-A1A4* (D). P1 indicating the promoter of the *sol* operon and ORF L were previously proposed by Fischer et al. (Fischer *et al.*, 1993)

Fig. 3.2. Substrates and products profile under three different conditions for the control, *Δ adhE1* and *ΔadhE2* strains. (A) Carbon source consumption: glucose (blue) and glycerol (red). Product profiles in acidogenesis (B), solventogenesis (C), and alcohologenesis (D). For (B), (C) and (D), each histogram indicates different strains: control (red), *ΔadhE1* (green), and *ΔadhE2* (blue).

Fig. 3.3. Electron flux map of the control, *ΔadhE1* and *ΔadhE2* strains in acidogenesis (A), solventogenesis (B), and alcohologenesis (C). The arrows for hydrogenase (red), ferredoxin-NAD+ reductase (blue) and ferredoxin-NADP+ (green) *in vivo* fluxes are presented. All values are normalized to the flux of the initial carbon source (millimoles per gram of dry cell weight (DCW) per hour). Glucose flux is normalized to 100 for acidogenesis and solventogenesis, and the sum of glucose and half of the glycerol is normalized to 100 for alcohologenesis.

Fig. 3.4. Venn diagrams of representative genes with involved pathways, which matched the significance criteria (> 4-fold increase or decrease) in the *ΔadhE1* and *ΔadhE2* mutants. A

complete list of each metabolic condition is provided in the supplementary materials.

Supporting information

Supplementary experimental procedures and results

Table S3.1. Primers and strains used in this study

Table S3.2. Four-fold increased or decreased genes under acidogenesis in *ΔadhE1*

Table S3.3. Four-fold increased or decreased genes under acidogenesis in *ΔadhE2*

Table S3.4. Four-fold increased or decreased genes under solventogenesis in *ΔadhE1*

Table S3.5. Four-fold increased or decreased genes under solventogenesis in *ΔadhE2*

Table S3.6. Four-fold increased or decreased genes under alcohologenesis in *ΔadhE1*

Table S3.7. Four-fold increased or decreased genes under alcohologenesis in *ΔadhE2*

Fig. S3.1. PCR Verification of deletion of *adhE1* in *ΔadhE1* strain (A) and *adhE2* in *ΔadhE2* strain (B).

Fig. S3.2. Butanol pathway analysis of control (A), *ΔadhE1* (B), *ΔadhE2* (C) under acidogenesis, solventogenesis, and alcohologenesis

Fig. S3.3. Metabolic flux map of *ΔadhE1* under acidogenesis (A), *ΔadhE2* under acidogenesis (B), *ΔadhE1* under solventogenesis (C), *ΔadhE2* under solventogenesis (D), . *ΔadhE1* under alcohologenesis (E), *ΔadhE2* under alcohologenesis (F)

Dataset S1. Transcriptomic data of the total open reading frames (ORFs)

Table 3.1. Transcriptional changes of genes coding for the six key enzymes for alcohol production. The numbers of mRNA molecules per cell are shown as mean values ± SD from three biological replicates.

Metabolic state/gene	Control	*ΔadhE1*	*ΔadhE2*
Acidogenesis			
adhE1 (CA_P0162)	0.09±0.01	0±0	0.2±0.01
adhE2 (CA_P0035)	0.42±0.02	2.31±0.6	0±0
bdhA (CA_C3299)	8.15±0.32	4.33±1.03	5.76±0.2
bdhB (CA_C3298)	16.31±0.45	5.13±4.28	1.52±0.11
bdhC (CA_C3392)	8.63±0.94	7.55±0.28	17.65±0.44
pdc (CA_P0025)	5.6±0.81	1.74±0.1	3.23±0.24
Solventogenesis			
adhE1 (CA_P0162)	7.09±0.73	0±0	11.4±4.71
adhE2 (CA_P0035)	0.21±0.02	26.6±0.26	0±0
bdhA (CA_C3299)	8.22±1.33	4.62±0.06	7.55±0.75
bdhB (CA_C3298)	28.1±5.07	34.78±1.55	17.76±2.83
bdhC (CA_C3392)	11.28±1.68	12.52±0.36	9.16±0.67
pdc (CA_P0025)	5.17±2.78	6.59±0.3	6.23±1.03
Alcohologenesis			
adhE1 (CA_P0162)	0.13±0.01	0±0	0.18±0.01
adhE2 (CA_P0035)	68.6±12.95	62.56±7.58	0±0
bdhA (CA_C3299)	6.08±0.37	4.82±0.13	7.39±0.21
bdhB (CA_C3298)	14.33±2.65	16.96±0.25	15.16±0.46
bdhC (CA_C3392)	10.73±0.94	11.05±0.25	8.95±0.32
pdc (CA_P0025)	1.23±0.51	0.83±0.03	1.86±0.07

Table 3.2. Numbers of significantly changed genes by each gene deletion and genes exhibiting the same pattern of change for both deletions under three different metabolic states (the genes exhibiting the same pattern for both deletions under acidogenesis are listed in Table 3).

	Δ*adhE1*	Δ*adhE2*	Same pattern in Δ*adhE1* and Δ*adhE2*	Note[a]
Upregulation under acidogenesis	100	119	50	Most CymR regulons are included
Downregulation under acidogenesis	108	170	89	Most butanol response genes are included
Upregulation under solventogenesis	55	22	0	
Downregulation under solventogenesis	127	17	1	CA_C3612
Upregulation under alcohologenesis	1	35	0	
Downregulation under alcohologenesis	14	38	1	CA_C3274

[a]Representative features or locus number of the sole gene showing same pattern under certain condition are shown

Table 3.3. Genes exhibiting the same pattern of change for both deletions under acidogenesis

Locus number	Function	*ΔadhE1* /Control strain	*ΔadhE2* /Control strain	Note[a]
Upregulation				
CA_C0102	O-acetylhomoserine sulfhydrylase	28.70	20.49	CymR
CA_C0103	Adenylylsulfate kinase	32.55	22.06	CymR
CA_C0104	Adenylylsulfate reductase, subunit A	48.44	28.89	CymR
CA_C0105	Ferredoxin	30.78	21.84	CymR
CA_C0106	ABC-type probable sulfate transporter, periplasmic binding protein	26.09	14.54	CymR
CA_C0107	ABC-type sulfate transporter, ATPase component	22.86	13.03	CymR
CA_C0108	ABC-type probable sulfate transporter, permease protein	35.38	19.05	CymR
CA_C0109	Sulfate adenylate transferase, CysD subfamily	42.53	26.82	CymR
CA_C0110	GTPase, sulfate adenylate transferase subunit 1	54.78	42.48	CymR
CA_C0117	Chemotaxis protein cheY homolog	8.34	6.69	
CA_C0118	Chemotaxis protein cheA	11.00	8.24	
CA_C0119	Chemotaxis protein cheW	13.83	9.52	
CA_C0120	Membrane-associated methyl-accepting chemotaxis protein with HAMP domain	6.93	5.29	
CA_C0878	Amino acid ABC transporter permease component	5.61	4.04	CymR
CA_C0879	ABC-type polar amino acid transport system, ATPase component	8.29	5.60	CymR
CA_C0880	Periplasmic amino acid binding protein	9.50	6.50	CymR
CA_C0930	Cystathionine gamma-synthase	4.58	4.72	CymR
CA_C1392	Glutamine phosphoribosylpyrophosphate amidotransferase	4.20	4.47	
CA_C1394	Folate-dependent phosphoribosylglycinamide formyltransferase	4.11	4.57	
CA_C2072	Stage IV sporulation protein B, SpoIVB	∞	∞	
CA_C2235	Cysteine synthase/cystathionine beta-synthase, CysK	8.27	7.17	CymR
CA_C2236	Uncharacterized conserved protein of YjeB/RRF2 family	4.29	4.06	CymR encoding gene
CA_C2241	Cation transport P-type ATPase	7.92	7.62	
CA_C2242	Predicted transcriptional regulator, arsE family	5.01	5.22	

CA_C2521	Hypothetical protein, CF-41 family	4.33	5.70	
CA_C2533	Protein containing ChW-repeats	∞	∞	
CA_C2816	Hypothetical protein, CF-17 family	6.00	11.20	
CA_C3049	Glycosyltransferase	4.79	7.42	
CA_C3050	AMSJ/WSAK related protein, possibly involved in exopolysaccharide biosynthesis	4.70	8.25	
CA_C3051	Glycosyltransferase	5.16	9.60	
CA_C3052	Glycosyltransferase	5.59	9.91	
CA_C3053	Histidinol phosphatase related enzyme	7.03	10.94	
CA_C3054	Phosphoheptose isomerase	6.69	11.37	
CA_C3055	Sugar kinase	5.90	10.87	
CA_C3056	Nucleoside-diphosphate-sugar pyrophosphorylase	6.37	11.28	
CA_C3057	Glycosyltransferase	12.36	11.92	
CA_C3058	Mannose-1-phosphate guanylyltransferase	9.94	11.59	
CA_C3059	Sugar transferases	13.47	12.63	
CA_C3325	Periplasmic amino acid binding protein	18.24	10.68	CymR
CA_C3326	Amino acid ABC-type transporter, permease component	19.82	11.79	CymR
CA_C3327	Amino acid ABC-type transporter, ATPase component	28.33	16.73	CymR
CA_C3461	Hypothetical protein	4.52	16.79	
CA_C3556	Probable S-layer protein;	4.18	10.41	
CA_C3636	Oligopeptide ABC transporter, ATPase component	4.23	4.68	
CA_P0029	Permease MDR-related	∞	∞	
CA_P0030	Isochorismatase	385.91	81.89	
CA_P0031	Transcriptional activator HLYU, HTH of ArsR family	46.17	10.93	
CA_P0117	Possible beta-xylosidase diverged, family 5/39 of glycosyl hydrolases and alpha-amylase C (Greek key) C-terminal domain	56.53	4.94	
CA_P0118	Possible xylan degradation enzyme (glycosyl hydrolase family 30-like domain and Ricin B-like domain)	54.97	5.22	
CA_P0119	Possible xylan degradation enzyme (glycosyl hydrolase family 30-like domain and Ricin B-like domain)	46.44	4.23	
Downregulation				
CA_C0078	Accessory gene regulator protein B	0.04	0.00	
CA_C0079	Hypothetical protein	0.00	0.00	

CA_C0082	Predicted membrane protein	0.02	0.00	
CA_C0310	Regulators of stationary/sporulation gene expression, abrB B.subtilis ortholog	0.15	0.23	
CA_C0381	Methyl-accepting chemotaxis protein	0.18	0.13	
CA_C0437	Sensory transduction histidine kinase	0.15	0.23	
CA_C0537	Acetylxylan esterase, acyl-CoA esterase or GDSL lipase family, strong similarity to C-terminal region of endoglucanase E precursor	0.15	0.10	
CA_C0542	Methyl-accepting chemotaxis protein	0.21	0.08	
CA_C0658	Fe-S oxidoreductase	0.24	0.00	
CA_C0660	Hypothetical protein, CF-26 family	0.17	0.08	BuOH
CA_C0814	3-oxoacyl-[acyl-carrier-protein] synthase III	0.11	0.02	BuOH
CA_C0815	Methyl-accepting chemotaxis protein	0.13	0.04	BuOH
CA_C0816	Lipase-esterase related protein	0.17	0.04	BuOH
CA_C1010	Predicted phosphohydrolase, Icc family	0.21	0.04	BuOH
CA_C1022	Thioesterase II of alpha/beta hydrolase superfamily	0.22	0.11	
CA_C1078	Predicted phosphohydrolase, Icc family	0.17	0.04	BuOH
CA_C1079	Uncharacterized protein, related to enterotoxins of other Clostridiales	0.15	0.05	
CA_C1080	Uncharacterized protein, probably surface-located	0.11	0.01	
CA_C1081	Uncharacterized protein, probably surface-located	0.13	0.01	
CA_C1532	Protein containing ChW-repeats	0.22	0.08	
CA_C1766	Predicted sigma factor	0.19	0.00	
CA_C1775	Predicted membrane protein	0.16	0.05	
CA_C1868	Uncharacterized secreted protein, homolog YXKC Bacillus subtilis	0.22	0.18	
CA_C1989	ABC-type iron (III) transport system, ATPase component	0.18	0.11	BuOH
CA_C1991	Uncharacterized protein, YIIM family	0.23	0.10	BuOH
CA_C1993	Molybdenum cofactor biosynthesis enzyme MoaA, Fe-S oxidoreductase	0.23	0.18	BuOH
CA_C1994	Molybdopterin biosynthesis enzyme, MoaB	0.22	0.11	BuOH
CA_C1996	Hypothetical protein	0.19	0.08	BuOH
CA_C1997	Predicted glycosyltransferase	0.19	0.07	BuOH
CA_C1998	ABC-type transport system, ATPase component	0.19	0.07	BuOH

CA_C1999	Uncharacterized protein related to hypothetical protein Cj1507c from Campylobacter jejuni	0.20	0.07	BuOH
CA_C2000	Indolepyruvate ferredoxin oxidoreductase, subunit beta	0.19	0.06	BuOH
CA_C2001	Indolepyruvate ferredoxin oxidoreductase, subunit alpha	0.13	0.04	BuOH
CA_C2002	Predicted iron-sulfur flavoprotein	0.16	0.05	BuOH
CA_C2003	Predicted permease	0.16	0.08	BuOH
CA_C2004	Siderophore/Surfactin synthetase related protein	0.10	0.04	BuOH
CA_C2005	Siderophore/Surfactin synthetase related protein	0.12	0.05	BuOH
CA_C2006	Enzyme of siderophore/surfactin biosynthesis	0.15	0.07	BuOH
CA_C2007	Predicted glycosyltransferase	0.09	0.03	BuOH
CA_C2008	3-oxoacyl-(acyl-carrier-protein) synthase	0.11	0.04	BuOH
CA_C2009	3-Hydroxyacyl-CoA dehydrogenase	0.10	0.03	BuOH
CA_C2010	Predicted Fe-S oxidoreductase	0.09	0.03	BuOH
CA_C2011	Possible 3-oxoacyl-[acyl-carrier-protein] synthase III	0.12	0.03	BuOH
CA_C2012	Enoyl-CoA hydratase	0.12	0.04	BuOH
CA_C2013	Hypothetical protein	0.12	0.03	BuOH
CA_C2014	Predicted esterase	0.12	0.02	BuOH
CA_C2015	Hypothetical protein	0.15	0.04	BuOH
CA_C2016	Enoyl-CoA hydratase	0.12	0.02	BuOH
CA_C2017	Acyl carrier protein	0.15	0.03	BuOH
CA_C2018	Aldehyde:ferredoxin oxidoreductase	0.12	0.03	BuOH
CA_C2019	Malonyl CoA-acyl carrier protein transacylase	0.12	0.02	BuOH
CA_C2020	Molybdopterin biosynthesis enzyme, MoeA, fused to molibdopterin-binding domain	0.20	0.07	
CA_C2021	Molybdopterin biosynthesis enzyme, MoeA (short form)	0.24	0.06	
CA_C2023	Membrane protein, related to copy number protein COP from Clostridium perfringens plasmid pIP404 (GI:116928)	0.22	0.12	
CA_C2026	Predicted flavodoxin	0.20	0.09	
CA_C2107	Contains cell adhesion domain	0.20	0.08	
CA_C2293	Hypothetical secreted protein	0.13	0.10	
CA_C2581	6-pyruvoyl-tetrahydropterin synthase related domain; conserved membrane protein	0.24	0.11	BuOH
CA_C2663	Protein containing cell-wall hydrolase domain	0.23	0.09	
CA_C2695	Diverged Metallo-dependent hydrolase(Zn) of DD-Peptidase family; peptodoglycan-binding	0.17	0.12	BuOH

	domain			
CA_C2807	Endo-1,3(4)-beta-glucanase family 16	0.21	0.02	
CA_C2808	Beta-lactamase class C domain (PBPX family) containing protein	0.20	0.04	
CA_C2809	Predicted HD superfamily hydrolase	0.14	0.02	
CA_C2810	Possible glucoamylase (diverged), 15 family	0.14	0.01	
CA_C2944	N-terminal domain intergin-like repeats and c-terminal- cell wall-associated hydrolase domain	0.23	0.06	BuOH
CA_C3070	Glycosyltransferase	0.21	0.04	
CA_C3071	Glycosyltransferase	0.21	0.03	
CA_C3072	Mannose-1-phosphate guanylyltransferase	0.18	0.02	
CA_C3073	Sugar transferase involved in lipopolysaccharide synthesis	0.23	0.03	
CA_C3085	TPR-repeat-containing protein; Cell-adhesion domain;	0.25	0.12	
CA_C3086	Protein containing cell adhesion domain	0.20	0.11	
CA_C3251	Sensory transduction protein containing HD_GYP domain	0.20	0.11	
CA_C3264	Uncharacterized conserved protein, YTFJ B.subtilis ortholog	0.19	0.15	BuOH
CA_C3265	Predicted membrane protein	0.08	0.11	
CA_C3266	Hypothetical protein	0.07	0.07	
CA_C3267	Specialized sigma subunit of RNA polymerase	0.15	0.16	
CA_C3280	Possible surface protein, responsible for cell interaction; contains cell adhesion domain and ChW-repeats	0.23	0.14	
CA_C3408	NADH oxidase (two distinct flavin oxidoreductase domains)	0.03	0.02	
CA_C3409	Transcriptional regulators, LysR family	0.02	0.01	
CA_C3412	Predicted protein-S-isoprenylcysteine methyltransferase	0.22	0.06	
CA_C3422	Sugar:proton symporter (possible xylulose)	0.05	0.03	
CA_C3423	Acetyltransferase (ribosomal protein N-acetylase subfamily)	0.04	0.03	
CA_C3612	Hypothetical protein	0.18	0.00	BuOH
CA_P0053	Xylanase, glycosyl hydrolase family 10	0.24	0.09	BuOH
CA_P0054	Xylanase/chitin deacetylase family enzyme	0.24	0.07	BuOH
CA_P0057	Putative glycoportein or S-layer protein	0.21	0.13	BuOH
CA_P0135	Oxidoreductase	0.25	0.21	
CA_P0136	AstB/chuR/nirj-related protein	0.25	0.23	
CA_P0174	Membrane protein	0.25	0.14	

[a]CymR indicates CymR regulon, BuOH indicates the genes to be downregulated by butanol stress in an acidogenic chemostat in the study by Schwarz et al. (Schwarz *et al.*, 2012)

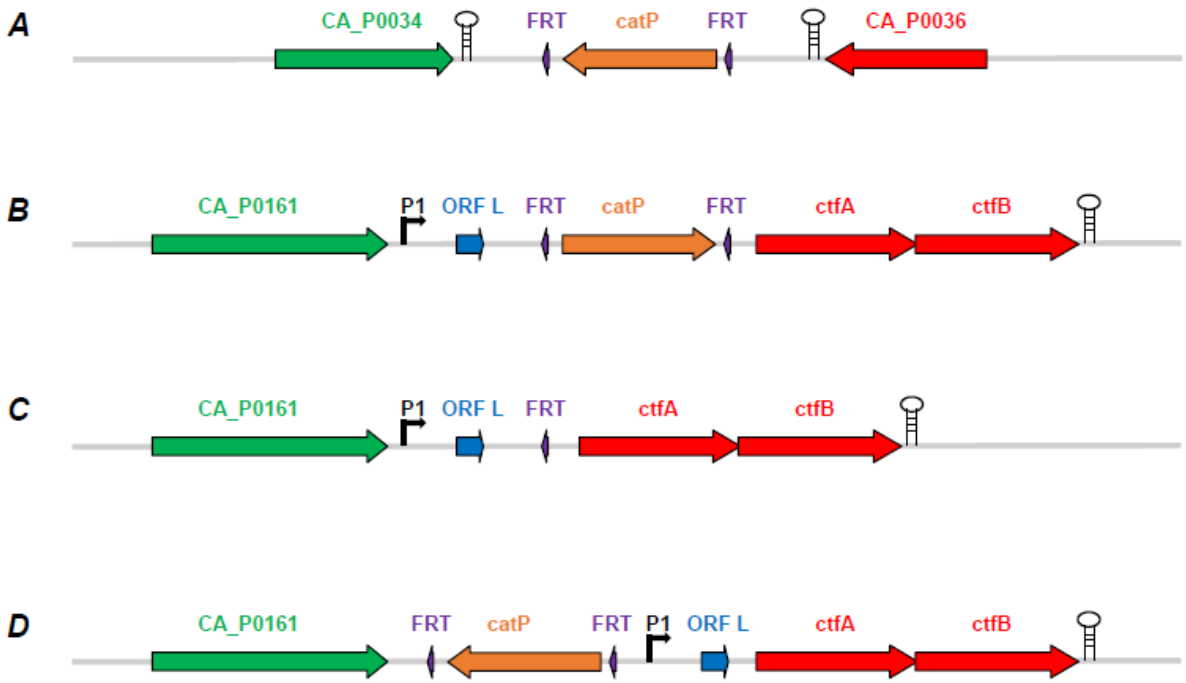

Fig. 3.1. . Construction of *ΔadhE1* and *ΔadhE2*. The single construction of *ΔadhE2* and three different constructions of *ΔadhE1* are described: *ΔCA_C1502ΔuppΔadhE2::catP* (A), *ΔCA_C1502ΔuppΔadhE1::catP* (B), *ΔCA_C1502ΔuppΔadhE1* (C), and *ΔCA_C1502ΔuppΔadhE1::catP-A1A4* (D). P1 indicating the promoter of the *sol* operon and ORF L were previously proposed by Fischer et al. (Fischer *et al.*, 1993)

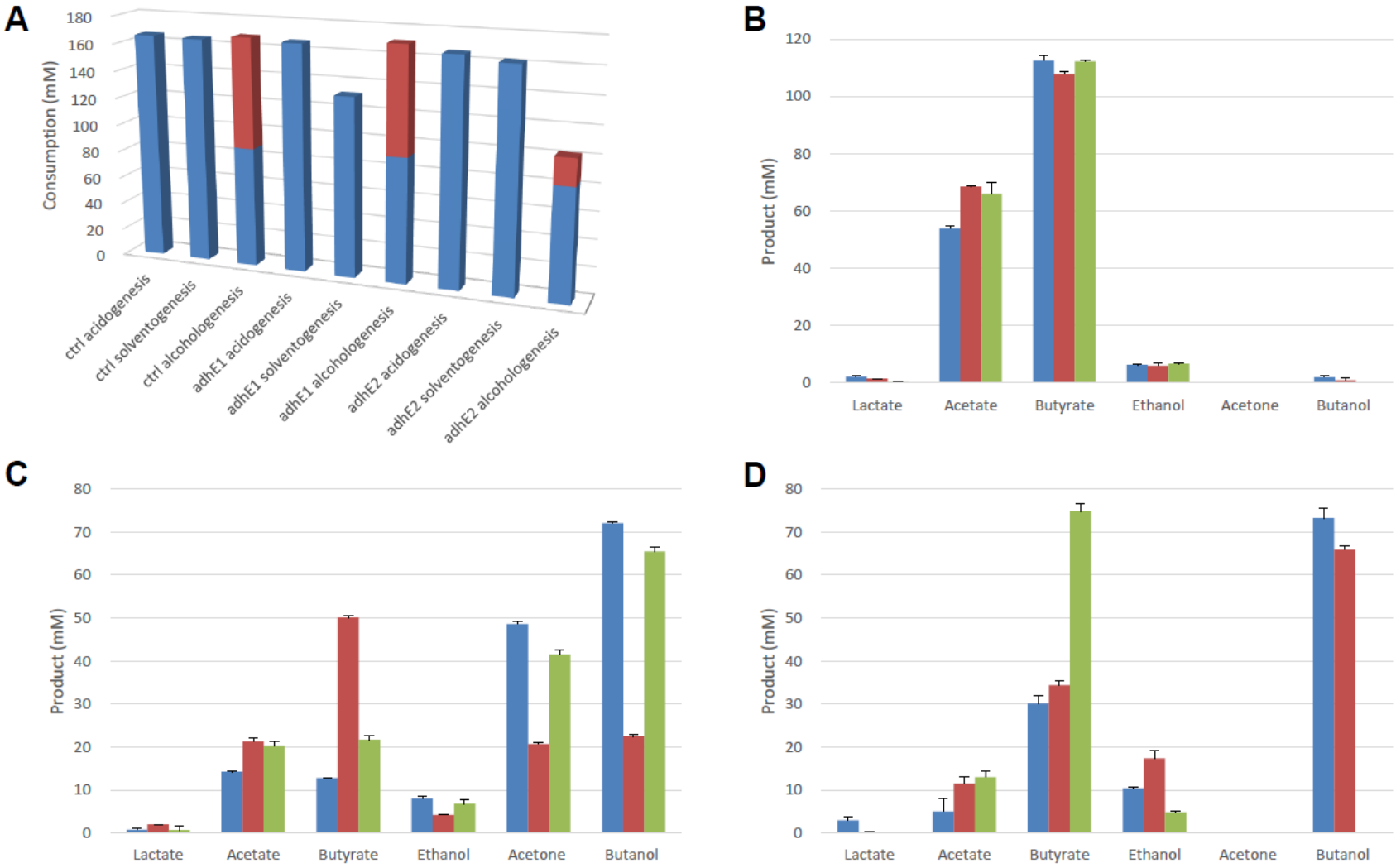

Fig. 3.2. Substrates and products profile under three different conditions for the control, *ΔadhE1* and *ΔadhE2* strains. (A) Carbon source

consumption: glucose (blue) and glycerol (red). Product profiles in acidogenesis (B), solventogenesis (C), and alcohologenesis (D). For (B), (C) and (D), each histogram indicates different strains: control (red), *ΔadhE1* (green), and *ΔadhE2* (blue).

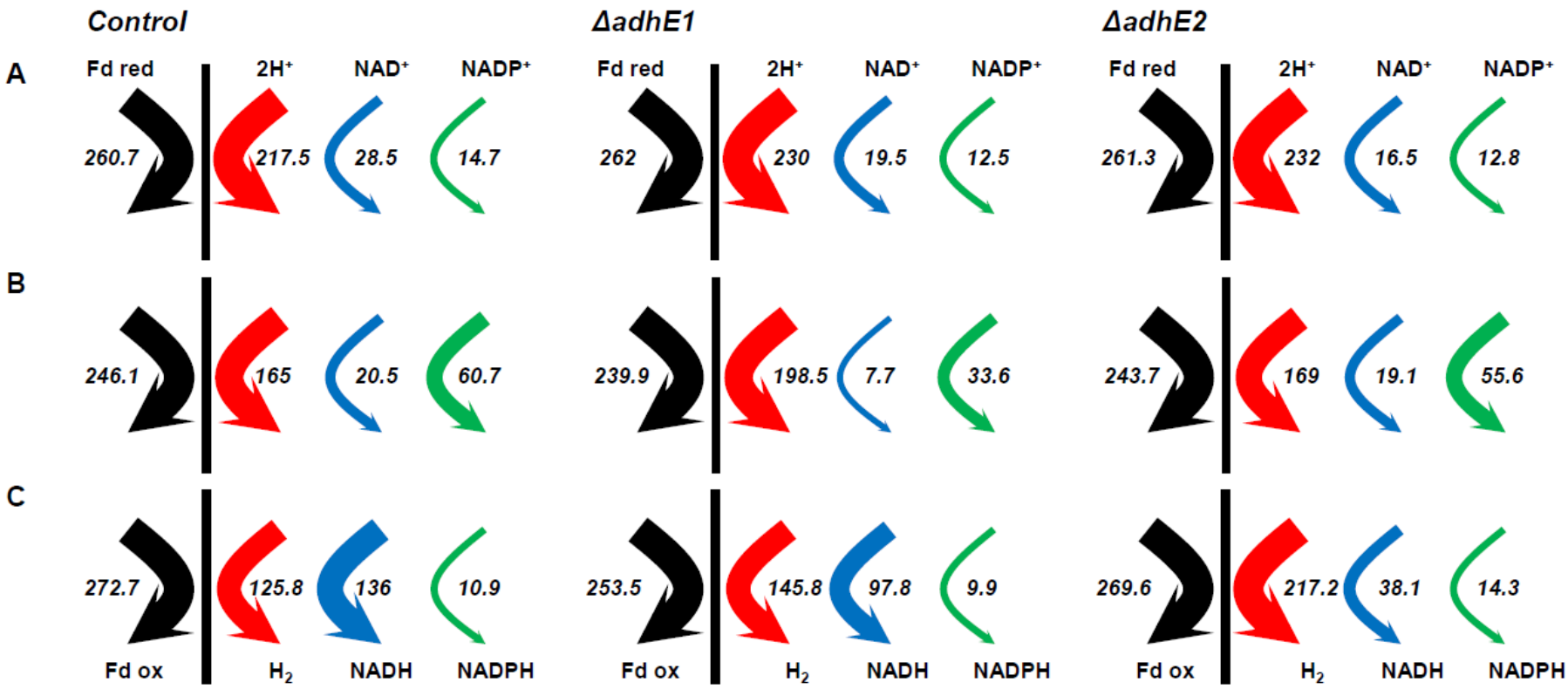

Fig. 3.3. Electron flux map of the control, *ΔadhE1* and *ΔadhE2* strains in acidogenesis (A), solventogenesis (B), and alcohologenesis (C). The arrows for hydrogenase (red), ferredoxin-NAD+ reductase (blue) and ferredoxin-NADP+ (green) *in vivo* fluxes are presented. All values are normalized to the flux of the initial carbon source (millimoles per gram of dry cell weight (DCW) per hour). Glucose flux is normalized to 100 for acidogenesis and solventogenesis, and the sum of glucose and half of the glycerol is normalized to 100 for alcohologenesis.

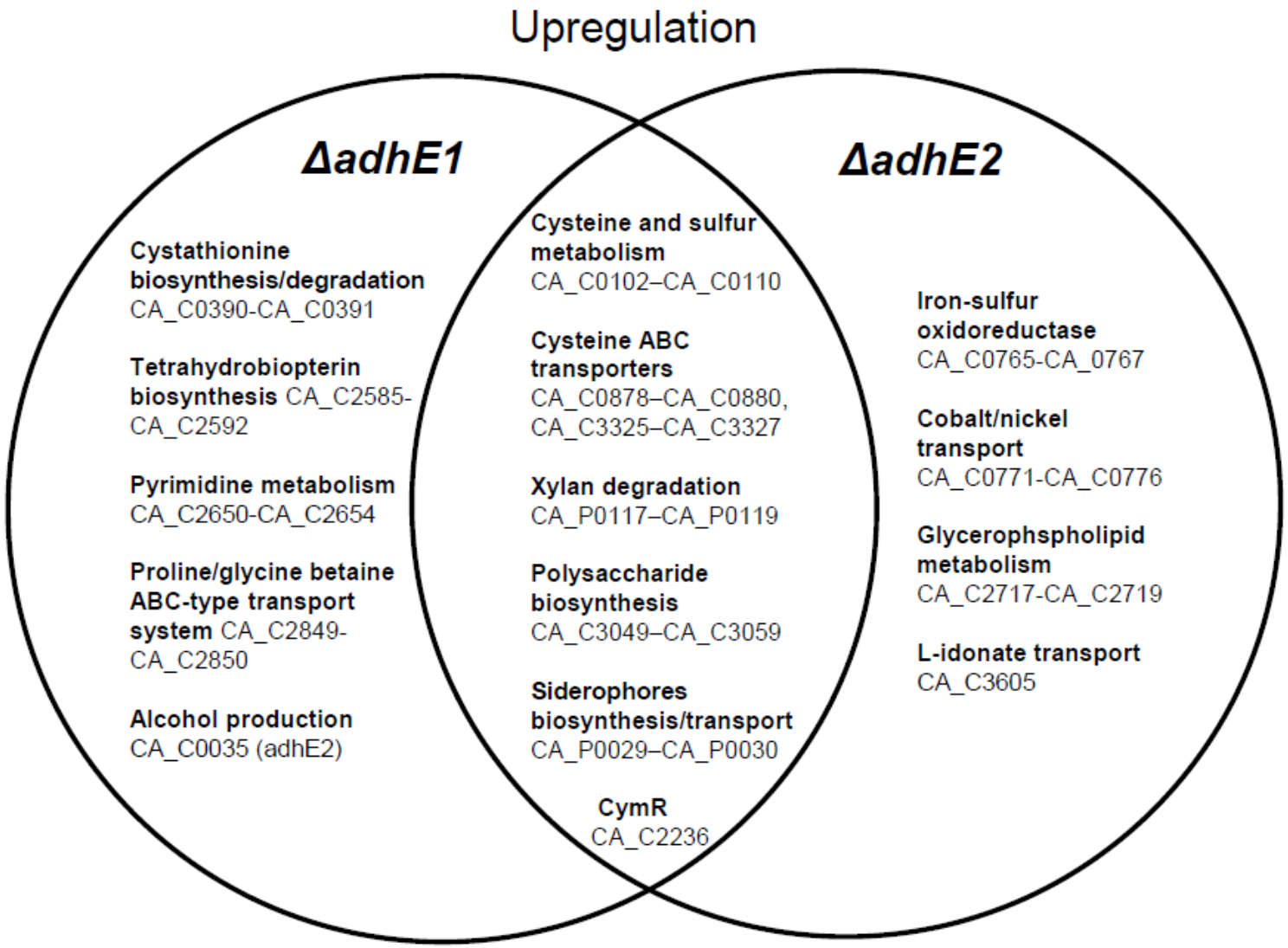
Upregulation
ΔadhE1
ΔadhE2
Cystathionine biosynthesis/degradation CA_C0390-CA_C0391
Tetrahydrobiopterin biosynthesis CA_C2585-CA_C2592
Pyrimidine metabolism CA_C2650-CA_C2654
Proline/glycine betaine ABC-type transport system CA_C2849-CA_C2850
Alcohol production CA_C0035 (adhE2)
Cysteine and sulfur metabolism CA_C0102–CA_C0110
Cysteine ABC transporters CA_C0878–CA_C0880, CA_C3325–CA_C3327
Xylan degradation CA_P0117–CA_P0119
Polysaccharide biosynthesis CA_C3049–CA_C3059
Siderophores biosynthesis/transport CA_P0029–CA_P0030
CymR CA_C2236
Iron-sulfur oxidoreductase CA_C0765-CA_0767
Cobalt/nickel transport CA_C0771-CA_C0776
Glycerophspholipid metabolism CA_C2717-CA_C2719
L-idonate transport CA_C3605

Fig.3.4.

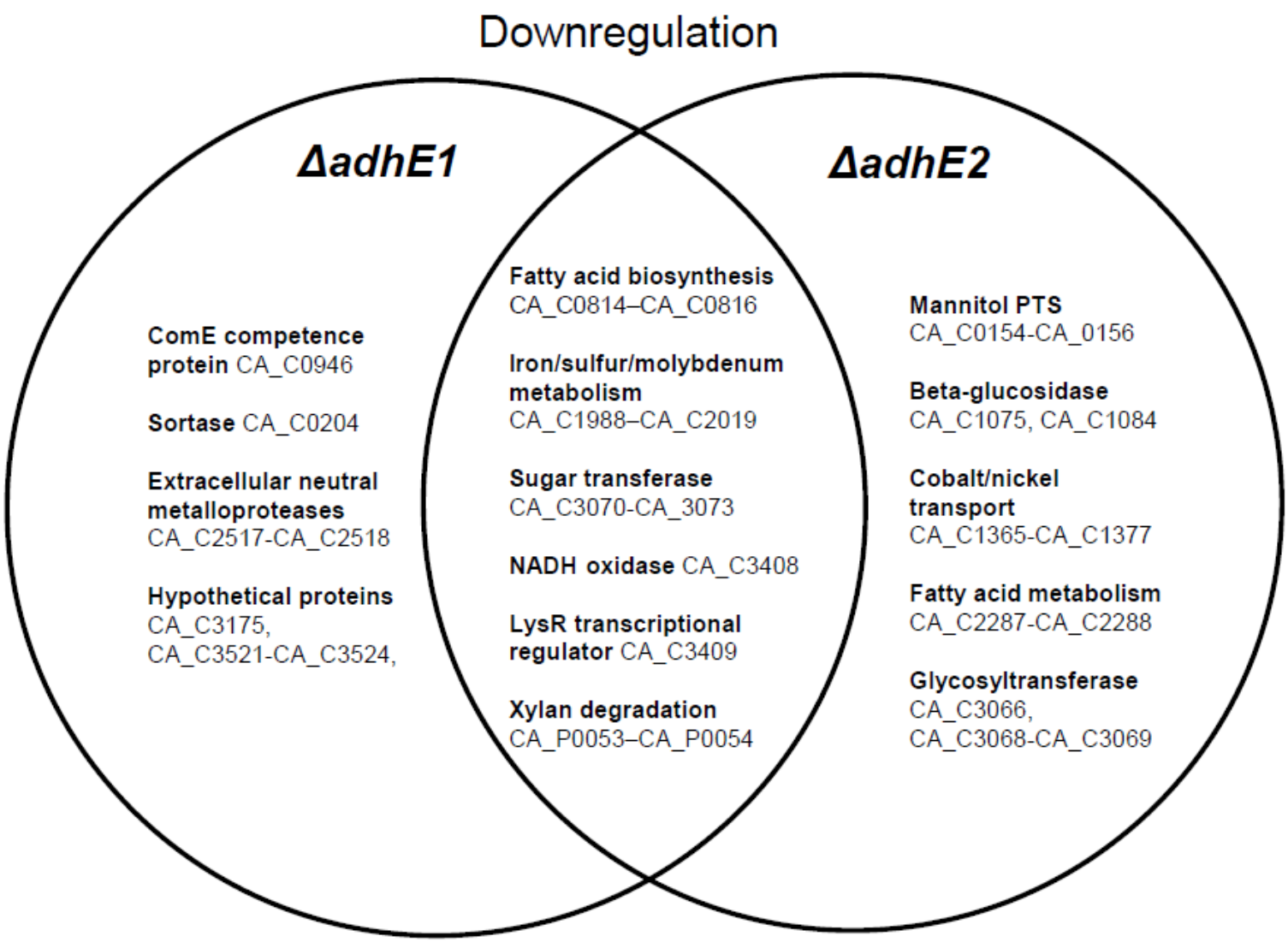
Downregulation
ΔadhE1
ΔadhE2
ComE competence protein CA_C0946
Sortase CA_C0204
Extracellular neutral metalloproteases CA_C2517-CA_C2518
Hypothetical proteins CA_C3175, CA_C3521-CA_C3524,
Fatty acid biosynthesis CA_C0814–CA_C0816
Iron/sulfur/molybdenum metabolism CA_C1988–CA_C2019
Sugar transferase CA_C3070-CA_3073
NADH oxidase CA_C3408
LysR transcriptional regulator CA_C3409
Xylan degradation CA_P0053–CA_P0054
Mannitol PTS CA_C0154-CA_0156
Beta-glucosidase CA_C1075, CA_C1084
Cobalt/nickel transport CA_C1365-CA_C1377
Fatty acid metabolism CA_C2287-CA_C2288
Glycosyltransferase CA_C3066, CA_C3068-CA_C3069

Fig.3.4.

Fig. 3.4. Venn diagrams of representative genes with involved pathways, which matched the significance criteria (> 4-fold increase or decrease) in the *ΔadhE1* and *ΔadhE2* mutants. A complete list of each metabolic condition is provided in the supplementary materials.

Supporting Information

Experimental procedures

Plasmid constructions

All primers used in this study are listed in Table S1. The allelic exchange method described by Croux *et al*. (Croux *et al.*, 2016) was used for deletion of target genes.

Construction of pSOS95-upp

The pSOS95-upp plasmid was constructed from the pSOS95-upp-DldhA-catP*a plasmid initially designed for the deletion of the *ldhA* gene. The pSOS95-upp-DldhA-catP* plasmid was constructed as follows. First two DNA fragments surrounding the *ldhA* gene (CA_C0267) were amplified by PCR using *C. acetobutylicum* ATCC824 total gDNA as template and two pairs of oligonucleotides as primers with the Phusion DNA Polymerase. Using pairs of primers ldhA-1/ldhA-2 and ldhA-3/ldhA-4, two 1 kb DNA fragments were obtained respectively. Both primers ldhA-1 and ldhA-4 introduce a *BamHI* site while primers ldhA-2 and ldhA-3 have complementary 5' extended sequences which introduce a *StuI* site. DNA fragments ldhA-1/ ldhA-2 and ldhA-3/ ldhA-4 were joined in a PCR fusion with primers ldhA-1 and ldhA-4 and the resulting fragment was cloned into the pSC-B vector (Agilent) to generate pSCB-DldhA.

The Pptb-catP* cassette containing the modified antibiotic resistance catP gene under the control of the *C. acetobutylicum* phosphotransbutyrylase (ptb) promoter and flanked by two FRT sequences was obtained by PCR amplification with the Phusion DNA Polymerase using pSOS94-catP* plasmid (Sillers *et al.*, 2008a) as template and FRT-CM-F1 and FRT-CM-F2 oligonucleotides as primers. This 1.2 kb fragment was then cloned into the pSC-B vector to give the pSCB-FRT-catP* plasmid.

The 1kb *SmaI*/*HindIII* fragment from pSCB-FRT-catP* blunt-ended by klenow treatment was then cloned into the unique *StuI* site of the pSCB-DldhA to give the resulting pSCB-DldhA-FRT-

catP*plasmid.

The 3.8 kb *BspHI*/*ClaI* blunt-ended by klenow treatment fragment from pSCB-DldhA-FRT-catP* was finally cloned into the *PstI*/E*coRI* digested and blunt ended pSOS95 backbone to give the pSOS95-DldhA-FRT-catP* plasmid.

The *upp* gene (CA_C2879) was amplified by PCR using *C. acetobutylicum ATCC824* total DNA as template and oligonucleotides Rep-upp-F and Rep-upp-F as primers with the Phusion DNA Polymerase. After *PvuII* digestion, the 0.7 kb resulting fragment was cloned into the *ClaI* digested and Klenow treated pSOS95-DldhA-FRT-catP* plasmid. The clones showing an insertion of the *upp* gene in the same orientation of that of the MLSR gene, *i.e.* resulting in the formation of an artificial bicistronic operon, were selected, and the final plasmid was named pSOS95-upp-DldhA-catP*.

After a *BamHI* digestion of the pSOS95-upp-DldhA-catP* plasmid to remove the specific region for *ldhA* deletion, and a self-ligation of the large fragment (5.6 kb), the pSOS95-upp plasmid was obtained, that can be subsequently used as a parental vector for the cloning into the unique *BamHI* site of others deletions-replacement cassettes (see deletion of *adhE1* and deletion of *adhE2*)

Construction of pSOS95-upp-flp

The 0.7 kb *PvuII* fragment containing the *upp* gene (see *ldhA* deletion) was cloned into the *ClaI* digested and blunt-ended (T4 DNA Polymerase) pSOS-catP* plasmid (Sillers *et al.*, 2008a). The clones showing an insertion of the *upp* gene in the same orientation of that of the MLSR gene, *ie* resulting in the formation of an artificial bicistronic operon were selected, and the final plasmid named pSOS95-catP*-upp

The 1.6 kb *SalI* fragment from pCLF1 (WO2008040387) carrying the *Flp* gene under the control of the *C. acetobutylicum* thiolase (*thlA*) promoter was then introduced into the *SalI* digested and dephosphorylated pSOS95-catP*-upp backbone (catP* removing) to give the pSOS95-upp-Flp plasmid,

designed for the removing of catP* antibiotic resistance cassette based on Flp-FRT recombination system.

Deletion of adhE1

Two DNA fragments surrounding the *adhE1* gene (CA_P0162) were amplified by PCR using *C. acetobutylicum* ATCC824 total DNA as template and two pairs of oligonucleotides as primers with the Phusion DNA Polymerase. Using pairs of primers adhE1-1/adhE1-2 and adhE1-3/adhE1-4, 1.1 kb and 1.2 kb DNA fragments were obtained respectively. Both primers adhE1-1 and adhE1-4 introduce a *BglII* site while primers adhE1-2 and adhE1-3 have complementary 5' extended sequences which introduce a *StuI* site. adhE1-2 was designed to amplify upstream of start codon (included) and downstream of stop codon (included) of *adhE1* to conserve P1 promoter and ORF L and also to amplify entire 60bp between stop codon of *adhE1* and start codon of *ctfA*.

DNA fragments adhE1-1/adhE1-2 and adhE1-3/adhE1-4 were joined in a low cycle PCR fusion with Phusion DNA polymerase and primers adhE1-1 and adhE1-4, and the resulting fragment was cloned into the Zero Blunt TOPO vector to generate the TOPO-DadhE1 plasmid. The 1.2 kb *StuI* fragment from the previously described pSCB-FRT-catP*carrying the FRT-Pptb-catP* cassette was introduced at the unique *StuI* site of TOPO-DadhE1, to generate the TOPO-DadhE1-FRT-catP* plasmid.

The 3.5 kb *BglII* fragment from TOPO-DadhE1-FRT-catP* was then cloned into the *BamHI* digested pSOS95-upp (see above) to give the final pREP-Delta adhE1-catP*-upp plasmid.

The final constructed plasmid, pREP-Delta adhE1-catP*-upp, was introduced into *ΔCA_C1502 Δupp* strain to yield *ΔCA_C1502 Δupp ΔadhE1::catP* strain exerting a polar effect on *ctfAB*, parts of *sol* operon as well as *adhE1*, resulting in loss of acetone production ability.

In order to obtain the *catP* cassette (that contains transcriptional terminator) removed strain,

pSOS95-upp-flp plasmid was introduced into *ΔCA_C1502 Δupp ΔadhE1::catP* strain. The continued polar effect on acetone formation in spite of the removal of *catP* cassette leaded to attempts to alter the location of *sol* operon promoter to downstream of the latter FRT site that is a putative transcriptional terminator. The plasmid, pREP-Delta adhE1-A1A4, for alteration of the location of *sol* promoter was constructed using the following procedure: a 1.3 kb FRT-Pptb-catP* fragment was amplified using the pREP-DadhE1-catP*-upp plasmid as template and the oligonucleotides AdhE1-A1 and AdhE1-A2 as primers, and a 6.5 kb fragment containing the *sol* promoter region was amplified using the *C. acetobutylicum* ATCC824 total gDNA as template and the oligonucleotides AdhE1-A3 and AdhE1-A4 as primers.

Both primers AdhE1-A2 and AdhE1-A3 have self-complementary 5' extended sequences and the DNA fragments AdhE1-A-1/ AdhE1-A-2 and AdhE1-A-3/ AdhE1-A-4 were joined in a PCR fusion with primers AdhE1-A-1 and AdhE1-A-4.

Both primers AdhE1-A1 and AdhE1-A4 have 5' extended sequence complementary to the pREP-Delta adhE1-catP-upp, thus after DpnI treatment, the resulting fused A1/A4 fragment was cloned into the pREP-Delta adhE1-catP-upp digested by *StuI* and *ClaI* using the GENEART Seamless Cloning and Assembly Kit (Invitrogen) to give the final pREP-Delta adhE1-A1A4 plasmid. This plasmid was then introduced into *ΔCA_C1502Δupp* strain to yield the *ΔCA_C1502ΔuppΔadhE1::catP-A1A4* strain.

Deletion of adhE2

For the *adhE2* (CA_P0035) replacement-deletion, the pREP-Delta adhE2-catP*-upp was constructed using the same procedures as for pREP-Delta adhE1-catP*-upp, excepted that the 1 kb upstream and 0.9 kb downstream homology regions immediately surrounding the *adhE2*

gene (CA_P0035) were PCR amplified using pairs of primers adhE2-1/adhE2-2 and adhE2-3/adhE2-4, with *NruI* restriction site replacing *StuI* restriction site in the adhE2-2 and adhE2-3 primers.

Table S3.1. Primers, strains, and plasmids used in this study

Primer	Sequence
Ldh-1	AAAAGGATCCGCTTTAAAATTTGGAAAGAGGAAGTTGTG
Ldh-2	GGGGAGGCCTAAAAAGGGGGTTAGAAATCTTTAAAAATTTCTCTATAGAGCCCATC
Ldh-3	CCCCCTTTTTAGGCCTCCCCGGTAAAAGACCTAAACTCCAAGGGTGGAGGCTAGGTC
Ldh-4	AAAAGGATCCCCCATTGTGGAGAATATTCCAAAGAAGAAAATAATTGC
FRT-CM F1	TACAGGCCTTGAGCGATTGTGTAGGCTGGAGCTGCTTCGAAGTTCCTATACTTTCTAGAGAATAGGAACTTCGGAATAGGAACTTCGGTTGGAATGGCGTGTGTGTTAGCCAAAGCTCCTGCAGGTCG
FRT-CM F2	AACAGGCCTGGGATGTAACGCACTGAGAAGCCCATGGTCCATATGAATATCCTCCTTAGTTCCTATTCCGAAGTTCCTATTCTCTAGAAAGTATAGGAACTTCTCACACAGGAAACAGCTATGACCATG
REP-UPP F	AAAACAGCTGGGAGGAATGAAATAATGAGTAAAGTTACAC
REP-UPP R	AAAACAGCTGTTATTTTGTACCGAATAATCTATCTCCAGC
adhE1-0	5’-CCAGCCTAATGTAGGTATATCCTACG-3’
adhE1-1	AAAAAGATCTGCTTTAGACGCAGAACCTGAAAAACCCTC

adhE1-2	GGGGAGGCCTAAAAAGGGGG**TTA**CATTTCTTGCGAGTAACAAGAG AATTTTTTTTGAGC
adhE1-3	CCCCCTTTTTAGGCCTCCCCGCACTAGATGATCAATGCACAGGCGC
adhE1-4	AAAAAGATCTGTAACATCTACGTGACCACCACGG
adhE1-5	CATTTACTAAATCCATAGCTCCACCC
adhE1-A1	TAAATTTAAAGATTTAGGCATAGAAATCGATGATAAAAAAATACTT AACGGAAAATTTTTAGTATAACTGGGATGTAACGCACTGAGAAGC CC
adhE1-A2	CTTAATTTGTAGACTTCTGAAATAATACTACATTTGAGCGATTGTGT AGGCTGGAGCTGC
adhE1-A3	ATGTAGTATTATTTCAGAAGTCTACAAATTAAG
adhE1-A4	TAAAAAGTAGTTGAAATATGAAGGTTTACATAAATATACACTTCTT TCTAAAATATTTATTATATTTTAAAAATAATGTC
adhE1-3D	AACTATGGCAGGTATGGCATCCGC
adhE1-5R	GTCTTCAACTAAGCCCATACCGG
adhE2-0	TATCTGGAAGCGGAAGTATAGGTGG
adhE2-1	AAAAAGATCTAGATTTAATTGTAAGCGGCTCTTCCCG
adhE2-2	GGGGTCGCGAAAAAAGGGGGTTATTCTTTTTGATTTGTAACTTTCA TTTATATACACTCC
adhE2-3	CCCCCTTTTTTCGCGACCCCGATAAAATGTCAGAGCTTGCTTTTGAT GACC
adhE2-4	AAAAAGATCTGGTGCTATTACAGGAACGCTTATGGC
adhE2-5	GGGGTACATCAGCGTATATAAGACC

adhE2-3D	GAAGCATATGTTTCGGTTATGGCTACGG
adhE2-5R	TTCTTTCTTTAGCTGCGGCTATGGCAC
FLPI-D	AAAAGGATCCAAAAGGAGGGATTAAAATGCCACAATTTGGTATATTATGTAAAACACCACCT
FLPI-R	AAATGGCGCCGCGTACTTATATGCGTCTATTTATGTAGGATGAAAGGTA

Strain or plasmid	**Relevant characteristics**	**Source**
***C. acetobutylicum* ATCC 824**		
ΔCA_C1502Δupp	Deletion of *upp* gene (CA_C2879) encoding uracil phosphoribosyl transferase and *CA_C1502* gene encoding the type II restriction endonuclease, control strain in this study	(Croux *et al.*, 2016, Yoo *et al.*, 2015)
ΔCA_C1502ΔuppΔadhE1::catP	Replacement of *adhE1* gene (CA_P0162) by the *catP* cassette	This study
ΔCA_C1502ΔuppΔadhE1	Derived from *ΔCA_C1502 Δupp ΔadhE1::catP*, *catP* cassette removed	This study
ΔCA_C1502ΔuppΔadhE1::catP-A1A4	Derived from *ΔCA_C1502 ΔuppΔadhE1::catP*, sol operon promoter location changed from upstream of the latter FRT to downstream of that, used for the chemostats	This study

ΔCA_C1502ΔuppΔadhE2::catP	Replacement of *adhE2* gene (CA_P0035) by the *catP* cassette, used for the chemostats	This study
E. coli		
Top10		Invitrogen
Plasmid		
pSOS95		(Tummala *et al.*, 1999)
pSOS95-MLS^r	Acetone operon Pthl-ctfA-ctfB-adc eliminated, MLS^r	(Zigha, 2013)
pSOS95-upp	Derived from pSOS95-MLS^r, upp gene inserted	(Zigha, 2013)
pREP-Delta adhE1-catP-upp	Derived from pSOS95-upp, adhE1-catP cassette inserted	This study
pSOS95-upp-flp S2	Derived from pSOS95-upp, flp gene inserted	(Zigha, 2013, Croux *et al.*, 2016)
pREP-Delta adhE1-A1A4	Derived from pREP-Delta adhE1-catP-upp, sol operon promoter location changed from upstream of the latter FRT to downstream of that	This study
pREP-Delta adhE2-catP-upp	Derived from pREPcel48A::upp-catP-11, adhE2-catP cassette inserted	This study

Antibiotic resistance cassette

FRT-CatP cassette	Amplified from pSOS94-Cm^c using primer FRT-CM F1 and FRT-CM F2	(Sillers *et al.*, 2008a)

Table S3.2. Four-fold increased or decreased genes under acidogenesis in *ΔadhE1*

Gene number	Function	adhE1 /Ctrl	Control	adhE1
Increase				
CAC0102	O-acetylhomoserine sulfhydrylase	28.7	0.06±0	1.79±0.75
CAC0103	Adenylylsulfate kinase	32.55	0.07±0	2.17±1.03
CAC0104	Adenylylsulfate reductase, subunit A	48.44	0.06±0	3.08±1.47
CAC0105	Ferredoxin	30.78	0.07±0	2.14±0.96
CAC0106	ABC-type probable sulfate transporter, periplasmic binding protein	26.09	0.12±0	3.07±1.56
CAC0107	ABC-type sulfate transporter, ATPase component	22.86	0.07±0.01	1.61±0.88
CAC0108	ABC-type probable sulfate transporter, permease protein	35.38	0.07±0	2.49±1.45
CAC0109	Sulfate adenylate transferase, CysD subfamily	42.53	0.08±0	3.59±2.17
CAC0110	GTPase, sulfate adenylate transferase subunit 1	54.78	0.14±0.01	7.47±4.57
CAC0117	Chemotaxis protein cheY homolog	8.34	0.07±0	0.57±0.18
CAC0118	Chemotaxis protein cheA	11	0.07±0.01	0.78±0.25
CAC0119	Chemotaxis protein cheW	13.83	0.08±0.01	1.12±0.36
CAC0120	Membrane-associated methyl-accepting chemotaxis protein with HAMP domain	6.93	0.07±0	0.52±0.17
CAC0390	Cystathionine gamma-synthase	4.77	0.69±0.03	3.3±0.61
CAC0391	Cystathionine beta-lyase	4.6	0.26±0.01	1.19±0.15
CAC0422	Transcriptional antiterminator licT	4.72	1.08±0.27	5.09±2.35
CAC0423	Fusion: PTS system, beta-glucosides specific IIABC component	5.45	7.23±1.07	39.43±21.61
CAC0424	Fructokinase	5.59	2.8±0.18	15.65±7.99
CAC0425	Sucrase-6-phosphate hydrolase (gene sacA)	6.42	1.55±0.21	9.98±5.38

CAC0466	Hypothetical protein	∞	0±0	0.27±0.17
CAC0467	Uncharacterized membrane protein, homolog of YDAH B.subtilis	18.03	0.09±0	1.69±0.64
CAC0468	HAD superfamily hydrolase	20.33	0.1±0.01	1.94±0.93
CAC0751	Permease	9.95	0.57±0.03	5.67±0.06
CAC0818	Diguanylate cyclase/phosphodiesterase domain (GGDEF) containing protein	7.68	0.09±0.01	0.67±0.26
CAC0878	Amino acid ABC transporter permease component	5.61	0.13±0	0.7±0.34
CAC0879	ABC-type polar amino acid transport system, ATPase component	8.29	0.79±0.03	6.52±3.32
CAC0880	Periplasmic amino acid binding protein	9.5	0.68±0.06	6.44±3.18
CAC0930	Cystathionine gamma-synthase	4.58	0.13±0.04	0.61±0.14
CAC1031	FeoB-like GTPase, responsible for iron uptake	4.24	0.21±0.01	0.89±0.13
CAC1032	Predicted transcriptional regulator	4.44	0.13±0.01	0.59±0.2
CAC1353	Phosphotransferase system IIC component, possibly N-acetylglucosamine-specific	5.55	0.3±0.02	1.68±0.36
CAC1387	Membrane associated chemotaxis sensory transducer protein (MSP domain and HAMP domain)	10.86	0.17±0.01	1.84±0.64
CAC1392	Glutamine phosphoribosylpyrophosphate amidotransferase	4.2	0.53±0.03	2.21±0.23
CAC1394	Folate-dependent phosphoribosylglycinamide formyltransferase	4.11	0.34±0.02	1.39±0.08
CAC1405	Beta-glucosidase	5.16	6±0.61	30.95±15.6
CAC1406	Transcriptional antiterminator (BglG family)	4.41	11.33±2.2	49.91±22.5
CAC1407	PTS system, beta-glucosides-specific IIABC component	13.76	0.29±0.04	4.03±2.51
CAC1408	Phospho-beta-glucosidase	15.57	0.39±0.06	6.11±3.77
CAC1524	Methyl-accepting chemotaxis-like domain (chemotaxis sensory transducer)	8.14	0.07±0	0.6±0.21

CAC1525	Uncharacterized protein, homolog of PHNB E.coli	8.72	0.07±0	0.65±0.23
CAC1862	Hypothetical protein	6.54	0.14±0.01	0.89±0.31
CAC1863	Hypothetical protein	10.43	0.07±0	0.75±0.31
CAC2072	Stage IV sporulation protein B, SpoIVB	∞	0±0	0.39±0.03
CAC2235	Cysteine synthase/cystathionine beta-synthase, CysK	8.27	3.22±0.22	26.61±5.08
CAC2236	Uncharacterized conserved protein of YjeB/RRF2 family	4.29	2.22±0.49	9.5±0.84
CAC2241	Cation transport P-type ATPase	7.92	0.44±0.04	3.51±0.95
CAC2242	Predicted transcriptional regulator, arsE family	5.01	0.15±0.03	0.74±0.11
CAC2521	Hypothetical protein, CF-41 family	4.33	0.21±0.01	0.9±0.07
CAC2533	Protein containing ChW-repeats	∞	0±0	0.72±0.26
CAC2585	6-pyruvoyl-tetrahydropterin synthase related domain; conserved membrane protein	17.69	0.07±0	1.25±0.4
CAC2586	Predicted membrane protein	19.16	0.07±0	1.25±0.44
CAC2587	GGDEF domain containing protein	∞	0±0	0.22±0.04
CAC2588	Glycosyltransferase	51.95	0.15±0.01	7.86±2.82
CAC2589	Glycosyltransferase	20.76	0.06±0	1.33±0.53
CAC2590	Uncharacterized conserved membrane protein;	28.44	0.06±0	1.77±0.69
CAC2591	Hypothetical protein, CF-41 family	∞	0±0	2.61±1.01
CAC2592	6-pyruvoyl-tetrahydropterin synthase related domain; conserved membrane protein	28.02	0.09±0.01	2.39±1.02
CAC2605	Transcriptional regulator (TetR/AcrR family)	28.28	0.13±0.01	3.73±1.4
CAC2650	Dihydroorotate dehydrogenase	6.08	0.41±0.02	2.5±0.08
CAC2651	Dihydroorotate dehydrogenase electron transfer subunit	8.24	0.25±0.02	2.09±0.16
CAC2652	Orotidine-5'-phosphate decarboxylase	8.55	0.54±0.04	4.6±0.58
CAC2653	Aspartate carbamoyltransferase regulatory subunit	8.43	0.85±0.02	7.17±0.22

CAC2654	Aspartate carbamoyltransferase catalytic subunit	7.26	0.7±0.01	5.1±0.08
CAC2816	Hypothetical protein, CF-17 family	6	0.1±0	0.57±0.13
CAC2849	Proline/glycine betaine ABC-type transport system, permease component fused to periplasmic component	6.81	1.83±0.08	12.44±0.65
CAC2850	Proline/glycine betaine ABC-type transport system, ATPase component	6.96	1.74±0.19	12.12±0.56
CAC2937	Ketopantoate reductase PanE/ApbA	4.83	0.11±0	0.52±0.06
CAC3049	Glycosyltransferase	4.79	0.09±0	0.43±0.07
CAC3050	AMSJ/WSAK related protein, possibly involved in exopolysaccharide biosynthesis	4.7	0.11±0	0.5±0.09
CAC3051	Glycosyltransferase	5.16	0.11±0	0.55±0.09
CAC3052	Glycosyltransferase	5.59	0.12±0	0.65±0.11
CAC3053	Histidinol phosphatase related enzyme	7.03	0.17±0.01	1.16±0.18
CAC3054	Phosphoheptose isomerase	6.69	0.23±0.01	1.55±0.35
CAC3055	Sugar kinase	5.9	0.31±0.01	1.85±0.34
CAC3056	Nucleoside-diphosphate-sugar pyrophosphorylase	6.37	0.39±0.03	2.49±0.61
CAC3057	Glycosyltransferase	12.36	0.36±0.03	4.41±1.19
CAC3058	Mannose-1-phosphate guanylyltransferase	9.94	0.3±0.01	2.98±0.62
CAC3059	Sugar transferases	13.47	0.77±0.03	10.43±2.79
CAC3325	Periplasmic amino acid binding protein	18.24	0.11±0	1.93±0.82
CAC3326	Amino acid ABC-type transporter, permease component	19.82	0.11±0.01	2.11±0.98
CAC3327	Amino acid ABC-type transporter, ATPase component	28.33	0.56±0.1	15.77±7.65
CAC3461	Hypothetical protein	4.52	0.24±0.03	1.11±0.22
CAC3556	Probable S-layer protein;	4.18	1.92±0.24	8.04±1.07
CAC3636	Oligopeptide ABC transporter, ATPase component	4.23	0.97±0.07	4.11±1.17

CAC3647	Transition state regulatory protein AbrB	4.92	0.75±0.03	3.69±0.69
CAP0028	HTH transcriptional regulator TetR family	13.55	0.44±0.03	6.03±0.34
CAP0029	Permease MDR-related	∞	0±0	12.2±1.27
CAP0030	Isochorismatase	385.91	0.06±0	24.38±3.46
CAP0031	Transcriptional activator HLYU, HTH of ArsR family	46.17	0.69±0.38	32.04±4.76
CAP0032	Rhodanese-like domain	4.22	0.15±0.01	0.63±0.07
CAP0033	Hypothetical protein	4.76	0.91±0.03	4.35±0.48
CAP0035	Aldehyde-alcohol dehydrogenase, ADHE1	5.44	0.42±0.02	2.31±0.6
CAP0071	Possible xylan degradation enzyme (alpha/beta hydrolase domain and ricin-B-like domain)	4.38	0.07±0	0.31±0.12
CAP0114	Possible beta-xylosidase, family 43 of glycosyl hydrolases	16.44	0.23±0.03	3.85±1.87
CAP0115	Endo-1,4-beta-xylanase XynD B.subtilis ortholog (family 43 glycosyl hydrolase and cellulose-binding domain)	19.51	0.3±0.03	5.9±2.78
CAP0116	Xylanase, glycosyl hydrolase family 10	32.42	0.11±0.01	3.69±1.3
CAP0117	Possible beta-xylosidase diverged, family 5/39 of glycosyl hydrolases and alpha-amylase C (Greek key) C-terminal domain	56.53	0.24±0.03	13.65±4.85
CAP0118	Possible xylan degradation enzyme (glycosyl hydrolase family 30-like domain and Ricin B-like domain)	54.97	0.22±0.02	11.95±4.91
CAP0119	Possible xylan degradation enzyme (glycosyl hydrolase family 30-like domain and Ricin B-like domain)	46.44	0.12±0.01	5.59±2.18
CAP0120	Possible xylan degradation enzyme (glycosyl hydrolase family 43-like domain, cellulose-binding domain and Ricin B-like domain)	36.19	0.1±0.01	3.53±1.31
Decrease				
CAC0029	Distantly related to cell wall-associated hydrolases, similar to yycO Bacillus subtilis	0.22	5.15±0.37	1.12±0.84

CAC0035	Serine/threonine phosphatase (inactivated protein)	0.25	1.57±0.06	0.39±0.18
CAC0078	Accessory gene regulator protein B	0.04	1.82±0.62	0.07±0.02
CAC0079	Hypothetical protein	0	40.95±4.74	0.19±0.19
CAC0082	Predicted membrane protein	0.02	40.84±3.37	0.8±0.66
CAC0141	Membrane permease, predicted cation efflux pumps	0.24	8.01±0.63	1.89±0.66
CAC0204	Sortase (surface protein transpeptidase), YHCS B.subtilis ortholog	0.18	3.65±0.24	0.66±0.29
CAC0205	Predicted phosphohydrolases, Icc family	0.21	16.4±0.6	3.48±3.13
CAC0206	Uncharacterized conserved membrane protein	0.17	5.06±0.47	0.84±0.42
CAC0310	Regulators of stationary/sporulation gene expression, abrB B.subtilis ortholog	0.15	7.79±3.79	1.14±0.52
CAC0353	2,3-cyclic-nucleotide 2'phosphodiesterase (duplication)	0.19	2.19±0.05	0.43±0.29
CAC0381	Methyl-accepting chemotaxis protein	0.18	2.07±0.05	0.37±0.22
CAC0403	Secreted protein contains fibronectin type III domains	0.25	0.6±0.03	0.15±0.02
CAC0437	Sensory transduction histidine kinase	0.15	1.44±0.02	0.22±0.13
CAC0537	Acetylxylan esterase, acyl-CoA esterase or GDSL lipase family, strong similarity to C-terminal region of endoglucanase E precursor	0.15	20.85±1.01	3.07±1.79
CAC0542	Methyl-accepting chemotaxis protein	0.21	1.74±0.17	0.37±0.36
CAC0658	Fe-S oxidoreductase	0.24	0.73±0.04	0.18±0.03
CAC0660	Hypothetical protein, CF-26 family	0.17	5.73±0.37	0.95±0.24
CAC0746	Secreted protease metal-dependent protease	0.16	4.11±0.14	0.68±0.18
CAC0814	3-oxoacyl-[acyl-carrier-protein] synthase III	0.11	6.25±0.26	0.72±0.43
CAC0815	Methyl-accepting chemotaxis protein	0.13	3.4±0.06	0.43±0.28
CAC0816	Lipase-esterase related protein	0.17	3.77±0.12	0.66±0.49

CAC0946	ComE-like protein, Metallo beta-lactamase superfamily hydrolase, secreted	0.18	7.6±0.56	1.35±1.22
CAC1010	Predicted phosphohydrolase, Icc family	0.21	6.5±0.44	1.37±0.85
CAC1022	Thioesterase II of alpha/beta hydrolase superfamily	0.22	0.87±0.03	0.19±0.12
CAC1078	Predicted phosphohydrolase, Icc family	0.17	6.77±0.47	1.18±0.74
CAC1079	Uncharacterized protein, related to enterotoxins of other Clostridiales	0.15	1.27±0.2	0.19±0.08
CAC1080	Uncharacterized protein, probably surface-located	0.11	20.76±0.39	2.37±1.73
CAC1081	Uncharacterized protein, probably surface-located	0.13	7.47±0.13	1.01±0.7
CAC1532	Protein containing ChW-repeats	0.22	1.98±0.08	0.44±0.25
CAC1766	Predicted sigma factor	0.19	0.34±0.03	0.06±0
CAC1775	Predicted membrane protein	0.16	5.53±0.37	0.87±0.61
CAC1868	Uncharacterized secreted protein, homolog YXKC Bacillus subtilis	0.22	1.01±0.1	0.22±0.14
CAC1989	ABC-type iron (III) transport system, ATPase component	0.18	2.78±0.1	0.5±0.18
CAC1991	Uncharacterized protein, YIIM family	0.23	1.66±0.1	0.39±0.15
CAC1993	Molybdenum cofactor biosynthesis enzyme MoaA, Fe-S oxidoreductase	0.23	0.45±0.02	0.1±0.04
CAC1994	Molybdopterin biosynthesis enzyme, MoaB	0.22	0.82±0.09	0.18±0.07
CAC1996	Hypothetical protein	0.19	1.45±0.16	0.28±0.12
CAC1997	Predicted glycosyltransferase	0.19	1.45±0.03	0.28±0.12
CAC1998	ABC-type transport system, ATPase component	0.19	1.31±0.1	0.24±0.13
CAC1999	Uncharacterized protein related to hypothetical protein Cj1507c from Campylobacter jejuni	0.2	1.14±0.07	0.23±0.12
CAC2000	Indolepyruvate ferredoxin oxidoreductase, subunit beta	0.19	1.48±0.05	0.27±0.15
CAC2001	Indolepyruvate ferredoxin oxidoreductase, subunit alpha	0.13	5.57±0.13	0.75±0.32
CAC2002	Predicted iron-sulfur flavoprotein	0.16	1.97±0.06	0.31±0.13

CAC2003	Predicted permease	0.16	0.89±0.02	0.14±0.05
CAC2004	Siderophore/Surfactin synthetase related protein	0.1	4.01±0.25	0.42±0.1
CAC2005	Siderophore/Surfactin synthetase related protein	0.12	2.22±0.3	0.27±0.08
CAC2006	Enzyme of siderophore/surfactin biosynthesis	0.15	0.96±0.19	0.15±0.05
CAC2007	Predicted glycosyltransferase	0.09	5.87±0.14	0.51±0.13
CAC2008	3-oxoacyl-(acyl-carrier-protein) synthase	0.11	2.25±0.14	0.26±0.05
CAC2009	3-Hydroxyacyl-CoA dehydrogenase	0.1	3.83±0.14	0.37±0.12
CAC2010	Predicted Fe-S oxidoreductase	0.09	5.38±0.16	0.49±0.2
CAC2011	Possible 3-oxoacyl-[acyl-carrier-protein] synthase III	0.12	3.32±0.16	0.41±0.15
CAC2012	Enoyl-CoA hydratase	0.12	2.31±0.07	0.28±0.13
CAC2013	Hypothetical protein	0.12	4.33±0.23	0.54±0.27
CAC2014	Predicted esterase	0.12	5.18±0.07	0.63±0.3
CAC2015	Hypothetical protein	0.15	2.28±0.08	0.33±0.16
CAC2016	Enoyl-CoA hydratase	0.12	13.81±0.63	1.7±0.83
CAC2017	Acyl carrier protein	0.15	3.51±0.12	0.51±0.29
CAC2018	Aldehyde:ferredoxin oxidoreductase	0.12	3.69±0.15	0.46±0.22
CAC2019	Malonyl CoA-acyl carrier protein transacylase	0.12	5.07±0.78	0.61±0.31
CAC2020	Molybdopterin biosynthesis enzyme, MoeA, fused to molibdopterin-binding domain	0.2	1.26±0.13	0.25±0.13
CAC2021	Molybdopterin biosynthesis enzyme, MoeA (short form)	0.24	2.88±0.54	0.7±0.28
CAC2023	Membrane protein, related to copy number protein COP from Clostridium perfringens plasmid pIP404 (GI:116928)	0.22	0.81±0.01	0.18±0.08
CAC2026	Predicted flavodoxin	0.2	3.83±0.2	0.77±0.49
CAC2107	Contains cell adhesion domain	0.2	0.87±0.03	0.18±0.15
CAC2293	Hypothetical secreted protein	0.13	2.47±0.26	0.31±0.23

CAC2517	Extracellular neutral metalloprotease, NPRE	0.17	1.63±0.16	0.27±0.07
CAC2518	Extracellular neutral metalloprotease, NPRE (fragment or C-term. domain)	0.22	1.53±0.37	0.33±0.18
CAC2581	6-pyruvoyl-tetrahydropterin synthase related domain; conserved membrane protein	0.24	0.73±0.01	0.17±0.08
CAC2663	Protein containing cell-wall hydrolase domain	0.23	1.65±0.06	0.38±0.2
CAC2695	Diverged Metallo-dependent hydrolase(Zn) of DD-Peptidase family; peptodoglycan-binding domain	0.17	2.79±0.11	0.47±0.35
CAC2807	Endo-1,3(4)-beta-glucanase family 16	0.21	78.48±1.92	16.84±17.3
CAC2808	Beta-lactamase class C domain (PBPX family) containing protein	0.2	2.67±0.25	0.53±0.27
CAC2809	Predicted HD superfamily hydrolase	0.14	4.61±0.4	0.66±0.33
CAC2810	Possible glucoamylase (diverged), 15 family	0.14	15.81±1.25	2.26±1.21
CAC2944	N-terminal domain intergin-like repeats and c-terminal- cell wall-associated hydrolase domain	0.23	5.72±0.45	1.32±0.61
CAC3070	Glycosyltransferase	0.21	4.34±0.23	0.9±0.81
CAC3071	Glycosyltransferase	0.21	5.54±0.28	1.15±1.04
CAC3072	Mannose-1-phosphate guanylyltransferase	0.18	9.16±0.51	1.6±1.49
CAC3073	Sugar transferase involved in lipopolysaccharide synthesis	0.23	4.21±0.85	0.96±0.91
CAC3085	TPR-repeat-containing protein; Cell-adhesion domain;	0.25	2.01±0.12	0.49±0.43
CAC3086	Protein containing cell adhesion domain	0.2	3.81±0.28	0.75±0.58
CAC3175	Hypothetical protein	0.21	3.62±2.52	0.76±0.12
CAC3251	Sensory transduction protein containing HD_GYP domain	0.2	1.91±0.03	0.39±0.27
CAC3264	Uncharacterized conserved protein, YTFJ B.subtilis ortholog	0.19	78.48±1.92	14.92±1.31
CAC3265	Predicted membrane protein	0.08	2.24±0.13	0.19±0.02
CAC3266	Hypothetical protein	0.07	8.71±0.16	0.63±0.03

CAC3267	Specialized sigma subunit of RNA polymerase	0.15	0.78±0.02	0.11±0
CAC3280	Possible surface protein, responsible for cell interaction; contains cell adhesion domain and ChW-repeats	0.23	0.55±0.07	0.13±0.05
CAC3408	NADH oxidase (two distinct flavin oxidoreductase domains)	0.03	5.91±0.22	0.16±0.07
CAC3409	Transcriptional regulators, LysR family	0.02	23.82±2.8	0.38±0.26
CAC3412	Predicted protein-S-isoprenylcysteine methyltransferase	0.22	1.55±0.04	0.33±0.19
CAC3422	Sugar:proton symporter (possible xylulose)	0.05	5.86±0.67	0.3±0.02
CAC3423	Acetyltransferase (ribosomal protein N-acetylase subfamily)	0.04	8.08±0.35	0.36±0.03
CAC3521	Hypothetical protein	0.14	8.82±0.24	1.23±0.46
CAC3522	Hypothetical protein, CF-7 family	0.14	6.64±0.43	0.95±0.29
CAC3523	Hypothetical protein, CF-7 family	0.15	2.36±0.17	0.36±0.08
CAC3524	Hypothetical protein, CF-7 family	0.19	2.35±0.08	0.45±0.11
CAC3558	Probable S-layer protein;	0.24	1.84±0.21	0.44±0.18
CAC3612	Hypothetical protein	0.18	0.85±0.07	0.16±0.05
CAP0053	Xylanase, glycosyl hydrolase family 10	0.24	1.05±0.13	0.25±0.06
CAP0054	Xylanase/chitin deacetylase family enzyme	0.24	1.88±0.26	0.44±0.04
CAP0057	Putative glycoportein or S-layer protein	0.21	2.53±0.14	0.54±0.02
CAP0135	Oxidoreductase	0.25	16.08±0.99	3.94±2.61
CAP0136	AstB/chuR/nirj-related protein	0.25	2.99±0.1	0.74±0.42
CAP0148	Phospholipase C	0.22	1.04±0.06	0.23±0.11
CAP0174	Membrane protein	0.25	1.06±0.23	0.26±0.13

Table S3.3. Four-fold increased or decreased genes under acidogenesis in *ΔadhE2*

Gene number	Function	adhE2 /Ctrl	Control	adhE2
Increase				
CAC0040	Uncharacterized small conserved protein, homolog of yfjA/yukE B.subtilis	4.11	4.33±0.11	17.78±0.79
CAC0041	Uncharacterized small conserved protein, homolog of yfjA/yukE B.subtilis	4.14	0.1±0.01	0.42±0.06
CAC0042	Hypothetical protein, CF-1 family	5.71	0.93±0.02	5.34±0.19
CAC0043	Hypothetical protein, CF-3 family	5.79	0.54±0.03	3.12±0.29
CAC0044	Predicted membrane protein	5.49	0.86±0.06	4.71±0.28
CAC0045	TPR-repeat-containing protein	5.11	0.35±0.02	1.8±0.04
CAC0047	Uncharacterized small conserved protein, homolog of yfjA/yukE B.subtilis	4.91	0.77±0.03	3.79±0.12
CAC0048	Hypothetical protein, CF-17 family	5.19	0.73±0.03	3.79±0.17
CAC0049	Hypothetical protein, CF-17 family	4.18	0.14±0.02	0.59±0.11
CAC0056	Hypothetical protein	5.48	2.06±0.28	11.29±0.91
CAC0057	Hypothetical protein	5.29	5.97±0.54	31.56±1.37
CAC0058	Hypothetical protein	5.39	5.86±0.64	31.6±0.97
CAC0059	Hypothetical protein	5.48	2.89±0.14	15.81±1.9
CAC0060	Predicted membrane protein	4.96	1.93±0.07	9.58±0.56
CAC0061	Phage-related protein, gp16	6.24	1.64±0.2	10.21±0.71
CAC0062	Phage-related protein	5.56	4.63±0.56	25.72±1.1
CAC0063	Phage-related protein	4.61	0.52±0.03	2.4±0.15
CAC0064	Hypothetical protein	4.39	0.96±0.08	4.23±0.29
CAC0065	Hypothetical protein	4.69	0.28±0.01	1.34±0.06
CAC0102	O-acetylhomoserine sulfhydrylase	20.49	0.06±0	1.28±0.08
CAC0103	Adenylylsulfate kinase	22.06	0.07±0	1.47±0.17

CAC0104	Adenylylsulfate reductase, subunit A	28.89	0.06±0	1.83±0.17
CAC0105	Ferredoxin	21.84	0.07±0	1.52±0.04
CAC0106	ABC-type probable sulfate transporter, periplasmic binding protein	14.54	0.12±0	1.71±0.05
CAC0107	ABC-type sulfate transporter, ATPase component	13.03	0.07±0.01	0.92±0.04
CAC0108	ABC-type probable sulfate transporter, permease protein	19.05	0.07±0	1.34±0.08
CAC0109	Sulfate adenylate transferase, CysD subfamily	26.82	0.08±0	2.26±0.04
CAC0110	GTPase, sulfate adenylate transferase subunit 1	42.48	0.14±0.01	5.79±0.35
CAC0116	Carbone-monoxide dehydrogenase, beta chain	6.2	0.64±0.16	3.95±1.53
CAC0117	Chemotaxis protein cheY homolog	6.69	0.07±0	0.46±0.04
CAC0118	Chemotaxis protein cheA	8.24	0.07±0.01	0.58±0.06
CAC0119	Chemotaxis protein cheW	9.52	0.08±0.01	0.77±0.08
CAC0120	Membrane-associated methyl-accepting chemotaxis protein with HAMP domain	5.29	0.07±0	0.39±0.04
CAC0208	Predicted membrane protein; CF-20 family	11.53	0.51±0.03	5.84±0.18
CAC0209	Predicted membrane protein; CF-20 family	10.41	0.21±0.01	2.16±0.03
CAC0539	Beta-mannanase ManB, contains ChW-repeats	18.97	0.1±0	1.99±0.1
CAC0540	Beta-mannanase ManB-like enzyme, contains ChW-repeats	28.45	0.22±0	6.21±0.27
CAC0623	Hypothetical protein	5.18	0.28±0.03	1.48±0.19
CAC0682	Ammonium transporter (membrane protein nrgA)	8.97	0.24±0.01	2.17±0.16
CAC0706	Endo-1,4-beta glucanase (fused to two ricin-B-like domains)	7.5	1.19±0.13	8.92±0.84
CAC0754	Hypothetical protein	7.48	0.1±0.01	0.73±0.12
CAC0765	Fe-S oxidoreductase	25.78	0.14±0.01	3.54±0.11
CAC0766	Predicted transcriptional regulator (MerR family)	34.25	0.31±0.04	10.58±0.43
CAC0767	Fe-S oxidoreductase	15.02	0.59±0.05	8.87±0.25

CAC0771	Cobalamin biosynthesis protein CbiM	8.86	0.29±0.03	2.52±0.09
CAC0772	Cobalt permease	8.2	0.14±0.01	1.14±0.04
CAC0773	ABC-type cobalt transport protein ATPase component	7.31	0.12±0.01	0.88±0.04
CAC0774	Uncharacterized conserved protein	5.83	0.09±0	0.5±0.02
CAC0775	ATP-utilizing enzyme of the PP-loop superfamily	8.86	0.25±0.02	2.23±0.01
CAC0776	NCAIR mutase (PurE)-related protein	9.98	0.47±0.02	4.71±0.22
CAC0777	Acetyltransferase (the isoleucine patch superfamily)	8.01	0.17±0.01	1.34±0.07
CAC0878	Amino acid ABC transporter permease component	4.04	0.13±0	0.51±0.03
CAC0879	ABC-type polar amino acid transport system, ATPase component	5.6	0.79±0.03	4.4±0.45
CAC0880	Periplasmic amino acid binding protein	6.5	0.68±0.06	4.41±0.4
CAC0930	Cystathionine gamma-synthase	4.72	0.13±0.04	0.63±0.02
CAC0931	Cysteine synthase	4.26	0.08±0.01	0.34±0.02
CAC1357	Uncharacterized predicted metal-binding protein	5.86	1.11±0.07	6.49±1.14
CAC1392	Glutamine phosphoribosylpyrophosphate amidotransferase	4.47	0.53±0.03	2.34±0.25
CAC1393	Phosphoribosylaminoimidazol (AIR) synthetase	4.07	0.32±0.02	1.31±0.06
CAC1394	Folate-dependent phosphoribosylglycinamide formyltransferase	4.57	0.34±0.02	1.54±0.07
CAC2072	Stage IV sporulation protein B, SpoIVB	∞	0±0	0.4±0
CAC2235	Cysteine synthase/cystathionine beta-synthase, CysK	7.17	3.22±0.22	23.06±1.97
CAC2236	Uncharacterized conserved protein of YjeB/RRF2 family	4.06	2.22±0.49	8.99±0.85
CAC2241	Cation transport P-type ATPase	7.62	0.44±0.04	3.38±0.12
CAC2242	Predicted transcriptional regulator, arsE family	5.22	0.15±0.03	0.77±0.04
CAC2456	Hypothetical protein, CF-40 family	6.09	1.82±0.11	11.08±0.47
CAC2457	Hypothetical protein	6.48	2.06±0.18	13.34±1.5

CAC2521	Hypothetical protein, CF-41 family	5.7	0.21±0.01	1.18±0.04
CAC2533	Protein containing ChW-repeats	∞	0±0	0.31±0.03
CAC2534	HD_GYP hydrolase domain fused to HD hydrolase domain	5.26	0.1±0.02	0.52±0.04
CAC2548	Reductase/isomerase/elongation factor common domain	7.43	0.09±0	0.65±0.02
CAC2717	Ethanolamine ammonia lyase small subunit	4.54	0.1±0	0.43±0.02
CAC2718	Ethanolamine ammonia lyase large subunit	5.74	0.09±0.02	0.54±0
CAC2719	Ethanolamin permease	∞	0±0	0.26±0.01
CAC2720	Sensory protein containing histidine kinase, PAS anf GAF domains	4.43	0.24±0.01	1.07±0.06
CAC2816	Hypothetical protein, CF-17 family	11.2	0.1±0	1.07±0.02
CAC3013	Hypothetical protein	4.66	0.28±0.01	1.28±0.12
CAC3045	CPSB/CAPC ortholog, PHP family hydrolase	5.47	0.17±0.01	0.93±0.04
CAC3047	Uncharacterized membrane protein, putative virulence factor MviN	4.79	0.19±0	0.9±0.03
CAC3048	Uncharacterized conserved membrane protein, possible transporter	6.64	0.1±0.01	0.65±0.02
CAC3049	Glycosyltransferase	7.42	0.09±0	0.67±0.02
CAC3050	AMSJ/WSAK related protein, possibly involved in exopolysaccharide biosynthesis	8.25	0.11±0	0.88±0.02
CAC3051	Glycosyltransferase	9.6	0.11±0	1.01±0.13
CAC3052	Glycosyltransferase	9.91	0.12±0	1.16±0.05
CAC3053	Histidinol phosphatase related enzyme	10.94	0.17±0.01	1.81±0.13
CAC3054	Phosphoheptose isomerase	11.37	0.23±0.01	2.63±0.07
CAC3055	Sugar kinase	10.87	0.31±0.01	3.4±0.05
CAC3056	Nucleoside-diphosphate-sugar pyrophosphorylase	11.28	0.39±0.03	4.4±0.1
CAC3057	Glycosyltransferase	11.92	0.36±0.03	4.25±0.18
CAC3058	Mannose-1-phosphate guanylyltransferase	11.59	0.3±0.01	3.48±0.14
CAC3059	Sugar transferases	12.63	0.77±0.03	9.77±0.39

CAC3234	Uncharacterized conserved protein, YVBJ B.subtilis ortholog with N-terminal C4-type Zn-finger domain	15.12	0.26±0.03	3.95±0.07
CAC3235	Uncharacterized conserved protein, YVBJ B.subtilis homolog	10.9	0.12±0	1.36±0.01
CAC3236	Possible transcriptional regulator from YAEG/LRPR family	4.41	1.05±0.1	4.63±0.32
CAC3274	Possible surface protein, responsible for cell interaction; contains cell adhesion domain and ChW-repeats	16.99	0.32±0.04	5.44±0.22
CAC3275	Possible surface protein, responsible for cell interaction; contains cell adhesion domain and ChW-repeats	5.25	0.13±0.01	0.66±0.06
CAC3325	Periplasmic amino acid binding protein	10.68	0.11±0	1.13±0.05
CAC3326	Amino acid ABC-type transporter, permease component	11.79	0.11±0.01	1.25±0.07
CAC3327	Amino acid ABC-type transporter, ATPase component	16.73	0.56±0.1	9.31±0.53
CAC3357	Hypothetical protein	4.47	0.24±0.02	1.09±0.05
CAC3458	Uncharacterized protein, homolog of B. anthracis (gi:48942631)	17.16	0.49±0.03	8.37±0.16
CAC3459	Homolog of cell division GTPase FtsZ, diverged	26.29	0.6±0.05	15.88±1.22
CAC3461	Hypothetical protein	16.79	0.24±0.03	4.11±0.14
CAC3556	Probable S-layer protein;	10.41	1.92±0.24	19.99±0.98
CAC3583	Predicted permease	4.01	0.32±0.03	1.28±0.1
CAC3585	ABC-type transporter, ATPase component	4.94	1.29±0.06	6.35±0.29
CAC3604	Dihydroxyacid dehydratase	99.3	0.2±0.01	20.26±0.92
CAC3605	High affinity gluconate/L-idonate permease	83.89	0.13±0.01	11.11±2.07
CAC3635	Oligopeptide ABC transporter, ATPase component	4.02	0.69±0.03	2.76±0.12
CAC3636	Oligopeptide ABC transporter, ATPase component	4.68	0.97±0.07	4.55±0.3
CAC3650	HD-GYP domain containing protein	4.35	0.91±0.03	3.96±0.22
CAP0001	Oxidoreductase	5.9	0.11±0	0.64±0.01
CAP0029	Permease MDR-related	∞	0±0	2.44±0.1

CAP0030	Isochorismatase	81.89	0.06±0	5.17±0.11
CAP0031	Transcriptional activator HLYU, HTH of ArsR family	10.93	0.69±0.38	7.59±0.24
CAP0106	1-deoxyxylulose-5-phosphate synthase, dehydrogenase	14.05	0.15±0	2.09±0.07
CAP0117	Possible beta-xylosidase diverged, family 5/39 of glycosyl hydrolases and alpha-amylase C (Greek key) C-terminal domain	4.94	0.24±0.03	1.19±0.06
CAP0118	Possible xylan degradation enzyme (glycosyl hydrolase family 30-like domain and Ricin B-like domain)	5.22	0.22±0.02	1.13±0.1
CAP0119	Possible xylan degradation enzyme (glycosyl hydrolase family 30-like domain and Ricin B-like domain)	4.23	0.12±0.01	0.51±0.05
Decrease				
CAC0078	Accessory gene regulator protein B	0	1.82±0.62	0±0
CAC0079	Hypothetical protein	0	40.95±4.74	0.07±0
CAC0081	Accessory gene regulator protein A	0.13	0.72±0.03	0.09±0
CAC0082	Predicted membrane protein	0	40.84±3.37	0.19±0
CAC0086	Muconate cycloisomerase related protein, ortholog of YKGB B.subtilis	0.15	1.06±0.09	0.16±0.02
CAC0149	Hypothetical protein	0.12	5.36±0.15	0.65±0.05
CAC0154	PTS system, mannitol-specific IIBC component (gene MtlA)	0.21	1.39±0.31	0.29±0.07
CAC0155	Putative regulator of the PTS system for mannitol (gene MltR)	0.24	1.85±0.33	0.44±0.07
CAC0156	PTS system, mannitol-specific IIA domain (Ntr-type) (gene MltF)	0.22	6.45±0.37	1.44±0.07
CAC0193	Uncharacterized conserved membrane protein, affecting LPS biosynthesis	0.2	3.31±0.49	0.67±0.08
CAC0310	Regulators of stationary/sporulation gene expression, abrB B.subtilis ortholog	0.23	7.79±3.79	1.76±0.26
CAC0381	Methyl-accepting chemotaxis protein	0.13	2.07±0.05	0.27±0
CAC0437	Sensory transduction histidine kinase	0.23	1.44±0.02	0.33±0.03
CAC0537	Acetylxylan esterase, acyl-CoA esterase or GDSL lipase family, strong similarity to C-terminal region of endoglucanase E	0.1	20.85±1.01	2.1±0.09

	precursor			
CAC0542	Methyl-accepting chemotaxis protein	0.08	1.74±0.17	0.14±0.01
CAC0543	Methyl-accepting chemotaxis protein	0.25	0.35±0.04	0.09±0
CAC0658	Fe-S oxidoreductase	0	0.73±0.04	0±0
CAC0659	Predicted Zn-dependent peptidase	0	0.52±0.09	0±0
CAC0660	Hypothetical protein, CF-26 family	0.08	5.73±0.37	0.48±0.11
CAC0663	Hypothetical protein	0.21	0.61±0.07	0.13±0.01
CAC0792	D-amino acid aminotransferase	0.15	1.47±0.14	0.23±0.01
CAC0804	Pectate lyase related protein, secreted	0	0.28±0.04	0±0
CAC0814	3-oxoacyl-[acyl-carrier-protein] synthase III	0.02	6.25±0.26	0.13±0
CAC0815	Methyl-accepting chemotaxis protein	0.04	3.4±0.06	0.12±0
CAC0816	Lipase-esterase related protein	0.04	3.77±0.12	0.15±0
CAC1009	Cell wall biogenesis enzyme (N-terminal domain related to N-Acetylmuramoyl-L-alanine amidase and C-terminal domain related to L-alanoyl-D-glutamate peptidase); peptodoglycan-binding domain	0	0.24±0.03	0±0
CAC1010	Predicted phosphohydrolase, Icc family	0.04	6.5±0.44	0.26±0.01
CAC1022	Thioesterase II of alpha/beta hydrolase superfamily	0.11	0.87±0.03	0.09±0
CAC1072	Fe-S oxidoreductase	0	0.21±0.01	0±0
CAC1075	Beta-glucosidase family protein	0.1	0.93±0.13	0.09±0.01
CAC1078	Predicted phosphohydrolase, Icc family	0.04	6.77±0.47	0.26±0.02
CAC1079	Uncharacterized protein, related to enterotoxins of other Clostridiales	0.05	1.27±0.2	0.06±0
CAC1080	Uncharacterized protein, probably surface-located	0.01	20.76±0.39	0.12±0.01
CAC1081	Uncharacterized protein, probably surface-located	0.01	7.47±0.13	0.09±0.01
CAC1084	Beta-glucosidase family protein	0.13	1.02±0.29	0.13±0.04
CAC1085	Alpha-glucosidase	0.17	1.44±0.19	0.24±0.03

CAC1086	Transcriptional regulators of NagC/XylR family	0.15	2.76±0.2	0.41±0.01
CAC1102	Predicted membrane protein	0.16	8.87±1.24	1.43±0.2
CAC1365	Cobalamin biosynthesis protein CbiM	0.16	1.56±0.05	0.25±0.02
CAC1366	Predicted membrane protein	0.18	1.23±0.06	0.22±0.01
CAC1367	Cobalt permease	0.2	0.78±0.01	0.16±0.01
CAC1368	Cobalt transport (ATPase component)	0.18	1.23±0.11	0.22±0.01
CAC1369	Histidinol-phosphate aminotransferase	0.13	4.55±0.54	0.6±0.02
CAC1370	Cobalamin biosynthesis protein CbiG	0.16	1.84±0.04	0.3±0.01
CAC1371	Possible kinase, diverged	0.16	1.86±0.03	0.3±0.01
CAC1372	Cobalamin biosynthesis enzyme CobT	0.16	1.98±0.08	0.33±0.01
CAC1373	Anaerobic Cobalt chelatase, cbiK	0.17	1.35±0.05	0.24±0
CAC1374	Cobyric acid synthase CbiP	0.17	1.79±0.08	0.3±0.01
CAC1375	Cobyrinic acid a,c-diamide synthase CobB	0.2	0.78±0.04	0.16±0.02
CAC1376	Precorrin isomerase, cbiC	0.24	0.62±0.03	0.15±0
CAC1377	Cobalamin biosynthesis protein CbiD	0.17	2.52±0.11	0.43±0.01
CAC1381	precorrin-6x reductase	0.21	1.82±0.09	0.38±0.01
CAC1532	Protein containing ChW-repeats	0.08	1.98±0.08	0.15±0
CAC1580	Hypothetical protein	0.25	3.33±0.13	0.82±0.06
CAC1766	Predicted sigma factor	0	0.34±0.03	0±0
CAC1768	Uncharacterized conserved protein, TraB family	0.12	0.81±0.04	0.1±0
CAC1775	Predicted membrane protein	0.05	5.53±0.37	0.27±0.03
CAC1868	Uncharacterized secreted protein, homolog YXKC Bacillus subtilis	0.18	1.01±0.1	0.18±0
CAC1988	Ferrichrome-binding periplasmic protein	0.17	0.77±0.03	0.13±0
CAC1989	ABC-type iron (III) transport system, ATPase component	0.11	2.78±0.1	0.3±0.01
CAC1990	ABC-type iron (III) transport system, permease component	0.19	0.48±0.01	0.09±0

CAC1991	Uncharacterized protein, YIIM family	0.1	1.66±0.1	0.17±0.01
CAC1992	Molybdenum cofactor biosynthesis enzyme, MoaC	0.18	0.45±0.03	0.08±0
CAC1993	Molybdenum cofactor biosynthesis enzyme MoaA, Fe-S oxidoreductase	0.18	0.45±0.02	0.08±0.01
CAC1994	Molybdopterin biosynthesis enzyme, MoaB	0.11	0.82±0.09	0.09±0
CAC1995	Hypothetical protein	0	0.25±0.04	0±0
CAC1996	Hypothetical protein	0.08	1.45±0.16	0.11±0
CAC1997	Predicted glycosyltransferase	0.07	1.45±0.03	0.11±0
CAC1998	ABC-type transport system, ATPase component	0.07	1.31±0.1	0.1±0
CAC1999	Uncharacterized protein related to hypothetical protein Cj1507c from Campylobacter jejuni	0.07	1.14±0.07	0.08±0
CAC2000	Indolepyruvate ferredoxin oxidoreductase, subunit beta	0.06	1.48±0.05	0.1±0
CAC2001	Indolepyruvate ferredoxin oxidoreductase, subunit alpha	0.04	5.57±0.13	0.2±0
CAC2002	Predicted iron-sulfur flavoprotein	0.05	1.97±0.06	0.09±0
CAC2003	Predicted permease	0.08	0.89±0.02	0.07±0
CAC2004	Siderophore/Surfactin synthetase related protein	0.04	4.01±0.25	0.16±0
CAC2005	Siderophore/Surfactin synthetase related protein	0.05	2.22±0.3	0.11±0.01
CAC2006	Enzyme of siderophore/surfactin biosynthesis	0.07	0.96±0.19	0.07±0
CAC2007	Predicted glycosyltransferase	0.03	5.87±0.14	0.16±0.01
CAC2008	3-oxoacyl-(acyl-carrier-protein) synthase	0.04	2.25±0.14	0.08±0
CAC2009	3-Hydroxyacyl-CoA dehydrogenase	0.03	3.83±0.14	0.1±0.01
CAC2010	Predicted Fe-S oxidoreductase	0.03	5.38±0.16	0.14±0
CAC2011	Possible 3-oxoacyl-[acyl-carrier-protein] synthase III	0.03	3.32±0.16	0.11±0
CAC2012	Enoyl-CoA hydratase	0.04	2.31±0.07	0.09±0
CAC2013	Hypothetical protein	0.03	4.33±0.23	0.12±0.01

CAC2014	Predicted esterase	0.02	5.18±0.07	0.13±0
CAC2015	Hypothetical protein	0.04	2.28±0.08	0.08±0
CAC2016	Enoyl-CoA hydratase	0.02	13.81±0.63	0.26±0.02
CAC2017	Acyl carrier protein	0.03	3.51±0.12	0.09±0.01
CAC2018	Aldehyde:ferredoxin oxidoreductase	0.03	3.69±0.15	0.11±0.01
CAC2019	Malonyl CoA-acyl carrier protein transacylase	0.02	5.07±0.78	0.1±0.01
CAC2020	Molybdopterin biosynthesis enzyme, MoeA, fused to molibdopterin-binding domain	0.07	1.26±0.13	0.08±0.01
CAC2021	Molybdopterin biosynthesis enzyme, MoeA (short form)	0.06	2.88±0.54	0.16±0.03
CAC2022	Molybdopterin biosynthesis enzyme, moaB	0.08	1.84±0.18	0.15±0.01
CAC2023	Membrane protein, related to copy number protein COP from Clostridium perfringens plasmid pIP404 (GI:116928)	0.12	0.81±0.01	0.1±0
CAC2024	Phosphatidylglycerophosphate synthase related protein (fragment)	0.1	1.22±0.06	0.13±0.01
CAC2025	Hypothetical protein	0.09	3.61±0.51	0.31±0.02
CAC2026	Predicted flavodoxin	0.09	3.83±0.2	0.33±0.02
CAC2040	ABC transported MDR-type, ATPase component	0.23	0.48±0.04	0.11±0.01
CAC2107	Contains cell adhesion domain	0.08	0.87±0.03	0.07±0
CAC2226	Enzyme of ILVE/PABC family (branched-chain amino acid aminotransferase/4-amino-4-deoxychorismate lyase)	0.19	7.98±0.85	1.53±0.07
CAC2252	Alpha-glucosidase fused to unknown alpha-amylase C-terminal. domain	0.04	78.48±1.92	3.17±0.27
CAC2287	Acyl-CoA reductase LuxC	0.21	0.71±0.08	0.15±0.01
CAC2288	Acyl-protein synthetase, luxE	0.19	0.94±0.12	0.18±0
CAC2289	Biotin carboxyl carrier protein	0	0.39±0	0±0
CAC2293	Hypothetical secreted protein	0.1	2.47±0.26	0.26±0.03
CAC2382	Single-strand DNA-binding protein, ssb	0.15	0.68±0.03	0.1±0.01
CAC2514	Beta galactosidase	0.24	0.54±0.01	0.13±0

CAC2580	Hypothetical protein, CF-41 family	0	0.2±0.01	0±0
CAC2581	6-pyruvoyl-tetrahydropterin synthase related domain; conserved membrane protein	0.11	0.73±0.01	0.08±0.01
CAC2584	Protein containing ChW-repeats	0.16	0.47±0.01	0.08±0
CAC2597	Hypothetical protein	0.24	1.04±0.02	0.25±0
CAC2610	L-fucose isomerase related protein	0.23	0.74±0.11	0.17±0.01
CAC2611	Hypothetical protein	0.24	0.74±0.06	0.18±0.02
CAC2663	Protein containing cell-wall hydrolase domain	0.09	1.65±0.06	0.15±0.01
CAC2695	Diverged Metallo-dependent hydrolase(Zn) of DD-Peptidase family; peptodoglycan-binding domain	0.12	2.79±0.11	0.33±0.04
CAC2722	RCC1 repeats protein (beta propeller fold)	0.19	1.01±0.02	0.19±0.02
CAC2805	Possible selenocysteine lyase (aminotransferase of NifS family)	0.1	0.83±0.07	0.08±0
CAC2806	Predicted phosphohydrolase, Icc family	0.08	78.48±1.92	6.56±0.11
CAC2807	Endo-1,3(4)-beta-glucanase family 16	0.02	78.48±1.92	1.62±0.18
CAC2808	Beta-lactamase class C domain (PBPX family) containing protein	0.04	2.67±0.25	0.09±0
CAC2809	Predicted HD superfamily hydrolase	0.02	4.61±0.4	0.08±0
CAC2810	Possible glucoamylase (diverged), 15 family	0.01	15.81±1.25	0.2±0.03
CAC2943	N-terminal domain intergin-like repeats and c-terminal - cell wall-associated hydrolase domain	0.14	0.53±0.05	0.07±0
CAC2944	N-terminal domain intergin-like repeats and c-terminal- cell wall-associated hydrolase domain	0.06	5.72±0.45	0.35±0.02
CAC3060	CPSC/CAPB subfamily ATPase	0.24	1.6±0.06	0.39±0.02
CAC3066	Glycosyltransferase	0.13	0.95±0.06	0.13±0.01
CAC3067	Predicted membrane protein	0	0.29±0.03	0±0
CAC3068	Glycosyltransferase	0.1	0.8±0.05	0.08±0.01
CAC3069	Predicted glycosyltransferase	0.08	0.81±0.04	0.07±0
CAC3070	Glycosyltransferase	0.04	4.34±0.23	0.15±0

CAC3071	Glycosyltransferase	0.03	5.54±0.28	0.18±0.01
CAC3072	Mannose-1-phosphate guanylyltransferase	0.02	9.16±0.51	0.22±0
CAC3073	Sugar transferase involved in lipopolysaccharide synthesis	0.03	4.21±0.85	0.13±0
CAC3085	TPR-repeat-containing protein; Cell-adhesion domain;	0.12	2.01±0.12	0.24±0.02
CAC3086	Protein containing cell adhesion domain	0.11	3.81±0.28	0.43±0.03
CAC3251	Sensory transduction protein containing HD_GYP domain	0.11	1.91±0.03	0.2±0
CAC3264	Uncharacterized conserved protein, YTFJ B.subtilis ortholog	0.15	78.48±1.92	11.7±0.94
CAC3265	Predicted membrane protein	0.11	2.24±0.13	0.24±0.03
CAC3266	Hypothetical protein	0.07	8.71±0.16	0.65±0.02
CAC3267	Specialized sigma subunit of RNA polymerase	0.16	0.78±0.02	0.12±0
CAC3279	Possible surface protein, responsible for cell interaction; contains cell adhesion domain and ChW-repeats	0.19	0.36±0.03	0.07±0.01
CAC3280	Possible surface protein, responsible for cell interaction; contains cell adhesion domain and ChW-repeats	0.14	0.55±0.07	0.08±0.01
CAC3298	NADH-dependent butanol dehydrogenase B (BDH II)	0.09	16.31±0.45	1.52±0.11
CAC3319	Signal transduction histidine kinase	0.06	3.14±0.66	0.19±0.02
CAC3320	Predicted secreted protein homolog of yjcM/yhbB B.subtilis	0.08	1.41±0.1	0.11±0.01
CAC3355	Polyketide synthase pksE (short-chain alcohol dehydrogenase,acyl-carrier-protein S-malonyltransferase,3-oxoacyl-(acyl-carrier-protein) synthase I domains)	0	0.4±0.02	0±0
CAC3408	NADH oxidase (two distinct flavin oxidoreductase domains)	0.02	5.91±0.22	0.1±0
CAC3409	Transcriptional regulators, LysR family	0.01	23.82±2.8	0.13±0
CAC3411	Homolog of plant auxin-responsive GH3-like protein	0	0.39±0.01	0±0
CAC3412	Predicted protein-S-isoprenylcysteine methyltransferase	0.06	1.55±0.04	0.09±0
CAC3422	Sugar:proton symporter (possible xylulose)	0.03	5.86±0.67	0.17±0.03

CAC3423	Acetyltransferase (ribosomal protein N-acetylase subfamily)	0.03	8.08±0.35	0.22±0.02
CAC3565	Uncharacterized secreted protein, containing cell adhesion domain	0.14	0.7±0.05	0.1±0
CAC3566	Hypothetical protein, CF-28 family	0.13	0.81±0.1	0.1±0
CAC3612	Hypothetical protein	0	0.85±0.07	0±0
CAC3613	Hypothetical protein	0.21	0.32±0.04	0.07±0
CAP0028	HTH transcriptional regulator TetR family	0.19	0.44±0.03	0.08±0
CAP0035	Aldehyde-alcohol dehydrogenase, ADHE1	0	0.42±0.02	0±0
CAP0053	Xylanase, glycosyl hydrolase family 10	0.09	1.05±0.13	0.1±0.01
CAP0054	Xylanase/chitin deacetylase family enzyme	0.07	1.88±0.26	0.14±0.01
CAP0057	Putative glycoportein or S-layer protein	0.13	2.53±0.14	0.33±0
CAP0058	Rare lipoprotein A RLPA releated protein	0.05	6.1±0.36	0.3±0.03
CAP0072	Hypothetical protein	0.09	1.45±0.08	0.13±0
CAP0098	Alpha-amylase, AmyB	0.19	1.38±0.17	0.26±0.02
CAP0135	Oxidoreductase	0.21	16.08±0.99	3.34±0.18
CAP0136	AstB/chuR/nirj-related protein	0.23	2.99±0.1	0.69±0.03
CAP0137	Similar to C-ter. fragment of UDP-glucuronosyltransferases, YpfP B.subtilis related	0.21	5.84±0.33	1.23±0.05
CAP0138	Diverged, distantly related to biotin carboxylase N-term. fragment.	0.25	5.38±0.07	1.33±0.07
CAP0160	Secreted protein containing cell-adhesion domains	0.2	0.54±0.07	0.11±0.01
CAP0174	Membrane protein	0.14	1.06±0.23	0.15±0

Table S3.4. Four-fold increased or decreased genes under solventogenesis in *ΔadhE1*

Gene number	Function	adhE1 /Ctrl	Control	adhE1
Increase				
CAC0102	O-acetylhomoserine sulfhydrylase	32.98	0.13±0.03	4.2±0.26
CAC0103	Adenylylsulfate kinase	50.51	0.1±0.02	5.14±0.31
CAC0104	Adenylylsulfate reductase, subunit A	64.43	0.12±0.02	7.62±0.27
CAC0105	Ferredoxin	44.64	0.14±0.03	6.36±0.07
CAC0106	ABC-type probable sulfate transporter, periplasmic binding protein	18.89	0.5±0.17	9.4±0.36
CAC0107	ABC-type sulfate transporter, ATPase component	41.92	0.11±0.01	4.52±0.13
CAC0108	ABC-type probable sulfate transporter, permease protein	52.22	0.13±0.02	6.53±0.46
CAC0109	Sulfate adenylate transferase, CysD subfamily	44.6	0.2±0.05	8.76±0.49
CAC0110	GTPase, sulfate adenylate transferase subunit 1	30.99	0.68±0.31	21.08±0.96
CAC0241	ABC-type multidrug transport system, ATP-ase compoment	6.71	0.09±0.02	0.61±0.02
CAC0243	Predicted permease	6.87	0.11±0.01	0.79±0.03
CAC0267	L-lactate dehydrogenase	5.1	0.55±0.17	2.83±0.05
CAC0403	Secreted protein contains fibronectin type III domains	5.32	0.17±0.09	0.93±0.05
CAC0409	Hypothetical protein	4.71	0.49±0.27	2.32±0.09
CAC0718	Ortholog ycnD B.subtilis, nitroreductase	5.2	0.67±0.36	3.48±0.16
CAC0867	Putative permease, ortholog yfkN B.subtilis	4.69	0.52±0.11	2.46±0.05
CAC0879	ABC-type polar amino acid transport system, ATPase component	5	0.82±0.09	4.12±0.08
CAC0880	Periplasmic amino acid binding protein	4.67	0.86±0.05	4±0.17
CAC0930	Cystathionine gamma-synthase	4.1	0.12±0.01	0.5±0.05
CAC0931	Cysteine synthase	4.4	0.1±0.01	0.43±0.02

CAC1283	Molecular chaperones DnaJ (HSP40 family)	4.33	7.34±3.4	31.8±0.28
CAC1284	SAM-dependent methyltransferase	4.43	0.61±0.2	2.72±0.18
CAC1356	Thiamine biosynthesis enzyme ThiH	7.7	1.96±1.44	15.11±0.26
CAC1547	Thioredoxin, trx	7.8	0.23±0.01	1.81±0.05
CAC1548	Thioredoxin reductase	9.47	1±0.07	9.44±0.07
CAC1549	Glutathione peroxidase	9.14	0.69±0.07	6.28±0.42
CAC1570	Glutathione peroxidase	7.45	0.26±0.11	1.95±0.01
CAC1571	Glutathione peroxidase	6.24	0.23±0.11	1.45±0.11
CAC1656	Hypothetical protein, CF-39 family	6.53	0.61±0.42	3.97±0.06
CAC1695	DNA-dependent RNA polymerase sigma subunit	4.86	0.16±0.01	0.75±0.04
CAC1696	Specialized DNA-dependent RNA polymerase sigma subunit	4.67	0.12±0.01	0.55±0.03
CAC1766	Predicted sigma factor	4.44	0.12±0.01	0.52±0.05
CAC2235	Cysteine synthase/cystathionine beta-synthase, CysK	4.06	2.46±0.13	9.99±0.22
CAC2456	Hypothetical protein, CF-40 family	5	0.31±0.1	1.55±0.1
CAC2457	Hypothetical protein	4.64	0.35±0.11	1.61±0.09
CAC2536	Glycosyltransferase	4.17	0.26±0.07	1.07±0.08
CAC2605	Transcriptional regulator (TetR/AcrR family)	4.8	0.14±0.04	0.66±0.02
CAC2906	Spore coat protein cotS related	4.9	0.06±0.02	0.32±0.02
CAC2991	Methionyl-tRNA synthetase	4.23	0.86±0.23	3.65±0.18
CAC3258	Hypothetical protein	4.58	0.16±0.05	0.71±0
CAC3266	Hypothetical protein	4.37	0.86±0.22	3.74±0.11
CAC3325	Periplasmic amino acid binding protein	10.14	0.32±0.11	3.21±0.05
CAC3326	Amino acid ABC-type transporter, permease component	11.64	0.32±0.11	3.73±0.15
CAC3327	Amino acid ABC-type transporter, ATPase component	10.54	2.56±1.07	26.98±2.27
CAC3550	Na+ ABC transporter, NATB	8.72	0.2±0.03	1.77±0.1

CAC3551	Na+ ABC transporter (ATP-binding protein), NATA	5.22	0.12±0.01	0.6±0.06
CAC3677	KDP operon transcriptional regulatory protein KdpE (CheY-like receiver domain and HTH-type DNA-binding domain)	7.61	1.06±0.06	8.1±0.38
CAC3678	Sensor protein KdpD (ATPase containing sensor domain and histidine kinase domain)	20.12	0.38±0.07	7.71±0.14
CAC3679	Uncharacterized protein of kdp operon, kdpX	32.53	0.61±0.26	20±0.67
CAC3680	K+-transporting ATPase, c chain	34.53	0.54±0.27	18.73±0.73
CAC3681	K+-transporting ATPase, b chain	32.53	0.2±0.09	6.65±0.36
CAC3682	K+-transporting ATPase, a chain	36.85	0.39±0.19	14.28±1.24
CAP0035	Aldehyde-alcohol dehydrogenase, ADHE1	125.83	0.21±0.02	26.6±0.26
CAP0044	Hypothetical protein	7.95	0.37±0.11	2.93±0.15
CAP0045	Glycosyl transferase	10.81	1.03±0.4	11.16±0.51
Decrease				
CAC0086	Muconate cycloisomerase related protein, ortholog of YKGB B.subtilis	0.17	2.27±0.3	0.38±0.01
CAC0149	Hypothetical protein	0.02	2.83±1.44	0.06±0
CAC0154	PTS system, mannitol-specific IIBC component (gene MtlA)	0.09	0.93±0.44	0.08±0
CAC0155	Putative regulator of the PTS system for mannitol (gene MltR)	0.07	1.32±0.61	0.1±0
CAC0156	PTS system, mannitol-specific IIA domain (Ntr-type) (gene MltF)	0.08	3.3±1.76	0.27±0.02
CAC0157	Mannitol-1-phosphate 5-dehydrogenase (gene MtlD)	0.1	1.26±0.72	0.12±0.01
CAC0164	ABC transporter, ATP binding-protein	0.07	2.24±0.92	0.15±0.01
CAC0165	Predicted ABC transporter, permease component	0.09	2.03±0.76	0.18±0.02
CAC0392	Peptodoglycan-binding domain	0.23	0.65±0.11	0.15±0.01
CAC0427	Glycerol-3-phosphate ABC-transporter, permease component	0.18	2.11±0.42	0.39±0.02
CAC0428	Sugar permease	0.21	16.27±3.86	3.38±0.1

CAC0435	Hypothetical protein	0.21	0.36±0.2	0.07±0.01
CAC0542	Methyl-accepting chemotaxis protein	0.21	3.47±0.15	0.73±0.05
CAC0553	Hypothetical protein, CF-8 family	0.22	4.72±1.57	1.03±0.02
CAC0554	Autolytic lysozime (1,4-beta-N-acetylmuramidase), family 25 of glycosyl hydrolases ; peptodoglycan-binding domain	0.21	2.37±0.71	0.51±0.01
CAC0706	Endo-1,4-beta glucanase (fused to two ricin-B-like domains)	0.22	0.49±0.2	0.11±0.01
CAC0707	RNA polymerase sigma-54 factor	0.21	2.88±0.5	0.6±0.02
CAC0751	Permease	0.14	0.95±0.61	0.13±0.01
CAC0814	3-oxoacyl-[acyl-carrier-protein] synthase III	0.23	7.59±1.03	1.74±0.12
CAC0815	Methyl-accepting chemotaxis protein	0.22	4.32±0.19	0.95±0.01
CAC0816	Lipase-esterase related protein	0.2	5.09±0.55	0.99±0.11
CAC1075	Beta-glucosidase family protein	0.05	2.2±0.63	0.11±0.01
CAC1078	Predicted phosphohydrolase, Icc family	0.23	6.91±3.39	1.59±0.05
CAC1079	Uncharacterized protein, related to enterotoxins of other Clostridiales	0.04	2.62±1.06	0.11±0.01
CAC1080	Uncharacterized protein, probably surface-located	0.03	18.01±8.43	0.55±0.01
CAC1081	Uncharacterized protein, probably surface-located	0.03	8.4±4.15	0.25±0.02
CAC1084	Beta-glucosidase family protein	0.08	1.21±0.63	0.09±0.01
CAC1085	Alpha-glucosidase	0.08	1.33±0.72	0.11±0.01
CAC1086	Transcriptional regulators of NagC/XylR family	0.09	2.31±1.16	0.2±0.01
CAC1231	Predicted dehydrogenase, YULF B.subtilis ortholog	0.09	2.51±0.87	0.23±0.02
CAC1232	Predicted lytic murein transglycosylase (N-term. LysM motif repeat domain)	0.08	1.47±0.57	0.12±0.02
CAC1319	Glycerol uptake facilitator protein, GLPF	0	0.4±0.09	0±0
CAC1320	Glycerol-3-phosphate responsive antiterminator (mRNA-binding), GLPP	0	0.25±0.03	0±0
CAC1321	Glycerol kinase, GLPK	0	0.39±0.11	0±0

CAC1322	Glycerol-3-phosphate dehydrogenase, GLPA	0.16	0.57±0.03	0.09±0
CAC1323	NAD(FAD)-dependent dehydrogenase	0.19	0.4±0.03	0.08±0
CAC1324	Uncharacterized predected metal-binding protein	0.05	1.23±1.23	0.07±0
CAC1346	L-arabinose isomerase	0	0.21±0.07	0±0
CAC1349	Aldose-1-epimerase	0.25	1.76±1.22	0.43±0.01
CAC1405	Beta-glucosidase	0.15	36.33±12.49	5.38±0.16
CAC1406	Transcriptional antiterminator (BglG family)	0.04	3.1±1.96	0.14±0.01
CAC1436	Hypothetical protein	0.18	1.49±0.62	0.27±0.01
CAC1454	Membrane associated histidine kinase-like ATPase	0.22	0.57±0.32	0.13±0
CAC1455	Two-component system regulator (CheY domain and HTH-like DNA-binding domain)	0.21	1.68±0.88	0.36±0
CAC1669	Carbon starvation protein	0.1	2.67±0.5	0.27±0.01
CAC1775	Predicted membrane protein	0.09	8.38±1.21	0.72±0.05
CAC1909	Ribonuclease D	0.22	0.31±0.13	0.07±0.01
CAC1988	Ferrichrome-binding periplasmic protein	0.21	1.98±0.61	0.41±0.03
CAC1989	ABC-type iron (III) transport system, ATPase component	0.23	5.22±1.52	1.22±0.08
CAC1990	ABC-type iron (III) transport system, permease component	0.23	0.98±0.26	0.23±0.01
CAC1991	Uncharacterized protein, YIIM family	0.23	3.03±1.07	0.7±0.02
CAC1993	Molybdenum cofactor biosynthesis enzyme MoaA, Fe-S oxidoreductase	0.2	0.96±0.37	0.2±0.01
CAC1994	Molybdopterin biosynthesis enzyme, MoaB	0.18	1.42±0.53	0.25±0.01
CAC1995	Hypothetical protein	0.22	0.46±0.19	0.1±0.02
CAC1996	Hypothetical protein	0.2	2.62±0.9	0.53±0.01
CAC1997	Predicted glycosyltransferase	0.21	2.72±1.04	0.56±0.02
CAC1998	ABC-type transport system, ATPase component	0.19	2.42±0.94	0.46±0.03
CAC1999	Uncharacterized protein related to hypothetical protein Cj1507c from	0.19	2.15±0.9	0.4±0.02

	Campylobacter jejuni			
CAC2000	Indolepyruvate ferredoxin oxidoreductase, subunit beta	0.17	2.65±1.09	0.44±0.06
CAC2001	Indolepyruvate ferredoxin oxidoreductase, subunit alpha	0.22	9.05±4.28	2±0.15
CAC2002	Predicted iron-sulfur flavoprotein	0.24	3.57±1.27	0.85±0.02
CAC2003	Predicted permease	0.21	1.7±0.84	0.36±0.03
CAC2004	Siderophore/Surfactin synthetase related protein	0.21	6.96±2.59	1.43±0.02
CAC2005	Siderophore/Surfactin synthetase related protein	0.19	4.06±1.57	0.76±0.02
CAC2006	Enzyme of siderophore/surfactin biosynthesis	0.22	1.65±0.59	0.37±0.01
CAC2007	Predicted glycosyltransferase	0.21	8.79±3.64	1.85±0.09
CAC2009	3-Hydroxyacyl-CoA dehydrogenase	0.22	6.35±1.95	1.42±0.06
CAC2010	Predicted Fe-S oxidoreductase	0.21	8.54±2.9	1.79±0.04
CAC2011	Possible 3-oxoacyl-[acyl-carrier-protein] synthase III	0.2	5.89±1.94	1.19±0.06
CAC2012	Enoyl-CoA hydratase	0.22	3.36±0.33	0.75±0.03
CAC2013	Hypothetical protein	0.19	8.36±2.44	1.56±0.02
CAC2014	Predicted esterase	0.19	8.21±2.59	1.58±0
CAC2015	Hypothetical protein	0.19	3.84±1.03	0.71±0.01
CAC2016	Enoyl-CoA hydratase	0.21	23.03±4.11	4.8±0.11
CAC2017	Acyl carrier protein	0.23	5.75±1.05	1.34±0.08
CAC2018	Aldehyde:ferredoxin oxidoreductase	0.18	6.52±2.32	1.16±0.14
CAC2019	Malonyl CoA-acyl carrier protein transacylase	0.19	6.63±2.11	1.29±0.03
CAC2020	Molybdopterin biosynthesis enzyme, MoeA, fused to molibdopterin-binding domain	0.15	0.85±0.32	0.12±0
CAC2021	Molybdopterin biosynthesis enzyme, MoeA (short form)	0.12	2.54±1.13	0.29±0.02
CAC2252	Alpha-glucosidase fused to unknown alpha-amylase C-terminal. domain	0.01	41.27±28.23	0.34±0.06
CAC2289	Biotin carboxyl carrier protein	0.2	0.45±0.06	0.09±0

CAC2514	Beta galactosidase	0.25	0.4±0.16	0.1±0
CAC2570	Predicted arabinogalactan endo-1,4-beta-galactosidase	0.09	4.75±1.31	0.43±0.02
CAC2610	L-fucose isomerase related protein	0.08	2.43±2.19	0.19±0
CAC2611	Hypothetical protein	0.07	2.57±2.57	0.19±0.01
CAC2774	Methyl-accepting chemotaxis protein with HAMP domain	0.14	3.25±1.35	0.45±0.03
CAC2805	Possible selenocysteine lyase (aminotransferase of NifS family)	0.21	0.39±0.14	0.08±0.01
CAC2806	Predicted phosphohydrolase, Icc family	0.1	79.67±1.72	7.74±1.19
CAC2807	Endo-1,3(4)-beta-glucanase family 16	0.04	64.7±11.05	2.77±1.21
CAC2808	Beta-lactamase class C domain (PBPX family) containing protein	0.16	1.79±0.66	0.29±0.01
CAC2809	Predicted HD superfamily hydrolase	0	1.45±1.12	0±0
CAC2810	Possible glucoamylase (diverged), 15 family	0.03	3.81±0.79	0.13±0.01
CAC2833	Uncharacterized conserved protein, YAEG family	0.06	1.14±0.4	0.07±0
CAC2834	Uncharacterized conserved protein, YHAD family	0.01	40.02±7.86	0.2±0.01
CAC2835	Gluconate permease, gntP	0	35.73±17.74	0.12±0.01
CAC2847	Ribosome-associated protein Y (PSrp-1)	0.23	14.71±4.59	3.34±0.15
CAC2891	Fusion of alpha-glucosidase (family 31 glycosyl hydrolase) and glycosidase (TreA/MalS family)	0.07	6.1±4.66	0.43±0.01
CAC2959	Galactokinase	0.09	8.67±3.42	0.76±0.05
CAC2960	UDP-galactose 4-epimerase	0.1	2.42±0.92	0.23±0.01
CAC2961	Galactose-1-phosphate uridyltransferase	0.14	2.81±0.83	0.4±0.02
CAC2962	Transcriptional regulators of the LacI family	0.19	5.49±2.78	1.07±0.06
CAC3032	Galactose mutarotase related enzyme	0.16	4.88±0.1	0.79±0.01
CAC3157	Tryptophan synthase alpha chain	0.25	3.02±2.11	0.75±0.08
CAC3158	Tryptophan synthase beta chain	0.19	14.1±10.61	2.67±0.26
CAC3159	Phosphoribosylanthranilate isomerase	0.12	9.4±6.76	1.12±0.12

CAC3160	Indole-3-glycerol phosphate synthase	0.12	5.36±4.12	0.63±0.06
CAC3161	Anthranilate phosphoribosyltransferase	0.12	4.06±2.91	0.47±0.03
CAC3162	Para-aminobenzoate synthase component II	0.08	6.09±4.75	0.47±0.02
CAC3163	Para-aminobenzoate synthase component I	0.09	1.64±1.18	0.14±0.01
CAC3236	Possible transcriptional regulator from YAEG/LRPR family	0.2	2.26±1.1	0.45±0.01
CAC3237	Multiple sugar-binding ABC-transporter, MSMX ATP-binding protein	0.23	1.42±0.56	0.33±0.02
CAC3362	Uncharacterized conserved membrane protein, YOAK B.subtilis homolog	0.21	0.62±0.05	0.13±0.02
CAC3425	PTS system, (possibly glucose-specific) IIBC component	0	0.23±0.12	0±0
CAC3489	Hypothetical protein	0.23	1.13±0.11	0.26±0.01
CAC3498	Sugar kinase, ribokinase family	0.19	0.46±0.16	0.09±0.02
CAC3612	Hypothetical protein	0.09	3.49±1.51	0.33±0.02
CAC3613	Hypothetical protein	0.18	0.83±0.5	0.15±0.01
CAC3617	Uncharacterized membrane protein, YHAG B.subtilis homolog	0.13	0.73±0.48	0.1±0
CAC3671	ABC-type sugar transport system, permease component	0	0.24±0.11	0±0
CAC3672	ABC-type sugar transport system, periplasmic sugar-binding component	0.2	0.31±0.13	0.06±0
CAP0066	Mannose-specific phosphotransferase system component IIAB	0.08	15.39±2.91	1.24±0.13
CAP0067	Mannose/fructose-specific phosphotransferase system component IIC	0.08	29.27±6.73	2.24±0.13
CAP0068	Mannose-specific phosphotransferase system component IID	0.06	17.54±3.27	1.04±0.03
CAP0069	Uncharacterized protein, homolog of Streptococcus salivarius (5669858)	0.08	5.56±2.78	0.45±0.09
CAP0072	Hypothetical protein	0.13	2.68±0.98	0.36±0.05
CAP0098	Alpha-amylase, AmyB	0.17	0.44±0.13	0.07±0.02
CAP0162	NAD+ dependent aldehyde dehydrogenase (adhE1)	0	7.09±0.73	0±0

Table S3.5. Four-fold increased or decreased genes under solventogenesis in *ΔadhE2*

Gene number	Function	adhE2 /Ctrl	Control	adhE2
Increase				
CAC1043	Xre family DNA-binding domain and TPR-repeat containing protein	4.13	0.1±0.01	0.43±0.23
CAC1880	Hypothetical protein, CF-35 family	4.29	0.12±0.01	0.52±0.32
CAC1881	Hypothetical protein	4.83	0.11±0.01	0.55±0.36
CAC1885	Hypothetical protein	∞	0±0	0.32±0.21
CAC1886	Uncharacterized phage related protein	∞	0±0	0.42±0.28
CAC1887	Hypothetical protein	∞	0±0	0.38±0.26
CAC1888	Uncharacterized phage related protein	∞	0±0	1.08±0.82
CAC1892	Hypothetical protein	∞	0±0	0.32±0.21
CAC1893	ClpP family serine protease, possible phage related	∞	0±0	1.41±1.07
CAC1894	Phage-related, head portal protein	∞	0±0	0.29±0.19
CAC1897	Phage-related, Zn finger domain containing protein	∞	0±0	0.29±0.19
CAC1945	Phage related anti-repressor protein	∞	0±0	0.22±0.13
CAC2438	Predicted phosphatase	4.26	0.17±0.09	0.73±0.81
CAC3234	Uncharacterized conserved protein, YVBJ B.subtilis ortholog with N-terminal C4-type Zn-finger domain	4.79	0.23±0.06	1.11±0.9
CAC3236	Possible transcriptional regulator from YAEG/LRPR family	8.76	2.26±1.1	19.75±17.13
CAC3237	Multiple sugar-binding ABC-transporter, MSMX ATP-binding protein	7.44	1.42±0.56	10.6±8.4
CAC3379	Uncharacterized protein, YQFW B.subtilis homolog	4.37	0.78±0.57	3.41±3.85
CAC3604	Dihydroxyacid dehydratase	122.68	0.18±0.04	22.11±12.55
CAC3605	High affinity gluconate/L-idonate permease	127.91	0.13±0.03	16.54±10.3
CAP0029	Permease MDR-related	20.5	0.14±0.09	2.88±0.72

CAP0030	Isochorismatase	22.96	0.23±0.15	5.29±1.7
CAP0031	Transcriptional activator HLYU, HTH of ArsR family	9.57	0.69±0.15	6.62±2.03
Decrease				
CAC0014	Aminotransferase	0.09	3.73±1.51	0.34±0.03
CAC0015	D-3-phosphoglycerate dehydrogenase	0.08	6.29±2.56	0.51±0.08
CAC0016	Related to HTH domain of SpoOJ/ParA/ParB/repB family, involved in chromosome partitioning	0.14	1.66±1.48	0.23±0.01
CAC0017	Seryl-tRNA synthetase	0.11	1.04±0.51	0.12±0.01
CAC0078	Accessory gene regulator protein B	0	1.99±0.03	0±0
CAC0079	Hypothetical protein	0	68.44±1.59	0.1±0.03
CAC0082	Predicted membrane protein	0.02	42.74±3.17	0.81±0.4
CAC1634	Flagellin	0.25	2.42±1.98	0.6±0.25
CAC2569	NimC/NimA family protein	0.22	7.73±3.94	1.71±0.39
CAC3408	NADH oxidase (two distinct flavin oxidoreductase domains)	0.04	6.6±0.71	0.28±0.13
CAC3409	Transcriptional regulators, LysR family	0.02	20.17±3.06	0.48±0.33
CAC3422	Sugar:proton symporter (possible xylulose)	0.02	9.01±2.14	0.16±0.07
CAC3423	Acetyltransferase (ribosomal protein N-acetylase subfamily)	0.03	10.41±1.56	0.28±0.06
CAC3424	Transcriptional regulator, RpiR family	0.23	1.71±0.18	0.39±0.07
CAC3612	Hypothetical protein	0.22	3.49±1.51	0.75±0.45
CAP0028	HTH transcriptional regulator TetR family	0.18	0.45±0.05	0.08±0
CAP0035	NADH-dependent aldehyde/alcohol dehydrogenase (adhE2)	0	0.21±0.02	0±0

Table S3.6. Four-fold increased or decreased genes under alcohologenesis in *ΔadhE1*

Gene number	Function	adhE2 /Ctrl	Control	adhE2
Increase				
CAC0078	Accessory gene regulator protein B	4.32	0.54±0.2	2.32±0.13
Decrease				
CAC0422	Transcriptional antiterminator licT	0.11	2.55±1.5	0.27±0.02
CAC0423	Fusion: PTS system, beta-glucosides specific IIABC component	0.01	14.55±9.31	0.1±0.01
CAC0424	Fructokinase	0.02	5.66±3.62	0.09±0.01
CAC0425	Sucrase-6-phosphate hydrolase (gene sacA)	0.02	3.33±2.1	0.07±0
CAC0426	Transcriptional regulator (HTH_ARAC-domain)	0.13	47.23±26.81	5.92±0.61
CAC0751	Permease	0.17	3.83±0.22	0.64±0.04
CAC1406	Transcriptional antiterminator (BglG family)	0.14	25.57±13.31	3.45±0.42
CAC1407	PTS system, beta-glucosides-specific IIABC component	0.12	0.9±0.51	0.11±0.01
CAC1408	Phospho-beta-glucosidase	0.12	1.23±0.68	0.15±0.01
CAC3274	Possible surface protein, responsible for cell interaction; contains cell adhesion domain and ChW-repeats	0.17	1.43±0.94	0.24±0.02
CAC3459	Homolog of cell division GTPase FtsZ, diverged	0.23	1.79±1.12	0.41±0.02
CAP0029	Permease MDR-related	0	0.81±0.53	0±0
CAP0030	Isochorismatase	0.04	1.84±1.26	0.08±0
CAP0031	Transcriptional activator HLYU, HTH of ArsR family	0.25	2.5±1.37	0.62±0.07

Table S3.7. Four-fold increased or decreased genes under alcohologenesis in *ΔadhE2*

Gene number	Function	adhE2 /Ctrl	Control	adhE2
Increase				
CAC0265	Transcriptional regulator, GntR family	4.39	0.91±0.05	4±0.08
CAC0266	ABC transporter, ATP-binding protein	4.97	0.41±0.06	2.05±0.06
CAC0375	PLP-dependent aminotransferase (gene patA)	4.1	3.77±0.32	15.45±0.98
CAC0682	Ammonium transporter (membrane protein nrgA)	11.43	0.31±0.05	3.53±0.19
CAC1107	Hypothetical protein, CF-36 family	4.52	0.08±0.02	0.37±0.02
CAC1130	Hypothetical protein	4.78	0.08±0.02	0.39±0
CAC1131	Hypothetical protein	4.91	0.08±0.02	0.41±0.01
CAC1600	Methyl-accepting chemotaxis-like protein (chemotaxis sensory transducer)	4.95	0.99±0.6	4.88±0.16
CAC1601	Methyl-accepting chemotaxis-like protein (chemotaxis sensory transducer)	5.64	0.58±0.3	3.3±0.16
CAC1634	Flagellin	4.53	1.99±1.39	9.03±1.02
CAC1705	Periplasmic phosphate-binding protein	27.3	0.27±0.09	7.33±0.53
CAC1706	Phosphate permease	6.66	0.08±0.03	0.56±0.09
CAC1707	Permease component of ATP-dependent phosphate uptake system	11.24	0.09±0.01	1.05±0.1
CAC1708	ATPase component of ABC-type phosphate transport system	20.22	0.13±0.01	2.64±0.15
CAC1709	Phosphate uptake regulator	5.83	0.12±0.02	0.69±0.03
CAC2203	Possible hook-associated protein, flagellin family	4.42	12.36±8.44	54.69±3.54
CAC2717	Ethanolamine ammonia lyase small subunit	4.1	0.12±0	0.48±0.02
CAC2718	Ethanolamine ammonia lyase large subunit	5.11	0.12±0.01	0.59±0.03
CAC2746	Membrane associated methyl-accepting chemotaxis protein (with HAMP domain)	6.76	0.22±0.12	1.49±0.03
CAC3352	Membrane associated methyl-accepting chemotaxis protein with HAMP domain	4.79	0.62±0.32	2.96±0.19

CAC3604	Dihydroxyacid dehydratase	297.03	0.19±0.03	57.09±1
CAC3605	High affinity gluconate/L-idonate permease	301.06	0.13±0.01	38.52±4.31
CAP0029	Permease MDR-related	11.43	0.81±0.53	9.28±0.99
CAP0030	Isochorismatase	14.44	1.84±1.26	26.58±0.98
CAP0031	Transcriptional activator HLYU, HTH of ArsR family	10.71	2.5±1.37	26.77±2.14
CAP0036	Uncharacterized, ortholog of YgaT gene of B.subtillis	9.55	1.97±0.18	18.8±1.04
CAP0037	Uncharacterized, ortholog of YgaS gene of B.subtillis	8.94	1.61±0.11	14.43±0.9
CAP0045	Glycosyl transferase	5.06	0.64±0.08	3.25±0.15
CAP0087	HTH transcriptional regulator TetR/AcrR family	13.65	0.84±0.09	11.53±0.47
CAP0088	3-oxoacyl-acyl-carrier protein synthase	21.46	2.45±0.23	52.58±2.19
CAP0167	Specialized sigma factor (SigF/SigE family)	5.32	0.42±0.25	2.22±0.22
CAP0169	Hypothetical protein, CF-45 family	5.77	0.15±0.07	0.87±0.15
CAP0170	Hypothetical protein, CF-46 family	8.35	0.08±0.01	0.69±0.13
CAP0171	Hypothetical protein, CF-45 family	7.01	0.1±0.02	0.67±0.15
CAP0172	Hypothetical protein, CF-46 family	6.71	0.4±0.11	2.69±0.77
Decrease				
CAC0078	Accessory gene regulator protein B	0	0.54±0.2	0±0
CAC0079	Hypothetical protein	0	10.91±8.15	0±0
CAC0082	Predicted membrane protein	0.03	15.51±5.65	0.43±0.03
CAC0316	Ornithine carbomoyltransferase	0.11	6.54±1.37	0.75±0.03
CAC0380	Periplasmic amino acid-binding protein	0.21	7.74±1.74	1.63±0.08
CAC0706	Endo-1,4-beta glucanase (fused to two ricin-B-like domains)	0.14	5.11±2.59	0.69±0.08
CAC0973	Argininosuccinate synthase	0.11	10.23±0.45	1.15±0.09
CAC0974	Argininosuccinate lyase	0.1	11.11±0.44	1.11±0

CAC1319	Glycerol uptake facilitator protein, GLPF	0.23	35.83±8.36	8.34±1.13
CAC1320	Glycerol-3-phosphate responsive antiterminator (mRNA-binding), GLPP	0.2	16.28±3.56	3.26±0.51
CAC1321	Glycerol kinase, GLPK	0.21	27.85±6.42	5.83±0.61
CAC1322	Glycerol-3-phosphate dehydrogenase, GLPA	0.18	59.33±8.11	10.51±1.61
CAC1323	NAD(FAD)-dependent dehydrogenase	0.23	58.91±8.35	13.49±1.21
CAC1324	Uncharacterized predected metal-binding protein	0.22	40.66±1.55	8.97±0.95
CAC1405	Beta-glucosidase	0.11	16.94±4.45	1.78±0.11
CAC1888	Uncharacterized phage related protein	0.19	0.48±0.15	0.09±0
CAC1893	ClpP family serine protease, possible phage related	0.19	0.56±0.14	0.1±0.01
CAC2388	N-acetylornithine aminotransferase	0.1	6.84±0.09	0.68±0.04
CAC2389	Acetylglutamate kinase	0.24	0.48±0.12	0.11±0.01
CAC2390	N-acetyl-gamma-glutamyl-phosphate reductase	0.17	1.55±0.26	0.26±0.01
CAC2391	Ornithine acetyltransferase	0.2	2.86±0.63	0.57±0.02
CAC2456	Hypothetical protein, CF-40 family	0.08	3.72±1.92	0.31±0.03
CAC2457	Hypothetical protein	0.1	3.66±1.91	0.38±0.01
CAC2469	Lactoylglutathione lyase (fragment)	0.23	0.92±0.24	0.21±0.02
CAC2470	Uncharacterized Zn-finger protein	0.25	1.94±0.4	0.48±0.03
CAC2511	Predicted membrane protein	0.24	0.46±0.22	0.11±0
CAC2644	Carbamoylphosphate synthase large subunit	0.22	2.31±0.23	0.51±0.08
CAC2645	Carbamoylphosphate synthase small subunit	0.23	0.53±0.12	0.12±0.02
CAC3160	Indole-3-glycerol phosphate synthase	0.24	2.58±0.63	0.63±0.06
CAC3274	Possible surface protein, responsible for cell interaction; contains cell adhesion domain and ChW-repeats	0.15	1.43±0.94	0.21±0.03
CAC3408	NADH oxidase (two distinct flavin oxidoreductase domains)	0.04	3.28±1.4	0.12±0
CAC3409	Transcriptional regulators, LysR family	0.02	9.93±2.4	0.15±0.01

CAC3422	Sugar:proton symporter (possible xylulose)	0.07	2.71±0.43	0.19±0.01
CAC3423	Acetyltransferase (ribosomal protein N-acetylase subfamily)	0.08	3.19±0.7	0.27±0.01
CAC3486	Multimeric flavodoxin WrbA family protein	0.23	2.28±1.03	0.52±0.03
CAC3618	ABC-type polar amino acid transport system, ATPase component	0.22	4.89±0.41	1.09±0.02
CAP0028	HTH transcriptional regulator TetR family	0.24	0.53±0.07	0.13±0.01
CAP0035	NADH-dependent aldehyde/alcohol dehydrogenase (adhE2)	0	68.6±12.95	0±0

A

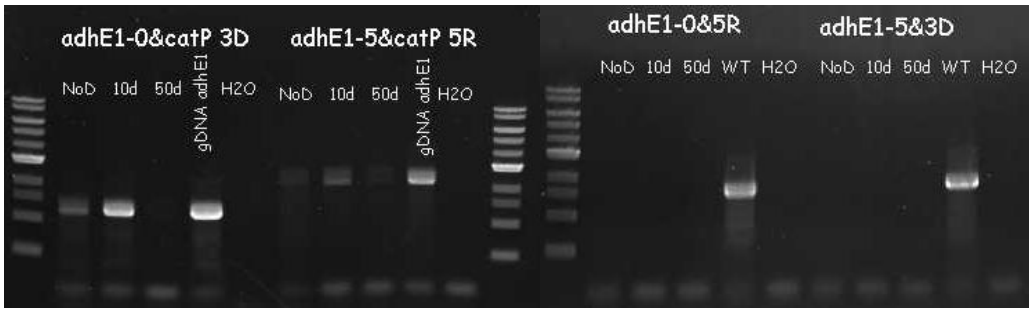

B

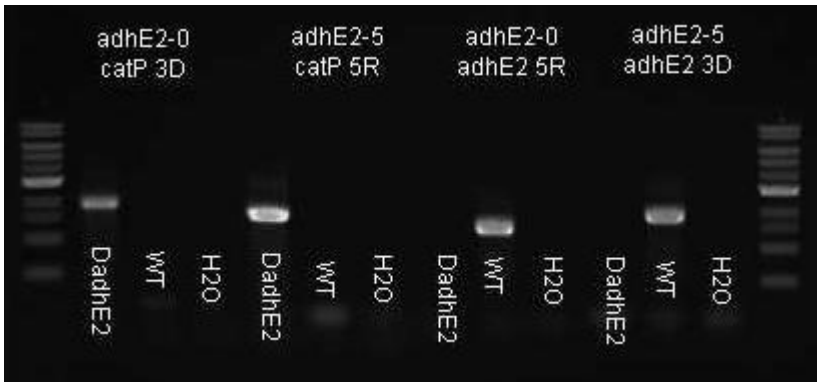

Fig. S3.1. PCR Verification of deletion of *adhE1* in *ΔadhE1* strain (A) and *adhE2* in *Δadhe2* strain (B). adhEX-0 is 5' external primer. adhEX-5 is 3' external primer. adhEX-5R/3D are located on target gene. catP 5R/3D are located on catP cassette. Abbreviations used in this figure: Nod, Non diluted culture; 10d, 10 times diluted culture; 50d, 50 times diluted culture; WT, genomic DNA of *C. acetobutylicum* ATCC 824; gDNA *adhE1*, genomic DNA of *Δadhe1*; DadhE2. Genomic DNA of *ΔadhE2*.

Acidogenesis

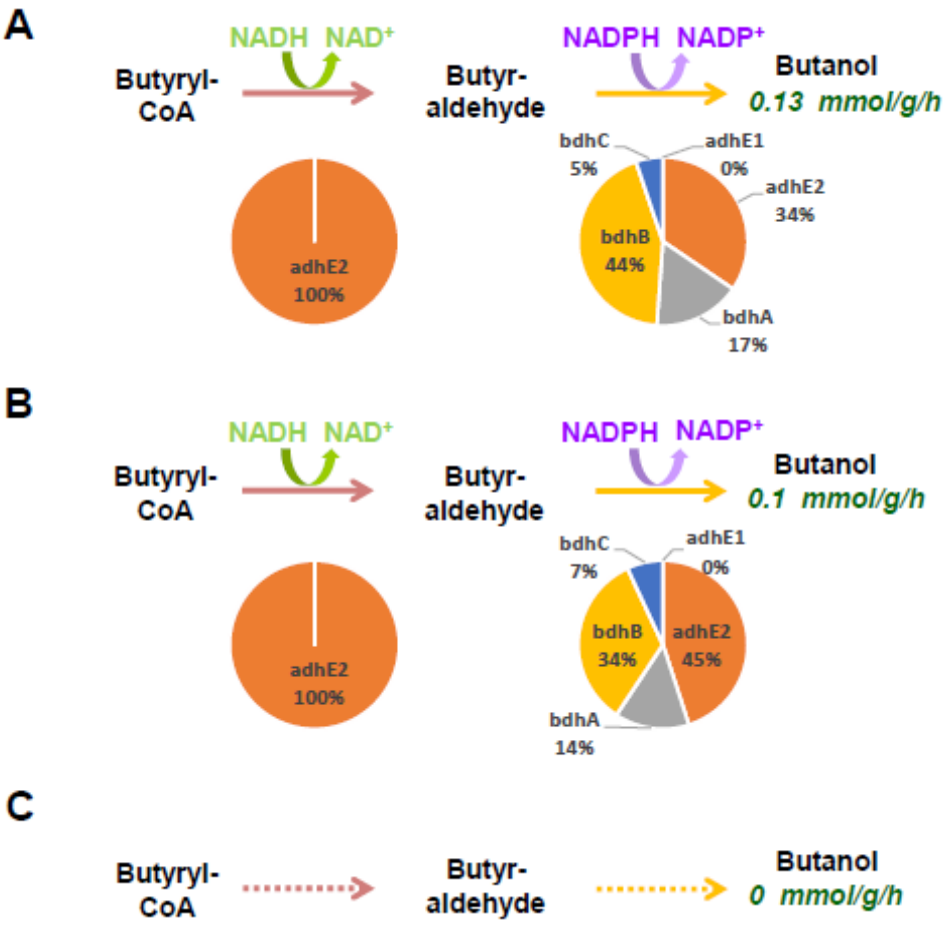

Fig. S3.2. Butanol pathway analysis of control (A), *ΔadhE1* (B), *ΔadhE2* (C) under acidogenesis, solventogenesis, and alcohologenesis. Activity distributions of the five enzymes are shown for each step under the arrows. The primary cofactors used for each step are shown over the arrows. Butanol flux is indicated under the word "Butanol."

Solventogenesis

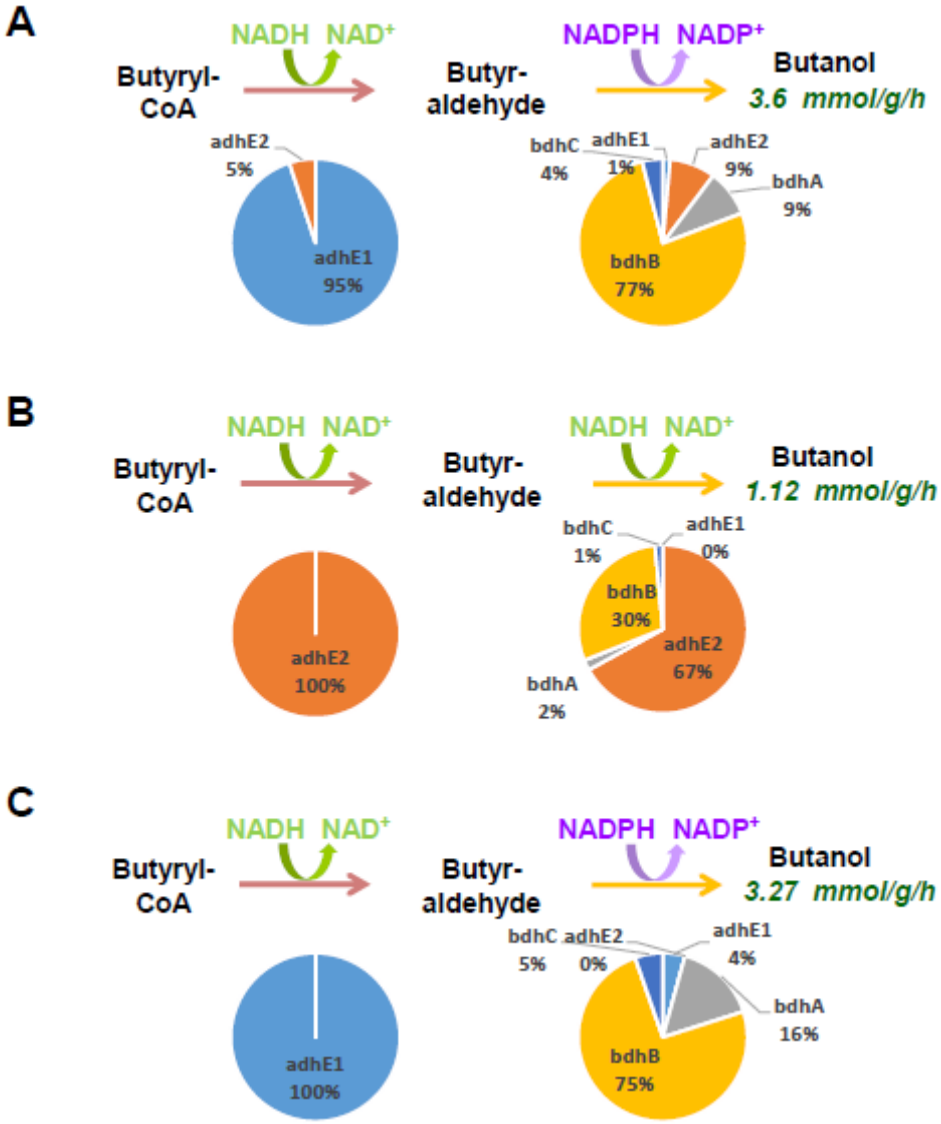

Fig. S3.2. Butanol pathway analysis of control (A), *ΔadhE1* (B), *ΔadhE2* (C) under acidogenesis, solventogenesis, and alcohologenesis. Activity distributions of the five enzymes are shown for each step under the arrows. The primary cofactors used for each step are shown over the arrows. Butanol flux is indicated under the word "Butanol."

Alcohologenesis

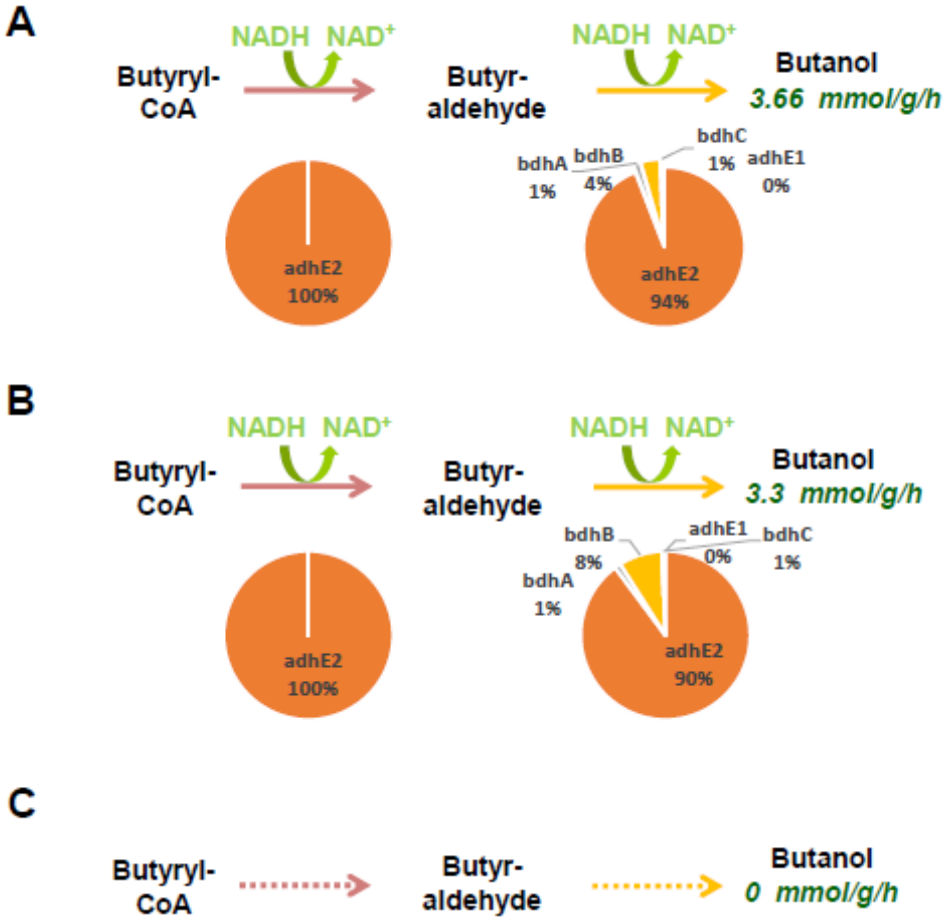

Fig. S3.2. Butanol pathway analysis of control (A), *ΔadhE1* (B), *ΔadhE2* (C) strains under acidogenesis, solventogenesis, and alcohologenesis. Activity distributions of the five enzymes are shown for each step under the arrows. The primary cofactors used for each step are shown over the arrows. Butanol flux is indicated under the word "Butanol."

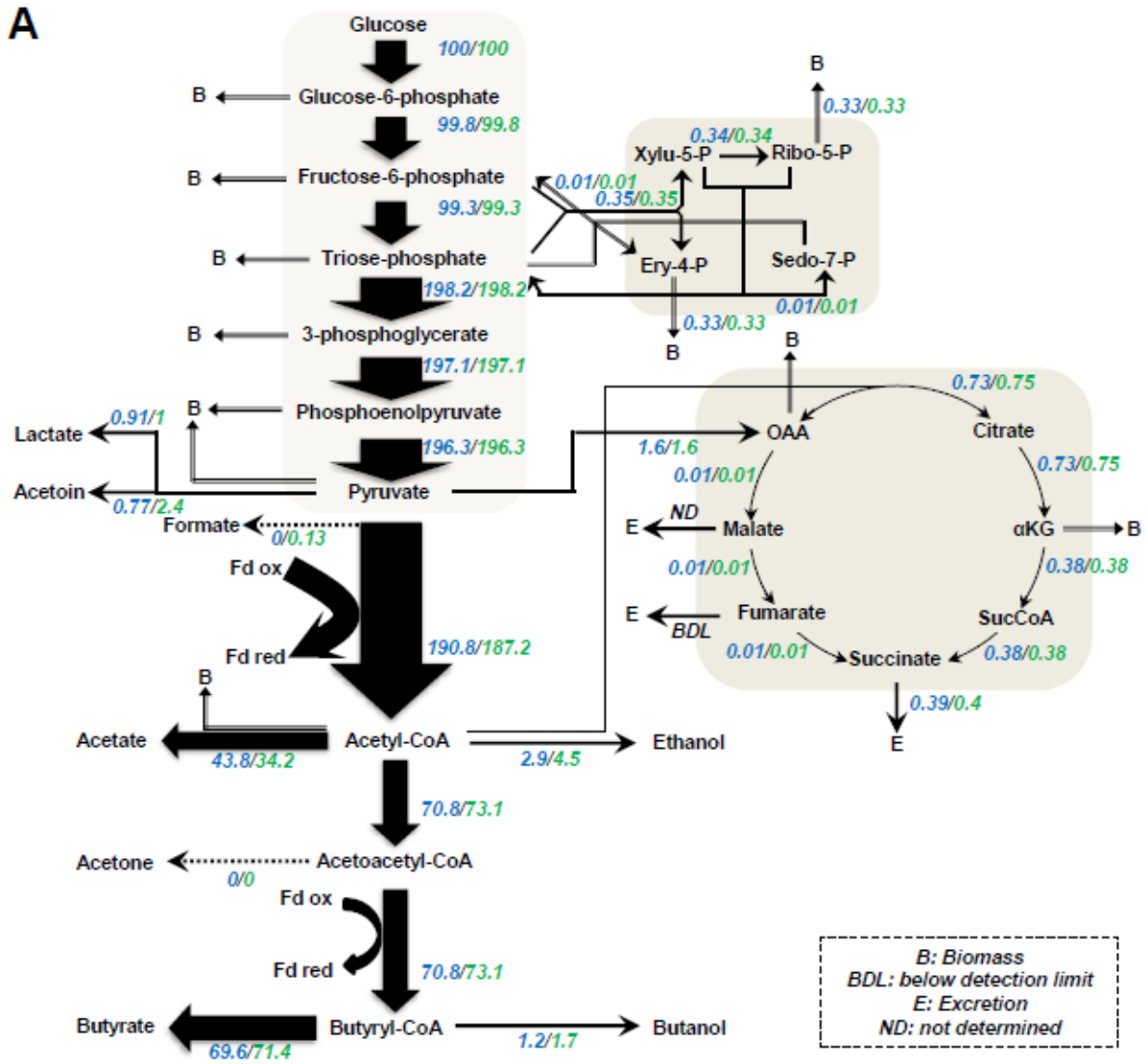

Fig. S3.3. Metabolic flux map of *ΔadhE1* under acidogenesis (A), *ΔadhE2* under acidogenesis (B), *ΔadhE1* under solventogenesis (C), *ΔadhE2* under solventogenesis (D), . *ΔadhE1* under alcohologenesis (E), *ΔadhE2* under alcohologenesis (F). All values are normalized to the flux of the initial carbon source (mmol/gDCW/h). Glucose flux is normalized as 100 for acidogenesisand solventogenesis, and the sum of glucose and half of the glycerol normalized as 100 for alcohologenesis. The values of corresponding mutant are shown in blue letter, and that of control strain are shown in green letter.

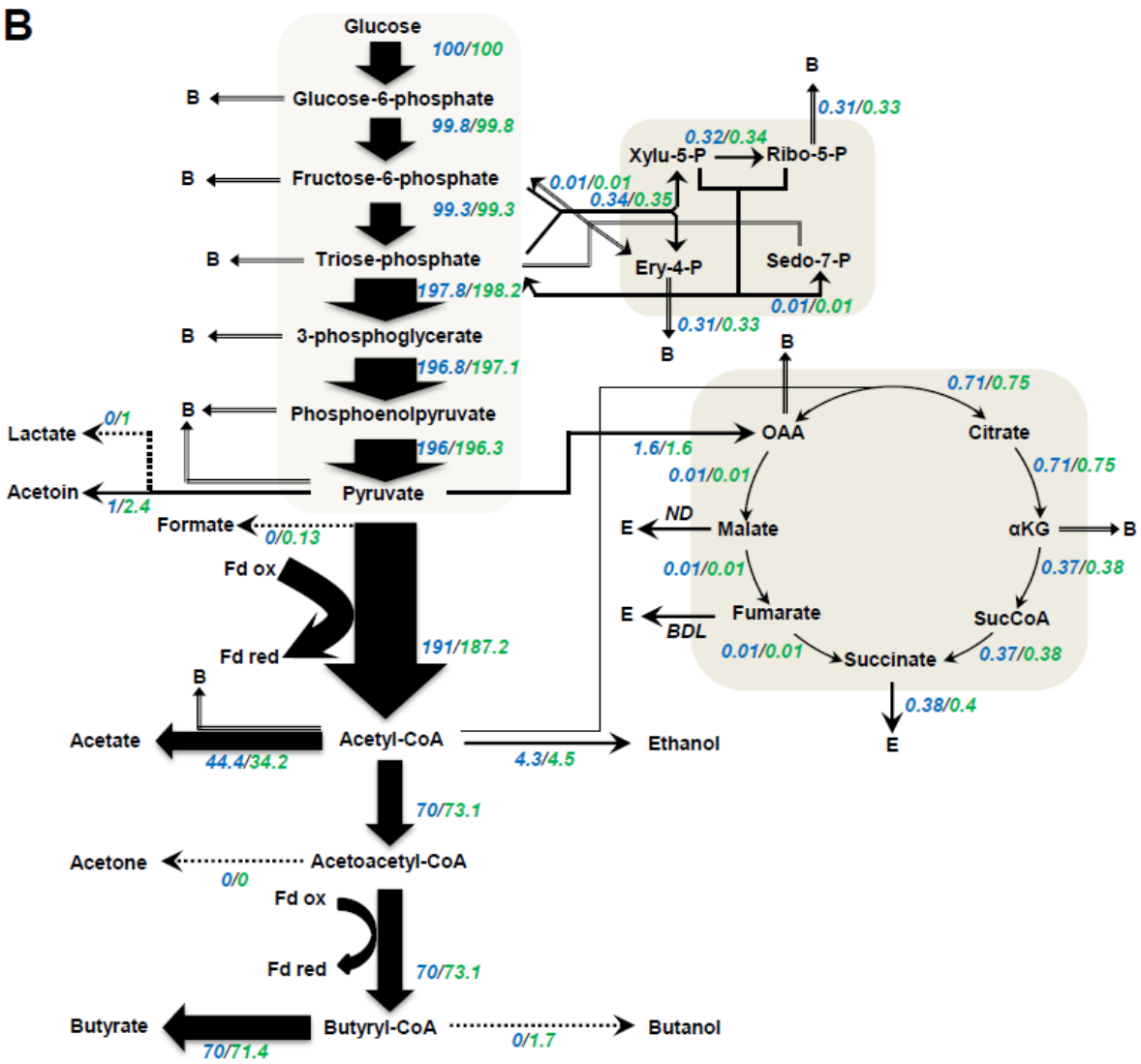

Fig. S3.3. Metabolic flux map of *ΔadhE1* under acidogenesis (A), *ΔadhE2* under acidogenesis (B), *ΔadhE1* under solventogenesis (C), *ΔadhE2* under solventogenesis (D), . *ΔadhE1* under alcohologenesis (E), *ΔadhE2* under alcohologenesis (F). All values are normalized to the flux of the initial carbon source (mmol/gDCW/h). Glucose flux is normalized as 100 for acidogenesisand solventogenesis, and the sum of glucose and half of the glycerol normalized as 100 for alcohologenesis. The values of corresponding mutant are shown in blue letter, and that of control strain are shown in green letter.

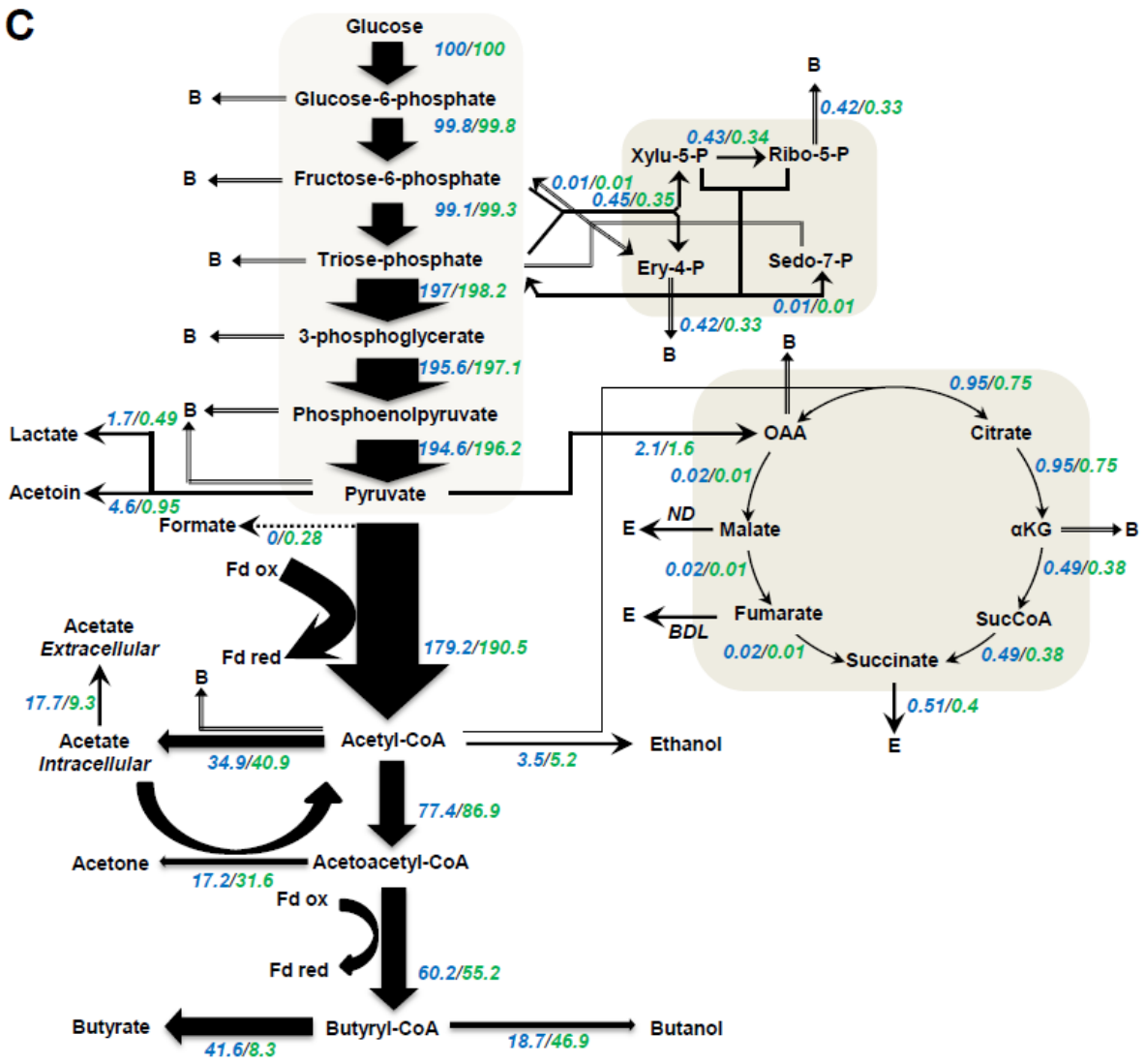

Fig. S3.3. Metabolic flux map of *ΔadhE1* under acidogenesis (A), *ΔadhE2* under acidogenesis (B), *ΔadhE1* under solventogenesis (C), *ΔadhE2* under solventogenesis (D), . *ΔadhE1* under alcohologenesis (E), *ΔadhE2* under alcohologenesis (F). All values are normalized to the flux of the initial carbon source (mmol/gDCW/h). Glucose flux is normalized as 100 for acidogenesisand solventogenesis, and the sum of glucose and half of the glycerol normalized as 100 for alcohologenesis. The values of corresponding mutant are shown in blue letter, and that of control strain are shown in green letter.

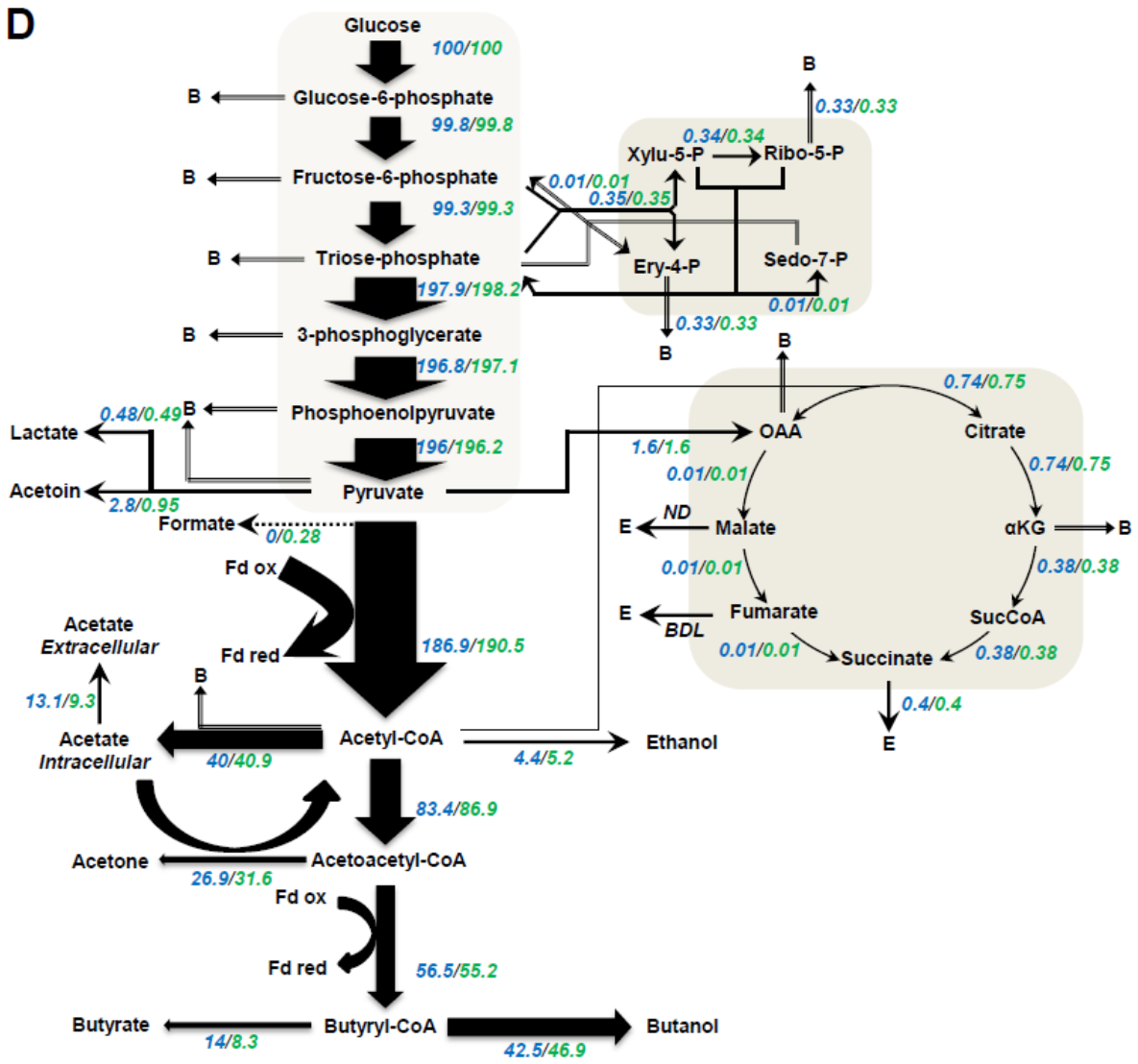

Fig. S3.3. Metabolic flux map of *ΔadhE1* under acidogenesis (A), *ΔadhE2* under acidogenesis (B), *ΔadhE1* under solventogenesis (C), *ΔadhE2* under solventogenesis (D), . *ΔadhE1* under alcohologenesis (E), *ΔadhE2* under alcohologenesis (F). All values are normalized to the flux of the initial carbon source (mmol/gDCW/h). Glucose flux is normalized as 100 for acidogenesisand solventogenesis, and the sum of glucose and half of the glycerol normalized as 100 for alcohologenesis. The values of corresponding mutant are shown in blue letter, and that of control strain are shown in green letter.

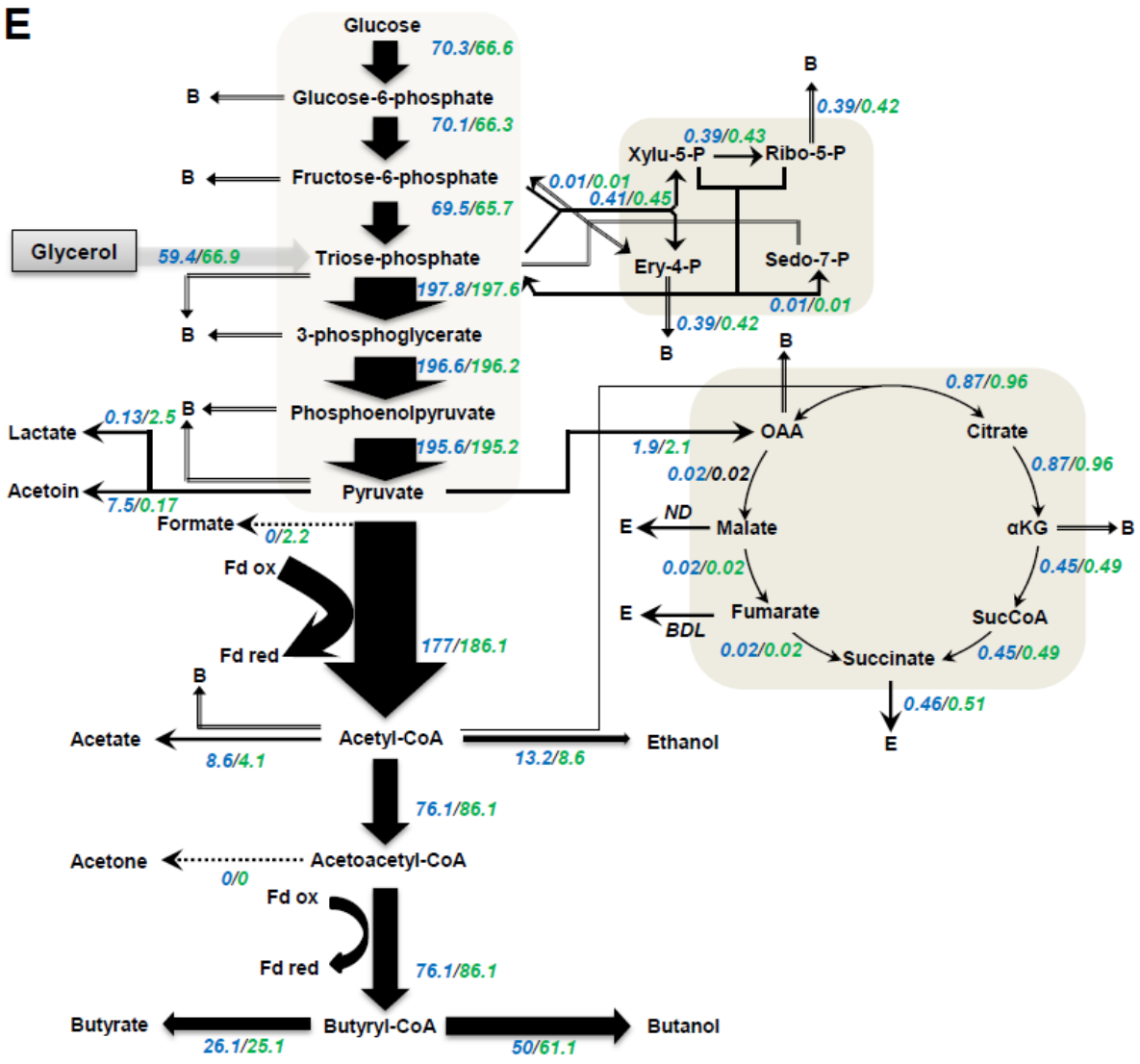

Fig. S3.3. Metabolic flux map of *ΔadhE1* under acidogenesis (A), *ΔadhE2* under acidogenesis (B), *ΔadhE1* under solventogenesis (C), *ΔadhE2* under solventogenesis (D), . *ΔadhE1* under alcohologenesis (E), *ΔadhE2* under alcohologenesis (F). All values are normalized to the flux of the initial carbon source (mmol/gDCW/h). Glucose flux is normalized as 100 for acidogenesisand solventogenesis, and the sum of glucose and half of the glycerol normalized as 100 for alcohologenesis. The values of corresponding mutant are shown in blue letter, and that of control strain are shown in green letter.

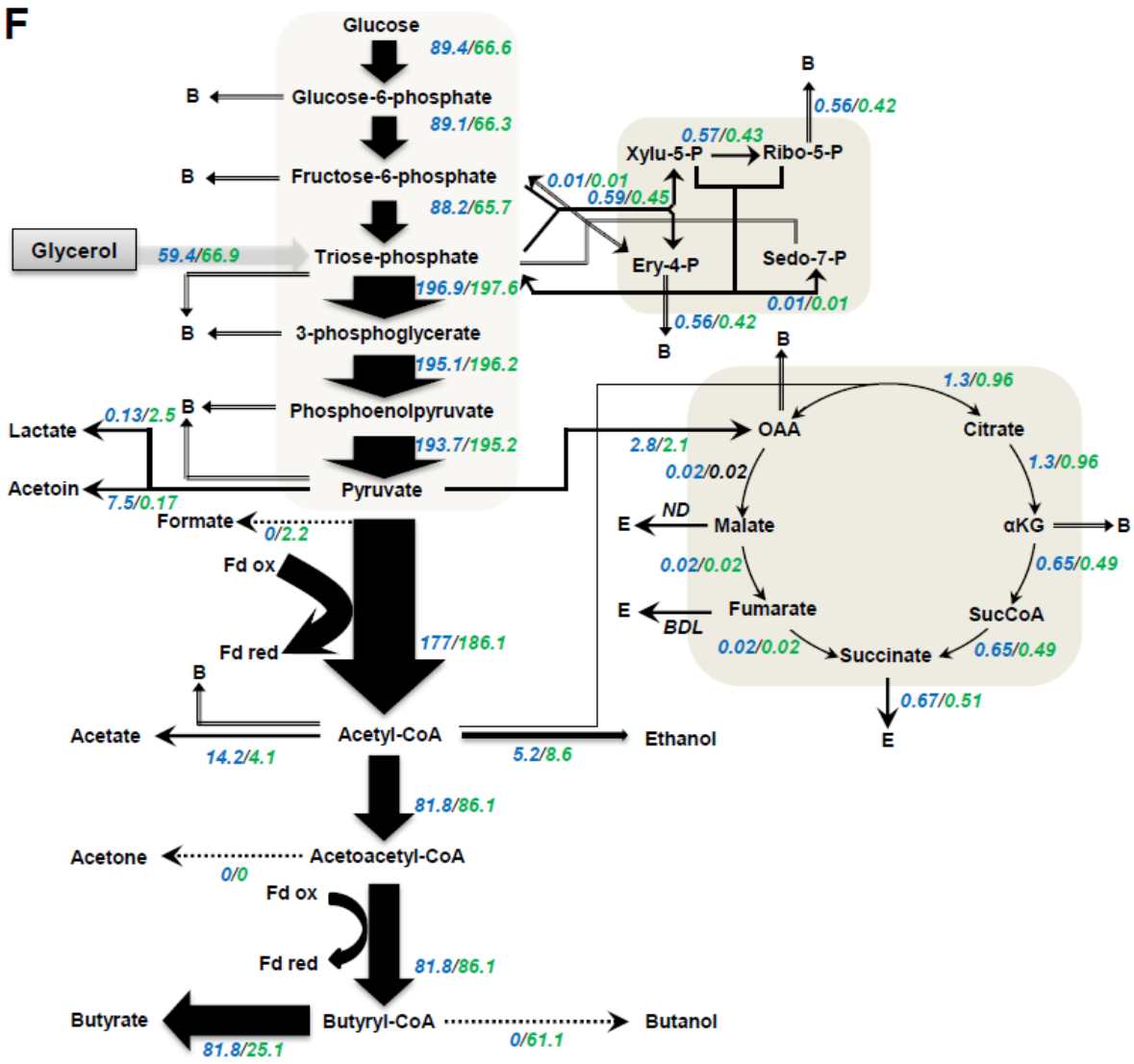

Fig. S3.3. Metabolic flux map of *ΔadhE1* under acidogenesis (A), *ΔadhE2* under acidogenesis (B), *ΔadhE1* under solventogenesis (C), *ΔadhE2* under solventogenesis (D), . *ΔadhE1* under alcohologenesis (E), *ΔadhE2* under alcohologenesis (F). All values are normalized to the flux of the initial carbon source (mmol/gDCW/h). Glucose flux is normalized as 100 for acidogenesisand solventogenesis, and the sum of glucose and half of the glycerol normalized as 100 for alcohologenesis. The values of corresponding mutant are shown in blue letter, and that of control strain are shown in green letter.

Chapter 4

Results and discussion part 3- Δ*buk*Δ*ptb* strain

Analysis of butyrate pathway mutant of *Clostridium acetobutylicum* by a quantitative system-scale approach

Not submitted as of April, 2016

Abstract

Clostridium acetobutylicum possesses two homologous *buk* genes, *buk1* or *buk1* and *buk2*, which encode butyrate kinases involved in the last step of butyrate formation. To investigate the contribution of *buk1* in detail, an in-frame deletion mutant was constructed. However, in all the *Δbuk* mutants obtained, partial deletions of the upstream *ptb* gene were always observed and very low phosphotransbutyrylase and the butyrate kinase activities were measured. This demonstrates that i) *buk* (CA_C3075) is the key butyrate kinase encoding gene and that *buk2* (CA_C1660) that is poorly transcribed (Yoo *et al.*, 2015) only play a minor role and ii) strongly suggests that a *Δbuk* mutant is not viable if the *ptb* gene is not also inactivated probably due to butyryl-phosphate accumulation that might be toxic for the cell.

One of the *ΔbukΔptb* mutant was subjected to quantitative transcriptomic (mRNA molecules/cell) and fluxomic analyses in acidogenic, solventogenic and alcohologenic chemostat cultures. Beside the low butyrate production, drastic changes in metabolic fluxes were also observed for the mutant: 1) under acidogenic conditions the primary metabolite was butanol, 2) under solventogenesis, a 58% increased butanol production was obtained compared to control strain under same condition and a very high yield of butanol formation was reached, 3) under alcohologenesis, the major product was lactate. Furthermore, at the transcriptional level, *adhE2*, encoding an aldehyde/alcohol dehydrogenase known as a gene specifically expressed in alcohologenesis, was surprisingly highly expressed in all the metabolic states in the mutant.

The results presented here not only support the key role of *buk* and *ptb* in butyrate formation but also highlight the metabolic flexibility of *C. acetobutylicum* to genetic alteration of its primary metabolism.

1. Introduction

Clostridium acetobutylicum is now considered the model organism for the study of solventogenic Clostridia (Nair *et al.*, 1994b, Lutke-Eversloh & Bahl, 2011b). The superiority of butanol over ethanol as an alternative biofuel has attracted research interest into *C. acetobutylicum* and other recombinant bacteria producing butanol as major products (Atsumi & Liao, 2008b).

In phosphate-limited chemostat cultures, *C. acetobutylicum* can be maintained in three different stable metabolic states (Vasconcelos *et al.*, 1994, Girbal *et al.*, 1995b, Girbal & Soucaille, 1994a, Girbal & Soucaille, 1998a, Bahl *et al.*, 1982a) without cellular differentiation (Grimmler *et al.*, 2011b): acidogenic (producing acetate and butyrate) when grown at neutral pH with glucose; solventogenic (producing acetone, butanol, and ethanol) when grown at low pH with glucose; and alcohologenic (forming butanol and ethanol but not acetone) when grown at neutral pH under conditions of high NAD(P)H availability (Girbal & Soucaille, 1994a, Peguin & Soucaille, 1995b, Girbal *et al.*, 1995b).

The molecular mechanisms of metabolic shifts and regulation of the primary metabolism of *C. acetobutylicum* have been studied but still largely remain to be elucidated. A number of metabolic mutants in acid or solvent formation pathways have been created to better understand the regulation of this bacterium's metabolism. In particular, butyrate kinase (*buk*) or phosphotransbutyrylase (*ptb*) mutants have attracted attention because the butanol formation pathway is in competition with the butyrate formation pathway (Sillers *et al.*, 2008b), as they share a branch point intermediate, butyryl-CoA. *C. acetobutylicum* possesses two butyrate kinase-encoding genes, *buk* or *buk1* (CA_C3075), which is part of the *ptb-buk* operon (Walter et al., 1993), and *buk2* (CA_C1660), which is transcribed as a monocistronic operon (Huang et al., 2000). Most of the *buk* or *ptb* mutants have been analyzed under batch conditions. Despite

the valuable insights achieved in those studies, many physiological parameters, such as specific growth rates, specific glucose consumption rates, pH, and cellular differentiation, as well as acids and butanol stress, change with time, making it difficult to understand many details of *buk* and *ptb* expression patterns. Recently, Honicke et al. (Honicke *et al.*, 2014b) reported a transcriptional analysis of a chemostat culture of *C. acetobutylicum* ptb::int (87) (obtained by ClosTron mutagenesis method) under acidogenesis and solventogenesis. However, no fluxomic analysis was supplied, and alcohologenic conditions (Girbal *et al.*, 1994b) were not studied.

To obtain targeted metabolic mutants for functional genomics studies or for metabolic engineering of clostridia known to be difficult to genetically manipulate, a few useful gene disruption methods have been established by several research groups. To date, one of the most commonly used methods is ClosTron, which is based on mobile group II introns (Lutke-Eversloh, 2014a, Heap *et al.*, 2007a). Although this technique has resulted in the successful construction of a number of mutants, it has vulnerable points, possibilities for intrinsic instability (Steiner et al., 2011), and polar effects on the integrated intron as well as limited availability for short-length target genes (Wang *et al.*, 2015, Al-Hinai *et al.*, 2012, Lutke-Eversloh, 2014a). Double-crossover allelic exchange methods, however, are free from these concerns (Croux *et al.*, 2016, Al-Hinai *et al.*, 2012).

The aim of this study was to perform a clean in-frame deletion of *buk* to characterize its role in butyrate formation. Furthermore, to study the metabolic flexibility of *C. acetobutylicum* in response to this gene deletion, a complete fluxomic and quantitative transcriptomic analysis was also performed under the three conditions known for the wild type strains as acidogenic, solventogenic and alcohologenic states. The results presented here not only support the key roles of *buk* and *ptb* in butyrate formation but also highlight the metabolic flexibility of *C.*

acetobutylicum to genetic alteration of its primary metabolism.

2. Materials and Methods

2.1 Bacterial strains and plasmid construction

As patented previously (Soucaille, 2008), all *ΔbukΔptb* strains were derived from the control strain *C. acetobutylicum* ATCC 824 ΔCA_C1502 *Δupp*, which was constructed for rapid gene knockout and gene knockin by the allelic exchange deletion method (Croux *et al.*, 2016). The strains and primers are described in the patent (Soucaille, 2008).

Culture conditions

All batch cultures were performed under strict anaerobic conditions in synthetic medium (MS), as previously described. *C. acetobutylicum* was stored in spore form at -20 °C after sporulation in MS medium. Heat shock was performed for spore germination by immersing a 30- or 60-mL culture vial into a water bath at 80 °C for 15 minutes.

All the phosphate-limited continuous cultivations were performed as previously described by (Vasconcelos *et al.*, 1994) and (Girbal *et al.*, 1995b) under the same conditions as the control strain study (Yoo *et al.*, 2015). The chemostat was fed a constant total of 995 mM carbon and maintained at a dilution rate of 0.05 h^{-1}. The maintained pH of the bioreactor and the supplied carbon sources of each metabolic state were as follows: for acidogenesis, pH 6.3, with 995 mM carbon from glucose; for solventogenesis, pH 4.4, with 995 mM carbon from glucose; and for alcohologenesis, pH 6.3, with 498 mM carbon from glucose and 498 mM carbon from glycerol.

2.2 RNA extraction & microarray

Total RNA isolation and microarray experiments were performed as previously described (Yoo *et al.*, 2015). Briefly, 3 mL of chemostat cultures were sampled, immediately frozen in liquid nitrogen, and ground with 2-mercaptoethanol. RNA was extracted using an RNeasy Midi kit (Qiagen, Courtaboeuf, France) and RNase-Free DNase Set (Qiagen) following the manufacturer's instructions. RNA quantity and integrity were monitored using an Agilent 2100 Bioanalyzer (Agilent Technologies, Massy, France) and a NanoDrop ND-1000 spectrophotometer (Labtech France, Paris, France) at 260 nm and 280 nm. All microarray procedures were performed per the manufacturer's protocol (Agilent One-Color Microarray-Based Exon Analysis).

2.3 Analytical methods

The optical density at 620 nm (OD620 nm) was monitored and used to calculate the biomass concentration with the correlation factor between dry cell weight and OD620 nm (path length 1 cm) of 0.28, which was used in the control strain study (Yoo *et al.*, 2015). The glucose, glycerol, acetate, butyrate, lactate, pyruvate, acetoin, acetone, ethanol, and butanol concentrations were determined using high-performance liquid chromatography (HPLC) coupled with a refractive index detector (RID) and a UV detector, as described by Dusséaux et al. (Dusseaux *et al.*, 2013)). The concentration of the eluent H2SO4 was changed to 0.5 mM to optimize the mobile phase for the control strain study (Yoo *et al.*, 2015).

2.4 Purification and identification of unknown metabolites

Two unknown metabolites, produced by the *ΔbukΔptb* strain under acidogenic conditions, were identified by analytical HPLC (see above) and purified by collecting fractions resulting from

ten successive injections on the analytical HPLC system. After neutralization of the two collected fractions by the addition of sodium hydroxide (5 mM), they were concentrated by evaporation at 40 °C under vacuum. Each of the two concentrated fractions were then verified for purity by analytical HPLC and analyzed by 1D and 2D NMR as previously described. The two unknown compounds were identified by NMR as 2-hydroxy-valerate and 2-keto-valerate. This was confirmed by running pure commercial compounds on the analytical HPLC.

2.5 Calculation of the contribution of different enzymes on the butanol flux

As published previously (Yoo *et al.*, 2016), the contribution of the 5 proteins potentially involved in the butanol pathway, namely AdhE1, AdhE2, BdhA, BdhB, and BdhC, was calculated by assuming that all five enzymes were functioning at their Vmax and using the calculated amount of each protein to determine the number of protein molecules per cell (Dataset S1).

2.6 Calculation of cytosolic protein concentrations (protein molecules per cell)

In a previously published work (Yoo et al., 2015), the quantified amounts of i) mRNA molecules per cell for all genes and ii) protein molecules per cell (for approximately 700 cytosolic proteins) for steady-state chemostat cultures (at a specific growth rate of 0.05 h^{-1}) of *C. acetobutylicum* under different physiological conditions were calculated. For 96% of the cytosolic proteins that could be quantified, a linear relationship was obtained, with an $R2 > 0.9$ when the numbers of protein molecules per cell were plotted against the numbers of mRNA molecules per cell. This result indicated that for steady-state continuous cultures run at the same specific growth rate and with the same total amount of supplied carbon, the rate of protein

turnover was proportional to the mRNA content for 96% of the genes. As the *Δbuk Δptb* strain was cultivated in chemostat culture at the same growth rate (0.05 h^{-1}), we used the absolute protein synthesis rates (kx) previously calculated for each of the 700 genes to calculate the amount of protein molecules per cell for each of these 700 genes in the *Δbuk Δptb* mutant (Dataset S1).

2.7 *Availability of data and material*

Microarray data can be accessed at GEO through accession number GSE69973.

3. Results and discussion

3.1 Construction of the Δbuk mutant strains

The strategy for the construction of the *Δbuk* mutant was relatively straightforward, as *buk* is the second gene of an operon composed of *ptb* (encoding a phosphotransbutyrylase) and *buk* (encoding a butyrate kinase) (Fontaine *et al.*, 2002b). The method used for the in-frame deletion of *buk* was the recently published allelic exchange method previously used for the creation of a marker-less restriction-less strain and for the deletion of several genes, including *ldhA*, *ctfAB*, *adhE1*, *adhE2* and *perR* (Fontaine *et al.*, 2002b). However, when this method was applied to the construction of the *Δbuk* mutant, we always observed some modification of the upstream *ptb* gene in parallel to the *buk* deletion (Fig. 1). The results obtained from four of the mutants are presented in Fig. 1. For the two first mutants, partial internal deletions of 90 and 320 bp, respectively, were observed in either the 5' or the 3' parts of the *ptb* gene. For the two other mutants, deletions of 605 and 808 bp, respectively, were observed in the 3' part of the *ptb* gene,

including the FRT site upstream of the *ery*^{R} marker. The phosphotransbutyrylase and the butyrate kinase activities were measured for the wild type and the four mutant strains. The data show that both activities were very low in all mutant strains (Fig. 1) (Data not shown). This demonstrates that *buk* (CA_C3075) is the key butyrate kinase-encoding gene and that *buk2* (CA_C1660), which is poorly transcribed (Yoo et al., 2015), only plays a minor role. It also strongly suggests that a *Δbuk* mutant is not viable if the *ptb* gene is not also inactivated, probably due to butyryl-phosphate accumulation that might be toxic for the cell.

Hereafter, *C. acetobutylicum ΔCA_C1502ΔbukΔptb320* (Fig. 1) is referred to as *ΔbukΔptb* and was used in all chemostat culture experiments.

3.2 Carbon and electron fluxes of the ΔbukΔptb mutant under different physiological conditions

The *ΔbukΔptb* mutant was first evaluated under acidogenic conditions and compared to previously published data for the control strain (Yoo et al., 2015). During this flux analysis, it turned out that the carbon balance was not closed by over 20%. It was already shown that butyrate pathway disrupted strains could demonstrate imbalanced carbon in batch cultures without pH control (68%) (Lehmann *et al.*, 2012b). The HPLC chromatogram of acidogenic cultures of the *ΔbukΔptb* mutants revealed two peaks corresponding to unknown compounds detected by both RID and UV. Those two compounds were purified by HPLC and analyzed by 1D and 2D NMR and unambiguously identified as 2-hydroxy-valerate for the major compound and 2-keto-valerate for the minor compound. 2-keto-valerate, an intermediate in the L-norvaline pathway, is a compound that has been shown to be produced by *Escherichia coli* during a shift from aerobic to anaerobic conditions (Soini *et al.*, 2008) due to both pyruvate

accumulation and repression of the leucine operon. The proposed pathway for the production of these two compounds is presented in Fig. 2. As previously described, *Serratia marcescens* (Kisumi et al., 1976) uses part of the L-leucine pathway (CA_C3171-3174 in *C. acetobutylicum*), and LdhA is proposed to catalyze the final reduction of 2-keto-valerate to 2-hydroxy-valerate.

In addition to the production of 2-hydroxy-valerate, the mutant strain demonstrated a profound change in its metabolism, with butyrate and acetate fluxes that were decreased by 93 and 30%, respectively, and lactate, ethanol and butanol fluxes that were increased by 8-, 4-, and 32-fold, respectively (Fig. 3, Fig. S2), compared to the control strain. These drastic flux changes were accompanied by a 4-fold decrease in hydrogen production and by other changes in electron fluxes (Fig. 4), which are described in detail below. The production of butanol of the *ΔbukΔptb* strain under acidogenesis is explained by the higher expression of *adhE2* (~185-fold higher than the control strain, with 79 mRNA molecules/cell) (Table 1, Dataset S1), while the expression of the *sol* operon was unchanged. The increase in lactate formation was associated with a 23-fold increase in *ldhA* expression. For the *ΔbukΔptb* mutant, the acetate flux decreased by 36% compared to the control strain (Fig. S2), although *pta-ack* (CA_C1742–CA_C1743) did not experience a significant transcriptional decrease (Dataset S1). Thus, flux is controlled at the enzyme level via a decrease in the acetyl-CoA pool, probably due to a 3-fold higher expression of most of the genes (CA_C2873 and CA_C2708–2712) coding for the enzymes converting acetyl-CoA to butyryl-CoA. A different result was previously obtained by (Harris *et al.*, 2000a) for a *buk* inactivated mutant of *C. acetobutylicum*, which showed a 56% increase in acetate production when cultured in batch mode.

The mutant strain was then evaluated under solventogenic conditions and compared to previously published data for the control strain (Yoo et al., 2015). Here again, the metabolism

was modified, with butyrate, acetate and acetone fluxes that were decreased by 74, 57, and 82%, respectively, and lactate, ethanol and butanol fluxes that were increased by 2-, 4-, and 1.5-fold, respectively (Fig. 3, Fig. S2), compared to the control strain. Such changes were accompanied by a 4-fold decrease in hydrogen production and by other changes in electron fluxes (Fig. 4), which are described in detail below. Interestingly, this mutant produced butanol at a glucose yield of 0.3 $g.g^{-1}$ (73% of the theoretical yield) and butanol + ethanol at a glucose yield of 0.35 $g.g^{-1}$ in continuous culture on a medium free of any organic nitrogen; these values have never before been obtained in this type of medium. A different result was previously obtained by (Honicke *et al.*, 2014b) for a *ptb*-inactivated mutant of *C. acetobutylicum*, which showed no changes in butanol and acetone production when cultured in chemostat culture under solventogenesis, suggesting that inactivation of both *ptb* and *buk* is necessary for the observed high solventogenic phenotype. The higher production of butanol and the lower production of acetone of the *ΔbukΔptb* strain under solventogenesis is explained by the higher *adhE2* expression (~360-fold higher than the control strain, with 77 mRNA molecules/cell) (Table 1, Dataset S1), while the expression of the sol operon was decreased 2.5-fold. The increase in lactate formation was associated with a 5.5-fold increase in *ldhA* expression. For the *ΔbukΔptb* mutant, the acetate flux decreased by 74% compared to the control strain (Fig. S2) and was associated with a 2-fold transcriptional decrease in the *pta-ack* (CA_C1742–CA_C1743) operon and 2-fold higher expression of most of the genes (CA_C3076–CA_C3075) coding for the enzymes converting acetyl-CoA to butyryl-CoA.

The mutant strain was also evaluated under alcohologenic conditions and compared to previously published data for the control strain (Yoo et al., 2015). The *ΔbukΔptb* mutant exhibited completely different behavior; a 3-fold decrease in glycerol consumption was associated with a 2-fold decrease in butanol flux, whereas lactate fluxes became the primary

fluxes (Fig. S2). Such drastic flux changes were accompanied by a 4-fold decrease in hydrogen production and by other changes in electron fluxes (Fig. 4), which are described in detail below. The lower glycerol consumption of the *ΔbukΔptb* strain is explained by the lower expression (15-65-fold decrease) of the gene cluster coding for glycerol transport and utilization (CA_C1319–CA_C1323). The increase in lactate formation was associated with a 9-fold increase in *ldhA* expression, but the lower production of butanol was not associated with lower *adhE2* expression.

The butanol pathway was analyzed for three different conditions in the *ΔbukΔptb* mutants (Fig. S1) by calculating the contribution of each of the five enzymes potentially involved in each of the two flux steps (see methods for the calculation).

Under acidogenesis, *adhE2* was highly expressed and *adhE1* was not expressed, and thus AdhE2 converts butyryl-CoA to butyraldehyde in the *ΔbukΔptb* mutant (Fig. S1). Similarly, with respect to the conversion of butyraldehyde to butanol in the mutant, AdhE2 (98% of the flux) was the main contributor (Fig. S1).

Under solventogenesis, regarding the conversion of butyryl-CoA to butyraldehyde in the *ΔbukΔptb* mutant, AdhE2 (88% of the flux) became the main contributor, with AdhE1 (12% of the flux) playing a minor role. Similarly, the main contributor to the conversion of butyraldehyde to butanol in the mutant was AdhE2 (98% of the flux) (Fig. S1). These results are in sharp contrast to the wild type strain, where the butyraldehyde dehydrogenase flux is largely attributable to AdhE1 (95% of the flux), and the butanol dehydrogenase flux is primarily attributable to BdhB (77% of the flux), BdhA (9% of the flux), and BdhC (4% of the flux), in decreasing order of activity.

Under alcohologenesis, the *ΔbukΔptb* mutant behaved the same as the control strain, as AdhE2

was responsible for both the conversion of butyryl-CoA to butyraldehyde and the conversion of butyraldehyde to butanol (Fig. S1).

The electron fluxes were analyzed for three different conditions in the *ΔbukΔptb* mutant (Fig. 4). Under acidogenesis and solventogenesis, the primary use of reduced ferredoxin was switched from hydrogen to NADH production in response to the high expression of *adhE2* in the mutant. Under acidogenesis and solventogenesis, the hydrogen production fluxes decreased by ~3 and 4-fold, respectively, while the fluxes of NADH production from reduced ferredoxin increased 4-and 10-fold, respectively (Fig. 4). Accordingly, as in solventogenesis of the mutant, the NADPH-dependent butanol dehydrogenases no longer played a major role, and the fluxes of NADPH production from reduced ferredoxin decreased 7-fold compared to the wild type strain. The decrease in hydrogen production was not attributable to the lower expression of *hydA* (CA_C0028), as 3- and 4.7-fold higher expression was observed under acidogenesis and solventogenesis, respectively. Furthermore, ferredoxin (encoded by *fdx1*, i.e., CA_C0303), a key redox partner of HydA, revealed similar numbers of mRNA molecules per cell compared to the control strain for the two conditions. Conversely, a potential multimeric flavodoxin encoded by CA_C3486 was highly expressed (44-fold increase for acidogenesis and 6-fold increase for solventogenesis compared to the control strain). This protein, in its reduced form, was previously suggested (Yoo et al., 2015) to be a better substrate for the ferredoxin NAD^+ reductase than for the hydrogenase, which could also explain the change in the electron fluxes observed in the *ΔbukΔptb* mutant under both acidogenesis and solventogenesis. In alcohologenesis, lactate was the main fermentation product of the *ΔbukΔptb* mutant, and both the hydrogenase and the ferredoxin-NAD^+ reductase fluxes decreased 4-fold and 2-fold, respectively. The low ferredoxin-NAD^+ reductase fluxes and butanol fluxes can be explained by the 5-fold down-regulation of CA_C3486, which encodes a potential multimeric fladoxin,

and the proposed physiological role stated above.

3.3 Common criteria used for quantitative transcriptomic analysis

To filter the data to obtain only significant results, the same criteria used to compare the wild-type strain under different physiological conditions (Yoo et al., 2015) were used to compare the mutant to the control strain. The first criterion was > 4.0-fold higher expression or > 4.0-fold lower expression in *ΔbukΔptb* than in the control strain under the same physiological conditions, and the second criterion was > 0.2 mRNA molecules per cell in at least one of the two strains being compared.

3.4 Genes affected by ΔbukΔptb deletion under acidogenesis

Under these conditions, 148 genes showed significantly increased expression, whereas 262 genes showed decreased expression in the *ΔbukΔptb* mutant. One of the highest increases in expression was revealed for an operon located on pSOL1 and composed of CA_P0029 encoding a permease (∞-fold, 0 mRNA molecules per cell in control strain, ~7 mRNA molecules per cell in *ΔbukΔptb*) and CA_P0030 (~250-fold) encoding an isochorismatase. The second highest increase was observed for *adhE2* expression (186-fold), as previously pointed out in the carbon and electron flux analysis section. An operon involved in cysteine and sulfur metabolism (CA_C0102–CA_C0110) and proposed by (Wang *et al.*, 2013b) to belong to the cysteine metabolism regulator (CymR) regulon was also highly upregulated (41-122-fold) in the *ΔbukΔptb* mutant. Similar results were previously reported by (Honicke *et al.*, 2014b) with their *ptb* mutant under the same conditions. A long operon, CA_C2585–2592, encoding 6-

pyruvovyl tetrahydrobiopterin synthases, glycosyl-transferases, and hypothetical proteins, was highly upregulated (21-∞-fold compared to the control strain). Another operon *pyrBIFZD* (CA_C2654–CA_C2650) related to pyrimidine and aspartate metabolism showed a ~10-fold increase. In addition to these operons, one long gene cluster, CA_C3045–CA_C3059, related to polysaccharide biosynthesis showed a ~2.3-13-fold increase.

The greatest decrease in expression was for a gene cluster, *agrBDCA* (CA_C0078-CA_C0081) (-∞~414-fold), coding for an *agr*-dependent quorum sensing system involved in the regulation of sporulation and granulose formation (Steiner *et al.*, 2012b). Furthermore, *spo0A* (CA_C2071), encoding the master regulator of sporulation in *C. acetobutylicum*, showed a ~5-fold decrease in expression. Moreover, among the three orphan histidine kinases (CA_C0323, CA_C0903, and CA_C3319) able to directly phosphorylate Spo0A in *C. acetobutylicum* (Al-Hinai et al., 2015), CA_C3319, which has the highest numbers of mRNA molecules per cell among the three genes in the control strain under all conditions, also showed significantly decreased expression (~33-fold) in *ΔbukΔptb*. This decreased gene expression is consistent with the fact that this strain poorly sporulate under acidogenesis and corroborates the asporogenous phenotype of the *spo0A* (Ravagnani *et al.*, 2000a) or CA_C3319 (Steiner et al., 2011) knockout strains.

CA_P0036 and CA_P0037, two genes located on pSOL1 that encode a cytoplasmic protein and a potential transcriptional regulator and are both highly transcribed and translated, respectively (Yoo et al., 2015), were highly downregulated (~27- and 33-fold, respectively) in *ΔbukΔptb.* Similar results were obtained when the control strain was switched from acidogenic to solventogenic or alcohologenic conditions (Yoo et al., 2015).

CA_C2806 and CA_C2807, encoding an Icc (Intracellular Chloride Chanel) family

phosphohydrolase and endo-1,3(4)-beta-glucanase, respectively, revealed ~59- and 203-fold decreases in *ΔbukΔptb*, while they achieved the highest numbers of mRNA molecules per cell in control strains under acidogenesis. In addition to CA_C2806, three other Icc family phosphohydrolases, namely CA_C0205, CA_C1010, and CA_C1078, also demonstrated considerable decreases in transcription (~13-, 57-, and 64-fold, respectively).

Curiously, three neighboring operons (CA_C1994–CA_C1988 related to iron/folate metabolism, CA_C2002–CA_C1995 related to molybdenum cofactor biosynthesis/ABC-type iron transport system, and CA_C2006–CA_C2003 involved in surfactin biosynthesis) demonstrated decreased expression (~5.2-∞-fold) under both acidogenesis and alcohologenesis in the mutant strain.

Two long gene clusters related to chemotaxis and motility (CA_C2139–CA_C2165 and CA_C2204–CA_C2225) did not demonstrate opposing expression patterns with *spo0A*, contrary to previous publications on asporogenous, non-solventogenic *C. acetobutylicum* strains (SKO1 and M5) (Tomas *et al.*, 2003b), and on *B. subtilis* (Fawcett et al., 2000), which reported inhibited expression by spo0A via indirect σ^D-mediated regulation. In *ΔbukΔptb*, the expression pattern of member genes of the clusters was either repressed or similar to the control strain when *spo0A* was repressed.

Lastly, CA_C1037, CA_P0054 and CA_P0053, encoding xylanases/chitin deacetylases and xylanase, were significantly repressed (~11-, 13- and 17-fold, respectively).

3.5 Genes affected by ΔbukΔptb deletion under solventogenesis

Under solventogenesis conditions, 45 genes showed significantly increased expression,

whereas 85 genes showed decreased expression in the *ΔbukΔptb* mutant. As written above, under acidogenic conditions, *adhE2*, CA_P0029 and CA_P0030 were also highly upregulated under solventogenic conditions (~361-, 49- and 75-fold respectively). The neighboring gene CA_P0031, encoding a potential transcriptional activator, was induced as well (~30-fold).

An operon, CA_C0111–CA_C0112, encoding a glutamine-binding protein fused to a glutamine permease and a glutamine ABC transporter ATP-binding protein, respectively, was upregulated (~5.6- and 5.9-fold). This operon was also induced by 0.9% butanol stress (~4.5-fold) in a previous study (Janssen *et al.*, 2012b); however, its expression remained unchanged in the *ΔbukΔptb* mutant under acidogenesis, producing approximately 0.55% butanol. Meanwhile, an operon, CA_C2850–CA_C2849, encoding a proline/glycine betaine ABC transporter, was induced in the *ΔbukΔptb* mutant under all conditions, as well as by butanol stress (Janssen *et al.*, 2012b).

As described in the section for acidogenesis, sporulation of this strain was not observed under acidogenesis or during a switch from acidogenesis to solventogenesis. We could observe sporulation, and then spores were washed out before reaching a steady state. The ability of the *ΔbukΔptb* strain to sporulate under solventogenesis was in agreement with the normal expression of *spo0A* and CA_C3319, encoding a key Spo0A kinase (Steiner et al., 2011).

A gene, CA_C2293, encoding a hypothetical secreted protein, was considerably upregulated not only in solventogenesis but also in acidogenesis and in alcohologenesis. This gene was previously shown to be upregulated in solventogenesis not only in its wild type (control) strain (Janssen *et al.*, 2010b, Yoo *et al.*, 2015) but also in response to acetate, butyrate, or butanol stress (Alsaker *et al.*, 2010a).

Similar to acidogenesis, an operon, pyrBIFZD, related to pyrimidine and aspartate metabolism,

showed ~15–20-fold increases. Moreover, CA_C2644–CA_C2645 (*carBA*) were upregulated as well (~5- and 3.9-fold). It was reported that many pyrimidine-biosynthesis genes, for instance, *pyrD*, *pyrF* and *pyrI*, are downregulated by 50 mM of butanol stress (Alsaker *et al.*, 2010a). Based on the fact that the butanol production of *ΔbukΔptb* in solventogenesis is over 100 mM, we could conclude that other factors in addition to butanol stress are regulating the expression of these pyrimidine biosynthesis genes.

Interestingly, *amyP* (CA_P0168), encoding an alpha-amylase, was induced by approximately 7.2-fold. This gene showed low numbers of mRNA molecules per cell (~0.34–0.64) in the control strain under all conditions, but in *ΔbukΔptb*, the numbers changed depending on the metabolic state (~0.09–2.4 mRNA molecules per cell).

The greatest decreased expression, except by infinite-fold, was noted for CA_P0151–CA_P0152, encoding an integrin-like repeat-containing lysozyme and a hypothetical protein (~17-fold decrease). Curiously, the mannitol phosphotransferase system (PTS)-related operon *mtlARFD* (CA_C0154–CA_C0157) was downregulated (~9-12-fold), and the downregulation was even stronger under alcohologenesis. Moreover, the mannose/fructose PTS-related operon *ptnA-manY*/*levF-ptnD* (CA_P0066–CA_P0068) showed more than 4-fold decreased expression under solventogenesis, and more striking decreases were observed under alcohologenesis, such as the mannitol PTS operon. As described in the acidogenesis section, three neighboring operons (CA_C1994–CA_C1988, CA_C2002–CA_C1995, and CA_C2006–CA_C2003) demonstrated decreased expression (~4.6-7.3-fold) under solventogenesis as well.

3.6 Genes affected by ΔbukΔptb deletion under alcohologenesis

Under alcohologenesis conditions, 138 genes showed significantly increased expression, whereas 313 genes showed decreased expression. As written above in the carbon and electron fluxes section, *ΔbukΔptb* poorly consumes glycerol due to the lower expression (15-65-fold decrease) of the gene cluster coding for glycerol transport and utilization (CA_C1319–CA_C1323).

As stated above for the *ΔbukΔptb* mutant under acidogenic conditions, CA_P0029, CA_P0030, CA_C0102–CA_C0110 (an operon involved in cysteine and sulfur metabolism), proposed by (Wang *et al.*, 2013b) to belong to the cysteine metabolism regulator (CymR) regulon, and CA_C2585–CA_C2592, a long gene cluster, were also highly upregulated (41-122-fold) under alcohologenic conditions.

Strikingly, an operon (CA_C3174–CA_C3169) involved in valine, leucine and isoleucine biosynthesis was strongly upregulated (~6.4-9-fold, > 21 mRNA molecules per cell for all structural genes). In particular, CA_C3170 scored the highest numbers of mRNA molecules per cell under alcohologenic conditions. The previous transcriptional study by (Janssen *et al.*, 2012b) showed significant up-regulation of this operon in response to butanol stress (Jones *et al.*, 2008b). On the other hand, an operon involved in aromatic amino acid biosynthesis, CA_C3163–CA_C3157, and a gene, CA_C3617, coding for a tryptophan transporter, were also strongly upregulated (~10-25-fold), although a previous study revealed that they were downregulated in response to butyrate or butanol stress (Alsaker *et al.*, 2010a). To date, unlike butanol and butyrate, the lactate stress response has not been studied in depth in *C. acetobutylicum*, owing to the small amount of lactate usually produced by this organism. However, the lactate stress response has been well studied in *Lactobacillus plantarum* (Huang

et al., 2016, Ingham *et al.*, 2008, Pieterse *et al.*, 2005). Concomitant increased expression of *cfa,* (CA_C0877) (~4.7-fold) encoding a cyclopropane fatty acid synthase, and genes encoding membrane proteins, such as CA_C0611–CA_C0612 (~6.4- and 5.5-fold), were detected. This result is in agreement with the higher cyclopropane fatty acid contents demonstrated in lactic acid-stressed *Lactobacillus plantarum* (Huang et al., 2016). It might be interesting in the future to also study the response of *C. acetobutylicum* to lactate stress via a combined transcriptomic and proteomic approach, as previously done for butyrate and butanol.

As stated above in the carbon and electron fluxes section, low expression (15-65-fold decrease) of the gene cluster coding for glycerol transport and utilization (CA_C1319–CA_C1323) was associated with low glycerol consumption of the *Δbuk Δptb* strain, and low butanol formation was associated with lower expression (5-fold downregulated) of CA_C3486, encoding a multimeric flavodoxin. Furthermore, several PTS genes were downregulated: CA_C0154-CA_C0156, mannitol; CA_C0383-CA_C0386, cellobiose; CA_C0570, glucose; CA_C1407-CA_C1408, beta-glucosides; and CA_C3087, PTS enzyme I.

4. Conclusions

To conclude, continuous chemostat cultures of *Δbuk Δptb* showed very drastic changes in both fluxes and mRNA profiles depending on the metabolic state. However, some genes, such as *adhE2* and *CA_P0029–CA_P0030,* seem to be more influenced by *buk-ptb* deletion than by the metabolic state given the similar numbers of mRNA molecules per cell (i.e. fold change among three conditions < 2) for all conditions, unlike the control strain (e.g. CA_P0030 showed a ~29-fold change between acidogenesis and alcohologenesis).

This study also demonstrates the metabolic flexibility of *C. acetobutylicum* in response to

genetic alteration of its primary metabolism. Furthermore, the information provided here will be important for the further metabolic engineering of *C. acetobutylicum* to develop a commercial process for the production of n-butanol.

Table 1. Gene expression change in primary metabolism in *Δbuk*Δ*ptb* under three metabolic conditions[a]

Gene number	Gene name.	Function	*Δbuk*/Ctrl Acidogenesis	Ctrl molecules per cell Acidogenesis	*Δbuk* molecules per cell Acidogenesis	*Δbuk*/Ctrl Solventogenesis	Ctrl molecules per cell Solventogenesis	*Δbuk* molecules per cell Solventogenesis	*Δbuk*/Ctrl Alcohologenesis	Ctrl molecules per cell Alcohologenesis	*Δbuk* molecules per cell Alcohologenesis
CA_C0028	hydA	Hydrogenase	3.06	3.61 ± 0.13	11.06 ± 0.99	4.65	1.39 ± 0.09	6.45 ± 0.11	1.55	6.62 ± 2.11	10.28 ± 0.44
CA_C0267	ldhA	L-lactate dehydrogenase	22.68	0.41 ± 0.02	9.28 ± 0.22	5.41	0.55 ± 0.17	3 ± 0.05	8.71	0.35 ± 0.03	3.06 ± 0.1
CA_C0303	fdx1	Ferredoxin	1.07	45.4 ± 2.19	48.41 ± 3.78	0.78	21.22 ± 3.03	16.55 ± 1.55	1.02	16.77 ± 1.51	17.03 ± 1.62
CA_C1660	buk2	Butyrate kinase 2	1.48	0.13 ± 0.03	0.19 ± 0.02	0.6	0.11 ± 0.02	0.06 ± 0	0.38	0.18 ± 0.01	0.07 ± 0
CA_C1742	pta	Phosphate acetyltransferase	1.04	4.95 ± 0.24	5.14 ± 0.63	0.58	6.38 ± 1.11	3.69 ± 0.11	0.62	5.91 ± 0.25	3.65 ± 0.12
CA_C1743	ack	Acetate kinase	0.89	13.62 ± 0.39	12.12 ± 0.17	0.59	16.26 ± 3.02	9.6 ± 0.14	0.61	14.02 ± 1.71	8.56 ± 0.31
CA_C2229	pfor	Pyruvate:ferredoxin oxidoreductase	1.37	53.1 ± 1.09	72.99 ± 3.04	0.92	65.85 ± 7.56	60.28 ± 6.88	0.41	49.49 ± 2.27	20.07 ± 0.62

CA_C2708	hbd	3-Hydroxybutyryl-CoA dehydrogenase	3.21	16.98 ± 1.15	54.48 ± 2.82	2.26	19.36 ± 5.09	43.75 ± 1.75	0.91	52.45 ± 7.22	47.59 ± 1.3
CA_C2709	etfA	Electron transfer flavoprotein subunit A	3.02	24.98 ± 0.09	75.54 ± 1.4	2.13	28.86 ± 6.35	61.46 ± 5.55	0.76	71.44 ± 2.65	54.08 ± 0.36
CA_C2710	etfB	Electron transfer flavoprotein subunit B	3.85	9.59 ± 0.09	36.94 ± 1.87	2.16	9.42 ± 1.63	20.37 ± 0.64	0.83	28.29 ± 2.78	23.52 ± 1.09
CA_C2711	bcd	Butyryl-CoA dehydrogenase	1.29	61.12 ± 1.91	78.81 ± 1.15	1.23	62.03 ± 6.11	76.25 ± 4.96	1.03	76.44 ± 4.11	78.6 ± 0.07
CA_C2712	crt	Crotonase	1.59	49.59 ± 1.51	78.81 ± 1.15	1.44	51.89 ± 7.02	74.89 ± 4.08	0.99	76.44 ± 4.11	75.93 ± 3.71
CA_C2873	thlA	Thiolase A	3.65	17.69 ± 0.26	64.6 ± 1.93	2.11	26.56 ± 3.73	56.07 ± 1.48	0.42	54.29 ± 1.07	22.66 ± 1
CA_C3075	buk	Butyrate kinase 1	0	74.68 ± 1.45	0 ± 0	0	57.6 ± 6.24	0 ± 0	0	68.87 ± 3.03	0 ± 0
CA_C3076	ptb	Phosphate butyryltransferase	1.18	37.32 ± 2.05	43.88 ± 2.25	1.33	30.38 ± 6.23	40.27 ± 0.81	0.94	33.95 ± 1.5	31.85 ± 1.04
CA_C3298	bdhB	NADPH-dependent alcohol dehydrogenase B	0.06	16.31 ± 0.45	1 ± 0.17	0.77	28.1 ± 5.07	21.67 ± 1	0.04	14.33 ± 2.65	0.61 ± 0.01
CA_C3299	bdhA	NADPH-dependent alcohol dehydrogenase A	0.28	8.15 ± 0.32	2.28 ± 0.09	0.57	8.22 ± 1.33	4.64 ± 0.27	0.51	6.08 ± 0.37	3.12 ± 0.27

CA_C3392	bdhC	NADPH-dependent alcohol dehydrogenase C	1.71	8.63 ± 0.94	14.77 ± 0.39	1.32	11.28 ± 1.68	14.91 ± 0.23	0.63	10.73 ± 0.94	6.75 ± 0.3
CA_C3486	CA_C3486	Multimeric flavodoxin	43.77	0.38 ± 0.05	16.58 ± 0.11	6.32	0.33 ± 0.1	2.06 ± 0.06	0.2	2.28 ± 1.03	0.46 ± 0.03
CA_P0025	pdc	Pyruvate decarboxylase	0.33	5.6 ± 0.81	1.83 ± 0.33	0.31	5.17 ± 2.78	1.62 ± 0.04	1.18	1.23 ± 0.51	1.46 ± 0.05
CA_P0035	adhE2	NADH-dependent aldehyde-alcohol dehydrogenase	185.75	0.42 ± 0.02	78.81 ± 1.15	360.69	0.21 ± 0.02	76.25 ± 4.96	1.15	68.6 ± 12.95	78.6 ± 0.07
CA_P0162	adhE1	NADH-dependent aldehyde dehydrogenase	1.43	0.09 ± 0.01	0.12 ± 0	0.43	7.09 ± 0.73	3.05 ± 0.05	1.57	0.13 ± 0.01	0.2 ± 0
CA_P0163	ctfA	CoA transferase subunit A	1.69	0.18 ± 0.02	0.3 ± 0.02	0.41	25.74 ± 2.58	10.55 ± 0.53	1.59	0.36 ± 0.08	0.57 ± 0.02
CA_P0164	ctfB	CoA transferase subunit B	1.62	0.12 ± 0.02	0.19 ± 0	0.41	10.25 ± 1.66	4.18 ± 0.09	1.65	0.18 ± 0.04	0.3 ± 0.01
CA_P0165	adc	Acetoacetate decarboxylase	0.11	3.99 ± 0.51	0.44 ± 0.16	0.33	11.14 ± 1.04	3.63 ± 0.23	0.17	1.98 ± 0.05	0.35 ± 0

[a]Data are expressed as mean ± SD (triplicate samples)

Figure legends

Fig.4.1. Ideal and 4 different types of ΔbukΔptb mutants.

(A) Ideal mutant, (B) Δ90 strain showing deletion in-frame in the 5' region of ptb (Δ30aa/301), (C) Δ300 strain showing deletion of 320bp in the 3' region of ptb (Δ135aa/301) and addition of an extrac C-term of 8aa, (D) Δ605 strain showing deletions of 605bp comprising the 3' region of ptb (Δ89aa/301) and FRT site, (E) Δ808 strain showing deletions of 808bp comprising the 3' region of ptb (Δ173aa/301) and FRT site. The red arrow indicates entire or partially deleted ptb, the green arrow indicates FRT site, and the blue arrow indicates entire erythromycin resistance gene.

Fig.4.2. Pathway to 2-hydroxy-valerate in *C. acetobutylicum*

Fig.4.3. Substrates and products profile under three different conditions for the control and ΔbukΔptb300strains. (A) Carbon source consumption: glucose (blue) and glycerol (red). Product profiles in acidogenesis(B), solventogenesis(C), and alcohologenesis(D). For (B), (C) and (D), each histogram indicates different strains: control (blue) and ΔbukΔptb300(green).

Fig.4.4. Electron flux map of the control and *ΔbukΔptb* strains in acidogenesis (A), solventogenesis (B), and alcohologenesis (C). The arrows for hydrogenase (red), ferredoxin-NAD+ reductase (blue) and ferredoxin-NADP+ (green) *in vivo* fluxes are presented. All values are normalized to the flux of the initial carbon source (millimoles per gram of dry cell weight (DCW) per hour). Glucose flux is normalized to 100 for acidogenesis and solventogenesis, and the sum of glucose and half of the glycerol is normalized to 100 for alcohologenesis.

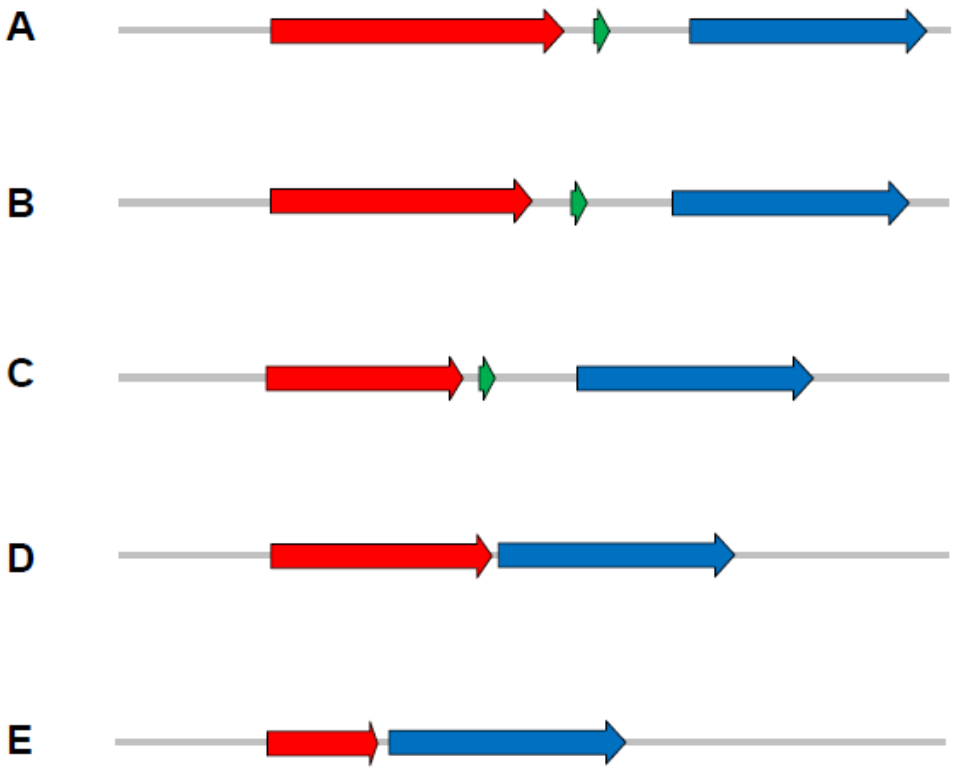

FIG 1. Ideal and 4 different types of ΔbukΔptb mutants.
(A) Ideal mutant, (B) Δ90 strain showing deletion in-frame in the 5' region of *ptb* (Δ30aa/301), (C) Δ300 strain showing deletion of 320bp in the 3' region of *ptb* (Δ135aa/301) and addition of an extra C-term of 8aa, (D) Δ605 strain showing deletions of 605bp comprising the 3' region of *ptb* (Δ89aa/301) and FRT site, (E) Δ808 strain showing deletions of 808bp comprising the 3' region of *ptb* (Δ173aa/301) and FRT site. The red arrow indicates entire or partially deleted *ptb,* the green arrow indicates FRT site, and the blue arrow indicates entire erythromycin resistance gene.

Fig. 4.1.

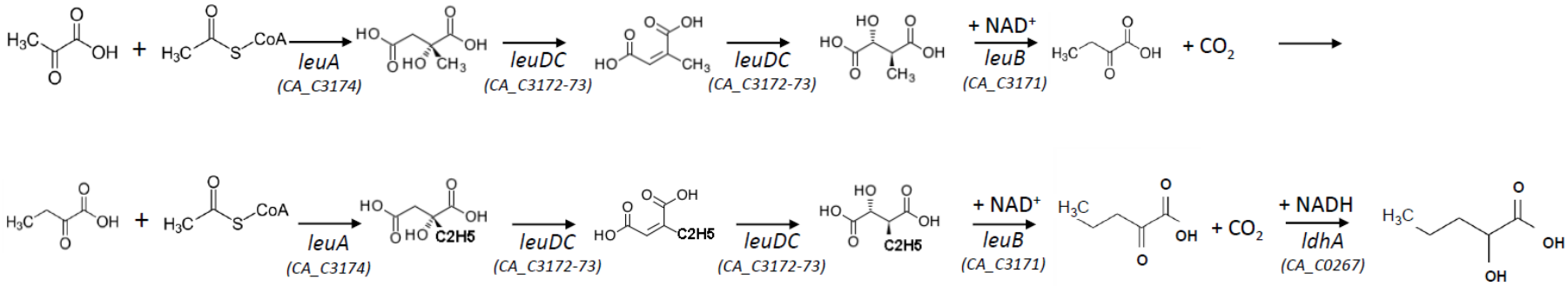

Fig.4.2. Pathway to 2-hydroxy-valerate in *C. acetobutylicum*

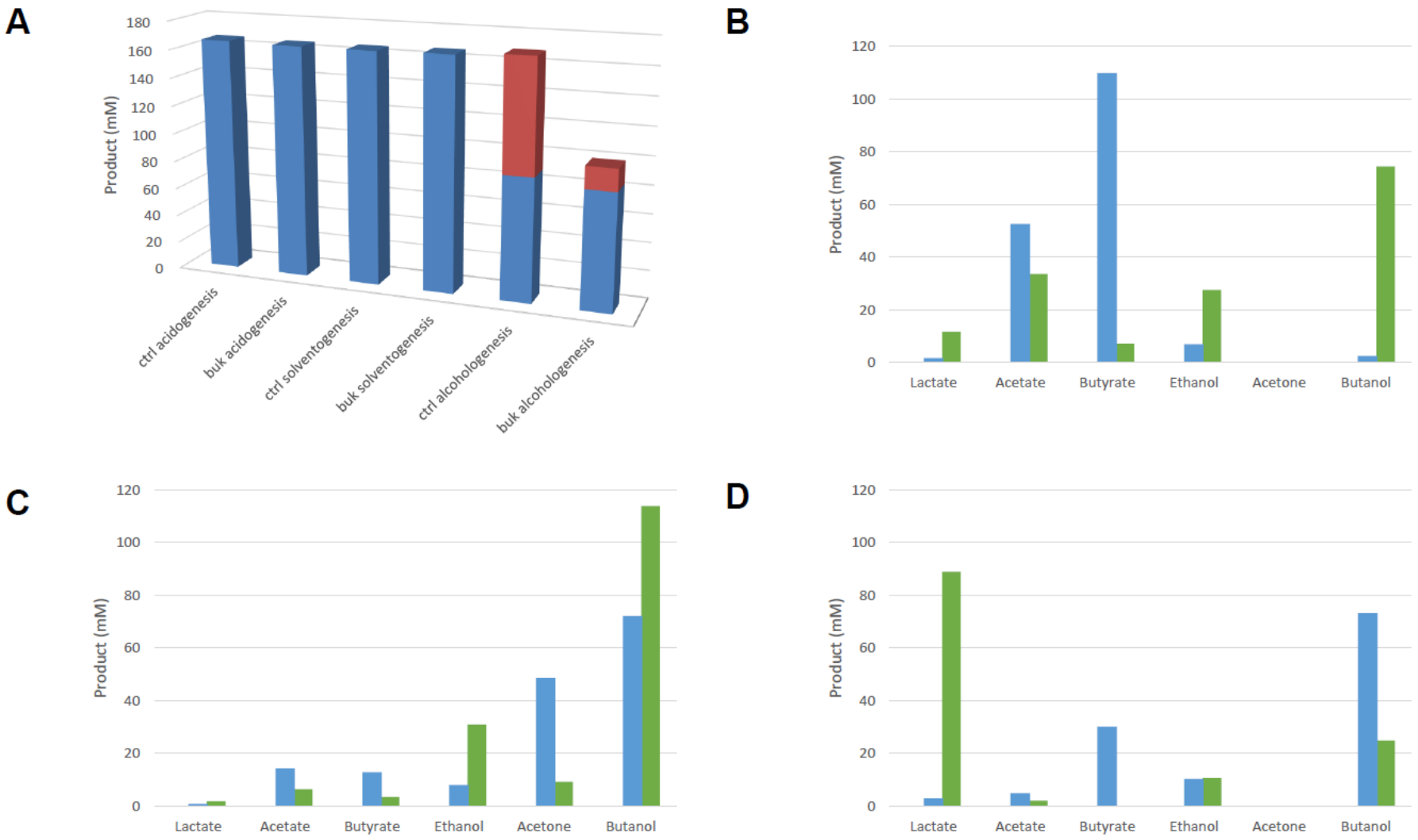

Fig.4.3. Substrates and products profile under three different conditions for the control and ΔbukΔptb300strains. (A) Carbon source

consumption: glucose (blue) and glycerol (red). Product profiles in acidogenesis(B), solventogenesis(C), and alcohologenesis(D). For (B), (C) and (D), each histogram indicates different strains: control (blue) and ΔbukΔptb300(green).

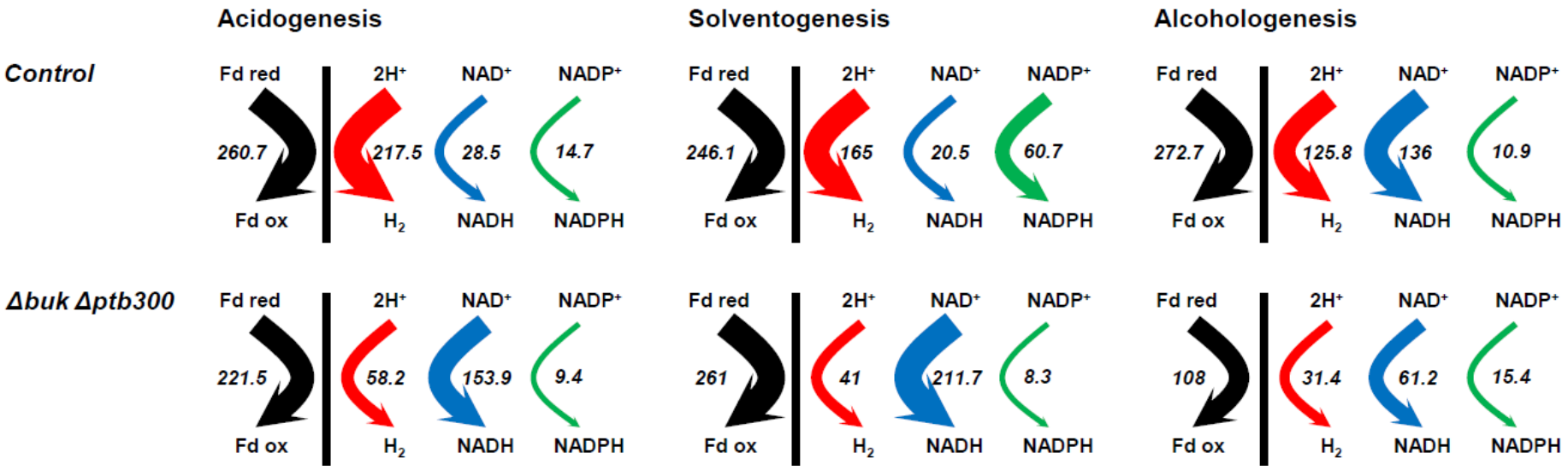

Fig.4.4. Electron flux map of the control and *Δbuk Δptb* strains in acidogenesis (A), solventogenesis (B), and alcohologenesis (C). The arrows for hydrogenase (red), ferredoxin-NAD+ reductase (blue) and ferredoxin-NADP+ (green) *in vivo* fluxes are presented. All values are normalized to the flux of the initial carbon source (millimoles per gram of dry cell weight (DCW) per hour). Glucose flux is normalized to 100 for acidogenesis and solventogenesis, and the sum of glucose and half of the glycerol is normalized to 100 for alcohologenesis.

Supporting information

Table S4.1. Four-fold increased genes under acidogenesis in *ΔbukΔptb*

Table S4.2. Four-fold decreased genes under acidogenesis in *ΔbukΔptb*

Table S4.3. Four-fold increased genes under solventogenesis in *ΔbukΔptb*

Table S4.4. Four-fold decreased genes under solventogenesis in *ΔbukΔptb*

Table S4.5. Four-fold increased genes under alcohologenesis in *ΔbukΔptb*

Table S4.6. Four-fold decreased genes under alcohologenesis in *ΔbukΔptb*

Fig.S4.1. Butanol pathway analysis of control (A) and *ΔbukΔptb* (B) under acidogenesis, solventogenesis, and alcohologenesis

Fig.S4.2 Metabolic flux map of control and ΔbukΔptb300 strains under three metabolic states. (A) control under acidogenesis, (B) ΔbukΔptb300under acidogenesis, (C) control under solventogenesis, (D) ΔbukΔptb300 under solventogenesis, (E) control under alcohologenesis, (F) ΔbukΔptb300under alcohologenesis. All values are normalized to the flux of the initial carbon source (mmol/gDCW/h). Glucose flux is normalized as 100 for acidogenesisandsolventogenesis, and the sum of glucose and half of the glycerol normalized as 100 for alcohologenesis. 2-KV, 2-keto-valerate; 2-HV, 2-hydroxyl-valerate.

Table S4.1. Four-fold increased genes under acidogenesis in *Δbuk*Δ*ptb*

Gene number	Function	*Δbuk* /Ctrl	Ctrl mRNA molecules per cell	*Δbuk* mRNA molecules per cell
Increase				
CAC0014	Aminotransferase	8.15	0.13 ± 0.01	1.06 ± 0.53
CAC0015	D-3-phosphoglycerate dehydrogenase	7.82	0.17 ± 0.02	1.35 ± 0.29
CAC0016	Related to HTH domain of SpoOJ/ParA/ParB/repB family, involved in chromosome partitioning	4.94	0.13 ± 0.01	0.64 ± 0.01
CAC0056	Hypothetical protein	5.63	2.06 ± 0.28	11.59 ± 0.82
CAC0057	Hypothetical protein	4.86	5.97 ± 0.54	28.98 ± 0.6
CAC0058	Hypothetical protein	5.24	5.86 ± 0.64	30.7 ± 0.39
CAC0059	Hypothetical protein	6.40	2.89 ± 0.14	18.47 ± 1.38
CAC0060	Predicted membrane protein	5.43	1.93 ± 0.07	10.49 ± 0.36
CAC0061	Phage-related protein, gp16	6.88	1.64 ± 0.2	11.27 ± 0.86
CAC0062	Phage-related protein	4.76	4.63 ± 0.56	22.06 ± 0.84
CAC0063	Phage-related protein	5.88	0.52 ± 0.03	3.05 ± 0.97
CAC0064	Hypothetical protein	5.04	0.96 ± 0.08	4.85 ± 0.33
CAC0065	Hypothetical protein	7.69	0.28 ± 0.01	2.19 ± 0.35
CAC0066	ABC transporter, ATP-binding protein	6.02	0.29 ± 0.03	1.74 ± 0.61
CAC0067	(FS) similar to ABC transporter (permease), YXDM B.subtilis ortholog	4.78	0.15 ± 0.02	0.72 ± 0.18
CAC0102	O-acetylhomoserine sulfhydrylase	41.29	0.06 ± 0	2.58 ± 0.49
CAC0103	Adenylylsulfate kinase	58.98	0.07 ± 0	3.93 ± 0.41
CAC0104	Adenylylsulfate reductase, subunit A	89.79	0.06 ± 0	5.7 ± 0.3
CAC0105	Ferredoxin	62.00	0.07 ± 0	4.31 ± 0.06
CAC0106	ABC-type probable sulfate transporter, periplasmic binding protein	43.95	0.12 ± 0	5.16 ± 0.29
CAC0107	ABC-type sulfate transporter, ATPase component	40.83	0.07 ± 0.01	2.87 ± 0.1
CAC0108	ABC-type probable sulfate transporter, permease protein	64.84	0.07 ± 0	4.57 ± 0.16
CAC0109	Sulfate adenylate transferase, CysD subfamily	84.10	0.08 ± 0	7.1 ± 0.19
CAC0110	GTPase, sulfate adenylate transferase subunit 1	121.97	0.14 ± 0.01	16.63 ± 0.45
CAC0117	Chemotaxis protein cheY homolog	5.93	0.07 ± 0	0.41 ± 0.01
CAC0118	Chemotaxis protein cheA	8.11	0.07 ± 0.01	0.57 ± 0
CAC0119	Chemotaxis protein cheW	9.95	0.08 ± 0.01	0.81 ± 0.05
CAC0120	Membrane-associated methyl-accepting chemotaxis protein with HAMP domain	5.57	0.07 ± 0	0.41 ± 0.03
CAC0267	L-lactate dehydrogenase	22.68	0.41 ± 0.02	9.28 ± 0.22

CAC0424	Fructokinase	4.59	2.8 ± 0.18	12.85 ± 0.89
CAC0425	Sucrase-6-phosphate hydrolase (gene sacA)	5.63	1.55 ± 0.21	8.74 ± 0.49
CAC0439	Hypothetical protein	11.16	0.12 ± 0.01	1.28 ± 0.45
CAC0456	ATP-dependent protease (lonA)	8.78	0.46 ± 0.04	4.07 ± 0.55
CAC0457	Transcriptional regulator, AcrR family	7.59	0.27 ± 0.03	2.03 ± 0.11
CAC0550	Possible sigma factor	7.19	0.08 ± 0	0.56 ± 0.07
CAC0551	Uncharacterized protein with possible cell attachment and effacing function; Cell-adhesion domain;	5.82	0.09 ± 0	0.55 ± 0.05
CAC0552	Protein containing cell-adhesion domain	5.98	2 ± 0.29	11.99 ± 0.22
CAC0557	Predicted Zn-dependent protease with possible chaperone function	4.32	0.06 ± 0	0.28 ± 0.05
CAC0570	PTS enzyme II, ABC component	4.55	4.45 ± 0.69	20.25 ± 1.89
CAC0623	Hypothetical protein	22.27	0.28 ± 0.03	6.35 ± 0.37
CAC0765	Fe-S oxidoreductase	17.33	0.14 ± 0.01	2.38 ± 0.38
CAC0766	Predicted transcriptional regulator (MerR family)	20.21	0.31 ± 0.04	6.25 ± 1.38
CAC0767	Fe-S oxidoreductase	8.43	0.59 ± 0.05	4.98 ± 0.91
CAC0771	Cobalamin biosynthesis protein CbiM	4.69	0.29 ± 0.03	1.34 ± 0.09
CAC0772	Cobalt permease	4.59	0.14 ± 0.01	0.64 ± 0.04
CAC0818	Diguanylate cyclase/phosphodiesterase domain (GGDEF) containing protein	13.93	0.09 ± 0.01	1.21 ± 0.09
CAC0878	Amino acid ABC transporter permease component	5.44	0.13 ± 0	0.68 ± 0.12
CAC0879	ABC-type polar amino acid transport system, ATPase component	7.13	0.79 ± 0.03	5.6 ± 0.82
CAC0880	Periplasmic amino acid binding protein	8.15	0.68 ± 0.06	5.53 ± 0.33
CAC0930	Cystathionine gamma-synthase	5.35	0.13 ± 0.04	0.72 ± 0.21
CAC0931	Cysteine synthase	7.64	0.08 ± 0.01	0.62 ± 0.29
CAC1023	Nicotinate-nucleotide pyrophosphorylase	4.66	1.38 ± 0.21	6.43 ± 0.65
CAC1025	Quinolinate synthase	4.05	4.4 ± 0.25	17.78 ± 1.12
CAC1039	Membrane protein, TerC homolog	4.66	0.16 ± 0.01	0.73 ± 0.02
CAC1101	Hypothetical protein, CF-34 family(identical)	5.23	1.48 ± 0.44	7.74 ± 0.08
CAC1229	Hypothetical protein, CF-34 family(identical)	4.73	2.09 ± 0.79	9.87 ± 0.64
CAC1322	Glycerol-3-phosphate dehydrogenase, GLPA	4.01	0.13 ± 0.01	0.51 ± 0.08
CAC1353	Phosphotransferase system IIC component, possibly N-acetylglucosamine-specific	8.04	0.3 ± 0.02	2.44 ± 0.87
CAC1387	Membrane associated chemotaxis sensory transducer protein (MSP domain and HAMP domain)	12.18	0.17 ± 0.01	2.06 ± 0.15
CAC1392	Glutamine phosphoribosylpyrophosphate amidotransferase	5.20	0.53 ± 0.03	2.73 ± 0.8
CAC1393	Phosphoribosylaminoimidazol (AIR) synthetase	4.32	0.32 ± 0.02	1.39 ± 0.19
CAC1394	Folate-dependent phosphoribosylglycinamide formyltransferase	5.03	0.34 ± 0.02	1.7 ± 0.3

CAC1407	PTS system, beta-glucosides-specific IIABC component	4.74	0.29 ± 0.04	1.39 ± 0.04
CAC1408	Phospho-beta-glucosidase	4.84	0.39 ± 0.06	1.9 ± 0.1
CAC1524	Methyl-accepting chemotaxis-like domain (chemotaxis sensory transducer)	8.01	0.07 ± 0	0.59 ± 0.06
CAC1525	Uncharacterized protein, homolog of PHNB E.coli	9.89	0.07 ± 0	0.74 ± 0.04
CAC1583	Predicted P-loop ATPase	4.32	0.64 ± 0.35	2.76 ± 1.54
CAC1845	Flagellar motor protein MotB	5.92	0.39 ± 0.02	2.33 ± 0.17
CAC1846	Flagellar motor component MotA	4.65	0.15 ± 0.01	0.7 ± 0.07
CAC1862	Hypothetical protein	4.62	0.14 ± 0.01	0.63 ± 0.01
CAC1863	Hypothetical protein	7.47	0.07 ± 0	0.54 ± 0.02
CAC2072	Stage IV sporulation protein B, SpoIVB	∞	0 ± 0	0.38 ± 0.04
CAC2112	Uracil permease UraA/PyrP	4.08	0.69 ± 0.05	2.8 ± 0.49
CAC2235	Cysteine synthase/cystathionine beta-synthase, CysK	7.49	3.22 ± 0.22	24.1 ± 2.27
CAC2236	Uncharacterized conserved protein of YjeB/RRF2 family	4.53	2.22 ± 0.49	10.04 ± 1.84
CAC2241	Cation transport P-type ATPase	10.63	0.44 ± 0.04	4.72 ± 0.07
CAC2242	Predicted transcriptional regulator, arsE family	9.04	0.15 ± 0.03	1.34 ± 0.34
CAC2388	N-acetylornithine aminotransferase	4.75	1.44 ± 0.18	6.82 ± 3.67
CAC2533	Protein containing ChW-repeats	∞	0 ± 0	0.34 ± 0.03
CAC2585	6-pyruvoyl-tetrahydropterin synthase related domain; conserved membrane protein	22.81	0.07 ± 0	1.61 ± 0.26
CAC2586	Predicted membrane protein	21.32	0.07 ± 0	1.39 ± 0.07
CAC2587	GGDEF domain containing protein	∞	0 ± 0	0.3 ± 0.03
CAC2588	Glycosyltransferase	46.94	0.15 ± 0.01	7.1 ± 1
CAC2589	Glycosyltransferase	25.21	0.06 ± 0	1.61 ± 0.05
CAC2590	Uncharacterized conserved membrane protein;	30.27	0.06 ± 0	1.88 ± 0.06
CAC2591	Hypothetical protein, CF-41 family	∞	0 ± 0	2.37 ± 0.19
CAC2592	6-pyruvoyl-tetrahydropterin synthase related domain; conserved membrane protein	27.79	0.09 ± 0.01	2.37 ± 0.07
CAC2603	Predicted membrane protein	∞	0 ± 0	0.26 ± 0.02
CAC2605	Transcriptional regulator (TetR/AcrR family)	31.56	0.13 ± 0.01	4.16 ± 0.22
CAC2650	Dihydroorotate dehydrogenase	11.41	0.41 ± 0.02	4.7 ± 0.91
CAC2651	Dihydroorotate dehydrogenase electron transfer subunit	9.75	0.25 ± 0.02	2.47 ± 0.78
CAC2652	Orotidine-5'-phosphate decarboxylase	10.64	0.54 ± 0.04	5.73 ± 2.22
CAC2653	Aspartate carbamoyltransferase regulatory subunit	9.17	0.85 ± 0.02	7.8 ± 3.53
CAC2654	Aspartate carbamoyltransferase catalytic subunit	8.64	0.7 ± 0.01	6.07 ± 2.7
CAC2816	Hypothetical protein, CF-17 family	6.26	0.1 ± 0	0.6 ± 0.04
CAC2821	Methyl-accepting chemotaxis protein	∞	0 ± 0	0.22 ± 0.02

CAC2833	Uncharacterized conserved protein, YAEG family	4.51	0.34 ± 0.04	1.54 ± 0.08
CAC2841	Conserved membrane protein, probable transporter, YPAA B.subtilis ortholog	11.17	0.37 ± 0.09	4.18 ± 0.99
CAC2849	Proline/glycine betaine ABC-type transport system, permease component fused to periplasmic component	6.35	1.83 ± 0.08	11.59 ± 0.77
CAC2850	Proline/glycine betaine ABC-type transport system, ATPase component	5.70	1.74 ± 0.19	9.92 ± 0.14
CAC2862	UDP-N-acetylglucosamine 1-carboxyvinyltransferase	4.16	0.09 ± 0.01	0.38 ± 0.03
CAC2863	Predicted membrane protein	7.83	0.07 ± 0	0.54 ± 0.08
CAC2871	FoF1-type ATP synthase A subunit	4.16	4.1 ± 0.2	17.07 ± 0.46
CAC2872	Predicted membrane protein in FoF1-type ATP synthase operon	10.57	0.51 ± 0.05	5.37 ± 0.37
CAC3013	Hypothetical protein	5.25	0.28 ± 0.01	1.45 ± 0.18
CAC3045	CPSB/CAPC ortholog, PHP family hydrolase	4.76	0.17 ± 0.01	0.81 ± 0.07
CAC3047	Uncharacterized membrane protein, putative virulence factor MviN	4.10	0.19 ± 0	0.77 ± 0.02
CAC3048	Uncharacterized conserved membrane protein, possible transporter	5.92	0.1 ± 0.01	0.58 ± 0.03
CAC3049	Glycosyltransferase	6.81	0.09 ± 0	0.62 ± 0.06
CAC3050	AMSJ/WSAK related protein, possibly involved in exopolysaccharide biosynthesis	6.93	0.11 ± 0	0.74 ± 0.06
CAC3051	Glycosyltransferase	7.46	0.11 ± 0	0.79 ± 0.08
CAC3052	Glycosyltransferase	8.06	0.12 ± 0	0.94 ± 0.14
CAC3053	Histidinol phosphatase related enzyme	9.62	0.17 ± 0.01	1.59 ± 0.2
CAC3054	Phosphoheptose isomerase	8.91	0.23 ± 0.01	2.06 ± 0.2
CAC3055	Sugar kinase	8.28	0.31 ± 0.01	2.59 ± 0.45
CAC3056	Nucleoside-diphosphate-sugar pyrophosphorylase	9.08	0.39 ± 0.03	3.54 ± 0.75
CAC3057	Glycosyltransferase	11.56	0.36 ± 0.03	4.12 ± 1.03
CAC3058	Mannose-1-phosphate guanylyltransferase	11.45	0.3 ± 0.01	3.44 ± 0.97
CAC3059	Sugar transferases	12.88	0.77 ± 0.03	9.97 ± 1.45
CAC3081	Spore-cortex-lytic enzyme, SLEB	5.59	0.09 ± 0	0.5 ± 0.04
CAC3082	Thioredoxin reductase	4.14	0.87 ± 0.07	3.62 ± 0.51
CAC3325	Periplasmic amino acid binding protein	29.41	0.11 ± 0	3.11 ± 0.07
CAC3326	Amino acid ABC-type transporter, permease component	31.67	0.11 ± 0.01	3.37 ± 0.05
CAC3327	Amino acid ABC-type transporter, ATPase component	36.84	0.56 ± 0.1	20.5 ± 1.02
CAC3343	Predicted Fe-S oxidoreductase	4.17	0.54 ± 0.02	2.27 ± 0.04
CAC3344	Uncharacterized protein, homolog of hypothetical protein (GI:5918205) from Pseudomonas stutzeri	4.46	0.22 ± 0.03	0.97 ± 0.2
CAC3345	Transcriptional regulator, AcrR family	4.12	0.35 ± 0.07	1.43 ± 0.56
CAC3359	Nitroreductase family protein fused to ferredoxin domain	4.28	0.6 ± 0.03	2.56 ± 0.22
CAC3362	Uncharacterized conserved membrane protein, YOAK B.subtilis homolog	5.41	0.26 ± 0.01	1.39 ± 0.56

CAC3461	Hypothetical protein	4.95	0.24 ± 0.03	1.21 ± 0.07
CAC3484	Short-chain alcohol dehydrogenase family protein	4.34	0.76 ± 0.02	3.28 ± 0.08
CAC3486	Multimeric flavodoxin WrbA family protein	43.77	0.38 ± 0.05	16.58 ± 0.11
CAC3599	Hypothetical protein	4.21	0.81 ± 0.37	3.39 ± 2.89
CAC3635	Oligopeptide ABC transporter, ATPase component	5.13	0.69 ± 0.03	3.52 ± 0.07
CAC3636	Oligopeptide ABC transporter, ATPase component	4.74	0.97 ± 0.07	4.6 ± 0.17
CAC3637	Oligopeptide ABC transporter, permease component	4.17	0.47 ± 0.04	1.95 ± 0.04
CAC3647	Transition state regulatory protein AbrB	11.08	0.75 ± 0.03	8.29 ± 3.63
CAC3649	Possible stage V sporulation protein T, transcriptional regulator AbrB homolog	7.28	0.08 ± 0.01	0.55 ± 0.34
CAP0028	HTH transcriptional regulator TetR family	9.58	0.44 ± 0.03	4.26 ± 0.47
CAP0029	Permease MDR-related	∞	0 ± 0	7.04 ± 0.68
CAP0030	Isochorismatase	249.10	0.06 ± 0	15.73 ± 1.36
CAP0031	Transcriptional activator HLYU, HTH of ArsR family	31.62	0.69 ± 0.38	21.94 ± 0.97
CAP0035	Aldehyde-alcohol dehydrogenase, ADHE1	185.75	0.42 ± 0.02	78.81 ± 1.15
CAP0099	DNA mismatch repair protein, MUTS fragment	5.04	0.34 ± 0.01	1.69 ± 0.18
CAP0106	1-deoxyxylulose-5-phosphate synthase, dehydrogenase	35.33	0.15 ± 0	5.24 ± 0.33
CAP0118	Possible xylan degradation enzyme (glycosyl hydrolase family 30-like domain and Ricin B-like domain)	4.19	0.22 ± 0.02	0.91 ± 0.06
CAP0119	Possible xylan degradation enzyme (glycosyl hydrolase family 30-like domain and Ricin B-like domain)	4.00	0.12 ± 0.01	0.48 ± 0.05
CAP0128	Permease, MDR related	17.68	0.11 ± 0	1.99 ± 0.09

Table S4.2. Four-fold decreased genes under acidogenesis in *⊿buk⊿ptb*

Gene number	Function	*Δbuk* /Ctrl	Ctrl mRNA molecules per cell	*Δbuk* mRNA molecules per cell
Decrease				
CAC0029	Distantly related to cell wall-associated hydrolases, similar to yycO Bacillus subtilis	0.06	5.15 ± 0.37	0.31 ± 0.07
CAC0030	Hypothetical protein	0.10	1.79 ± 0.11	0.17 ± 0.02
CAC0035	Serine/threonine phosphatase (inactivated protein)	0.13	1.57 ± 0.06	0.21 ± 0.02
CAC0037	MinD family ATPase from ParA/SOJ subfamily	0.23	0.4 ± 0.01	0.09 ± 0
CAC0038	Hypothetical protein	0.20	0.44 ± 0.03	0.09 ± 0
CAC0039	DNA segregation ATPase FtsK/SpoIIIE family protein, contains FHA domain	0.20	0.56 ± 0.03	0.11 ± 0
CAC0040	Uncharacterized small conserved protein, homolog of yfjA/yukE B.subtilis	0.09	4.33 ± 0.11	0.37 ± 0.08
CAC0042	Hypothetical protein, CF-1 family	0.15	0.93 ± 0.02	0.14 ± 0.01
CAC0043	Hypothetical protein, CF-3 family	0.22	0.54 ± 0.03	0.12 ± 0
CAC0044	Predicted membrane protein	0.22	0.86 ± 0.06	0.19 ± 0.01
CAC0078	Accessory gene regulator protein B	0.00	1.82 ± 0.62	0 ± 0
CAC0079	Hypothetical protein	0.00	40.95 ± 4.74	0.1 ± 0.01
CAC0081	Accessory gene regulator protein A	0.15	0.72 ± 0.03	0.1 ± 0
CAC0082	Predicted membrane protein	0.00	40.84 ± 3.37	0.18 ± 0.01
CAC0086	Muconate cycloisomerase related protein, ortholog of YKGB B.subtilis	0.12	1.06 ± 0.09	0.12 ± 0.02
CAC0122	Chemotaxis respons regulator (cheY)	0.24	3.43 ± 0.07	0.81 ± 0.06
CAC0138	ABC transporter, ATP-binding component	0.17	3.76 ± 0.25	0.62 ± 0.07
CAC0139	Predicted permease	0.16	4.63 ± 0.39	0.75 ± 0.06
CAC0140	Predicted permease	0.18	3.84 ± 0.25	0.68 ± 0.05
CAC0141	Membrane permease, predicted cation efflux pumps	0.14	8.01 ± 0.63	1.14 ± 0.04
CAC0156	PTS system, mannitol-specific IIA domain (Ntr-type) (gene MltF)	0.24	6.45 ± 0.37	1.54 ± 0.06
CAC0157	Mannitol-1-phosphate 5-dehydrogenase (gene MtlD)	0.25	2.41 ± 0.18	0.6 ± 0.08
CAC0175	Predicted sugar phosphate isomerase, homolog of eucaryotic glucokinase regulator	0.22	0.55 ± 0.03	0.12 ± 0.01
CAC0176	Oligopeptide-binding protein, periplasmic component	0.22	0.35 ± 0.04	0.08 ± 0.01
CAC0183	Transcriptional regulators of NagC/XylR (ROK) family, sugar kinase	0.24	1.25 ± 0.1	0.3 ± 0.03
CAC0193	Uncharacterized conserved membrane protein, affecting LPS biosynthesis	0.15	3.31 ± 0.49	0.5 ± 0.03
CAC0204	Sortase (surface protein transpeptidase), YHCS B.subtilis ortholog	0.10	3.65 ± 0.24	0.36 ± 0.05
CAC0205	Predicted phosphohydrolases, Icc family	0.08	16.4 ± 0.6	1.27 ± 0.03
CAC0206	Uncharacterized conserved membrane protein	0.06	5.06 ± 0.47	0.31 ± 0.04
CAC0310	Regulators of stationary/sporulation gene expression, abrB B.subtilis ortholog	0.17	7.79 ± 3.79	1.34 ± 0.63
CAC0324	TPR repeats containing protein	0.24	14.95 ± 0.45	3.56 ± 0.13
CAC0353	2,3-cyclic-nucleotide 2'phosphodiesterase (duplication)	0.09	2.19 ± 0.05	0.19 ± 0.01

CAC0381	Methyl-accepting chemotaxis protein	0.05	2.07 ± 0.05	0.11 ± 0
CAC0392	Peptodoglycan-binding domain	0.00	0.23 ± 0.03	0 ± 0
CAC0403	Secreted protein contains fibronectin type III domains	0.18	0.6 ± 0.03	0.11 ± 0.01
CAC0415	TPR-repeat-containing protein	0.19	11.49 ± 0.14	2.17 ± 0.35
CAC0428	Sugar permease	0.20	18.83 ± 0.66	3.7 ± 0.85
CAC0430	Glycerophosphoryl diester phosphodiesterase	0.24	14.78 ± 0.42	3.52 ± 0.55
CAC0437	Sensory transduction histidine kinase	0.09	1.44 ± 0.02	0.14 ± 0
CAC0488	Hypothetical protein	0.14	3.27 ± 0.59	0.44 ± 0.09
CAC0537	Acetylxylan esterase, acyl-CoA esterase or GDSL lipase family, strong similarity to C-terminal region of endoglucanase E precursor	0.03	20.85 ± 1.01	0.55 ± 0.04
CAC0542	Methyl-accepting chemotaxis protein	0.04	1.74 ± 0.17	0.07 ± 0
CAC0658	Fe-S oxidoreductase	0.09	0.73 ± 0.04	0.06 ± 0
CAC0659	Predicted Zn-dependent peptidase	0.12	0.52 ± 0.09	0.06 ± 0
CAC0660	Hypothetical protein, CF-26 family	0.13	5.73 ± 0.37	0.72 ± 0.03
CAC0706	Endo-1,4-beta glucanase (fused to two ricin-B-like domains)	0.23	1.19 ± 0.13	0.28 ± 0.01
CAC0746	Secreted protease metal-dependent protease	0.14	4.11 ± 0.14	0.56 ± 0.02
CAC0792	D-amino acid aminotransferase	0.10	1.47 ± 0.14	0.14 ± 0.01
CAC0804	Pectate lyase related protein, secreted	0.22	0.28 ± 0.04	0.06 ± 0
CAC0814	3-oxoacyl-[acyl-carrier-protein] synthase III	0.01	6.25 ± 0.26	0.08 ± 0
CAC0815	Methyl-accepting chemotaxis protein	0.02	3.4 ± 0.06	0.07 ± 0
CAC0816	Lipase-esterase related protein	0.02	3.77 ± 0.12	0.08 ± 0.01
CAC0842	Hypothetical protein, CF-28 family	0.00	0.21 ± 0.02	0 ± 0
CAC0843	Ribonuclease precursor (barnase), secreted.	0.25	5.2 ± 0.09	1.29 ± 0.27
CAC0946	ComE-like protein, Metallo beta-lactamase superfamily hydrolase, secreted	0.04	7.6 ± 0.56	0.3 ± 0.06
CAC1007	Predicted acetyltransferase	0.18	0.53 ± 0.09	0.1 ± 0.01
CAC1009	Cell wall biogenesis enzyme (N-terminal domain related to N-Acetylmuramoyl-L-alanine amidase and C-terminal domain related to L-alanoyl-D-glutamate peptidase); peptodoglycan-binding domain	0.00	0.24 ± 0.03	0 ± 0
CAC1010	Predicted phosphohydrolase, Icc family	0.02	6.5 ± 0.44	0.11 ± 0.01
CAC1022	Thioesterase II of alpha/beta hydrolase superfamily	0.10	0.87 ± 0.03	0.09 ± 0.02
CAC1037	Predicted xylanase/chitin deacetylase	0.09	8.94 ± 0.62	0.78 ± 0.05
CAC1072	Fe-S oxidoreductase	0.00	0.21 ± 0.01	0 ± 0
CAC1075	Beta-glucosidase family protein	0.09	0.93 ± 0.13	0.09 ± 0.01
CAC1078	Predicted phosphohydrolase, Icc family	0.02	6.77 ± 0.47	0.11 ± 0
CAC1079	Uncharacterized protein, related to enterotoxins of other Clostridiales	0.00	1.27 ± 0.2	0 ± 0
CAC1080	Uncharacterized protein, probably surface-located	0.00	20.76 ± 0.39	0.07 ± 0.01
CAC1081	Uncharacterized protein, probably surface-located	0.01	7.47 ± 0.13	0.07 ± 0
CAC1084	Beta-glucosidase family protein	0.12	1.02 ± 0.29	0.12 ± 0.03
CAC1085	Alpha-glucosidase	0.12	1.44 ± 0.19	0.17 ± 0.01

CAC1086	Transcriptional regulators of NagC/XylR family	0.10	2.76 ± 0.2	0.28 ± 0.02
CAC1102	Predicted membrane protein	0.06	8.87 ± 1.24	0.52 ± 0.09
CAC1103	Possible metal-binding domain, related to a correspondent domain of site-specific recombinase	0.21	0.92 ± 0.09	0.19 ± 0.01
CAC1214	Xre family DNA-binding domain and TPR-repeat containing protein	0.12	2.84 ± 0.22	0.34 ± 0.01
CAC1312	Hypothetical protein	0.10	1.07 ± 0.21	0.1 ± 0.01
CAC1313	Hypothetical protein	0.15	0.57 ± 0.04	0.08 ± 0
CAC1315	Peptodoglycan-binding domain containing protein	0.21	0.37 ± 0.04	0.08 ± 0
CAC1328	Thoesterase II (fragment)	0.00	0.24 ± 0.02	0 ± 0
CAC1365	Cobalamin biosynthesis protein CbiM	0.16	1.56 ± 0.05	0.25 ± 0
CAC1366	Predicted membrane protein	0.15	1.23 ± 0.06	0.18 ± 0.01
CAC1367	Cobalt permease	0.16	0.78 ± 0.01	0.13 ± 0
CAC1368	Cobalt transport (ATPase component)	0.14	1.23 ± 0.11	0.18 ± 0.02
CAC1369	Histidinol-phosphate aminotransferase	0.10	4.55 ± 0.54	0.47 ± 0.08
CAC1370	Cobalamin biosynthesis protein CbiG	0.13	1.84 ± 0.04	0.24 ± 0.01
CAC1371	Possible kinase, diverged	0.13	1.86 ± 0.03	0.24 ± 0.03
CAC1372	Cobalamin biosynthesis enzyme CobT	0.12	1.98 ± 0.08	0.24 ± 0.02
CAC1373	Anaerobic Cobalt chelatase, cbiK	0.16	1.35 ± 0.05	0.21 ± 0.02
CAC1374	Cobyric acid synthase CbiP	0.15	1.79 ± 0.08	0.27 ± 0.01
CAC1375	Cobyrinic acid a,c-diamide synthase CobB	0.20	0.78 ± 0.04	0.15 ± 0
CAC1376	Precorrin isomerase, cbiC	0.21	0.62 ± 0.03	0.13 ± 0.01
CAC1377	Cobalamin biosynthesis protein CbiD	0.15	2.52 ± 0.11	0.37 ± 0.05
CAC1378	Precorrin-6B methylase CbiT	0.20	0.74 ± 0.03	0.15 ± 0.01
CAC1381	precorrin-6x reductase	0.18	1.82 ± 0.09	0.33 ± 0.01
CAC1382	precorrin-3 methylase	0.23	0.69 ± 0.05	0.16 ± 0.01
CAC1532	Protein containing ChW-repeats	0.04	1.98 ± 0.08	0.08 ± 0
CAC1544	Cytidine deaminase, cdd	0.20	10.88 ± 0.28	2.18 ± 0.26
CAC1545	Deoxyribose-phosphate aldolase	0.19	6.71 ± 0.13	1.28 ± 0.17
CAC1546	Pyrimidine-nucleoside phosphorylase	0.25	2.7 ± 0.11	0.67 ± 0.08
CAC1600	Methyl-accepting chemotaxis-like protein (chemotaxis sensory transducer)	0.14	1.11 ± 0.11	0.16 ± 0.02
CAC1601	Methyl-accepting chemotaxis-like protein (chemotaxis sensory transducer)	0.19	0.86 ± 0.05	0.16 ± 0.01
CAC1634	Flagellin	0.21	3 ± 0.29	0.64 ± 0.02
CAC1766	Predicted sigma factor	0.00	0.34 ± 0.03	0 ± 0
CAC1768	Uncharacterized conserved protein, TraB family	0.09	0.81 ± 0.04	0.07 ± 0
CAC1775	Predicted membrane protein	0.02	5.53 ± 0.37	0.09 ± 0
CAC1817	Stage V sporulation protein, spoVS	0.16	6.81 ± 0.22	1.06 ± 0.29
CAC1868	Uncharacterized secreted protein, homolog YXKC Bacillus subtilis	0.07	1.01 ± 0.1	0.07 ± 0.01
CAC1869	Predicted transcriptional regulator	0.00	0.21 ± 0.01	0 ± 0
CAC1988	Ferrichrome-binding periplasmic protein	0.15	0.77 ± 0.03	0.11 ± 0
CAC1989	ABC-type iron (III) transport system, ATPase component	0.09	2.78 ± 0.1	0.24 ± 0.03

CAC1990	ABC-type iron (III) transport system, permease component	0.16	0.48 ± 0.01	0.08 ± 0
CAC1991	Uncharacterized protein, YIIM family	0.10	1.66 ± 0.1	0.17 ± 0
CAC1992	Molybdenum cofactor biosynthesis enzyme, MoaC	0.19	0.45 ± 0.03	0.09 ± 0
CAC1993	Molybdenum cofactor biosynthesis enzyme MoaA, Fe-S oxidoreductase	0.17	0.45 ± 0.02	0.07 ± 0.01
CAC1994	Molybdopterin biosynthesis enzyme, MoaB	0.12	0.82 ± 0.09	0.1 ± 0.01
CAC1995	Hypothetical protein	0.00	0.25 ± 0.04	0 ± 0
CAC1996	Hypothetical protein	0.07	1.45 ± 0.16	0.1 ± 0
CAC1997	Predicted glycosyltransferase	0.06	1.45 ± 0.03	0.09 ± 0
CAC1998	ABC-type transport system, ATPase component	0.06	1.31 ± 0.1	0.07 ± 0
CAC1999	Uncharacterized protein related to hypothetical protein Cj1507c from Campylobacter jejuni	0.06	1.14 ± 0.07	0.07 ± 0
CAC2000	Indolepyruvate ferredoxin oxidoreductase, subunit beta	0.05	1.48 ± 0.05	0.08 ± 0
CAC2001	Indolepyruvate ferredoxin oxidoreductase, subunit alpha	0.02	5.57 ± 0.13	0.14 ± 0.02
CAC2002	Predicted iron-sulfur flavoprotein	0.04	1.97 ± 0.06	0.08 ± 0
CAC2003	Predicted permease	0.07	0.89 ± 0.02	0.06 ± 0
CAC2004	Siderophore/Surfactin synthetase related protein	0.03	4.01 ± 0.25	0.12 ± 0.01
CAC2005	Siderophore/Surfactin synthetase related protein	0.05	2.22 ± 0.3	0.1 ± 0.01
CAC2006	Enzyme of siderophore/surfactin biosynthesis	0.06	0.96 ± 0.19	0.06 ± 0
CAC2007	Predicted glycosyltransferase	0.02	5.87 ± 0.14	0.11 ± 0.01
CAC2008	3-oxoacyl-(acyl-carrier-protein) synthase	0.03	2.25 ± 0.14	0.07 ± 0
CAC2009	3-Hydroxyacyl-CoA dehydrogenase	0.02	3.83 ± 0.14	0.07 ± 0.02
CAC2010	Predicted Fe-S oxidoreductase	0.02	5.38 ± 0.16	0.1 ± 0.01
CAC2011	Possible 3-oxoacyl-[acyl-carrier-protein] synthase III	0.02	3.32 ± 0.16	0.07 ± 0.01
CAC2012	Enoyl-CoA hydratase	0.03	2.31 ± 0.07	0.06 ± 0
CAC2013	Hypothetical protein	0.02	4.33 ± 0.23	0.09 ± 0.01
CAC2014	Predicted esterase	0.02	5.18 ± 0.07	0.09 ± 0.01
CAC2015	Hypothetical protein	0.03	2.28 ± 0.08	0.06 ± 0
CAC2016	Enoyl-CoA hydratase	0.01	13.81 ± 0.63	0.15 ± 0.01
CAC2017	Acyl carrier protein	0.02	3.51 ± 0.12	0.07 ± 0
CAC2018	Aldehyde:ferredoxin oxidoreductase	0.02	3.69 ± 0.15	0.07 ± 0
CAC2019	Malonyl CoA-acyl carrier protein transacylase	0.01	5.07 ± 0.78	0.07 ± 0.01
CAC2020	Molybdopterin biosynthesis enzyme, MoeA, fused to molibdopterin-binding domain	0.06	1.26 ± 0.13	0.07 ± 0.01
CAC2021	Molybdopterin biosynthesis enzyme, MoeA (short form)	0.04	2.88 ± 0.54	0.11 ± 0.01
CAC2022	Molybdopterin biosynthesis enzyme, moaB	0.05	1.84 ± 0.18	0.1 ± 0.01
CAC2023	Membrane protein, related to copy number protein COP from Clostridium perfringens plasmid pIP404 (GI:116928)	0.00	0.81 ± 0.01	0 ± 0
CAC2024	Phosphatidylglycerophosphate synthase related protein (fragment)	0.07	1.22 ± 0.06	0.08 ± 0.01
CAC2025	Hypothetical protein	0.04	3.61 ± 0.51	0.14 ± 0.02
CAC2026	Predicted flavodoxin	0.03	3.83 ± 0.2	0.13 ± 0.02
CAC2040	ABC transported MDR-type, ATPase component	0.16	0.48 ± 0.04	0.08 ± 0.01

CAC2071	Spo0A protein, (CheY-like receiver domain and HTH-type DNA binding domain)	0.20	3.61 ± 0.18	0.74 ± 0.33
CAC2107	Contains cell adhesion domain	0.00	0.87 ± 0.03	0 ± 0
CAC2181	Hypothetical protein	0.18	1.07 ± 0.03	0.19 ± 0.01
CAC2182	Hypothetical protein	0.19	1.37 ± 0.06	0.25 ± 0.05
CAC2183	Uncharacterized protein, posible homoloh of YJFB B. subtilis	0.23	1.04 ± 0.01	0.24 ± 0.03
CAC2200	Uncharacterized conserved protein	0.23	1.62 ± 0.13	0.37 ± 0.05
CAC2201	Hypothetical protein	0.23	1.41 ± 0.08	0.33 ± 0.05
CAC2216	Flagellar switch protein FliM	0.20	19.15 ± 1.3	3.9 ± 0.25
CAC2217	Chemotaxis signal transduction protein CheW	0.21	17.76 ± 1.74	3.8 ± 0.35
CAC2218	Chemotaxis signal receiving protein CheY	0.20	23.33 ± 1.27	4.7 ± 0.37
CAC2219	Chemotaxis protein CheC	0.24	5.77 ± 0.26	1.37 ± 0.06
CAC2220	Chemotaxis histidine kinase, CheA (contains CheW-like adaptor domain)	0.21	24.08 ± 1.74	5.03 ± 0.4
CAC2221	Chemotaxis protein methyltransferase, cheR	0.16	20.21 ± 0.89	3.14 ± 0.21
CAC2222	Chemotaxis protein CheB, (CheY-like receiver domain and methylesterase domain)	0.20	3.73 ± 0.33	0.74 ± 0.05
CAC2223	Chemotaxis protein CheD	0.21	3.6 ± 0.35	0.74 ± 0.06
CAC2224	Chemotaxis protein CheW	0.21	4.41 ± 0.67	0.91 ± 0.03
CAC2225	Uncharacterized conserved protein	0.24	3.39 ± 0.13	0.8 ± 0.04
CAC2226	Enzyme of ILVE/PABC family (branched-chain amino acid aminotransferase/4-amino-4-deoxychorismate lyase)	0.12	7.98 ± 0.85	0.94 ± 0.09
CAC2252	Alpha-glucosidase fused to unknown alpha-amylase C-terminal. domain	0.01	78.48 ± 1.92	0.72 ± 0.03
CAC2287	Acyl-CoA reductase LuxC	0.15	0.71 ± 0.08	0.11 ± 0.01
CAC2288	Acyl-protein synthetase, luxE	0.12	0.94 ± 0.12	0.11 ± 0.01
CAC2289	Biotin carboxyl carrier protein	0.00	0.39 ± 0	0 ± 0
CAC2293	Hypothetical secreted protein	0.00	2.47 ± 0.26	0 ± 0
CAC2382	Single-strand DNA-binding protein, ssb	0.10	0.68 ± 0.03	0.07 ± 0.01
CAC2456	Hypothetical protein, CF-40 family	0.25	1.82 ± 0.11	0.45 ± 0.01
CAC2507	Predicted membrane protein	0.17	12.98 ± 0.9	2.27 ± 0.24
CAC2508	Nitroreductase family protein	0.14	54.55 ± 1.47	7.8 ± 1.25
CAC2509	Predicted acetyltransferase	0.22	12.1 ± 0.48	2.7 ± 0.31
CAC2514	Beta galactosidase	0.15	0.54 ± 0.01	0.08 ± 0.01
CAC2517	Extracellular neutral metalloprotease, NPRE	0.07	1.63 ± 0.16	0.12 ± 0.01
CAC2518	Extracellular neutral metalloprotease, NPRE (fragment or C-term. domain)	0.11	1.53 ± 0.37	0.17 ± 0.03
CAC2580	Hypothetical protein, CF-41 family	0.00	0.2 ± 0.01	0 ± 0
CAC2581	6-pyruvoyl-tetrahydropterin synthase related domain; conserved membrane protein	0.00	0.73 ± 0.01	0 ± 0
CAC2584	Protein containing ChW-repeats	0.14	0.47 ± 0.01	0.07 ± 0
CAC2597	Hypothetical protein	0.14	1.04 ± 0.02	0.15 ± 0.01
CAC2620	HD-GYP hydrolase domain containing protein	0.21	0.36 ± 0.03	0.08 ± 0.01
CAC2663	Protein containing cell-wall hydrolase domain	0.04	1.65 ± 0.06	0.07 ± 0

CAC2695	Diverged Metallo-dependent hydrolase(Zn) of DD-Peptidase family; peptodoglycan-binding domain	0.03	2.79 ± 0.11	0.08 ± 0.01
CAC2716	Predicted glycosyl transferase from UDP-glucuronosyltransferase family	0.16	1.76 ± 0.19	0.28 ± 0
CAC2722	RCC1 repeats protein (beta propeller fold)	0.10	1.01 ± 0.02	0.1 ± 0
CAC2805	Possible selenocysteine lyase (aminotransferase of NifS family)	0.00	0.83 ± 0.07	0 ± 0
CAC2806	Predicted phosphohydrolase, Icc family	0.02	78.48 ± 1.92	1.34 ± 0.42
CAC2807	Endo-1,3(4)-beta-glucanase family 16	0.00	78.48 ± 1.92	0.39 ± 0.11
CAC2808	Beta-lactamase class C domain (PBPX family) containing protein	0.00	2.67 ± 0.25	0 ± 0
CAC2809	Predicted HD superfamily hydrolase	0.02	4.61 ± 0.4	0.07 ± 0
CAC2810	Possible glucoamylase (diverged), 15 family	0.01	15.81 ± 1.25	0.12 ± 0
CAC2891	Fusion of alpha-glucosidase (family 31 glycosyl hydrolase) and glycosidase (TreA/MalS family)	0.23	3.76 ± 0.41	0.85 ± 0.02
CAC2943	N-terminal domain intergin-like repeats and c-terminal - cell wall-associated hydrolase domain	0.00	0.53 ± 0.05	0 ± 0
CAC2944	N-terminal domain intergin-like repeats and c-terminal- cell wall-associated hydrolase domain	0.03	5.72 ± 0.45	0.16 ± 0.01
CAC3060	CPSC/CAPB subfamily ATPase	0.22	1.6 ± 0.06	0.36 ± 0.02
CAC3066	Glycosyltransferase	0.11	0.95 ± 0.06	0.1 ± 0.01
CAC3067	Predicted membrane protein	0.00	0.29 ± 0.03	0 ± 0
CAC3068	Glycosyltransferase	0.09	0.8 ± 0.05	0.07 ± 0
CAC3069	Predicted glycosyltransferase	0.00	0.81 ± 0.04	0 ± 0
CAC3070	Glycosyltransferase	0.02	4.34 ± 0.23	0.08 ± 0.01
CAC3071	Glycosyltransferase	0.01	5.54 ± 0.28	0.08 ± 0.01
CAC3072	Mannose-1-phosphate guanylyltransferase	0.01	9.16 ± 0.51	0.09 ± 0.02
CAC3073	Sugar transferase involved in lipopolysaccharide synthesis	0.02	4.21 ± 0.85	0.07 ± 0.02
CAC3075	Butyrate kinase, BUK	0.00	74.68 ± 1.45	0 ± 0
CAC3085	TPR-repeat-containing protein; Cell-adhesion domain;	0.04	2.01 ± 0.12	0.09 ± 0
CAC3086	Protein containing cell adhesion domain	0.04	3.81 ± 0.28	0.16 ± 0
CAC3165	Hypothetical protein	0.19	3.82 ± 0.21	0.74 ± 0.17
CAC3251	Sensory transduction protein containing HD_GYP domain	0.04	1.91 ± 0.03	0.08 ± 0.01
CAC3264	Uncharacterized conserved protein, YTFJ B.subtilis ortholog	0.06	78.48 ± 1.92	4.75 ± 0.66
CAC3265	Predicted membrane protein	0.07	2.24 ± 0.13	0.17 ± 0.04
CAC3266	Hypothetical protein	0.06	8.71 ± 0.16	0.51 ± 0.04
CAC3267	Specialized sigma subunit of RNA polymerase	0.18	0.78 ± 0.02	0.14 ± 0.02
CAC3279	Possible surface protein, responsible for cell interaction; contains cell adhesion domain and ChW-repeats	0.00	0.36 ± 0.03	0 ± 0
CAC3280	Possible surface protein, responsible for cell interaction; contains cell adhesion domain and ChW-repeats	0.00	0.55 ± 0.07	0 ± 0
CAC3298	NADH-dependent butanol dehydrogenase B (BDH II)	0.06	16.31 ± 0.45	1 ± 0.17
CAC3319	Signal transduction histidine kinase	0.03	3.14 ± 0.66	0.1 ± 0.01
CAC3320	Predicted secreted protein homolog of yjcM/yhbB B.subtilis	0.06	1.41 ± 0.1	0.08 ± 0

CAC3355	Polyketide synthase pksE (short-chain alcohol dehydrogenase,acyl-carrier-protein S-malonyltransferase,3-oxoacyl-(acyl-carrier-protein) synthase I domains)	0.00	0.4 ± 0.02	0 ± 0
CAC3373	Pectin methylesterase	0.24	1.61 ± 0.07	0.38 ± 0.05
CAC3408	NADH oxidase (two distinct flavin oxidoreductase domains)	0.02	5.91 ± 0.22	0.1 ± 0
CAC3409	Transcriptional regulators, LysR family	0.01	23.82 ± 2.8	0.14 ± 0.01
CAC3411	Homolog of plant auxin-responsive GH3-like protein	0.00	0.39 ± 0.01	0 ± 0
CAC3412	Predicted protein-S-isoprenylcysteine methyltransferase	0.00	1.55 ± 0.04	0 ± 0
CAC3422	Sugar:proton symporter (possible xylulose)	0.06	5.86 ± 0.67	0.33 ± 0.01
CAC3423	Acetyltransferase (ribosomal protein N-acetylase subfamily)	0.05	8.08 ± 0.35	0.38 ± 0.01
CAC3521	Hypothetical protein	0.07	8.82 ± 0.24	0.64 ± 0.04
CAC3522	Hypothetical protein, CF-7 family	0.07	6.64 ± 0.43	0.44 ± 0.03
CAC3523	Hypothetical protein, CF-7 family	0.08	2.36 ± 0.17	0.19 ± 0.02
CAC3524	Hypothetical protein, CF-7 family	0.12	2.35 ± 0.08	0.28 ± 0.03
CAC3557	Probable S-layer protein;	0.07	1.56 ± 0.15	0.11 ± 0
CAC3558	Probable S-layer protein;	0.05	1.84 ± 0.21	0.1 ± 0
CAC3565	Uncharacterized secreted protein, containing cell adhesion domain	0.11	0.7 ± 0.05	0.08 ± 0.01
CAC3566	Hypothetical protein, CF-28 family	0.10	0.81 ± 0.1	0.08 ± 0.01
CAC3581	HAD superfamily hydrolase	0.11	1.09 ± 0.23	0.12 ± 0.03
CAC3612	Hypothetical protein	0.00	0.85 ± 0.07	0 ± 0
CAC3613	Hypothetical protein	0.21	0.32 ± 0.04	0.07 ± 0
CAC3683	Penicillin-binding protein 2 (serine-type D-Ala-D-Ala carboxypeptidase)	0.24	1.35 ± 0.08	0.32 ± 0.01
CAP0026	Hypothetical protein	0.21	18.09 ± 0.83	3.83 ± 0.37
CAP0036	Uncharacterized, ortholog of YgaT gene of B.subtillis	0.04	78.48 ± 1.92	2.92 ± 0.19
CAP0037	Uncharacterized, ortholog of YgaS gene of B.subtillis	0.03	78.48 ± 1.92	2.4 ± 0.18
CAP0053	Xylanase, glycosyl hydrolase family 10	0.08	1.05 ± 0.13	0.08 ± 0
CAP0054	Xylanase/chitin deacetylase family enzyme	0.06	1.88 ± 0.26	0.11 ± 0.01
CAP0057	Putative glycoportein or S-layer protein	0.15	2.53 ± 0.14	0.37 ± 0.02
CAP0058	Rare lipoprotein A RLPA releated protein	0.04	6.1 ± 0.36	0.26 ± 0.01
CAP0065	Predicted secreted metalloprotease	0.25	0.54 ± 0.01	0.13 ± 0.01
CAP0072	Hypothetical protein	0.10	1.45 ± 0.08	0.14 ± 0.03
CAP0086	Permease, MDR related, probably tetracycline resistance protein	0.24	1.18 ± 0.05	0.29 ± 0.03
CAP0112	Hypothetical protein	0.24	2.28 ± 0.17	0.56 ± 0.06
CAP0133	Antibiotic-resistance protein, alpha/beta superfamily hydrolase	0.21	2.78 ± 0.2	0.58 ± 0.02
CAP0134	Hypothetical protein	0.15	1.59 ± 0.17	0.24 ± 0.01
CAP0135	Oxidoreductase	0.07	16.08 ± 0.99	1.18 ± 0.07
CAP0136	AstB/chuR/nirj-related protein	0.11	2.99 ± 0.1	0.32 ± 0.01
CAP0137	Similar to C-ter. fragment of UDP-glucuronosyltransferases, YpfP B.subtilis related	0.09	5.84 ± 0.33	0.53 ± 0.08

CAP0138	Diverged, distantly related to biotin carboxylase N-term. fragment.	0.10	5.38 ± 0.07	0.56 ± 0.08
CAP0148	Phospholipase C	0.08	1.04 ± 0.06	0.09 ± 0.01
CAP0149	Xre family DNA-binding domain and TRP-repeats containing protein	0.25	0.67 ± 0.26	0.16 ± 0.04
CAP0151	Integrin-like repeats domain fused to lysozyme, LYCV glycosyl hydrolase	0.11	1.17 ± 0.07	0.13 ± 0.01
CAP0152	Hypothetical protein, CF-6 family	0.13	1.2 ± 0.1	0.16 ± 0.01
CAP0160	Secreted protein containing cell-adhesion domains	0.18	0.54 ± 0.07	0.1 ± 0.01
CAP0165	Acetoacetate decarboxylase	0.11	3.99 ± 0.51	0.44 ± 0.16
CAP0173	Archaeal-type Fe-S oxidoreductase	0.00	0.29 ± 0.07	0 ± 0
CAP0174	Membrane protein	0.09	1.06 ± 0.23	0.09 ± 0.02

Table S4.3. Four-fold increased genes under solventogenesis in *ΔbukΔptb*

Gene number	Function	*Δbuk* /Ctrl	Ctrl mRNA molecules per cell	*Δbuk* mRNA molecules per cell
Increase				
CAC0028	Hydrogen dehydrogenase	4.65	1.39 ± 0.09	6.45 ± 0.11
CAC0111	Glutamine-binding periplasmic protein fused to glutamine permease	5.62	2.24 ± 0.11	12.61 ± 0.37
CAC0112	Glutamine ABC transporter (ATP-binding protein)	5.90	1.34 ± 0.08	7.93 ± 0.14
CAC0267	L-lactate dehydrogenase	5.41	0.55 ± 0.17	3 ± 0.05
CAC0467	Uncharacterized membrane protein, homolog of YDAH B.subtilis	8.81	0.07 ± 0.01	0.58 ± 0.04
CAC0468	HAD superfamily hydrolase	10.65	0.06 ± 0.01	0.68 ± 0.01
CAC0469	Spore maturation protein A (gene spmA)	5.33	0.06 ± 0	0.34 ± 0
CAC0570	PTS enzyme II, ABC component	4.41	2.6 ± 0.97	11.48 ± 0.5
CAC0751	Permease	4.69	0.95 ± 0.61	4.44 ± 0.12
CAC1162	Hypothetical protein, CF-11 family	5.07	0.17 ± 0.01	0.86 ± 0.03
CAC1165	Hypothetical protein	4.53	0.16 ± 0.02	0.73 ± 0.01
CAC1353	Phosphotransferase system IIC component, possibly N-acetylglucosamine-specific	6.06	0.13 ± 0.01	0.78 ± 0.02
CAC1695	DNA-dependent RNA polymerase sigma subunit	6.14	0.16 ± 0.01	0.95 ± 0.04
CAC2112	Uracil permease UraA/PyrP	4.39	0.66 ± 0.05	2.89 ± 0.04
CAC2113	Uracil phosphoribosyltransferase	4.34	0.92 ± 0.01	4.01 ± 0.16
CAC2635	Hypothetical protein	4.71	0.56 ± 0.17	2.65 ± 0.04
CAC2644	Carbamoylphosphate synthase large subunit	4.97	2.01 ± 0.34	9.99 ± 0.04
CAC2648	Uncharacterized conserved membrane protein	10.48	0.1 ± 0.02	1.04 ± 0.07
CAC2649	Uncharacterized conserved membrane protein	18.66	0.21 ± 0.07	4.01 ± 0.06
CAC2650	Dihydroorotate dehydrogenase	19.89	0.87 ± 0.21	17.37 ± 0.61
CAC2651	Dihydroorotate dehydrogenase electron transfer subunit	19.36	0.54 ± 0.14	10.38 ± 0.26
CAC2652	Orotidine-5'-phosphate decarboxylase	18.27	1.26 ± 0.33	23 ± 0.34
CAC2653	Aspartate carbamoyltransferase regulatory subunit	14.74	2.31 ± 0.67	34.05 ± 0.47
CAC2654	Aspartate carbamoyltransferase catalytic subunit	15.96	1.69 ± 0.43	26.91 ± 0.45
CAC2681	Hypothetical protein	10.36	2.2 ± 0.8	22.78 ± 0.76
CAC2682	Hypothetical protein	8.62	0.09 ± 0.01	0.76 ± 0.05
CAC2683	Related to spore coat protein F	4.88	0.07 ± 0.01	0.33 ± 0.04
CAC2849	Proline/glycine betaine ABC-type transport system, permease component fused to periplasmic component	8.13	0.95 ± 0.18	7.73 ± 0.38
CAC2850	Proline/glycine betaine ABC-type transport system, ATPase component	7.71	0.83 ± 0.08	6.38 ± 0.11
CAC2872	Predicted membrane protein in FoF1-type ATP synthase operon	4.95	1.67 ± 0.6	8.25 ± 0.27
CAC3019	Sensory transduction protein with GGDEF and EAL domains	5.12	0.28 ± 0.05	1.42 ± 0.03
CAC3174	2-isopropylmalate synthase	5.26	1.8 ± 0.16	9.49 ± 0.36

CAC3437	Predicted membrane-associated Zn-dependent protease, HtpX family (BlaR subfamily)	4.20	0.94 ± 0.25	3.94 ± 0.1
CAC3438	Transcriptional regulator, (BlaI/MecI subfamily)	4.35	0.65 ± 0.18	2.84 ± 0.01
CAC3486	Multimeric flavodoxin WrbA family protein	6.32	0.33 ± 0.1	2.06 ± 0.06
CAC3658	Uncharacterized conserved membrane protein, SapB/MtgC family	5.61	0.13 ± 0.02	0.71 ± 0.05
CAC3659	S-adenosylmethionine-dependent methyltransferase	4.13	0.26 ± 0.04	1.07 ± 0.02
CAP0029	Permease MDR-related	48.61	0.14 ± 0.09	6.83 ± 0.18
CAP0030	Isochorismatase	74.57	0.23 ± 0.15	17.18 ± 0.61
CAP0031	Transcriptional activator HLYU, HTH of ArsR family	29.86	0.69 ± 0.15	20.65 ± 0.36
CAP0035	Aldehyde-alcohol dehydrogenase, ADHE1	360.69	0.21 ± 0.02	76.25 ± 4.96
CAP0045	Glycosyl transferase	4.16	1.03 ± 0.4	4.29 ± 0.11
CAP0099	DNA mismatch repair protein, MUTS fragment	8.31	0.22 ± 0.01	1.86 ± 0.05
CAP0106	1-deoxyxylulose-5-phosphate synthase, dehydrogenase	8.28	0.14 ± 0.05	1.15 ± 0.05
CAP0168	Alpha-amylase	7.21	0.34 ± 0.05	2.43 ± 0.04

Table S4.4. Four-fold decreased genes under solventogenesis in *Δbuk Δptb*

Gene number	Function	*Δbuk* /Ctrl	Ctrl mRNA molecules per cell	*Δbuk* mRNA molecules per cell
Decrease				
CAC0086	Muconate cycloisomerase related protein, ortholog of YKGB B.subtilis	0.22	2.27 ± 0.3	0.49 ± 0.04
CAC0149	Hypothetical protein	0.14	2.83 ± 1.44	0.4 ± 0.01
CAC0154	PTS system, mannitol-specific IIBC component (gene MtlA)	0.09	0.93 ± 0.44	0.08 ± 0
CAC0155	Putative regulator of the PTS system for mannitol (gene MltR)	0.09	1.32 ± 0.61	0.11 ± 0
CAC0156	PTS system, mannitol-specific IIA domain (Ntr-type) (gene MltF)	0.09	3.3 ± 1.76	0.28 ± 0.03
CAC0157	Mannitol-1-phosphate 5-dehydrogenase (gene MtlD)	0.11	1.26 ± 0.72	0.14 ± 0.01
CAC0164	ABC transporter, ATP binding-protein	0.19	2.24 ± 0.92	0.43 ± 0.03
CAC0165	Predicted ABC transporter, permease component	0.19	2.03 ± 0.76	0.38 ± 0.01
CAC0273	2-isopropylmalate synthase	0.12	2.23 ± 0.56	0.26 ± 0.02
CAC0274	Aspartate ammonia-lyase (aspartase) gene ansB(aspA)	0.20	1.49 ± 0.49	0.3 ± 0.01
CAC0332	Beta-mannanase	0.17	0.66 ± 0.34	0.11 ± 0
CAC0542	Methyl-accepting chemotaxis protein	0.18	3.47 ± 0.15	0.64 ± 0.01
CAC0718	Ortholog ycnD B.subtilis, nitroreductase	0.18	0.67 ± 0.36	0.12 ± 0
CAC0910	Probably cellulosomal scaffolding protein precursor, secreted; cellulose-binding and cohesin domain;	0.21	3.42 ± 0.97	0.72 ± 0.03
CAC0912	Possible non-processive endoglucanase family 5, secreted; CelA homolog secreted; dockerin domain;	0.22	2.83 ± 1.01	0.62 ± 0.01
CAC1079	Uncharacterized protein, related to enterotoxins of other Clostridiales	0.17	2.62 ± 1.06	0.45 ± 0.01
CAC1080	Uncharacterized protein, probably surface-located	0.13	18.01 ± 8.43	2.42 ± 0.03
CAC1081	Uncharacterized protein, probably surface-located	0.17	8.4 ± 4.15	1.42 ± 0.1
CAC1084	Beta-glucosidase family protein	0.18	1.21 ± 0.63	0.21 ± 0.01
CAC1085	Alpha-glucosidase	0.21	1.33 ± 0.72	0.28 ± 0.02
CAC1086	Transcriptional regulators of NagC/XylR family	0.23	2.31 ± 1.16	0.54 ± 0.05
CAC1232	Predicted lytic murein transglycosylase (N-term. LysM motif repeat domain)	0.20	1.47 ± 0.57	0.29 ± 0.03
CAC1233	Chemotaxis protein CheV ortholog (CheW-like adaptor domain and CheY-like reciever domain)	0.20	0.52 ± 0.35	0.11 ± 0
CAC1349	Aldose-1-epimerase	0.24	1.76 ± 1.22	0.42 ± 0.02
CAC1548	Thioredoxin reductase	0.18	1 ± 0.07	0.18 ± 0
CAC1549	Glutathione peroxidase	0.24	0.69 ± 0.07	0.17 ± 0
CAC1634	Flagellin	0.08	2.42 ± 1.98	0.2 ± 0.01
CAC1669	Carbon starvation protein	0.16	2.67 ± 0.5	0.44 ± 0.01
CAC1988	Ferrichrome-binding periplasmic protein	0.14	1.98 ± 0.61	0.27 ± 0.01
CAC1989	ABC-type iron (III) transport system, ATPase component	0.14	5.22 ± 1.52	0.75 ± 0.05

CAC1990	ABC-type iron (III) transport system, permease component	0.17	0.98 ± 0.26	0.16 ± 0.01
CAC1991	Uncharacterized protein, YIIM family	0.15	3.03 ± 1.07	0.46 ± 0.02
CAC1992	Molybdenum cofactor biosynthesis enzyme, MoaC	0.19	0.78 ± 0.3	0.15 ± 0
CAC1993	Molybdenum cofactor biosynthesis enzyme MoaA, Fe-S oxidoreductase	0.15	0.96 ± 0.37	0.14 ± 0
CAC1994	Molybdopterin biosynthesis enzyme, MoaB	0.16	1.42 ± 0.53	0.23 ± 0
CAC1995	Hypothetical protein	0.22	0.46 ± 0.19	0.1 ± 0.01
CAC1996	Hypothetical protein	0.16	2.62 ± 0.9	0.42 ± 0.01
CAC1997	Predicted glycosyltransferase	0.16	2.72 ± 1.04	0.45 ± 0.03
CAC1998	ABC-type transport system, ATPase component	0.16	2.42 ± 0.94	0.38 ± 0.01
CAC1999	Uncharacterized protein related to hypothetical protein Cj1507c from Campylobacter jejuni	0.15	2.15 ± 0.9	0.32 ± 0.01
CAC2000	Indolepyruvate ferredoxin oxidoreductase, subunit beta	0.14	2.65 ± 1.09	0.37 ± 0.01
CAC2001	Indolepyruvate ferredoxin oxidoreductase, subunit alpha	0.16	9.05 ± 4.28	1.42 ± 0.01
CAC2002	Predicted iron-sulfur flavoprotein	0.18	3.57 ± 1.27	0.63 ± 0.01
CAC2003	Predicted permease	0.19	1.7 ± 0.84	0.32 ± 0.01
CAC2004	Siderophore/Surfactin synthetase related protein	0.17	6.96 ± 2.59	1.22 ± 0.04
CAC2005	Siderophore/Surfactin synthetase related protein	0.18	4.06 ± 1.57	0.73 ± 0.01
CAC2006	Enzyme of siderophore/surfactin biosynthesis	0.21	1.65 ± 0.59	0.34 ± 0.01
CAC2007	Predicted glycosyltransferase	0.21	8.79 ± 3.64	1.8 ± 0.05
CAC2008	3-oxoacyl-(acyl-carrier-protein) synthase	0.24	2.82 ± 0.3	0.67 ± 0.02
CAC2009	3-Hydroxyacyl-CoA dehydrogenase	0.19	6.35 ± 1.95	1.18 ± 0.01
CAC2010	Predicted Fe-S oxidoreductase	0.19	8.54 ± 2.9	1.63 ± 0.04
CAC2011	Possible 3-oxoacyl-[acyl-carrier-protein] synthase III	0.20	5.89 ± 1.94	1.17 ± 0.04
CAC2012	Enoyl-CoA hydratase	0.24	3.36 ± 0.33	0.8 ± 0.01
CAC2013	Hypothetical protein	0.22	8.36 ± 2.44	1.82 ± 0.02
CAC2014	Predicted esterase	0.24	8.21 ± 2.59	1.97 ± 0.03
CAC2015	Hypothetical protein	0.23	3.84 ± 1.03	0.9 ± 0.02
CAC2018	Aldehyde:ferredoxin oxidoreductase	0.18	6.52 ± 2.32	1.15 ± 0.05
CAC2181	Hypothetical protein	0.21	0.79 ± 0.57	0.16 ± 0.02
CAC2182	Hypothetical protein	0.20	0.88 ± 0.59	0.18 ± 0.01
CAC2184	Uncharacterized protein, homolog HI1244 from Haemophilus influenzae	0.16	0.54 ± 0.42	0.09 ± 0
CAC2185	Uncharacterized protein, homolog HI1244 from Haemophilus influenzae	0.12	1.62 ± 1.2	0.19 ± 0.01
CAC2203	Possible hook-associated protein, flagellin family	0.12	16.38 ± 13.09	2.02 ± 0.07
CAC2252	Alpha-glucosidase fused to unknown alpha-amylase C-terminal. domain	0.14	41.27 ± 28.23	5.73 ± 0.32
CAC2293	Hypothetical secreted protein	0.08	18.17 ± 5.58	1.49 ± 0.05
CAC2569	NimC/NimA family protein	0.16	7.73 ± 3.94	1.23 ± 0.07
CAC2570	Predicted arabinogalactan endo-1,4-beta-galactosidase	0.23	4.75 ± 1.31	1.07 ± 0.06
CAC2610	L-fucose isomerase related protein	0.22	2.43 ± 2.19	0.55 ± 0.03
CAC2611	Hypothetical protein	0.19	2.57 ± 2.57	0.5 ± 0.04

CAC2746	Membrane associated methyl-accepting chemotaxis protein (with HAMP domain)	0.00	0.2 ± 0.15	0 ± 0
CAC2774	Methyl-accepting chemotaxis protein with HAMP domain	0.25	3.25 ± 1.35	0.8 ± 0.03
CAC2807	Endo-1,3(4)-beta-glucanase family 16	0.18	64.7 ± 11.05	11.37 ± 0.55
CAC2835	Gluconate permease, gntP	0.23	35.73 ± 17.74	8.09 ± 0.44
CAC3075	Butyrate kinase, BUK	0.00	57.6 ± 6.24	0 ± 0
CAC3352	Membrane associated methyl-accepting chemotaxis protein with HAMP domain	0.25	0.65 ± 0.39	0.16 ± 0
CAC3556	Probable S-layer protein;	0.20	3.58 ± 1.76	0.73 ± 0.02
CAC3557	Probable S-layer protein;	0.09	3.35 ± 1.38	0.29 ± 0.01
CAC3558	Probable S-layer protein;	0.08	3.34 ± 1.56	0.27 ± 0.01
CAC3612	Hypothetical protein	0.19	3.49 ± 1.51	0.67 ± 0.04
CAP0026	Hypothetical protein	0.24	28.08 ± 13.9	6.7 ± 0.2
CAP0066	Mannose-specific phosphotransferase system component IIAB	0.24	15.39 ± 2.91	3.71 ± 0.17
CAP0067	Mannose/fructose-specific phosphotransferase system component IIC	0.23	29.27 ± 6.73	6.81 ± 0.26
CAP0068	Mannose-specific phosphotransferase system component IID	0.23	17.54 ± 3.27	3.99 ± 0.27
CAP0151	Integrin-like repeats domain fused to lysozyme, LYCV glycosyl hydrolase	0.06	3.91 ± 2.45	0.23 ± 0.01
CAP0152	Hypothetical protein, CF-6 family	0.06	4.49 ± 2.8	0.26 ± 0.01
CAP0167	Specialized sigma factor (SigF/SigE family)	0.20	0.85 ± 0.77	0.17 ± 0

Table S4.5. Four-fold increased genes under alcohologenesis in *ΔbukΔptb*

Gene number	Function	*Δbuk* /Ctrl	Ctrl mRNA molecules per cell	*Δbuk* mRNA molecules per cell
Increase				
CAC0101	Methyl-accepting chemotaxis protein	∞	0 ± 0	0.21 ± 0
CAC0115	Uncharacterized protein, Yje/RRF2 family	4.59	1.6 ± 0.17	7.36 ± 1.07
CAC0116	Carbone-monoxide dehydrogenase, beta chain	5.74	1.49 ± 0.41	8.53 ± 2.14
CAC0117	Chemotaxis protein cheY homolog	4.78	0.11 ± 0.03	0.54 ± 0.08
CAC0158	Glucoseamine-fructose-6-phosphate aminotransferase (gene glmS)	4.43	1.88 ± 0.13	8.31 ± 0.32
CAC0162	Transcriptional regulator MarR/EmrR family	4.16	0.32 ± 0.06	1.35 ± 0.01
CAC0267	L-lactate dehydrogenase	8.71	0.35 ± 0.03	3.06 ± 0.1
CAC0458	Permease	10.23	0.15 ± 0.01	1.52 ± 0.01
CAC0608	Diaminopimelate decarboxilase, lisA	6.68	0.45 ± 0.03	2.98 ± 0.08
CAC0610	Hypothetical protein	∞	0 ± 0	0.22 ± 0.01
CAC0611	Predicted membrane protein, YohK family	6.38	0.08 ± 0.01	0.52 ± 0.01
CAC0612	Predicted membrane protein YohJ family	5.48	0.1 ± 0.01	0.57 ± 0.01
CAC0626	Tryptophan-tRNA synthetase, trpS	10.96	0.34 ± 0.02	3.73 ± 0.34
CAC0627	Transcriptional regulator, MarR/EmrR family	5.87	0.86 ± 0.02	5.08 ± 0.33
CAC0687	Serine acetyltransferase	4.59	1.01 ± 0.05	4.65 ± 0.08
CAC0688	1-acyl-sn-glycerol-3-phosphate acyltransferase	4.61	0.28 ± 0.02	1.27 ± 0.09
CAC0689	Predicted endonuclease, gene nth	4.01	0.43 ± 0.01	1.71 ± 0.08
CAC0708	Putative transcriptional regulator	4.28	2.59 ± 0.77	11.09 ± 0.16
CAC0744	Na+/H+ antiporter, ortholog YQKI B.subtilis	5.85	0.17 ± 0.01	0.97 ± 0.01
CAC0769	Uncharacterized conserved protein	8.22	0.2 ± 0.02	1.68 ± 0.17
CAC0770	Glycerol uptake facilitator protein, permease	8.13	0.12 ± 0.02	0.96 ± 0.12
CAC0818	Diguanylate cyclase/phosphodiesterase domain (GGDEF) containing protein	22.50	0.08 ± 0	1.86 ± 0.07
CAC0843	Ribonuclease precursor (barnase), secreted.	12.35	0.29 ± 0.06	3.64 ± 0.05
CAC0844	Barstar-like protein ribonuclease (barnase) inhibitor	15.72	0.31 ± 0.06	4.92 ± 0.07
CAC0869	Thioredoxine reductase	4.09	0.82 ± 0.04	3.34 ± 0.29
CAC0877	Cyclopropane fatty acid synthase	4.75	0.09 ± 0.02	0.45 ± 0.01
CAC0878	Amino acid ABC transporter permease component	6.06	0.19 ± 0.02	1.18 ± 0.05
CAC0879	ABC-type polar amino acid transport system, ATPase component	6.20	1.67 ± 0.19	10.35 ± 0.19
CAC0880	Periplasmic amino acid binding protein	6.93	1.66 ± 0.14	11.52 ± 0.12
CAC0892	DAHP synthase related protein	6.17	10.44 ± 1.12	64.43 ± 1.82
CAC0893	Prephenate dehydrogenase	7.22	1.7 ± 0.14	12.23 ± 0.88
CAC0894	3-dehydroquinate synthetase	8.52	0.99 ± 0.07	8.39 ± 1.03
CAC0895	5-enolpyruvylshikimate-3-phosphate synthase	7.46	2.34 ± 0.17	17.42 ± 1.42
CAC0896	Chorismate synthase	8.07	1.53 ± 0.1	12.34 ± 0.75

CAC0897	Fusion: chorismate mutase and shikimate 5-dehydrogenase	8.07	0.9 ± 0.12	7.23 ± 0.32
CAC0898	Shikimate kinase	4.88	4.07 ± 0.16	19.88 ± 0.94
CAC0899	3-dehydroquinate dehydratase II	6.13	0.44 ± 0.04	2.71 ± 0.14
CAC0929	SAM-dependent methyltransferase	6.17	0.11 ± 0.01	0.71 ± 0.04
CAC0930	Cystathionine gamma-synthase	8.85	0.3 ± 0.04	2.69 ± 0.17
CAC0931	Cysteine synthase	10.41	0.18 ± 0.02	1.85 ± 0.08
CAC1145	Hypothetical protein	4.25	0.11 ± 0.02	0.47 ± 0.03
CAC1356	Thiamine biosynthesis enzyme ThiH	10.85	0.94 ± 0.23	10.24 ± 0.15
CAC1387	Membrane associated chemotaxis sensory transducer protein (MSP domain and HAMP domain)	8.88	0.16 ± 0.02	1.43 ± 0.02
CAC1390	Phosphoribosylcarboxyaminoimidazole (NCAIR) mutase	4.44	6.23 ± 0.38	27.7 ± 1.29
CAC1391	Phosphoribosylaminoimidazolesuccinocarboxamide (SAICAR) synthase	4.15	6.95 ± 0.74	28.86 ± 1.32
CAC1392	Glutamine phosphoribosylpyrophosphate amidotransferase	6.84	1.42 ± 0.1	9.73 ± 0.15
CAC1393	Phosphoribosylaminoimidazol (AIR) synthetase	5.98	0.75 ± 0.07	4.48 ± 0.24
CAC1394	Folate-dependent phosphoribosylglycinamide formyltransferase	7.47	0.91 ± 0.05	6.78 ± 0.17
CAC1395	AICAR transformylase/IMP cyclohydrolase	6.26	1.01 ± 0.04	6.3 ± 0.4
CAC1396	Phosphoribosylamine-glycine ligase	4.92	0.44 ± 0.01	2.19 ± 0.02
CAC1448	tetracycline resistance protein, tetQ family, GTPase	6.00	0.17 ± 0.02	0.99 ± 0.04
CAC1525	Uncharacterized protein, homolog of PHNB E.coli	4.30	0.08 ± 0.01	0.36 ± 0.02
CAC1583	Predicted P-loop ATPase	7.63	0.31 ± 0.09	2.34 ± 0.23
CAC1584	Metal-dependent hydrolase of the beta-lactamase superfamily	4.03	1.06 ± 0.05	4.28 ± 0.09
CAC1590	2-oxoglutarate/malate translocator	5.64	0.08 ± 0.02	0.44 ± 0.01
CAC1609	Zn-finger containing protein	9.85	1.94 ± 0.69	19.11 ± 0.37
CAC1610	Branched-chain amino acid permease	75.11	0.1 ± 0.02	7.63 ± 0.11
CAC1655	bifunctional enzyme phosphoribosylformylglycinamidine (FGAM) synthase (synthetase domain/glutamine amidotransferase domain)	6.59	1.18 ± 0.3	7.77 ± 0.26
CAC1666	Predicted membrane protein	4.51	0.48 ± 0.17	2.15 ± 0.1
CAC1667	HD family hydrolase, diverged	4.43	0.3 ± 0.11	1.32 ± 0.05
CAC1685	Uncharacterized protein from YceG family	4.43	1.54 ± 0.18	6.84 ± 0.41
CAC1686	S-adenosylmethionine-dependent methyltransferase	4.43	1.58 ± 0.19	6.98 ± 0.12
CAC1687	Collagenase family protease	4.30	1.64 ± 0.12	7.05 ± 0.42
CAC1821	Adenylosuccinate lyase	5.86	1.62 ± 0.25	9.49 ± 0.22
CAC1845	Flagellar motor protein MotB	4.24	0.67 ± 0.02	2.83 ± 0.02
CAC1855	Hypothetical protein	4.14	0.07 ± 0.01	0.28 ± 0.02
CAC1863	Hypothetical protein	∞	0 ± 0	0.31 ± 0
CAC2392	Uncharacterized ABC transporter, ATPase component	4.43	0.08 ± 0.01	0.35 ± 0
CAC2393	Uncharacterized ABC transporter, ATPase component	4.50	0.11 ± 0.01	0.51 ± 0.01
CAC2542	FAD/FMN-containing dehydrogenase	6.46	0.4 ± 0.3	2.57 ± 0.22

CAC2543	Electron-transferring flavoprotein large subunit	5.68	0.66 ± 0.58	3.76 ± 0.17
CAC2544	Electron-transferring flavoprotein small subunit	6.62	0.42 ± 0.34	2.77 ± 0.05
CAC2585	6-pyruvoyl-tetrahydropterin synthase related domain; conserved membrane protein	58.89	0.07 ± 0.01	4.05 ± 0.14
CAC2586	Predicted membrane protein	68.71	0.06 ± 0	4.32 ± 0.15
CAC2587	GGDEF domain containing protein	∞	0 ± 0	0.63 ± 0.05
CAC2588	Glycosyltransferase	114.28	0.14 ± 0.01	16.15 ± 0.26
CAC2589	Glycosyltransferase	∞	0 ± 0	3.15 ± 0.13
CAC2590	Uncharacterized conserved membrane protein;	55.38	0.07 ± 0.01	3.83 ± 0.13
CAC2591	Hypothetical protein, CF-41 family	80.58	0.06 ± 0.01	5 ± 0.03
CAC2592	6-pyruvoyl-tetrahydropterin synthase related domain; conserved membrane protein	35.12	0.09 ± 0.02	3.18 ± 0.09
CAC2605	Transcriptional regulator (TetR/AcrR family)	70.34	0.12 ± 0.02	8.21 ± 0.13
CAC2650	Dihydroorotate dehydrogenase	4.40	1.25 ± 0.14	5.48 ± 0.45
CAC2688	Alpha/beta superfamily hydrolase (possible chloroperoxidase)	∞	0 ± 0	0.23 ± 0
CAC2717	Ethanolamine ammonia lyase small subunit	4.51	0.12 ± 0	0.53 ± 0.05
CAC2718	Ethanolamine ammonia lyase large subunit	5.35	0.12 ± 0.01	0.62 ± 0.05
CAC2752	Uncharacterized membrane protein, YPAA B.subtilis ortholog	5.87	0.42 ± 0.09	2.48 ± 0.1
CAC2821	Methyl-accepting chemotaxis protein	∞	0 ± 0	0.31 ± 0
CAC2924	Uncharacterized protein, possibly involved in thiamine biosynthesis	4.19	0.39 ± 0.08	1.63 ± 0.25
CAC2991	Methionyl-tRNA synthetase	6.77	0.64 ± 0.07	4.34 ± 0.51
CAC3010	ATP-dependent RNA helicase (superfamily II), YDBR B.subtilis ortholog	4.20	0.62 ± 0.16	2.59 ± 0.07
CAC3038	Isoleucyl-tRNA synthetase	15.18	1.91 ± 0.11	28.95 ± 0.88
CAC3045	CPSB/CAPC ortholog, PHP family hydrolase	4.13	0.35 ± 0.01	1.43 ± 0.05
CAC3047	Uncharacterized membrane protein, putative virulence factor MviN	4.51	0.34 ± 0.01	1.53 ± 0.05
CAC3048	Uncharacterized conserved membrane protein, possible transporter	4.99	0.2 ± 0.01	1.01 ± 0.02
CAC3049	Glycosyltransferase	4.70	0.21 ± 0.01	0.99 ± 0.02
CAC3050	AMSJ/WSAK related protein, possibly involved in exopolysaccharide biosynthesis	4.15	0.26 ± 0.02	1.07 ± 0.07
CAC3051	Glycosyltransferase	4.09	0.28 ± 0.02	1.14 ± 0.06
CAC3082	Thioredoxin reductase	4.13	1.48 ± 0.09	6.11 ± 0.84
CAC3155	Uncharacterized conserved protein, THY1 family	7.47	0.18 ± 0.01	1.37 ± 0.04
CAC3156	Uncharacterized conserved protein, YACZ B.subtilis ortholog	9.37	0.25 ± 0.01	2.33 ± 0.07
CAC3157	Tryptophan synthase alpha chain	19.29	1.48 ± 0.25	28.46 ± 1.34
CAC3158	Tryptophan synthase beta chain	10.01	6.77 ± 1.12	67.73 ± 0.47
CAC3159	Phosphoribosylanthranilate isomerase	17.49	4.29 ± 1.02	75.14 ± 4.89
CAC3160	Indole-3-glycerol phosphate synthase	19.62	2.58 ± 0.63	50.51 ± 1.42
CAC3161	Anthranilate phosphoribosyltransferase	24.46	1.55 ± 0.3	37.99 ± 3.63
CAC3162	Para-aminobenzoate synthase component II	21.02	1.94 ± 0.38	40.79 ± 5.27
CAC3163	Para-aminobenzoate synthase component I	23.11	0.59 ± 0.1	13.7 ± 0.98
CAC3169	Acetolactate synthase large subunit	7.46	6.46 ± 1.42	48.18 ± 0.7

CAC3170	Dihydroxy-acid dehydratase	6.43	12.23 ± 3.25	78.6 ± 0.07
CAC3171	Isopropylmalate dehydrogenase	6.74	7.96 ± 1.71	53.65 ± 0.38
CAC3172	3-isopropylmalate dehydratase, small subunit	8.23	2.65 ± 0.76	21.82 ± 0.38
CAC3173	3-Isopropylmalate dehydratase, large subunit	6.79	7.82 ± 1.75	53.08 ± 4.74
CAC3174	2-isopropylmalate synthase	8.99	3.7 ± 1	33.22 ± 0.47
CAC3175	Hypothetical protein	8.37	1.28 ± 0.06	10.75 ± 0.17
CAC3269	ABC-type MDR transport system, ATPase component	4.73	0.22 ± 0.06	1.03 ± 0.04
CAC3276	Ribonucleotide reductase beta subunit	8.62	0.38 ± 0.08	3.24 ± 0.09
CAC3277	Ribonucleotide reductase alpha subunit	6.27	0.18 ± 0.03	1.1 ± 0.11
CAC3281	ABC-type multidrug/protein/lipid transport system, ATPase component	4.46	0.83 ± 0.11	3.72 ± 0.16
CAC3282	ABC-type multidrug/protein/lipid transport system, ATPase component	4.43	0.72 ± 0.07	3.19 ± 0.15
CAC3306	Thiol peroxidase, TPX	5.63	0.55 ± 0.07	3.09 ± 0.4
CAC3325	Periplasmic amino acid binding protein	7.61	0.73 ± 0.22	5.58 ± 0.12
CAC3326	Amino acid ABC-type transporter, permease component	7.13	0.77 ± 0.21	5.53 ± 0.45
CAC3327	Amino acid ABC-type transporter, ATPase component	4.45	5.3 ± 1.2	23.56 ± 0.23
CAC3387	Pectate lyase	4.24	0.12 ± 0.01	0.49 ± 0.02
CAC3414	ABC-type multidrug/protein/lipid transport system, ATPase component	4.29	0.14 ± 0.02	0.6 ± 0.02
CAC3415	ABC-type multidrug/protein/lipid transport system, ATPase component	4.25	0.13 ± 0.01	0.56 ± 0
CAC3453	Lysine-specific permease	6.20	0.6 ± 0.11	3.7 ± 0.11
CAC3481	Transcriptional regulator, AcrR family	4.82	0.17 ± 0.01	0.82 ± 0.01
CAC3513	Hypothetical protein	5.66	0.16 ± 0.03	0.9 ± 0.03
CAC3589	Uncharacterized conserved membrane protein, YHGE B.subtilis ortholog	4.73	0.62 ± 0.45	2.91 ± 0.05
CAC3599	Hypothetical protein	7.51	0.81 ± 0.13	6.05 ± 0.34
CAC3600	Dihydrodipicolinate synthase	8.36	0.4 ± 0.03	3.32 ± 0.19
CAC3617	Uncharacterized membrane protein, YHAG B.subtilis homolog	10.59	0.34 ± 0.09	3.56 ± 0.59
CAC3647	Transition state regulatory protein AbrB	4.52	0.84 ± 0.2	3.81 ± 0.13
CAP0028	HTH transcriptional regulator TetR family	7.04	0.53 ± 0.07	3.73 ± 0.17
CAP0029	Permease MDR-related	13.14	0.81 ± 0.53	10.68 ± 0.32
CAP0030	Isochorismatase	19.37	1.84 ± 1.26	35.66 ± 1.1
CAP0031	Transcriptional activator HLYU, HTH of ArsR family	16.66	2.5 ± 1.37	41.64 ± 1.35

Table S4.6. Four-fold decreased genes under alcohologenesis in *ΔbukΔptb*

Gene number	Function	*Δbuk* /Ctrl	Ctrl mRNA molecules per cell	*Δbuk* mRNA molecules per cell
Decrease				
CAC0029	Distantly related to cell wall-associated hydrolases, similar to yycO Bacillus subtilis	0.14	1.88 ± 0.11	0.26 ± 0.01
CAC0030	Hypothetical protein	0.20	0.8 ± 0.11	0.16 ± 0.01
CAC0035	Serine/threonine phosphatase (inactivated protein)	0.19	0.86 ± 0.17	0.16 ± 0
CAC0040	Uncharacterized small conserved protein, homolog of yfjA/yukE B.subtilis	0.06	4.42 ± 2.71	0.28 ± 0.01
CAC0042	Hypothetical protein, CF-1 family	0.10	1.42 ± 0.82	0.14 ± 0.01
CAC0043	Hypothetical protein, CF-3 family	0.13	0.95 ± 0.54	0.12 ± 0
CAC0044	Predicted membrane protein	0.12	1.51 ± 0.86	0.19 ± 0.01
CAC0045	TPR-repeat-containing protein	0.20	0.57 ± 0.3	0.11 ± 0
CAC0047	Uncharacterized small conserved protein, homolog of yfjA/yukE B.subtilis	0.19	1.33 ± 0.71	0.25 ± 0.02
CAC0048	Hypothetical protein, CF-17 family	0.19	1.25 ± 0.69	0.24 ± 0.02
CAC0078	Accessory gene regulator protein B	0.00	0.54 ± 0.2	0 ± 0
CAC0079	Hypothetical protein	0.00	10.91 ± 8.15	0 ± 0
CAC0081	Accessory gene regulator protein A	0.20	0.67 ± 0.18	0.13 ± 0
CAC0082	Predicted membrane protein	0.01	15.51 ± 5.65	0.18 ± 0.01
CAC0086	Muconate cycloisomerase related protein, ortholog of YKGB B.subtilis	0.10	0.63 ± 0.1	0.07 ± 0
CAC0138	ABC transporter, ATP-binding component	0.16	3.2 ± 0.1	0.5 ± 0.01
CAC0139	Predicted permease	0.18	3.68 ± 0.27	0.67 ± 0.02
CAC0140	Predicted permease	0.18	3.12 ± 0.23	0.57 ± 0.01
CAC0141	Membrane permease, predicted cation efflux pumps	0.15	5.38 ± 0.7	0.8 ± 0.02
CAC0149	Hypothetical protein	0.03	5.58 ± 1.22	0.15 ± 0.02
CAC0154	PTS system, mannitol-specific IIBC component (gene MtlA)	0.03	2.53 ± 0.62	0.07 ± 0.01
CAC0155	Putative regulator of the PTS system for mannitol (gene MltR)	0.02	3.29 ± 0.77	0.08 ± 0.01
CAC0156	PTS system, mannitol-specific IIA domain (Ntr-type) (gene MltF)	0.02	8.64 ± 2.56	0.14 ± 0.01
CAC0157	Mannitol-1-phosphate 5-dehydrogenase (gene MtlD)	0.03	3.32 ± 0.68	0.08 ± 0
CAC0164	ABC transporter, ATP binding-protein	0.07	1.83 ± 0.52	0.13 ± 0.01
CAC0165	Predicted ABC transporter, permease component	0.11	1.45 ± 0.33	0.16 ± 0
CAC0183	Transcriptional regulators of NagC/XylR (ROK) family, sugar kinase	0.21	0.66 ± 0.2	0.14 ± 0.01
CAC0193	Uncharacterized conserved membrane protein, affecting LPS biosynthesis	0.05	6.61 ± 4.03	0.35 ± 0.01
CAC0194	Glycosyltransferase involved in cell wall biogenesis	0.21	0.38 ± 0.2	0.08 ± 0
CAC0205	Predicted phosphohydrolases, Icc family	0.17	1.05 ± 0.18	0.17 ± 0
CAC0206	Uncharacterized conserved membrane protein	0.00	0.21 ± 0.08	0 ± 0
CAC0231	Transcripcional regulator of sugar metabolism	0.15	1.56 ± 0.23	0.23 ± 0
CAC0232	1-phosphofructokinase (fructoso 1-phosphate kinase)	0.12	3.05 ± 0.38	0.37 ± 0.04

CAC0233	PTS system, IIA component	0.08	7.34 ± 0.75	0.56 ± 0.02
CAC0234	PTS system, fructoso-specific IIBC component	0.07	4.69 ± 0.44	0.31 ± 0.02
CAC0304	Chemotaxis motility protein A, gene motA	0.24	2.63 ± 1.49	0.62 ± 0.01
CAC0316	Ornithine carbomoyltransferase	0.09	6.54 ± 1.37	0.58 ± 0.02
CAC0332	Beta-mannanase	0.20	6.01 ± 1.08	1.19 ± 0.02
CAC0353	2,3-cyclic-nucleotide 2'phosphodiesterase (duplication)	0.16	0.54 ± 0.18	0.09 ± 0.01
CAC0381	Methyl-accepting chemotaxis protein	0.12	1.06 ± 0.52	0.13 ± 0
CAC0383	PTS cellobiose-specific component IIA	0.00	0.22 ± 0.01	0 ± 0
CAC0384	PTS system, cellobiose-specific component BII	0.00	0.58 ± 0.11	0 ± 0
CAC0385	Beta-glucosidase	0.00	0.93 ± 0.18	0 ± 0
CAC0386	PTS cellobiose-specific component IIC	0.00	0.27 ± 0.06	0 ± 0
CAC0387	Hypothetical protein	0.22	0.48 ± 0	0.11 ± 0
CAC0422	Transcriptional antiterminator licT	0.06	2.55 ± 1.5	0.16 ± 0.01
CAC0423	Fusion: PTS system, beta-glucosides specific IIABC component	0.02	14.55 ± 9.31	0.27 ± 0.05
CAC0424	Fructokinase	0.02	5.66 ± 3.62	0.14 ± 0.01
CAC0425	Sucrase-6-phosphate hydrolase (gene sacA)	0.03	3.33 ± 2.1	0.11 ± 0.01
CAC0426	Transcriptional regulator (HTH_ARAC-domain)	0.10	47.23 ± 26.81	4.73 ± 0.28
CAC0435	Hypothetical protein	0.00	0.29 ± 0.04	0 ± 0
CAC0488	Hypothetical protein	0.14	2.37 ± 0.86	0.33 ± 0.01
CAC0531	Transcriptional regulator, RpiR family	0.14	4.82 ± 1.04	0.68 ± 0.01
CAC0532	PTS system, arbutin-like IIBC component	0.09	0.74 ± 0.05	0.07 ± 0.01
CAC0533	Maltose-6'-phosphate glucosidase (glvA)	0.03	4.86 ± 0.84	0.15 ± 0.02
CAC0537	Acetylxylan esterase, acyl-CoA esterase or GDSL lipase family, strong similarity to C-terminal region of endoglucanase E precursor	0.03	11.06 ± 3.98	0.38 ± 0.01
CAC0542	Methyl-accepting chemotaxis protein	0.08	0.83 ± 0.81	0.06 ± 0
CAC0544	Permease	0.10	0.7 ± 0.44	0.07 ± 0
CAC0552	Protein containing cell-adhesion domain	0.14	5.47 ± 1.06	0.74 ± 0.03
CAC0553	Hypothetical protein, CF-8 family	0.12	9.89 ± 0.47	1.17 ± 0.02
CAC0554	Autolytic lysozime (1,4-beta-N-acetylmuramidase), family 25 of glycosyl hydrolases ; peptodoglycan-binding domain	0.15	5.43 ± 0.3	0.8 ± 0.04
CAC0555	Predicted membrane protein	0.21	0.75 ± 0.23	0.16 ± 0
CAC0561	Cellulase CelE ortholog; dockerin domain;	0.23	0.37 ± 0.04	0.08 ± 0
CAC0562	Predicted membrane protein	0.07	8.74 ± 5.09	0.66 ± 0.04
CAC0563	Predicted membrane protein	0.11	3.7 ± 2.15	0.4 ± 0.01
CAC0570	PTS enzyme II, ABC component	0.15	6.68 ± 2.09	1.03 ± 0.05
CAC0590	Riboflavin biosynthesis protein RIBD (pirimidine deaminase and pirimidine reductase)	0.20	19.46 ± 8.27	3.8 ± 0.04
CAC0591	Riboflavin synthase alpha chain	0.23	4.11 ± 1.55	0.93 ± 0.03
CAC0592	Riboflavin biosynthes protein RIBA (GTPcyclohydrolase/3,4-dihydroxy-2-butanone 4-phosphate synthase)	0.21	6.87 ± 2.75	1.46 ± 0.08
CAC0593	Riboflavin synthase beta-chain	0.23	8.51 ± 3.92	1.93 ± 0.06

CAC0663	Hypothetical protein	0.18	0.92 ± 0.25	0.17 ± 0.01
CAC0706	Endo-1,4-beta glucanase (fused to two ricin-B-like domains)	0.03	5.11 ± 2.59	0.13 ± 0
CAC0707	RNA polymerase sigma-54 factor	0.09	6.83 ± 1.45	0.62 ± 0.01
CAC0746	Secreted protease metal-dependent protease	0.12	3.06 ± 0.52	0.37 ± 0.01
CAC0792	D-amino acid aminotransferase	0.10	1.51 ± 0.33	0.15 ± 0
CAC0804	Pectate lyase related protein, secreted	0.00	0.21 ± 0.02	0 ± 0
CAC0814	3-oxoacyl-[acyl-carrier-protein] synthase III	0.07	1.01 ± 0.45	0.07 ± 0.01
CAC0815	Methyl-accepting chemotaxis protein	0.08	1.01 ± 0.62	0.09 ± 0
CAC0816	Lipase-esterase related protein	0.09	1.05 ± 0.54	0.1 ± 0
CAC0861	ABC-type multidrug transport system, ATPase component	0.22	1.95 ± 0.96	0.42 ± 0.01
CAC0862	Transmembrane protein	0.16	2.32 ± 1.19	0.38 ± 0.01
CAC0863	Sensory transduction histidine kinase	0.13	2.73 ± 1.38	0.36 ± 0.03
CAC0882	Predicted membrane protein, hemolysin III homolog	0.04	5.14 ± 0.24	0.21 ± 0.01
CAC0946	ComE-like protein, Metallo beta-lactamase superfamily hydrolase, secreted	0.15	0.86 ± 0.15	0.13 ± 0
CAC0973	Argininosuccinate synthase	0.18	10.23 ± 0.45	1.84 ± 0.02
CAC0974	Argininosuccinate lyase	0.21	11.11 ± 0.44	2.3 ± 0.17
CAC1010	Predicted phosphohydrolase, Icc family	0.04	1.97 ± 0.72	0.08 ± 0.01
CAC1022	Thioesterase II of alpha/beta hydrolase superfamily	0.24	0.39 ± 0.14	0.09 ± 0
CAC1037	Predicted xylanase/chitin deacetylase	0.22	4.77 ± 0.24	1.03 ± 0.06
CAC1075	Beta-glucosidase family protein	0.00	1.35 ± 0.68	0 ± 0
CAC1078	Predicted phosphohydrolase, Icc family	0.04	2.19 ± 0.87	0.08 ± 0
CAC1079	Uncharacterized protein, related to enterotoxins of other Clostridiales	0.00	0.29 ± 0.12	0 ± 0
CAC1080	Uncharacterized protein, probably surface-located	0.00	5.02 ± 3.61	0 ± 0
CAC1081	Uncharacterized protein, probably surface-located	0.03	2.05 ± 1.73	0.06 ± 0
CAC1084	Beta-glucosidase family protein	0.00	0.82 ± 0.14	0 ± 0
CAC1085	Alpha-glucosidase	0.07	1.04 ± 0.25	0.08 ± 0
CAC1086	Transcriptional regulators of NagC/XylR family	0.08	1.88 ± 0.37	0.16 ± 0
CAC1102	Predicted membrane protein	0.14	4.72 ± 1.04	0.68 ± 0.04
CAC1214	Xre family DNA-binding domain and TPR-repeat containing protein	0.19	3.94 ± 0.55	0.74 ± 0.02
CAC1231	Predicted dehydrogenase, YULF B.subtilis ortholog	0.21	3.91 ± 0.14	0.83 ± 0.03
CAC1232	Predicted lytic murein transglycosylase (N-term. LysM motif repeat domain)	0.18	2.17 ± 0.08	0.39 ± 0.01
CAC1304	Uncharacterized conserved protein, predicted metal-binding	0.24	2.69 ± 0.2	0.64 ± 0.03
CAC1312	Hypothetical protein	0.13	0.82 ± 0.06	0.11 ± 0.01
CAC1313	Hypothetical protein	0.17	0.54 ± 0	0.09 ± 0.01
CAC1315	Peptodoglycan-binding domain containing protein	0.19	0.43 ± 0.07	0.08 ± 0.01
CAC1319	Glycerol uptake facilitator protein, GLPF	0.02	35.83 ± 8.36	0.55 ± 0.03
CAC1320	Glycerol-3-phosphate responsive antiterminator (mRNA-binding), GLPP	0.02	16.28 ± 3.56	0.34 ± 0.01
CAC1321	Glycerol kinase, GLPK	0.02	27.85 ± 6.42	0.45 ± 0.02
CAC1322	Glycerol-3-phosphate dehydrogenase, GLPA	0.06	59.33 ± 8.11	3.84 ± 0.16

CAC1323	NAD(FAD)-dependent dehydrogenase	0.06	58.91 ± 8.35	3.56 ± 0.32
CAC1324	Uncharacterized predected metal-binding protein	0.06	40.66 ± 1.55	2.56 ± 0.09
CAC1339	Possible sugar-proton symporter	0.15	0.47 ± 0.05	0.07 ± 0
CAC1345	D-xylose-proton symporter	0.10	0.63 ± 0.08	0.07 ± 0
CAC1346	L-arabinose isomerase	0.00	0.5 ± 0.05	0 ± 0
CAC1347	Transaldolase, TAL	0.10	1.13 ± 0.07	0.11 ± 0
CAC1348	Transketolase, TKT	0.14	1.27 ± 0.04	0.17 ± 0
CAC1349	Aldose-1-epimerase	0.10	2.19 ± 0.1	0.22 ± 0
CAC1365	Cobalamin biosynthesis protein CbiM	0.17	2.33 ± 0.55	0.39 ± 0.01
CAC1366	Predicted membrane protein	0.16	1.61 ± 0.35	0.25 ± 0.01
CAC1367	Cobalt permease	0.18	0.98 ± 0.22	0.18 ± 0
CAC1368	Cobalt transport (ATPase component)	0.14	1.85 ± 0.42	0.25 ± 0.01
CAC1369	Histidinol-phosphate aminotransferase	0.10	6.26 ± 1.23	0.61 ± 0.01
CAC1370	Cobalamin biosynthesis protein CbiG	0.18	2.2 ± 0.37	0.4 ± 0.01
CAC1371	Possible kinase, diverged	0.17	2.24 ± 0.38	0.39 ± 0.01
CAC1372	Cobalamin biosynthesis enzyme CobT	0.18	2.11 ± 0.39	0.39 ± 0.01
CAC1373	Anaerobic Cobalt chelatase, cbiK	0.22	1.57 ± 0.27	0.34 ± 0.01
CAC1374	Cobyric acid synthase CbiP	0.20	2.1 ± 0.4	0.43 ± 0.01
CAC1377	Cobalamin biosynthesis protein CbiD	0.22	2.89 ± 0.41	0.64 ± 0.01
CAC1405	Beta-glucosidase	0.02	16.94 ± 4.45	0.27 ± 0.03
CAC1406	Transcriptional antiterminator (BglG family)	0.01	25.57 ± 13.31	0.36 ± 0.02
CAC1407	PTS system, beta-glucosides-specific IIABC component	0.08	0.9 ± 0.51	0.07 ± 0.01
CAC1408	Phospho-beta-glucosidase	0.07	1.23 ± 0.68	0.09 ± 0.01
CAC1411	Similar to toxic anion resistance protein terA, ortholog of YCEH B.subtilis	0.18	1.29 ± 0.66	0.23 ± 0
CAC1412	Methyl methane sulfonate/mytomycin C/UV resistance protein, GSP18 (YCEE) B.subtilis ortholog, TerE family protein	0.12	1.74 ± 0.92	0.21 ± 0.01
CAC1413	Similar to C-terminal fragment of toxic anion resistance protein terA	0.13	1.89 ± 1	0.25 ± 0.01
CAC1414	TerE family protein, ortholog of stress responce protein SCP2 (YCEC) B.subtilis	0.14	2.74 ± 1.43	0.38 ± 0.02
CAC1415	TerC family protein, ortholog of stress responce protein	0.22	1.61 ± 0.83	0.35 ± 0.01
CAC1454	Membrane associated histidine kinase-like ATPase	0.22	0.88 ± 0.15	0.19 ± 0
CAC1455	Two-component system regulator (CheY domain and HTH-like DNA-binding domain)	0.20	2.05 ± 0.39	0.41 ± 0.01
CAC1531	Uncharacterized conserved protein	0.20	0.4 ± 0.1	0.08 ± 0
CAC1532	Protein containing ChW-repeats	0.09	0.97 ± 0.45	0.09 ± 0
CAC1554	Heavy-metal-associated domain (N-terminus) and membrane-bounded cytochrome biogenesis cycZ-like domain, possible membrane copper tolerance protein	0.05	2.52 ± 1.67	0.12 ± 0
CAC1579	Methyl-accepting chemotaxis-like protein (chemotaxis sensory transducer)	0.20	1.25 ± 0.42	0.25 ± 0.01
CAC1580	Hypothetical protein	0.12	5.05 ± 1.45	0.61 ± 0.01
CAC1600	Methyl-accepting chemotaxis-like protein (chemotaxis sensory transducer)	0.11	0.99 ± 0.6	0.11 ± 0

CAC1601	Methyl-accepting chemotaxis-like protein (chemotaxis sensory transducer)	0.22	0.58 ± 0.3	0.13 ± 0
CAC1634	Flagellin	0.15	1.99 ± 1.39	0.29 ± 0.01
CAC1768	Uncharacterized conserved protein, TraB family	0.20	0.35 ± 0.08	0.07 ± 0
CAC1775	Predicted membrane protein	0.10	0.96 ± 0.25	0.09 ± 0
CAC1817	Stage V sporulation protein, spoVS	0.07	8.29 ± 0.78	0.57 ± 0.04
CAC1868	Uncharacterized secreted protein, homolog YXKC Bacillus subtilis	0.14	0.47 ± 0.15	0.07 ± 0
CAC1886	Uncharacterized phage related protein	0.00	0.24 ± 0.05	0 ± 0
CAC1888	Uncharacterized phage related protein	0.18	0.48 ± 0.15	0.09 ± 0
CAC1893	ClpP family serine protease, possible phage related	0.16	0.56 ± 0.14	0.09 ± 0
CAC2001	Indolepyruvate ferredoxin oxidoreductase, subunit alpha	0.16	1 ± 0.65	0.16 ± 0.01
CAC2002	Predicted iron-sulfur flavoprotein	0.18	0.49 ± 0.33	0.09 ± 0
CAC2003	Predicted permease	0.00	0.25 ± 0.15	0 ± 0
CAC2004	Siderophore/Surfactin synthetase related protein	0.15	0.98 ± 0.68	0.15 ± 0
CAC2005	Siderophore/Surfactin synthetase related protein	0.24	0.52 ± 0.34	0.13 ± 0
CAC2007	Predicted glycosyltransferase	0.12	1.2 ± 0.83	0.14 ± 0
CAC2008	3-oxoacyl-(acyl-carrier-protein) synthase	0.15	0.5 ± 0.33	0.08 ± 0
CAC2009	3-Hydroxyacyl-CoA dehydrogenase	0.09	0.82 ± 0.57	0.07 ± 0
CAC2010	Predicted Fe-S oxidoreductase	0.08	1.16 ± 0.82	0.09 ± 0.01
CAC2011	Possible 3-oxoacyl-[acyl-carrier-protein] synthase III	0.11	0.74 ± 0.46	0.09 ± 0
CAC2012	Enoyl-CoA hydratase	0.11	0.57 ± 0.35	0.06 ± 0
CAC2013	Hypothetical protein	0.09	1.05 ± 0.58	0.09 ± 0
CAC2014	Predicted esterase	0.07	1.2 ± 0.68	0.09 ± 0
CAC2015	Hypothetical protein	0.11	0.58 ± 0.3	0.07 ± 0
CAC2016	Enoyl-CoA hydratase	0.04	3.37 ± 2.05	0.13 ± 0
CAC2017	Acyl carrier protein	0.08	0.97 ± 0.57	0.07 ± 0
CAC2018	Aldehyde:ferredoxin oxidoreductase	0.07	1.03 ± 0.55	0.07 ± 0
CAC2019	Malonyl CoA-acyl carrier protein transacylase	0.00	1.33 ± 0.71	0 ± 0
CAC2020	Molybdopterin biosynthesis enzyme, MoeA, fused to molibdopterin-binding domain	0.10	0.6 ± 0.21	0.06 ± 0
CAC2021	Molybdopterin biosynthesis enzyme, MoeA (short form)	0.04	1.69 ± 0.55	0.07 ± 0
CAC2022	Molybdopterin biosynthesis enzyme, moaB	0.09	1.06 ± 0.33	0.1 ± 0
CAC2023	Membrane protein, related to copy number protein COP from Clostridium perfringens plasmid pIP404 (GI:116928)	0.00	0.49 ± 0.14	0 ± 0
CAC2024	Phosphatidylglycerophosphate synthase related protein (fragment)	0.11	0.76 ± 0.21	0.08 ± 0
CAC2025	Hypothetical protein	0.05	2.45 ± 0.52	0.13 ± 0
CAC2026	Predicted flavodoxin	0.06	2.45 ± 0.37	0.16 ± 0.01
CAC2043	Hypothetical protein	0.00	0.35 ± 0.12	0 ± 0
CAC2107	Contains cell adhesion domain	0.13	0.75 ± 0.34	0.1 ± 0
CAC2153	Flagellar protein flbD	0.20	12.96 ± 6.5	2.56 ± 0.08
CAC2154	Flagellar hook protein FlgE.	0.14	8.05 ± 1.81	1.15 ± 0.04

CAC2155	Hypothetical protein	0.12	13.11 ± 4.08	1.52 ± 0.02
CAC2156	Flagellar hook assembly protein FlgD	0.14	15.69 ± 4.65	2.14 ± 0.04
CAC2157	Flagellar hook-length control protein fliK	0.18	11.3 ± 3.48	2.04 ± 0.06
CAC2203	Possible hook-associated protein, flagellin family	0.16	12.36 ± 8.44	2 ± 0.02
CAC2226	Enzyme of ILVE/PABC family (branched-chain amino acid aminotransferase/4-amino-4-deoxychorismate lyase)	0.11	4.66 ± 1.2	0.53 ± 0.02
CAC2241	Cation transport P-type ATPase	0.04	8.91 ± 1.09	0.33 ± 0.02
CAC2242	Predicted transcriptional regulator, arsE family	0.06	1.53 ± 0.2	0.09 ± 0
CAC2252	Alpha-glucosidase fused to unknown alpha-amylase C-terminal. domain	0.00	52.44 ± 12.92	0.15 ± 0.01
CAC2293	Hypothetical secreted protein	0.17	0.66 ± 0.48	0.11 ± 0
CAC2382	Single-strand DNA-binding protein, ssb	0.18	0.35 ± 0.02	0.06 ± 0
CAC2388	N-acetylornithine aminotransferase	0.09	6.84 ± 0.09	0.61 ± 0.03
CAC2390	N-acetyl-gamma-glutamyl-phosphate reductase	0.23	1.55 ± 0.26	0.36 ± 0.03
CAC2391	Ornithine acetyltransferase	0.24	2.86 ± 0.63	0.7 ± 0.04
CAC2433	HtrA-like serine protease (with PDZ domain)	0.08	46.33 ± 10.88	3.88 ± 0.07
CAC2455	Hypothetical protein, CF-13 family	0.00	0.23 ± 0.1	0 ± 0
CAC2456	Hypothetical protein, CF-40 family	0.10	3.72 ± 1.92	0.38 ± 0.01
CAC2457	Hypothetical protein	0.11	3.66 ± 1.91	0.41 ± 0.01
CAC2469	Lactoylglutathione lyase (fragment)	0.16	0.92 ± 0.24	0.15 ± 0
CAC2470	Uncharacterized Zn-finger protein	0.15	1.94 ± 0.4	0.29 ± 0
CAC2511	Predicted membrane protein	0.18	0.46 ± 0.22	0.08 ± 0
CAC2514	Beta galactosidase	0.00	0.3 ± 0.06	0 ± 0
CAC2517	Extracellular neutral metalloprotease, NPRE	0.18	0.64 ± 0.32	0.11 ± 0.01
CAC2535	Predicted protein of beta-propeller fold	0.22	0.74 ± 0.4	0.16 ± 0
CAC2536	Glycosyltransferase	0.18	0.86 ± 0.48	0.15 ± 0
CAC2570	Predicted arabinogalactan endo-1,4-beta-galactosidase	0.09	4.26 ± 1.17	0.37 ± 0.02
CAC2581	6-pyruvoyl-tetrahydropterin synthase related domain; conserved membrane protein	0.00	0.33 ± 0.15	0 ± 0
CAC2584	Protein containing ChW-repeats	0.00	0.38 ± 0.12	0 ± 0
CAC2597	Hypothetical protein	0.22	0.78 ± 0.31	0.17 ± 0.01
CAC2610	L-fucose isomerase related protein	0.06	1.31 ± 0.23	0.08 ± 0
CAC2611	Hypothetical protein	0.08	1.18 ± 0.26	0.09 ± 0.01
CAC2612	Xylulose kinase	0.12	0.63 ± 0.07	0.08 ± 0
CAC2620	HD-GYP hydrolase domain containing protein	0.00	0.4 ± 0.24	0 ± 0
CAC2663	Protein containing cell-wall hydrolase domain	0.16	0.56 ± 0.16	0.09 ± 0
CAC2695	Diverged Metallo-dependent hydrolase(Zn) of DD-Peptidase family; peptodoglycan-binding domain	0.10	0.93 ± 0.41	0.09 ± 0
CAC2774	Methyl-accepting chemotaxis protein with HAMP domain	0.21	0.73 ± 0.13	0.16 ± 0
CAC2805	Possible selenocysteine lyase (aminotransferase of NifS family)	0.00	0.52 ± 0.01	0 ± 0
CAC2806	Predicted phosphohydrolase, Icc family	0.00	68.92 ± 1.3	0.16 ± 0.01

CAC2807	Endo-1,3(4)-beta-glucanase family 16	0.00	49.05 ± 15.33	0.06 ± 0
CAC2808	Beta-lactamase class C domain (PBPX family) containing protein	0.00	1.05 ± 0.44	0 ± 0
CAC2809	Predicted HD superfamily hydrolase	0.04	1.64 ± 0.82	0.06 ± 0
CAC2810	Possible glucoamylase (diverged), 15 family	0.00	4.5 ± 1.62	0 ± 0
CAC2828	Nudix (MutT) family hydrolase/pyrophosphatase	0.24	2.67 ± 0.15	0.63 ± 0.02
CAC2833	Uncharacterized conserved protein, YAEG family	0.00	0.51 ± 0.28	0 ± 0
CAC2834	Uncharacterized conserved protein, YHAD family	0.01	31 ± 21.13	0.29 ± 0.01
CAC2835	Gluconate permease, gntP	0.01	25.35 ± 17.48	0.17 ± 0
CAC2847	Ribosome-associated protein Y (PSrp-1)	0.21	32.75 ± 6.27	6.9 ± 0.24
CAC2891	Fusion of alpha-glucosidase (family 31 glycosyl hydrolase) and glycosidase (TreA/MalS family)	0.02	6.35 ± 1.38	0.1 ± 0
CAC2943	N-terminal domain intergin-like repeats and c-terminal - cell wall-associated hydrolase domain	0.00	0.27 ± 0.03	0 ± 0
CAC2944	N-terminal domain intergin-like repeats and c-terminal- cell wall-associated hydrolase domain	0.08	1.46 ± 0.13	0.12 ± 0
CAC2959	Galactokinase	0.11	1.2 ± 0.13	0.13 ± 0
CAC2960	UDP-galactose 4-epimerase	0.20	0.43 ± 0.03	0.08 ± 0
CAC2998	TPR-repeat-containing protein	0.15	2.23 ± 0.25	0.33 ± 0
CAC3066	Glycosyltransferase	0.15	0.85 ± 0.47	0.13 ± 0.01
CAC3067	Predicted membrane protein	0.25	0.25 ± 0.11	0.06 ± 0
CAC3068	Glycosyltransferase	0.10	0.64 ± 0.31	0.06 ± 0
CAC3069	Predicted glycosyltransferase	0.00	0.72 ± 0.29	0 ± 0
CAC3070	Glycosyltransferase	0.02	3.15 ± 1.34	0.06 ± 0
CAC3071	Glycosyltransferase	0.00	4.07 ± 1.55	0 ± 0
CAC3072	Mannose-1-phosphate guanylyltransferase	0.00	5.2 ± 1.51	0 ± 0
CAC3073	Sugar transferase involved in lipopolysaccharide synthesis	0.00	2.73 ± 0.7	0 ± 0
CAC3075	Butyrate kinase, BUK	0.00	68.87 ± 3.03	0 ± 0
CAC3085	TPR-repeat-containing protein; Cell-adhesion domain;	0.12	0.74 ± 0.02	0.09 ± 0
CAC3086	Protein containing cell adhesion domain	0.11	1.36 ± 0.15	0.15 ± 0.01
CAC3087	Phosphoenolpyruvate-protein kinase (PTS system enzyme I)	0.04	39.14 ± 22.32	1.6 ± 0.02
CAC3251	Sensory transduction protein containing HD_GYP domain	0.09	0.96 ± 0.3	0.09 ± 0
CAC3274	Possible surface protein, responsible for cell interaction; contains cell adhesion domain and ChW-repeats	0.10	1.43 ± 0.94	0.15 ± 0.01
CAC3279	Possible surface protein, responsible for cell interaction; contains cell adhesion domain and ChW-repeats	0.23	0.28 ± 0.13	0.06 ± 0
CAC3280	Possible surface protein, responsible for cell interaction; contains cell adhesion domain and ChW-repeats	0.15	0.49 ± 0.27	0.07 ± 0.01
CAC3298	NADH-dependent butanol dehydrogenase B (BDH II)	0.04	14.33 ± 2.65	0.61 ± 0.01
CAC3319	Signal transduction histidine kinase	0.03	2.58 ± 0.5	0.08 ± 0
CAC3320	Predicted secreted protein homolog of yjcM/yhbB B.subtilis	0.08	0.93 ± 0.24	0.07 ± 0
CAC3408	NADH oxidase (two distinct flavin oxidoreductase domains)	0.04	3.28 ± 1.4	0.13 ± 0

CAC3409	Transcriptional regulators, LysR family	0.02	9.93 ± 2.4	0.21 ± 0.02
CAC3412	Predicted protein-S-isoprenylcysteine methyltransferase	0.00	0.64 ± 0.05	0 ± 0
CAC3422	Sugar:proton symporter (possible xylulose)	0.03	2.71 ± 0.43	0.09 ± 0
CAC3423	Acetyltransferase (ribosomal protein N-acetylase subfamily)	0.03	3.19 ± 0.7	0.1 ± 0
CAC3425	PTS system, (possibly glucose-specific) IIBC component	0.15	0.43 ± 0.05	0.06 ± 0
CAC3426	6-phospho-alpha-glucosidase	0.12	0.81 ± 0.05	0.1 ± 0.02
CAC3486	Multimeric flavodoxin WrbA family protein	0.20	2.28 ± 1.03	0.46 ± 0.03
CAC3498	Sugar kinase, ribokinase family	0.00	0.43 ± 0.03	0 ± 0
CAC3521	Hypothetical protein	0.07	6.11 ± 0.63	0.43 ± 0.01
CAC3522	Hypothetical protein, CF-7 family	0.07	5.28 ± 0.51	0.37 ± 0.01
CAC3523	Hypothetical protein, CF-7 family	0.10	1.74 ± 0.23	0.18 ± 0
CAC3524	Hypothetical protein, CF-7 family	0.16	1.74 ± 0.29	0.28 ± 0
CAC3557	Probable S-layer protein;	0.23	0.55 ± 0.3	0.12 ± 0
CAC3558	Probable S-layer protein;	0.17	0.59 ± 0.34	0.1 ± 0
CAC3565	Uncharacterized secreted protein, containing cell adhesion domain	0.19	0.4 ± 0.14	0.08 ± 0
CAC3566	Hypothetical protein, CF-28 family	0.15	0.58 ± 0.21	0.09 ± 0
CAC3581	HAD superfamily hydrolase	0.17	0.75 ± 0.21	0.12 ± 0.01
CAC3582	Hypothetical protein	0.04	11.19 ± 7.64	0.42 ± 0.01
CAC3583	Predicted permease	0.06	2.28 ± 1.57	0.13 ± 0
CAC3584	Predicted permease	0.03	9.28 ± 6.32	0.31 ± 0.01
CAC3585	ABC-type transporter, ATPase component	0.02	11.96 ± 8.25	0.28 ± 0.02
CAC3628	Oligopeptide ABC transporter, ATPase component	0.18	4.67 ± 0.42	0.86 ± 0.01
CAC3629	Oligopeptide ABC transporter, ATPase component	0.21	3.47 ± 0.66	0.74 ± 0.02
CAC3630	Oligopeptide ABC transporter, permease component	0.19	2.94 ± 0.51	0.56 ± 0.02
CAC3631	Oligopeptide ABC transporter, permease component	0.20	3.41 ± 0.57	0.67 ± 0.05
CAC3632	Oligopeptide ABC transporter, periplasmic substrate-binding component	0.14	5.14 ± 0.71	0.73 ± 0.06
CAC3650	HD-GYP domain containing protein	0.09	2.68 ± 0.06	0.23 ± 0
CAC3671	ABC-type sugar transport system, permease component	0.00	0.42 ± 0.03	0 ± 0
CAC3672	ABC-type sugar transport system, periplasmic sugar-binding component	0.15	0.47 ± 0.05	0.07 ± 0.01
CAC3683	Penicillin-binding protein 2 (serine-type D-Ala-D-Ala carboxypeptidase)	0.23	1.45 ± 0.11	0.34 ± 0.01
CAP0053	Xylanase, glycosyl hydrolase family 10	0.00	0.54 ± 0.02	0 ± 0
CAP0054	Xylanase/chitin deacetylase family enzyme	0.10	0.8 ± 0.03	0.08 ± 0.01
CAP0058	Rare lipoprotein A RLPA releated protein	0.09	1.85 ± 0.34	0.17 ± 0
CAP0065	Predicted secreted metalloprotease	0.14	0.7 ± 0.07	0.1 ± 0
CAP0066	Mannose-specific phosphotransferase system component IIAB	0.01	32.06 ± 7.25	0.24 ± 0.05
CAP0067	Mannose/fructose-specific phosphotransferase system component IIC	0.01	55.44 ± 10.81	0.4 ± 0.07
CAP0068	Mannose-specific phosphotransferase system component IID	0.01	39.27 ± 9.88	0.35 ± 0.07

CAP0069	Uncharacterized protein, homolog of Streptococcus salivarius (5669858)	0.03	8.42 ± 0.36	0.22 ± 0
CAP0072	Hypothetical protein	0.11	0.72 ± 0.07	0.08 ± 0
CAP0085	Hypothetical secreted protein (fragment)	0.17	1.06 ± 0.05	0.18 ± 0.01
CAP0086	Permease, MDR related, probably tetracycline resistance protein	0.13	1.51 ± 0.12	0.2 ± 0
CAP0098	Alpha-amylase, AmyB	0.03	2.34 ± 0.24	0.08 ± 0.01
CAP0102	Membrane protein	0.05	5.04 ± 2.34	0.25 ± 0.01
CAP0133	Antibiotic-resistance protein, alpha/beta superfamily hydrolase	0.20	2.38 ± 0.27	0.48 ± 0.02
CAP0134	Hypothetical protein	0.16	1.08 ± 0.23	0.18 ± 0.01
CAP0135	Oxidoreductase	0.08	10.43 ± 1.91	0.78 ± 0.02
CAP0136	AstB/chuR/nirj-related protein	0.11	2.08 ± 0.43	0.22 ± 0
CAP0137	Similar to C-ter. fragment of UDP-glucuronosyltransferases, YpfP B.subtilis related	0.09	3.59 ± 0.46	0.32 ± 0.01
CAP0138	Diverged, distantly related to biotin carboxylase N-term. fragment.	0.12	3.46 ± 0.31	0.41 ± 0.02
CAP0148	Phospholipase C	0.21	0.31 ± 0.07	0.07 ± 0
CAP0151	Integrin-like repeats domain fused to lysozyme, LYCV glycosyl hydrolase	0.11	0.86 ± 0.56	0.1 ± 0
CAP0152	Hypothetical protein, CF-6 family	0.12	0.92 ± 0.59	0.11 ± 0
CAP0160	Secreted protein containing cell-adhesion domains	0.18	0.47 ± 0.15	0.09 ± 0
CAP0165	Acetoacetate decarboxylase	0.17	1.98 ± 0.05	0.35 ± 0
CAP0166	Hypothetical protein	0.22	0.33 ± 0.18	0.07 ± 0
CAP0167	Specialized sigma factor (SigF/SigE family)	0.18	0.42 ± 0.25	0.07 ± 0.01
CAP0168	Alpha-amylase	0.15	0.64 ± 0.08	0.09 ± 0
CAP0174	Membrane protein	0.16	0.6 ± 0.07	0.09 ± 0.01

Acidogenesis

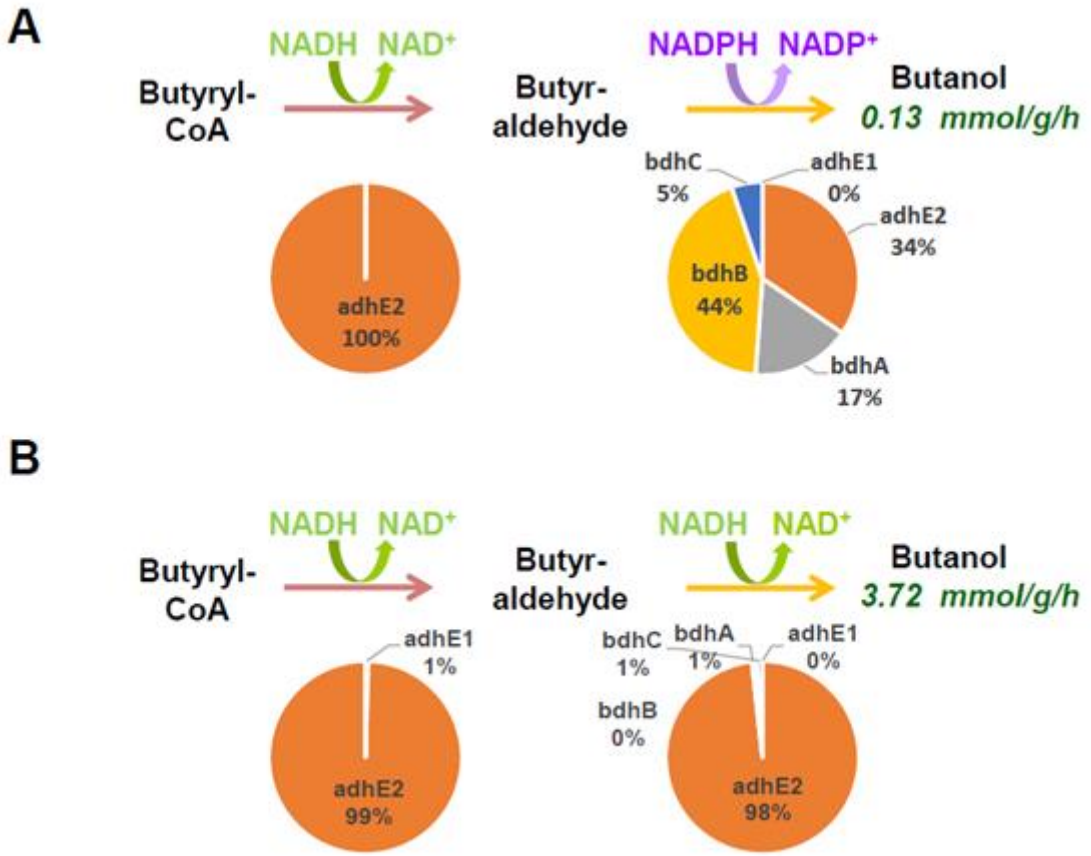

Fig.S.4.1. Butanol pathway analysis of control (A), *ΔbukΔ*ptb (B)

Solventogenesis

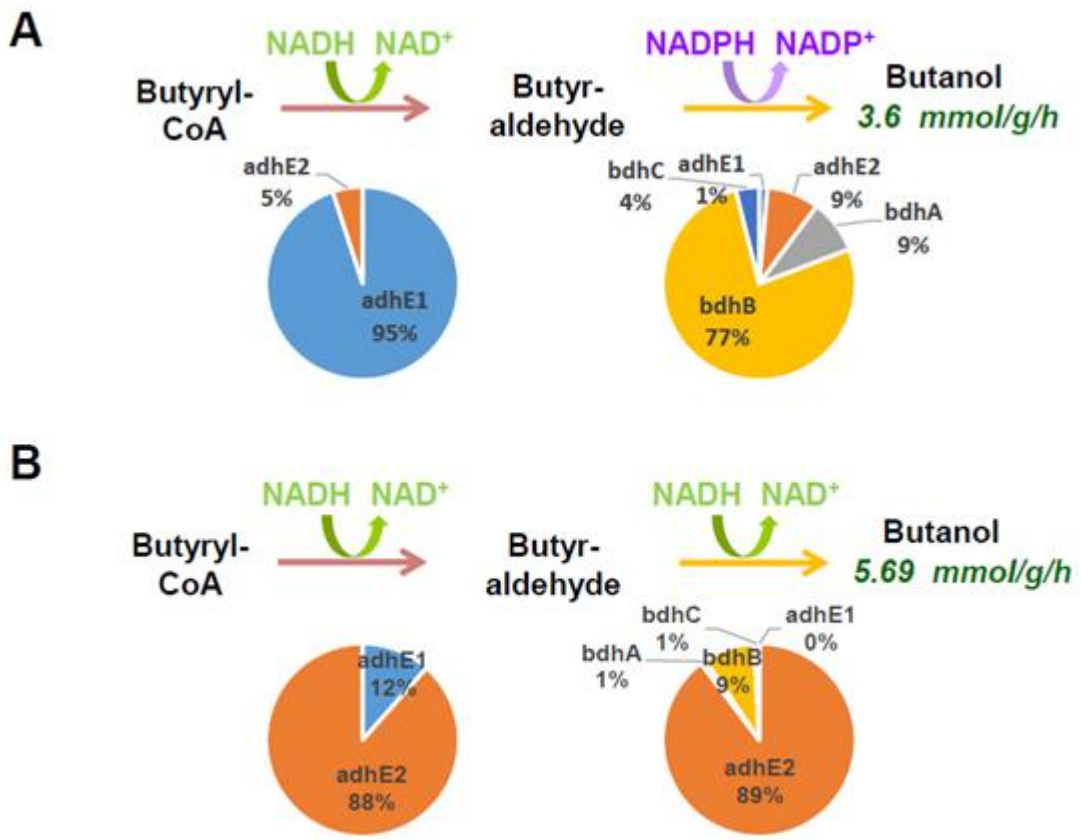

Fig.S.4.1. Butanol pathway analysis of control (A), *ΔbukΔ*ptb (B)

Alcohologenesis

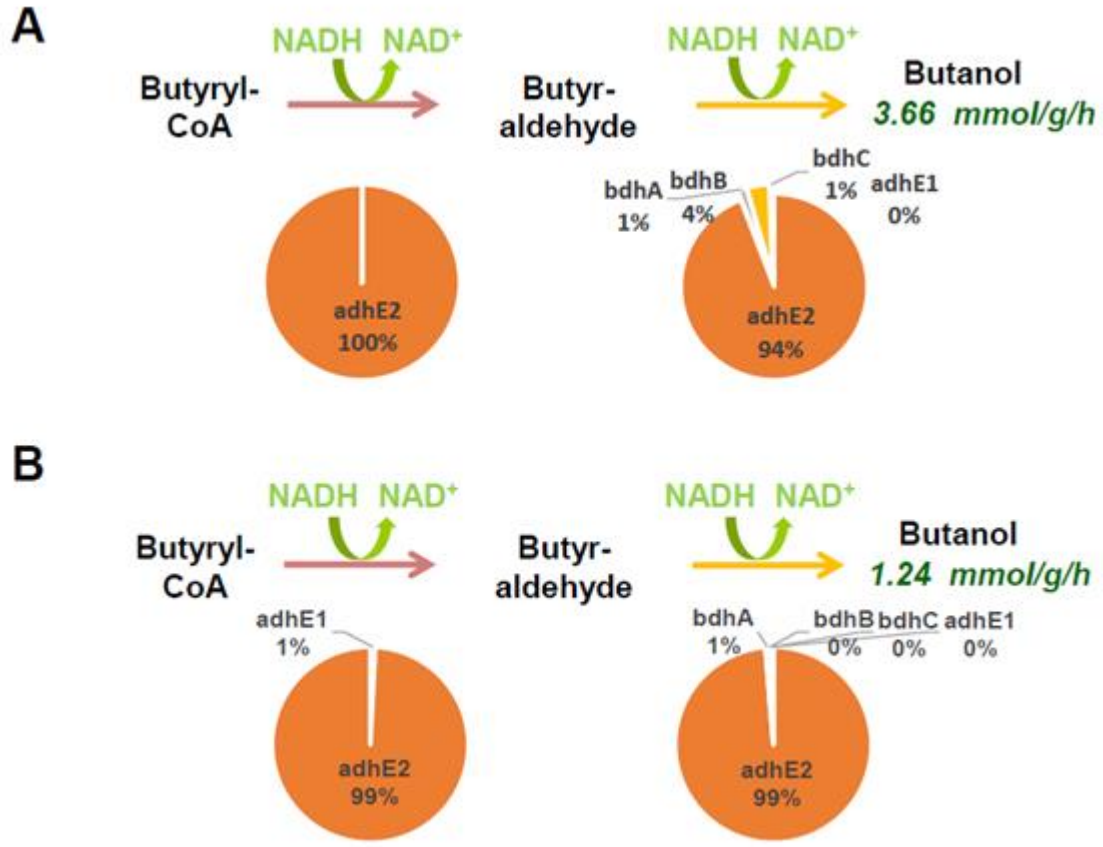

Fig.S.4.1. Butanol pathway analysis of control (A), *ΔbukΔ*ptb (B)

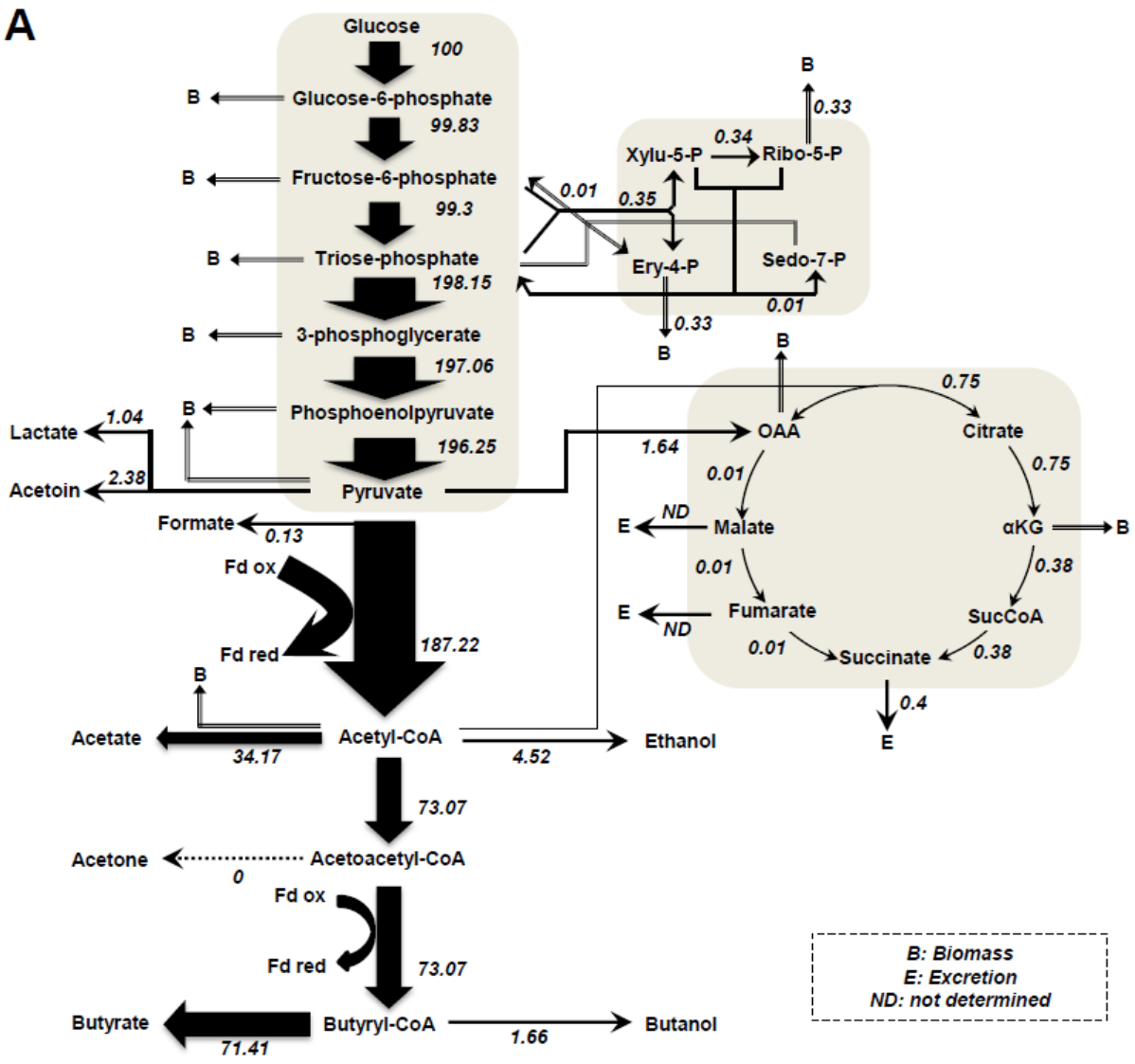

Fig.S4.2 Metabolic flux map of control and ΔbukΔptb300 strains under three metabolic states. (A) control under acidogenesis, (B) ΔbukΔptb300under acidogenesis, (C) control under solventogenesis, (D) ΔbukΔptb300 under solventogenesis, (E) control under alcohologenesis, (F) ΔbukΔptb300under alcohologenesis. All values are normalized to the flux of the initial carbon source (mmol/gDCW/h). Glucose flux is normalized as 100 for acidogenesisandsolventogenesis, and the sum of glucose and half of the glycerol normalized as 100 for alcohologenesis. 2-KV, 2-keto-valerate; 2-HV, 2-hydroxyl-valerate.

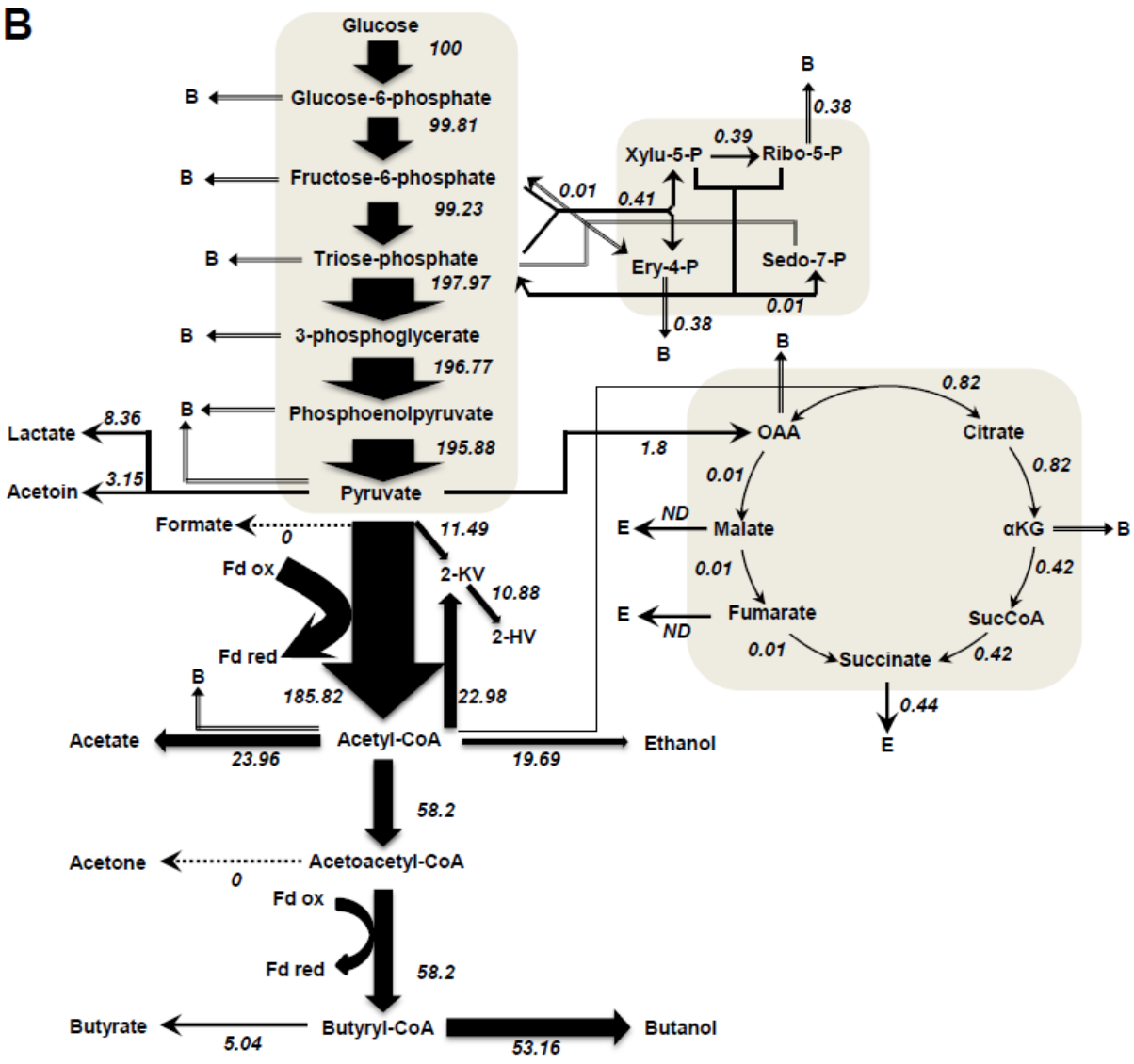

Fig.S4.2 Metabolic flux map of control and ΔbukΔptb300 strains under three metabolic states. (A) control under acidogenesis, (B) ΔbukΔptb300under acidogenesis, (C) control under solventogenesis, (D) ΔbukΔptb300 under solventogenesis, (E) control under alcohologenesis, (F) ΔbukΔptb300under alcohologenesis. All values are normalized to the flux of the initial carbon source (mmol/gDCW/h). Glucose flux is normalized as 100 for acidogenesisandsolventogenesis, and the sum of glucose and half of the glycerol normalized as 100 for alcohologenesis. 2-KV, 2-keto-valerate; 2-HV, 2-hydroxyl-valerate.

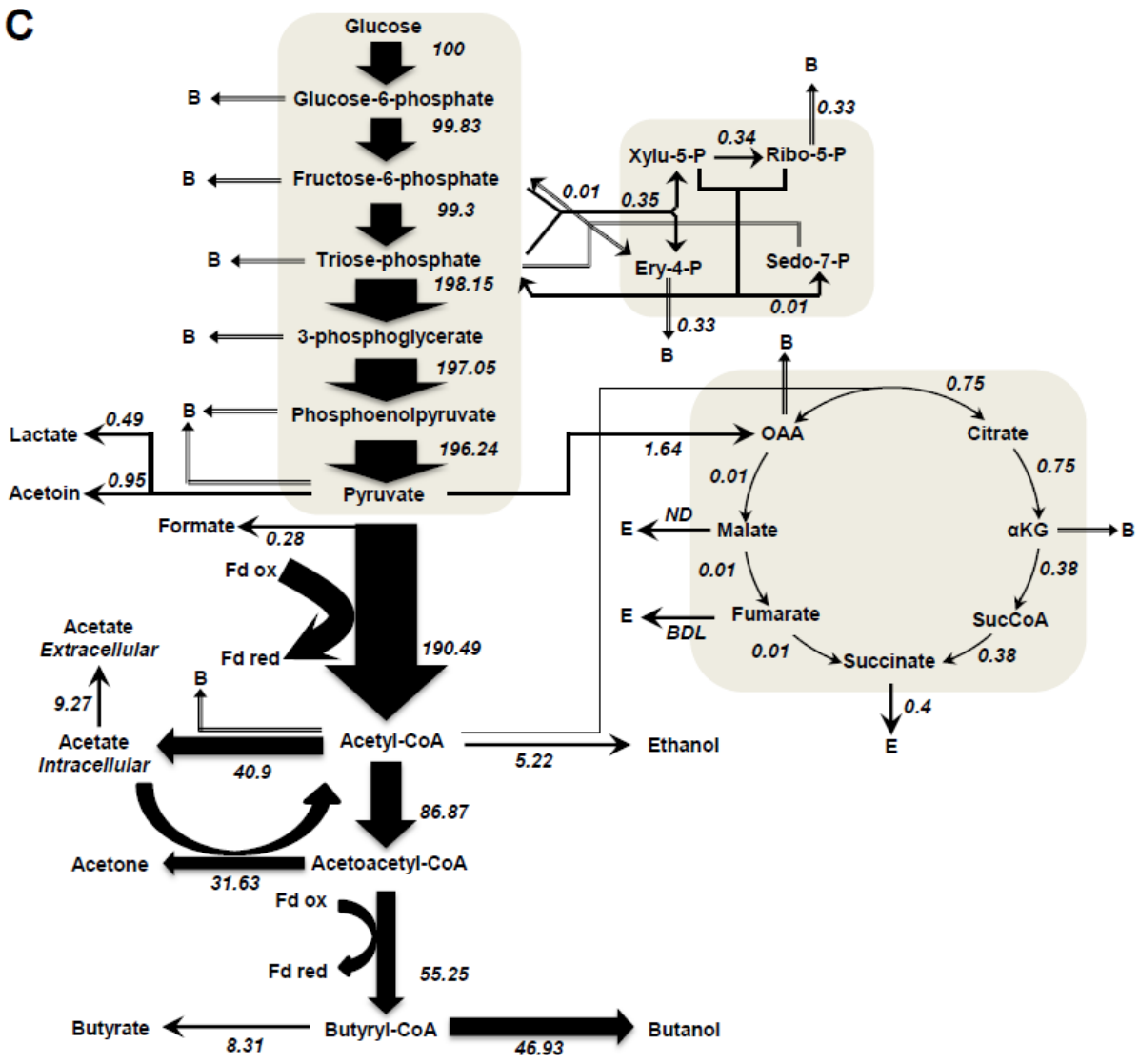

Fig.S4.2 Metabolic flux map of control and ΔbukΔptb300 strains under three metabolic states. (A) control under acidogenesis, (B) ΔbukΔptb300under acidogenesis, (C) control under solventogenesis, (D) ΔbukΔptb300 under solventogenesis, (E) control under alcohologenesis, (F) ΔbukΔptb300under alcohologenesis. All values are normalized to the flux of the initial carbon source (mmol/gDCW/h). Glucose flux is normalized as 100 for acidogenesisandsolventogenesis, and the sum of glucose and half of the glycerol normalized as 100 for alcohologenesis. 2-KV, 2-keto-valerate; 2-HV, 2-hydroxyl-valerate.

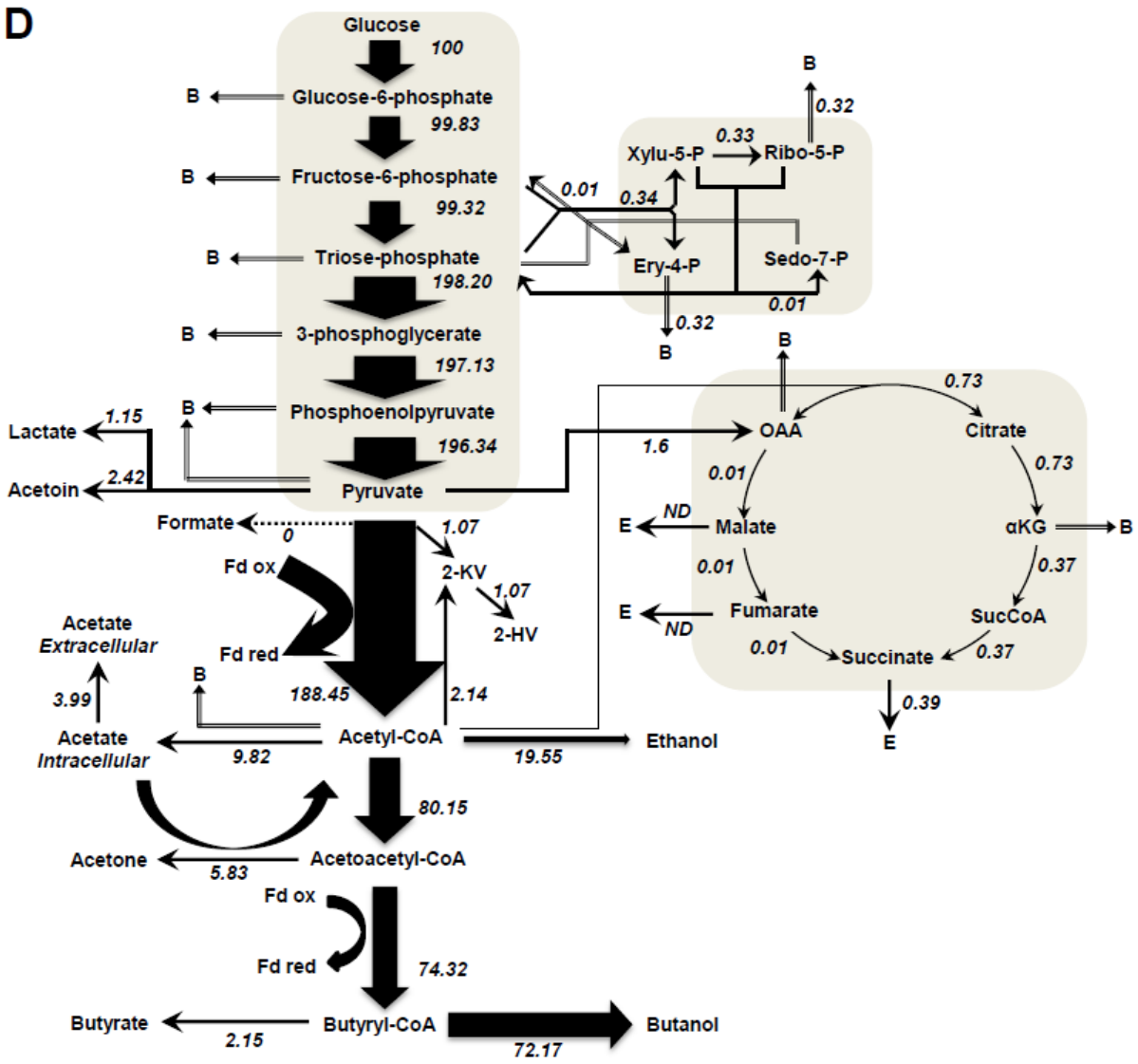

Fig.S4.2 Metabolic flux map of control and ΔbukΔptb300 strains under three metabolic states. (A) control under acidogenesis, (B) ΔbukΔptb300under acidogenesis, (C) control under solventogenesis, (D) ΔbukΔptb300 under solventogenesis, (E) control under alcohologenesis, (F) ΔbukΔptb300under alcohologenesis. All values are normalized to the flux of the initial carbon source (mmol/gDCW/h). Glucose flux is normalized as 100 for acidogenesisandsolventogenesis, and the sum of glucose and half of the glycerol normalized as 100 for alcohologenesis. 2-KV, 2-keto-valerate; 2-HV, 2-hydroxyl-valerate.

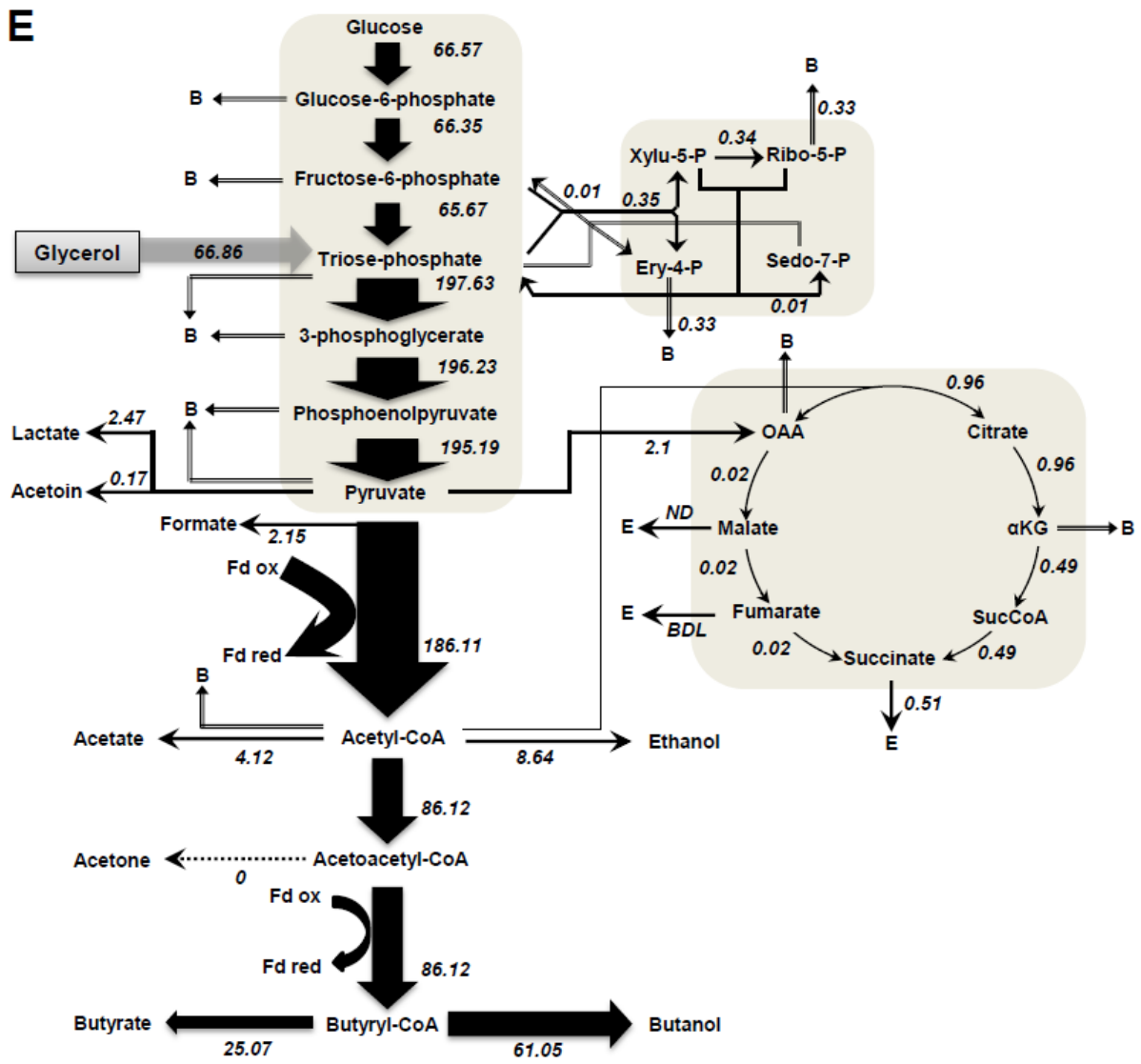

Fig.S4.2 Metabolic flux map of control and ΔbukΔptb300 strains under three metabolic states. (A) control under acidogenesis, (B) ΔbukΔptb300under acidogenesis, (C) control under solventogenesis, (D) ΔbukΔptb300 under solventogenesis, (E) control under alcohologenesis, (F) ΔbukΔptb300under alcohologenesis. All values are normalized to the flux of the initial carbon source (mmol/gDCW/h). Glucose flux is normalized as 100 for acidogenesisandsolventogenesis, and the sum of glucose and half of the glycerol normalized as 100 for alcohologenesis. 2-KV, 2-keto-valerate; 2-HV, 2-hydroxyl-valerate.

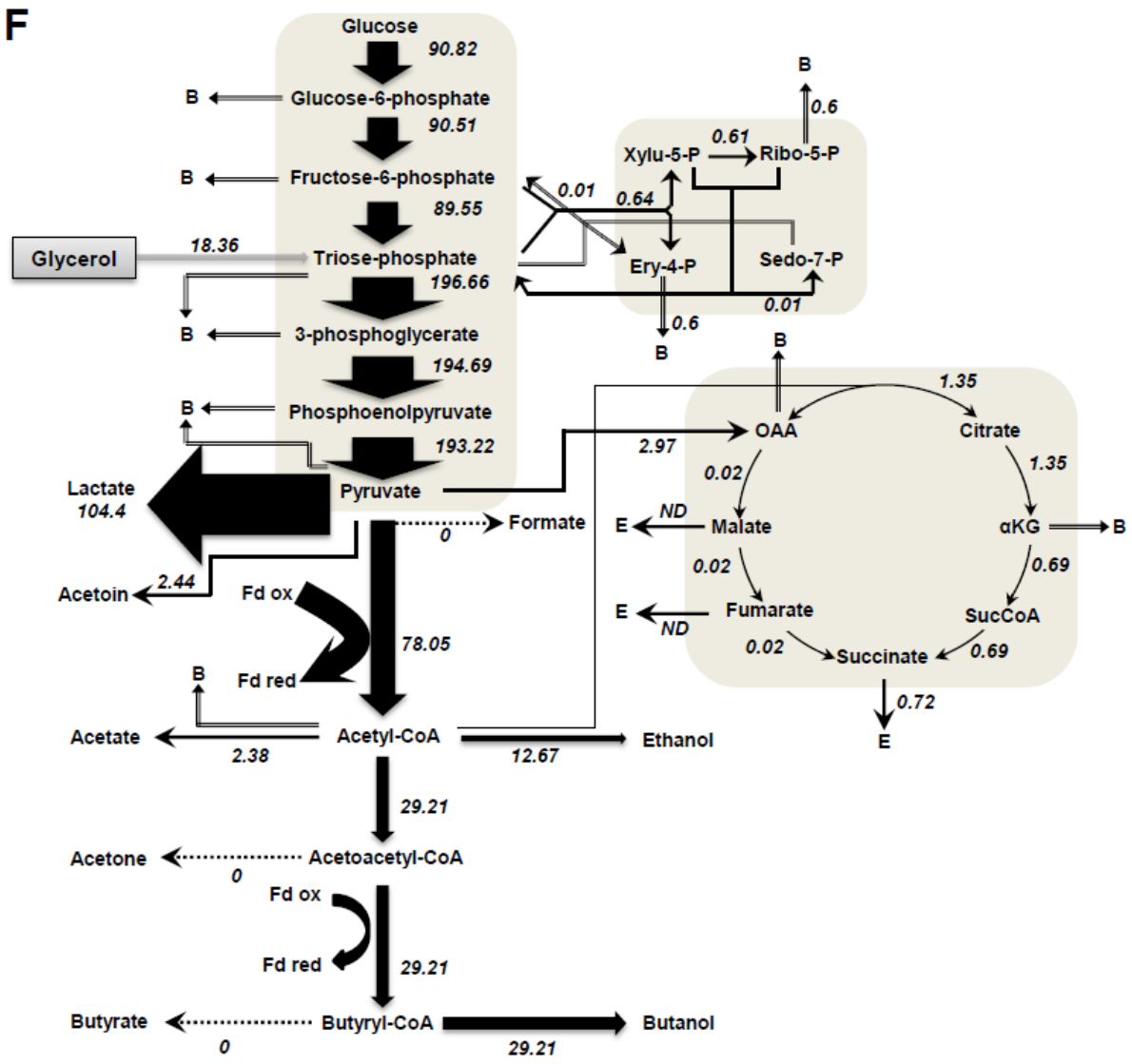

Fig.S4.2 Metabolic flux map of control and ΔbukΔptb300 strains under three metabolic states. (A) control under acidogenesis, (B) ΔbukΔptb300under acidogenesis, (C) control under solventogenesis, (D) ΔbukΔptb300 under solventogenesis, (E) control under alcohologenesis, (F) ΔbukΔptb300under alcohologenesis. All values are normalized to the flux of the initial carbon source (mmol/gDCW/h). Glucose flux is normalized as 100 for acidogenesisandsolventogenesis, and the sum of glucose and half of the glycerol normalized as 100 for alcohologenesis. 2-KV, 2-keto-valerate; 2-HV, 2-hydroxyl-valerate.

Chapter 5

General conclusion and future perspectives

5.1. General conclusion and future perspectives

The objective of this work was to acquire a better knowledge of the physiology of *Clostridium acetobutylicum* by combining a system scale approach and the construction and characterization of specific metabolic mutants.

An improved Genome Scale Model containing new and validated biochemical data was developed in conjunction with quantitative transcriptomic and proteomic analyses to obtain accurate fluxomic data. To access to quantitative data, the "omics" methods used have to be either improved or developed. Furthermore, for the first time to our knowledge, complementary analyses were done in order to express the genes expression data in number of molecules of mRNA and cytoplasmic protein per cell, numbers which are more relevant for the understanding of the cell physiology. These "omics" data allowed for i) the determination of the distribution of carbon and electron fluxes, ii) the elucidation of the different genes/enzymes involved in the primary metabolism of *C. acetobutylicum* and iii) a better understanding of the regulation of *C. acetobutylicum* primary metabolism under different physiological conditions.

Three metabolic mutants, Δ*adhE1*, Δ*adhE2* and Δ*ptb-buk* were constructed and physiologically characterized using the quantitative transcriptomic, proteomic and fluxomic approach developed before for the wild type strain.

C. acetobutylicum possesses two homologous *adhE* genes, *adhE1* and *adhE2*, coding for bifunctional aldehyde/alcohol dehydrogenases which have been proposed to be responsible for butanol production in solventogenic and alcohologenic cultures, respectively. These roles were confirmed by the study of the Δ*adhE1* and Δ*adhE2* mutants but in addition AdhE2 was shown to partly replace AdhE1 under solventogenesis in Δ*adhE1*, demonstrating the metabolic flexibility of *C. acetobutylicum* in response to genetic alterations of its primary metabolism. In

addition, it is reported in this thesis that many genes revealed the same patterns of change in gene expression in both the *ΔadhE1* and *ΔadhE*2 mutants, some of the genes are linked to regulons like CymR for example. This study would be enhanced by gene sequence analysis of all the genes showing same pattern to find unknown regulon or by the determination of relationship between CymR and *adhE1*/*adhE2* inactivation.

The study of the Δ*ptb-buk* mutant, revealed the production of 2-hydroxy-valerate under acidogenesis and at a lower level under solventogenesis. This compound has never been described to be produced by *C. acetobutylicum*. We proposed as already described in *Serratia marcescens* (Kisumi M, et al, J Biochem. 1976, 79: 1021-1028) that i) pyruvate is converted to 2-keto-valerate using part of the L-leucine pathway (CAC3171-3174, in *C. acetobutylicum*) and ii) LdhA catalyzes the final reduction of 2-keto-valerate to 2-hydroxy-valerate. To demonstrate this hypothetical pathway, double knockout mutants combining Δ*ptb-buk* and Δ*leuA* (CAC3174) or Δ*ldhA* (CAC0267) will have to be constructed and analyzed from a metabolic point of view. In addition, although *buk*/*ptb* inactivated strains were studied by several research groups, the high butanol yield, observed for phosphate limited solventogenic cultures obtained in this thesis was never reported before. The reason for this is due to different fermentation conditions in each study. Traditionally, many studies including *buk*/*ptb* related ones in *C. acetobutylicum* are carried out in batch cultures under excess of all nutrients. The study of Honicke et al. presented continuous culture of a *ptb* muant under solventogenic conditions, however the butanol yield remained unchanged compare to the control strain. Since the chemostat conditions (concentration of the limiting nutrients, dilution rates…) of two aforementioned research groups, were slightly different, it might be the reason for the highly different butanol yields of *buk*/*ptb* mutants. To develop a commercial process for the production of butanol, optimization of fermentation condition should be combined with

metabolically engineered strains.

In conclusion, both the physiological information provided by this study that will help to further metabolically engineer *C. acetobutylicum* and the fermentation medium used for the continuous culture for maximizing the butanol yield should be very helpful for the optimization of commercial process for the production of butanol.

References

Al-Hinai, M.A., A.G. Fast & E.T. Papoutsakis, (2012) Novel system for efficient isolation of Clostridium double-crossover allelic exchange mutants enabling markerless chromosomal gene deletions and DNA integration. *Appl. Environ. Microbiol.* **78**: 8112-8121.

Al-Hinai, M.A., S.W. Jones & E.T. Papoutsakis, (2015) The Clostridium sporulation programs: diversity and preservation of endospore differentiation. *Microbiol. Mol. Biol. Rev.* **79**: 19-37.

Alsaker, K.V. & E.T. Papoutsakis, (2005) Transcriptional program of early sporulation and stationary-phase events in Clostridium acetobutylicum. *J Bacteriol* **187**: 7103-7118.

Alsaker, K.V., C. Paredes & E.T. Papoutsakis, (2010a) Metabolite stress and tolerance in the production of biofuels and chemicals: gene-expression-based systems analysis of butanol, butyrate, and acetate stresses in the anaerobe Clostridium acetobutylicum. *Biotechnol. Bioeng.* **105**: 1131-1147.

Alsaker, K.V., C. Paredes & E.T. Papoutsakis, (2010b) Metabolite stress and tolerance in the production of biofuels and chemicals: gene-expression-based systems analysis of butanol, butyrate, and acetate stresses in the anaerobe Clostridium acetobutylicum. *Biotechnol Bioeng* **105**: 1131-1147.

Amador-Noguez, D., I.A. Brasg, X.J. Feng, N. Roquet & J.D. Rabinowitz, (2011) Metabolome remodeling during the acidogenic-solventogenic transition in Clostridium acetobutylicum. *Appl Environ Microbiol* **77**: 7984-7997.

Amador-Noguez, D., X.J. Feng, J. Fan, N. Roquet, H. Rabitz & J.D. Rabinowitz, (2010) Systems-level metabolic flux profiling elucidates a complete, bifurcated tricarboxylic acid cycle in Clostridium acetobutylicum. *J Bacteriol* **192**: 4452-4461.

Apfel, H., (2012) Salmonella marker vaccine. In.: Google Patents, pp.

Atsumi, S., T. Hanai & J.C. Liao, (2008) Non-fermentative pathways for synthesis of branched-chain higher alcohols as biofuels. *Nature* **451**: 86-89.

Atsumi, S. & J.C. Liao, (2008a) Metabolic engineering for advanced biofuels production from Escherichia coli. *Curr Opin Biotechnol* **19**: 414-419.

Atsumi, S. & J.C. Liao, (2008b) Metabolic engineering for advanced biofuels production from Escherichia coli. *Curr. Opin. Biotechnol.* **19**: 414-419.

Au, J., J. Choi, S.W. Jones, K.P. Venkataramanan & M.R. Antoniewicz, (2014) Parallel labeling experiments validate Clostridium acetobutylicum metabolic network model for C metabolic flux analysis. *Metab Eng* **26C**: 23-33.

Bahl, H., W. Andersch & G. Gottschalk, (1982a) Continuous production of acetone and butanol by Clostridium acetobutylicum in a two-stage phosphate limited chemostat. *Eur. J. Appl. Microbiol. Biotechnol.* **15**: 201-205.

Bahl, H., W. Andersch & G. Gottschalk, (1982b) Continuous production of acetone and butanol by Clostridium acetobutylicum in a two-stage phosphate limited chemostat. *European journal of applied microbiology and biotechnology* **15**: 201-205.

Borodina, I., P. Krabben & J. Nielsen, (2005) Genome-scale analysis of Streptomyces coelicolor A3(2) metabolism. *Genome Res* **15**: 820-829.

Boynton, Z.L., G.N. Bennet & F.B. Rudolph, (1996) Cloning, sequencing, and expression of clustered genes encoding beta-hydroxybutyryl-coenzyme A (CoA) dehydrogenase, crotonase, and butyryl-CoA dehydrogenase from Clostridium acetobutylicum ATCC 824. *J Bacteriol* **178**: 3015-3024.

Breitling, R., D. Vitkup & M.P. Barrett, (2008) New surveyor tools for charting microbial

metabolic maps. *Nat Rev Microbiol* **6**: 156-161.
Bremer, H. & P.P. Dennis, (1996) Modulation of chemical composition and other parameters of the cell by growth rate. in Escherichia coli and Salmonella typhimurium: cellular and molecular biology, eds Neidhardt F. C., Curtiss III R., Ingraham J. L., Lin E. C. C., Low K. B., Magasanik B., Reznikoff W. S., Riley M., Schaechter M., Umbarger H. E. (American Society for Microbiology, Washington, D.C.) 2nd ed. . pp 1553–1569.
Caspi, R., H. Foerster, C.A. Fulcher, R. Hopkinson, J. Ingraham, P. Kaipa, M. Krummenacker, S. Paley, J. Pick, S.Y. Rhee, C. Tissier, P. Zhang & P.D. Karp, (2006) MetaCyc: a multiorganism database of metabolic pathways and enzymes. *Nucleic Acids Res* **34**: D511-516.
Cooksley, C.M., Y. Zhang, H. Wang, S. Redl, K. Winzer & N.P. Minton, (2012) Targeted mutagenesis of the Clostridium acetobutylicum acetone-butanol-ethanol fermentation pathway. *Metab Eng* **14**: 630-641.
Cornillot, E., C. Croux & P. Soucaille, (1997a) Physical and genetic map of the Clostridium acetobutylicum ATCC 824 chromosome. *Journal of bacteriology* **179**: 7426-7434.
Cornillot, E., R.V. Nair, E.T. Papoutsakis & P. Soucaille, (1997b) The genes for butanol and acetone formation in Clostridium acetobutylicum ATCC 824 reside on a large plasmid whose loss leads to degeneration of the strain. *J Bacteriol* **179**: 5442-5447.
Cornillot, E. & P. Soucaille, (1996) Solvent-forming genes in clostridia. *Nature* **380**: 489-489.
Covert, M.W., C.H. Schilling & B. Palsson, (2001) Regulation of gene expression in flux balance models of metabolism. *J Theor Biol* **213**: 73-88.
Croux, C., R. Figge & P. Soucaille, (2012) Process for chromosomal integration and DNA sequence replacement in clostridia. In.: Google Patents, pp.
Croux, C., N.P.T. Nguyen, J. Lee, C. Raynaud, F. Saint-Prix, M. Gonzalez-Pajuelo, I. Meynial-Salles & P. Soucaille, (2016) Construction of a restriction-less, marker-less mutant useful for functional genomic and metabolic engineering of the biofuel producer Clostridium acetobutylicum. *Biotechnology for Biofuel* **9**: 21.
Dürre, P., (2004) *Handbook on clostridia*. CRC Press.
Dürre, P., (2007) Biobutanol: an attractive biofuel. *Biotechnology Journal* **2**: 1525-1534.
Dürre, P., (2008) Fermentative butanol production. *Annals of the New York Academy of Sciences* **1125**: 353-362.
Dürre, P., (2011) Fermentative production of butanol—the academic perspective. *Current opinion in biotechnology* **22**: 331-336.
Dürre, P., A. Kuhn, M. Gottwald & G. Gottschalk, (1987) Enzymatic investigations on butanol dehydrogenase and butyraldehyde dehydrogenase in extracts of Clostridium acetobutylicum. *Applied microbiology and biotechnology* **26**: 268-272.
Dash, S., T.J. Mueller, K.P. Venkataramanan, E.T. Papoutsakis & C.D. Maranas, (2014) Capturing the response of Clostridium acetobutylicum to chemical stressors using a regulated genome-scale metabolic model. *Biotechnol Biofuels* **7**: 144.
Desai, R.P. & E.T. Papoutsakis, (1999) Antisense RNA strategies for metabolic engineering of Clostridium acetobutylicum. *Appl Environ Microbiol* **65**: 936-945.
Dingman, D.W. & A.L. Sonenshein, (1987) Purification of aconitase from Bacillus subtilis and correlation of its N-terminal amino acid sequence with the sequence of the citB gene. *J Bacteriol* **169**: 3062-3067.
Durre, P., (2007) Biobutanol: an attractive biofuel. *Biotechnol J* **2**: 1525-1534.
Dusseaux, S., C. Croux, P. Soucaille & I. Meynial-Salles, (2013) Metabolic engineering of Clostridium acetobutylicum ATCC 824 for the high-yield production of a biofuel composed of an isopropanol/butanol/ethanol mixture. *Metab Eng* **18**: 1-8.
Edwards, J.S., R.U. Ibarra & B.O. Palsson, (2001) In silico predictions of Escherichia coli

metabolic capabilities are consistent with experimental data. *Nat Biotechnol* **19**: 125-130.
Ezeji, T.C., N. Qureshi & H.P. Blaschek, (2007) Bioproduction of butanol from biomass: from genes to bioreactors. *Curr Opin Biotechnol* **18**: 220-227.
Fawcett, P., P. Eichenberger, R. Losick & P. Youngman, (2000) The transcriptional profile of early to middle sporulation in Bacillus subtilis. *Proc. Natl. Acad. Sci. U. S. A.* **97**: 8063-8068.
Feist, A.M., C.S. Henry, J.L. Reed, M. Krummenacker, A.R. Joyce, P.D. Karp, L.J. Broadbelt, V. Hatzimanikatis & B.O. Palsson, (2007) A genome-scale metabolic reconstruction for Escherichia coli K-12 MG1655 that accounts for 1260 ORFs and thermodynamic information. *Mol Syst Biol* **3**: 121.
Ferras, E., M. Minier & G. Goma, (1986) Acetonobutylic fermentation: improvement of performances by coupling continuous fermentation and ultrafiltration. *Biotechnol Bioeng* **28**: 523-533.
Fischer, R.J., J. Helms & P. Durre, (1993) Cloning, sequencing, and molecular analysis of the sol operon of Clostridium acetobutylicum, a chromosomal locus involved in solventogenesis. *J Bacteriol* **175**: 6959-6969.
Fontaine, L., I. Meynial-Salles, L. Girbal, X. Yang, C. Croux & P. Soucaille, (2002a) Molecular characterization and transcriptional analysis of adhE2, the gene encoding the NADH-dependent aldehyde/alcohol dehydrogenase responsible for butanol production in alcohologenic cultures of Clostridium acetobutylicum ATCC 824. *J Bacteriol* **184**: 821-830.
Fontaine, L., I. Meynial-Salles, L. Girbal, X. Yang, C. Croux & P. Soucaille, (2002b) Molecular characterization and transcriptional analysis of adhE2, the gene encoding the NADH-dependent aldehyde/alcohol dehydrogenase responsible for butanol production in alcohologenic cultures of Clostridium acetobutylicum ATCC 824. *J. Bacteriol.* **184**: 821-830.
Foster, M.W., L.D. Morrison, J.L. Todd, L.D. Snyder, J.W. Thompson, E.J. Soderblom, K. Plonk, K.J. Weinhold, R. Townsend, A. Minnich & M.A. Moseley, (2015) Quantitative proteomics of bronchoalveolar lavage fluid in idiopathic pulmonary fibrosis. *J Proteome Res* **14**: 1238-1249.
Girbal, L., (1994) Etudes biochimique et physiologique de la production de solvants chez Clostridium acetobutylicum. In., pp.
Girbal, L., C. Croux, I. Vasconcelos & P. Soucaille, (1995a) Regulation of metabolic shifts in Clostridium acetobutylicum ATCC 824. *FEMS Microbiology Reviews* **17**: 287-297.
Girbal, L. & P. Soucaille, (1994a) Regulation of Clostridium acetobutylicum metabolism as revealed by mixed-substrate steady-state continuous cultures: role of NADH/NAD ratio and ATP pool. *J. Bacteriol.* **176**: 6433-6438.
Girbal, L. & P. Soucaille, (1994b) Regulation of Clostridium acetobutylicum metabolism as revealed by mixed-substrate steady-state continuous cultures: role of NADH/NAD ratio and ATP pool. *J Bacteriol* **176**: 6433-6438.
Girbal, L. & P. Soucaille, (1998a) Regulation of solvent production in Clostridium acetobutylicum. *Trends Biotechnol.* **16**: 11-16.
Girbal, L. & P. Soucaille, (1998b) Regulation of solvent production in Clostridium acetobutylicum. *Trends in Biotechnology* **16**: 11-16.
Girbal, L., I. Vasconcelos, S. Saint-Amans & P. Soucaille, (1995b) How neutral red modified carbon and electron flow in Clostridium acetobutylicum grown in chemostat culture at neutral pH. *FEMS Microbiol. Rev.* **16**: 151-162.
Girbal, L., I. Vasconcelos, S. Saint-Amans & P. Soucaille, (1995c) How neutral red modified

carbon and electron flow in Clostridium acetobutylicum grown in chemostat culture at neutral pH. *FEMS microbiology reviews* **16**: 151-162.

Girbal, L., I. Vasconcelos, S. Saint-Amans & P. Soucaille, (1995d) How neutral red modified carbon and electron flow in Clostridium acetobutylicum grown in chemostat culture at neutral pH. *FEMS Microbiology Reviews* **16**: 151-162.

Girbal, L., I. Vasconcelos, S. Saintamans & P. Soucaille, (1995e) How Neutral Red Modified Carbon and Electron Flow in *Clostridium acetobutylicum* Grown in Chemostat Culture at Neutral pH. *FEMS Microbiology Reviews* **16**: 151-162.

Girbal, L., I. Vasconcelos & P. Soucaille, (1994a) Transmembrane pH of Clostridium acetobutylicum is inverted (more acidic inside) when the in vivo activity of hydrogenase is decreased. *J Bacteriol* **176**: 6146-6147.

Girbal, L., I. Vasconcelos & P. Soucaille, (1994b) Transmembrane pH of Clostridium acetobutylicum is inverted (more acidic inside) when the in vivo activity of hydrogenase is decreased. *J. Bacteriol.* **176**: 6146-6147.

Girbal, L., G. von Abendroth, M. Winkler, P.M. Benton, I. Meynial-Salles, C. Croux, J.W. Peters, T. Happe & P. Soucaille, (2005) Homologous and heterologous overexpression in Clostridium acetobutylicum and characterization of purified clostridial and algal Fe-only hydrogenases with high specific activities. *Appl Environ Microbiol* **71**: 2777-2781.

Gorwa, M.F., C. Croux & P. Soucaille, (1996) Molecular characterization and transcriptional analysis of the putative hydrogenase gene of Clostridium acetobutylicum ATCC 824. *J Bacteriol* **178**: 2668-2675.

Green, E.M. & G.N. Bennett, (1996) Inactivation of an aldehyde/alcohol dehydrogenase gene from Clostridium acetobutylicum ATCC 824. *Appl Biochem Biotechnol* **57-58**: 213-221.

Green, E.M., Z.L. Boynton, L.M. Harris, F.B. Rudolph, E.T. Papoutsakis & G.N. Bennett, (1996) Genetic manipulation of acid formation pathways by gene inactivation in Clostridium acetobutylicum ATCC 824. *Microbiology* **142 (Pt 8)**: 2079-2086.

Grimmler, C., C. Held, W. Liebl & A. Ehrenreich, (2010) Transcriptional analysis of catabolite repression in Clostridium acetobutylicum growing on mixtures of D-glucose and D-xylose. *J Biotechnol* **150**: 315-323.

Grimmler, C., H. Janssen, D. Krausse, R.J. Fischer, H. Bahl, P. Durre, W. Liebl & A. Ehrenreich, (2011a) Genome-wide gene expression analysis of the switch between acidogenesis and solventogenesis in continuous cultures of Clostridium acetobutylicum. *J Mol Microbiol Biotechnol* **20**: 1-15.

Grimmler, C., H. Janssen, D. Krauβe, R.-J. Fischer, H. Bahl, P. Dürre, W. Liebl & A. Ehrenreich, (2011b) Genome-wide gene expression analysis of the switch between acidogenesis and solventogenesis in continuous cultures of Clostridium acetobutylicum. *J. Mol. Microbiol. Biotechnol.* **20**: 1-15.

Grimmler, C., H. Janssen, D. Krauβe, R.-J. Fischer, H. Bahl, P. Dürre, W. Liebl & A. Ehrenreich, (2011c) Genome-wide gene expression analysis of the switch between acidogenesis and solventogenesis in continuous cultures of Clostridium acetobutylicum. *Journal of molecular microbiology and biotechnology* **20**: 1-15.

Guerrini, O., B. Burlat, C. Leger, B. Guigliarelli, P. Soucaille & L. Girbal, (2008) Characterization of two 2[4Fe4S] ferredoxins from Clostridium acetobutylicum. *Curr Microbiol* **56**: 261-267.

Hönicke, D., H. Janssen, C. Grimmler, A. Ehrenreich & T. Lütke-Eversloh, (2012) Global transcriptional changes of< i> Clostridium acetobutylicum</i> cultures with increased butanol: acetone ratios. *New biotechnology* **29**: 485-493.

Hanson, R. & J. Phillips, (1981) Chemical composition. *Manual of methods for general*

bacteriology. American Society for Microbiology, Washington, DC: 328-364.
Harris, L.M., R.P. Desai, N.E. Welker & E.T. Papoutsakis, (2000a) Characterization of recombinant strains of the Clostridium acetobutylicum butyrate kinase inactivation mutant: need for new phenomenological models for solventogenesis and butanol inhibition? *Biotechnol. Bioeng.* **67**: 1-11.
Harris, L.M., R.P. Desai, N.E. Welker & E.T. Papoutsakis, (2000b) Characterization of recombinant strains of the Clostridium acetobutylicum butyrate kinase inactivation mutant: need for new phenomenological models for solventogenesis and butanol inhibition? *Biotechnol Bioeng* **67**: 1-11.
Harris, L.M., N.E. Welker & E.T. Papoutsakis, (2002) Northern, morphological, and fermentation analysis of spo0A inactivation and overexpression in Clostridium acetobutylicum ATCC 824. *J Bacteriol* **184**: 3586-3597.
Haus, S., S. Jabbari, T. Millat, H. Janssen, R.-J. Fischer, H. Bahl, J.R. King & O. Wolkenhauer, (2011) A systems biology approach to investigate the effect of pH-induced gene regulation on solvent production by Clostridium acetobutylicum in continuous culture. *BMC systems biology* **5**: 10.
Heap, J.T., O.J. Pennington, S.T. Cartman, G.P. Carter & N.P. Minton, (2007a) The ClosTron: a universal gene knock-out system for the genus Clostridium. *J. Microbiol. Methods* **70**: 452-464.
Heap, J.T., O.J. Pennington, S.T. Cartman, G.P. Carter & N.P. Minton, (2007b) The ClosTron: a universal gene knock-out system for the genus Clostridium. *J Microbiol Methods* **70**: 452-464.
Heinemann, M., A. Kummel, R. Ruinatscha & S. Panke, (2005) In silico genome-scale reconstruction and validation of the Staphylococcus aureus metabolic network. *Biotechnol Bioeng* **92**: 850-864.
Henry, C.S., L.J. Broadbelt & V. Hatzimanikatis, (2007) Thermodynamics-based metabolic flux analysis. *Biophys J* **92**: 1792-1805.
Hillmann, F., C. Doring, O. Riebe, A. Ehrenreich, R.J. Fischer & H. Bahl, (2009) The role of PerR in O2-affected gene expression of Clostridium acetobutylicum. *J Bacteriol* **191**: 6082-6093.
Honicke, D., T. Lutke-Eversloh, Z. Liu, D. Lehmann, W. Liebl & A. Ehrenreich, (2014a) Chemostat cultivation and transcriptional analyses of Clostridium acetobutylicum mutants with defects in the acid and acetone biosynthetic pathways. *Appl Microbiol Biotechnol* **98**: 9777-9794.
Honicke, D., T. Lutke-Eversloh, Z. Liu, D. Lehmann, W. Liebl & A. Ehrenreich, (2014b) Chemostat cultivation and transcriptional analyses of Clostridium acetobutylicum mutants with defects in the acid and acetone biosynthetic pathways. *Appl. Microbiol. Biotechnol.* **98**: 9777-9794.
Hou, S., S.W. Jones, L.H. Choe, E.T. Papoutsakis & K.H. Lee, (2013) Workflow for quantitative proteomic analysis of Clostridium acetobutylicum ATCC 824 using iTRAQ tags. *Methods* **61**: 269-276.
Hu, K., M. Zhao, T. Zhang, M. Zha, C. Zhong, Y. Jiang & J. Ding, (2013) Structures of trans-2-enoyl-CoA reductases from Clostridium acetobutylicum and Treponema denticola: insights into the substrate specificity and the catalytic mechanism. *Biochem J* **449**: 79-89.
Huang, K.X., S. Huang, F.B. Rudolph & G.N. Bennett, (2000) Identification and characterization of a second butyrate kinase from Clostridium acetobutylicum ATCC 824. *J. Mol. Microbiol. Biotechnol.* **2**: 33-38.
Huang, R., M. Pan, C. Wan, N.P. Shah, X. Tao & H. Wei, (2016) Physiological and

transcriptional responses and cross protection of Lactobacillus plantarum ZDY2013 under acid stress. *J. Dairy Sci.* **99**: 1002-1010.

Iddar, A., F. Valverde, A. Serrano & A. Soukri, (2002) Expression, purification, and characterization of recombinant nonphosphorylating NADP-dependent glyceraldehyde-3-phosphate dehydrogenase from Clostridium acetobutylicum. *Protein Expr Purif* **25**: 519-526.

Ingham, C.J., M. Beerthuyzen & J. van Hylckama Vlieg, (2008) Population heterogeneity of Lactobacillus plantarum WCFS1 microcolonies in response to and recovery from acid stress. *Appl. Environ. Microbiol.* **74**: 7750-7758.

Jang, Y.S., M.J. Han, J. Lee, J.A. Im, Y.H. Lee, E.T. Papoutsakis, G. Bennett & S.Y. Lee, (2014a) Proteomic analyses of the phase transition from acidogenesis to solventogenesis using solventogenic and non-solventogenic Clostridium acetobutylicum strains. *Appl Microbiol Biotechnol* **98**: 5105-5115.

Jang, Y.S., J.A. Im, S.Y. Choi, J.I. Lee & S.Y. Lee, (2014b) Metabolic engineering of Clostridium acetobutylicum for butyric acid production with high butyric acid selectivity. *Metab Eng* **23**: 165-174.

Janssen, H., C. Doring, A. Ehrenreich, B. Voigt, M. Hecker, H. Bahl & R.J. Fischer, (2010a) A proteomic and transcriptional view of acidogenic and solventogenic steady-state cells of Clostridium acetobutylicum in a chemostat culture. *Appl Microbiol Biotechnol* **87**: 2209-2226.

Janssen, H., C. Doring, A. Ehrenreich, B. Voigt, M. Hecker, H. Bahl & R.J. Fischer, (2010b) A proteomic and transcriptional view of acidogenic and solventogenic steady-state cells of Clostridium acetobutylicum in a chemostat culture. *Appl. Microbiol. Biotechnol.* **87**: 2209-2226.

Janssen, H., C. Grimmler, A. Ehrenreich, H. Bahl & R.J. Fischer, (2012a) A transcriptional study of acidogenic chemostat cells of Clostridium acetobutylicum--solvent stress caused by a transient n-butanol pulse. *J Biotechnol* **161**: 354-365.

Janssen, H., C. Grimmler, A. Ehrenreich, H. Bahl & R.J. Fischer, (2012b) A transcriptional study of acidogenic chemostat cells of Clostridium acetobutylicum--solvent stress caused by a transient n-butanol pulse. *J. Biotechnol.* **161**: 354-365.

Jones, D.T., (2001) Applied acetone–butanol fermentation. *Clostridia: biotechnology and medical applications*: 125-168.

Jones, D.T., A. van der Westhuizen, S. Long, E.R. Allcock, S.J. Reid & D.R. Woods, (1982) Solvent Production and Morphological Changes in Clostridium acetobutylicum. *Appl Environ Microbiol* **43**: 1434-1439.

Jones, D.T. & D.R. Woods, (1986a) Acetone-butanol fermentation revisited. *Microbiological reviews* **50**: 484.

Jones, D.T. & D.R. Woods, (1986b) Acetone-butanol fermentation revisited. *Microbiol Rev* **50**: 484-524.

Jones, S.W., C.J. Paredes, B. Tracy, N. Cheng, R. Sillers, R.S. Senger & E.T. Papoutsakis, (2008a) The transcriptional program underlying the physiology of clostridial sporulation. *Genome Biol* **9**: R114.

Jones, S.W., C.J. Paredes, B. Tracy, N. Cheng, R. Sillers, R.S. Senger & E.T. Papoutsakis, (2008b) The transcriptional program underlying the physiology of clostridial sporulation. *Genome Biol.* **9**: R114.

Jones, S.W., B.P. Tracy, S.M. Gaida & E.T. Papoutsakis, (2011) Inactivation of sigmaF in Clostridium acetobutylicum ATCC 824 blocks sporulation prior to asymmetric division and abolishes sigmaE and sigmaG protein expression but does not block solvent formation. *J Bacteriol* **193**: 2429-2440.

Kanehisa, M., S. Goto, M. Hattori, K.F. Aoki-Kinoshita, M. Itoh, S. Kawashima, T. Katayama, M. Araki & M. Hirakawa, (2006) From genomics to chemical genomics: new developments in KEGG. *Nucleic Acids Res* **34**: D354-357.

Karberg, M., H. Guo, J. Zhong, R. Coon, J. Perutka & A.M. Lambowitz, (2001) Group II introns as controllable gene targeting vectors for genetic manipulation of bacteria. *Nature biotechnology* **19**: 1162-1167.

Kisumi, M., M. Sugiura, J. Kato & I. Chibata, (1976) L-Norvaline and L-homoisoleucine formation by Serratia marcescens. *J. Biochem.* **79**: 1021-1028.

Lautier, T., P. Ezanno, C. Baffert, V. Fourmond, L. Cournac, J.C. Fontecilla-Camps, P. Soucaille, P. Bertrand, I. Meynial-Salles & C. Leger, (2011) The quest for a functional substrate access tunnel in FeFe hydrogenase. *Faraday Discuss* **148**: 385-407; discussion 421-341.

Leang, C., T. Ueki, K.P. Nevin & D.R. Lovley, (2013) A genetic system for Clostridium ljungdahlii: a chassis for autotrophic production of biocommodities and a model homoacetogen. *Appl Environ Microbiol* **79**: 1102-1109.

Lee, J., Y.S. Jang, S.J. Choi, J.A. Im, H. Song, J.H. Cho, Y. Seung do, E.T. Papoutsakis, G.N. Bennett & S.Y. Lee, (2012) Metabolic engineering of Clostridium acetobutylicum ATCC 824 for isopropanol-butanol-ethanol fermentation. *Appl Environ Microbiol* **78**: 1416-1423.

Lee, J., H. Yun, A.M. Feist, B.O. Palsson & S.Y. Lee, (2008a) Genome-scale reconstruction and in silico analysis of the Clostridium acetobutylicum ATCC 824 metabolic network. *Appl Microbiol Biotechnol* **80**: 849-862.

Lee, J.Y., Y.S. Jang, J. Lee, E.T. Papoutsakis & S.Y. Lee, (2009) Metabolic engineering of Clostridium acetobutylicum M5 for highly selective butanol production. *Biotechnol J* **4**: 1432-1440.

Lee, S.Y., J.H. Park, S.H. Jang, L.K. Nielsen, J. Kim & K.S. Jung, (2008b) Fermentative butanol production by Clostridia. *Biotechnol Bioeng* **101**: 209-228.

Lehmann, D., D. Honicke, A. Ehrenreich, M. Schmidt, D. Weuster-Botz, H. Bahl & T. Lutke-Eversloh, (2012a) Modifying the product pattern of Clostridium acetobutylicum: physiological effects of disrupting the acetate and acetone formation pathways. *Appl Microbiol Biotechnol* **94**: 743-754.

Lehmann, D. & T. Lutke-Eversloh, (2011) Switching Clostridium acetobutylicum to an ethanol producer by disruption of the butyrate/butanol fermentative pathway. *Metab Eng* **13**: 464-473.

Lehmann, D., N. Radomski & T. Lütke-Eversloh, (2012b) New insights into the butyric acid metabolism of Clostridium acetobutylicum. *Appl. Microbiol. Biotechnol.* **96**: 1325-1339.

Li, F., C.H. Hagemeier, H. Seedorf, G. Gottschalk & R.K. Thauer, (2007) Re-citrate synthase from Clostridium kluyveri is phylogenetically related to homocitrate synthase and isopropylmalate synthase rather than to Si-citrate synthase. *J Bacteriol* **189**: 4299-4304.

Li, F., J. Hinderberger, H. Seedorf, J. Zhang, W. Buckel & R.K. Thauer, (2008) Coupled ferredoxin and crotonyl coenzyme A (CoA) reduction with NADH catalyzed by the butyryl-CoA dehydrogenase/Etf complex from Clostridium kluyveri. *J Bacteriol* **190**: 843-850.

Lutke-Eversloh, T., (2014a) Application of new metabolic engineering tools for Clostridium acetobutylicum. *Appl. Microbiol. Biotechnol.* **98**: 5823-5837.

Lutke-Eversloh, T., (2014b) Application of new metabolic engineering tools for Clostridium acetobutylicum. *Appl Microbiol Biotechnol* **98**: 5823-5837.

Lutke-Eversloh, T. & H. Bahl, (2011a) Metabolic engineering of Clostridium acetobutylicum:

recent advances to improve butanol production. *Curr Opin Biotechnol* **22**: 634-647.
Lutke-Eversloh, T. & H. Bahl, (2011b) Metabolic engineering of Clostridium acetobutylicum: recent advances to improve butanol production. *Curr. Opin. Biotechnol.* **22**: 634-647.
Magdeldin, S., S. Enany, Y. Yoshida, B. Xu, Y. Zhang, Z. Zureena, I. Lokamani, E. Yaoita & T. Yamamoto, (2014) Basics and recent advances of two dimensional- polyacrylamide gel electrophoresis. *Clin Proteomics* **11**: 16.
Mao, S., Y. Luo, G. Bao, Y. Zhang, Y. Li & Y. Ma, (2011) Comparative analysis on the membrane proteome of Clostridium acetobutylicum wild type strain and its butanol-tolerant mutant. *Molecular BioSystems* **7**: 1660-1677.
Mao, S., Y. Luo, T. Zhang, J. Li, G. Bao, Y. Zhu, Z. Chen, Y. Zhang, Y. Li & Y. Ma, (2010) Proteome reference map and comparative proteomic analysis between a wild type Clostridium acetobutylicum DSM 1731 and its mutant with enhanced butanol tolerance and butanol yield. *Journal of proteome research* **9**: 3046-3061.
McAnulty, M.J., J.Y. Yen, B.G. Freedman & R.S. Senger, (2012) Genome-scale modeling using flux ratio constraints to enable metabolic engineering of clostridial metabolism in silico. *BMC Syst Biol* **6**: 42.
McCoy, E., E. Fred, W. Peterson & E. Hastings, (1926) A Cultural Study of the Acetone Butyl Alcohol Organism One Plate. *Journal of Infectious Diseases* **39**: 457-483.
Mermelstein, L.D. & E.T. Papoutsakis, (1993) In vivo methylation in Escherichia coli by the Bacillus subtilis phage phi 3T I methyltransferase to protect plasmids from restriction upon transformation of Clostridium acetobutylicum ATCC 824. *Appl Environ Microbiol* **59**: 1077-1081.
Miller, J.A., V. Menon, J. Goldy, A. Kaykas, C.K. Lee, K.A. Smith, E.H. Shen, J.W. Phillips, E.S. Lein & M.J. Hawrylycz, (2014) Improving reliability and absolute quantification of human brain microarray data by filtering and scaling probes using RNA-Seq. *BMC Genomics* **15**: 154.
Monot, F., J.R. Martin, H. Petitdemange & R. Gay, (1982) Acetone and Butanol Production by Clostridium acetobutylicum in a Synthetic Medium. *Appl Environ Microbiol* **44**: 1318-1324.
Nölling, J., G. Breton, M.V. Omelchenko, K.S. Makarova, Q. Zeng, R. Gibson, H.M. Lee, J. Dubois, D. Qiu & J. Hitti, (2001) Genome sequence and comparative analysis of the solvent-producing bacterium Clostridium acetobutylicum. *Journal of bacteriology* **183**: 4823-4838.
Nair, R.V., G.N. Bennett & E.T. Papoutsakis, (1994a) Molecular characterization of an aldehyde/alcohol dehydrogenase gene from Clostridium acetobutylicum ATCC 824. *J Bacteriol* **176**: 871-885.
Nair, R.V., G.N. Bennett & E.T. Papoutsakis, (1994b) Molecular characterization of an aldehyde/alcohol dehydrogenase gene from Clostridium acetobutylicum ATCC 824. *J. Bacteriol.* **176**: 871-885.
Nair, R.V., E.M. Green, D.E. Watson, G.N. Bennett & E.T. Papoutsakis, (1999) Regulation of the sol locus genes for butanol and acetone formation in Clostridium acetobutylicum ATCC 824 by a putative transcriptional repressor. *J Bacteriol* **181**: 319-330.
Neidhardt, F.C. & H.E. Umbarger, (1996) *Chemical composition of E. coli. in Escherichia coli and Salmonella typhimurium: cellular and molecular biology, eds Neidhardt F. C., Curtiss III R., Ingraham J. L., Lin E. C. C., Low K. B., Magasanik B., Reznikoff W. S., Riley M., Schaechter M., Umbarger H. E. (American Society for Microbiology, Washington, D.C.) 2nd ed. pp 13-16.* .
Nelson, D.L., A.L. Lehninger & M.M. Cox, (2008) *Lehninger principles of biochemistry*. Macmillan.

Ni, Y. & Z. Sun, (2009) Recent progress on industrial fermentative production of acetone-butanol-ethanol by Clostridium acetobutylicum in China. *Appl Microbiol Biotechnol* **83**: 415-423.

Nolling, J., G. Breton, M.V. Omelchenko, K.S. Makarova, Q. Zeng, R. Gibson, H.M. Lee, J. Dubois, D. Qiu, J. Hitti, Y.I. Wolf, R.L. Tatusov, F. Sabathe, L. Doucette-Stamm, P. Soucaille, M.J. Daly, G.N. Bennett, E.V. Koonin & D.R. Smith, (2001) Genome sequence and comparative analysis of the solvent-producing bacterium Clostridium acetobutylicum. *J Bacteriol* **183**: 4823-4838.

Novick, A. & L. Szilard, (1950) Experiments with the Chemostat on spontaneous mutations of bacteria. *Proc Natl Acad Sci U S A* **36**: 708-719.

Oh, Y.-K., B.O. Palsson, S.M. Park, C.H. Schilling & R. Mahadevan, (2007) Genome-scale reconstruction of metabolic network in Bacillus subtilis based on high-throughput phenotyping and gene essentiality data. *Journal of Biological Chemistry* **282**: 28791-28799.

Orth, J.D., I. Thiele & B.O. Palsson, (2010) What is flux balance analysis? *Nat Biotechnol* **28**: 245-248.

Papoutsakis, E.T., (2008) Engineering solventogenic clostridia. *Curr Opin Biotechnol* **19**: 420-429.

Paredes, C.J., I. Rigoutsos & E.T. Papoutsakis, (2004) Transcriptional organization of the Clostridium acetobutylicum genome. *Nucleic Acids Res* **32**: 1973-1981.

Paredes, C.J., R.S. Senger, I.S. Spath, J.R. Borden, R. Sillers & E.T. Papoutsakis, (2007) A general framework for designing and validating oligomer-based DNA microarrays and its application to Clostridium acetobutylicum. *Appl Environ Microbiol* **73**: 4631-4638.

Pasteur, L., (1862) Quelques résultats nouveaux relatifs aux fermentations acétique et butyrique. *Bull Soc Chim Paris*: 52-53.

Peguin, S. & P. Soucaille, (1995a) Modulation of Carbon and Electron Flow in Clostridium acetobutylicum by Iron Limitation and Methyl Viologen Addition. *Appl Environ Microbiol* **61**: 403-405.

Peguin, S. & P. Soucaille, (1995b) Modulation of carbon and electron flow in Clostridium acetobutylicum by iron limitation and methyl viologen addition. *Appl. Environ. Microbiol.* **61**: 403-405.

Peterson, G.L., (1983) Determination of total protein. *Methods Enzymol* **91**: 95-119.

Pieterse, B., R.J. Leer, F.H. Schuren & M.J. van der Werf, (2005) Unravelling the multiple effects of lactic acid stress on Lactobacillus plantarum by transcription profiling. *Microbiology* **151**: 3881-3894.

Pramanik, J. & J.D. Keasling, (1997) Stoichiometric model of Escherichia coli metabolism: incorporation of growth-rate dependent biomass composition and mechanistic energy requirements. *Biotechnol Bioeng* **56**: 398-421.

Rao, G. & R. Mutharasan, (1987) Altered Electron Flow in Continuous Cultures of Clostridium acetobutylicum Induced by Viologen Dyes. *Appl Environ Microbiol* **53**: 1232-1235.

Ravagnani, A., K.C. Jennert, E. Steiner, R. Grunberg, J.R. Jefferies, S.R. Wilkinson, D.I. Young, E.C. Tidswell, D.P. Brown, P. Youngman, J.G. Morris & M. Young, (2000a) Spo0A directly controls the switch from acid to solvent production in solvent-forming clostridia. *Mol. Microbiol.* **37**: 1172-1185.

Ravagnani, A., K.C. Jennert, E. Steiner, R. Grunberg, J.R. Jefferies, S.R. Wilkinson, D.I. Young, E.C. Tidswell, D.P. Brown, P. Youngman, J.G. Morris & M. Young, (2000b) Spo0A directly controls the switch from acid to solvent production in solvent-forming clostridia. *Mol Microbiol* **37**: 1172-1185.

Roos, J.W., J.K. McLaughlin & E.T. Papoutsakis, (1985) The effect of pH on nitrogen supply,

cell lysis, and solvent production in fermentations of Clostridium acetobutylicum. *Biotechnol Bioeng* **27**: 681-694.
Sabathé, F., A. Bélaïch & P. Soucaille, (2002) Characterization of the cellulolytic complex (cellulosome) of Clostridium acetobutylicum. *FEMS microbiology letters* **217**: 15-22.
Sakamoto, N., A.M. Kotre & M.A. Savageau, (1975) Glutamate dehydrogenase from Escherichia coli: purification and properties. *J Bacteriol* **124**: 775-783.
Sauer, U. & P. Dürre, (1995) Differential induction of genes related to solvent formation during the shift from acidogenesis to solventogenesis in continuous culture of Clostridium acetobutylicum. *FEMS microbiology letters* **125**: 115-120.
Schaffer, S., N. Isci, B. Zickner & P. Durre, (2002) Changes in protein synthesis and identification of proteins specifically induced during solventogenesis in Clostridium acetobutylicum. *Electrophoresis* **23**: 110-121.
Schardinger, F., (1905) Bacillus macerans, ein Aceton bildender Rottebacillus. *Zbl Bakteriol Parasitenkd Infektionskr Hyg Abt II* **14**: 772-781.
Schilling, C.H., J.S. Edwards & B.O. Palsson, (1999) Toward metabolic phenomics: analysis of genomic data using flux balances. *Biotechnol Prog* **15**: 288-295.
Schmidt, C.N. & L. Jervis, (1980) Affinity purification of glutamate synthase from Escherichia coli. *Anal Biochem* **104**: 127-129.
Schreiber, W. & P. Durre, (1999) The glyceraldehyde-3-phosphate dehydrogenase of Clostridium acetobutylicum: isolation and purification of the enzyme, and sequencing and localization of the gap gene within a cluster of other glycolytic genes. *Microbiology* **145 (Pt 8)**: 1839-1847.
Schwarz, K., T. Fiedler, R.J. Fischer & H. Bahl, (2007) A Standard Operating Procedure (SOP) for the preparation of intra- and extracellular proteins of Clostridium acetobutylicum for proteome analysis. *J Microbiol Methods* **68**: 396-402.
Schwarz, K.M., W. Kuit, C. Grimmler, A. Ehrenreich & S.W. Kengen, (2012) A transcriptional study of acidogenic chemostat cells of Clostridium acetobutylicum–Cellular behavior in adaptation to n-butanol. *Journal of biotechnology* **161**: 366-377.
Senger, R.S. & E.T. Papoutsakis, (2008a) Genome-scale model for Clostridium acetobutylicum: Part I. Metabolic network resolution and analysis. *Biotechnol Bioeng* **101**: 1036-1052.
Senger, R.S. & E.T. Papoutsakis, (2008b) Genome-scale model for Clostridium acetobutylicum: Part II. Development of specific proton flux states and numerically determined sub-systems. *Biotechnol Bioeng* **101**: 1053-1071.
Servinsky, M.D., J.T. Kiel, N.F. Dupuy & C.J. Sund, (2010) Transcriptional analysis of differential carbohydrate utilization by Clostridium acetobutylicum. *Microbiology* **156**: 3478-3491.
Shao, L., S. Hu, Y. Yang, Y. Gu, J. Chen, W. Jiang & S. Yang, (2007) Targeted gene disruption by use of a group II intron (targetron) vector in Clostridium acetobutylicum. *Cell Res* **17**: 963-965.
Sillers, R., A. Chow, B. Tracy & E.T. Papoutsakis, (2008a) Metabolic engineering of the non-sporulating, non-solventogenic Clostridium acetobutylicum strain M5 to produce butanol without acetone demonstrate the robustness of the acid-formation pathways and the importance of the electron balance. *Metab Eng* **10**: 321-332.
Sillers, R., A. Chow, B. Tracy & E.T. Papoutsakis, (2008b) Metabolic engineering of the non-sporulating, non-solventogenic Clostridium acetobutylicum strain M5 to produce butanol without acetone demonstrate the robustness of the acid-formation pathways and the importance of the electron balance. *Metab. Eng.* **10**: 321-332.
Sivagnanam, K., V.G. Raghavan, M. Shah, R.L. Hettich, N.C. Verberkmoes & M.G. Lefsrud, (2011) Comparative shotgun proteomic analysis of Clostridium acetobutylicum from

butanol fermentation using glucose and xylose. *Proteome Sci* **9**: 66.
Soini, J., C. Falschlehner, C. Liedert, J. Bernhardt, J. Vuoristo & P. Neubauer, (2008) Norvaline is accumulated after a down-shift of oxygen in Escherichia coli W3110. *Microb Cell Fact* **7**: 30.
Soucaille, P., (2008) Process for the biological production of n-butanol with high yield. In.: Google Patents, pp.
Soucaille, P., R. Figge & C. Croux, (2014) Process for chromosomal integration and DNA sequence replacement in clostridia. In., pp. WO/2008/040387.
Steiner, E., A.E. Dago, D.I. Young, J.T. Heap, N.P. Minton, J.A. Hoch & M. Young, (2011) Multiple orphan histidine kinases interact directly with Spo0A to control the initiation of endospore formation in Clostridium acetobutylicum. *Mol. Microbiol.* **80**: 641-654.
Steiner, E., J. Scott, N.P. Minton & K. Winzer, (2012a) An agr quorum sensing system that regulates granulose formation and sporulation in Clostridium acetobutylicum. *Appl Environ Microbiol* **78**: 1113-1122.
Steiner, E., J. Scott, N.P. Minton & K. Winzer, (2012b) An agr quorum sensing system that regulates granulose formation and sporulation in Clostridium acetobutylicum. *Appl. Environ. Microbiol.* **78**: 1113-1122.
Stols, L. & M.I. Donnelly, (1997) Production of succinic acid through overexpression of NAD(+)-dependent malic enzyme in an Escherichia coli mutant. *Appl Environ Microbiol* **63**: 2695-2701.
Storici, F. & C.V. Bruschi, (2000) Involvement of the inverted repeat of the yeast 2-micron plasmid in Flp site-specific and RAD52-dependent homologous recombination. *Mol Gen Genet* **263**: 81-89.
Sullivan, L. & G.N. Bennett, (2006) Proteome analysis and comparison of Clostridium acetobutylicum ATCC 824 and Spo0A strain variants. *J Ind Microbiol Biotechnol* **33**: 298-308.
Sulzenbacher, G., K. Alvarez, R.H. Van Den Heuvel, C. Versluis, S. Spinelli, V. Campanacci, C. Valencia, C. Cambillau, H. Eklund & M. Tegoni, (2004) Crystal structure of E.coli alcohol dehydrogenase YqhD: evidence of a covalently modified NADP coenzyme. *J Mol Biol* **342**: 489-502.
Tan, Y., Z.-Y. Liu, Z. Liu, H.-J. Zheng & F.-L. Li, (2015) Comparative transcriptome analysis between csrA-disruption Clostridium acetobutylicum and its parent strain. *Molecular BioSystems* **11**: 1434-1442.
Tangney, M. & W.J. Mitchell, (2000) Analysis of a catabolic operon for sucrose transport and metabolism in Clostridium acetobutylicum ATCC 824. *J Mol Microbiol Biotechnol* **2**: 71-80.
Teller, J.K., R.J. Smith, M.J. McPherson, P.C. Engel & J.R. Guest, (1992) The glutamate dehydrogenase gene of Clostridium symbiosum. Cloning by polymerase chain reaction, sequence analysis and over-expression in Escherichia coli. *Eur J Biochem* **206**: 151-159.
Thormann, K., L. Feustel, K. Lorenz, S. Nakotte & P. Durre, (2002) Control of butanol formation in Clostridium acetobutylicum by transcriptional activation. *J Bacteriol* **184**: 1966-1973.
Tomas, C.A., K.V. Alsaker, H.P. Bonarius, W.T. Hendriksen, H. Yang, J.A. Beamish, C.J. Paredes & E.T. Papoutsakis, (2003a) DNA array-based transcriptional analysis of asporogenous, nonsolventogenic Clostridium acetobutylicum strains SKO1 and M5. *J Bacteriol* **185**: 4539-4547.
Tomas, C.A., K.V. Alsaker, H.P. Bonarius, W.T. Hendriksen, H. Yang, J.A. Beamish, C.J. Paredes & E.T. Papoutsakis, (2003b) DNA array-based transcriptional analysis of

asporogenous, nonsolventogenic Clostridium acetobutylicum strains SKO1 and M5. *J. Bacteriol.* **185**: 4539-4547.

Tomas, C.A., J. Beamish & E.T. Papoutsakis, (2004) Transcriptional analysis of butanol stress and tolerance in Clostridium acetobutylicum. *J Bacteriol* **186**: 2006-2018.

Tracy, B.P., S.W. Jones & E.T. Papoutsakis, (2011) Inactivation of sigmaE and sigmaG in Clostridium acetobutylicum illuminates their roles in clostridial-cell-form biogenesis, granulose synthesis, solventogenesis, and spore morphogenesis. *J Bacteriol* **193**: 1414-1426.

Tummala, S.B., N.E. Welker & E.T. Papoutsakis, (1999) Development and characterization of a gene expression reporter system for Clostridium acetobutylicum ATCC 824. *Appl Environ Microbiol* **65**: 3793-3799.

Vanoni, M.A., L. Nuzzi, M. Rescigno, G. Zanetti & B. Curti, (1991) The kinetic mechanism of the reactions catalyzed by the glutamate synthase from Azospirillum brasilense. *Eur J Biochem* **202**: 181-189.

Vasconcelos, I., L. Girbal & P. Soucaille, (1994) Regulation of carbon and electron flow in Clostridium acetobutylicum grown in chemostat culture at neutral pH on mixtures of glucose and glycerol. *J Bacteriol* **176**: 1443-1450.

Venkataramanan, K.P., S.W. Jones, K.P. McCormick, S.G. Kunjeti, M.T. Ralston, B.C. Meyers & E.T. Papoutsakis, (2013) The Clostridium small RNome that responds to stress: the paradigm and importance of toxic metabolite stress in C. acetobutylicum. *BMC Genomics* **14**: 849.

Venkataramanan, K.P., L. Min, S. Hou, S.W. Jones, M.T. Ralston, K.H. Lee & E.T. Papoutsakis, (2015) Complex and extensive post-transcriptional regulation revealed by integrative proteomic and transcriptomic analysis of metabolite stress response in Clostridium acetobutylicum. *Biotechnology for biofuels* **8**: 1-29.

Waghmare, S.K., V. Caputo, S. Radovic & C.V. Bruschi, (2003) Specific targeted integration of kanamycin resistance-associated nonselectable DNA in the genome of the yeast Saccharomyces cerevisiae. *Biotechniques* **34**: 1024-1028, 1033.

Walter, K.A., G.N. Bennett & E.T. Papoutsakis, (1992) Molecular characterization of two Clostridium acetobutylicum ATCC 824 butanol dehydrogenase isozyme genes. *J Bacteriol* **174**: 7149-7158.

Walter, K.A., R.V. Nair, J.W. Cary, G.N. Bennett & E.T. Papoutsakis, (1993) Sequence and arrangement of two genes of the butyrate-synthesis pathway of Clostridium acetobutylicum ATCC 824. *Gene* **134**: 107-111.

Wang, P., M. Jin & G. Zhu, (2012) Biochemical and molecular characterization of NAD(+)-dependent isocitrate dehydrogenase from the ethanologenic bacterium Zymomonas mobilis. *FEMS Microbiol Lett* **327**: 134-141.

Wang, Q., K.P. Venkataramanan, H. Huang, E.T. Papoutsakis & C.H. Wu, (2013a) Transcription factors and genetic circuits orchestrating the complex, multilayered response of Clostridium acetobutylicum to butanol and butyrate stress. *BMC Syst Biol* **7**: 120.

Wang, Q., K.P. Venkataramanan, H. Huang, E.T. Papoutsakis & C.H. Wu, (2013b) Transcription factors and genetic circuits orchestrating the complex, multilayered response of Clostridium acetobutylicum to butanol and butyrate stress. *BMC Syst. Biol.* **7**: 120.

Wang, Y., Z.-T. Zhang, S.-O. Seo, K. Choi, T. Lu, Y.-S. Jin & H.P. Blaschek, (2015) Markerless chromosomal gene deletion in Clostridium beijerinckii using CRISPR/Cas9 system. *J. Biotechnol.* **200**: 1-5.

Weizmann, C., (1915) Improvements in the bacterial fermentation of carbohydrates and in

bacterial cultures for the same. *Br. Patent* **4845**.
Welch, R.W., F.B. Rudolph & E.T. Papoutsakis, (1989) Purification and characterization of the NADH-dependent butanol dehydrogenase from Clostridium acetobutylicum (ATCC 824). *Arch Biochem Biophys* **273**: 309-318.
Wiesenborn, D.P., F.B. Rudolph & E.T. Papoutsakis, (1989a) Coenzyme A transferase from Clostridium acetobutylicum ATCC 824 and its role in the uptake of acids. *Appl Environ Microbiol* **55**: 323-329.
Wiesenborn, D.P., F.B. Rudolph & E.T. Papoutsakis, (1989b) Phosphotransbutyrylase from Clostridium acetobutylicum ATCC 824 and its role in acidogenesis. *Appl Environ Microbiol* **55**: 317-322.
Wietzke, M. & H. Bahl, (2012) The redox-sensing protein Rex, a transcriptional regulator of solventogenesis in Clostridium acetobutylicum. *Appl Microbiol Biotechnol* **96**: 749-761.
Yoo, M., G. Bestel-Corre, C. Croux, A. Riviere, I. Meynial-Salles & P. Soucaille, (2015) A Quantitative System-Scale Characterization of the Metabolism of Clostridium acetobutylicum. *mBio* **6**: e01808-01815.
Yoo, M., C. Croux, I. Meynial-Salles & P. Soucaille, (2016) Elucidation of the roles of adhE1 and adhE2 in the primary metabolism of Clostridium acetobutylicum by combining in-frame gene deletion and a quantitative system-scale approach. *Biotechnol Biofuels* **9**: 92.
Zigha, A., (2013) A process for butanol production. In.: Google Patents, pp.
Zingaro, K.A. & E. Terry Papoutsakis, (2013) GroESL overexpression imparts Escherichia coli tolerance to i-, n-, and 2-butanol, 1,2,4-butanetriol and ethanol with complex and unpredictable patterns. *Metab Eng* **15**: 196-205.

Publications

Yoo et al. (2015) A Quantitative System-Scale Characterization of the Metabolism of Clostridium acetobutylicum. mBio 6: e01808-01815.

Yoo et al. (2016) Elucidation of the roles of adhE1 and adhE2 in the primary metabolism of Clostridium acetobutylicum by combining in-frame gene deletion and a quantitative system-scale approach. Biotechnol Biofuels 9: 92.

RESEARCH ARTICLE

A Quantitative System-Scale Characterization of the Metabolism of *Clostridium acetobutylicum*

Minyeong Yoo,[a,b,c] Gwenaelle Bestel-Corre,[d] Christian Croux,[a,b,c] Antoine Riviere,[a,b,c] Isabelle Meynial-Salles,[a,b,c] Philippe Soucaille[a,b,c,d]

Université de Toulouse, INSA, UPS, INP, LISBP, Toulouse, France[a]; INRA, UMR792, Toulouse, France[b]; CNRS, UMR5504, Toulouse, France[c]; Metabolic Explorer, Biopôle Clermont-Limagne, Saint Beauzire, France[d]

ABSTRACT **Engineering industrial microorganisms for ambitious applications, for example, the production of second-generation biofuels such as butanol, is impeded by a lack of knowledge of primary metabolism and its regulation. A quantitative system-scale analysis was applied to the biofuel-producing bacterium *Clostridium acetobutylicum*, a microorganism used for the industrial production of solvent. An improved genome-scale model, *i*Cac967, was first developed based on thorough biochemical characterizations of 15 key metabolic enzymes and on extensive literature analysis to acquire accurate fluxomic data. In parallel, quantitative transcriptomic and proteomic analyses were performed to assess the number of mRNA molecules per cell for all genes under acidogenic, solventogenic, and alcohologenic steady-state conditions as well as the number of cytosolic protein molecules per cell for approximately 700 genes under at least one of the three steady-state conditions. A complete fluxomic, transcriptomic, and proteomic analysis applied to different metabolic states allowed us to better understand the regulation of primary metabolism. Moreover, this analysis enabled the functional characterization of numerous enzymes involved in primary metabolism, including (i) the enzymes involved in the two different butanol pathways and their cofactor specificities, (ii) the primary hydrogenase and its redox partner, (iii) the major butyryl coenzyme A (butyryl-CoA) dehydrogenase, and (iv) the major glyceraldehyde-3-phosphate dehydrogenase. This study provides important information for further metabolic engineering of *C. acetobutylicum* to develop a commercial process for the production of *n*-butanol.**

IMPORTANCE **Currently, there is a resurgence of interest in *Clostridium acetobutylicum*, the biocatalyst of the historical Weizmann process, to produce *n*-butanol for use both as a bulk chemical and as a renewable alternative transportation fuel. To develop a commercial process for the production of *n*-butanol via a metabolic engineering approach, it is necessary to better characterize both the primary metabolism of *C. acetobutylicum* and its regulation. Here, we apply a quantitative system-scale analysis to acidogenic, solventogenic, and alcohologenic steady-state *C. acetobutylicum* cells and report for the first time quantitative transcriptomic, proteomic, and fluxomic data. This approach allows for a better understanding of the regulation of primary metabolism and for the functional characterization of numerous enzymes involved in primary metabolism.**

Received 20 October 2015 **Accepted** 26 October 2015 **Published** 24 November 2015

Citation Yoo M, Bestel-Corre G, Croux C, Riviere A, Meynial-Salles I, Soucaille P. 2015. A quantitative system-scale characterization of the metabolism of *Clostridium acetobutylicum*. mBio 6(6):e01808-15. doi:10.1128/mBio.01808-15.

Invited Editor Eleftherios T. Papoutsakis, University of Delaware **Editor** Sang Yup Lee, Korea Advanced Institute of Science and Technology

Address correspondence to Philippe Soucaille, philippe.soucaille@insa-toulouse.fr.

Clostridium acetobutylicum is a Gram-positive, spore-forming anaerobic bacterium capable of converting various sugars and polysaccharides to organic acids (acetate and butyrate) and solvents (acetone, butanol, and ethanol). Due to its importance in the industrial production of the bulk chemicals acetone and butanol (1–3) and its potential use in the production of *n*-butanol, a promising biotechnology-based liquid fuel with several advantages over ethanol (4, 5), much research has focused on understanding (i) the regulation of solvent formation (6–13), (ii) the ability to tolerate butanol (14–17), and (iii) the molecular mechanism of strain degeneration in *C. acetobutylicum* (18, 19). The complete genome sequence of *C. acetobutylicum* ATCC 824 has been published (20), and numerous transcriptomic and proteomic studies have been performed to date (21–26). Although most of these transcriptomic studies have been performed using two-color microarrays (25, 27–29), RNA deep sequencing (RNA-seq) has recently been used, allowing a more accurate quantification of transcripts as well as the determination of transcription start sites and 5′ untranscribed regions (5′ UTRs) (17, 30). With regard to proteomic studies of *C. acetobutylicum*, 2-dimensional gel electrophoresis (2-DGE) (22, 24, 31–33) is typically employed. 2-DGE is popular and generates substantially valuable data; however, limitations of this method, such as low reproducibility, narrow dynamic range, and low throughput, remain (34). Recently, more quantitative approaches have been developed using two-dimensional liquid chromatography–tandem mass spectrometry (2D-LC-MS/MS) (35) or iTRAQ tags (36).

In general, transcriptomic and/or proteomic studies of *C. acetobutylicum* have been focused on understanding (i) the transcriptional program underlying spore formation (21, 23), (ii) the re-

sponse or adaptation to butanol and butyrate stress (14–17), and (iii) the regulation of primary metabolism (21–23, 25, 35, 37).

Furthermore, to elucidate the molecular mechanisms of endospore formation, microarrays (21, 23) have been used extensively in combination with the downregulation of sigma factors by antisense RNA (23) or inactivation by gene knockout (38, 39). Initially, investigations of the response of *C. acetobutylicum* to butanol and butyrate stress employed microarrays (14–16) followed by RNA deep sequencing (RNA-seq) to quantify both mRNA and small noncoding RNAs (sRNA) (17), and quantitative transcriptomic and proteomic approaches were later combined (40). Based on one of these studies (16), regulons and DNA-binding motifs of stress-related transcription factors as well as transcriptional regulators controlling stress-responsive amino acid and purine metabolism and their regulons have been identified. Furthermore, integrative proteomic-transcriptomic analysis has revealed the complex expression patterns of a large fraction of the proteome that could be explained only by involving specific molecular mechanisms of posttranscriptional regulation (40).

The regulation of solvent formation in *C. acetobutylicum* has been extensively studied in batch cultures using transcriptomic (21, 23, 25) and/or proteomic (24, 35) approaches. Despite the valuable insights achieved in those studies, many physiological parameters, such as specific growth rates, specific glucose consumption rates, pH, and cellular differentiation, as well as butyrate and butanol stress, change with time, making it difficult to understand many details of the expression pattern.

In phosphate-limited chemostat cultures, *C. acetobutylicum* can be maintained in three different stable metabolic states (6, 8–10, 41) without cellular differentiation (37): acidogenic (producing acetate and butyrate) when grown at neutral pH on glucose, solventogenic (producing acetone, butanol, and ethanol) when grown at low pH on glucose, and alcohologenic (forming butanol and ethanol but not acetone) when grown at neutral pH under conditions of high NAD(P)H availability. Indeed, because the cells are maintained under steady-state conditions with constant endogenous and exogenous parameters such as a specific growth rate and specific substrate consumption rate, chemostat culture is the preferred fermentation method by which to achieve standardized conditions with a maximum degree of reproducibility. Transcriptional analysis of the transition from an acidogenic to a solventogenic state (37), as well as transcriptomic and proteomic analyses of acidogenic and solventogenic (22) phosphate-limited chemostat cultures, has already been performed using two-color microarrays for transcriptomic analysis and 2-DGE for proteomic analysis, methods that are semiquantitative. However, a systems biology approach, combining more than two quantitative "omic" analyses of chemostat cultures of *C. acetobutylicum*, has never been performed.

Therefore, the aim of this study was to apply a quantitative system-scale analysis to acidogenic, solventogenic, and alcohologenic steady-state *C. acetobutylicum* cells to provide new insight into the metabolism of this bacterium. We first developed an improved genome-scale model (GSM), including a thorough biochemical characterization of 15 key metabolic enzymes, to obtain accurate fluxomic data. We then applied quantitative transcriptomic and proteomic approaches to better characterize the distribution of carbon and electron fluxes under different physiological conditions and the regulation of *C. acetobutylicum* metabolism.

TABLE 1 Comparison of GSMs of *C. acetobutylicum*[a]

Model statistic	No. of genes, reactions, or metabolites in GSM:				
	Senger et al. (56, 57)	Lee et al. (58)	McAnulty et al. (46)	Dash et al. (45)	*i*Cac967
Genes	474	432	490	802	967
Reactions	552	502	794	1,462	1,231
Metabolites	422	479	707	1,137	1,058

[a] The numbers of genes, reactions, and metabolites present in four previous GSMs of *C. acetobutylicum* and *i*Cac967 are shown.

RESULTS AND DISCUSSION

Improving upon current GSMs for metabolic flux analysis. The *i*Cac967 model for *C. acetobutylicum* ATCC 824 spans 967 genes and includes 1,058 metabolites participating in 1,231 reactions (Table 1; also see Data Set S1 in the supplemental material). All reactions are elementally and charge balanced. The *i*Cac967 model is the result of an extensive literature analysis associated with the biochemical characterization of many key metabolic enzymes in an attempt to better understand the distribution of carbon and electron fluxes. The previously uncharacterized butyryl coenzyme A (butyryl-CoA) dehydrogenase (BCD) encoded by *bcd-etfB-etfA* (CA_C2711, CA_C2710, and CA_C2709, respectively) (42) was biochemically characterized via homologous expression of the encoding operon in *C. acetobutylicum* and the purification of the enzyme complex (Table 2; see also Fig. S1). We demonstrated that the butyryl-CoA dehydrogenase of *C. acetobutylicum* is a strictly NADH-dependent enzyme and that ferredoxin is needed for the reaction to proceed. To study the stoichiometry of the reaction, the concentrations of NADH (see Fig. S1A) and crotonyl-CoA (see Fig. S1B) were modulated using constant concentrations of purified ferredoxin (CA_C0303) and hydrogenase (CA_C0028). Based on the initial slope in Fig. S1B in the supplemental material, it was calculated that in the presence of excess crotonyl-CoA, 2.15 mol of NADH was required for the formation of 1 mol of H_2; from the initial slope in Fig. S1A in the supplemental material, it was calculated that in the presence of excess NADH, 1.25 mol of crotonyl-CoA was required for the formation of 1 mol of H_2. The results indicate that under fully coupled conditions, approximately 1 mol of ferredoxin is reduced by 2 mol of NADH and 1 mol of crotonyl-CoA, similar to the butyryl-CoA dehydrogenase of *Clostridium kluyveri* (43). Although the possibility that this enzyme might consume 2 mol of NADH and produce 1 mol of reduced ferredoxin in *C. acetobutylicum* was previously presented as a hypothesis (44), it has not been demonstrated to date, nor has it been integrated in the recently published GSMs (45, 46). This result has strong implications for the distribution of electron fluxes, as discussed below in the metabolic flux analysis section.

The second key enzyme that remained uncharacterized was the bifunctional alcohol-aldehyde dehydrogenase (AdhE1 or Aad, encoded by CA_P0162), an enzyme involved in the last two steps of butanol and ethanol formation during solventogenic culturing of *C. acetobutylicum* (47, 48). First, *adhE1* and *adhE2* (as a positive control) were individually heterologously expressed in *Escherichia coli*, after which AdhE1 and AdhE2 were purified as tag-free proteins (Table 2) for biochemical characterization. We demonstrated that *in vitro*, AdhE1 possesses high NADH-dependent butyraldehyde dehydrogenase activity but surprisingly very low butanol dehydrogenase activity with both NADH and NADPH; in

TABLE 2 Activities of purified key metabolic enzymes

Locus no.	Gene name	Enzyme activity	Activity (U/mg)[a]
CA_C3299	*bdhA*	Butanol dehydrogenase	NADH (0.15 ± 0.05), NADPH (2.57 ± 0.45)
CA_C3298	*bdhB*	Butanol dehydrogenase	NADH (0.18 ± 0.02), NADPH (2.95 ± 0.36)
CA_C3392	*bdhC*	Butanol dehydrogenase	NADH (0.24 ± 0.04), NADPH (2.21 ± 0.41)
CA_P0162	*adhE1*	Butanol dehydrogenase	NADH (0.04 ± 0.02), NADPH (not detected)
CA_P0035	*adhE2*	Butanol dehydrogenase	NADH (4.8 ± 0.42), NADPH (0.12 ± 0.01)
CA_P0162	*adhE1*	Butyraldehyde dehydrogenase	NADH (2.27 ± 0.21), NADPH (0.08 ± 0.01)
CA_P0035	*adhE2*	Butyraldehyde dehydrogenase	NADH (2.5 ± 0.31), NADPH (0.07 ± 0.01)
CA_C2711-CA_C2709	*bcd-etfB-etfA*	Butyryl-CoA dehydrogenase	NADH (0.569 ± 0.08), NADPH (not detected)
CA_C1673-CA_C1674	*gltA/gltB*	Glutamate synthase	NADH (0.61 ± 0.16), NADPH (0.051 ± 0.01)
CA_C0737	*gdh*	Glutamate dehydrogenase	NADH (41.2 ± 3.4), NADPH (0.12 ± 0.01)
CA_C0970	*citA*	*Re*-citrate synthase	1.9 ± 0.14
CA_C0971	*citB*	Aconitase	6.5 ± 0.52
CA_C0972	*citC*	Isocitrate dehydrogenase	NADH (104 ± 6.8), NADPH (7.1 ± 0.43)
CA_C1589	*malS1*	Malic enzyme	NADH (156 ± 9.6), NADPH (3.4 ± 0.24)
CA_C1596	*malS2*	Malic enzyme	NADH (142 ± 12.7), NADPH (2.9 ± 0.34)

[a] One unit is the amount of enzyme that consumes 1 μmol of substrate per min.

contrast, AdhE2 possesses both high butyraldehyde and butanol dehydrogenase activities with NADH. The three potential alcohol dehydrogenases, BdhA, BdhB, and BdhC (49), encoded by *bdhA*, *bdhB*, and *bdhC* (CA_C3299, CA_C3298, and CA_C3392), respectively, were heterologously expressed in *E. coli* and then characterized after purification as tag-free proteins (Table 2). The three enzymes were demonstrated to be primarily NADPH-dependent butanol dehydrogenases, results which do not agree with the previous characterizations of BDHI and BDHII (later demonstrated to be encoded by *bdhA* and *bdhB*), which were reported to be NADH dependent (49, 50). However, in agreement with our findings, all of the key amino acids of the two GGGS motifs at positions 37 to 40 and 93 to 96 involved in the NADPH binding of YqhD, a strictly NADPH-dependent alcohol dehydrogenase (51), are perfectly conserved in the three *C. acetobutylicum* alcohol dehydrogenases. Furthermore, these results are also in line with previously published data from two different research groups (9, 52) showing that in a crude extract of solventogenic *C. acetobutylicum* cultures, the butanol dehydrogenase activity measured in the physiological direction is mainly NADPH dependent. As discussed below, *C. acetobutylicum* must utilize at least one of these alcohol dehydrogenases to produce butanol and ethanol under solventogenic conditions, which implies that 1 mol of NADPH is needed for each mole of butanol and ethanol produced under solventogenic conditions.

The cofactor specificity of the ammonium assimilation pathway that proceeds via glutamine 2-oxoglutarate aminotransferase (GOGAT) encoded by *gltA* and *gltB* (CA_C1673 and CA_C1674, respectively) and glutamate dehydrogenase (GDH) encoded by *gdh* (CA_C0737) was also characterized. The *gltA-gltB* and *gdh* genes were expressed in *C. acetobutylicum* and *E. coli*, respectively, and GOGAT and GDH were purified (Table 2). Both enzymes were found to be NADH dependent, in contrast to the corresponding enzymes in *E. coli*, which are NADPH dependent (53, 54).

The functions of the three genes (CA_C0970, CA_C0971, and CA_C0972) proposed (55) to encode the first three steps of the oxidative branch of the tricarboxylic acid (TCA) cycle were unambiguously characterized. CA_C0970, CA_C0971, and CA_C0972 were individually expressed in *E. coli*, and their gene products were purified (Table 2); the genes were demonstrated to encode an *Re*-citrate synthase (CitA), an aconitase (CitB), and an NADH-dependent isocitrate dehydrogenase (CitC), respectively.

Finally, we characterized the cofactor specificity of the two malic enzymes encoded by CA_C1589 and CA_C1596, two almost-identical genes that differ by only two nucleotides. Not surprisingly, the specific activities of the two purified enzymes are almost identical, and both enzymes are NADH dependent (Table 2).

The *i*Cac967 model statistics and those of all other published models for *C. acetobutylicum* (45, 46, 56–58) are shown in Table 1. *i*Cac967 has 20% more genes than the most recently published model by Dash et al. (45) but fewer metabolites and reactions, as some reactions described by these authors were not validated by our extensive literature analysis or were inappropriate in the context of anaerobic metabolism, for example, R0013 (NADPH + O_2 + H^+ + 2-octaprenylphenol → H_2O + $NADP^+$ + 2-octaprenyl-6-hydroxyphenol) and R0293 (H_2O + O_2 + sarcosine → H_2O_2 + glycine + formaldehyde). Furthermore, we applied our GSM to the butyrate kinase knockout mutant (59) and the M5 degenerate strain (60) (which has lost the pSOL1 plasmid) and successfully predicted their phenotypes (see Table S1 in the supplemental material).

Quantitative transcriptomic and proteomic analyses of *C. acetobutylicum* under stable acidogenic, solventogenic, and alcohologenic conditions. (i) General considerations. Quantitative transcriptomic and proteomic analyses were performed on phosphate-limited chemostat cultures of *C. acetobutylicum* maintained in three different stable metabolic states: acidogenic, solventogenic, and alcohologenic (6, 7, 9, 10). The total amount of DNA, RNA, and protein contents (expressed in grams per gram of dry cell weight [DCW]) and the number of cells per gram of DCW were experimentally determined for each steady-state condition under phosphate limitation at a dilution rate of 0.05 h^{-1}. These numbers were not significantly different among the steady-state conditions, in agreement with previous studies (61, 62) on *E. coli* that have shown that the biomass composition is not dependent on the carbon source but is strictly dependent on the specific growth rate. According to all of the values, the average contents of DNA (1.92 ± 0.03), mRNA ([9.41 ± 0.94] × 10^3), and protein

($[6.26 \pm 0.18] \times 10^6$) molecules per cell were calculated. Noticeably, the total number of mRNA molecules per cell was only 2.4 times higher than the total number of open reading frames (ORFs) (3,916). In *E. coli*, the situation was even worse, with a total number of mRNA molecules per cell (1,380) 3 times lower than the total number of ORFs (4,194) (61).

For each gene, we sought to quantify the number of mRNA molecules per cell. For this purpose, we used Agilent's one-color microarray-based gene expression analysis, as a recent study (63) demonstrated a linear relationship between the amounts of transcript determined by this method and those determined by the RNA-seq method. The minimum number of mRNA molecules per cell detected was around 0.06 while the maximum number was around 80. It was observed that a large number of genes have less than 0.2 mRNA molecule per cell (for 37.1%, 36.8%, and 37.2% of the genes under acidogenic, solventogenic, and alcohologenic conditions, respectively). This result indicates that for these genes, there is either (i) heterogeneity among different cells, such that some cells contain one transcript and others do not, or (ii) a high mRNA degradation rate. Genes that showed a value of mRNA molecules per cell of <0.2 under all three conditions were excluded from further analysis.

The purpose of this study was also to quantify the number of cytoplasmic protein molecules per cell. Different quantitative methods using either 2D-protein gels (26) or peptide analysis by two-dimensional high-performance liquid chromatography (2D HPLC) coupled with tandem mass spectrometry (MS/MS) with peptide labeling (36, 40) have been developed for *C. acetobutylicum*. In collaboration with the Waters Company, we adapted a recently published method (64) using label-free peptide analysis after shotgun trypsin hydrolysis of cytosolic proteins. For approximately 700 cytosolic proteins, it was possible to quantify the number of protein molecules per cell in at least one of the three steady states. This number is approximately 4 times higher than the number of cytosolic proteins detected in phosphate-limited acidogenic and solventogenic chemostat cultures by Janssen et al. (22) but similar to the number of cytosolic proteins detected by Venkataramanan et al. (40) by iTRAQ. Furthermore, the minimum number of protein molecules per cell detected was around 200 while the maximum number was approximately 300,000. For 96% of the cytosolic proteins that could be quantified, a linear relationship was obtained, with an R^2 value of >0.9, when the numbers of protein molecules per cell were plotted against the numbers of mRNA molecules per cell (see Data Set S2 in the supplemental material). This result indicated that for steady-state continuous cultures run at the same specific growth rate and with the same total amount of carbon supplied, the rate of protein turnover is proportional to the mRNA content for 96% of the genes. This result is not necessarily surprising, as it has previously been shown for other microorganisms such as *E. coli* (65) that the numbers of ribosomes and tRNAs per cell are dependent on the specific growth rate and not on the carbon source. The absolute protein synthesis rates for approximately 700 genes were calculated by assuming that the rate of protein degradation is negligible compared to the rate of protein synthesis (see Data Set S2). These values varied from 0.0007 s^{-1} for CA_C3723 (*ssb* encoding a single-stranded DNA-binding protein) to 0.95 s^{-1} for CA_C0877 (*cfa* encoding a cyclopropane fatty acid synthase). Interestingly, the rate of protein synthesis appears to correlate inversely with the average number of mRNA molecules per cell (see Data Set S2).

(ii) Comparison of solventogenic versus acidogenic steady-state cells. Solventogenic cells were first comprehensively compared to acidogenic cells via quantitative transcriptomic and proteomic analyses. The complete transcriptomic and proteomic results are provided in Data Set S2 in the supplemental material. A similar study in phosphate-limited chemostat cultures was previously performed by Janssen et al. (22) using semiquantitative transcriptomic (two-color microarrays) and proteomic (2-DGE) methods. Among the 95 genes shown by Janssen et al. to be upregulated, we qualitatively confirmed upregulation for 68; among the 53 genes shown by Janssen et al. to be downregulated, we qualitatively confirmed downregulation for 27. What might explain the differences between the two studies? First, the culture conditions were slightly different in terms of dilution rate (0.075 h^{-1} for the work of Janssen et al., 0.05 h^{-1} in our study), phosphate limitation (0.5 mM for the work of Janssen et al., 0.7 mM in our study), and the pH of the acidogenic culture (5.7 for the work of Janssen et al., 6.3 in our study), leading to a larger amount of glucose consumed and thus a larger amount of products formed in our study. We are confident regarding the validity of our results because we found agreement quantitatively with the transcriptomic data whenever proteins were detected by our method, and thus, quantitative proteomic data were available. Below, we discuss these data in more detail, and striking differences in mRNA molecules per cell are highlighted in Fig. S2A in the supplemental material.

In total, 64 genes matched the significance criteria of $\geq$4.0-fold-higher expression in solventogenesis than in acidogenesis as well as >0.2 mRNA molecules per cell under at least one of the two conditions (see Table S2 in the supplemental material). In particular, high values (~80- to 150-fold) were documented for the *sol* operon genes (CA_P0162-CA_P0164) and confirmed by the proteomic analysis, in agreement with (i) the requirement of AdhE1 and CoA-transferase subunits for the production of solvents under solventogenic conditions (12, 47, 48, 66) and (ii) the previous study by Janssen et al. (22). Elevated upregulation (4- to 40-fold) of genes involved in serine biosynthesis (CA_C0014-CA_C0015), seryl-tRNA synthesis (CA_C0017), and arginine biosynthesis (CA_C2388) was detected at the mRNA level and confirmed by the proteomic analysis, in agreement with a previous metabolomic study in batch culture (67), which reported higher intracellular concentrations of serine and arginine in solventogenic cells. Interestingly, all these genes were previously shown to be upregulated in response to butanol stress (16), although these results were not confirmed by proteomic analysis (40). In addition, an ~4- to 8-fold upregulation of genes involved in purine biosynthesis (CA_C1392-CA_C1395, CA_C1655, and CA_C2445) was detected at the mRNA level and confirmed by the proteomic analysis. Similar to the results in the study by Janssen et al. (22), an ~5-fold upregulation of a gluconate dehydrogenase (CA_C2607) was detected; however, as this protein was not detected, this was not confirmed by proteomic analysis.

As reported in previous studies (22, 37), we found elevated upregulations (~4- to 16-fold) of the genes involved in the production of (i) a nonfunctional cellulosome (CA_C0910-CA_C0918 and CA_C0561) (20, 68) and (ii) noncellulosomal pectate lyase-encoding genes (CA_P0056 and CA_C0574) at the mRNA level. However, these results could not be verified by proteomic analysis, as exoproteome analysis was not performed in

this study. All these genes, except CA_P0056, were also shown to be upregulated in response to a butanol stress (16).

Importantly, *spo0A* (CA_C2071), encoding a regulator of sporulation and solvent production (69–71), showed an increase in expression at the level of both mRNA and protein molecules per cell. This increased expression does not agree with previous chemostat culture studies by Grimmler et al. (37) and Janssen et al. (22) but does agree with batch culture studies (21, 25) and also supports the common notion of Spo0A acting as a master regulator of solventogenesis. *hsp18* (CA_C3714), encoding a gene product involved in solvent tolerance (72), also exhibited an ~4.5-fold increase in mRNA and protein molecules per cell, in agreement with a previous butanol stress study (40). A striking difference between the study by Janssen et al. and ours was observed with regard to the level of this chaperone, which in contrast to our study showing an ~4.5-fold increase under solventogenesis, was decreased (~5-fold) in the study by Janssen et al. (22). Nonetheless, this difference appears to be due to the limitation of 2-DGE, because 3 different proteins could be detected in the "Hsp18 spot" and transcriptional changes in *hsp18* did not correlate with the proteomic data (22); in contrast, our quantitative transcriptomic and proteomic data showed good correlation ($R^2 > 0.9$).

The detailed results of the 45 ORFs that exhibited ≥4.0-fold decreases in numbers of mRNA molecules per cell under solventogenic versus acidogenic conditions and of a number with >0.2 mRNA molecules per cell under at least one of the two conditions are given in Table S2 in the supplemental material. Significantly, in this metabolic state, various genes involved in the assimilation of different carbon sources were downregulated. For example, the highest decrease (~6- to 70-fold) at the mRNA level was observed for genes (CA_C0422-CA_C0426) involved in sucrose transport, metabolism, and the regulation of these genes, which was confirmed by the proteomic analysis. In addition, two genes involved in mannan (CA_C0332) and maltose (CA_C0533) metabolism exhibited 4- and 10-fold decreases, respectively, in their mRNA levels. Because acidogenic culture reached glucose limitation but a small amount of glucose remained in solventogenic culture (similar to our previous publication [9]), this phenomenon can be explained by a release of catabolite repression in acidogenic cultures. The similar high expression observed for CA_C0422-CA_C0426, CA_C0332, and CA_C0533 in alcohologenic and acidogenic cultures that were glucose limited is in agreement with this hypothesis. Two genes located on the megaplasmid pSOL1 (CA_P0036 and CA_P0037), encoding a cytosolic protein of unknown function and a potential transcriptional regulator, respectively, exhibited particularly high scores corresponding to an ~60- to 70-fold decrease, which is in good agreement with the proteomic data and the previous study by Janssen et al. (22). Interestingly, under all conditions, these two proteins are present at a 1:1 molar ratio. Furthermore, three genes involved in cysteine (CA_C2783) and methionine (CA_C1825 and CA_C0390) biosynthesis exhibited ~5-fold decreases in their numbers of mRNA and protein molecules per cell in agreement with a previous metabolomics study by Amador-Noguez et al. (67), showing an ~5-fold decrease in intracellular methionine in solventogenesis.

(iii) Comparison of alcohologenic versus acidogenic steady-state cells. Alcohologenic cells were comprehensively compared to acidogenic cells by quantitative transcriptomic and proteomic analyses. The complete transcriptomic results are listed in Data Set S2, and striking differences are highlighted in Fig. S2B, both in the supplemental material. In total, 52 genes matched the significance criterion of ≥4.0-fold-higher expression in alcohologenesis than in acidogenesis as well as >0.2 mRNA molecules per cell under at least one of the two conditions (see Table S3). In particular, high values (~55- to 520-fold) were documented for the gene cluster coding for glycerol transport and utilization (CA_C1319-CA_C1323) and confirmed by the proteomic analysis, in agreement with the requirement of GlpK (glycerol kinase) and GlpAB (glycerol-3-phosphate dehydrogenase) for glycerol utilization in alcohologenic metabolism (6, 9). High upregulation (160-fold) of *adhE2* (CA_P0035), which is involved in alcohol production under alcohologenic conditions (66), was detected and correlated with a high AdhE2 protein concentration. Interestingly, CA_C3486, which encodes a multimeric flavodoxin, was also highly expressed (~6-fold) and may participate in redistribution of the electron flux in favor of butanol under alcohologenic conditions. Of note, ~20- to 70-fold upregulation of a gene cluster involved in sulfate transport, reduction, and incorporation to produce cysteine (CA_C0102-CA_C0110); ~4-fold upregulation of *cysK* (CA_C2235), which is also involved in cysteine synthesis; and ~7- to 10-fold upregulation of an operon (CA_C3325-CA_C3327) involved in cysteine transport were detected at the mRNA level and confirmed by the proteomic analysis for the cytosolic proteins detected (CA_C0102-CA_C0104, CA_C0107, CA_C0109-CA_C0110, CA_C2235, and CA_C3327). All of these genes/operons were shown to possess a CymR-binding site in their promoter regions, and some have been shown to be upregulated in response to butanol stress (16).

An ~3- to 5-fold upregulation of an operon involved in histidine synthesis and histidyl-tRNA synthesis (CA_C0935-CA_C0943) and 5-fold upregulation of a gene involved in arginine biosynthesis (CA_C2388) were also detected at the mRNA level and confirmed by the proteomic analysis. These genes were also shown to be upregulated under solventogenic conditions (this study) and in response to butanol stress (16).

The detailed results of the 64 ORFs that exhibited a ≥4.0-fold decrease in transcript levels under alcohologenic versus acidogenic conditions and >0.2 mRNA molecules per cell under at least one of the two conditions are given in Table S3 in the supplemental material. The highest decrease (~70-fold) at the mRNA level was observed for an operon (CA_C0427-CA_C0430) involved in glycerol-3-phosphate transport and coding for a glycerophosphoryl diester phosphodiesterase, which was confirmed by the cytosolic protein analysis. As observed under solventogenic conditions, CA_P0036 and CA_P0037 exhibited ~40- to 50-fold-lower expression levels, which agrees well with the proteomic data. Furthermore, an operon involved in phosphate uptake (CA_C1705-CA_C1709), an operon encoding an indolepyruvate ferredoxin oxidoreductase (CA_C2000-CA_C2001), and a gene encoding a pyruvate decarboxylase (CA_P0025) exhibited ~80- to 350-fold, ~4- to 5-fold, and ~4-fold decreases, respectively, at the mRNA level, confirmed by the proteomic analysis. Additionally, two clusters of genes involved in fatty acid biosynthesis/degradation (CA_C2004-CA_C2017) exhibited ~3.5- to 6-fold decreases at the mRNA level, a result that could not be confirmed by the proteomic analysis as the corresponding proteins were not detected.

Metabolic flux analysis of *C. acetobutylicum* under stable acidogenic, solventogenic, and alcohologenic conditions. To perform a metabolic flux analysis of *C. acetobutylicum* under stable acidogenic, solventogenic, and alcohologenic conditions,

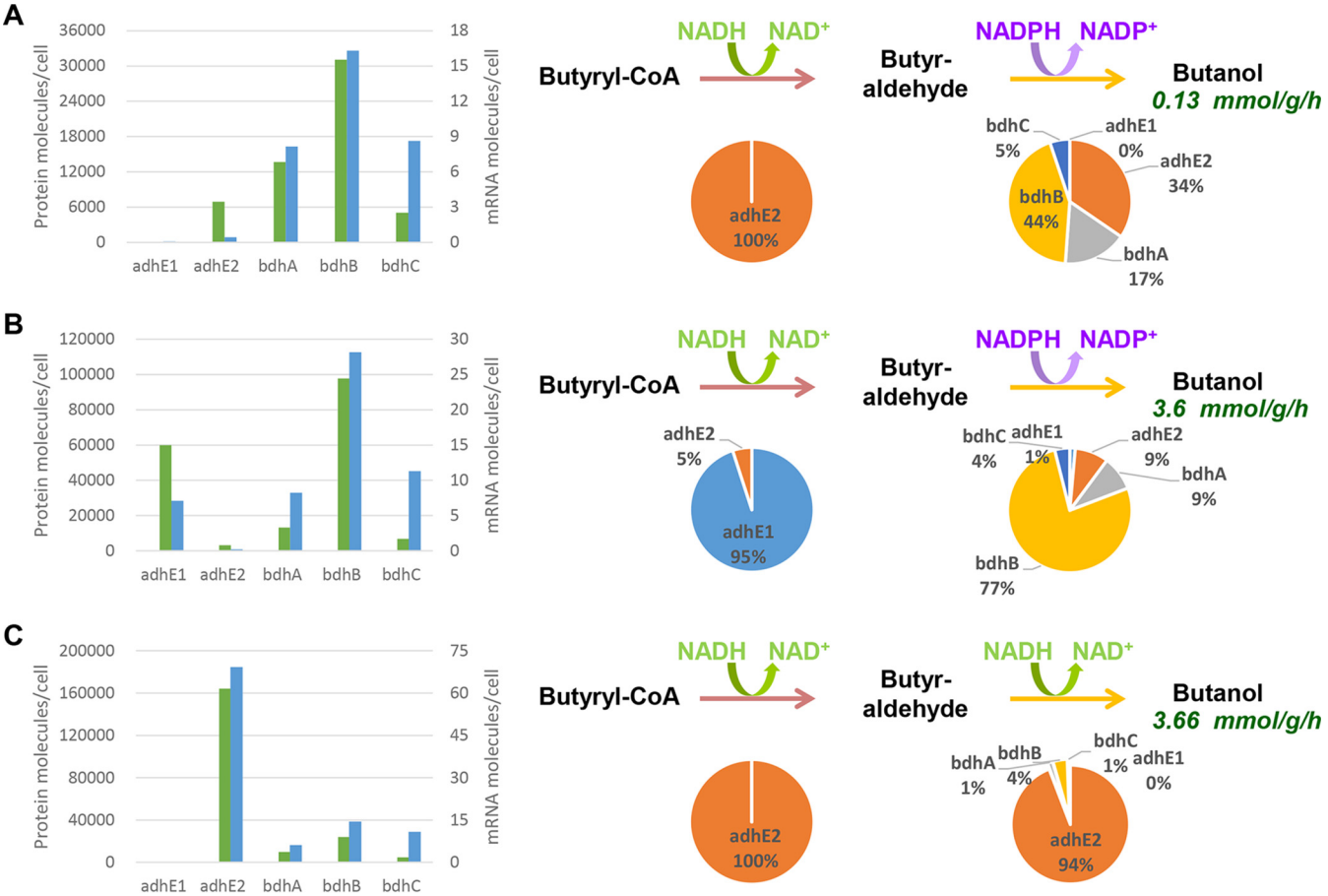

FIG 1 Butanol pathway analysis under acidogenesis (A), solventogenesis (B), and alcohologenesis (C). (Left) Numbers of mRNA (blue) and protein (green) molecules per cell for the five enzymes potentially involved in butanol production. (Right) Activity distributions of the five enzymes are shown for each step under the arrows. The primary cofactors used for each step are shown over the arrows. Butanol flux is indicated under the word "Butanol."

*i*Cac967 was combined with our transcriptomic and proteomic data. As a first simple example, we present how the gene responsible for pyruvate ferredoxin oxidoreductase (PFOR) activity was identified. This gene encodes a key enzyme in the glycolytic pathway that decarboxylates pyruvate to produce reduced ferredoxin, CO_2, and acetyl-CoA. Two putative PFOR-encoding genes (CA_C2229 and CA_C2499) were identified in our GSM (see Data Set S1 in the supplemental material). Under all conditions, only CA_C2229 was transcribed (average of 56 mRNA molecules per cell) and translated (average of 166,000 protein molecules per cell).

As a second simple example, we present how the main enzyme responsible for crotonyl-CoA reduction to butyryl-CoA was identified. Two different enzymes can potentially catalyze this reaction: the BCD complex encoded by *bcd*, *etfB*, and *etfA* (CA_C2711, CA_C2710, and CA_C2709, respectively) which consumes 2 moles of NADH and produces 1 mole of reduced ferredoxin (see Fig. S1 in the supplemental material) and TER (*trans*-2-enoyl-CoA reductase) encoded by CA_C0642, which consumes only 1 mole of NADH (73). Under all conditions, *bcd* was much more highly transcribed than CA_C0642 (67 versus 1.2 mRNA molecules per cell) and in terms of proteins BCD was detected at higher levels (average of 113,000 protein molecules per cell), whereas TER was below the detection limit of the method.

As a complex example, we also present the actors in the different butanol pathways and their cofactor specificities. Five proteins could potentially be involved in the last two steps of butanol formation. AdhE1 retains only NADH-dependent aldehyde dehydrogenase activity, whereas AdhE2 is a bifunctional NADH-dependent aldehyde-alcohol dehydrogenase (66); BdhA, BdhB, and BdhC are NADPH-dependent alcohol dehydrogenases. For each of the three conditions and for each of the abovementioned genes and their corresponding proteins, the number of mRNA molecules per cell and the number of protein molecules per cell were measured. The percentage of the total butanol flux due to each of the five enzymes was calculated by assuming that all five enzymes function at their V_{max} and using the amount of each protein per cell. The results are presented in Fig. 1. Under acidogenic conditions, the entire butyraldehyde dehydrogenase flux is due to AdhE2, whereas the butanol dehydrogenase flux is primarily due to BdhB and BdhA. Under solventogenic conditions, the butyraldehyde dehydrogenase flux is largely due to AdhE1, whereas the butanol dehydrogenase flux is primarily due to BdhB, BdhA, and BdhC, in decreasing order of activity. Finally, under alcohologenic conditions, all of the flux of butyraldehyde dehydrogenase activity and most of that of butanol dehydrogenase activity are due to AdhE2. In summary, the last two steps of butanol production consume 1 mole of NADH and 1 mole of NADPH

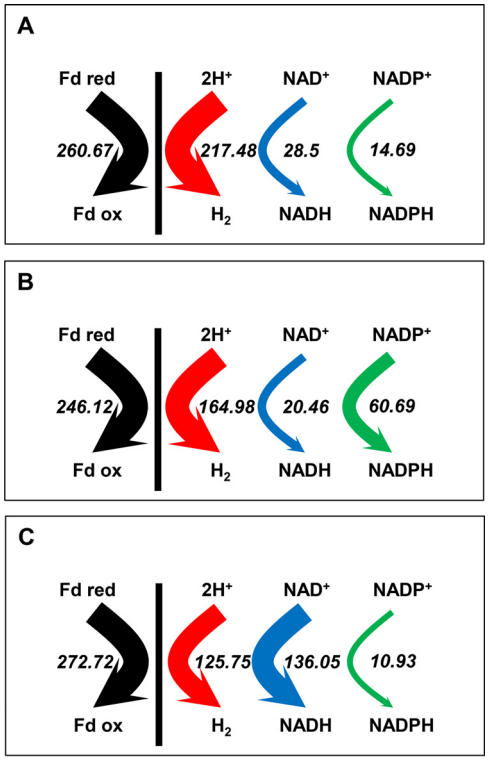

FIG 2 Electron flux map: acidogenesis (A), solventogenesis (B), and alcohologenesis (C). The hydrogenase (red), ferredoxin-NAD^+ reductase (blue), and ferredoxin-$NADP^+$ (green) *in vivo* fluxes are presented. All values are normalized to the flux of the initial carbon source (millimoles per gram [DCW] per hour). Glucose flux is normalized as 100 for acidogenesis and solventogenesis, and the sum of glucose and half of the glycerol is normalized as 100 for alcohologenesis.

under acidogenic and solventogenic conditions and 2 moles of NADH under alcohologenic conditions (Fig. 1). These results have strong implications for the distribution of electron fluxes and the use of reduced ferredoxin under the respective studied conditions. Under acidogenic conditions, reduced ferredoxin is primarily used to produce hydrogen, and only a small fraction is used to produce the NADH needed for butyrate formation and the NADPH needed for anabolic reactions (Fig. 2A). However, under alcohologenic conditions, reduced ferredoxin is primarily used to produce the NADH needed for alcohol formation (Fig. 2C); under solventogenic conditions, although reduced ferredoxin is predominantly utilized for hydrogen production, a significant amount is used for the NADPH formation needed for the final step of alcohol formation by BdhB, BdhA, and BdhC, as *C. acetobutylicum* has no oxidative pentose phosphate pathway (*zwf*, encoding glucose 6-phosphate-dehydrogenase, is absent) to produce NADPH (Fig. 2B and 3). Although the enzymes converting reduced ferredoxin to NADPH or NADH, namely, ferredoxin-$NADP^+$ reductase and ferredoxin-NAD^+ reductase, and their corresponding genes are unknown, they likely play key roles in alcohol formation under solventogenic and alcohologenic conditions, respectively.

A fourth example of metabolic flux analysis is the identification of the hydrogen production pathway. Three hydrogenases are potentially involved: two Fe-Fe hydrogenases, HydA (encoded by CA_C0028) and HydB (encoded by CA_C3230), and one Ni-Fe hydrogenase, HupSL (encoded by CA_P0141-CA_P0142). The *hydB* and the *hupSL* genes are not expressed under all three conditions, nor were the HydB and HupSL proteins detected by quantitative proteomic analysis. As HydA is the only hydrogenase present, how can the lower observed flux in H_2 production under solventogenic and alcohologenic conditions (compared to acidogenic conditions) be explained? Under solventogenic conditions, there is a 3-fold decrease in the expression of *hydA*; this is associated with a 2-fold decrease in the expression of *fdx1* (CA_C0303), which encodes the primary ferredoxin, the key redox partner for the hydrogenase. As these results were confirmed by the proteomic analysis, they may explain the 1.3-fold decrease in H_2 production under solventogenic conditions compared to acidogenic conditions (Fig. 2B). Nonetheless, under alcohologenic conditions a 1.7-fold decrease in H_2 production (compared to acidogenic conditions) is associated with a 1.8-fold-higher expression of *hydA*, a 3-fold decrease in the expression of *fdx1*, and a 6-fold increase in the expression of CA_C3486, which encodes a multimeric flavodoxin, another potential redox partner for the hydrogenase. In fact, the reduced multimeric flavodoxin may be a better substrate for the ferredoxin-NAD^+ reductase than for the primary hydrogenase, as was previously shown for reduced neutral red (8). This result would explain the low flux in hydrogen production and the high flux in ferredoxin-NAD^+ reductase production under alcohologenic metabolism obtained through growth either in glucose-glycerol mixtures or in glucose in the presence of neutral red (8).

A fifth example of metabolic flux analysis is the glyceraldehyde-3-phosphate oxidation pathway. Two glyceraldehyde-3-phosphate dehydrogenases are potentially involved: GapC (encoded by CA_C0709) (74), which phosphorylates and produces NADH, and GapN (encoded by CA_C3657) (75), which is nonphosphorylating and produces NADPH. For each of the three conditions and each of the genes studied, the numbers of mRNA molecules and protein molecules per cell were measured. The percentage of the total glycolytic flux due to each of the enzymes was calculated by assuming that both enzymes function at their previously published V_{max} levels (74, 75) and using the amount of each protein per cell. Here, results are presented for only solventogenic metabolism, though qualitatively, the conclusions were the same for all conditions: *gapN* is poorly expressed compared to *gapC* (0.56 versus 66 mRNA molecules per cell; 3,500 versus 190,000 protein molecules per cell) (see Data Set S2 in the supplemental material), and GapN would be responsible for less than 5% of the glycolytic flux.

Two fluxes involved in anaplerotic reactions, namely, those for pyruvate carboxylase (encoded by CA_C2660) and NADH-dependent malic enzymes (encoded by CA_C1589 and CA_C1596), could not be solved using our GSM analysis coupled with transcriptomic and proteomic analyses. All of the genes studied were transcribed and translated under all conditions, and because all fermentations occurred under a high partial pressure of CO_2, malic enzymes could function in both malate production from pyruvate and malate decarboxylation to pyruvate, depending on the NADH/NAD^+ and pyruvate/malate ratios. Using ^{13}C labeling in a *C. acetobutylicum* batch culture, Au et al. (76) demonstrated that malic enzymes function in the malate-to-pyruvate direction but that this flux accounted for less than 5% of the pyruvate carboxylase flux. In Fig. 3 and in Fig. S3 in the supplemental

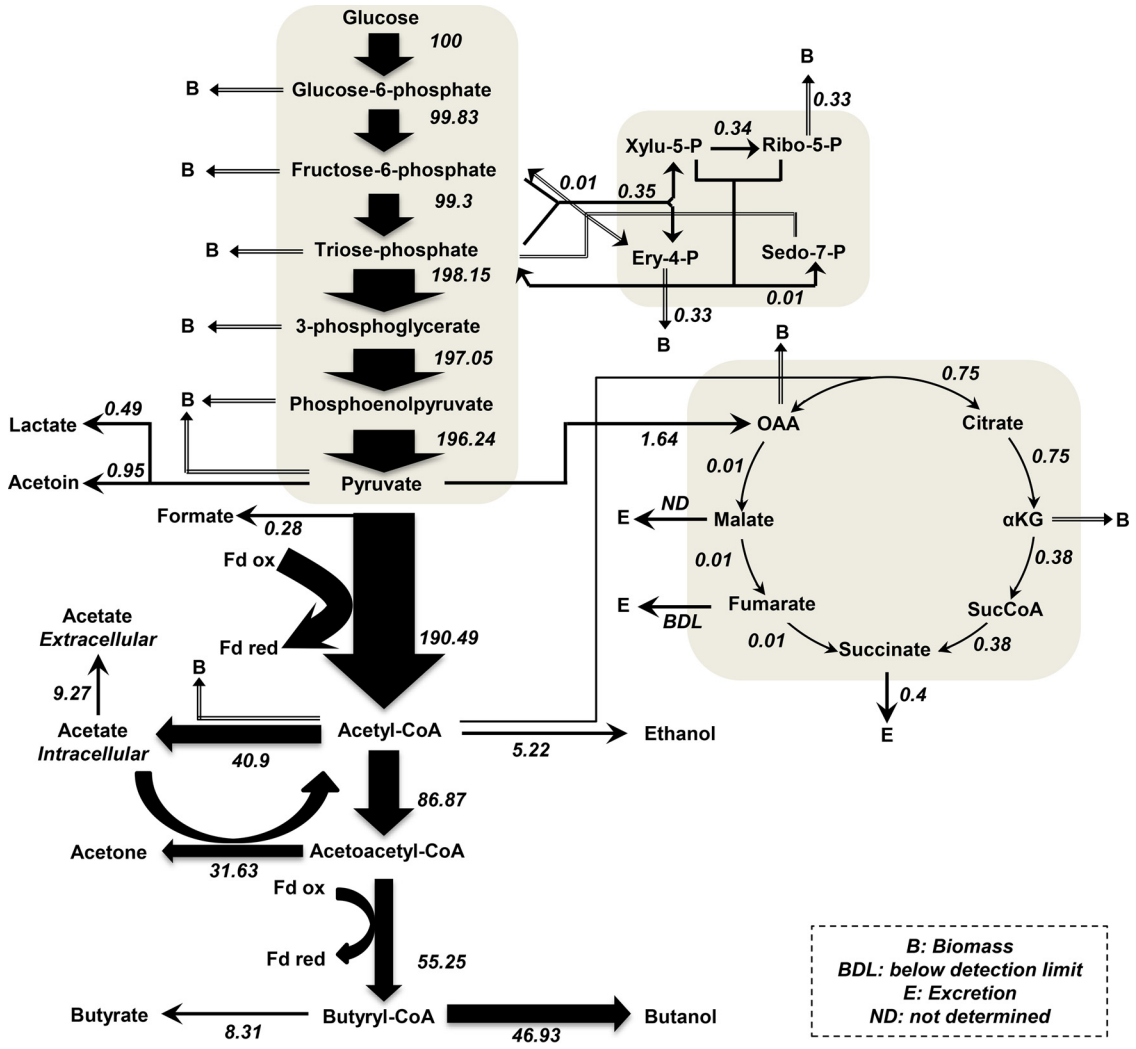

FIG 3 Metabolic flux map of *C. acetobutylicum* in solventogenesis. All values are normalized to the flux of the initial carbon source, glucose (millimoles per gram of DCW per hour). Metabolic flux maps of *C. acetobutylicum* in acidogenesis and in alcohologenesis are presented in Fig. S3 in the supplemental material.

material, the anaplerotic fluxes presented are net anaplerotic fluxes, which were attributed to pyruvate carboxylase.

The flux in the oxidative branch of the TCA cycle was much higher than that in the reductive branch (Fig. 3; see also Fig. S3 in the supplemental material). In agreement with the ^{13}C labeling flux data reported by Amador-Noguez et al. (55), who demonstrated the flux from oxaloacetate to malate, but in contrast to the report by Au et al. (76), in which no flux could be measured through this enzyme, under all three conditions, we measured ~1,000 malate dehydrogenase (CA_C0566) protein molecules per cell that could catalyze the first step of the TCA reductive branch (see Data Set S2).

Conclusion. In this work, an improved GSM containing new and validated biochemical data was developed in conjunction with quantitative transcriptomic and proteomic analyses to obtain accurate fluxomic data. These "omics" data allowed for (i) the determination of the distribution of carbon and electron fluxes, (ii) the elucidation of the different genes/enzymes involved in the primary metabolism of *C. acetobutylicum*, and (iii) a better understanding of the regulation of *C. acetobutylicum* primary metabolism under different physiological conditions. The information provided in this study will be important for the further metabolic engineering of *C. acetobutylicum* to develop a commercial process for the production of *n*-butanol.

MATERIALS AND METHODS

Chemicals and other reagents. All chemicals were of reagent grade and were purchased from Sigma-Aldrich Chimie (Saint-Quentin Fallavier, France) or from VWR Prolabo (Fontenay sous Bois, France). All gases used for gas flushing of the medium and for the anaerobic chamber were of the highest purity available and were obtained from Air Liquide (Paris, France). All restriction enzymes and Crimson *Taq* DNA polymerase used for colony PCR were supplied by New England Biolabs (MA, USA) and were used according to the manufacturer's instructions. DNA fragments for vector constructions were amplified using Phusion high-fidelity DNA polymerase (New England Biolabs).

Culture conditions. (i) Batch culture. All liquid cultures of *C. acetobutylicum* ATCC 824 Δ*CA_C1502* Δ*upp* (P. Soucaille, R. Figge, and R. Croux, 2014, U.S. Patent 8,628,967) were performed in 30-ml or 60-ml glass vials under strict anaerobic conditions in clostridium growth medium (CGM) as described previously (77) or in synthetic medium (MS) as

described previously (6). *C. acetobutylicum* was stored in spore form at −20°C after sporulation in MS medium. Heat shock was performed for spore germination by immersing the bottle in a water bath at 80°C for 15 min.

(ii) Continuous culture. The conditions described previously by Vasconcelos et al. (6) and Girbal et al. (9) were used for the phosphate-limited continuous culture of *C. acetobutylicum* fed a constant total carbon amount of 995 mM. The cultures were maintained under acidogenesis (pH 6.3, 995 mM carbon from glucose), solventogenesis (pH 4.4, 995 mM carbon from glucose), and alcohologenesis (pH 6.3, 498 mM carbon from glucose and 498 mM carbon from glycerol).

RNA extraction and microarray. For transcriptomic analysis, 3-ml samples were collected from chemostat cultures and immediately frozen in liquid nitrogen. The frozen cell cultures were ground promptly with 2-mercaptoethanol in a liquid nitrogen-cooled mortar. RNA was extracted using an RNeasy midikit (Qiagen, Courtaboeuf, France) according to the manufacturer's instructions with the supplementation of DNase treatment using the RNase-free DNase set (Qiagen). RNA quantity and composition were analyzed using an Agilent 2100 bioanalyzer (Agilent Technologies, Massy, France) and a NanoDrop ND-1000 spectrophotometer (Labtech France, Paris, France) at 260 nm and 280 nm. All microarray procedures were performed according to the manufacturer's protocol (Agilent one-color microarray-based exon analysis). Briefly, the RNAs were labeled with a low-input Quick Amp labeling kit and hybridized following a one-color microarray-based gene expression analysis protocol. The slides were scanned using a Tecan MS200 scanner and analyzed using Feature Extraction V.11.5.1.1.

Protein extraction and analysis. For proteomic analysis, 20-ml samples were collected from chemostat cultures and treated according to the standard operating procedures developed by Schwarz et al. (78) for the extraction of intracellular proteins, except that phenylmethylsulfonyl fluoride (PMSF) was not added. Samples of 200 μg of each of the lyophilized protein extracts were dissolved at 80°C in 100 μl of 0.1% RapiGest (Waters) in water. Disulfide bonds were reduced with the addition of dithiothreitol (DTT) at 2 mM and incubation at 60°C for 15 min. Cysteine residues were carboxyamidomethylated with the addition of iodoacetamide to a concentration of 10 mM and incubated in the dark at room temperature. Proteolytic digestion was performed with trypsin (10 μg/ml) at 37°C for 12 h. Protein hydrolysates were acidified with 5 μl of concentrated trifluoroacetic acid (TFA), incubated at 37°C for 20 min, and centrifuged at 18,000 × *g* for 2 min to remove the RapiGest precipitate. The supernatant was collected. Postdigestion samples at a concentration of 2 μg/μl were mixed at a ratio of 1:1 with 40 fmol/μl phosphorylase *b* internal standard tryptic digest in 200 mM ammonium formate buffer.

Quantitative two-dimensional reversed-phase liquid chromatography-tandem mass spectrometry (LC/LC-MS/MS) was performed at a high-low-pH reversed-phase/reversed-phase configuration using a nanoAcquity ultraperformance liquid chromatography (UPLC)/UPLC system (Waters Corp.) coupled with a Synapt G2 HDMS mass spectrometer (Waters Corp.) and nano-electrospray ionization, as previously described by Foster et al. (64).

Raw MS data were processed either using a Mascot Distiller (version 2.4.3.1) for peptide and protein identification and isobaric quantification or using a Progenesis QI (Nonlinear Dynamics, United Kingdom) for label-free quantification. The MS/MS spectra were searched against the UniProt *Clostridium acetobutylicum* database using the Mascot search engine (version 2.4.1) with the following search parameters: full tryptic specificity, up to two missed cleavage sites, carbamidomethylation of cysteine residues as a fixed modification, and N-terminal methionine oxidation as a variable modification.

Determination of DNA, mRNA, and protein contents. DNA and protein contents were measured in cells grown in a chemostat culture after centrifugation (4,000 × *g*, 10 min, 4°C) and washed twice with Milli-Q water. Protein content was determined via the Biuret method (79). The DNA content was determined after incubation with perchloric acid (0.5 M, 70 to 80°C, 15 to 20 min), as described by Hanson and Phillips (80). The RNA content was determined using the protocol described above for the microarrays.

Measurement of fermentation parameters. Biomass concentration was determined both by counting the number of cells per milliliter, as previously described (81), and by the DCW method after centrifugation (16,000 × *g*, 5 min, room temperature), two washes with Milli-Q water, and drying under vacuum at 80°C. The concentrations of glucose, glycerol, acetate, butyrate, lactate, pyruvate, acetoin, acetone, ethanol, and butanol were determined based on high-performance liquid chromatography (HPLC), as described by Dusséaux et al. (82), except that the concentration of H_2SO_4 was changed to 0.5 mM, as required for mobile phase optimization. The concentrations of formate and fumarate were measured using a formate assay kit (Sigma-Aldrich) and a fumarate assay kit (Sigma-Aldrich), according to the manufacturer's instructions.

Metabolic enzyme expression and purification. Information on metabolic enzyme expression and purification is provided as Text S1 in the supplemental material.

Microarray data accession number. The microarray data can be accessed at GEO through accession number GSE69973.

SUPPLEMENTAL MATERIAL

Supplemental material for this article may be found at http://mbio.asm.org/lookup/suppl/doi:10.1128/mBio.01808-15/-/DCSupplemental.

Text S1, DOCX file, 0.03 MB.
Data Set S1, XLSX file, 0.2 MB.
Data Set S2, XLSX file, 2.1 MB.
Figure S1, PDF file, 0.03 MB.
Figure S2, PDF file, 0.2 MB.
Figure S3, PDF file, 0.1 MB.
Figure S4, PDF file, 0.1 MB.
Table S1, DOCX file, 0.01 MB.
Table S2, DOCX file, 0.03 MB.
Table S3, DOCX file, 0.03 MB.

ACKNOWLEDGMENTS

We thank Jean-Louis Uribelarrea, Sophie Lamarre, and Lidwine Trouilh for help with the data analysis.

This work was financially supported by the European Community's Seventh Framework Program "CLOSTNET" (PEOPLE-ITN-2008-237942) to Minyeong Yoo.

REFERENCES

1. **Jones DT**. 2001. Applied acetone-butanol fermentation, p 125–168. In Bahl H, Dürre P (ed), Clostridia: biotechnology and medical applications. Wiley-VCH Verlag GmbH, Weinheim, Germany.
2. **Jones DT, Woods DR**. 1986. Acetone-butanol fermentation revisited. Microbiol Res **50:**484–524.
3. **Jones DT, van der Westhuizen A, Long S, Allcock ER, Reid SJ, Woods DR**. 1982. Solvent production and morphological changes in *Clostridium acetobutylicum*. Appl Environ Microbiol **43:**1434–1439.
4. **Dürre P**. 2007. Biobutanol: an attractive biofuel. Biotechnol J **2:**1525–1534. http://dx.doi.org/10.1002/biot.200700168.
5. **Ni Y, Sun Z**. 2009. Recent progress on industrial fermentative production of acetone-butanol-ethanol by *Clostridium acetobutylicum* in China. Appl Microbiol Biotechnol **83:**415–423. http://dx.doi.org/10.1007/s00253-009-2003-y.
6. **Vasconcelos I, Girbal L, Soucaille P**. 1994. Regulation of carbon and electron flow in *Clostridium acetobutylicum* grown in chemostat culture at neutral pH on mixtures of glucose and glycerol. J Bacteriol **176:**1443–1450.
7. **Girbal L, Soucaille P**. 1994. Regulation of *Clostridium acetobutylicum* metabolism as revealed by mixed-substrate steady-state continuous cultures: role of NADH/NAD ratio and ATP pool. J Bacteriol **176:**6433–6438.
8. **Girbal L, Vasconcelos I, Saint-Amans S, Soucaille P**. 1995. How neutral red modified carbon and electron flow in *Clostridium acetobutylicum*

grown in chemostat culture at neutral pH. FEMS Microbiol Rev **16:** 151–162. http://dx.doi.org/10.1111/j.1574-6976.1995.tb00163.x.
9. **Girbal L, Croux C, Vasconcelos I, Soucaille P.** 1995. Regulation of metabolic shifts in *Clostridium acetobutylicum* ATCC 824. FEMS Microbiol Rev 17:287–297. http://dx.doi.org/10.1111/j.1574-6976.1995.tb00212.x.
10. **Girbal L, Soucaille P.** 1998. Regulation of solvent production in *Clostridium acetobutylicum*. Trends Biotechnol **16:**11–16. http://dx.doi.org/10.1016/S0167-7799(97)01141-4.
11. **Wiesenborn DP, Rudolph FB, Papoutsakis ET.** 1989. Phosphotransbutyrylase from *Clostridium acetobutylicum* ATCC 824 and its role in acidogenesis. Appl Environ Microbiol **55:**317–322.
12. **Wiesenborn DP, Rudolph FB, Papoutsakis ET.** 1989. Coenzyme A transferase from *Clostridium acetobutylicum* ATCC 824 and its role in the uptake of acids. Appl Environ Microbiol **55:**323–329.
13. **Sauer U, Dürre P.** 1995. Differential induction of genes related to solvent formation during the shift from acidogenesis to solventogenesis in continuous culture of *Clostridium acetobutylicum*. FEMS Microbiol Lett **125:** 115–120. http://dx.doi.org/10.1111/j.1574-6968.1995.tb07344.x.
14. **Janssen H, Grimmler C, Ehrenreich A, Bahl H, Fischer R.** 2012. A transcriptional study of acidogenic chemostat cells of *Clostridium acetobutylicum*—solvent stress caused by a transient n-butanol pulse. J Biotechnol **161:**354–365. http://dx.doi.org/10.1016/j.jbiotec.2012.03.027.
15. **Schwarz KM, Kuit W, Grimmler C, Ehrenreich A, Kengen SWM.** 2012. A transcriptional study of acidogenic chemostat cells of *Clostridium acetobutylicum*—cellular behavior in adaptation to n-butanol. J Biotechnol **161:**366–377. http://dx.doi.org/10.1016/j.jbiotec.2012.03.018.
16. **Wang Q, Venkataramanan K, Huang H, Papoutsakis ET, Wu CH.** 2013. Transcription factors and genetic circuits orchestrating the complex, multilayered response of *Clostridium acetobutylicum* to butanol and butyrate stress. BMC Syst Biol **7:**120. http://dx.doi.org/10.1186/1752-0509-7-120.
17. **Venkataramanan KP, Jones SW, McCormick KP, Kunjeti SG, Ralston MT, Meyers BC, Papoutsakis ET.** 2013. The clostridium small RNome that responds to stress: the paradigm and importance of toxic metabolite stress in C. acetobutylicum. BMC Genomics **14:**849. http://dx.doi.org/10.1186/1471-2164-14-849.
18. **Cornillot E, Soucaille P.** 1996. Solvent-forming genes in Clostridia. Nature **380:**489. http://dx.doi.org/10.1038/380489a0.
19. **Cornillot E, Nair RV, Papoutsakis ET, Soucaille P.** 1997. The genes for butanol and acetone formation in *Clostridium acetobutylicum* ATCC 824 reside on a large plasmid whose loss leads to degeneration of the strain. J Bacteriol **179:**5442–5447.
20. **Nolling J, Breton G, Omelchenko MV, Makarova KS, Zeng Q, Gibson R, Lee HM, Dubois J, Qiu D, Hitti J, Wolf YI, Tatusov RL, Sabathe F, Doucette-Stamm L, Soucaille P, Daly MJ, Bennett GN, Koonin EV, Smith DR.** 2001. Genome sequence and comparative analysis of the solvent-producing bacterium *Clostridium acetobutylicum*. J Bacteriol **183:** 4823–4838. http://dx.doi.org/10.1128/JB.183.16.4823-4838.2001.
21. **Alsaker KV, Papoutsakis ET.** 2005. Transcriptional program of early sporulation and stationary-phase events in *Clostridium acetobutylicum*. J Bacteriol **187:**7103–7118. http://dx.doi.org/10.1128/JB.187.20.7103-7118.2005.
22. **Janssen H, Döring C, Ehrenreich A, Voigt B, Hecker M, Bahl H, Fischer R.** 2010. A proteomic and transcriptional view of acidogenic and solventogenic steady-state cells of *Clostridium acetobutylicum* in a chemostat culture. Appl Microbiol Biotechnol **87:**2209–2226. http://dx.doi.org/10.1007/s00253-010-2741-x.
23. **Jones SW, Paredes CJ, Tracy B, Cheng N, Sillers R, Senger RS, Papoutsakis ET.** 2008. The transcriptional program underlying the physiology of clostridial sporulation. Genome Biol **9:**R114. http://dx.doi.org/10.1186/gb-2008-9-7-r114.
24. **Sullivan L, Bennett GN.** 2006. Proteome analysis and comparison of *Clostridium acetobutylicum* ATCC 824 and Spo0A strain variants. J Ind Microbiol Biotechnol **33:**298–308. http://dx.doi.org/10.1007/s10295-005-0050-7.
25. **Tomas CA, Alsaker KV, Bonarius HPJ, Hendriksen WT, Yang H, Beamish JA, Paredes CJ, Papoutsakis ET.** 2003. DNA array-based transcriptional analysis of asporogenous, nonsolventogenic *Clostridium acetobutylicum* strains SKO1 and M5. J Bacteriol **185:**4539–4547. http://dx.doi.org/10.1128/JB.185.15.4539-4547.2003.
26. **Schaffer S, Isci N, Zickner B, Dürre P.** 2002. Changes in protein synthesis and identification of proteins specifically induced during solventogenesis in *Clostridium acetobutylicum*. Electrophoresis **23:**110–121. http://dx.doi.org/10.1002/1522-2683(200201)23:1<110::AID-ELPS110>3.0.CO;2-G.
27. **Paredes CJ, Senger RS, Spath IS, Borden JR, Sillers R, Papoutsakis ET.** 2007. A general framework for designing and validating oligomer-based DNA microarrays and its application to *Clostridium acetobutylicum*. Appl Environ Microbiol **73:**4631–4638. http://dx.doi.org/10.1128/AEM.00144-07.
28. **Servinsky MD, Kiel JT, Dupuy NF, Sund CJ.** 2010. Transcriptional analysis of differential carbohydrate utilization by *Clostridium acetobutylicum*. Microbiology **156:**3478–3491. http://dx.doi.org/10.1099/mic.0.037085-0.
29. **Grimmler C, Held C, Liebl W, Ehrenreich A.** 2010. Transcriptional analysis of catabolite repression in *Clostridium acetobutylicum* growing on mixtures of D-glucose and D-xylose. J Biotechnol **150:**315–323. http://dx.doi.org/10.1016/j.jbiotec.2010.09.938.
30. **Tan Y, Liu Z, Liu Z, Zheng H, Li F.** 2015. Comparative transcriptome analysis between csrA-disruption *Clostridium acetobutylicum* and its parent strain. Mol Biosyst **11:**1434–1442. http://dx.doi.org/10.1039/C4MB00600C.
31. **Mao S, Luo Y, Zhang T, Li J, Bao G, Zhu Y, Chen Z, Zhang Y, Li Y, Ma Y.** 2010. Proteome reference map and comparative proteomic analysis between a wild type *Clostridium acetobutylicum* DSM 1731 and its mutant with enhanced butanol tolerance and butanol yield. J Proteome Res **9:**3046–3061. http://dx.doi.org/10.1021/pr9012078.
32. **Mao S, Luo Y, Bao G, Zhang Y, Li Y, Ma Y.** 2011. Comparative analysis on the membrane proteome of *Clostridium acetobutylicum* wild type strain and its butanol-tolerant mutant. Mol Biosyst **7:**1660–1677. http://dx.doi.org/10.1039/c0mb00330a.
33. **Jang Y, Han M, Lee J, Im JA, Lee YH, Papoutsakis ET, Bennett G, Lee SY.** 2014. Proteomic analyses of the phase transition from acidogenesis to solventogenesis using solventogenic and non-solventogenic *Clostridium acetobutylicum* strains. Appl Microbiol Biotechnol **98:**5105–5115. http://dx.doi.org/10.1007/s00253-014-5738-z.
34. **Magdeldin S, Enany S, Yoshida Y, Xu B, Zhang Y, Zureena Z, Lokamani I, Yaoita E, Yamamoto T.** 2014. Basics and recent advances of two dimensional-polyacrylamide gel electrophoresis. Clin Proteomics **11:**16. http://dx.doi.org/10.1186/1559-0275-11-16.
35. **Sivagnanam K, Raghavan VG, Shah M, Hettich RL, Verberkmoes NC, Lefsrud MG.** 2011. Comparative shotgun proteomic analysis of *Clostridium acetobutylicum* from butanol fermentation using glucose and xylose. Proteome Sci **9:**66. http://dx.doi.org/10.1186/1477-5956-9-66.
36. **Hou S, Jones SW, Choe LH, Papoutsakis ET, Lee KH.** 2013. Workflow for quantitative proteomic analysis of *Clostridium acetobutylicum* ATCC 824 using iTRAQ tags. Methods **61:**269–276. http://dx.doi.org/10.1016/j.ymeth.2013.03.013.
37. **Grimmler C, Janssen H, Krauβe D, Fischer R, Bahl H, Dürre P, Liebl W, Ehrenreich A.** 2011. Genome-wide gene expression analysis of the switch between acidogenesis and solventogenesis in continuous cultures of *Clostridium acetobutylicum*. J Mol Microbiol Biotechnol **20:**1–15. http://dx.doi.org/10.1159/000320973.
38. **Tracy BP, Jones SW, Papoutsakis ET.** 2011. Inactivation of sigmaE and sigmaG in *Clostridium acetobutylicum* illuminates their roles in clostridial-cell-form biogenesis, granulose synthesis, solventogenesis, and spore morphogenesis. J Bacteriol **193:**1414–1426. http://dx.doi.org/10.1128/JB.01380-10.
39. **Jones SW, Tracy BP, Gaida SM, Papoutsakis ET.** 2011. Inactivation of sigmaF in *Clostridium acetobutylicum* ATCC 824 blocks sporulation prior to asymmetric division and abolishes sigmaE and sigmaG protein expression but does not block solvent formation. J Bacteriol **193:**2429–2440. http://dx.doi.org/10.1128/JB.00088-11.
40. **Venkataramanan KP, Min L, Hou S, Jones SW, Ralston MT, Lee KH, Papoutsakis ET.** 2015. Complex and extensive post-transcriptional regulation revealed by integrative proteomic and transcriptomic analysis of metabolite stress response in *Clostridium acetobutylicum*. Biotechnol Biofuels **8:**1–29. http://dx.doi.org/10.1186/s13068-015-0260-9.
41. **Bahl H, Andersch W, Gottschalk G.** 1982. Continuous production of acetone and butanol by *Clostridium acetobutylicum* in a two-stage phosphate limited chemostat. Eur J Appl Microbiol Biotechnol **15:**201–205. http://dx.doi.org/10.1007/BF00499955.
42. **Boynton ZL, Bennet GN, Rudolph FB.** 1996. Cloning, sequencing, and expression of clustered genes encoding beta-hydroxybutyryl-coenzyme A (CoA) dehydrogenase, crotonase, and butyryl-CoA dehydrogenase from *Clostridium acetobutylicum* ATCC 824. J Bacteriol **178:**3015–3024.

43. **Li F, Hinderberger J, Seedorf H, Zhang J, Buckel W, Thauer RK**. 2008. Coupled ferredoxin and crotonyl coenzyme A (CoA) reduction with NADH catalyzed by the butyryl-CoA dehydrogenase/Etf complex from *Clostridium kluyveri*. J Bacteriol **190:**843–850. http://dx.doi.org/10.1128/JB.01417-07.
44. **Sillers R, Chow A, Tracy B, Papoutsakis ET**. 2008. Metabolic engineering of the non-sporulating, non-solventogenic *Clostridium acetobutylicum* strain M5 to produce butanol without acetone demonstrate the robustness of the acid-formation pathways and the importance of the electron balance. Metab Eng **10:**321–332. http://dx.doi.org/10.1016/j.ymben.2008.07.005.
45. **Dash S, Mueller TJ, Venkataramanan KP, Papoutsakis ET, Maranas CD**. 2014. Capturing the response of *Clostridium acetobutylicum* to chemical stressors using a regulated genome-scale metabolic model. Biotechnol Biofuels **7:**144. http://dx.doi.org/10.1186/s13068-014-0144-4.
46. **McAnulty MJ, Yen JY, Freedman BG, Senger RS**. 2012. Genome-scale modeling using flux ratio constraints to enable metabolic engineering of clostridial metabolism in silico. BMC Syst Biol **6:**42. http://dx.doi.org/10.1186/1752-0509-6-42.
47. **Nair RV, Bennett GN, Papoutsakis ET**. 1994. Molecular characterization of an aldehyde/alcohol dehydrogenase gene from *Clostridium acetobutylicum* ATCC 824. J Bacteriol **176:**871–885.
48. **Fischer RJ, Helms J, Durre P**. 1993. Cloning, sequencing, and molecular analysis of the sol operon of *Clostridium acetobutylicum*, a chromosomal locus involved in solventogenesis. J Bacteriol **175:**6959–6969.
49. **Walter KA, Bennett GN, Papoutsakis ET**. 1992. Molecular characterization of two *Clostridium acetobutylicum* ATCC 824 butanol dehydrogenase isozyme genes. J Bacteriol **174:**7149–7158.
50. **Welch RW, Rudolph FB, Papoutsakis ET**. 1989. Purification and characterization of the NADH-dependent butanol dehydrogenase from *Clostridium acetobutylicum* (ATCC 824). Arch Biochem Biophys **273:**309–318. http://dx.doi.org/10.1016/0003-9861(89)90489-X.
51. **Sulzenbacher G, Alvarez K, Van Den Heuvel RHH, Versluis C, Spinelli S, Campanacci V, Valencia C, Cambillau C, Eklund H, Tegoni M**. 2004. Crystal structure of E.coli alcohol dehydrogenase YqhD: evidence of a covalently modified NADP coenzyme. J Mol Biol **342:**489–502. http://dx.doi.org/10.1016/j.jmb.2004.07.034.
52. **Durre P, Kuhn A, Gottwald M, Gottschalk G**. 1987. Enzymatic investigations on butanol dehydrogenase and butyraldehyde dehydrogenase in extracts of *Clostridium acetobutylicum*. Appl Microbiol Biotechnol **26:**268–272. http://dx.doi.org/10.1007/BF00286322.
53. **Schmidt CNG, Jervis L**. 1980. Affinity purification of glutamate synthase from Escherichia coli. Anal Biochem **104:**127–129. http://dx.doi.org/10.1016/0003-2697(80)90286-9.
54. **Sakamoto N, Kotre AM, Savageau MA**. 1975. Glutamate dehydrogenase from *Escherichia coli*: purification and properties. J Bacteriol **124:**775–783.
55. **Amador-Noguez D, Feng X-, Fan J, Roquet N, Rabitz H, Rabinowitz JD**. 2010. Systems-level metabolic flux profiling elucidates a complete, bifurcated tricarboxylic acid cycle in *Clostridium acetobutylicum*. J Bacteriol **192:**4452–4461. http://dx.doi.org/10.1128/JB.00490-10.
56. **Senger RS, Papoutsakis ET**. 2008. Genome-scale model for *Clostridium acetobutylicum*: part I. Metabolic network resolution and analysis. Biotechnol Bioeng **101:**1036–1052. http://dx.doi.org/10.1002/bit.22010.
57. **Senger RS, Papoutsakis ET**. 2008. Genome-scale model for *Clostridium acetobutylicum*: part II. Development of specific proton flux states and numerically determined sub-systems. Biotechnol Bioeng **101:**1053–1071. http://dx.doi.org/10.1002/bit.22009.
58. **Lee J, Yun H, Feist AM, Palsson BØ, Lee SY**. 2008. Genome-scale reconstruction and in silico analysis of the *Clostridium acetobutylicum* ATCC 824 metabolic network. Appl Microbiol Biotechnol **80:**849–862. http://dx.doi.org/10.1007/s00253-008-1654-4.
59. **Harris LM, Desai RP, Welker NE, Papoutsakis ET**. 2000. Characterization of recombinant strains of the *Clostridium acetobutylicum* butyrate kinase inactivation mutant: need for new phenomenological models for solventogenesis and butanol inhibition? Biotechnol Bioeng **67:**1–11. http://dx.doi.org/10.1002/(SICI)1097-0290(20000105)67:1<1::AID-BIT1>3.0.CO;2-G.
60. **Lee JY, Jang Y, Lee J, Papoutsakis ET, Lee SY**. 2009. Metabolic engineering of *Clostridium acetobutylicum* M5 for highly selective butanol production. Biotechnol J **4:**1432–1440. http://dx.doi.org/10.1002/biot.200900142.
61. **Neidhardt FC, Umbarger HE**. 1996. Chemical composition of *E. coli*, p 13–16. In Neidhardt FC, Curtiss R, III, Ingraham JL, Lin ECC, Low KB, Magasanik B, Reznikoff WS, Riley M, Schaechter M, Umbarger HE (ed), *Escherichia coli* and *Salmonella*: cellular and molecular biology, 2nd ed. American Society for Microbiology, Washington, DC.
62. **Pramanik J, Keasling JD**. 1997. Stoichiometric model of Escherichia coli metabolism: incorporation of growth-rate dependent biomass composition and mechanistic energy requirements. Biotechnol Bioeng **56:**398–421.
63. **Miller JA, Menon V, Goldy J, Kaykas A, Lee C, Smith KA, Shen EH, Phillips JW, Lein ES, Hawrylycz MJ**. 2014. Improving reliability and absolute quantification of human brain microarray data by filtering and scaling probes using RNA-Seq. BMC Genomics **15:**154. http://dx.doi.org/10.1186/1471-2164-15-154.
64. **Foster MW, Morrison LD, Todd JL, Snyder LD, Thompson JW, Soderblom EJ, Plonk K, Weinhold KJ, Townsend R, Minnich A, Moseley MA**. 2015. Quantitative proteomics of bronchoalveolar lavage fluid in idiopathic pulmonary fibrosis. J Proteome Res **14:**1238–1249. http://dx.doi.org/10.1021/pr501149m.
65. **Bremer H, Dennis PP**. 1996. Modulation of chemical composition and other parameters of the cell by growth rate, p 1553–1569. In Neidhardt FC, Curtiss R, III, Ingraham JL, Lin ECC, Low KB, Magasanik B, Reznikoff WS, Riley M, Schaechter M, Umbarger HE (ed), *Escherichia coli* and *Salmonella*: cellular and molecular biology, 2nd ed. American Society for Microbiology, Washington, DC.
66. **Fontaine L, Meynial-Salles I, Girbal L, Yang X, Croux C, Soucaille P**. 2002. Molecular characterization and transcriptional analysis of *adhE2*, the gene encoding the NADH-dependent aldehyde/alcohol dehydrogenase responsible for butanol production in alcohologenic cultures of *Clostridium acetobutylicum* ATCC 824. J Bacteriol **184:**821–830. http://dx.doi.org/10.1128/JB.184.3.821-830.2002.
67. **Amador-Noguez D, Brasg IA, Feng X-, Roquet N, Rabinowitz JD**. 2011. Metabolome remodeling during the acidogenic-solventogenic transition in *Clostridium acetobutylicum*. Appl Environ Microbiol **77:**7984–7997. http://dx.doi.org/10.1128/AEM.05374-11.
68. **Sabathé F, Bélaïch A, Soucaille P**. 2002. Characterization of the cellulolytic complex (cellulosome) of *Clostridium acetobutylicum*. FEMS Microbiol Lett **217:**15–22. http://dx.doi.org/10.1111/j.1574-6968.2002.tb11450.x.
69. **Harris LM, Welker NE, Papoutsakis ET**. 2002. Northern, morphological, and fermentation analysis of spo0A inactivation and overexpression in *Clostridium acetobutylicum* ATCC 824. J Bacteriol **184:**3586–3597. http://dx.doi.org/10.1128/JB.184.13.3586-3597.2002.
70. **Ravagnani A, Jennert KCB, Steiner E, Grunberg R, Jefferies JR, Wilkinson SR, Young DI, Tidswell EC, Brown DP, Youngman P, Morris JG, Young M**. 2000. Spo0A directly controls the switch from acid to solvent production in solvent-forming clostridia. Mol Microbiol **37:**1172–1185. http://dx.doi.org/10.1046/j.1365-2958.2000.02071.x.
71. **Thormann K, Feustel L, Lorenz K, Nakotte S, Durre P**. 2002. Control of butanol formation in *Clostridium acetobutylicum* by transcriptional activation. J Bacteriol **184:**1966–1973. http://dx.doi.org/10.1128/JB.184.7.1966-1973.2002.
72. **Tomas CA, Beamish J, Papoutsakis ET**. 2004. Transcriptional analysis of butanol stress and tolerance in *Clostridium acetobutylicum*. J Bacteriol **186:**2006–2018. http://dx.doi.org/10.1128/JB.186.7.2006-2018.2004.
73. **Hu K, Zhao M, Zhang T, Zha M, Zhong C, Jiang Y, Ding J**. 2013. Structures of trans-2-enoyl-CoA reductases from *Clostridium acetobutylicum* and *Treponema denticola*: insights into the substrate specificity and the catalytic mechanism. Biochem J **449:**79–89. http://dx.doi.org/10.1042/BJ20120871.
74. **Schreiber W, Durre P**. 1999. The glyceraldehyde-3-phosphate dehydrogenase of *Clostridium acetobutylicum*: isolation and purification of the enzyme, and sequencing and localization of the gap gene within a cluster of other glycolytic genes. Microbiology **145:**1839–1847. http://dx.doi.org/10.1099/13500872-145-8-1839.
75. **Iddar A, Valverde F, Serrano A, Soukri A**. 2002. Expression, purification, and characterization of recombinant nonphosphorylating NADP-dependent glyceraldehyde-3-phosphate dehydrogenase from *Clostridium acetobutylicum*. Protein Expr Purif **25:**519–526. http://dx.doi.org/10.1016/S1046-5928(02)00032-3.
76. **Au J, Choi J, Jones SW, Venkataramanan KP, Antoniewicz MR**. 2014. Parallel labeling experiments validate *Clostridium acetobutylicum* metabolic network model for C metabolic flux analysis. Metab Eng **26:**23–33. http://dx.doi.org/10.1016/j.ymben.2014.08.002.

77. **Roos JW, McLaughlin JK, Papoutsakis ET**. 1985. The effect of pH on nitrogen supply, cell lysis, and solvent production in fermentations of *Clostridium acetobutylicum*. Biotechnol Bioeng **27:**681–694. http://dx.doi.org/10.1002/bit.260270518.
78. **Schwarz K, Fiedler T, Fischer R, Bahl H**. 2007. A standard operating procedure (SOP) for the preparation of intra- and extracellular proteins of *Clostridium acetobutylicum* for proteome analysis. J Microbiol Methods **68:**396–402. http://dx.doi.org/10.1016/j.mimet.2006.09.018.
79. **Peterson GL**. 1983. Determination of total protein. Methods Enzymol **91:**95–119.
80. **Hanson R, Phillips J**. 1981. Chemical composition, p 328–364. In Gerhardt P, Murray RGE, Costilow RN, Nester EW, Wood WA, Krieg NR, Phillips GB (ed), Manual of methods for general bacteriology. American Society for Microbiology, Washington, DC.
81. **Ferras E, Minier M, Goma G**. 1986. Acetonobutylic fermentation: improvement of performances by coupling continuous fermentation and ultrafiltration. Biotechnol Bioeng **28:**523–533. http://dx.doi.org/10.1002/bit.260280408.
82. **Dusséaux S, Croux C, Soucaille P, Meynial-Salles I**. 2013. Metabolic engineering of *Clostridium acetobutylicum* ATCC 824 for the high-yield production of a biofuel composed of an isopropanol/butanol/ethanol mixture. Metab Eng **18:**1–8. http://dx.doi.org/10.1016/j.ymben.2013.03.003.

Yoo et al. Biotechnol Biofuels (2016) 9:92
DOI 10.1186/s13068-016-0507-0

Biotechnology for Biofuels

RESEARCH Open Access

Elucidation of the roles of *adhE1* and *adhE2* in the primary metabolism of *Clostridium acetobutylicum* by combining in-frame gene deletion and a quantitative system-scale approach

Minyeong Yoo[1,2,3], Christian Croux[1,2,3], Isabelle Meynial-Salles[1,2,3] and Philippe Soucaille[1,2,3,4*]

Abstract

Background: *Clostridium acetobutylicum* possesses two homologous *adhE* genes, *adhE1* and *adhE2*, which have been proposed to be responsible for butanol production in solventogenic and alcohologenic cultures, respectively. To investigate their contributions in detail, in-frame deletion mutants of each gene were constructed and subjected to quantitative transcriptomic (mRNA molecules/cell) and fluxomic analyses in acidogenic, solventogenic, and alcohologenic chemostat cultures.

Results: Under solventogenesis, compared to the control strain, only Δ*adhE1* mutant exhibited significant changes showing decreased butanol production and transcriptional expression changes in numerous genes. In particular, *adhE2* was over expressed (126-fold); thus, AdhE2 can partially replace AdhE1 for butanol production (more than 30 % of the in vivo butanol flux) under solventogenesis. Under alcohologenesis, only Δ*adhE2* mutant exhibited striking changes in gene expression and metabolic fluxes, and butanol production was completely lost. Therefore, it was demonstrated that AdhE2 is essential for butanol production and thus metabolic fluxes were redirected toward butyrate formation. Under acidogenesis, metabolic fluxes were not significantly changed in both mutants except the complete loss of butanol formation in Δ*adhE2*, but numerous changes in gene expression were observed. Furthermore, most of the significantly up- or down-regulated genes under this condition showed the same pattern of change in both mutants.

Conclusions: This quantitative system-scale analysis confirms the proposed roles of AdhE1 and AdhE2 in butanol formation that AdhE1 is the key enzyme under solventogenesis, whereas AdhE2 is the key enzyme for butanol formation under acidogenesis and alcohologenesis. Our study also highlights the metabolic flexibility of *C. acetobutylicum* to genetic alterations of its primary metabolism.

Keywords: AdhE, Butanol, *Clostridium acetobutylicum*, System-scale analysis

Background

Clostridium acetobutylicum is now considered as the model organism for the study of solventogenic Clostridia [1, 2]. The superiority of butanol over ethanol as an alternative biofuel has attracted research interest into *C. acetobutylicum* and other recombinant bacteria producing butanol as major products [3].

In phosphate-limited chemostat cultures, *C. acetobutylicum* can be maintained in three different stable metabolic states [4–8] without cellular differentiation [9]: acidogenic (producing acetate and butyrate) when grown at neutral pH with glucose; solventogenic (producing

*Correspondence: philippe.soucaille@insa-toulouse.fr
[4] Metabolic Explorer, Biopôle Clermont-Limagne, Saint Beauzire, France
Full list of author information is available at the end of the article

acetone, butanol, and ethanol) when grown at low pH with glucose; and alcohologenic (forming butanol and ethanol but not acetone) when grown at neutral pH under conditions of high NAD(P)H availability [5, 6, 10].

AdhE1 (CA_P0162 gene product, also referred to as Aad) has long been considered as an NADH-dependent bifunctional alcohol/aldehyde dehydrogenase responsible for alcohol formation in solventogenic *C. acetobutylicum* cultures [1, 2, 11]. Recently, however, AdhE1 was purified and shown to have lost most of its alcohol dehydrogenase activity despite its NADH-dependent aldehyde dehydrogenase activity [12].

Prior to the identification of *adhE2* (CA_P0035), the existence of alcohologenesis-specific gene(s) responsible for alcohol formation was predicted because (i) there was high NADH-dependent butanol dehydrogenase activity in alcohologenesis versus high NADPH-dependent butanol dehydrogenase activity in solventogenesis [5, 7] and (ii) previously identified genes related to butanol production (*bdhA*, *bdhB*, *adhE1*) were not induced in alcohologenic cultures [13]. The *adhE2* gene is the second aldehyde/alcohol dehydrogenase-encoding gene and is carried by the pSol1 megaplasmid, as is *adhE1* [14]. The two genes are not clustered, in contrast to the observations for *C. ljungdahlii* [15] and their expression patterns differ [9, 12]. *adhE1, ctfA,* and *ctfB* (CA_P0163 and CA_P0164) form the *sol* operon [1, 11]; *ctfA* and *ctfB* encode the CoA-transferase responsible for the first step of acetone formation, while the second step, catalyzed by acetoacetate decarboxylase, is encoded by *adc* (CA_P0165), located downstream of the *sol* operon. However, *adc* is transcribed under the control of its own promoter, which is oriented in the opposite direction of the *sol* operon [11].

In the three metabolic states, the contributions of the different enzymes responsible for the butyraldehyde dehydrogenase and butanol dehydrogenase activities to butanol flux have recently been characterized [12]. Under acidogenesis, the low butanol flux is catalyzed by AdhE2 (100 %) for butyraldehyde dehydrogenase activity, while BdhB and BdhA are responsible for butanol dehydrogenase activity. Under solventogenesis, AdhE1 (95 %; the other 5 % is contributed by AdhE2) is the key player responsible for butyraldehyde dehydrogenase activity, while BdhB, BdhA, and BdhC are responsible for butanol dehydrogenase activity. Under alcohologenesis, AdhE2 plays a major role in both butyraldehyde dehydrogenase (100 %) and butanol dehydrogenase activities. In the study of Cooksley et al. [16], *adhE1* and *adhE2* knockout mutants were (i) constructed using the ClosTron method [17] and (ii) phenotypically characterized in batch culture using Clostridium basal medium (CBMS) without pH adjustment. The *adhE1* knockout mutant obtained in their study exhibited low ethanol and no butanol formation along with scant acetone production; these findings were consistent with the polar effect of the intron on *ctfAB* transcription [16]. Using the *adhE2* knockout mutant, no alteration of solvent production was observed; however, the *adhE2* knockout mutant has not been evaluated under alcohologenic conditions, under which it is normally thought to play a major role [14].

The aim of this study was to perform clean individual in-frame deletions of *adhE1* and *adhE2* to characterize their roles in butanol formation in the three different metabolic states in more detail. Furthermore, to study the metabolic flexibility of *C. acetobutylicum* in response to each of these gene deletions, a complete fluxomic and quantitative transcriptomic analysis was also performed in the three conditions known for the wild-type strains: acidogenic, solventogenic, and alcohologenic states. The results presented here not only support our previous studies [12, 14] on the roles of AdhE1 and AdhE2 in butanol formation in different metabolic states but also highlight the metabolic flexibility of *C. acetobutylicum* to genetically alter its primary metabolism.

Results and discussion

Construction of *ΔadhE1* and *ΔadhE2* mutant strains

Construction of the *ΔadhE2* mutant was relatively straightforward, as *adhE2* is expressed in a monocistronic operon [14] (Fig. 1a). However, the position of *adhE1* as the first gene of the *sol* operon made the construction of *ΔadhE1* more complicated because the transcription of downstream *ctfAB* genes could be affected. Figure 1b–d shows different configurations of the *sol* operon promoter, *ctfAB* genes, and either *catP* cassette with two FRT (Flippase Recognition Target) sites or a single FRT site remaining after Flippase (Flp)-FRT recombination of the three different types of *ΔadhE1* mutants generated in this study. The first constructed *ΔadhE1* mutant, *ΔCA_C1502ΔuppΔadhE1::catP* (Fig. 1b), was unable to form acetone as predicted because a transcriptional terminator was included in the *catP* cassette, which is located upstream of *ctfAB* encoding the acetoacetyl coenzyme A:acetate/butyrate:coenzyme A transferase that is responsible for the first specific step of acetone formation [11]. However, after removing the *catP* cassette from *ΔCA_C1502ΔuppΔadhE1::catP*, acetone production was unexpectedly not recovered in *ΔCA_C1502ΔuppΔadhE1* (Fig. 1c). The presence of the megaplasmid pSOL1 was confirmed by the production of ethanol and butanol under alcohologenic conditions and was attributed to *adhE2* expression. By sequencing the pSOL1 region around the *adhE1* deletion, we confirmed that there was no mutation in the *sol* promoter, *ctfAB* and *adc* (encoding acetoacetate decarboxylase, which is responsible for the last step of acetone production). Based on these results, the possibility of unsuspected

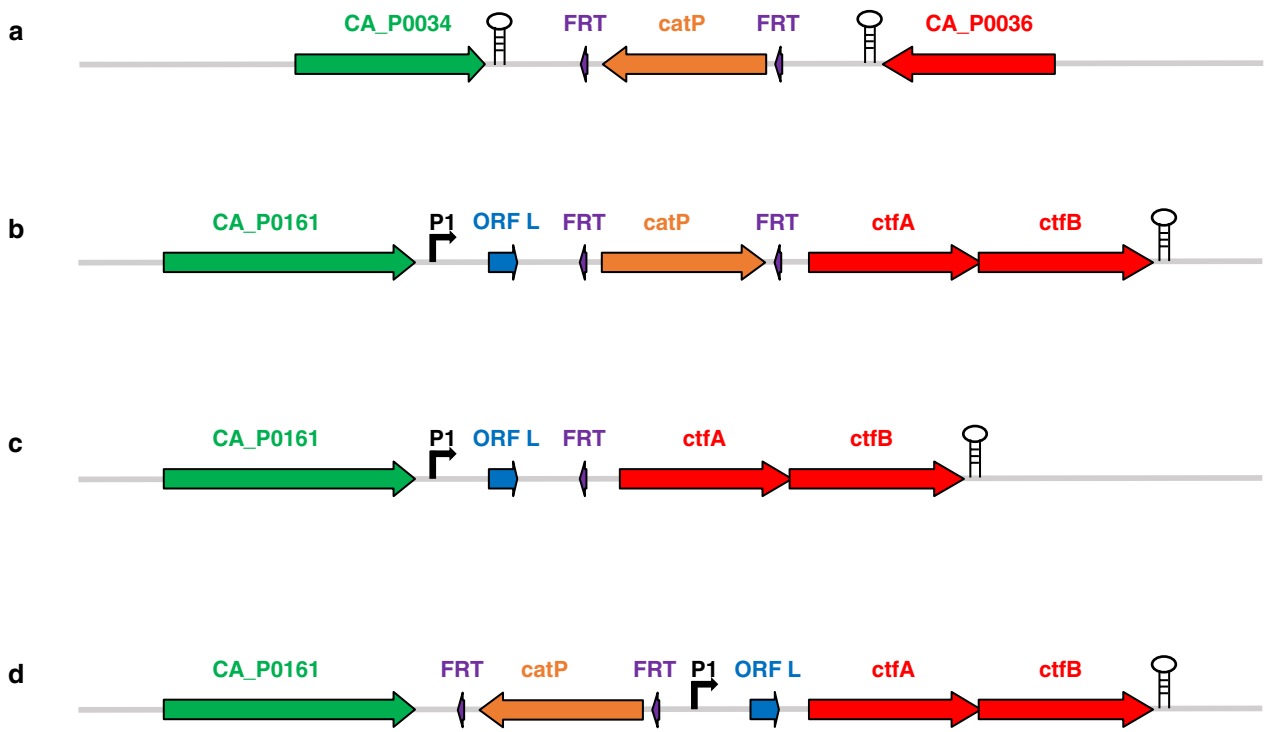

Fig. 1 Construction of *ΔadhE1 and ΔadhE2*. The single construction of *ΔadhE2 and* three different constructions of *ΔadhE1* are described: *ΔCA_C1502ΔuppΔadhE2::catP* (**a**), *ΔCA_C1502ΔuppΔadhE1::catP* (**b**), *ΔCA_C1502ΔuppΔadhE1* (**c**), and *ΔCA_C1502ΔuppΔadhE1::catP-A1A4* (**d**). P1 indicating the promoter of the *sol* operon and ORF L were previously proposed by Fischer et al. [11]

early transcriptional termination by the FRT site remaining after *catP* removal was deduced. To confirm the early termination of transcription by an FRT site and to eliminate this polar effect on acetone production, a new plasmid was constructed to position both of the FRT sites carried by the *catP* cassette upstream of the *sol* operon promoter and was used to construct the *ΔadhE1* mutant *ΔCA_C1502ΔuppΔadhE1::catP-A1A4* mutant (Fig. 1d). Consistent with our hypothesis, this last *ΔadhE1* mutant recovered acetone production (Fig. 2, Additional file 1: Fig. S3). To the best of our knowledge, the potential role of an FRT site as a transcriptional terminator was reported once in *Salmonella* [18] and twice in yeast [19, 20], although the FRT site is not generally recognized as possessing this additional activity. However, the high score of the FRT site hit from the "Dimers and Hairpin Loops analysis" in Vector NTI software (Invitrogen) and the detection of this activity upon deleting *adhE1* in *C. acetobutylicum* unambiguously demonstrate that the FRT site can function as a transcriptional terminator.

Hereafter, *C. acetobutylicum ΔCA_C1502ΔuppΔadhE1::catP-A1A4* (Fig. 1d) is referred to as *ΔadhE1* in all the chemostat culture experiments.

Carbon and electron fluxes of *ΔadhE1* and *ΔadhE2* mutants under different physiological conditions

The *ΔadhE1* and *ΔadhE2* mutants were first evaluated under acidogenic conditions and compared to previously published data for the control strain [12]. All the strains behaved the same, and no significant changes in the metabolic fluxes were recorded (Additional file 1: Fig. S3), except that butanol production was completely abolished in the *ΔadhE2* mutant strain (Fig. 2, Additional file 1: Fig. S3).

The two mutant strains were then evaluated under solventogenic conditions and compared to previously published data for the control strain [12]. The control and *ΔadhE2* strains behaved the same, with no significant change in metabolic fluxes (Additional file 1: Fig. S3). However, the *ΔadhE1* mutant exhibited a completely different behavior. In the first phase, before the "pseudo steady state" was reached, this mutant exhibited considerable fluctuations in growth, glucose consumption, and metabolite profiles. Under "pseudo steady state conditions," the butanol and acetone fluxes were stable, while the butyrate flux showed fluctuations between 2.2 and 2.9 mmol g^{-1} h^{-1}. In *ΔadhE1*, the butanol, ethanol, and

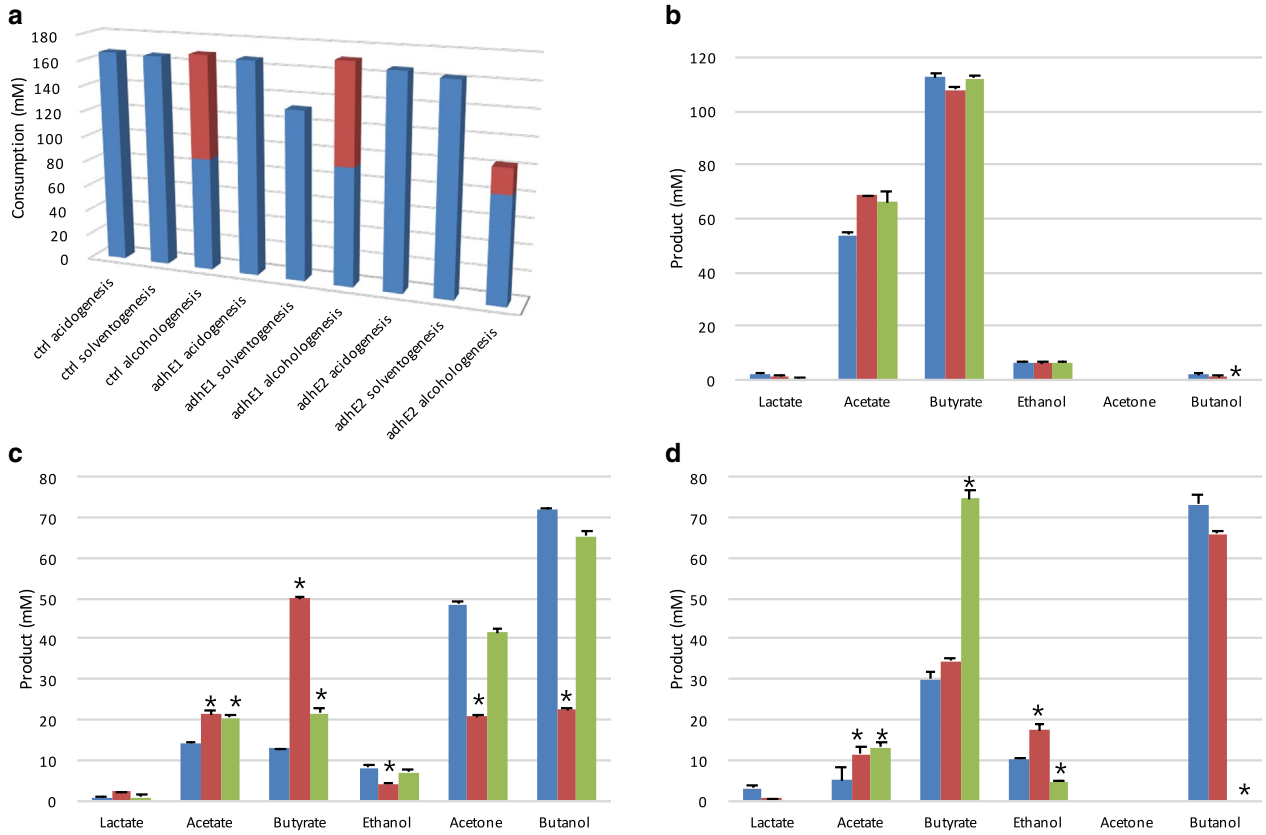

Fig. 2 Substrates and products profile under three different conditions for the control, *ΔadhE1* and *ΔadhE2* strains. **a** Carbon source consumption: glucose (*blue*) and glycerol (*red*). Product profiles in acidogenesis (**b**), solventogenesis (**c**), and alcohologenesis (**d**). For (**b**), (**c**), and (**d**), each histogram indicates different strains: control (*blue*), *ΔadhE1* (*red*), and *ΔadhE2* (*green*). Each *error bar* indicates the SEM from the mean of duplicate samples. *The value is significantly different from the value of the control at the 1 % level based on the *P* value obtained from Student's T-test

acetone fluxes decreased by 60, 49, and 46 %, respectively (Additional file 1: Fig. S3), compared to the control strain; thus, the acetone and ethanol fluxes were not reduced as greatly as the butanol fluxes. These results support the previously proposed [1, 11, 12, 14] key role of AdhE1 in butanol production under solventogenic conditions and demonstrate that an *adhE1* knockout strain with no polar effect on *ctfAB* transcription can still produce acetone. The level of *ctfAB* expression was 3-fold higher in the *adhE1* knockout compared to the control strain. This indicates that the lower flux of acetone production is the result of a control at the enzyme level due to a lower acetoacetyl-CoA concentration and/or higher acetyl-CoA/butyryl-CoA concentrations. The remaining ability of the *ΔadhE1* strain to produce butanol under solventogenesis is explained by the higher *adhE2* expression (~127-fold higher than the control strain, but only 25 mRNA molecules/cell) (Table 1, Additional file 2: Dataset S1). For the *ΔadhE1* mutant, the butyrate flux increased by 5-fold compared to the control strain (Additional file 1: Fig. S3), although neither *ptb-buk* (CA_C3076–CA_C3075) nor *buk2* (CA_C1660) experienced a significant transcriptional increase (Additional file 2: Dataset S1). Thus, flux is controlled at the enzyme level via an increase in the butyryl-CoA pool due to the lower flux in the butanol pathway. However, as the AdhE2 level in the mutant is the same as the AdhE1 level in the control (6.31×10^4 versus 5.99×10^4 protein molecules/cell), the lower flux of butanol production can be explained by (i) a lower catalytic efficiency of AdhE2 for butyryl-CoA and/or NADH or (ii) a lower intracellular pH under solventogenic conditions that would be less optimal for AdhE2 that is normally expressed under alcohologenic conditions at neutral pH. The second hypothesis can be eliminated as the previously measured intracellular pH [4, 21] in solventogenic and alcohologenic cells are relatively close (5.5 and 5.95, respectively) as the ΔpH is inverted (more acidic inside) under alcohologenic conditions [6]. Finally, as we will see below, the fact that ethanol flux is less affected than the butanol flux might be explained by the existence of an ethanol flux through the Pdc (pyruvate decarboxylase, encoded by CA_P0025) and bdhA/BdhB.

Table 1 Transcriptional changes of genes coding for the six key enzymes for alcohol production

Metabolic state/gene	Control	*ΔadhE1*	*ΔadhE2*
Acidogenesis			
adhE1 (CA_P0162)	0.09 ± 0.01	0 ± 0	0.2 ± 0.01
adhE2 (CA_P0035)	0.42 ± 0.02	2.31 ± 0.6	0 ± 0
bdhA (CA_C3299)	8.15 ± 0.32	4.33 ± 1.03	5.76 ± 0.2
bdhB (CA_C3298)	16.31 ± 0.45	5.13 ± 4.28	1.52 ± 0.11
bdhC (CA_C3392)	8.63 ± 0.94	7.55 ± 0.28	17.65 ± 0.44
pdc (CA_P0025)	5.6 ± 0.81	1.74 ± 0.1	3.23 ± 0.24
Solventogenesis			
adhE1 (CA_P0162)	7.09 ± 0.73	0 ± 0	11.4 ± 4.71
adhE2 (CA_P0035)	0.21 ± 0.02	26.6 ± 0.26	0 ± 0
bdhA (CA_C3299)	8.22 ± 1.33	4.62 ± 0.06	7.55 ± 0.75
bdhB (CA_C3298)	28.1 ± 5.07	34.78 ± 1.55	17.76 ± 2.83
bdhC (CA_C3392)	11.28 ± 1.68	12.52 ± 0.36	9.16 ± 0.67
pdc (CA_P0025)	5.17 ± 2.78	6.59 ± 0.3	6.23 ± 1.03
Alcohologenesis			
adhE1 (CA_P0162)	0.13 ± 0.01	0 ± 0	0.18 ± 0.01
adhE2 (CA_P0035)	68.6 ± 12.95	62.56 ± 7.58	0 ± 0
bdhA (CA_C3299)	6.08 ± 0.37	4.82 ± 0.13	7.39 ± 0.21
bdhB (CA_C3298)	14.33 ± 2.65	16.96 ± 0.25	15.16 ± 0.46
bdhC (CA_C3392)	10.73 ± 0.94	11.05 ± 0.25	8.95 ± 0.32
pdc (CA_P0025)	1.23 ± 0.51	0.83 ± 0.03	1.86 ± 0.07

The numbers of mRNA molecules per cell are shown as mean values ± SD from three biological replicates

The two mutant strains were also evaluated under alcohologenic conditions and compared to previously published data for the control strain [12]. The control and *ΔadhE1* strains behaved the same, with no significant changes in metabolic fluxes (Additional file 1: Fig. S3). However, the *ΔadhE2* mutant exhibited a completely different behavior; no flux toward butanol was detected, whereas fluxes toward butyrate became the primary fluxes, as opposed to butanol in the control strain (Additional file 1: Fig. S3). In addition, acetate levels increased by ~3-fold, and such changes were accompanied by changes in electron fluxes (Fig. 3), which are described in detail below. These phenomena were not observed by Cooksley et al. [16] with their *adhE2* knockout mutant, as they performed batch fermentation without promoting alcohologenic conditions. As *adhE1* was not expressed under the "alcohologenic conditions" of the *ΔadhE2* mutant, the physiological function of *adhE2* does not appear to be compensated by *adhE1* (Table 1). To verify that loss of the butanol-producing ability under alcohologenesis did not result from loss of the pSOL1 megaplasmid [22, 23] but rather from the deletion of *adhE2*, the culture was switched to solventogenic conditions before the experiment was ended; under solventogenic conditions, high butanol and acetone production fluxes were recovered (data not shown).

The butanol pathway was analyzed for three different conditions in the respective mutants (Additional file 1: Fig. S2) by calculating the contribution of each of the five enzymes potentially involved in each of the two steps to the fluxes (see methods for the calculation).

Under acidogenesis, *adhE1* was not expressed, and thus AdhE1 could not replace AdhE2 for the conversion of butyryl-CoA to butyraldehyde in the *ΔadhE2* mutant (Additional file 1: Fig. S2). This failure of AdhE1 to replace AdhE2 led to the absence of butanol production in the *ΔadhE1* mutant, which behaved the same as the control strain, leaving AdhE2 responsible for all the conversion. The *ΔadhE1* mutant behaved the same as the control strain with respect to the conversion of butyraldehyde to butanol under these conditions, and AdhE2 (45 % of the flux), BdhB (34 % of the flux), and BdhA (14 % of the flux) were the main contributors (Additional file 1: Fig. S2). The *ΔadhE2* mutant was not analyzed because it does not produce butanol.

Under solventogenesis, AdhE2 replaced AdhE1 for the conversion of butyryl-CoA to butyraldehyde in the *ΔadhE1* mutant, while in the *ΔadhE2* mutant, which behaved the same as the control strain, AdhE1 was responsible for all the conversion. The two main contributors to the conversion of butyraldehyde to butanol under these conditions were AdhE2 (67 % of the flux) and BdhB (30 % of the flux) in the *ΔadhE1* mutant, while in the *ΔadhE2* mutant, which behaved the same as the control strain, BdhB (75 % of the flux) and BdhA (16 % of the flux) were the main contributors (Additional file 1: Fig. S2).

Under alcohologenesis, *adhE1* was not expressed (Table 1, Additional file 2: Dataset S1), and thus, AdhE1 could not replace AdhE2 for the conversion of butyryl-CoA to butyraldehyde in the *ΔadhE2* mutant. This failure of AdhE1 to replace AdhE2 led to the absence of butanol production, while in the *ΔadhE1* mutant, which behaved the same as the control strain, AdhE2 was responsible for all the conversion. The *ΔadhE1* mutant behaved the same as the control strain with respect to the conversion of butyraldehyde to butanol under these conditions, and AdhE2 was the main contributor (Additional file 1: Fig. S2). The *ΔadhE2* mutant was not analyzed because it does not produce butanol.

Two possible routes are known for the conversion of pyruvate to acetaldehyde in *C. acetobutylicum*: (i) a two-step reaction by pyruvate:ferredoxin oxidoreductase (PFOR) and acetaldehyde dehydrogenase via acetyl-CoA production or (ii) a one-step reaction by pyruvate decarboxylase (Pdc, encoded by CA_P0025) [24]. In the wild-type strain, the former route is considered as the primary pathway [2, 25]. Under acidogenic and alcohologenic

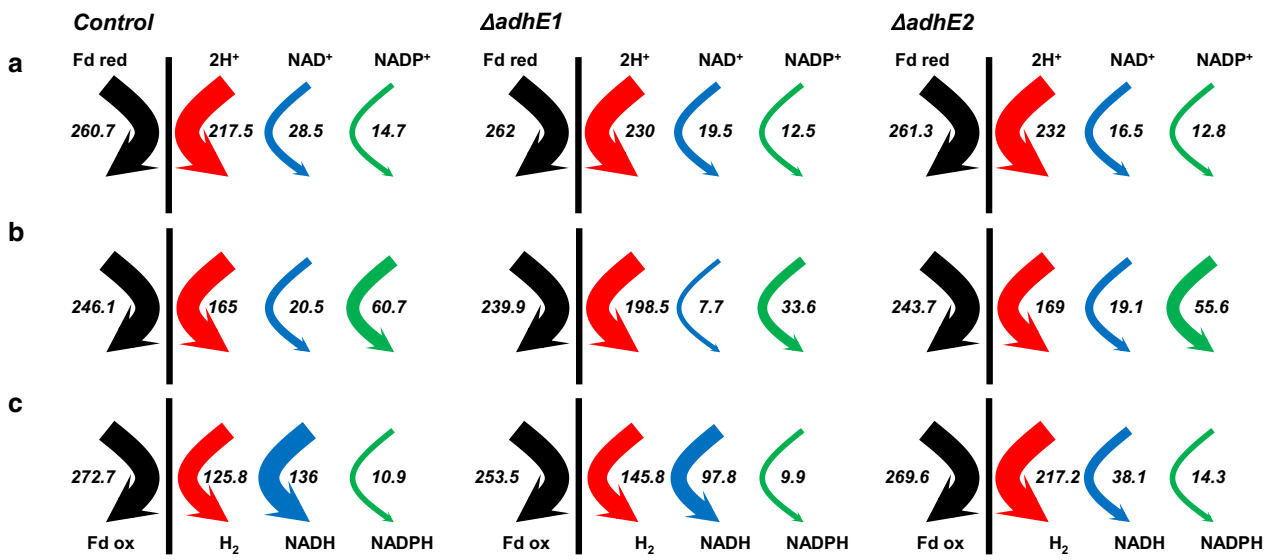

Fig. 3 Electron flux map of the control, *ΔadhE1* and *ΔadhE2* strains in acidogenesis (**a**), solventogenesis (**b**), and alcohologenesis (**c**). The *arrows* for hydrogenase (*red*), ferredoxin-NAD + reductase (*blue*), and ferredoxin-NADP + (*green*) in vivo fluxes are presented. All values are normalized to the flux of the initial carbon source [millimoles per gram of dry cell weight (DCW) per hour]. Glucose flux is normalized to 100 for acidogenesis and solventogenesis, and the sum of glucose and half of the glycerol is normalized to 100 for alcohologenesis

conditions of the *ΔadhE2* mutant, ethanol production was observed, but no butanol production was detected (Fig. 2, Additional file 1: Fig. S3). As previously reported [12], AdhE1 retains only aldehyde dehydrogenase activity, whereas AdhE2 possesses both aldehyde and alcohol dehydrogenases activities. Thus, the ethanol production of the *ΔadhE2* mutant suggests that the latter route is active. In other words, Pdc could be functional, and the ethanol dehydrogenase activity in acidogenesis could be due to BdhA, BdhB, or BdhC (Table 1). The same pathway might also be functional in solventogenesis and explains why in the *ΔadhE1* mutant the ethanol flux was less affected than the butanol flux.

Because the predominant use of reduced ferredoxin is for hydrogen production [12], no significant effects were observed under acidogenesis in both the *ΔadhE1* and *ΔadhE2* mutants with respect to electron flux (Fig. 3). In addition, solventogenesis of the *ΔadhE2* mutant exhibited similar flux levels to the control strain due to the small contribution of AdhE2 (5 % for butyraldehyde dehydrogenase function and 9 % for butanol dehydrogenase function) under these conditions in the control strain. However, under the same conditions as for *ΔadhE1*, both the fluxes for NADH, known as the partner of AdhE1 and AdhE2, and for NADPH, known as the partner of BdhA, BdhB, and BdhC, were reduced (by ~2.7-fold and 1.8-fold, respectively) due to decreased carbon fluxes toward alcohols (Fig. 3, Additional file 1: Fig. S3). The most striking changes were observed in the *ΔadhE2* mutant under alcohologenesis, in which the primary use of reduced ferredoxin was switched from NADH to hydrogen production. The absence of butanol formation resulted in a ~3.6-fold decreased flux toward NADH production and a 1.7-fold increased flux toward hydrogen production (Fig. 3).

Common criteria used for quantitative transcriptomic analysis

To filter the data from only significant results, the same criteria used to compare the wild-type strain under different physiological conditions [12] were used to compare the mutants to the control strain. The first criterion was >4.0-fold higher expression or >4.0-fold lower expression in *ΔadhE1* or *ΔadhE2* than in the control strain under the same physiological condition, and the second criterion was >0.2 mRNA molecules per cell in at least one of the two strains being compared.

Genes affected by *adhE1* or *adhE2* deletion under acidogenesis

As alcohols are minor products under acidogenesis, the deletion of *adhE1* or *adhE2* did not significantly alter the metabolic flux map (Additional file 1: Fig. S3). However, a surprisingly large number of genes (100 genes increased in *ΔadhE1*, 108 genes decreased in *ΔadhE1*, 119 genes increased in *ΔadhE2*, 170 genes decreased in *ΔadhE2*) showed significant changes in mRNA molecules/cell in response to the deletion of each gene (Table 2). Furthermore, 50 genes (>4-fold increase) and 87 genes (>4-fold

decrease) revealed the same patterns of change in both the *ΔadhE1* and *ΔadhE*2 mutants (Table 2). The primary metabolism-related genes that influence metabolic fluxes did not exhibit significant changes, whereas mostly subordinate metabolism-related genes were affected (Additional file 1: Table S2, Additional file 1: S3, and Fig. 4).

Interestingly, a large portion (18 genes showed >a 4-fold increase, and 2 genes showed a >2.8-fold increase out of 30 genes proposed by Wang et al. [26]) of the cysteine metabolism regulator (CymR) regulon showed significantly increased expression in both mutants under acidogenesis (CymR regulons are indicated in Table 3). In particular, an operon involved in cysteine and sulfur metabolism (CA_C0102–CA_C0110) showed a >10-fold increase in both mutants. This operon was reported to respond to butyrate/butanol stresses and to be up-regulated under alcohologenesis in wild-type strains [12, 26, 27] and under solventogenesis in the *Δptb* mutant [28]. In addition, the expression of two putative cysteine ABC transporter operons belonging to the CymR regulon [26, 27], namely CA_C0878–CA_C0880 and CA_C3325–CA_C3327), was also up-regulated.

A long gene cluster linked to iron/sulfur/molybdenum metabolism (CA_C1988–CA_C2019) exhibited significantly decreased expression (except for CA_C1988, CA_C1990, CA_C1992 and CA_C1995, for which some values were below the significance criterion of 4-fold but were higher than 3-fold) (Table 3, Additional file 2: Dataset S1). A part of this cluster, CA_C1988–CA_C1996, was previously reported to be down-regulated under oxygen-exposed conditions [29]. Moreover, this cluster was shown by Schwarz et al. [30] to be repressed by butanol stress in an acidogenic chemostat.

Transcriptional changes due to *adhE1* or *adhE2* deletion under solventogenesis

Under solventogenesis, a drastic change in fluxes was observed in the *ΔadhE1* mutant, while the fluxes remained unchanged in the *ΔadhE2* mutant; additionally, as expected, more genes showed significant changes in *ΔadhE1* than in *ΔadhE2* (Table 2, Additional file 1: Table S4, Additional file 1: S5). Specifically, in *ΔadhE1,* 55 genes were up-regulated, and 127 genes were down-regulated (Table 2). In *ΔadhE2*, 22 genes were up-regulated, and 17 genes were down-regulated (Table 2). In contrast to the observations previously made under acidogenesis, no gene was significantly increased in both the *ΔadhE1* and *ΔadhE*2 mutants, and only 1 gene (CA_C3612, encoding a hypothetical protein) was significantly decreased in both mutants.

In *ΔadhE1*, the CA_C0102–CA_C0110 operon which was shown to be up-regulated in acidogenesis and belongs to the CymR regulon, was also up-regulated by >18-fold under solventogenesis (Additional file 1: Table S4). However, the up-regulation of this operon (under alcohologenesis in the control strain, acidogenesis and solventogenesis in *ΔadhE1*, or acidogenesis in *ΔadhE2*) did not have striking shared features with the main product profile.

Interestingly, expression of the *natAB* operon (CA_C3551–CA_C3550) (>10-fold), encoding a potential Na^+-ABC transporter, and the *kdp* gene cluster (CA_C3678–CA_C3682), encoding a potential K^+ transporter (>20-fold), was highly up-regulated under solventogenesis (Additional file 1: Table S4, Additional file 2: Dataset S1) in *ΔadhE1*. The *natAB* operon and the *kdp* gene cluster have previously been reported to be up-regulated by both acetate and butyrate stress [27]. As the ability of the *ΔadhE1* mutant to produce butanol was highly affected and as butyrate and acetate were the primary fermentation products (Fig. 2), this strain struggled to survive under acidic conditions (i.e., under the pH of 4.4 for solventogenesis); consequently, genes involved in ion transport were up-regulated.

The operon CA_P0029–CA_P0030, which potentially encodes a transporter and an isochorismatase, was up-regulated under acidogenesis in both mutants as well as

Table 2 Numbers of significantly changed genes by each gene deletion and genes exhibiting the same pattern of change for both deletions under three different metabolic states (the genes exhibiting the same pattern for both deletions under acidogenesis are listed in Table 3)

	Δ*adhE1*	Δ*adhE2*	Same pattern in Δ*adhE1* and Δ*adhE2*	Note[a]
Up-regulation under acidogenesis	100	119	50	Most CymR regulons are included
Down-regulation under acidogenesis	108	170	89	Most butanol response genes are included
Up-regulation under solventogenesis	55	22	0	
Down-regulation under solventogenesis	127	17	1	CA_C3612
Up-regulation under alcohologenesis	1	35	0	
Down-regulation under alcohologenesis	14	38	1	CA_C3274

[a] Representative features or locus number of the sole gene showing same pattern under certain condition are shown

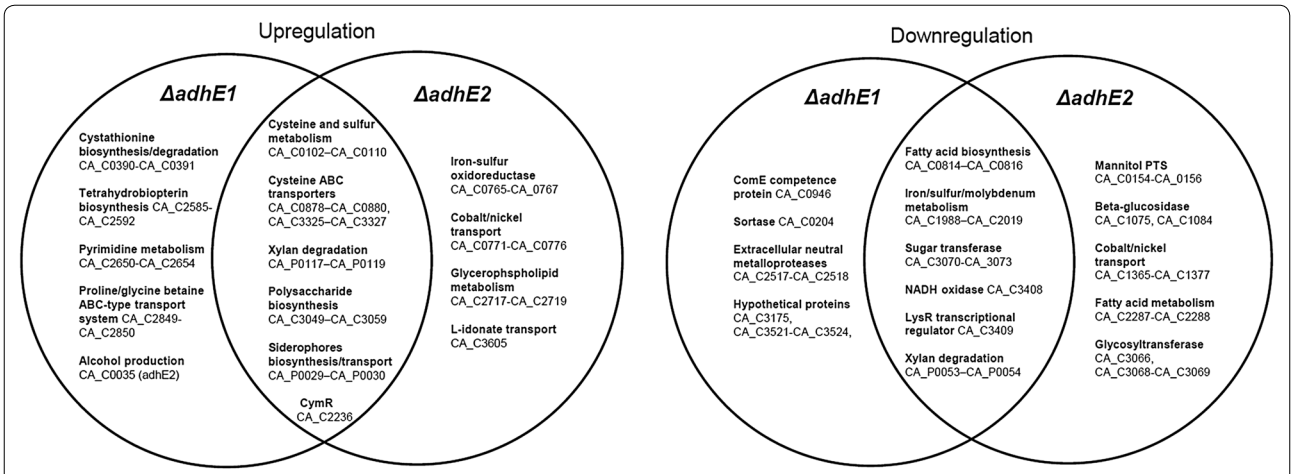

Fig. 4 Venn diagrams of representative genes with involved pathways, which matched the significance criteria (>4-fold increase or decrease) in the *ΔadhE1* and *ΔadhE2* mutants. A complete list of each metabolic condition is provided in the Additional file 2

under solventogenesis in *ΔadhE2* (>20-fold) (Table 2, Additional file 1: Table S5). Two neighboring genes, CA_C3604 (*ilvD*), encoding dihydroxyacid dehydratase linked to valine/leucine/isoleucine biosynthesis, and CA_C3605 (*gntP*), encoding high affinity gluconate/L-idonate permease, exhibited striking increases (>120-fold) (Additional file 1: Table S5) in *ΔadhE2*.

As described above, the solventogenic culture of *ΔadhE1* has a lower glucose consumption rate than the control strain (Fig. 2) and consequently more glucose remained unconsumed in the medium. Accordingly, numerous genes related to sugar metabolism were down-regulated under this metabolic state. For instance, all the structural genes on the mannitol phosphotransferase system (PTS)-related operon *mtlARFD* (CA_C0154–CA_C0157) and the mannose PTS-related operon (CA_P0066–CA_P0068) were decreased by >10-fold (Additional file 1: Table S4).

Interestingly, one of two operons encoding a quorum-sensing system and putatively involved in sporulation, CA_C0078–CA_C0079 (*agrBD*) [31], was strongly down-regulated (infinity-fold for CA_C0078 and 667-fold for CA_C0078) in *ΔadhE2* relative to the control strain (Additional file 1: Table S5). However, the other operon, CA_C0080–CA_C0081 (*agrCA*), did not significantly change (<3-fold decreases) (Additional file 2: Dataset S1). Quantitatively, less than 1 *agrCA* mRNA molecule was found per cell, whereas more than 1 *agrBD* mRNA molecule was found per cell under all conditions in the control strain [12]. These different expression levels are not surprising because *agrBD* and *agrCA* are independently transcribed [31–33]. In addition, *agrBD* was repressed under all conditions in *ΔadhE2*, although the sporulation of this mutant was not affected (Additional file 2: Dataset S1).

Transcriptional changes due to *adhE1* or *adhE2* deletion under alcohologenesis

Under alcohologenesis, a drastic change in fluxes was observed in the *ΔadhE2* mutant, while in the *ΔadhE1* mutant, the fluxes remained unchanged. As expected, more genes showed significant changes in the *ΔadhE2* mutant than in the *ΔadhE1* mutant (Table 2). Specifically, in *ΔadhE1*, only 1 gene was up-regulated (*agrB),* and 14 genes were down-regulated, while in *ΔadhE2,* 35 genes were up-regulated, and 38 genes were down-regulated.

The most dynamic changes in the *ΔadhE2* mutant were observed in CA_C3604 (*ilvD*, 297-fold) and CA_C3605 (*gntP*, 301-fold) (Additional file 1: Table S7). As mentioned previously, these genes were highly up-regulated (>84-fold) under all the conditions in the *ΔadhE2* mutant (Additional file 2: Dataset S1). Interestingly, two genes located immediately downstream of *adhE2,* CA_P0036, which encodes a cytosolic protein of unknown function, and CA_P0037, which encodes a potential transcriptional regulator, exhibited a ~ 9-fold increase under alcohologenesis (Additional file 1: Table S7) in *ΔadhE2.*

A sucrose metabolism operon comprising *scrAKB* (CA_C0423–CA_C0425), encoding a PTS IIBCA domain on a single gene, fructokinase and sucrose-6-P hydrolase [35, 36], was strikingly down-regulated (>47-fold) (Additional file 1: Table S6). Moreover, the gene immediately upstream, *scrT* (CA_C0422) (encoding a putative transcriptional antiterminator), and the gene downstream, CA_C0426, encoding a putative AraC-type of regulator, were also decreased, by 9.3-fold and 8-fold, respectively (Additional file 1: Table S6). The similar expression patterns of CA_C0422, CA_C0426, and *scrAKB* support the hypotheses of previous studies regarding their roles in regulating *scrAKB* [35, 36].

Table 3 Genes exhibiting the same pattern of change for both deletions under acidogenesis

Locus number	Function	*ΔadhE1*/Control strain	*ΔadhE2*/Control strain	Note[a]
Up-regulation				
CA_C0102	O-acetylhomoserine sulfhydrylase	28.70	20.49	CymR
CA_C0103	Adenylylsulfate kinase	32.55	22.06	CymR
CA_C0104	Adenylylsulfate reductase, subunit A	48.44	28.89	CymR
CA_C0105	Ferredoxin	30.78	21.84	CymR
CA_C0106	ABC-type probable sulfate transporter, periplasmic binding protein	26.09	14.54	CymR
CA_C0107	ABC-type sulfate transporter, ATPase component	22.86	13.03	CymR
CA_C0108	ABC-type probable sulfate transporter, permease protein	35.38	19.05	CymR
CA_C0109	Sulfate adenylate transferase, CysD subfamily	42.53	26.82	CymR
CA_C0110	GTPase, sulfate adenylate transferase subunit 1	54.78	42.48	CymR
CA_C0117	Chemotaxis protein cheY homolog	8.34	6.69	
CA_C0118	Chemotaxis protein cheA	11.00	8.24	
CA_C0119	Chemotaxis protein cheW	13.83	9.52	
CA_C0120	Membrane-associated methyl-accepting chemotaxis protein with HAMP domain	6.93	5.29	
CA_C0878	Amino acid ABC transporter permease component	5.61	4.04	CymR
CA_C0879	ABC-type polar amino acid transport system, ATPase component	8.29	5.60	CymR
CA_C0880	Periplasmic amino acid binding protein	9.50	6.50	CymR
CA_C0930	Cystathionine gamma-synthase	4.58	4.72	CymR
CA_C1392	Glutamine phosphoribosylpyrophosphate amidotransferase	4.20	4.47	
CA_C1394	Folate-dependent phosphoribosylglycinamide formyltransferase	4.11	4.57	
CA_C2072	Stage IV sporulation protein B, SpoIVB	∞	∞	
CA_C2235	Cysteine synthase/cystathionine beta-synthase, CysK	8.27	7.17	CymR
CA_C2236	Uncharacterized conserved protein of YjeB/RRF2 family	4.29	4.06	CymR encoding gene
CA_C2241	Cation transport P-type ATPase	7.92	7.62	
CA_C2242	Predicted transcriptional regulator, arsE family	5.01	5.22	
CA_C2521	Hypothetical protein, CF-41 family	4.33	5.70	
CA_C2533	Protein containing ChW-repeats	∞	∞	
CA_C2816	Hypothetical protein, CF-17 family	6.00	11.20	
CA_C3049	Glycosyltransferase	4.79	7.42	
CA_C3050	AMSJ/WSAK-related protein, possibly involved in exopolysaccharide biosynthesis	4.70	8.25	
CA_C3051	Glycosyltransferase	5.16	9.60	
CA_C3052	Glycosyltransferase	5.59	9.91	
CA_C3053	Histidinol phosphatase-related enzyme	7.03	10.94	
CA_C3054	Phosphoheptose isomerase	6.69	11.37	
CA_C3055	Sugar kinase	5.90	10.87	
CA_C3056	Nucleoside-diphosphate-sugar pyrophosphorylase	6.37	11.28	
CA_C3057	Glycosyltransferase	12.36	11.92	
CA_C3058	Mannose-1-phosphate guanylyltransferase	9.94	11.59	

Table 3 continued

Locus number	Function	*ΔadhE1*/Control strain	*ΔadhE2*/Control strain	Note[a]
CA_C3059	Sugar transferases	13.47	12.63	
CA_C3325	Periplasmic amino acid binding protein	18.24	10.68	CymR
CA_C3326	Amino acid ABC-type transporter, permease component	19.82	11.79	CymR
CA_C3327	Amino acid ABC-type transporter, ATPase component	28.33	16.73	CymR
CA_C3461	Hypothetical protein	4.52	16.79	
CA_C3556	Probable S-layer protein;	4.18	10.41	
CA_C3636	Oligopeptide ABC transporter, ATPase component	4.23	4.68	
CA_P0029	Permease MDR-related	∞	∞	
CA_P0030	Isochorismatase	385.91	81.89	
CA_P0031	Transcriptional activator HLYU, HTH of ArsR family	46.17	10.93	
CA_P0117	Possible beta-xylosidase diverged, family 5/39 of glycosyl hydrolases and alpha-amylase C (Greek key) C-terminal domain	56.53	4.94	
CA_P0118	Possible xylan degradation enzyme (glycosyl hydrolase family 30-like domain and Ricin B-like domain)	54.97	5.22	
CA_P0119	Possible xylan degradation enzyme (glycosyl hydrolase family 30-like domain and Ricin B-like domain)	46.44	4.23	
Down-regulation				
CA_C0078	Accessory gene regulator protein B	0.04	0.00	
CA_C0079	Hypothetical protein	0.00	0.00	
CA_C0082	Predicted membrane protein	0.02	0.00	
CA_C0310	Regulators of stationary/sporulation gene expression, abrB B.subtilis ortholog	0.15	0.23	
CA_C0381	Methyl-accepting chemotaxis protein	0.18	0.13	
CA_C0437	Sensory transduction histidine kinase	0.15	0.23	
CA_C0537	Acetylxylan esterase, acyl-CoA esterase or GDSL lipase family, strong similarity to C-terminal region of endoglucanase E precursor	0.15	0.10	
CA_C0542	Methyl-accepting chemotaxis protein	0.21	0.08	
CA_C0658	Fe-S oxidoreductase	0.24	0.00	
CA_C0660	Hypothetical protein, CF-26 family	0.17	0.08	BuOH
CA_C0814	3-oxoacyl-[acyl-carrier-protein] synthase III	0.11	0.02	BuOH
CA_C0815	Methyl-accepting chemotaxis protein	0.13	0.04	BuOH
CA_C0816	Lipase-esterase-related protein	0.17	0.04	BuOH
CA_C1010	Predicted phosphohydrolase, Icc family	0.21	0.04	BuOH
CA_C1022	Thioesterase II of alpha/beta hydrolase superfamily	0.22	0.11	
CA_C1078	Predicted phosphohydrolase, Icc family	0.17	0.04	BuOH
CA_C1079	Uncharacterized protein, related to enterotoxins of other Clostridiales	0.15	0.05	
CA_C1080	Uncharacterized protein, probably surface-located	0.11	0.01	
CA_C1081	Uncharacterized protein, probably surface-located	0.13	0.01	
CA_C1532	Protein containing ChW-repeats	0.22	0.08	
CA_C1766	Predicted sigma factor	0.19	0.00	
CA_C1775	Predicted membrane protein	0.16	0.05	

Table 3 continued

Locus number	Function	*ΔadhE1*/Control strain	*ΔadhE2*/Control strain	Note[a]
CA_C1868	Uncharacterized secreted protein, homolog YXKC Bacillus subtilis	0.22	0.18	
CA_C1989	ABC-type iron (III) transport system, ATPase component	0.18	0.11	BuOH
CA_C1991	Uncharacterized protein, YIIM family	0.23	0.10	BuOH
CA_C1993	Molybdenum cofactor biosynthesis enzyme MoaA, Fe-S oxidoreductase	0.23	0.18	BuOH
CA_C1994	Molybdopterin biosynthesis enzyme, MoaB	0.22	0.11	BuOH
CA_C1996	Hypothetical protein	0.19	0.08	BuOH
CA_C1997	Predicted glycosyltransferase	0.19	0.07	BuOH
CA_C1998	ABC-type transport system, ATPase component	0.19	0.07	BuOH
CA_C1999	Uncharacterized protein related to hypothetical protein Cj1507c from Campylobacter jejuni	0.20	0.07	BuOH
CA_C2000	Indolepyruvate ferredoxin oxidoreductase, subunit beta	0.19	0.06	BuOH
CA_C2001	Indolepyruvate ferredoxin oxidoreductase, subunit alpha	0.13	0.04	BuOH
CA_C2002	Predicted iron-sulfur flavoprotein	0.16	0.05	BuOH
CA_C2003	Predicted permease	0.16	0.08	BuOH
CA_C2004	Siderophore/Surfactin synthetase-related protein	0.10	0.04	BuOH
CA_C2005	Siderophore/Surfactin synthetase-related protein	0.12	0.05	BuOH
CA_C2006	Enzyme of siderophore/surfactin biosynthesis	0.15	0.07	BuOH
CA_C2007	Predicted glycosyltransferase	0.09	0.03	BuOH
CA_C2008	3-oxoacyl-(acyl-carrier-protein) synthase	0.11	0.04	BuOH
CA_C2009	3-Hydroxyacyl-CoA dehydrogenase	0.10	0.03	BuOH
CA_C2010	Predicted Fe-S oxidoreductase	0.09	0.03	BuOH
CA_C2011	Possible 3-oxoacyl-[acyl-carrier-protein] synthase III	0.12	0.03	BuOH
CA_C2012	Enoyl-CoA hydratase	0.12	0.04	BuOH
CA_C2013	Hypothetical protein	0.12	0.03	BuOH
CA_C2014	Predicted esterase	0.12	0.02	BuOH
CA_C2015	Hypothetical protein	0.15	0.04	BuOH
CA_C2016	Enoyl-CoA hydratase	0.12	0.02	BuOH
CA_C2017	Acyl carrier protein	0.15	0.03	BuOH
CA_C2018	Aldehyde:ferredoxin oxidoreductase	0.12	0.03	BuOH
CA_C2019	Malonyl CoA-acyl carrier protein transacylase	0.12	0.02	BuOH
CA_C2020	Molybdopterin biosynthesis enzyme, MoeA, fused to molybdopterin-binding domain	0.20	0.07	
CA_C2021	Molybdopterin biosynthesis enzyme, MoeA (short form)	0.24	0.06	
CA_C2023	Membrane protein, related to copy number protein COP from Clostridium perfringens plasmid pIP404 (GI:116,928)	0.22	0.12	
CA_C2026	Predicted flavodoxin	0.20	0.09	
CA_C2107	Contains cell adhesion domain	0.20	0.08	
CA_C2293	Hypothetical secreted protein	0.13	0.10	
CA_C2581	6-pyruvoyl-tetrahydropterin synthase-related domain; conserved membrane protein	0.24	0.11	BuOH
CA_C2663	Protein containing cell wall hydrolase domain	0.23	0.09	

Table 3 continued

Locus number	Function	*ΔadhE1*/Control strain	*ΔadhE2*/Control strain	Note[a]
CA_C2695	Diverged Metallo-dependent hydrolase(Zn) of DD-Peptidase family; peptodoglycan-binding domain	0.17	0.12	BuOH
CA_C2807	Endo-1,3(4)-beta-glucanase family 16	0.21	0.02	
CA_C2808	Beta-lactamase class C domain (PBPX family) containing protein	0.20	0.04	
CA_C2809	Predicted HD superfamily hydrolase	0.14	0.02	
CA_C2810	Possible glucoamylase (diverged), 15 family	0.14	0.01	
CA_C2944	N-terminal domain intergin-like repeats and c-terminal- cell wall-associated hydrolase domain	0.23	0.06	BuOH
CA_C3070	Glycosyltransferase	0.21	0.04	
CA_C3071	Glycosyltransferase	0.21	0.03	
CA_C3072	Mannose-1-phosphate guanylyltransferase	0.18	0.02	
CA_C3073	Sugar transferase involved in lipopolysaccharide synthesis	0.23	0.03	
CA_C3085	TPR-repeat-containing protein; Cell adhesion domain	0.25	0.12	
CA_C3086	Protein containing cell adhesion domain	0.20	0.11	
CA_C3251	Sensory transduction protein containing HD_GYP domain	0.20	0.11	
CA_C3264	Uncharacterized conserved protein, YTFJ B.subtilis ortholog	0.19	0.15	BuOH
CA_C3265	Predicted membrane protein	0.08	0.11	
CA_C3266	Hypothetical protein	0.07	0.07	
CA_C3267	Specialized sigma subunit of RNA polymerase	0.15	0.16	
CA_C3280	Possible surface protein, responsible for cell interaction; contains cell adhesion domain and ChW-repeats	0.23	0.14	
CA_C3408	NADH oxidase (two distinct flavin oxidoreductase domains)	0.03	0.02	
CA_C3409	Transcriptional regulators, LysR family	0.02	0.01	
CA_C3412	Predicted protein-S-isoprenylcysteine methyltransferase	0.22	0.06	
CA_C3422	Sugar:proton symporter (possible xylulose)	0.05	0.03	
CA_C3423	Acetyltransferase (ribosomal protein N-acetylase subfamily)	0.04	0.03	
CA_C3612	Hypothetical protein	0.18	0.00	BuOH
CA_P0053	Xylanase, glycosyl hydrolase family 10	0.24	0.09	BuOH
CA_P0054	Xylanase/chitin deacetylase family enzyme	0.24	0.07	BuOH
CA_P0057	Putative glycoprotein or S-layer protein	0.21	0.13	BuOH
CA_P0135	Oxidoreductase	0.25	0.21	
CA_P0136	AstB/chuR/nirj-related protein	0.25	0.23	
CA_P0174	Membrane protein	0.25	0.14	

[a] CymR indicates CymR regulon, BuOH indicates the genes to be down-regulated by butanol stress in an acidogenic chemostat in the study by Schwarz et al. [30]

As expected based on the reduced consumption of glycerol (approximately one-fourth of the control strain) (Fig. 2) in *ΔadhE2*, the gene cluster for glycerol transport and utilization (CA_C1319-CA_C1322) was down-regulated (>4.3-fold) under these conditions (Additional file 1: Table S7).

Most arginine biosynthesis-related genes known to respond negatively to butanol and butyrate stress [26] (i.e., CA_C0316 (*argF/I*), CA_C0973–CA_C0974 (*argGH*), CA_C2389–CA_C2388 (*argBD*), CA_C2390–CA_C2391 (*argCJ*), CA_C2644 (*carB*), and CA_C2645 (*carA*)) were significantly down-regulated (>4-fold decrease) (Additional file 1: Table S7) in *ΔadhE2*. As "alcohologenic cultures" of *ΔadhE2* produced 70 mM of butyrate and no butanol (Fig. 2), this down-regulation is consistent with the high butyrate stress (50 mM) response [26].

CA_C3486, which encodes a multimeric flavodoxin, was decreased by 4.4-fold in *ΔadhE2* (Additional file 1: Table S7), resulting in a loss of butanol production under alcohologenesis. This finding is consistent with the proposed hypothesis [12] that under alcohologenesis, the gene product of CA_C3486 may function as a redox partner between the hydrogenase and ferredoxin-NAD^+ reductase and may participate in the redistribution of electron fluxes in favor of butanol formation.

Conclusions

The results presented here support the hypothesis of the roles of AdhE1 and AdhE2 in butanol formation, namely that AdhE1 is the key enzyme for butanol formation in solventogenesis and that AdhE2 is the key enzyme for butanol formation in alcohologenesis. Furthermore, this study also demonstrates the metabolic flexibility of *C. acetobutylicum* in response to genetic alteration of its primary metabolism.

Methods

Bacterial strains and plasmid construction

All *C. acetobutylicum* strains used in this study and in the control study were constructed from the *C. acetobutylicum* ATCC 824 Δ*CA_C1502* Δ*upp* mutant strain, which was constructed for rapid gene knockout and gene knockin [38]. Detailed procedures, including all strains and primers used, are described in the online supporting information (Supplementary experimental procedures).

Culture conditions

All batch cultures were performed under strict anaerobic conditions in synthetic medium (MS), as previously described [4]. *C. acetobutylicum* was stored in spore form at −20 °C after sporulation in MS medium. Heat shock was performed for spore germination by immersing the 30- or 60-mL bottle into a water bath at 80 °C for 15 min.

All the phosphate-limited continuous cultivations were performed as previously described by Vasconcelos et al. [4] and Girbal et al. [21] like in the control strain study [12]. The chemostat was fed a constant total of 995 mM of carbon and maintained at a dilution rate of 0.05 h^{-1}. The maintained pH of the bioreactor and the supplied carbon sources of each metabolic state were as follows: for acidogenesis, pH 6.3, with 995 mM of carbon from glucose; for solventogenesis, pH 4.4, with 995 mM of carbon from glucose; and for alcohologenesis, pH 6.3, with 498 mM of carbon from glucose and 498 mM of carbon from glycerol.

RNA extraction and microarray

Total RNA isolation and microarray experiments were performed as previously described [12]. Briefly, 3 mL of chemostat cultures was sampled, immediately frozen in liquid nitrogen and ground with 2-mercaptoethanol. RNA was extracted by using an RNeasy Midi kit (Qiagen, Courtaboeuf, France) and RNase-Free DNase Set (Qiagen) per the manufacturer's protocol. The RNA quantity and integrity were monitored using an Agilent 2100 Bioanalyzer (Agilent Technologies, Massy, France) and a NanoDrop ND-1000 spectrophotometer (Labtech France, Paris, France) at 260 and 280 nm. All microarray procedures were performed per the manufacturer's protocol (Agilent One-Color Microarray-Based Exon Analysis).

Analytical methods

The optical density at 620 nm (OD620 nm) was monitored and used to calculate the biomass concentration with the correlation factor between dry cell weight and OD620 nm (path length 1 cm) of 0.28, which was experimentally determined from continuous cultures and was used in a control strain study [12]. The glucose, glycerol, acetate, butyrate, lactate, pyruvate, acetoin, acetone, ethanol, and butanol concentrations were determined using high-performance liquid chromatography (HPLC), as described by Dusséaux et al. [39]. The concentration of the eluent H_2SO_4 was changed to 0.5 mM, as this concentration was required to optimize the mobile phase for the control strain study [12].

Calculation of the cytosolic proteins concentration (protein molecules per cell)

In a previously published work [12], we quantified the amount of (i) mRNA molecules per cell for all genes and (ii) protein molecules per cell (for approximately 700 cytosolic proteins) for steady-state chemostat cultures (at a specific growth rate of 0.05 h^{-1}) of *C. acetobutylicum* under different physiological conditions. For 96 % of the cytosolic proteins that could be quantified, a

linear relationship was obtained, with an $R^2 > 0.9$, when the numbers of protein molecules per cell were plotted against the numbers of mRNA molecules per cell. This result indicated that for steady-state continuous cultures run at the same specific growth rate and with the same total amount of carbon supplied, the rate of protein turnover is proportional to the mRNA content for 96 % of the genes. As the mutants were cultivated in chemostat culture at the same growth rate (0.05 h^{-1}), we used the absolute protein synthesis rates previously calculated [12] for each of the 700 genes to calculate the amount of protein molecule per cell for each of these 700 genes in the different mutants. (Additional file 2: Dataset S1).

Calculation of the contribution of different enzymes on the butanol flux

The contribution of the 5 proteins potentially involved in the butanol pathway, namely AdhE1, AdhE2, BdhA, BdhB, and BdhC, was made as previously described [12] by assuming that all five enzymes function at their Vmax and using the calculated amount of each protein per cell (Additional file 2: Dataset S1).

Additional files

Additional file 1. Supplementary experimental procedures and results.

Additional file 2. Dataset S1. Transcriptomic data of the total open reading frames (ORFs).

Abbreviations

Flp: flippase; FRT: flippase recognition target; catP: chloramphenicol acetyltransferase.

Authors' contributions

CC, IMS, and PS conceived the study; MY performed all the experimental work. MY and PS performed the data analysis and drafted the manuscript. PS supervised the work. All authors read and approved the final manuscript.

Author details

[1] INSA, UPS, INP, LISBP, Université de Toulouse, Toulouse, France. [2] INRA, UMR792, Toulouse, France. [3] CNRS, UMR5504, Toulouse, France. [4] Metabolic Explorer, Biopôle Clermont-Limagne, Saint Beauzire, France.

Acknowledgements

We thank Sophie Lamarre and Lidwine Trouilh for help with the data analysis.

Availability of supporting data

Microarray data can be accessed at GEO through accession number GSE69973.

Competing interests

The authors declare that they have no competing interests.

Consent for publication

Not applicable.

Ethical Approval and Consent to participate

Not applicable.

Funding

This work was financially supported by the European Community's Seventh Framework Program "CLOSTNET" (PEOPLE-ITN-2008-237,942) to Minyeong Yoo.

Received: 4 February 2016 Accepted: 12 April 2016
Published online: 26 April 2016

References

1. Nair RV, Bennett GN, Papoutsakis ET. Molecular characterization of an aldehyde/alcohol dehydrogenase gene from Clostridium acetobutylicum ATCC 824. J Bacteriol. 1994;176(3):871–85.
2. Lutke-Eversloh T, Bahl H. Metabolic engineering of Clostridium acetobutylicum: recent advances to improve butanol production. Curr Opin Biotechnol. 2011;22(5):634–47.
3. Atsumi S, Liao JC. Metabolic engineering for advanced biofuels production from Escherichia coli. Curr Opin Biotechnol. 2008;19(5):414–9.
4. Vasconcelos I, Girbal L, Soucaille P. Regulation of carbon and electron flow in Clostridium acetobutylicum grown in chemostat culture at neutral pH on mixtures of glucose and glycerol. J Bacteriol. 1994;176(5):1443–50.
5. Girbal L, Vasconcelos I, Saint-Amans S, Soucaille P. How neutral red modified carbon and electron flow in Clostridium acetobutylicum grown in chemostat culture at neutral pH. FEMS Microbiol Rev. 1995;16(2):151–62.
6. Girbal L, Soucaille P. Regulation of Clostridium acetobutylicum metabolism as revealed by mixed-substrate steady-state continuous cultures: role of NADH/NAD ratio and ATP pool. J Bacteriol. 1994;176(21):6433–8.
7. Girbal L, Soucaille P. Regulation of solvent production in Clostridium acetobutylicum. Trends Biotechnol. 1998;16(1):11–6.
8. Bahl H, Andersch W, Gottschalk G. Continuous production of acetone and butanol by Clostridium acetobutylicum in a two-stage phosphate limited chemostat. Eur J Appl Microbiol Biotechnol. 1982;15(4):201–5.
9. Grimmler C, Janssen H, Krauße D, Fischer R-J, Bahl H, Dürre P, Liebl W, Ehrenreich A. Genome-wide gene expression analysis of the switch between acidogenesis and solventogenesis in continuous cultures of Clostridium acetobutylicum. J Mol Microbiol Biotechnol. 2011;20(1):1–15.
10. Peguin S, Soucaille P. Modulation of Carbon and Electron Flow in Clostridium acetobutylicum by Iron Limitation and Methyl Viologen Addition. Appl Environ Microbiol. 1995;61(1):403–5.
11. Fischer RJ, Helms J, Durre P. Cloning, sequencing, and molecular analysis of the sol operon of Clostridium acetobutylicum, a chromosomal locus involved in solventogenesis. J Bacteriol. 1993;175(21):6959–69.
12. Yoo M, Bestel-Corre G, Croux C, Riviere A, Meynial-Salles I, Soucaille P. A Quantitative System-Scale Characterization of the Metabolism of Clostridium acetobutylicum. *MBio* 2015, 6(6):e01808–01815.
13. Sauer U, Dürre P. Differential induction of genes related to solvent formation during the shift from acidogenesis to solventogenesis in continuous culture of Clostridium acetobutylicum. FEMS Microbiol Lett. 1995;125(1):115–20.
14. Fontaine L, Meynial-Salles I, Girbal L, Yang X, Croux C, Soucaille P. Molecular characterization and transcriptional analysis of adhE2, the gene encoding the NADH-dependent aldehyde/alcohol dehydrogenase responsible for butanol production in alcohologenic cultures of Clostridium acetobutylicum ATCC 824. J Bacteriol. 2002;184(3):821–30.
15. Leang C, Ueki T, Nevin KP, Lovley DR. A genetic system for Clostridium ljungdahlii: a chassis for autotrophic production of biocommodities and a model homoacetogen. Appl Environ Microbiol. 2013;79(4):1102–9.
16. Cooksley CM, Zhang Y, Wang H, Redl S, Winzer K, Minton NP. Targeted mutagenesis of the Clostridium acetobutylicum acetone-butanol-ethanol fermentation pathway. Metab Eng. 2012;14(6):630–41.
17. Heap JT, Pennington OJ, Cartman ST, Carter GP, Minton NP. The ClosTron: a universal gene knock-out system for the genus Clostridium. J Microbiol Methods. 2007;70(3):452–64.
18. Apfel H. Salmonella marker vaccine. In.: Google Patents; 2012.
19. Waghmare SK, Caputo V, Radovic S, Bruschi CV. Specific targeted integration of kanamycin resistance-associated nonselectable DNA in the genome of the yeast Saccharomyces cerevisiae. Biotechniques 2003, 34(5):1024–1028, 1033.

20. Storici F, Bruschi CV. Involvement of the inverted repeat of the yeast 2-micron plasmid in Flp site-specific and RAD52-dependent homologous recombination. Mol Gen Genet. 2000;263(1):81–9.
21. Girbal L, Croux C, Vasconcelos I, Soucaille P. Regulation of metabolic shifts in Clostridium acetobutylicum ATCC 824. FEMS Microbiol Rev. 1995;17(3):287–97.
22. Cornillot E, Nair RV, Papoutsakis ET, Soucaille P. The genes for butanol and acetone formation in Clostridium acetobutylicum ATCC 824 reside on a large plasmid whose loss leads to degeneration of the strain. J Bacteriol. 1997;179(17):5442–7.
23. Cornillot E, Soucaille P. Solvent-forming genes in clostridia. Nature. 1996;380(6574):489–489.
24. Atsumi S, Hanai T, Liao JC. Non-fermentative pathways for synthesis of branched-chain higher alcohols as biofuels. Nature. 2008;451(7174):86–9.
25. Lehmann D, Lutke-Eversloh T. Switching Clostridium acetobutylicum to an ethanol producer by disruption of the butyrate/butanol fermentative pathway. Metab Eng. 2011;13(5):464–73.
26. Wang Q, Venkataramanan KP, Huang H, Papoutsakis ET, Wu CH. Transcription factors and genetic circuits orchestrating the complex, multilayered response of Clostridium acetobutylicum to butanol and butyrate stress. BMC Syst Biol. 2013;7:120.
27. Alsaker KV, Paredes C, Papoutsakis ET. Metabolite stress and tolerance in the production of biofuels and chemicals: gene-expression-based systems analysis of butanol, butyrate, and acetate stresses in the anaerobe Clostridium acetobutylicum. Biotechnol Bioeng. 2010;105(6):1131–47.
28. Honicke D, Lutke-Eversloh T, Liu Z, Lehmann D, Liebl W, Ehrenreich A. Chemostat cultivation and transcriptional analyses of Clostridium acetobutylicum mutants with defects in the acid and acetone biosynthetic pathways. Appl Microbiol Biotechnol. 2014;98(23):9777–94.
29. Hillmann F, Doring C, Riebe O, Ehrenreich A, Fischer RJ, Bahl H. The role of PerR in O2-affected gene expression of Clostridium acetobutylicum. J Bacteriol. 2009;191(19):6082–93.
30. Schwarz KM, Kuit W, Grimmler C, Ehrenreich A, Kengen SW. A transcriptional study of acidogenic chemostat cells of Clostridium acetobutylicum–Cellular behavior in adaptation to n-butanol. J Biotechnol. 2012;161(3):366–77.
31. Steiner E, Scott J, Minton NP, Winzer K. An agr quorum sensing system that regulates granulose formation and sporulation in Clostridium acetobutylicum. Appl Environ Microbiol. 2012;78(4):1113–22.
32. Alsaker KV, Papoutsakis ET. Transcriptional program of early sporulation and stationary-phase events in Clostridium acetobutylicum. J Bacteriol. 2005;187(20):7103–18.
33. Paredes CJ, Rigoutsos I, Papoutsakis ET. Transcriptional organization of the Clostridium acetobutylicum genome. Nucleic Acids Res. 2004;32(6):1973–81.
34. Liu D, Chen Y, Ding F, Guo T, Xie J, Zhuang W, Niu H, Shi X, Zhu C, Ying H. Simultaneous production of butanol and acetoin by metabolically engineered Clostridium acetobutylicum. Metab Eng. 2015;27:107–14.
35. Tangney M, Mitchell WJ. Analysis of a catabolic operon for sucrose transport and metabolism in Clostridium acetobutylicum ATCC 824. J Mol Microbiol Biotechnol. 2000;2(1):71–80.
36. Servinsky MD, Kiel JT, Dupuy NF, Sund CJ. Transcriptional analysis of differential carbohydrate utilization by Clostridium acetobutylicum. Microbiology. 2010;156(11):3478–91.
37. Fischer RJ, Oehmcke S, Meyer U, Mix M, Schwarz K, Fiedler T, Bahl H. Transcription of the pst operon of Clostridium acetobutylicum is dependent on phosphate concentration and pH. J Bacteriol. 2006;188(15):5469–78.
38. Croux C, Nguyen NPT, Lee J, Raynaud C, Saint-Prix F, Gonzalez-Pajuelo M, Meynial-Salles I, Soucaille P. Construction of a restriction-less, marker-less mutant useful for functional genomic and metabolic engineering of the biofuel producer Clostridium acetobutylicum. Biotechnol Biofuel. 2016;9:21.
39. Dusseaux S, Croux C, Soucaille P, Meynial-Salles I. Metabolic engineering of Clostridium acetobutylicum ATCC 824 for the high-yield production of a biofuel composed of an isopropanol/butanol/ethanol mixture. Metab Eng. 2013;18:1–8.